

LARSA4D

Sample and Verification Problems



LARSA 4D Sample and Verification Problems

A manual for

LARSA 4D
Finite Element Analysis and Design Software

Last Revised May 24, 2023

Copyright (C) 2001-2022 LARSA, Inc. All rights reserved. Information in this document is subject to change without notice and does not represent a commitment on the part of LARSA, Inc. The software described in this document is furnished under a license or nondisclosure agreement. No part of the documentation may be reproduced or transmitted in any form or by any means, electronic or mechanical including photocopying, recording, or information storage or retrieval systems, for any purpose without the express written permission of LARSA, Inc.

Table of Contents

Samples for Linear Elastic Static Analysis	13
L01: 2D Truss with Static Loads	17
Solution Comparison	17
L02: Beam with Elastic Supports	19
Solution Comparison	20
L03: Beam on Elastic Foundation	21
Solution Comparison	23
Theoretical Results	24
L04: Space Truss Static Analysis	27
Solution Comparison	28
L05: 2D Truss with Thermal Load	29
Solution Comparison	29
L06: Static Analysis of a Space Frame	31
Solution Comparison	33
L07: Plate Thermal Analysis	35
Solution Comparison	36
L08: Shell-Bending of a Tapered Cantilever	37
Solution Comparison	38
L10: Tie Beam without Geometric Stiffening	39
Solution Comparison	40
L11: Circular Plate with a Hole Static Analysis	41
Solution Comparison	42
References	42
L12: Hemispherical Shell Static Analysis	43
Solution Comparison	45
References	45
L13: Cylindrical Roof Static Analysis	47
Reference	48
Solution Comparison	48
L14: 2D Truss - Thermal Loads and Settlement	51
Solution Comparison	52
L16: Nonlinear Thermal Load	53
Solution Comparison	53
L17: Plane Stress Element-Straight Beam with Static Loads	55
Problem Description	55
Loading	55
Solution Comparison	56
Conclusion	61
L18: Shell-Straight Beam with Static Loads	63
Problem Description	63

Results	65
References	71
L19: Shell-Twisted Beam with Static Loads	73
Problem Description	73
Loading	73
Solution Comparison	74
References	74
L20: Shell-Cylinder with Internal Pressure	75
Problem Description	75
Solution Comparison	76
References	76
L21: Shell-Patch Test with Prescribed Displacements	79
Problem Description	79
Loading	79
Solution Comparison	80
References	82
L22: Shell-Patch Test Using Thermal Loading	83
Problem Description	83
Results	84
References	86
L23: Shell-Plate on Elastic Foundation	87
Problem Description	87
Solution Comparison	87
References	88
L24: Shell-Curved Beam with Static Loads	89
Problem Description	89
Loading	90
Solution Comparison	90
References	92
L25: Shell-Rectangular Plate with Static Loads	93
Problem Description	93
Solution Comparison	94
References	96
L26: Shell-Scordelis-Lo Roof with Static Loads	99
Problem Description	99
Loading	99
Solution Comparison	99
L27: Thermal Stresses in a Plate	109
Problem Description	109
Solution Comparison	109
References	110
L28: Shell-Temperature Gradient Through Shell Thickness	111
Problem Description	111
Results	112

References	113
L29: Solid-Straight Beam with Static Loads	115
Problem Description	115
Data	115
Loading	116
Solution Comparison	127
L30: Solid-Twisted Beam with Static Loads	129
Problem Description	129
Loading	129
Solution Comparison	130
L31: Non-Prismatic Beam with Nonlinear Thermal Load	131
Problem Description	131
Solution Comparison	133
L32: Isotropic Plate Cantilever using an Orthotropic Material	137
Definition	
Problem Description	137
Solution Comparison	142
L33: Cantilever with Orthotropic Material	145
Problem Description	145
Solution Comparison	149
L35: Plate Initial Strain Load	151
Problem Description	151
Solution Comparison	152
Samples for Nonlinear Elastic Static Analysis	155
N01: Tie Beam with Geometric Stiffening	157
Solution Comparison	158
Reference	158
N02: Cable with Hanging Loads	159
Solution Comparison	159
N03: Beam on an Elastic Soil Foundation	161
Solution Comparison	161
Reference	162
N04: Truss with Misaligned Supports - Nonlinear Static	163
Solution Comparison	163
N05: Nonlinear Analysis of Cable Roof	165
Solution Comparison	165
N06: Diamond Shaped Frame - Geometric Nonlinear	167
Reference	168
Solution Comparison	168
N07: Diamond Shaped Frame - Geometric Nonlinear -	169
Incremental Joint Displacement Loading	
Reference	170
Solution Comparison	170

N08: A High Arch Structure - Geometric Nonlinear	171
Solution Comparison	172
Reference	172
N09: Thermal Expansion to Close a Gap	173
Solution Comparison	173
N13: Straight Cantilever Girder with Nonlinear Shell Elements in Membrane Action	175
Problem Description	175
Solution Comparison	176
References	177
N14: Straight Cantilever Girder with Nonlinear Shell Elements in Plate Action	179
Problem Description	179
Solution Comparison	180
References	181
N15: Slit Annular Plate with Vertical Load	183
Problem Description	183
Solution Comparison	184
References	185
N22: Rail-Structure Interaction (RSI) under thermal loads	187
Background	187
Model	187
Solution and comparison	188
References	190
Samples for Eigenvalue Analysis	191
E01: Triangular Cantilever Plate Eigenvalues	193
Solution Comparison	195
Reference	195
E02: Square Cantilever Plate Eigenvalues	197
Solution Comparison	199
E03: Beam Eigenvalues	201
Solution Comparison	201
E04: Cantilever Beam Eigenvalues	203
Solution Comparison	203
E05: Rectangular Cantilever Plate Eigenvalues	205
Solution Comparison	207
E06: Mass Spring Model Eigenvalues	209
Solution Comparison	211
E07: 2D Frame (Wilson & Bathe) Eigenvalues	213
Solution Comparison	214
References	214
E08: ASME Frame Eigenvalues	215

Solution Comparison	216
References	217
E09: Natural Frequencies of a Torsional System	219
Solution Comparison	219
Samples for Stressed Eigenvalue Analysis	221
ES01: Vibrations of Axially Loaded Beam - Nonlinear	223
Solution Comparison	224
Samples for Response Spectra Analysis	225
RSA01: 2D Frame with Static and Seismic Loads	227
Solution Comparison	230
References	233
Samples for Time History Analysis	235
TH01: Spring Mass System Time History Analysis	237
Solution Comparison	238
TH02: Beam with Concentrated Mass & Dynamic Load	239
Solution Comparison	240
TH03: Cantilever Beam Time History Analysis	243
Solution Comparison	245
References	246
TH04: Dynamic Analysis of a Bridge	247
Solution Comparison	248
References	248
TH05: Two Dimensional Frame with Linear Viscous Damper	249
Background	249
Problem Description	249
Nonlinear Dashpots	253
Limitations	255
References	255
TH15: Rolling Stock Analysis	257
Model Setup	257
Rolling Stock Analysis	260
Moving Load Analysis	262
Comparison of Results	263
Dynamic Effect	264
TH18: Hysteretic Spring Time History Analysis	267
Modeling	269
Case 1: Hysteretic spring with bilinear backbone curve and without stiffness and strength degradation	269
Case 2: Hysteretic spring with bilinear backbone curve and stiffness degradation	271
Case 3: Hysteretic spring with bilinear backbone curve and ductility-based strength degradation	271

Case 4: Hysteretic spring with bilinear backbone curve and energy based strength degradation	272
Case 5: Hysteretic spring with trilinear backbone curve and vertex-oriented polygonal hysteretic model (PHM)	272
Case 6: Hysteretic spring with trilinear backbone curve and yield-oriented PHM	273
Case 7: Hysteretic spring with trilinear backbone curve, yield-oriented PHM, and slip	274
References	274
TH19: Simple frame with friction damper	277
Background	277
Model	277
Solution and Comparison	279
References	282
TH20: Vehicle-Track-Structure Interaction Analysis	285
Background	285
Model	285
VTSI Analysis	286
Rolling Stock Analysis	288
Moving Load Analysis	289
Solution and comparison	289
References	291
Samples for Staged Construction Analysis	293
S01: Creep Effects - Simple Span Concrete Beam	295
S02: Creep and Shrinkage - Cantilevers Loaded at Different Times	297
S03: Creep and Shrinkage - Use CEB-FIP model code 1990 in S02	299
S04: Creep and Shrinkage - Connect Aging Cantilevers	301
S05: Creep and Shrinkage - Use CEB-FIP model code 1990 in sample S04	303
S06: 3-Span Post-Tension Deck	305
S07: Composite I-Girder with Time-Dependent Effects	311
Cross-Section Definition	311
Model Geometry	311
Construction Sequence	311
Verification of Cross-Section Properties	312
Verification of Self-Weight Loading	312
Verification of the Time Effect on Elastic Modulus	314
Verification of Shrinkage	315
S08: Time-Dependent Material Properties Effects	317
Problem Definition	317
Modeling	318
Construction Sequence	321

Verification of Creep	321
Verification of Shrinkage	328
S08b: Time-Dependent Material Properties Effects	333
Problem Definition	333
Modeling	334
Construction Sequence	339
Verification of Creep	339
Verification of Shrinkage	341
S08c: Time-Dependent Material Properties Effects	345
Problem Definition	345
Modeling	346
Verification of Creep	347
S08d: Time-Dependent Material Properties Effects	351
Problem Definition	351
Modeling	352
Construction Sequence	353
Verification of Elastic Modulus	354
S09: Shells with Time-Dependent Material Effects	359
Problem Definition	359
Modeling	360
Verification of Creep	362
Verification of Shrinkage	362
Verification of Elastic Modulus Change	363
S09b: Shells with Time-Dependent Material Effects (Orthotropic Material)	365
Problem Definition	365
Modeling	366
Verification of Creep	367
Verification of Shrinkage	368
Verification of Elastic Modulus Change	368
Samples for Influence-Based Analysis	369
INF01: AASHTO LFD Simple Span	371
Model Setup	371
Result Case Setup	372
Accessing Results	373
Solution Comparison	375
INF02: AASHTO LFD Three Span	377
Model Setup	377
Span Break Markers	379
Result Case Setup	380
Accessing Results	382
INF10: Influence Surface	385
Model Setup	385
Result Case Setup	385

Accessing Results	385
Samples for Steel Bridge Design and Rating	387
SBD06: Straight Steel Plate Girder Bridge with 90 Degree Skew (LFD)	389
Problem Details	389
Dead Load	392
Live Load	392
Model Generation	394
Compound Element Result Extraction	398
Non-Composite and Composite Dead Load Analysis Results	399
2) Influence Surface Based Live Load Analysis	404
SBD07: Curved Steel Plate Girder Bridge With 60 Degree Skew (LFD)	417
Problem Details	417
Dead Load	420
Live Load	420
Model Generation	422
Compound Element Result Extraction	426
Non-Composite and Composite Dead Load Analysis Results	427
2) Influence Surface Based Live Load Analysis	433
SBD08: Three-Span Continuous Horizontally Curved Composite Steel Tub-Girder Bridge	445
Problem Details	445
Dead Load	452
Live Load	452
Load Combinations	452
Modeling and Code Check in LARSA 4D - Steel Bridge Module (SBM)	453
References	498
Samples for Composite Construction	499
C01: Single Span with Roller under Vertical Load	501
Cross-Section Definition	501
Model	503
Cross-Sectional Properties	504
Self-Weight Loading	505
C02: Staged Construction Analysis	509
Composite Sequence States	509
Self-Weight Loading	510
Standard Staged Construction Analysis	511
C03: Time-Dependent Material Properties	517
Cross-Section Definition	517
Model	517
Cross-Sectional Properties	518
Self-Weight Loading	519

Time Effect on Elastic Modulus	520
Shrinkage	522
Creep	525
References	525
C04: Thermal Loads	527
Cross-Section Definition	527
Model	529
Analysis of Thermal Loads	529
Uniform Thermal Load	530
Linear Gradient Thermal Load	531
Nonlinear Gradient Thermal Load	533
Samples for Buckling Analysis	537
B01: Torsional Buckling of Crucifix Section with Shell Elements	539
Problem Description	539
Solution Comparison	540
References	540
B02: Lateral Buckling of I Section with Shell Elements	541
Problem Description	541
Solution Comparison	542
References	542
B03: Lateral Torsional Buckling of C Section with Shell Elements	543
Problem Description	543
Solution Comparison	544
References	544

Samples for Linear Elastic Static Analysis

These samples provide an overview of the linear elastic static analysis.

For More Information, please refer to the following documentation.

- For help on linear static analysis, see Linear Static Analysis in *LARSA 4D Reference Manual*.

L01: 2D Truss with Static Loads	17
Solution Comparison	17
L02: Beam with Elastic Supports	19
Solution Comparison	20
L03: Beam on Elastic Foundation	21
Solution Comparison	23
Theoretical Results	24
L04: Space Truss Static Analysis	27
Solution Comparison	28
L05: 2D Truss with Thermal Load	29
Solution Comparison	29
L06: Static Analysis of a Space Frame	31
Solution Comparison	33
L07: Plate Thermal Analysis	35
Solution Comparison	36
L08: Shell-Bending of a Tapered Cantilever	37
Solution Comparison	38
L10: Tie Beam without Geometric Stiffening	39
Solution Comparison	40
L11: Circular Plate with a Hole Static Analysis	41
Solution Comparison	42
References	42
L12: Hemispherical Shell Static Analysis	43
Solution Comparison	45

References	45
L13: Cylindrical Roof Static Analysis	47
Reference	48
Solution Comparison	48
L14: 2D Truss - Thermal Loads and Settlement	51
Solution Comparison	52
L16: Nonlinear Thermal Load	53
Solution Comparison	53
L17: Plane Stress Element-Straight Beam with Static Loads	55
Problem Description	55
Loading	55
Solution Comparison	56
Conclusion	61
L18: Shell-Straight Beam with Static Loads	63
Problem Description	63
Results	65
References	71
L19: Shell-Twisted Beam with Static Loads	73
Problem Description	73
Loading	73
Solution Comparison	74
References	74
L20: Shell-Cylinder with Internal Pressure	75
Problem Description	75
Solution Comparison	76
References	76
L21: Shell-Patch Test with Prescribed Displacements	79
Problem Description	79
Loading	79
Solution Comparison	80
References	82
L22: Shell-Patch Test Using Thermal Loading	83
Problem Description	83
Results	84
References	86
L23: Shell-Plate on Elastic Foundation	87
Problem Description	87
Solution Comparison	87

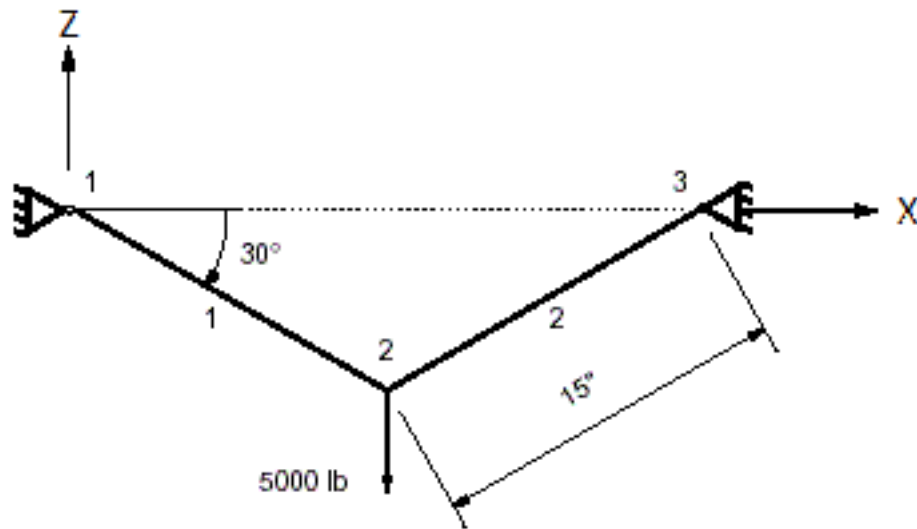
References	88
L24: Shell-Curved Beam with Static Loads	89
Problem Description	89
Loading	90
Solution Comparison	90
References	92
L25: Shell-Rectangular Plate with Static Loads	93
Problem Description	93
Solution Comparison	94
References	96
L26: Shell-Scordelis-Lo Roof with Static Loads	99
Problem Description	99
Loading	99
Solution Comparison	99
L27: Thermal Stresses in a Plate	109
Problem Description	109
Solution Comparison	109
References	110
L28: Shell-Temperature Gradient Through Shell Thickness	111
Problem Description	111
Results	112
References	113
L29: Solid-Straight Beam with Static Loads	115
Problem Description	115
Data	115
Loading	116
Solution Comparison	127
L30: Solid-Twisted Beam with Static Loads	129
Problem Description	129
Loading	129
Solution Comparison	130
L31: Non-Prismatic Beam with Nonlinear Thermal Load	131
Problem Description	131
Solution Comparison	133
L32: Isotropic Plate Cantilever using an Orthotropic Material	137
Definition	
Problem Description	137
Solution Comparison	142

L33: Cantilever with Orthotropic Material	145
Problem Description	145
Solution Comparison	149
L35: Plate Initial Strain Load	151
Problem Description	151
Solution Comparison	152

L01: 2D Truss with Static Loads

This is a two-dimensional truss support. The truss structure consists of two steel truss bars and is subjected to a vertical load of P . Ignore the self-weight of the elements. Determine the force in each bar and the vertical deflection at the point of the applied load.

Example Project: The example described here can be found in the Linear Elastic Static folder of your LARSA 4D Samples directory (generally My Documents\LARSA Projects\Samples) in the file L01.



2D Truss Model

The 2-D model consists of 3 joints and 2 truss elements. The joints 1 and 3 are pin supports. The truss structure is modeled in the XZ plane. All rotational degrees of freedom and the translational displacement in the Global Y-direction are eliminated from the analysis.

The material property data is given:

Modulus of Elasticity = 30,000,000 psi

and sectional property data:

Area = 0.50 in².

The vertical load of 5000 lb is applied in the negative Global Z-direction at joint 2.

Linear static analysis with one load case is performed.

Solution Comparison

Sources:

- Timoshenko, S., Strength of Materials Part I, D. Van Nostrand Co., 1955, p.10.
- LARSA 4D

	Timoshenko	LARSA
Axial Force @ I-end (lb)	5000 (Tension)	-5000
Vertical Deflection @ 2(in)	0.12 (Down)	-0.12

For More Information, please refer to the following documentation.

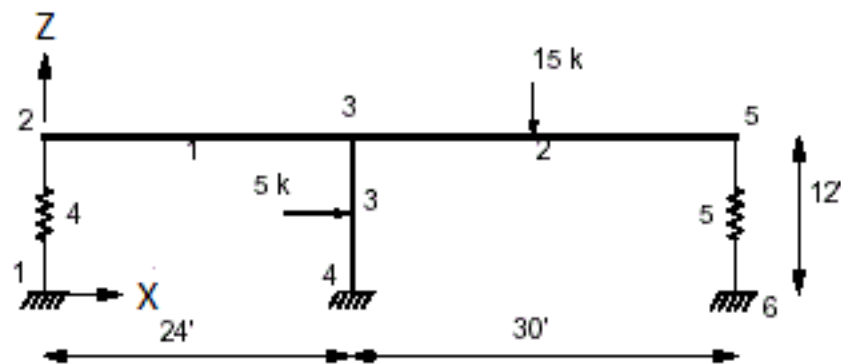
- For help on linear static analysis, see Linear Static Analysis in *LARSA 4D Reference Manual*.

L02: Beam with Elastic Supports

A two-span beam is supported at an interior point by a column and with yielding elastic supports at the two exterior points. The beam is continuous and the column is pin-connected to the beam.

The beam is subjected to a vertical point load and the column is subjected to a horizontal point load. Determine the deflections and reactions.

Example Project: The example described here can be found in the Linear Elastic Static folder of your LARSA 4D Samples directory (generally My Documents\LARSA Projects\Samples) in the file L02.



2D Model

The 2D model consists of 6 joints, 3 beam elements and 2 spring elements. This is a plane frame analysis. The translational displacement in Global Y-direction and rotations about Global X and Z-directions can be deleted from the analysis. The joints 1, 4 and 6 are fixed supports.

The material property data is given:

Modulus of Elasticity = 30,000,000 psi

and sectional property data:

Area = 0.125 ft²

I_{zz} = 0.263 ft⁴ for beams

Area = 0.175 ft²

I_{zz} = 0.193 ft⁴ for columns

The spring constant for the springs is given as:

k = 1200 kip/ft

The member loads applied on beams are:

P = -15 kips on beam # 2 @ mid-span in Global Y

P = -5 kips on beam #3 @ mid-span in Global X

Linear static analysis with one load case is performed.

Solution Comparison

Sources:

- Beaufait, F.W., et al., "Computer Methods of Structural Analysis," Prentice-Hall, 197-210.
- LARSA 4D

	Beaufait	LARSA
U2 & U3 & U5 ($\times 10^{-3}$ ft)	1.079	1.079
V2 ($\times 10^{-3}$ ft)	1.7873	1.787
V3 ($\times 10^{-3}$ ft)	-0.1803	-0.1803
V5 ($\times 10^{-3}$ ft)	-4.8202	-4.8204
R2 ($\times 10^{-3}$ rad)	0.0992	0.0992
R3 ($\times 10^{-3}$ rad)	-0.4443	-0.4443
R5 ($\times 10^{-3}$ rad)	0.3615	0.3615
Reaction V @ Joint 1 (kip)	-2.1	-2.144
Reaction H @ Joint 4 (kip)	-5.0	-5.0
Reaction V @ Joint 4 (kip)	11.3	11.360
Reaction M @ Joint 4 (kip)	30.	30.
Reaction V @ Joint 6 (kip)	5.8	5.7845

U denotes the displacement in horizontal direction and V denotes the displacement in vertical direction. **R** is the rotation. **Reaction V** is the vertical force at the support joint and Reaction H is the horizontal force. **Reaction M** is the support moment.

For More Information, please refer to the following documentation.

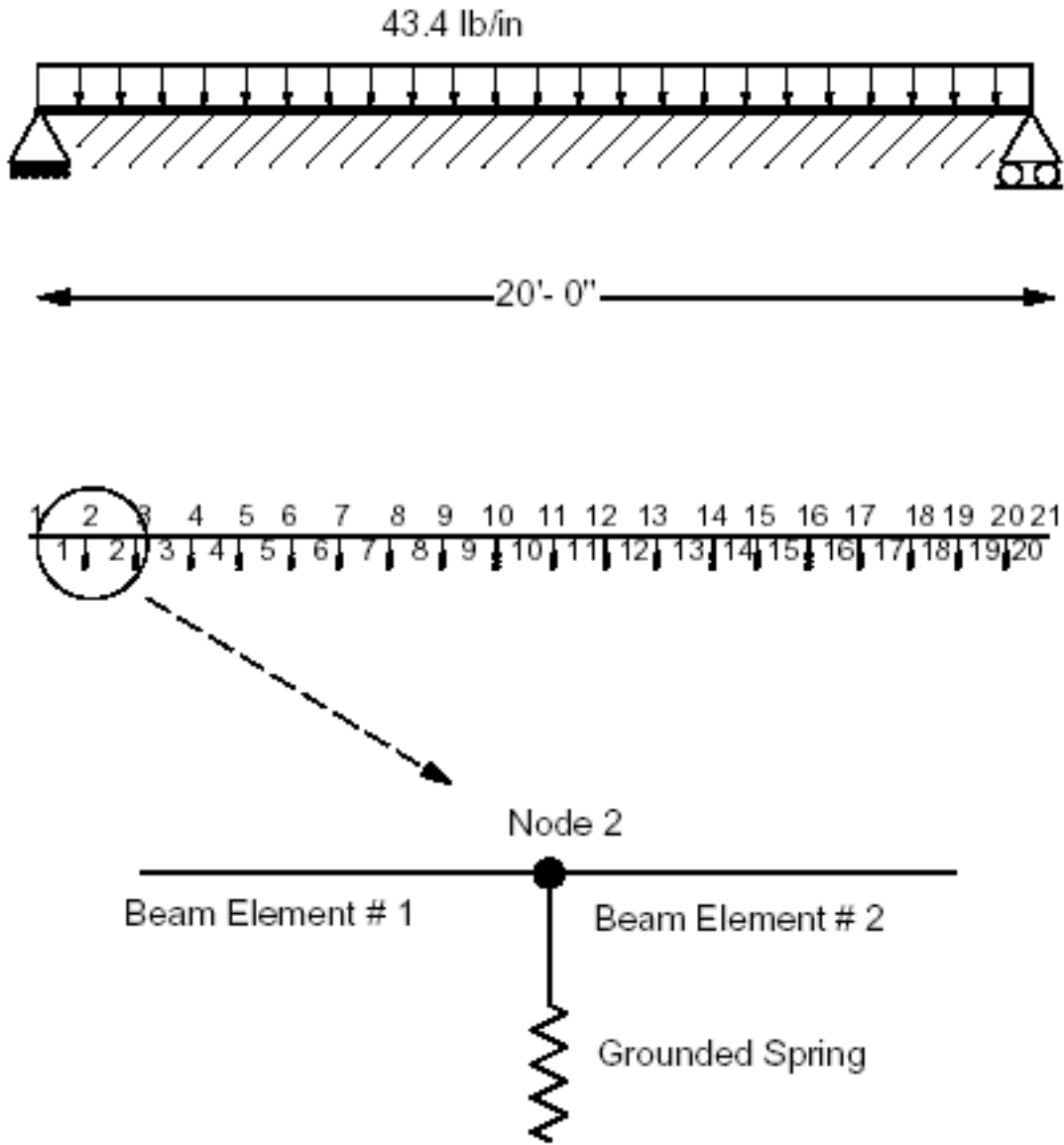
- For help on linear static analysis, see Linear Static Analysis in *LARSA 4D Reference Manual*.

L03: Beam on Elastic Foundation

A simply supported beam is uniformly loaded and is on an elastic foundation. The beam cross section is rectangular with moment of inertia of 30 in^4 . The elastic modulus of the beam is $30 \times 10^6 \text{ psi}$. The span length is 240 inches. The uniform load is 43.4 lb/in. The foundation modulus (i.e. distributed reaction for a deflection of unity) is 26.041667 psi (lb/in^2).

Determine the transverse deflections and bending moments along the beam.

Example Project: The example described here can be found in the Linear Elastic Static folder of your LARSA 4D Samples directory (generally My Documents\LARSA Projects\Samples) in the file L03.



Beam on Elastic Foundation

The model consists of 21 joints, 20 beam elements and 19 grounded springs using a 2D model in the global XZ plane. The degrees of freedom for Y translation, X and Z rotations can be deleted from the analysis. Joint 1 is a pin support and joint 21 is a roller support.

The material data is given as:

Modulus of Elasticity = 30,000,000 lb/in²

and sectional property data as:

A = 7.11 in²

I_{zz} = 30 in⁴

The member orientation angle is 90 degrees.

A distributed load of 43.4 lb/inch is applied in the vertical (Z)- direction as uniform beam load on all beam elements. Linear static analysis with one (1) load case is performed.

The foundation support is modeled using a set of foundation springs with stiffness of 312.50 lb/in in the vertical (Z) direction. The spring constant is computed as the product of the foundation modulus and tributary area for each joint. At all joints the tributary area is 12 inches (width of the beam) by 1 inch (unit length). Therefore, the spring constant for a grounded spring element is:

$$k = (\text{Foundation Modulus}) \times (\text{Tributary Area})$$

$$k = (26.041667) \times (12)$$

$$k = 312.50 \text{ lb/in}$$

In this example, linear grounded spring elements are used and linear static analysis is performed. Since we know the solution will yield the vertical displacement as downward with soil resistance active at all joints, we can use linear static analysis. However, the foundations can be subject to loads causing uplifts and loss of soil contact. It is more appropriate to model the soil as compression-only foundation elements and perform nonlinear static analysis.

Solution Comparison

Sources:

- Timoshenko, S. and Wionowsky-Krieger, S., "Theory of Plates and Shells", McGraw-Hill Book Co., N.Y., 1959.
- "EASE2 - Elastic Analysis for Structural Engineering - Example Problem Manual," Engineering Analysis Corporation, 1981, pp. 1.05.
- LARSA 4D

	Timoshenko	EASE2	LARSA
Vertical Displacements			
Station=0	0.0000	0.0000	0.0000
Station=12	-0.1693	-0.169	-0.1693
Station=24	-0.3331	-0.332	-0.3331
Station=36	-0.4870	-0.486	-0.4870
Station=48	-0.6270	-0.625	-0.6270
Station=60	-0.7502	-0.748	-0.7502
Station=72	-0.8541	-0.852	-0.8541
Station=84	-0.9367	-0.935	-0.9367
Station=96	-0.9967	-0.995	-0.9967
Station=108	-1.0331	-1.031	-1.0331
Station=120	-1.0453	-1.043	-1.0453
Bending Moment (lb-inch)			
Station=0.	0		0
Station=6.	17872		17885
Station=18.	49247		49287

	Timoshenko	EASE2	LARSA
Station=30.	75317		75380
Station=42.	96673		96762
Station=54.	113870		113983
Station=66.	127407		127537
Station=78.	137705		137849
Station=90.	145119		145270
Station=102.	149901		150066
Station=114.	152254		152419

The displacements are in inches with negative displacement as downward.

The moments tabulated are at the mid-points of the beam elements. These moments can be listed using the **Member Force** tool in the postprocessor **Numerical Results** window. Choose the **Number of Stations** as 3 and the station 2 of each beam element will correspond to the mid-point of the element.

Theoretical Results

The theoretical results for the transverse deflection and the bending moments are computed using the following equations.

With the assumption that the reaction of the foundation at any point is proportional to the deflection, the governing differential equation is:

$$EI (d^4w/dx^4) = q - k w$$

The solution of this equation from reference

$$w(x) = (q/k) + C1 [\sin(2bx/L) \sinh(2bx/L)] + C4 [\cos(2bx/L) \cosh(2bx/L)]$$

where

$$b = (L/2) [k / (4EI)]^{1/4}$$

and

$$C1 = -(q/k) (2 \sin b \sinh b) / (\cos 2b + \cosh 2b)$$

$$C4 = -(q/k) (2 \cos b \cosh b) / (\cos 2b + \cosh 2b)$$

The moment at any point x on the beam is:

$$M(x) = -EI (d^2w/dx^2)$$

Substituting w(x) in the above equation, we obtain:

$$M(x) = -EI (8b^2 / L^2) [C1 \cos (2bx/L) \cosh (2bx/L) - C4 \sin (2bx/L) \sinh (2bx/L)]$$

The joint displacements in Z direction as computed by LARSA compare very well with the analytical values. The bending moments compare well also. The reactions are automatically computed and the sum of the reactions balance the total applied load.

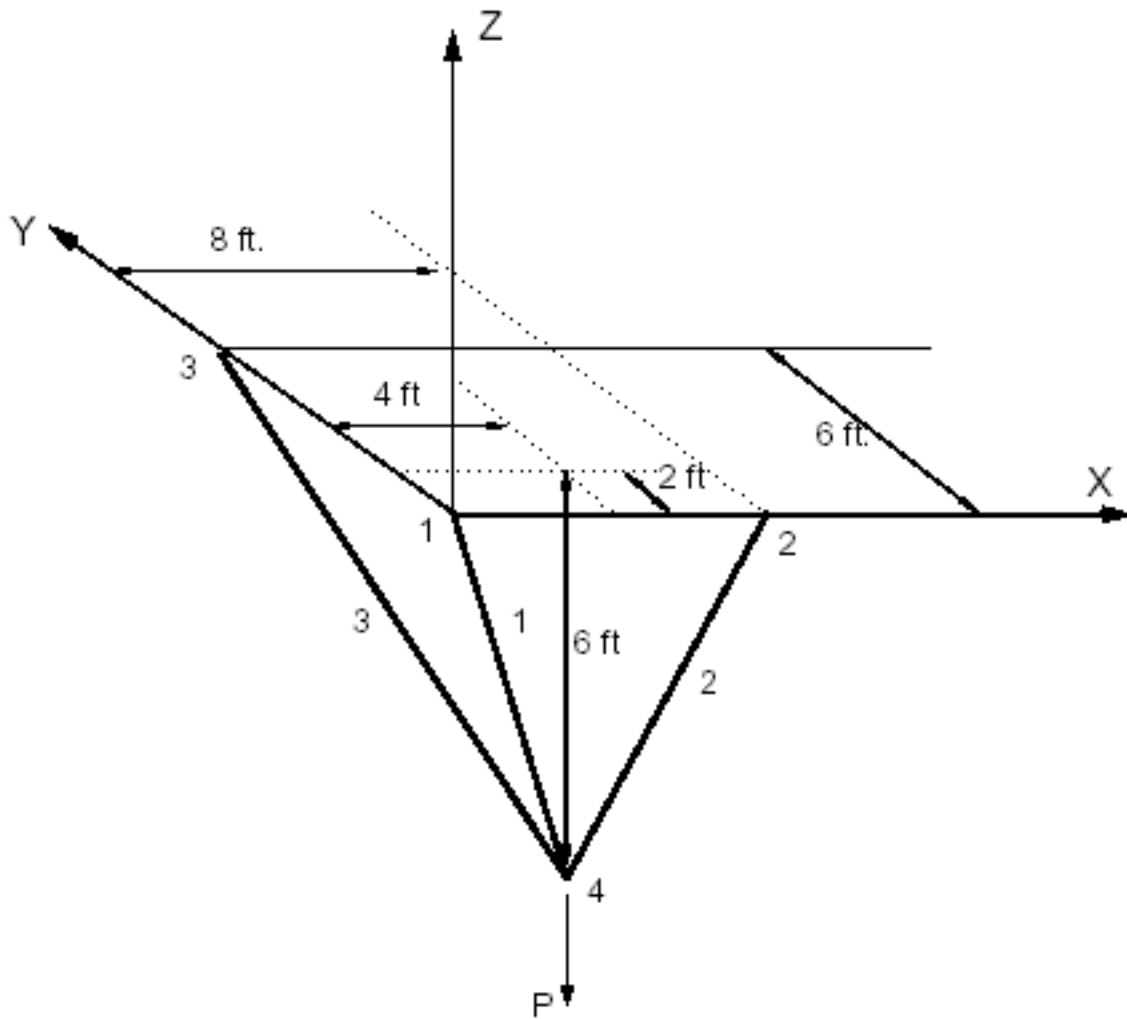
For More Information, please refer to the following documentation.

- For help on linear static analysis, see Linear Static Analysis in *LARSA 4D Reference Manual*.

L04: Space Truss Static Analysis

Three element space truss supports 50 lb load. The bars are attached to the ceiling. The truss elements are steel ($E = 30 \times 10^6$ psi) and the cross-sectional area of each element is 1 in^2 . Determine the axial force in each bar.

Example Project: The example described here can be found in the Linear Elastic Static folder of your LARSA 4D Samples directory (generally My Documents\LARSA Projects\Samples) in the file L04.



Space Truss

The model consists of 4 joints and 3 truss elements. The rotational degrees of freedom are deleted from the 3D model. The joints 1, 2 and 3 are pin supports.

The material property data is given as:

Modulus of Elasticity = $30,000,000 \text{ lb/in}^2$

The sectional property data for the truss bar is:

Area of each truss bar = 1 in²

The load of 50 lb is applied in the vertical Global Z-direction. The applied load is:

Load P @ Joint 4 in Z = -50 lb

Linear static analysis with one (1) load case is performed.

All truss elements are in tension.

Solution Comparison

Sources:

- Beer, F.P., and Johnston, Jr., E.R., "Vector Mechanics for Engineers, Statics and Dynamics," McGraw-Hill Book Co., Inc. New York, 1962, p. 47.
- LARSA 4D

	Beer	LARSA
Truss force F1 (lb)	10.4	10.4
Truss force F2 (lb)	31.2	31.2
Truss force F3 (lb)	22.9	22.9

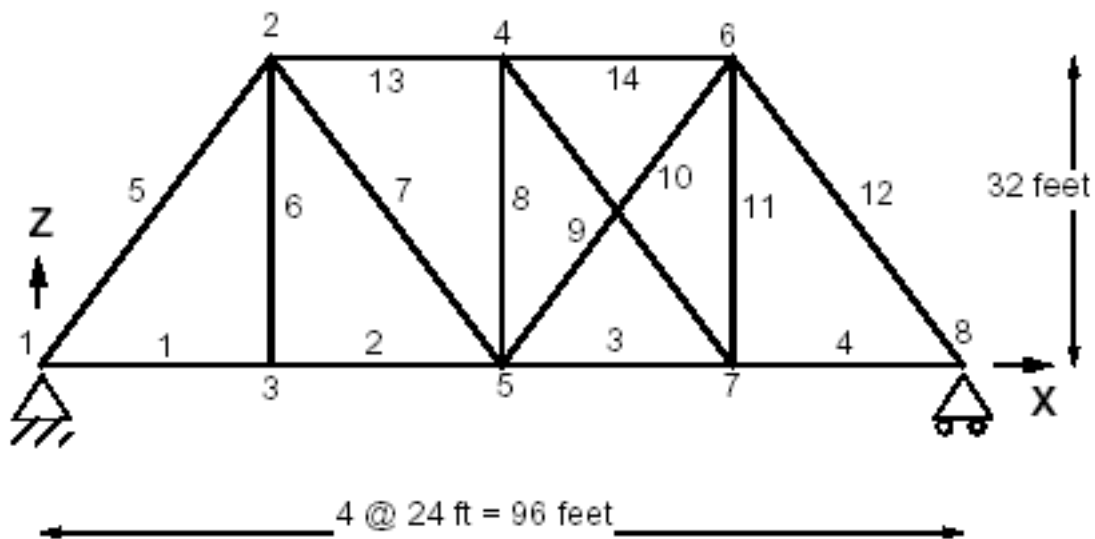
For More Information, please refer to the following documentation.

- For help on linear static analysis, see Linear Static Analysis in *LARSA 4D Reference Manual*.

L05: 2D Truss with Thermal Load

This is a two dimensional truss structure with 32 feet height and 96 feet span. The top chord of the truss is subjected to temperature rise of 50 degrees Fahrenheit. The coefficient of thermal expansion for the material is 0.0000065 in/in/F. The elastic modulus is 30,000,000 psi. Determine the member forces in the structure.

Example Project: The example described here can be found in the Linear Elastic Static folder of your LARSA 4D Samples directory (generally My Documents\LARSA Projects\Samples) in the file L05.



Joints and Members for 2D Truss Model

The material properties of the truss are given as:

Modulus of Elasticity = 30,000,000 lb/in²

Coefficient of Thermal Expansion = 0.0000065 in/in/oF

The sectional properties are:

Area = 24 in² Designation = S1 Top & Bottom

Area = 32 in² Designation = S2 Vertical Bars

Area = 40 in² Designation = S3 Diagonal Bars

The truss model has 8 joints and 12 truss elements. The rotations (about X, Y and Z) and translation in Y-direction are eliminated. Joint 1 is pin support and joint 8 is a roller in horizontal direction.

The temperature rise on the top chord is specified for elements 13 and 14.

Solution Comparison

Sources:

- Hsieh, Y.Y., "Elementary Theory of Structures," Prentice-Hall, Inc., 1970, pp. 200-202.
- LARSA 4D

	Hsieh	LARSA
F1,F2	0.00	0.00
F3	-21.1	-21.06
F4,F5,F6,F7	0.00	0.00
F8	-28.1	-28.08
F9	+35.1	+35.1
F10	+35.1	+35.1
F11	-28.1	-28.08
F12,F13	0.00	0.00
F14	-21.1	-21.06

Tensile force has positive magnitude. All forces are in kips.

For More Information, please refer to the following documentation.

- For help on linear static analysis, see Linear Static Analysis in *LARSA 4D Reference Manual*.

L06: Static Analysis of a Space Frame

A space frame having three members and four joints is subjected to static force loading. Points A and D are fully restrained. All members have the same cross-sectional properties. The loads on the frame consist of a force $2P$ in the positive X direction at point B, a force P in the negative Y direction at point C, and a moment PL in the negative Z sense at C. Determine the final displaced shape of the structure. Include the effect of shearing deformations.

$$E = 200 \times 10^6 \text{ kN/m}^2$$

$$G = 80 \times 10^6 \text{ kN/m}^2$$

$$L = 3\text{m}$$

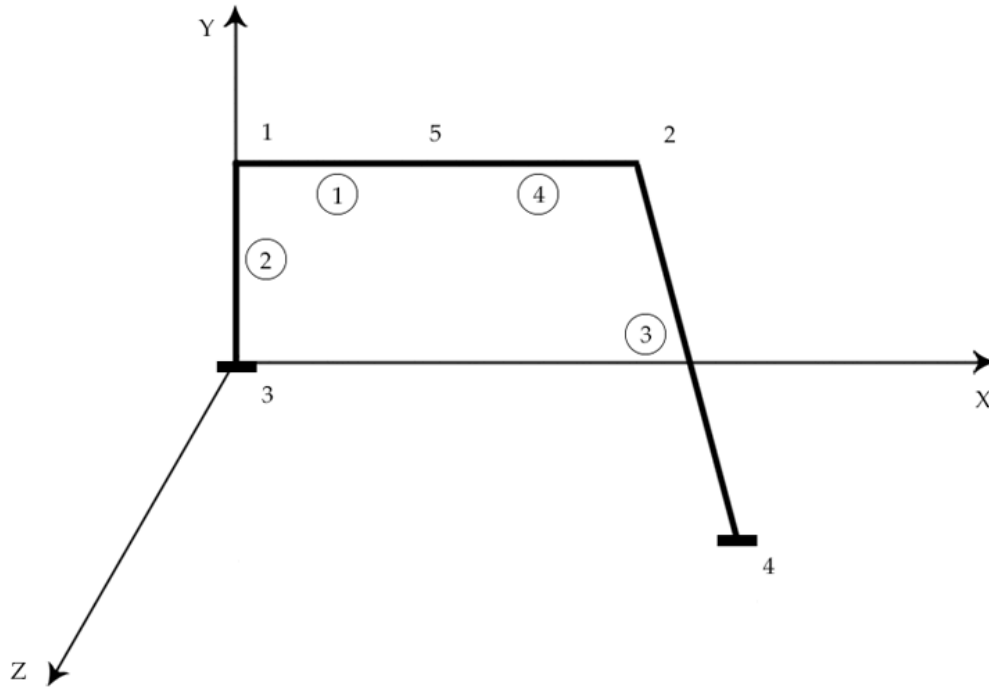
$$A = 0.01\text{m}^2$$

$$I_{xx} = 2 \times 10^{-3}\text{m}^4$$

$$I_{zz} = I_{yy} = 1 \times 10^{-3}\text{m}^4$$

$$P = 60 \text{ kN}$$

Example Project: The example described here can be found in the Linear Elastic Static folder of your LARSA 4D Samples directory (generally My Documents\LARSA Projects\Samples) in the file L06.



Joints and Members

	ux,1[m]	uy,1[m]	uz,1[m]	rotx,1[rad]	roty,1[rad]	rotz,1[rad]
Reference	-0.859E-03	0.578E-04	0.501E-02	0.239E-02	-0.162E-02	0.681E-03
IDARC	-0.859E-03	0.578E-04	0.501E-02	0.239E-02	-0.162E-02	0.681E-03
Difference	None	None	None	None	None	None
	Fx,1[kN]	Fy,1[kN]	Fz,1[kN]	Mx,1[kNm]	My,1[kNm]	Mz,1[kNm]
Reference	105.548	-38.509	-126.013	29.464	86.569	-67.100
IDARC	105.548	-38.509	-126.013	29.464	86.569	-67.100
Difference	None	None	None	None	None	None

Solution Comparison

Sources:

- Weaver, Gere, Weaver Jr., Matrix Analysis of Framed Structures, 1990, p.354.
- Reinhorn, Simenonov, Mylonakis, Reichman, IDARC-BRIDGE: A computational Platform for Seismic Damage Assessment of Bridge Structures, MCEER, 1998, p.113.
- LARSA 4D

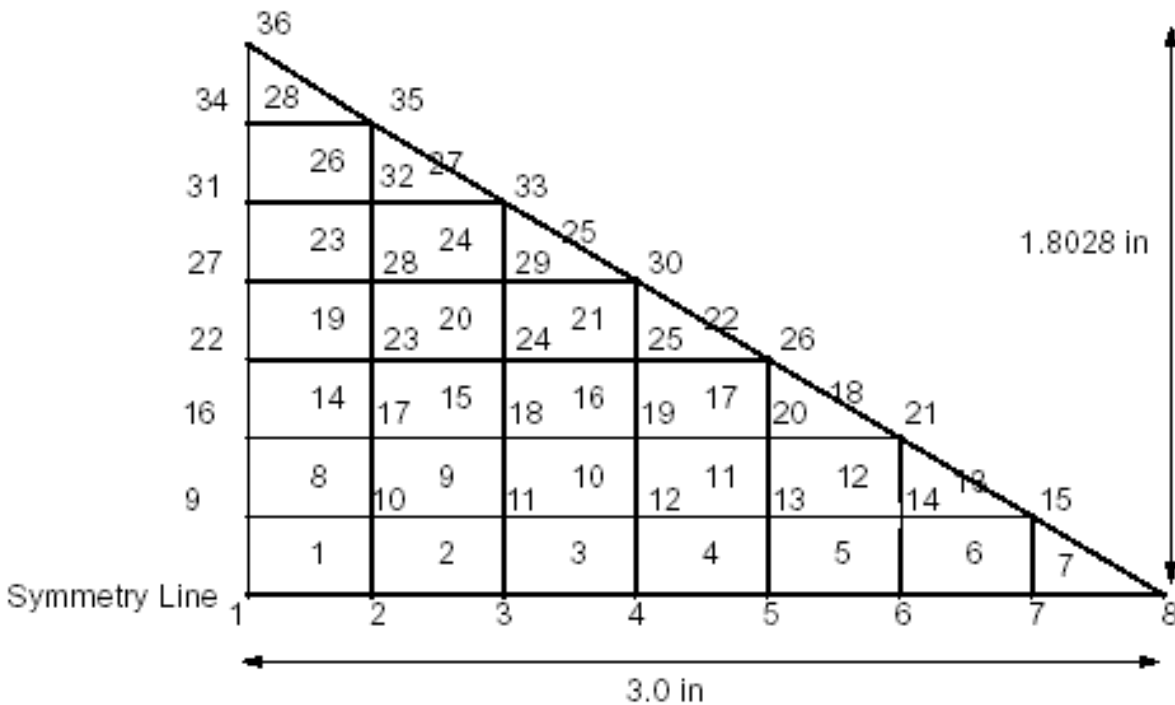
For More Information, please refer to the following documentation.

- For help on linear static analysis, see Linear Static Analysis in *LARSA 4D Reference Manual*.

L07: Plate Thermal Analysis

An equilateral triangular plate is simply supported at the edges. The plate is subjected to temperature variation along the thickness. The variation of temperature from top to bottom is 450o F. The coefficient of thermal expansion is 0.000012 in/in/oF. The material elastic modulus and Poisson's Ratio are 10,000,000 psi and 0.30 respectively. Determine the deflections along the base which is on X-axis.

Example Project: The example described here can be found in the Linear Elastic Static folder of your LARSA 4D Samples directory (generally My Documents\LARSA Projects\Samples) in the file L07.



Joints and Shell Elements for Triangular Plate

Due to the symmetry, half of the plate is taken for the model. The model has 36 joints and 28 plate elements.

The edges from joint 1 to 36 and 8 to 36 are the simply supported edges. The restraints for the joints from 1 to 8 are specified to preserve the symmetry of the plate.

Linear static analysis with one (1) load case is performed.

Modulus of Elasticity = 10,000,000 psi

Poisson's Ratio = 0.30

Shear Modulus = 3,841,615 psi

Coefficient of Thermal Expansion = 0.000012 in/in/oF

Plate Thickness = 0.10 inch

Temperature Gradient = 450o F for 0.10 inch thickness

The temperature gradient is the change of temperature for the unit thickness of the plate. The variation through 0.10 inches is 450 o F, then for one inch thick (unit thickness), the temperature gradient is 4500 o F.

Solution Comparison

Sources:

- Maulbetsch, J.L., "Thermal Stresses in Plates", Journal of Applied Mechanics, Vol. 57, June 1935, pp. A141-A146.
- LARSA 4D

	Maulbetsch	LARSA
Ux @ x = 0.403 (in)	0.01590	0.01586
Ux @ x = 0.836 (in)	0.02290	0.02287
Ux @ x = 1.269 (in)	0.02224	0.02224
Ux @ x = 1.702 (in)	0.01677	0.01678
Ux @ x = 2.135 (in)	0.00934	0.00937
Ux @ x = 2.568 (in)	0.00280	0.00283

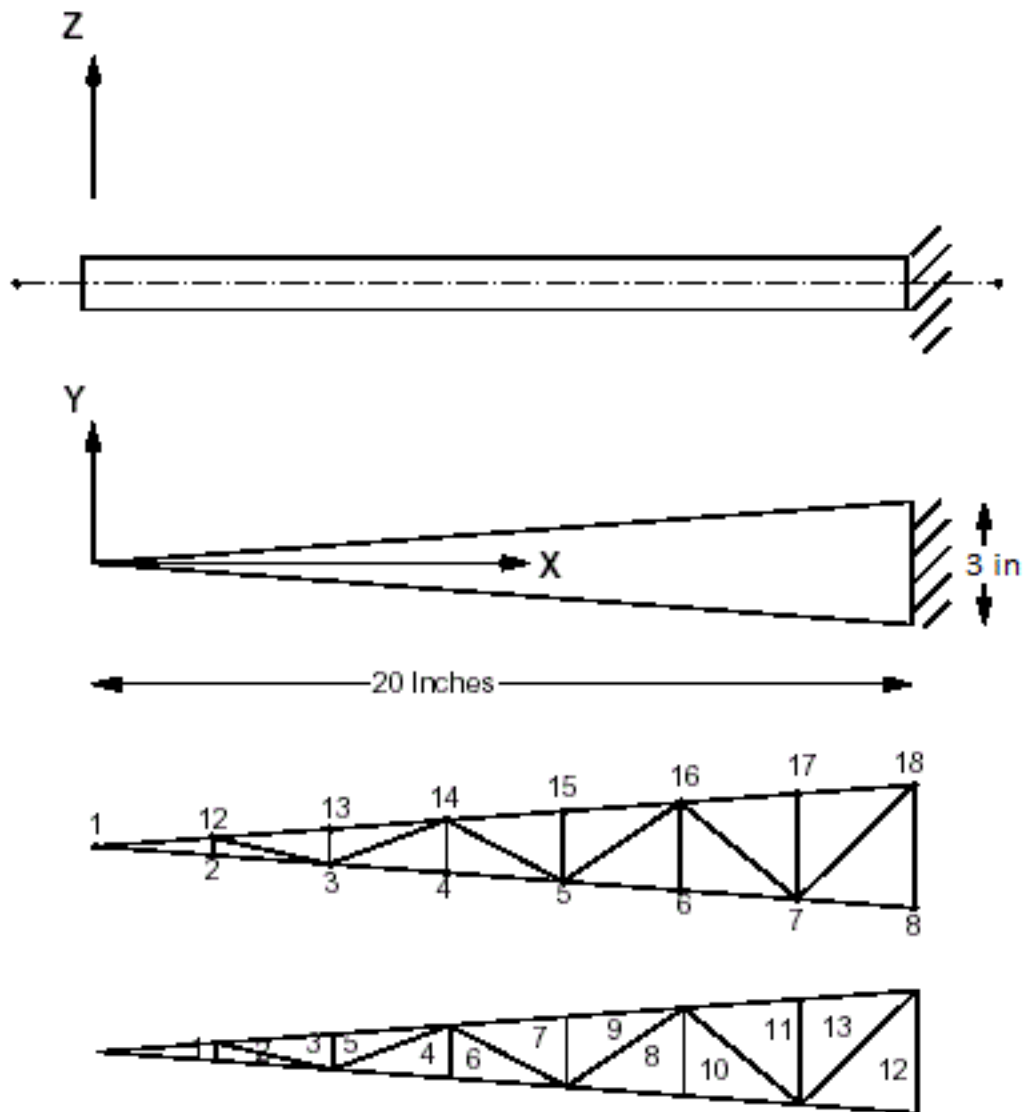
For More Information, please refer to the following documentation.

- For help on linear static analysis, see Linear Static Analysis in *LARSA 4D Reference Manual*.

L08: Shell-Bending of a Tapered Cantilever

A tapered beam of rectangular cross-section is subjected to a load P at its tip. The beam is steel with 20 inches of span. The load P is 10 lbs. Determine the maximum deflection and the stress using shell elements.

Example Project: The example described here can be found in the Linear Elastic Static folder of your LARSA 4D Samples directory (generally My Documents\LARSA Projects\Samples) in the file L08.



Tapered Beam Model with Shell Elements

The model has 15 joints and 13 plate elements. The 3-node (triangular) plate elements are used in the model. The joints 8 and 18 are fixed supports.

Linear static analysis with one (1) load case is performed.

Modulus of Elasticity = 30,000,000 psi

Poisson's Ratio = 0.0

G = 15,000,000 psi

Plate Thickness = 0.50 inches

Span = 20 inches

P = 10 lb. (applied in the negative Z direction at joint 1)

Solution Comparison

Sources:

- Harris, p. 114, problem 61.
- LARSA 4D

	Harris	LARSA
Deflection (in)	-0.04267	-0.04323
Moment (lb-in/in)	66.66	68.67
Stress (psi)	1600.	1648.

The section modulus of the plate is 0.04167 in³. The stress is computed using the following relationship:

$$s = M / S$$

where

M = Bending moment

S = Section modulus

For More Information, please refer to the following documentation.

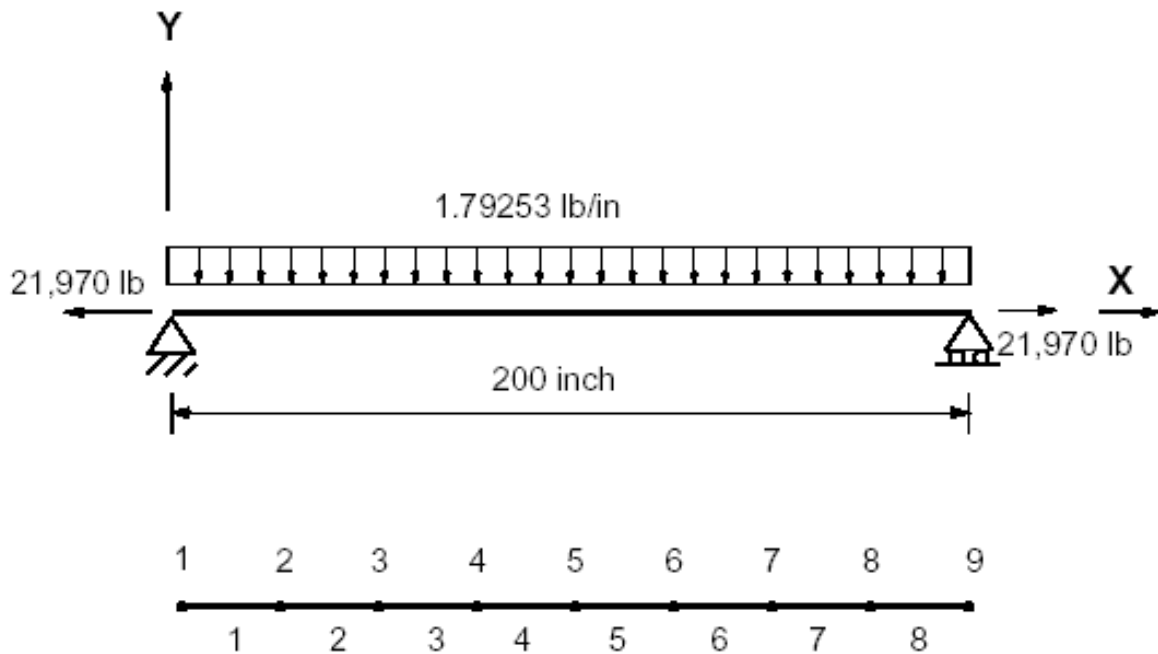
- For help on linear static analysis, see Linear Static Analysis in *LARSA 4D Reference Manual*.

L10: Tie Beam without Geometric Stiffening

A tie beam is subjected to the action of a tensile force and a uniform lateral load. The tensile force is 21,970 lbs and the uniform lateral load is 1.79253 lb/in. The beam is steel and has a square section of 2.5 in by 2.5 in. Determine the maximum deflection, maximum bending moment and the slope at the lefthand support.

Example Project: The example described here can be found in the Linear Elastic Static folder of your LARSA 4D Samples directory (generally My Documents\LARSA Projects\Samples) in the file L10.

Significance of geometric stiffening becomes evident when the results of the linear static analysis and nonlinear static analysis (Sample Problem N01) are compared.



Tie Beam Geometry and Loading

The model used has 9 joints and 8 beam elements. The tensile force is specified as an external joint force acting at joint 9. The uniform load is specified as an external beam loading.

The data given for the problem is:

Modulus of Elasticity = 30,000,000 lb/in²

Span = 200 inches

A = 6.25 in²

I_{zz} = 3.2552 in⁴

Uniform Load = 1.79253 lb/in (applied as beam load)

Tensile Force S = 21,970 lb (applied at joint 9 in X)

Linear static analysis with one (1) load case is performed.

Solution Comparison

Sources:

- Timoshenko, S., "Strength of Materials, Part II", 3rd Edition, D. Van Nostrand Co., Inc., New York, p. 42.
- LARSA 4D

	Timoshenko	LARSA
Vertical Disp @ Joint 5 (in)	-0.382406	-0.382407
Rotation @ Joint 1 (rad)	-0.0061185	-0.00611852
Moment @ I-end of Beam 5 (in-lb)	-8962.65	-8962.65

The linear static analysis ignores the geometric stiffening effect of the beam. For comparison of the results to the nonlinear static analysis, refer to Problem 11.

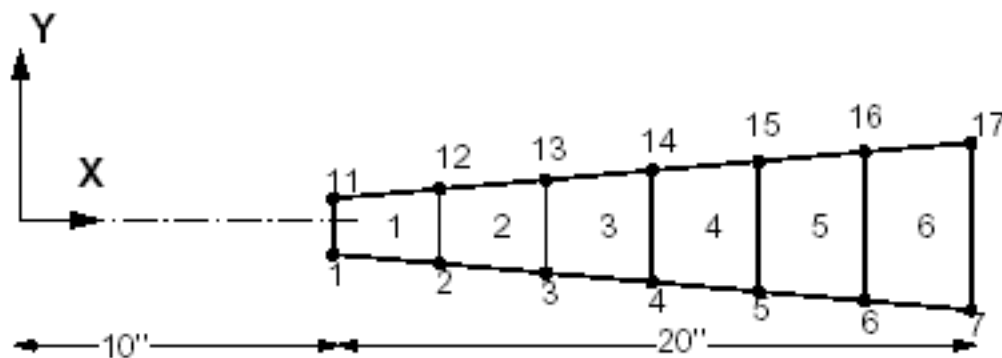
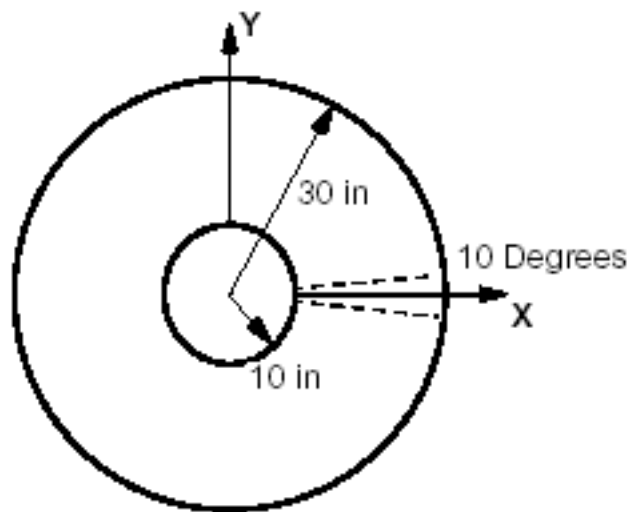
For More Information, please refer to the following documentation.

- For help on linear static analysis, see Linear Static Analysis in *LARSA 4D Reference Manual*.

L11: Circular Plate with a Hole Static Analysis

A circular plate with a center hole is built-in along the inner edge (i.e. fixed). The plate is subjected to bending by a moment applied along the outer edge. Determine the maximum deflection and slope of the plate. Also determine the moment near the inner and outer edges.

Example Project: The example described here can be found in the Linear Elastic Static folder of your LARSA 4D Samples directory (generally My Documents\LARSA Projects\Samples) in the file L11.



Circular Plate with a Hole

The circular plate is axisymmetric and only a small sector of the complete plate is needed for the analysis. We will use a 10 degree segment for approximating the circular boundary with a straight edge.

The model has 14 joints and 6 shell elements. The joints are numbered from 1 to 7 and 11 to 17. The plate elements are 4-node elements.

The uniform moment of 10 in-lb/in is equivalent to a total moment of 52.3598 in-lb for the 10 degree segment. The moment is applied at joints 7 and 17 as joint loads with magnitude of $M_y = -26.1799387$ in-lb. Linear static analysis with one load case is performed.

Modulus of Elasticity = 30,000,000 psi

Poisson's Ratio = 0.30

Shear Modulus = 11,538,461 psi

Plate Thickness = 0.25 inches

Radius (inner) = 10 inches

Radius (outer) = 30 inches

The model is defined using cylindrical coordinates with R, Q and Z. The joints 1 to 7 are at $Q = -5$ degrees and 11 to 17 are at $Q = +5$ degrees. The joint displacement directions are also defined in cylindrical R, Q and Z directions.

The model is created in LARSA 4D using the Classic and MITC4 plate element behaviors.

Solution Comparison

Displacement at the outer edge and bending moment at the indicated locations are compared. In LARSA 4D, the moments are taken from the center of the nearest plate.

Result	Timoshenko	Classic	MITC4
Rotation (rad)	0.0490577	0.04933	0.04910
Deflection (in)	-0.0045089	-0.0045044	-0.0045104
M (x=10.86) (in-lb/in)	-13.74	-13.12	-13.15
M (x=27.2) (in-lb/in)	-10.12	-10.06	-10.11

References

- Timoshenko, S., "Strength of Materials, Part II", 3rd Edition, D. Van Nostrand Co., Inc., New York, p. 111.

For More Information, please refer to the following documentation.

- For help on linear static analysis, see Linear Static Analysis in *LARSA 4D Reference Manual*.

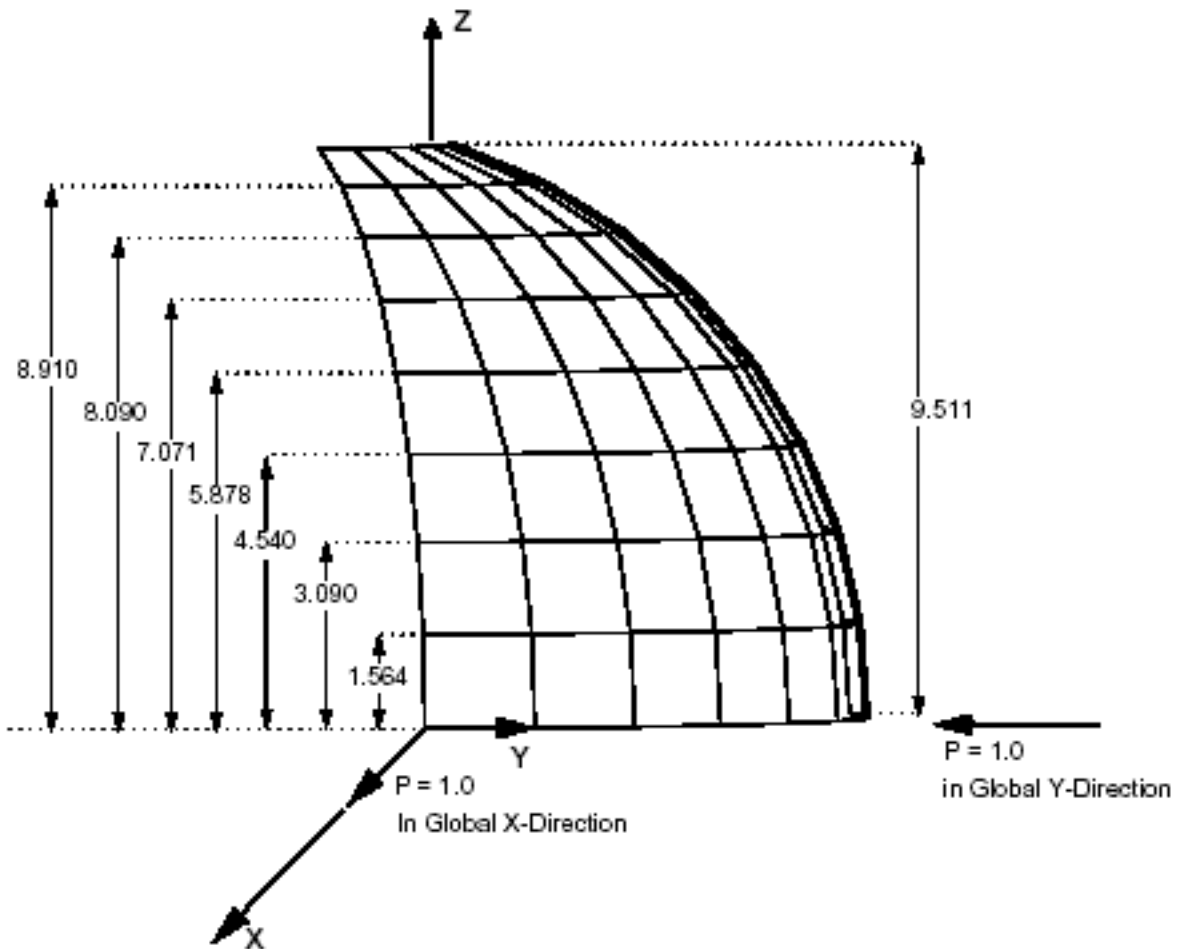
L12: Hemispherical Shell Static Analysis

A hemispherical shell is subjected to point loads at the lower two edges. The shell is 0.04 inches thick and the radius is 10.0 inches. The modulus of elasticity is 6.825×10^7 and Poisson's Ratio 0.30.

The top of the sphere is open at a vertical elevation of 9.511 inches. The elevation of the opening corresponds to an angle of 72 degrees when measured from the vertical axis Z.

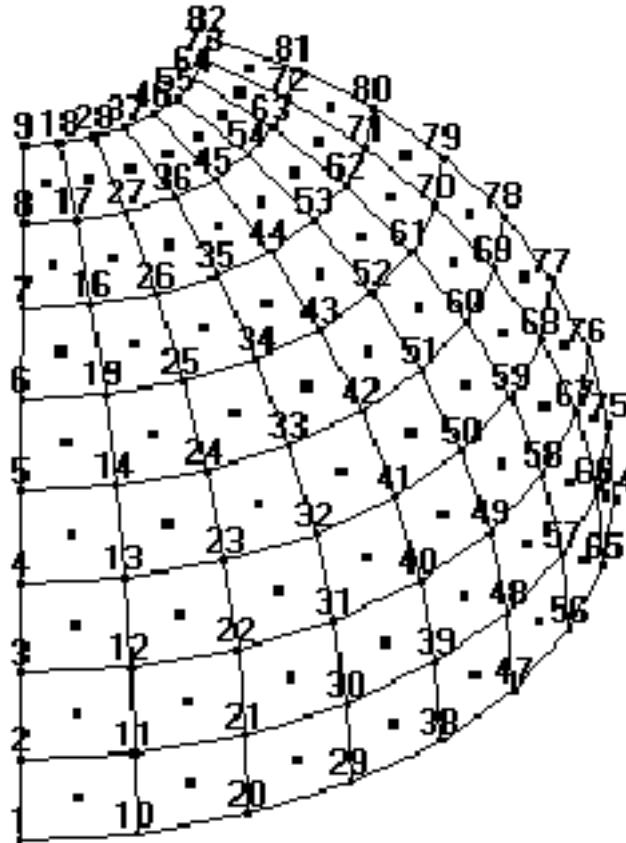
Determine the displacement at the point of application of loads at joints 1 and 74.

Example Project: The example described here can be found in the Linear Elastic Static folder of your LARSA 4D Samples directory (generally My Documents\LARSA Projects\Samples) in the file L12.



Hemispherical Shell Mesh

A quarter of the hemispherical shell is used as a model. The model consists of 8 x 8 mesh of shell elements with the horizontal mesh of 11.25 degrees and the vertical mesh of 9 degrees.



FE Model Nodes

The boundary conditions are prescribed for the symmetry. The joints along the edge from joint 1 to 9 are restrained for translation in the Global Y-direction and for rotations about Global X and Z-directions. Similarly, the joints along the edge from joint 74 to 82 are restrained for translation in the Global X-direction and for rotations about the Global Y and Z-directions. Joint 38 at the lower center of the free edge is restrained to prevent unstable solution.

The geometry, material and section property data of the shell is:

Modulus of Elasticity = 68,250,000 psi

Poisson's Ratio = 0.30

Shear Modulus = 26,250,000 psi

Shell Thickness = 0.04 inch

Radius of the Hemisphere = 10 inch

Solution Comparison

The model is created in LARSA 4D using the Classic and MITC4 plate element behaviors. For validation, independent analytical results and results from SAP90 are also listed below. The displacement reported is at the point of application of the load and in the direction of the load.

Result	MacNeal	Classic	MITC4	SAP90
Displacement U_1 (inch)	0.094	0.0938	0.0925	0.0937

Both LARSA 4D element behaviors gives similiar results with the references. MacNeal suggests a value of 0.094 for comparison of the results with the theoretical lower bound of 0.0924.

References

- MacNeal, R.H. and Harder, R.C., "A Proposed Standard Set of Problems to Test Finite Element Accuracy," *Finite Elements Analysis and Design 1* (1985), pp. 3-20, North-Holland.
- Computers & Structures Inc., "SAP90 Structural Analysis Verification Manual", October, 1990, 18-1.

For More Information, please refer to the following documentation.

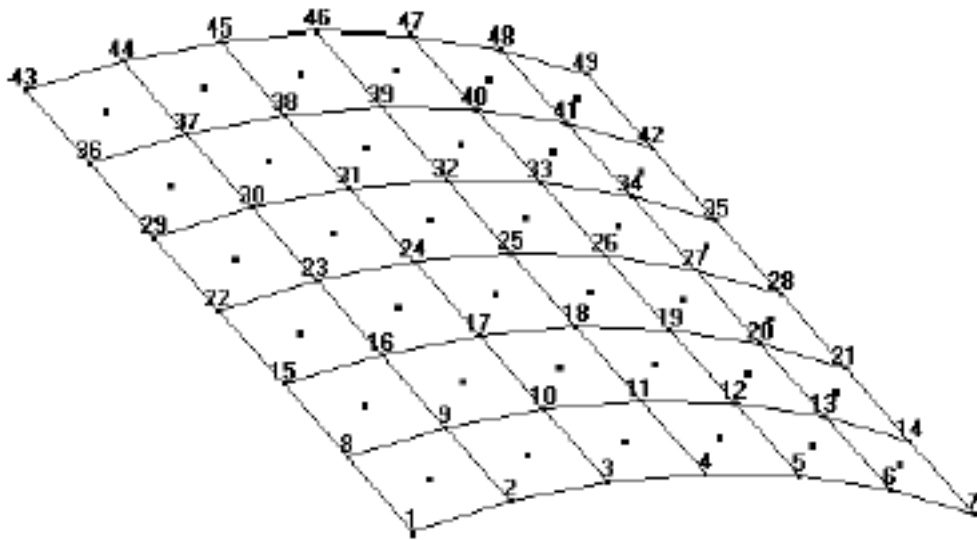
- For help on linear static analysis, see Linear Static Analysis in *LARSA 4D Reference Manual*.

L13: Cylindrical Roof Static Analysis

A reinforced concrete cylindrical roof (barrel vault) is subjected to a uniform load. It has a length of 50 feet, a thickness of 0.25 feet, a radius of 25 feet and an 80 degree arc length. A 90 lb/ft² uniform downward load is to be applied.

Determine the vertical displacement at the center of the free edge i.e. at joint 49 of the model.

Example Project: The example described here can be found in the Linear Elastic Static folder of your LARSA 4D Samples directory (generally My Documents\LARSA Projects\Samples) in the file L13.



FE Mesh

Due to symmetry of the structure and loading, a quarter of the cylindrical shell (as shown above) is used as a model. It consists of 6 x 6 mesh of shell elements.

The edge from joint 1 to 7 is simply supported and from 7 to 49 is free.

The boundary conditions along the edges from joint 1 to 43 and 43 to 49 are prescribed for symmetry. Here are the joint restraints specified for preserving symmetry:

Joints 1 to 7 XT YT ZR

Edge Joints 1 to 43 XT YR ZR

Joints 43 to 49 ZT XR YR

The material property of the shell is:

Modulus of Elasticity = 432,000,000 psf

Poisson's Ratio = 0.00

Shear Modulus = 216,000,000 psf

The uniform downward load of 90 lb/ft² is equivalent to specifying a gravity loading in Global Y-direction with:

Weight Density = 360 lb/ft³

For a shell thickness of 0.25 ft and weight density of 360 lb/ft³, this combination gives the desired 90 lb/ft² uniform loading in Global Y-direction.

The input for the model should be generated using a cylindrical coordinate system.

Reference

- MacNeal, R.H. and Harder, R.C., "A Proposed Standard Set of Problems to Test Finite Element Accuracy," Finite Elements in Analysis and Design 1 (1985), pp.3-20, North-Holland.
- Zienkiewicz, O. C., "The Finite Element Method," McGraw-Hill, 1977.

Solution Comparison

Sources:

- Computers & Structures Inc., "SAP90 Structural Analysis Verification Manual", October, 1990, 16-1.
- Theory
- LARSA 4D

	SAP90	Theory	LARSA
Axial Z-Displacement in feet at the Support Joints 1-7			
Location=0.00(deg)	0.0000	0.0004	0.0000
Location=6.67(deg)	0.0005	0.0009	0.0005
Location=13.33(deg)	0.0018	0.0020	0.0018
Location=20.00(deg)	0.0029	0.0030	0.0029
Location=26.67(deg)	0.0024	0.0021	0.0024
Location=33.33(deg)	-0.0017	-0.0016	-0.0017
Location=40.00(deg)	-0.0118	-0.0120	-0.0118
Vertical Y-Displacement in feet at the Center Joints 43-49			
Location=0.00(deg)	0.046	0.045	0.047
Location=6.67(deg)	0.031	0.027	0.031
Location=13.33(deg)	-0.013	-0.018	-0.013
Location=20.00(deg)	-0.078	-0.082	-0.079
Location=26.67(deg)	-0.155	-0.155	-0.157
Location=33.33(deg)	-0.234	-0.241	-0.236
Location=40.00(deg)	-0.307	-0.309	-0.309
Moments Mx (lb-ft/ft) at the Central Section Shell 31-36			
Location=3.33(deg)	-2038	-2045	-2004

	SAP90	Theory	LARSA
Location=10.00(deg)	-1796	-1810	-1772
Location=16.67(deg)	-1329	-1310	-1321
Location=23.33(deg)	-727	-715	-730
Location=30.00(deg)	-186	-165	-192
Location=36.67(deg)	14	+25	16
Twisting Moments Mxy (lb-ft/lb) at the Support Shell 1-6			
Location=3.33(deg)	-225	-190	-177
Location=10.00(deg)	-529	-525	-520
Location=16.67(deg)	-840	-835	-828
Location=23.33(deg)	-1082	-1120	-1063
Location=30.00(deg)	-1215	-1265	-1187
Location=36.67(deg)	-1241	-1265	-1198

The midside vertical displacement computed by LARSA is -0.309 feet agreeing well with the theoretical value of -0.309.

Important note: The bending and twisting moments from the Reference and theory are reported for the edge of the plate whereas the values from LARSA are at the center of each plate element. Since the bending and twisting moments are expected to be slightly lower at the center (about 2 feet from the edge) of the plate than the values at the edge, the results from LARSA are agreeing well with theory and Reference.

For More Information, please refer to the following documentation.

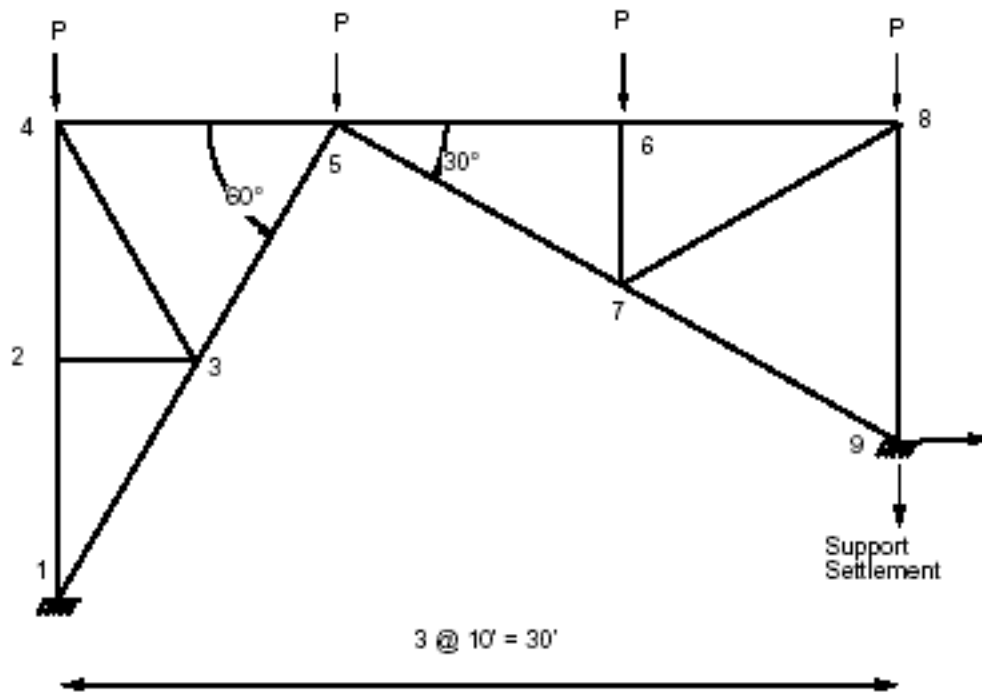
- For help on linear static analysis, see Linear Static Analysis in *LARSA 4D Reference Manual*.

L14: 2D Truss - Thermal Loads and Settlement

2D truss shown below is subjected to various loads. In case 1, the truss is subjected to a uniform temperature rise of 70 degrees Fahrenheit. In case 2, concentrated forces of 10,000 lb. each are applied at the joints of the top chord of the truss. In addition to applied loads, the right support undergoes some settlement relative to the support. The vertical settlement is 0.01 ft down and the horizontal settlement is 0.01 ft towards right. In case 2, the temperature drops 40 degrees F.

Calculate the vertical deflection at the top hinge (at Joint 5).

Example Project: The example described here can be found in the Linear Elastic Static folder of your LARSA 4D Samples directory (generally My Documents\LARSA Projects\Samples) in the file L14.



2D Truss and FE Model Joints

The material properties for the truss bars are:

Modulus of Elasticity = 30,000,000 psi

Coefficient of Thermal Expansion = 0.0000065

The section property for the truss bars is:

$A_{xx} = 2.0 \text{ in}^2$

The finite element model consists of 14 truss elements. Linear static analysis is performed with 2 primary load cases.

Solution Comparison

Translational displacement in global direction at Joint 5 (in feet):

Sources:

- Timoshenko, S.P. and Young, D.H., "Theory of Structures," 2nd ed., McGraw-Hill, New York, 1965, pp. 266-267.
- LARSA 4D

	Timoshenko	LARSA
Load Case 1	+0.158	+0.158
Load Case 2	-0.223	-0.223

The comparison of the results is excellent.

For More Information, please refer to the following documentation.

- For help on linear static analysis, see Linear Static Analysis in *LARSA 4D Reference Manual*.

L16: Nonlinear Thermal Load

The three-span continuous concrete beam is subjected to a thermal load that is uniform along the length of the member but varies along the vertical axis of the cross-section. The nonlinear variation causes self-equilibrating stresses.

Example Project: The example described here can be found in the Linear Elastic Static folder of your LARSA 4D Samples directory (generally My Documents\LARSA Projects\Samples) in the file L16.

The three-span continuous concrete beam in the figure below is subjected to a nonlinear thermal gradient. The member has a T-shaped cross-section (1.6m depth, 2.8 m width, 0.4 m web thickness, 0.2 m flange thickness). The material has a modulus of elasticity of $3 \times 10^8 \text{ N/m}^2$ and a coefficient of thermal expansion of $10 \times 10^{-6} \text{ 1/}^\circ\text{C}$.

The spans are 21 m, 27 m, and 21 m.

The thermal load is uniform along the length of the member but it varies as a fifth-order parabola along the depth of the section, from a maximum of 25°C at the top fiber to 0°C at a depth of 1.2 m and below. The temperature change as a function of depth, measured from the top of the section, is given by the equation:

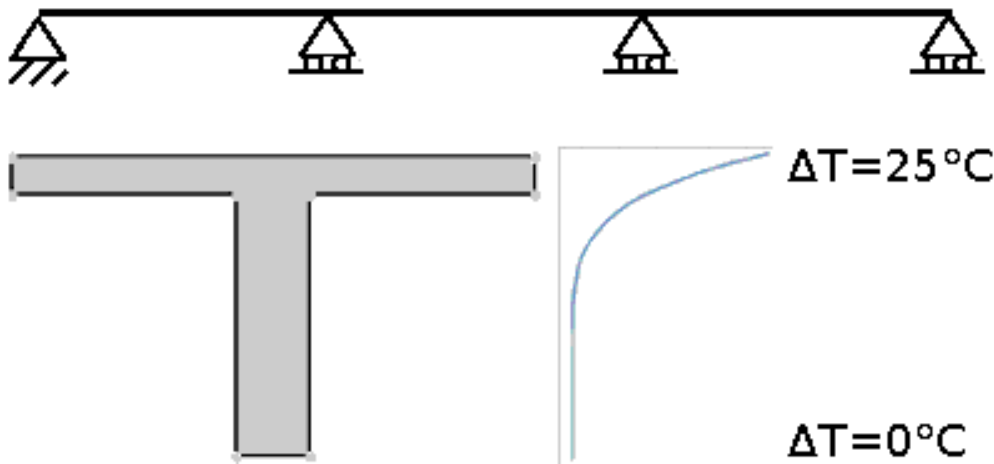
$$\Delta T = 4.21 \times 25 \times ((3/4 - y/1.6)^5) \text{ (}^\circ\text{C)}$$

for $y < 1.2 \text{ m}$, and $\Delta T = 0$ in $1.2 \text{ m} \leq y \leq 1.6 \text{ m}$.

The nonlinear gradient creates self-equilibrating stresses.

Calculate the total stress at a fiber.

The model, cross-section, and thermal gradient are depicted in the figure below:



3-Span Beam, X-Section and Temperature Variation

Solution Comparison

Stress at the top fiber, centroid, and bottom fiber (at mid-span locations) are reported in the table below. Units are N/mm^2 .

Sources:

- Structural Analysis 4th edition, example 5-3, page 132. A. Ghali and A.M. Neville.
- LARSA 4D

	Ghali	LARSA
Top Fiber	-5.20 MPa	-5.19 MPa
Centroid	2.16 MPa	2.17 MPa
Bottom Fiber	3.49 MPa	3.50 MPa

The comparison of the results is excellent.

For More Information, please refer to the following documentation.

- For help on linear static analysis, see Linear Static Analysis in *LARSA 4D Reference Manual*.
- For help on member thermal loads, see Member Thermal Loads in *LARSA 4D Reference Manual*.

L17: Plane Stress Element-Straight Beam with Static Loads

A straight cantilever beam, modeled with plane stress elements, is subjected to unit forces at the tip in the X and Y directions and a unit moment at the tip about the Y direction, each in a different load case. Please note that this example is an extreme case presented for testing and verification of the plane plate elements. Plane plate elements are not in general intended for use in modeling a beam with a 2 to 1 depth-to-width ratio. The problem is modeled with classic, bilinear, drilling and incompatible plates with different mesh sizes. The solutions are compared to independent solutions from MacNeal and Harder 1985.

Example Project: The example described here can be found in the LinearStatic folder of your LARSA 4D Samples directory (generally My Documents\LARSA Projects\Samples) in the file L17.

Problem Description

The basic geometry, properties and loadings are as described in MacNeal and Harder 1985. The cantilever beam is 6 inches long, 0.2 inch wide parallel to the Z direction, and 0.1 inch wide parallel to the Y direction. For testing elements with incompatible bending modes and drilling degrees of freedom, three different models meshed with six elements are used as suggested in MacNeal and Harder 1985. Model A uses rectangular elements, model B uses trapezoidal elements, and model C uses parallelogram elements. For testing classic and bilinear plates, a triangular model, model D, with 12 triangle elements is added to the mix.

Model Diagrams

Material properties of the cantilever beam, namely the elastic modulus E and Poisson's ratio ν are defined as follows:

$$E = 10,000,000 \text{ lb/in}^2$$

$$\nu = 0.3$$

Loading

Three load cases are created for each model, applying a unit axial force, a unit in-plane force, and a unit in-plane moment at the tip of the cantilever, respectively. The in-plane moment is applied as a couple of forces in the X direction.

The independent solution is derived using elementary beam theory that assumes no local Poisson's effect occurring at the support. The beam is modeled to match this assumption by applying an in-plane force equal to the applied tip load in the opposite direction to model the reaction without Poisson's effect.

In the LARSA 4D models the U_x and U_z degrees of freedom are active; all other degrees of freedom are inactive. For models with drilling plates rotations in R_y direction are set active as drilling elements have this rotation degree of freedom. At the fixed end, joint 1 is restrained in the U_x and U_z degrees of freedom and joint 8 is restrained in the U_x degrees of freedom only. Joint 8 is not restrained in the U_z degrees of freedom to avoid imposing the unwanted local Poisson's effect on the model.

Load Case	Load Type	Load
1	Axial Extension	$F_x = +0.5$ lb at joints 7 and 14
2	In-Plane Shear and Bending	$F_z = +0.5$ lb at joints 7 and 14 $F_z = -0.5$ lb at joint 8
3	In-Plane Moment	$F_x = -5$ lb at joint 7 $F_x = +5$ lb at joint 14

Solution Comparison

Plates with Incompatible Bending Modes

First, models A, B, and C are modeled with plate elements with the incompatible membrane type. The following table presents the results of solutions to these models and their comparisons to the independent results.

Comparison of Solutions of Models A-C using Plates with Incompatible Bending Modes for Different Mesh Sizes

Load Type	Model and Element Shape	Output Parameter	Independent	LARSA4D	Percent Difference
Axial Extension	A - Rectangle	$U_x @$ Joint 14	3.000E-05	3.00E-05	0%
Axial Extension	B - Trapezoid	$U_x @$ Joint 14	3.000E-05	3.00E-05	0%
Axial Extension	C - Parallelogram	$U_x @$ Joint 14	3.000E-05	3.00E-05	0%
In-Plane Shear and Bending	A - Rectangle	$U_{xz} @$ Joint 14	0.1081	0.1073	0.7%
In-Plane Shear and Bending	B - Trapezoid	$U_x @$ Joint 14	0.1081	0.0247	77.1%
In-Plane Shear and bending	C - Parallelogram	$U_x @$ Joint 14	0.1081	0.0874	19.1%
In-Plane Moment	A - Rectangle	$U_x @$ Joint 14	9.000E-04	0.00090	0%
In-Plane Moment	B - Trapezoid	$U_x @$ Joint 14	9.000E-04	0.000015	98.3%
In-Plane Moment	C - Parallelogram	$U_x @$ Joint 14	9.000E-04	0.00076	91.5%

Model A which uses rectangular elements with the incompatible bending modes membrane type gives close results to the independent solutions in all load cases. However models B and C get close to the independent solution only in the axial extension load case.

Accurate results can be obtained from these models by breaking the trapezoidal elements into smaller ones. Smaller trapezoidal elements will have straighter angles between opposite edges and the aspect ratio of these elements will be closer to one. First we break the first and last elements of models B and C to see if the trapezoidal elements are the problem and parallelogram elements work correctly.

The following table presents the solutions of models B and C with or without breaking the first and last trapezoidal elements and their comparisons to the independent solutions. In the models with broken elements, named F-L, the first and the last trapezoidal elements are broken into four smaller ones. If we break the first and last elements of Model B, the trapezoidal model, we get better results than the unbroken case. However the results are not close proximity to the independent solutions. If break the first and last elements of Model C, the parallelogram model, we get better results than the unbroken case and the results are close to the independent solutions. This confirms that the shape of trapezoidal elements are the problem and not the shape of parallelogram elements.

Comparison of Solutions of Models B and C with or without Breaking of Trapezoidal Elements

	In-Plane Shear and Bending		In-Plane Moment	
	LARSA 4D	Percent Difference	LARSA 4D	Percent Difference
B - Trapezoid 6x1	2.47E-02	-77.1%	1.54E-04	-82.9%
B - Trapezoid F-L	4.93E-02	-54.4%	3.25E-04	-63.9%
C - Parallelogram 6x1	8.75E-02	-19.1%	7.68E-04	-14.7%
C - Parallelogram F-L	1.08E-01	-0.2%	9.02E-04	-0.1%

If break all elements of model B into 4 trapezoids, we can achieve close proximity to the independent solution. The following table presents the comparison of results for model B meshed into 96 elements to model B meshed into 6 elements. The finely meshed model gives close proximity results to the independent solutions, showing the importance of the shapes of trapezoidal elements.

Comparison of Solutions of Model B for Course (6x1) and Fine (24x1) Meshes

	In-Plane Shear and Bending		In-Plane Moment	
	LARSA 4D	Percent Difference	LARSA 4D	Percent Difference
B - Trapezoid 6x1	2.47E-02	-77.1%	1.54E-04	-82.9%
B - Trapezoid 24x1	1.08E-01	0.1%	9.01E-04	0.1%

Plates With Drilling Degrees of Freedoms

The following tables summarizes the results and their differences from the independent solutions, for models A, B, C solved using plates with the drilling membrane type. Results for models with different mesh sizes are also presented to show the effects of element size.

For axial extension all models provide correct results. For in-plane shear and bending and in-plane moment only rectangular elements can get close to 2% range of independent solutions. For all element geometries increasing mesh

size increases the solution accuracy. Rectangular elements can get in 1% range of the independent results with a mesh size of 48x2. Trapezoidal model can get in 3% range of the independent results with a mesh size of 48x2 and 1% range with a mesh size of 96x4. Parallelogram model can get in 6% range of the independent results with a mesh size of 48x2 and 0.5% range with a mesh size of 96x4.

**Comparison of Solutions of Models A-C using Plates with
Drilling Degrees of Freedom for Different Mesh Sizes**

	Axial Extension		In-Plane Shear and Bending		In-Plane Moment	
	LARSA 4D	Percent Difference	LARSA 4D	Percent Difference	LARSA 4D	Percent Difference
A - Rectangular 6x1	3.00E-05	0.0%	1.05E-01	-2.4%	8.84E-04	-1.7%
A - Rectangular 48x2	3.00E-05	0.0%	1.07E-01	-0.8%	8.93E-04	-0.8%
B - Trapezoid 6x1	3.00E-05	0.0%	1.63E-02	-84.9%	1.04E-04	-88.4%
B - Trapezoid 48x2	3.00E-05	0.0%	1.05E-01	-3.3%	8.70E-04	-3.3%
B - Trapezoid 96x4	3.00E-05	0.0%	1.09E-01	1.2%	9.05E-04	0.5%
C - Parallelogram 6x1	3.00E-05	0.0%	7.04E-02	-34.9%	6.44E-04	-28.4%
C - Parallelogram 48x2	3.00E-05	0.0%	1.02E-01	-5.6%	8.46E-04	-6.0%
C - Parallelogram 96x4	3.00E-05	0.0%	1.09E-01	0.5%	8.98E-04	-0.3%

Classic Plates

After solving models A, B, and C using plate elements with incompatible modes and drilling degrees of freedom, they are solved using the membrane type classic. Furthermore, model D that uses triangular elements is solved and its results are compared to the results of other models and independent solutions. The Following tables summarizes the results for models A, B, C and D solved with classic plates for different mesh sizes and their comparisons to the independent solutions.

For axial extension all models provide correct results. For in-plane shear and bending and in-plane moment only rectangular meshes can give results close proximity to the independent solutions. The trapezoidal models give results within 4% range of the independent results with a mesh size of 24x1 and within 1% range with a mesh size of 48x2. Similar to the models with incompatible bending modes, parallelogram models give better results than trapezoidal results using classical plates. Parallelogram models can get in 1% range of independent solutions with a mesh size of 24x1. Triangle models need considerably more elements to get in close range of independent solutions. A 96 element model gets in 70% range and a 768 element model can get in 20% range.

Comparison of Solutions of Models A-D with Classic Plates for Different Mesh Sizes

	Axial Extension		In-Plane Shear and Bending		In-Plane Moment	
	LARSA 4D	Percent Difference	LARSA 4D	Percent Difference	LARSA 4D	Percent Difference
A - Rectangular 6x1	3.00E-05	0%	1.07E-01	-1%	9.00E-04	0%
B - Trapezoid 6x1	3.00E-05	0%	1.36E-02	-87%	9.18E-05	-90%
B - Trapezoid 24x1	3.00E-05	0%	1.04E-01	-4%	8.64E-04	-4%
B - Trapezoid 48x2	3.00E-05	0%	1.08E-01	0%	8.98E-04	0%
C - Parallelogram 6x1	3.00E-05	0%	7.62E-02	-30%	6.95E-04	-23%
C - Parallelogram 24x1	3.00E-05	0%	1.08E-01	-1%	8.96E-04	0%
C - Parallelogram 48x2	3.00E-05	0%	1.08E-01	0%	8.98E-04	0%
D - Triangle 12	3.00E-05	0%	2.82E-05	-100%	2.82E-05	-97%
D - Triangle 96	3.00E-05	0%	3.23E-02	-70%	2.68E-04	-70%
D - Triangle 768	3.00E-05	0%	8.70E-02	-20%	7.22E-04	-20%

Bilinear Plates

The following tables summarize the results for models A, B, C and D solved with bilinear plates for different mesh sizes and their differences from the independent solutions. For axial extension all models provide correct results. For in-plane shear and bending and in-plane moment none of the models can get in close proximity to the independent results with a mesh size of 6x1 for quad elements and 12 for triangular elements. However increasing mesh size increases the solution accuracy. Rectangular elements can get in 3% range of the independent results with a mesh size of 96x4. Trapezoidal model can get in 11% range of the independent results with a mesh size of 96x4. Parallelogram model can get in 20% range of the independent results with a mesh size of 96x4. Triangle models give similar results to the triangles models with classic plates. A 96 element model gets in 70% range and a 768 element element model can get in 20% range.

Comparison of Solutions of Models A-D with Bilinear Plates for Different Mesh Sizes

	Axial Extension		In-Plane Shear and Bending		In-Plane Moment	
	LARSA 4D	Percent Difference	LARSA 4D	Percent Difference	LARSA 4D	Percent Difference
A - Rectangular 6x1	3.00E-05	0%	1.01E-02	-91%	8.40E-05	-91%
A - Rectangular 48x2	3.00E-05	0%	9.20E-02	-15%	7.66E-04	-15%
A - Rectangular 96x4	3.00E-05	0%	1.05E-01	-3%	8.72E-04	-3%
B - Trapezoid 6x1	3.00E-05	0%	2.99E-03	-97%	2.06E-05	-98%
B - Trapezoid 48x2	3.00E-05	0%	7.33E-02	-32%	6.06E-04	-33%
B - Trapezoid 96x4	3.00E-05	0%	9.74E-02	-10%	8.04E-04	-11%
C - Parallelogram 6x1	3.00E-05	0%	3.77E-03	-97%	2.82E-05	-97%
C - Parallelogram 48x2	3.00E-05	0%	5.72E-02	-47%	4.49E-04	-50%
C - Parallelogram 96x4	3.00E-05	0%	8.84E-02	-18%	7.17E-04	-20%

	Axial Extension		In-Plane Shear and Bending		In-Plane Moment	
D - Triangle 12	3.00E-05	0%	3.45E-03	-97%	2.82E-05	-97%
D - Triangle 96	3.00E-05	0%	3.23E-02	-70%	2.68E-04	-70%
D - Triangle 768	3.00E-05	0%	8.70E-02	-20%	7.22E-04	-20%

Conclusion

In this example, a plane cantilever beam subjected to axial, shear and bending, and moment loadings is modeled with different plate types and different mesh sizes. Furthermore, models with different element geometries are used to observe the effects of element shapes on the results. Results are compared to each other and solutions from independent sources.

The best results are achieved using plate elements with incompatible modes. Plates with incompatible modes are followed by classic plates, plates with drilling degrees of freedom and bilinear plates in terms of solution accuracy.

The shape of the element directly effects the accuracy of the results. For all plate types rectangular elements give the most accurate results. Furthermore, the more rectangular the element shape the better results are. For all plate types, quadrilateral element shapes give better results than triangular ones.

Sources:

- Cook and Young, "Advanced Mechanics of Materials," 1985, pp. 244.
- MacNeal, R.H. and Harder, R.L., "A Proposed Standard Set of Problems to Test Finite Element Accuracy," *Finite Elements Analysis and Design 1 (1985)*, pp. 3-20, North-Holland.
- SAP 2000, CSI Software Verification Example 3-002, "Plane-Straight Beam with Static Loads."

For More Information, please refer to the following documentation.

- For help on linear static analysis, see Linear Static Analysis in *LARSA 4D Reference Manual*.

L18: Shell-Straight Beam with Static Loads

A straight cantilever beam, modeled with shell elements with different configurations, is subjected to unit forces and moments at the tip in all orthogonal directions, each in a different load case. Tip deflections in the direction of loadings are tracked and compared with analytical results as well as SAP2000's. Please note that this example is an extreme case for testing shell elements since they are not intended for use in modeling a beam with a 2 to 1 depth-to-width ratio.

Example Project: The example described here can be found in the Linear Elastic Static folder of your LARSA 4D Samples directory (generally My Documents\LARSA Projects\Samples) in the file L18_Rectangular_Thin_Incompatible_6x1.

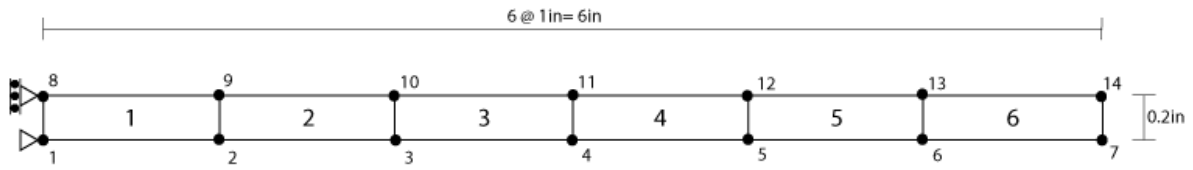
Problem Description

This problem is described in the paper "A Proposed Standard set of Problems to Test Finite Element Accuracy" by MacNeal and Harder (1985). The cantilever beam has a length of 6 inches (in X direction), a depth of 0.2 inches (in Z direction) and a width of 0.1 inches (in Y direction). This geometry is modeled with five different meshes and each mesh is excited with six different load cases. The meshes, loadings and material properties also conform to the paper mentioned above.

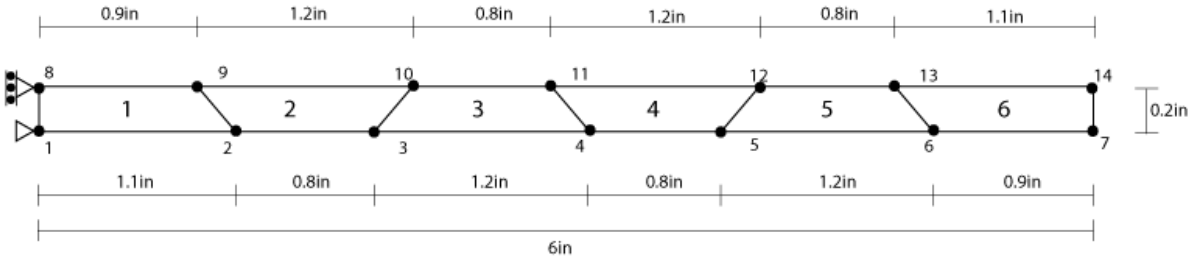
Mesh models

First three models use quadrilateral elements with different geometric irregularities and last two model use triangular elements with a varying degree of fineness. All models are shown in following figure. Sign convention for axes, node and element labels are also given in the figure.

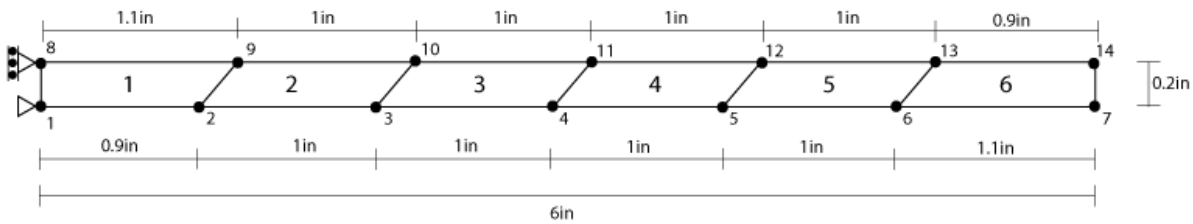
Model A - Rectangular Shaped Elements



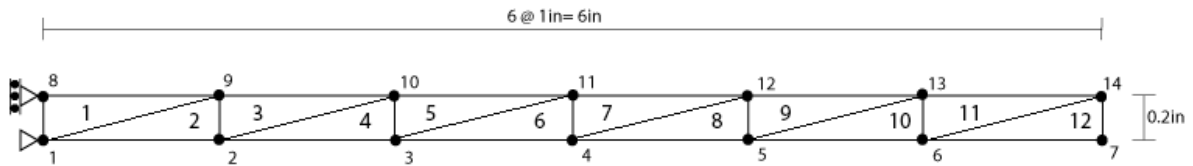
Model B - Trapezoidal Shaped Elements



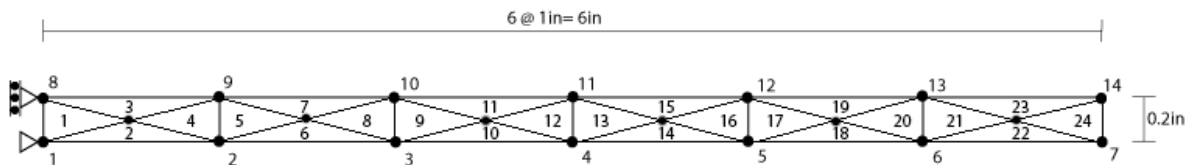
Model C - Parallelogram Shaped Elements



Model D - Triangular Shaped Elements



Model E - Triangular Shaped Elements



Mesh diagrams

Load cases

Six load cases are created for each model. These load cases apply a unit axial force, a unit in-plane force, unit out-of-plane force, a unit twisting moment, a unit in-plane moment and a unit out-of-plane moment at the tip of the

cantilever, respectively. The twisting moment is applied as a force couple in Y axis. The in-plane moment is applied as a force couple in X axis. Only the out-of-plane moment is applied as moments. The details of the loadings are given in following table.

Load Case	Load Type	Load
1	Axial extension	$F_x = +0.5$ lb at joint 7 and 14
2	In-plane shear and bending	$F_z = +0.5$ lb at joint 7 and 14, $F_z = -0.5$ lb at joint 8
3	Out-of-plane shear and bending	$F_y = +0.5$ lb at joint 7 and 14
4	Twisting moment	$F_y = -5$ lb at joint 7, $F_y = +5$ lb at joint 14
5	In-plane moment	$F_x = -5$ lb at joint 7, $F_x = +5$ lb at joint 14
6	Out-of-plane moment	$M_z = +0.5$ lb-in at joint 7 and 14

Material properties

$$E = 10,000,000 \text{ lb/in}^2$$

$$\nu = 0.3$$

$$G = 3,846,154 \text{ lb/in}^2$$

$$\text{Shell thickness} = 0.1 \text{ in}$$

Results

The independent solution is derived using elementary beam theory that assumes no local Poisson's effect at the support. The beam is modeled to match this assumption in LARSA 4D. At the fixed end, joint 1 is restrained in the U_x , U_y , U_z and R_z degrees of freedom and joint 8 is restrained in the U_x , U_y and R_z degrees of freedom. Joint 8 is not restrained in the U_z degree of freedom to avoid imposing unwanted local Poisson's effect into the model. Also, when the beam is loaded with in-plane shear, an in-plane force equal to half the applied tip load is applied to joint 8 in the opposite direction of the tip load. This special load at joint 8 is applied to model the reaction without the Poisson's effect.

The results are compared for four LARSA 4D plate element behaviors: Classic, Thin Plate, Thick Plate, and MITC4. For the Thin and Thick Plate, the Incompatible and Drilling membrane behaviors are combined with the bending behavior and reported in separate columns. The bilinear membrane behavior and the MITC4 behavior are known to suffer from the shear-locking phenomena which is relevant in the in-plane bending and moment load cases. The bilinear membrane behavior is therefore not included in this comparison, and MITC4 results are only reported for out of plane load cases.

The results reported in SAP2000's corresponding document are also given. It is important to note that all results are the averages of absolute values obtained from joints 7 and 14. The percentages in the parantheses next to the results indicate relative percentage errors.

Classic Element Behavior

Load Type	Mesh Type	Result	Independent	LARSA 4D
Axial extension	Rectangular	U_x (in)	0.00003	0.00003 (0%)
Axial extension	Trapezoidal	U_x (in)	0.00003	0.00003 (0%)
In-plane shear and bending	Rectangular	U_z (in)	0.10810	0.10733 (-1%)
In-plane shear and bending	Trapezoidal	U_z (in)	0.10810	0.01376 (-87%)
Out-of-plane shear and bending	Rectangular	U_y (in)	0.43210	0.42864 (-1%)
Out-of-plane shear and bending	Trapezoidal	U_y (in)	0.43210	0.41601 (-4%)
Twisting moment	Rectangular	U_y (in)	0.00341	0.00206 (-40%)
Twisting moment	Trapezoidal	U_y (in)	0.00341	0.00209 (-39%)
In-plane moment	Rectangular	U_x (in)	0.00090	0.00090 (0%)
In-plane moment	Trapezoidal	U_x (in)	0.00090	0.00009 (-90%)
Out-of-plane moment	Rectangular	R_z (rad)	0.03600	0.03600 (0%)
Out-of-plane moment	Trapezoidal	R_z (rad)	0.03600	0.03600 (0%)

Thin Plate Bending Behavior

Load Type	Mesh Type	Result	Independent	LARSA 4D <i>Incompatible</i>	LARSA 4D <i>Drilling</i>	SAP2000
Axial extension	Rectangular	U_x (in)	0.00003	0.00003 (0%)	0.00003 (0%)	0.00003 (0%)
Axial extension	Trapezoidal	U_x (in)	0.00003	0.00003 (0%)	0.00003 (0%)	0.00003 (0%)
Axial extension	Parallelogram	U_x (in)	0.00003	0.00003 (0%)	0.00003 (0%)	0.00003 (0%)
Axial extension	Triangular (12 elem.)	U_x (in)	0.00003		0.00003 (0%)	0.00003 (0%)
Axial extension	Triangular (24 elem.)	U_x (in)	0.00003		0.00003 (0%)	0.00003 (0%)

Load Type	Mesh Type	Result	Independent	LARSA 4D <i>Incompatible</i>	LARSA 4D <i>Drilling</i>	SAP2000
In-plane shear and bending	Rectangular	U_z (in)	0.10810	0.10733 (-1%)	0.10548 (-2%)	0.10720 (-1%)
In-plane shear and bending	Trapezoidal	U_z (in)	0.10810	0.02517 (-77%)	0.01655 (-85%)	0.02270 (-79%)
In-plane shear and bending	Parallelogram	U_z (in)	0.10810	0.08703 (-19%)	0.07009 (-35%)	0.08040 (-26%)
In-plane shear and bending	Triangular (12 elem.)	U_z (in)	0.10810		0.00345 (-97%)	0.00320 (-97%)
In-plane shear and bending	Triangular (24 elem.)	U_z (in)	0.10810		0.00705 (-93%)	0.00660 (-94%)
Out-of-plane shear and bending	Rectangular	U_y (in)	0.43210	0.43200 (0%)	0.43200 (0%)	0.43200 (0%)
Out-of-plane shear and bending	Trapezoidal	U_y (in)	0.43210	0.43217 (0%)	0.43217 (0%)	0.43220 (0%)
Out-of-plane shear and bending	Parallelogram	U_y (in)	0.43210	0.43219 (0%)	0.43219 (0%)	0.43220 (0%)
Out-of-plane shear and bending	Triangular (12 elem.)	U_y (in)	0.43210		0.42962 (-1%)	0.42960 (-1%)
Out-of-plane shear and bending	Triangular (24 elem.)	U_y (in)	0.43210		0.43137 (0%)	0.43140 (0%)
Twisting moment	Rectangular	U_y (in)	0.00341	0.00233 (-32%)	0.00233 (-32%)	0.00233 (-32%)
Twisting moment	Trapezoidal	U_y (in)	0.00341	0.00233 (-32%)	0.00233 (-32%)	0.00233 (-32%)
Twisting moment	Parallelogram	U_y (in)	0.00341	0.00233 (-32%)	0.00233 (-32%)	0.00233 (-32%)
Twisting moment	Triangular (12 elem.)	U_y (in)	0.00341		0.00231 (-32%)	0.00231 (-32%)

Load Type	Mesh Type	Result	Independent	LARSA 4D <i>Incompatible</i>	LARSA 4D <i>Drilling</i>	SAP2000
Twisting moment	Triangular (24 elem.)	U_y (in)	0.00341		0.00230 (-33%)	0.00230 (-33%)
In-plane moment	Rectangular	U_x (in)	0.00090	0.00090 (0%)	0.00088 (-2%)	0.00090 (0%)
In-plane moment	Trapezoidal	U_x (in)	0.00090	0.00015 (-83%)	0.00010 (-88%)	0.00014 (-85%)
In-plane moment	Parallelogram	U_x (in)	0.00090	0.00077 (-15%)	0.00064 (-28%)	0.00072 (-20%)
In-plane moment	Triangular (12 elem.)	U_x (in)	0.00090		0.00003 (-97%)	0.00003 (-97%)
In-plane moment	Triangular (24 elem.)	U_x (in)	0.00090		0.00006 (-93%)	0.00006 (-94%)
Out-of-plane moment	Rectangular	R_z (rad)	0.03600	0.03600 (0%)	0.03600 (0%)	0.03600 (0%)
Out-of-plane moment	Trapezoidal	R_z (rad)	0.03600	0.03600 (0%)	0.03600 (0%)	0.03600 (0%)
Out-of-plane moment	Parallelogram	R_z (rad)	0.03600	0.03600 (0%)	0.03600 (0%)	0.03600 (0%)
Out-of-plane moment	Triangular (12 elem.)	R_z (rad)	0.03600		0.03600 (0%)	0.03600 (0%)
Out-of-plane moment	Triangular (24 elem.)	R_z (rad)	0.03600		0.03600 (0%)	0.03600 (0%)

Thick Plate Bending Behavior

Load Type	Mesh Type	Result	Independent	LARSA 4D <i>Incompatible</i>	LARSA 4D <i>Drilling</i>	SAP2000
Axial extension	Rectangular	U_x (in)	0.00003	0.00003 (0%)	0.00003 (0%)	0.00003 (0%)
Axial extension	Trapezoidal	U_x (in)	0.00003	0.00003 (0%)	0.00003 (0%)	0.00003 (0%)
Axial extension	Parallelogram	U_x (in)	0.00003	0.00003 (0%)	0.00003 (0%)	0.00003 (0%)
Axial extension	Triangular (12 elem.)	U_x (in)	0.00003		0.00003 (0%)	0.00003 (0%)

Load Type	Mesh Type	Result	Independent	LARSA 4D <i>Incompatible</i>	LARSA 4D <i>Drilling</i>	SAP2000
Axial extension	Triangular (24 elem.)	U_x (in)	0.00003		0.00003 (0%)	0.00003 (0%)
In-plane shear and bending	Rectangular	U_z (in)	0.10810	0.10733 (-1%)	0.10548 (-2%)	0.10720 (-1%)
In-plane shear and bending	Trapezoidal	U_z (in)	0.10810	0.02517 (-77%)	0.01655 (-85%)	0.02270 (-79%)
In-plane shear and bending	Parallelogram	U_z (in)	0.10810	0.08703 (-19%)	0.07009 (-35%)	0.08040 (-26%)
In-plane shear and bending	Triangular (12 elem.)	U_z (in)	0.10810		0.00345 (-97%)	0.00320 (-97%)
In-plane shear and bending	Triangular (24 elem.)	U_z (in)	0.10810		0.00705 (-93%)	0.00660 (-94%)
Out-of-plane shear and bending	Rectangular	U_y (in)	0.43210	0.42882 (-1%)	0.42882 (-1%)	0.43210 (0%)
Out-of-plane shear and bending	Trapezoidal	U_y (in)	0.43210	0.42146 (-2%)	0.42146 (-2%)	0.43070 (0%)
Out-of-plane shear and bending	Parallelogram	U_y (in)	0.43210	0.42773 (-1%)	0.42773 (-1%)	0.43220 (0%)
Out-of-plane shear and bending	Triangular (12 elem.)	U_y (in)	0.43210		0.42829 (-1%)	0.43280 (0%)
Out-of-plane shear and bending	Triangular (24 elem.)	U_y (in)	0.43210		0.42871 (-1%)	0.42980 (-1%)
Twisting moment	Rectangular	U_y (in)	0.00341	0.00302 (-11%)	0.00302 (-11%)	0.00224 (-34%)
Twisting moment	Trapezoidal	U_y (in)	0.00341	0.00284 (-17%)	0.00284 (-17%)	0.00409 (20%)
Twisting moment	Parallelogram	U_y (in)	0.00341	0.00272 (-20%)	0.00272 (-20%)	0.00240 (-30%)

Load Type	Mesh Type	Result	Independent	LARSA 4D <i>Incompatible</i>	LARSA 4D <i>Drilling</i>	SAP2000
Twisting moment	Triangular (12 elem.)	U_y (in)	0.00341		0.00204 (-40%)	0.00466 (37%)
Twisting moment	Triangular (24 elem.)	U_y (in)	0.00341		0.00227 (-34%)	0.00458 (34%)
In-plane moment	Rectangular	U_x (in)	0.00090	0.00090 (0%)	0.00088 (-2%)	0.00090 (0%)
In-plane moment	Trapezoidal	U_x (in)	0.00090	0.00015 (-83%)	0.00010 (-88%)	0.00014 (-85%)
In-plane moment	Parallelogram	U_x (in)	0.00090	0.00077 (-15%)	0.00064 (-28%)	0.00072 (-20%)
In-plane moment	Triangular (12 elem.)	U_x (in)	0.00090		0.00003 (-97%)	0.00003 (-97%)
In-plane moment	Triangular (24 elem.)	U_x (in)	0.00090		0.00006 (-93%)	0.00006 (-94%)
Out-of-plane moment	Rectangular	R_z (rad)	0.03600	0.03600 (0%)	0.03600 (0%)	0.03600 (0%)
Out-of-plane moment	Trapezoidal	R_z (rad)	0.03600	0.03600 (0%)	0.03600 (0%)	0.03600 (0%)
Out-of-plane moment	Parallelogram	R_z (rad)	0.03600	0.03600 (0%)	0.03600 (0%)	0.03600 (0%)
Out-of-plane moment	Triangular (12 elem.)	R_z (rad)	0.03600		0.03600 (0%)	0.03600 (0%)
Out-of-plane moment	Triangular (24 elem.)	R_z (rad)	0.03600		0.03600 (0%)	0.03600 (0%)

MITC4 Element Behavior

Load Type	Mesh Type	Result	Independent	LARSA 4D
Axial extension	Rectangular	U_x (in)	0.00003	0.00003 (0%)
Axial extension	Trapezoidal	U_x (in)	0.00003	0.00003 (0%)
Axial extension	Parallelogram	U_x (in)	0.00003	0.00003 (0%)
Out-of-plane shear and bending	Rectangular	U_y (in)	0.43210	0.42873 (1%)
Out-of-plane shear and bending	Trapezoidal	U_y (in)	0.43210	0.42150(2%)

Load Type	Mesh Type	Result	Independent	LARSA 4D
Out-of-plane shear and bending	Parallelogram	U_y (in)	0.43210	0.42763 (1%)
Twisting moment	Rectangular	U_y (in)	0.00341	0.00236 (31%)
Twisting moment	Trapezoidal	U_y (in)	0.00341	0.00236 (31%)
Twisting moment	Parallelogram	U_y (in)	0.00341	0.00237 (31%)
Out-of-plane moment	Rectangular	R_z (rad)	0.03600	0.03600 (0%)
Out-of-plane moment	Trapezoidal	R_z (rad)	0.03600	0.03600 (0%)
Out-of-plane moment	Parallelogram	R_z (rad)	0.03600	0.03600 (0%)

References

- MacNeal, R.H. and Harder, R.L., "A Proposed Standard Set of Problems to Test Finite Element Accuracy," *Finite Elements Analysis and Design 1 (1985)*, pp. 3-20, North-Holland.
- Cook and Young, "Advanced Mechanics of Materials," 1985, pp. 244.
- SAP 2000, CSI Software Verification Example 2-002, "Shell-Straight Beam with Static Loads."

For More Information, please refer to the following documentation.

- For help on linear static analysis, see Linear Static Analysis in *LARSA 4D Reference Manual*.

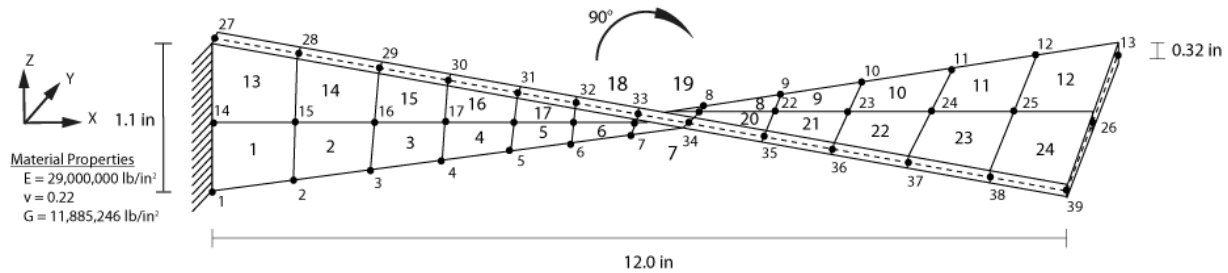
L19: Shell-Twisted Beam with Static Loads

A twisted cantilever beam, modeled with shell elements, is subjected to unit forces at the tip in the in-plane and out-of-plane directions, that is, the Y and Z directions, respectively. The in-plane and out-of-plane loads are applied in different load cases. The tip displacements in the direction of the load are compared with the results from an independent source (MacNeal and Harder 1985).

Example Project: The example described here can be found in the LinearElasticStatic folder of your LARSA 4D Samples directory (generally My Documents\LARSA Projects\Samples) in the file L19.

Problem Description

The geometry, properties and loading are as suggested in MacNeal and Harder 1985. The cantilever beam is twisted 90° from the root (fixed end) to the tip. It is 12 inches long, 1.1 inches wide and 0.32 inches thick. For modeling in LARSA 4D the twisted beam is meshed 2 x 12 (24 area objects total) as shown in the figure.



Model Diagrams

Loading

Two different load cases are applied to the model. In the first load case, IN, a unit force in the in-plane direction, direction Y is applied to the end of the model. In the second load case, OUT, a unit force in the out-of-plane direction, direction Z, is applied to the end of the model. The next table presents the joint loads used to model these two load cases.

Table 1: Joint Loads Used in the IN and OUT Load Cases

Load Case	Load
IN	$F_y = +0.25$ lb at joint 13 $F_y = +0.50$ lb at joint 26 $F_y = +0.25$ lb at joint 39
OUT	$F_z = +0.25$ lb at joint 13 $F_z = +0.50$ lb at joint 26 $F_z = +0.25$ lb at joint 39

Solution Comparison

In Table 2, results obtained from LARSA 4D using elements with the Classic behavior, the MITC4 behavior, and the Thin and Thick Plate bending behaviors with the Drilling membrane type are presented. (The Bilinear and Incompatible membrane types are unable to correctly solve this problem as they lack the necessary degrees of freedom.) In Table 3, comparison of these results to the solutions from the independent source are presented.

Table 2: End Joints Displacements Computed by LARSA 4D and Obtained from the Independent Source

Model	IN (in)	OUT (in)
Independent	5.43E-03	1.75E-03
Classic	4.05E-03	1.62E-03
MITC4	5.38E-03	1.61E-03
Thick Plate	5.41E-03	1.76E-03
Thin Plate	5.42E-03	1.77E-03

Table 3: Difference in End Joint Displacements Between LARSA 4D Results and Solutions from the Independent Source

Model	Difference IN (%)	Difference OUT (%)
Classic	-25.4%	-7.1%
MITC4	-1.0%	-7.8%
Thick Plate	-0.3%	0.4%
Thin Plate	-0.2%	1.2%

The solutions with the Classic element type differ from the results from the independent source by 25% in the in-plane load case and by -7.1% in the out-of-plane load case. The solutions with the Thick Plate behavior are in close proximity to the solution from the independent source: The Thick Plate results differ only 0.5% from the independent results for both load cases. Thin Plate results differ from the independent source by -0.2% for the in-plane load case and by 1.2% for the out-of-plane load case.

References

- MacNeal, R.H. and Harder, R.L., "A Proposed Standard Set of Problems to Test Finite Element Accuracy," *Finite Elements Analysis and Design 1 (1985)*, pp. 244, North-Holland.
- SAP 2000, CSI Software Verification Example 2-004, "Shell-Twisted Beam with Static Loads."

For More Information, please refer to the following documentation.

- For help on linear static analysis, see Linear Static Analysis in *LARSA 4D Reference Manual*.

L20: Shell-Cylinder with Internal Pressure

A cylinder is analyzed for an internal pressure load. The resulting radial outward displacement, vertical displacement at the top of the cylinder, and stresses are compared with hand calculated results based on formulas presented in Roark and Young 1975.

Problem Description

The cylinder is 200 inches tall and has a 60 inch radius. The wall thickness is 1 inch. The applied load is a uniform radial pressure of 1 k/in^2 on the inside face of the entire cylinder.

The local axes of all joints are oriented such that axis 1 points radially outward and axis 3 points upward. The joints at the base of the cylinder are restrained against translation in the local 2 and 3 directions while all other joints are restrained against translation in the local 2 direction. The local axes of all shells are oriented such that axis 3 points radially outward and axis 2 points upward.

Two different models are created for the analysis. The models are identical except for the shell element mesh. Model A uses an 8 x 16 mesh (height x circumference) and Model B uses a 24 x 48 mesh.

The MITC4 element behavior is used.

Material Properties

$E = 29,000 \text{ k/in}^2$

$\nu = 0.3$

$G = 11,154 \text{ k/in}^2$

Loading

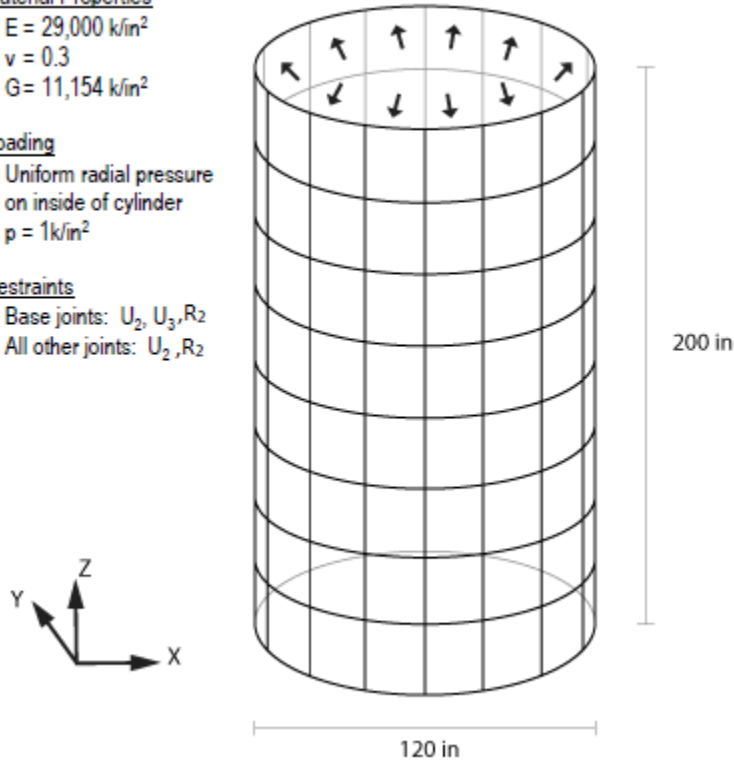
Uniform radial pressure
on inside of cylinder

$p = 1 \text{ k/in}^2$

Restraints

Base joints: U_2, U_3, R_2

All other joints: U_2, R_2



Model Diagram

Solution Comparison

Mesh	Result	Theoretical	LARSA 4D
8X16	U_1 (at any joint) in.	0.12414	0.12175
24X48	U_1 (at any joint) in.	0.12414	0.12387
8X16	U_3 (at any joint) in.	-0.12414	-0.12175
24X48	U_3 (at any joint) in.	-0.12414	-0.12387
8X16	σ_{11} (anywhere) k/in.^2	60	58.85
24X48	σ_{11} (anywhere) k/in.^2	60	59.87

References

- Roark and Young, "Roark's Formulas for Stress and Strain," 1975, pp. 448, Table 29, Item 1b

For More Information, please refer to the following documentation.

- For help on linear static analysis, see Linear Static Analysis in *LARSA 4D Reference Manual*.

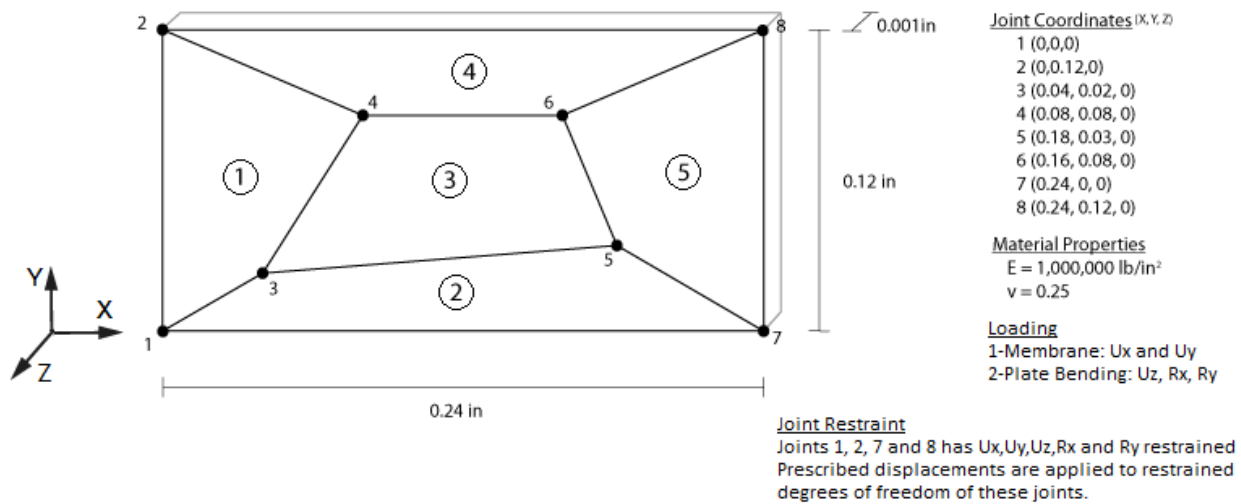
L21: Shell-Patch Test with Prescribed Displacements

In this example, a rectangular plate is modeled with irregular shaped shell elements and subjected to prescribed displacements that theoretically impose a constant stress field over the model. The membrane and plate bending stress components resulting from prescribed displacements are compared to the results from independent sources. Properties, geometry, and the loading are as described in MacNeal and Harder 1985.

Example Project: The example described here can be found in the LinearStatic folder of your LARSA 4D Samples directory (generally My Documents\LARSA Projects\Samples) in the file L21.

Problem Description

The rectangular plate is defined in the X-Y plane with 0.24 in width, 0.12 in height and 0.001 in thickness. The material used in modeling the plate has an elastic modulus of 1,000,000 lb/in² with a Poisson's ratio of 0.25. Joints and elements of the model are defined as presented in the next figure:



Loading

Because the model is flat, there is no coupling between the membrane and plate bending behaviors. Thus, separate load cases are used to test the the membrane and plate bending behaviors of the model.

In order to test the membrane behavior, prescribed displacements in X and Y directions to joints 1, 2, 7 and 8 are applied.

Prescribed Displacements to Test Membrane Behavior

Joint	X (in)	Y (in)	U _x (in)	U _y (in)
1	0	0	0	0
2	0	0.12	0.00006	0.00012
7	0.24	0	0.00024	0.00012
8	0.24	0.12	0.00030	0.00024

In order to test the membrane behavior, prescribed displacements in Z direction and prescribed rotations in X and Y directions to joints 1, 2, 7 and 8 are applied.

Prescribed Displacements to Test Bending Behavior

Joint	X (in)	Y (in)	U _z (in)	R _x (radians)	R _y (radians)
1	0	0	0	0	0
2	0	0.12	0.0000072	0.00012	-0.00006
7	0.24	0	0.0000288	0.00012	-0.00024
8	0.24	0.12	0.0000504	0.00024	-0.00030

Solution Comparison

The problem is solved using plates with the Classic element behavior, the Thin and Thick Plate combined with the Bilinear, Incompatible, and Drilling membrane behaviors, and the MITC4 element behavior.

The results are compared to the ones from independent sources. The independent membrane solution is based on Timoshenko and Goodier 1951 and the independent bending solution is based on Timoshenko and Woinowsky-Krieger 1959. The following tables summarize the results from these analysis and their comparison to the solution from independent sources.

Classic Element Behavior

Analysis Case	Stress Component	Independent	LARSA 4D
Membrane	σ_{xx} lb/in ²	1333	1336.4
Membrane	σ_{yy} lb/in ²	1333	1339
Membrane	σ_{xy} lb/in ²	400	401.8
Plate bend	M_{xx} lb-in/in	1.11E-07	1.09E-07
Plate Bend	M_{yy} lb-in/in	1.11E-07	1.01E-07
Plate Bend	M_{xy} lb-in/in	3.33-08	3.46E-08

Solutions obtained using shell elements with the Classic behavior are presented above. In this model, elemental stresses are not equal to each other, thus average values are presented. Although average values are close to the ones from independent sources, differences between element stresses are significantly high. For example, element stress σ_{xx} changes from 1156 lb/in² to 1460 lb/in² through the model.

Thin Plate Bending Behavior

Analysis Case	Stress Component	Independent	LARSA 4D - Bilinear	LARSA 4D - Drilling	LARSA 4D - Incompatible
Membrane	σ_{xx} lb/in ²	1333	1333	1333	1333
Membrane	σ_{yy} lb/in ²	1333	1333	1333	1333
Membrane	σ_{xy} lb/in ²	400	400	400	400
Plate bend	M_{xx} lb-in/in	1.11E-07	1.11E-07	1.11E-07	1.11E-07
Plate Bend	M_{yy} lb-in/in	1.11E-07	1.11E-07	1.11E-07	1.11E-07
Plate Bend	M_{xy} lb-in/in	3.33E-08	3.33E-08	3.33E-08	3.33E-08

Thick Plate Bending Behavior

Analysis Case	Stress Component	Independent	LARSA 4D - Bilinear	LARSA 4D - Drilling	LARSA 4D - Incompatible
Membrane	σ_{xx} lb/in ²	1333	1333	1333	1333
Membrane	σ_{yy} lb/in ²	1333	1333	1333	1333
Membrane	σ_{xy} lb/in ²	400	400	400	400
Plate bend	M_{xx} lb-in/in	1.11E-07	1.11E-07	1.11E-07	1.11E-07
Plate Bend	M_{yy} lb-in/in	1.11E-07	1.11E-07	1.11E-07	1.11E-07
Plate Bend	M_{xy} lb-in/in	3.33-08	3.33E-08	3.33E-08	3.33E-08

MITC4 Element Behavior

Analysis Case	Stress Component	Independent	LARSA 4D
Membrane	σ_{xx} lb/in ²	1333	1333
Membrane	σ_{yy} lb/in ²	1333	1333
Membrane	σ_{xy} lb/in ²	400	400
Plate bend	M_{xx} lb-in/in	1.11E-07	1.11E-07

Analysis Case	Stress Component	Independent	LARSA 4D
Plate Bend	M_{yy} lb-in/in	1.11E-07	1.11E-07
Plate Bend	M_{xy} lb-in/in	3.33-08	3.33E-08

Contrary to results from the Classic behavior, solutions obtained from the Thin and Thick Plate with Bilinear, Incompatible, and Drilling membrane types and from the MITC4 element behavior compare exactly to the independent solutions. In addition, stresses and moments are uniform through the entire model.

References

- MacNeal, R.H. and Harder, R.L., "A Proposed Standard Set of Problems to Test Finite Element Accuracy," *Finite Elements Analysis and Design 1 (1985)*
- Timoshenko and Goodier, "Theory of Elasticity," 1951, pp. 6.
- Timoshenko and Woinowsky-Krieger, "Theory of plates and shells," 1959, pp. 81.
- SAP 2000, CSI Software Verification Example 2-001, "Shell-Patch test With Prescribed Displacements."

For More Information, please refer to the following documentation.

- For help on linear static analysis, see Linear Static Analysis in *LARSA 4D Reference Manual*.

L22: Shell-Patch Test Using Thermal Loading

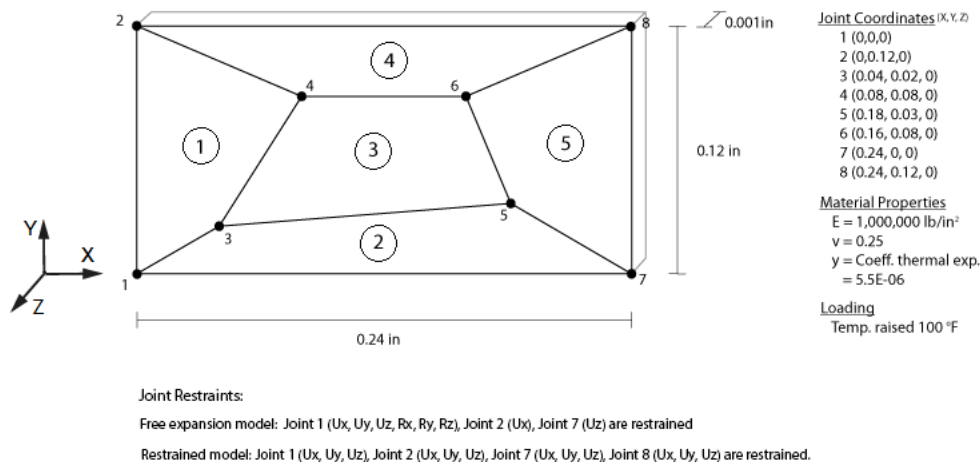
This is a patch test for plates suggested by MacNeal and Harder (1985). The model is a rectangular plate with a mesh of irregularly shaped elements. The plate is subjected to a uniform temperature gradient of +100°F constant through the thickness. The geometry and properties of the plate are equal to those described in problem L21. Joint displacements and stresses resulting from the temperature load are compared with theoretical solution reported by MacNeal and Harder.

Example Project: The example described here can be found in the Linear Elastic Static folder of your LARSA 4D Samples directory (generally My Documents\LARSA Projects\Samples) in the file L22_Restrained_Thin_Incompatible.

Problem Description

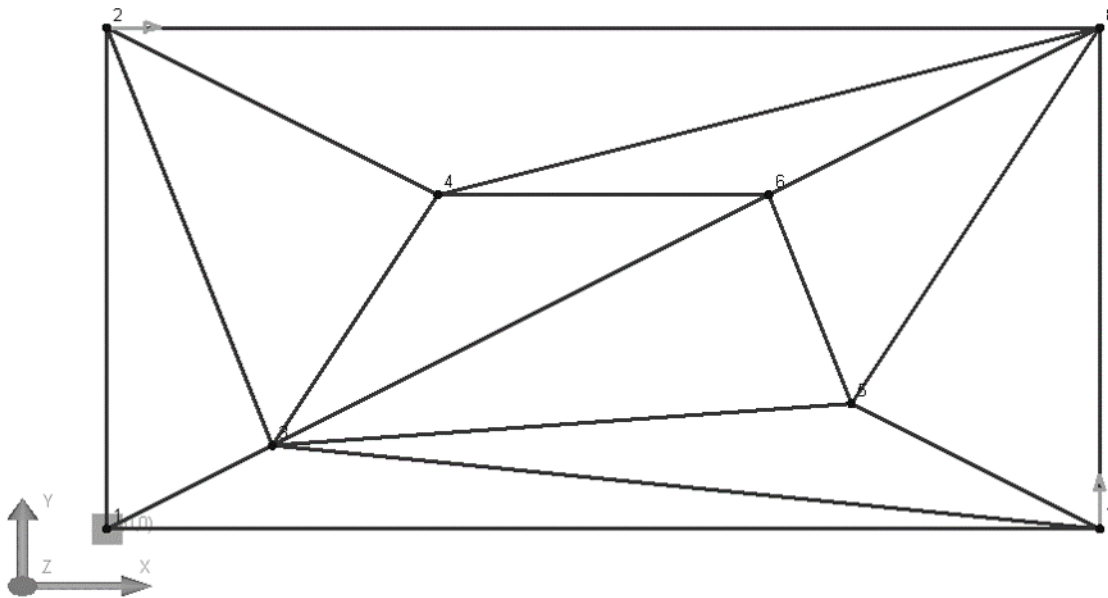
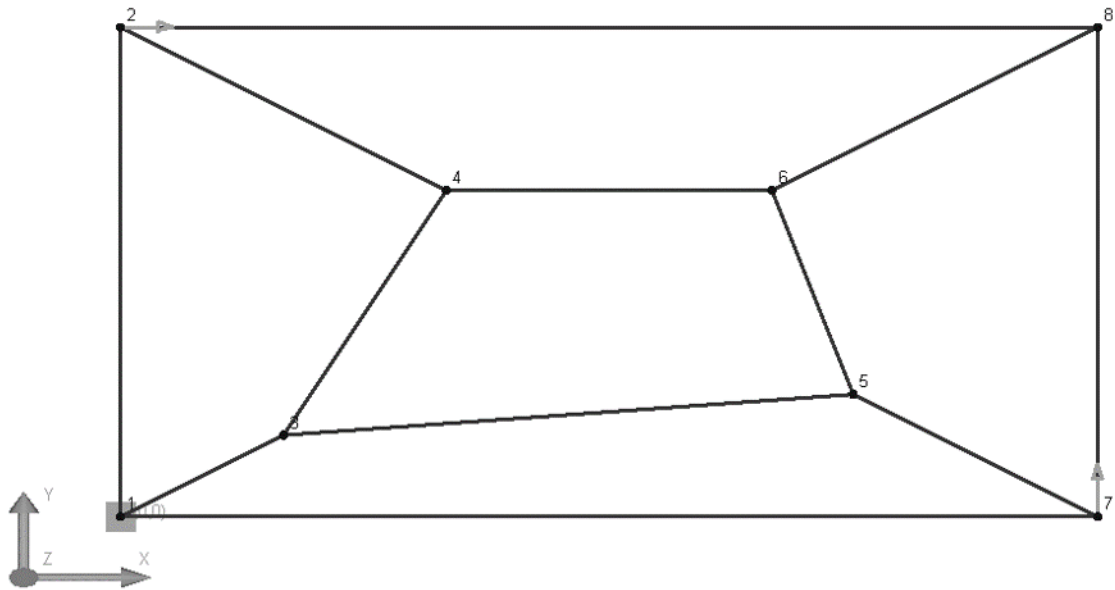
Two different models are created for this example. The models are alike, except for the joint restraints. The first model (namely free expansion) is restrained about all degrees of freedom at joint 1, thus allowing free expansion of the plate. For this model, joint 2 is restrained in U_x direction and joint 7 is restrained in U_y direction for stability conditions. Second model (namely restrained) is pinned at the four corner joints (Joints 1, 2, 7 and 8) and is not free to expand resulting in a stress increase in the elements.

The sign convention for the axes, joint and element labels, joint coordinates, material properties, loading and boundary conditions are specified in the following figure.



Model diagram

The example model is also created via triangular plates such that each quadrilateral element is divided into two triangular elements so joint IDs are not changed.



Model Meshes

Results

The problem is solved using plates with the Classic element behavior, the Thin Plate combined with the Bilinear, Incompatible, and Drilling membrane behaviors, and the MITC4 element behavior.

Percentages next to the results are percentages of deviation from the results of MacNeal and Harder.

Rectangular Plates with Thin Plate Bending Behavior

Model	Result	MacNeal and Harder	LARSA 4D <i>Bilinear</i>	LARSA 4D <i>Incompatible</i>	LARSA 4D <i>Drilling</i>
Free expansion	U_x @ joint 8 (in)	0.000132	0.000132 (0%)	0.000132 (0%)	0.000132 (0%)
Free expansion	U_y @ joint 8 (in)	0.000066	0.000066 (0%)	0.000066 (0%)	0.000066 (0%)
Free expansion	σ_{xx} @ joint 8 (lb/in ²)	0	0 (0%)	0 (0%)	0 (0%)
Free expansion	σ_{yy} @ joint 8 (lb/in ²)	0	0 (0%)	0 (0%)	0 (0%)
Restrained	U_x @ joint 8 (in)	0	0 (0%)	0 (0%)	0 (0%)
Restrained	U_y @ joint 8 (in)	0	0 (0%)	0 (0%)	0 (0%)
Restrained	σ_{xx} @ joint 8 (lb/in ²)	-733.33	-733.33 (0%)	-733.33 (0%)	-733.33 (0%)
Restrained	σ_{yy} @ joint 8 (lb/in ²)	-733.33	-733.33 (0%)	-733.33 (0%)	-733.33 (0%)

Triangular Plates with Thin Plate Bending Behavior and Bilinear Membrane Behavior

Model	Result	MacNeal and Harder	LARSA 4D
Free expansion	U_x @ joint 8 (in)	0.000132	0.000132 (0%)
Free expansion	U_y @ joint 8 (in)	0.000066	0.000066 (0%)
Free expansion	σ_{xx} @ joint 8 (lb/in ²)	0	0 (0%)
Free expansion	σ_{yy} @ joint 8 (lb/in ²)	0	0 (0%)
Restrained	U_x @ joint 8 (in)	0	0 (0%)
Restrained	U_y @ joint 8 (in)	0	0 (0%)
Restrained	σ_{xx} @ joint 8 (lb/in ²)	-733.33	-733.33 (0%)
Restrained	σ_{yy} @ joint 8 (lb/in ²)	-733.33	-733.33 (0%)

MITC4 Element Behavior

Model	Result	MacNeal and Harder	LARSA 4D
Free expansion	U_x @ joint 8 (in)	0.000132	0.000132 (0%)

Model	Result	MacNeal and Harder	LARSA 4D
Free expansion	$U_y @ \text{joint 8 (in)}$	0.000066	0.000066 (0%)
Free expansion	$\sigma_{xx} @ \text{joint 8 (lb/in}^2\text{)}$	0	0 (0%)
Free expansion	$\sigma_{yy} @ \text{joint 8 (lb/in}^2\text{)}$	0	0 (0%)
Restrained	$U_x @ \text{joint 8 (in)}$	0	0 (0%)
Restrained	$U_y @ \text{joint 8 (in)}$	0	0 (0%)
Restrained	$\sigma_{xx} @ \text{joint 8 (lb/in}^2\text{)}$	-733.33	-733.33 (0%)
Restrained	$\sigma_{yy} @ \text{joint 8 (lb/in}^2\text{)}$	-733.33	-733.33 (0%)

References

- MacNeal, R.H. and Harder, R.L., "A Proposed Standard Set of Problems to Test Finite Element Accuracy," *Finite Elements Analysis and Design 1 (1985)*, pp. 3-20, North-Holland.

For More Information, please refer to the following documentation.

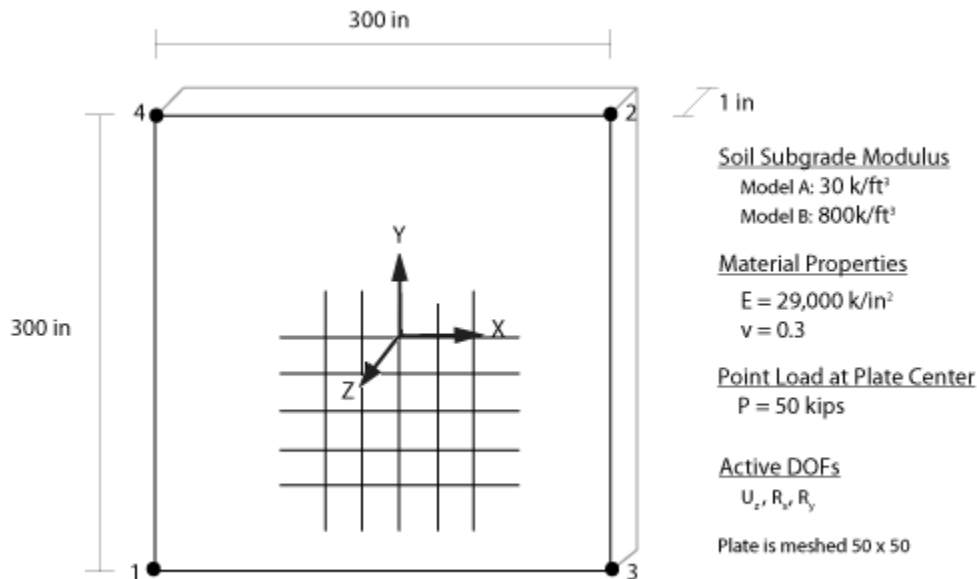
- For help on linear static analysis, see Linear Static Analysis in *LARSA 4D Reference Manual*.

L23: Shell-Plate on Elastic Foundation

An isolated 50 kip point load is acting on a one inch thick infinitely large plate that is support on a elastic foundation. Here, the infinitely large plate is modeled as 300 inches long by 300 inches wide and meshed 50 x 50 with a point load applied at the center of the plate. The plate deflection at the point load location is compared with independent hand calculated results that are computed using theory presented in Timoshenko and Woinowsky-Krieger 1959.

Problem Description

Two different models are created each using a different soil subgrade modulus. Model A uses a subgrade modulus of 30 k/ft³ while Model B uses a subgrade modulus of 800 k/ft³. Those values are chosen to represent approximate upper and lower bound sandy soil stiffnesses.



Model Diagrams

Solution Comparison

The problem is solved using plates with the MITC4 element behavior.

Model; and Modulus	Output parameter	Theoretical	LARSA 4D
A; (k = 300 k/ft ³)	U _z at center of plate in	-0.9205	-0.9122

Model; and Modulus	Output parameter	Theoretical	LARSA 4D
B ; ($k = 800 \text{ k/ft}^3$)	U_z at center of plate in	-0.1782	-0.1707

References

- Timoshenko and Woinowsky-Krieger, "Theory of Plates and Shells," 1959, pp. 275, Equation 185.

For More Information, please refer to the following documentation.

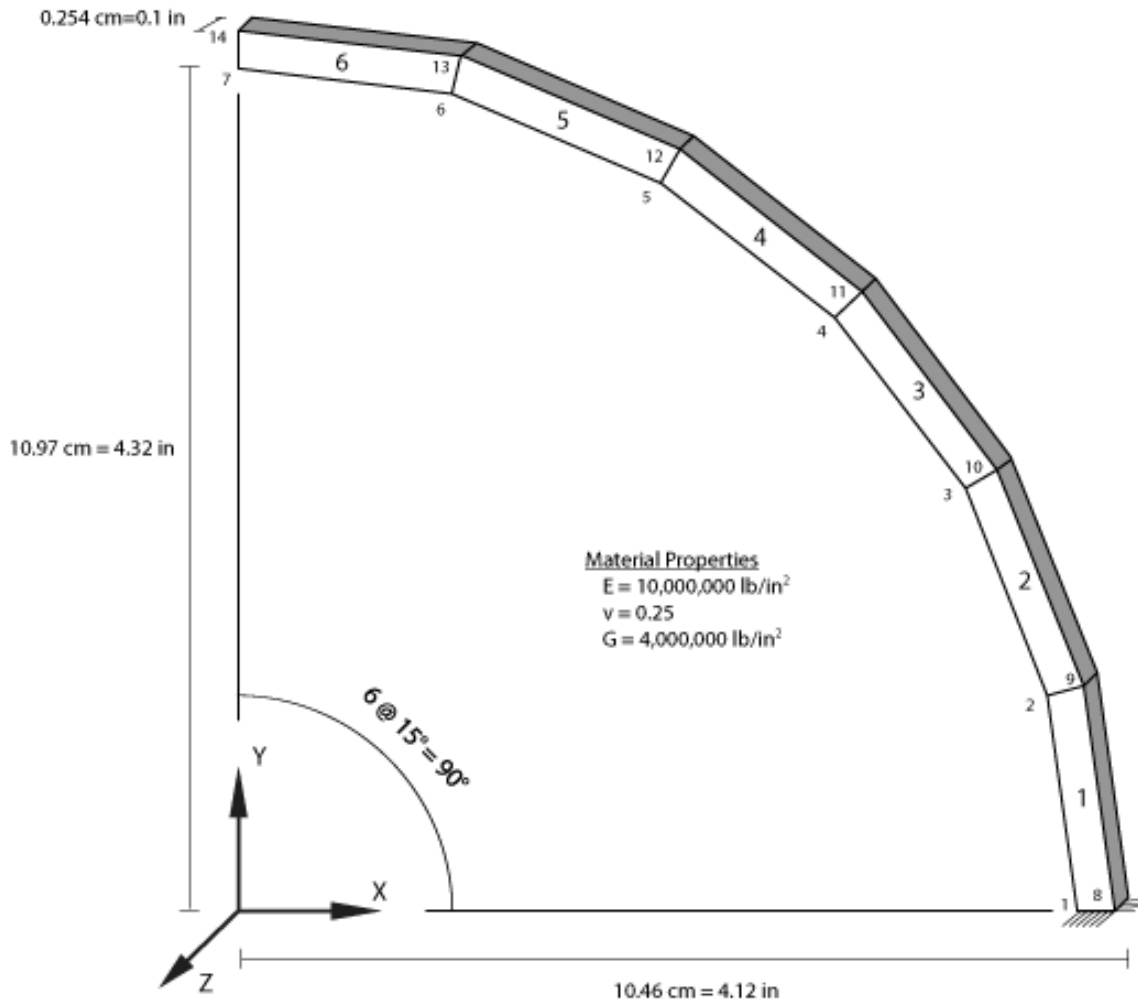
- For help on linear static analysis, see Linear Static Analysis in *LARSA 4D Reference Manual*.

L24: Shell-Curved Beam with Static Loads

In this example a curved cantilever beam, modeled with shell elements, is subjected to unit forces at the tip in the in-plane and out-plane directions, that is, the Y and Z directions, respectively. The in-plane and out-of-plane loads are applied in the different load cases.

Problem Description

The geometry, properties and loading are as suggested in MacNeal and Harder 1985. The cantilever beam is bent into a 90 degree arc. The inner radius is 4.12 inches and the outer is 4.32 inches. It is thus 0.2 inches wide and approximately 6.63 inches long at the centerline. In the Y direction the beam is 0.1 inches thick. For modeling in LARSA 4D, the curved beam is meshed into six elements, each corresponding a 15 degree arch.



Model Diagrams

Loading

Load Case	Load
IN	$F_y = +0.5 \text{ lb}$ at joints 7 and 14
OUT	$F_z = +0.5 \text{ lb}$ at joint 7 and 14

Solution Comparison

The problem is solved using plates with the Thin and Thick Plate combined with the Bilinear, Incompatible, and Drilling membrane behaviors, and the MITC4 element behavior.

Thin Plate Bending Behavior

Mesh Size	Load Case	Result	Theoretical	LARSA 4D Drilling	LARSA 4D Bilinear	LARSA 4D Incompatible	SAP2000
6x1	IN	U_y avg.of jnts 7 and 14	0.0886	0.0751	0.0064	0.0776	0.0773
90X1	IN	U_y avg.of jnts 91 and 182	0.0886	0.0841	0.0789	0.0885	0.0845
90x3	IN	U_y avg.of jnts 91 and 182	0.0886	0.0882	0.0833	0.0884	0.0884
6x1	OUT	U_z avg.of jnts 7 and 14	0.5004	0.4535	0.4535	0.4535	0.4535
90x1	OUT	U_z avg.of jnts 91 and 182	0.5004	0.4512	0.4512	0.4512	0.4514
90x3	OUT	U_z avg.of jnts 91 and 182	0.5004	0.4508	0.4508	0.4508	0.4510

For the out of plane load case, the deviation from the theoretical result is due to the shell theory used by LARSA 4D and the beam theory used for the theoretical solution.

Thick Plate Bending Behavior

Mesh Size	Load Case	Result	Theoretical	LARSA 4D Drilling	LARSA 4D Bilinear	LARSA 4D Incompatible	SAP2000
6x1	IN	U_y avg.of jnts 7 and 14	0.0886	0.0751	0.0064	0.0776	0.0773
90X1	IN	U_y avg.of jnts 91 and 182	0.0886	0.0841	0.0789	0.0885	0.0845
90x3	IN	U_y avg.of jnts 91 and 182	0.0886	0.0882	0.0833	0.0884	0.0884
6x1	OUT	U_z avg.of jnts 7 and 14	0.5004	1.3140	1.3140	1.3140	0.4298

Mesh Size	Load Case	Result	Theoretical	LARSA 4D Drilling	LARSA 4D Bilinear	LARSA 4D Incompatible	SAP2000
90x1	OUT	U_z avg.of jnts 91 and 182	0.5004	0.4898	0.4898	0.4898	0.4566
90x3	OUT	U_z avg.of jnts 91 and 182	0.5004	0.4964	0.4964	0.4964	0.4558

MITC4 Element Behavior

Mesh Size	Load Case	Result	Theoretical	LARSA 4D
6x1	IN	U_y avg.of jnts 7 and 14	0.0886	0.00641
90X1	IN	U_y avg.of jnts 91 and 182	0.0886	0.0790
90x3	IN	U_y avg.of jnts 91 and 182	0.0886	0.0834
6x1	OUT	U_z avg.of jnts 7 and 14	0.5004	0.4398
90x1	OUT	U_z avg.of jnts 91 and 182	0.5004	0.6748
90x3	OUT	U_z avg.of jnts 91 and 182	0.5004	0.4836

Results of LARSA 4D are acceptable comparing to theoretical results, if the mesh size is sufficient.

Increased mesh size reduces distortion from the curved geometry and improves the results.

References

- Cook and Young, "Advanced Mechanics of Materials," 1985, pp. 244.
- SAP 2000, CSI Software Verification Example 2-003, "Shell-Curved Beam with Static Loads."

For More Information, please refer to the following documentation.

- For help on linear static analysis, see Linear Static Analysis in *LARSA 4D Reference Manual*.

L25: Shell-Rectangular Plate with Static Loads

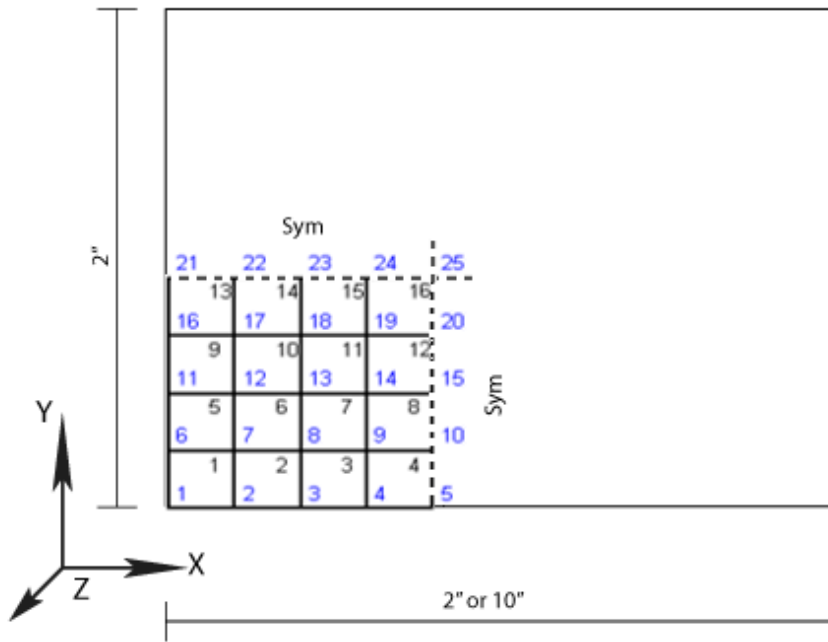
A rectangular plane, modeled with shell elements, is subjected to an out-of-plane point concentrated load, and an out-of-plane uniform load, which is the Z direction. The point concentrated and uniform loads are applied in different states.

Problem Description

The geometry, properties and loading for this problem are based on the publication by MacNeal and Harder 1985. The plate is 2 inches wide and modeled with both a 2 inch and 10 inch length. Modeled is a quarter plate, considering both a 4X4 and 16X16 mesh.

Active in the model are the degrees of freedom for the Z translational, along with the X and Y rotational displacements. In the 4X4 mesh, model symmetry situations are imposed by restraining the X rotational freedom at joints 22, 23, and 24; restraining the Y rotational freedom at joints 10, 15, and 20; and restraining both the X and Y rotational freedom at joint 25. The symmetry restraints used in the 16X16 mesh are similar the restraints used above in the 4X4 mesh. Since only a quarter of the plate is modeled, only a quarter of the specified concentrated load is applied to the center of the plate at joint 25.

Geometry, Properties, and Loading



Material Properties

$E = 17,472,00 \text{ ln/in}^2$
 $\nu = 0.3$
 $G = 6,720,00 \text{ lb/in}^2$

Section Properties

Thickness = 0.0001 in

Loading (in separate cases)

Uniform Load = 0.001 lb/in^2
 Center Point Load = 0.0001 lb

1 = Joint Number
7 = Area Object Number

Model Diagram

Solution Comparison

2"x2" Think Plate (U_z [in] center of plate)

Mesh	Edge Support	Load	Theoretical	LARSA 4D	SAP2000
4X4	Simple	Uniform	-4.06	-4.16	-4.06
16X16	Simple	Uniform	-4.06	-4.07	-4.06
4X4	Fixed	Uniform	-1.26	-1.32	-1.32
16X16	Fixed	Uniform	-1.26	-1.27	-1.27
4X4	Simple	Point	-11.60	-11.94	-11.94
16X16	Simple	Point	-11.60	-11.63	-11.63
4X4	Fixed	Point	-5.60	-5.90	-5.90
16X16	Fixed	Point	-5.60	-5.64	-5.64

2"x2" Thick Plate (U_z [in] center of plate)

Mesh	Edge Support	Load	Theoretical	LARSA 4D	SAP2000
4X4	Simple	Uniform	-4.06	-4.33	-4.03
16X16	Simple	Uniform	-4.06	-4.10	-4.06
4X4	Fixed	Uniform	-1.26	-1.34	-1.25
16X16	Fixed	Uniform	-1.26	-1.27	-1.27
4X4	Simple	Point	-11.60	-12.42	-11.61
16X16	Simple	Point	-11.60	-11.71	-11.61
4X4	Fixed	Point	-5.60	-6.08	-5.38
16X16	Fixed	Point	-5.60	-5.65	-5.61

2"x10" Thin Plate (U_z [in] center of plate)

Mesh	Edge Support	Load	Theoretical	LARSA 4D	SAP2000
4X4	Simple	Uniform	-12.97	-12.95	-12.86
16X16	Simple	Uniform	-12.97	-12.97	-12.96
4X4	Fixed	Uniform	-2.60	-2.60	-2.60
16X16	Fixed	Uniform	-2.60	-2.60	-2.60
4X4	Simple	Point	-16.95	-18.29	-18.12
16X16	Simple	Point	-16.95	-17.15	-17.15
4X4	Fixed	Point	-7.25	-7.79	-7.79
16X16	Fixed	Point	-7.25	-7.41	-7.41

2"x10" Thick Plate (U_z [in] center of plate)

Mesh	Edge Support	Load	Theoretical	LARSA 4D	SAP2000
4X4	Simple	Uniform	-12.97	-12.87	-12.87
16X16	Simple	Uniform	-12.97	-12.99	-12.97
4X4	Fixed	Uniform	-2.60	-2.60	-2.59
16X16	Fixed	Uniform	-2.60	-2.60	-2.60
4X4	Simple	Point	-16.95	-20.83	-16.27
16X16	Simple	Point	-16.95	-17.53	-16.92
4X4	Fixed	Point	-7.25	-8.49	-5.86

Mesh	Edge Support	Load	Theoretical	LARSA 4D	SAP2000
16X16	Fixed	Point	-7.25	-7.52	-7.11

2"x2" MITC4 Plate (U_z [in] center of plate)

Mesh	Edge Support	Load	Theoretical	LARSA 4D
4X4	Simple	Uniform	-4.06	-4.04
16X16	Simple	Uniform	-4.06	-4.05
4X4	Fixed	Uniform	-1.26	-1.25
16X16	Fixed	Uniform	-1.26	-1.26
4X4	Simple	Point	-11.60	-11.52
16X16	Simple	Point	-11.60	-11.58
4X4	Fixed	Point	-5.60	-5.40
16X16	Fixed	Point	-5.60	-5.60

2"x10" MITC4 Plate (U_z [in] center of plate)

Mesh	Edge Support	Load	Theoretical	LARSA 4D
4X4	Simple	Uniform	-12.97	-12.66
16X16	Simple	Uniform	-12.97	-12.93
4X4	Fixed	Uniform	-2.60	-2.48
16X16	Fixed	Uniform	-2.60	-2.59
4X4	Simple	Point	-16.95	-15.71
16X16	Simple	Point	-16.95	-16.82
4X4	Fixed	Point	-7.25	-5.97
16X16	Fixed	Point	-7.25	-7.12

References

- MacNeal, R.H., Harder, R.L.; "A Proposed Standard Set of Problems to Test Finite Element Accuracy", *Finite Elements in Analysis and Design 1 (1985) 3-20, North-Holand.*
- SAP 2000, CSI Software Verification Example 2-005, "Shell-Rectangular Plate with Static Loads"

For More Information, please refer to the following documentation.

- For help on linear static analysis, see Linear Static Analysis in *LARSA 4D Reference Manual*.

L26: Shell-Scordelis-Lo Roof with Static Loads

A single span cylindrical barrel vault roof is analyzed for gravity loads. First, the vertical deflection at the center of the free edge, displacement and bending moment results along the support and along the central section are computed and compared with published results from MacNeal and Harder 1985. The geometry, properties and loading are also based on this publication. Then, twisting moments at support section, transverse and longitudinal moments in central section are computed and compared with published results from Zienkiewicz 1977.

Example Project: The example described here can be found in the LinearStatic folder of your LARSA 4D Samples directory (generally My Documents\LARSA Projects\Samples) in the file L26.

Problem Description

The 3 inch thick roof spans longitudinally 50 feet between supports and is simply supported (U_x and U_y restrained) at its curved ends and is free along the straight edges. The roof has a 25 foot radius and a central angle of 40° . Only a quarter of the roof is modeled to take advantage of symmetry.

A 6 x 6 mesh is used for the quarter roof. In order to impose symmetry conditions, U_z and R_x degrees of freedom of joints 44 through 49; U_x and R_z degrees of freedom of joints 1, 8, 15, 22, 29 and 36; U_x , U_z , R_x and R_z degrees of freedom of joint 43 are restrained.

Model Diagrams

Loading

The loading for this problem is a 90 psf gravity load and is, in other words, a uniform load on the surface area in the -Y direction of 90 psf. Two different load cases are used in order to test two different types of loadings. First the gravity load is applied as self weight then it is applied as a uniform load. In order for the self weight and gravity loads to be 90 psf, the unit weight of the concrete is set to 360 lb/ft^3 .

Load Case	Load Type
SELF	Self Weight
UNIF	Uniform Load

Solution Comparison

Axial Deformation At Support

Here, axial displacements at support joints (joints 1, 2, 3, 4, 5, 6, 7) are computed and results are compared to solutions from the independent source. The model is analyzed using classical bending and classical membrane types, the thick

bending type and the thin bending type. For thick and thin bending types, bilinear, drilling and incompatible membrane types are used.

The following table presents the results from LARSA 4D and from MacNeal and Harder 1985 that are used as an independent source for comparison. Both load cases give exactly the same results as expected, thus only one table is provided for both of them.

Axial Deformations at Support

	U_{z1} (ft)	U_{z2} (ft)	U_{z3} (ft)	U_{z4} (ft)	U_{z5} (ft)	U_{z6} (ft)	U_{z7} (ft)
Independent	4.00E-04	1.00E-03	2.10E-03	3.00E-03	2.10E-03	-2.50E-03	-1.25E-02
Thick - Bilinear	4.70E-05	5.19E-04	1.66E-03	2.67E-03	2.19E-03	-1.58E-03	-1.10E-02
Thick - Drilling	6.00E-05	5.65E-04	1.79E-03	2.85E-03	2.34E-03	-1.69E-03	-1.18E-02
Thick - Incompatible	5.11E-05	5.58E-04	1.78E-03	2.86E-03	2.35E-03	-1.69E-03	-1.18E-02
Thin - Bilinear	4.37E-05	5.17E-04	1.66E-03	2.67E-03	2.20E-03	-1.58E-03	-1.10E-02
Thin- Drilling	5.08E-05	5.58E-04	1.79E-03	2.86E-03	2.36E-03	-1.69E-03	-1.18E-02
Thin - Incompatible	5.52E-05	5.61E-04	1.79E-03	2.86E-03	2.35E-03	-1.69E-03	-1.18E-02
Classical - Classical	3.11E-05	5.43E-04	1.78E-03	2.88E-03	2.38E-03	-1.68E-03	-1.18E-02

The following table presents the deviation of LARSA 4D results from the independent source. The percent differences are computed using the maximum independent value, 0.0125.

Percent Differences Between LARSA 4D Results and the Independent Source: Axial Deformations at Support

	U_{z1}	U_{z2}	U_{z3}	U_{z4}	U_{z5}	U_{z6}	U_{z7}
Thick - Bilinear	-2.8%	-3.8%	-3.5%	-2.7%	0.7%	7.4%	12.2%
Thick - Drilling	-2.7%	-3.5%	-2.5%	-1.2%	1.9%	6.4%	5.9%
Thick - Incompatible	-2.8%	-3.5%	-2.5%	-1.1%	2.0%	6.5%	5.7%
Thin - Bilinear	-2.9%	-3.9%	-3.5%	-2.7%	0.8%	7.4%	12.2%

	U _{z1}	U _{z2}	U _{z3}	U _{z4}	U _{z5}	U _{z6}	U _{z7}
Thin-Drilling	-2.8%	-3.5%	-2.5%	-1.1%	2.0%	6.5%	5.7%
Thin - Incompatible	-2.8%	-3.5%	-2.5%	-1.1%	2.0%	6.5%	5.8%
Classical - Classical	-3.0%	-3.7%	-2.5%	-1.0%	2.2%	6.6%	5.3%

All element types give results in close proximity to the independent solutions. Note that bilinear thin and thick shell elements give significantly worse results, compared to other element types. This can be considered normal as the bilinear membrane type is the simplest membrane type in LARSA 4D.

Vertical Displacement at Central Section

Here, vertical displacements at joints in the central section of the model (joints 43, 44, 45, 46, 47, 48, 49) are computed and results are compared to the solutions from the independent source. The model is analyzed using classical bending and membrane types, the thick bending type and the thin bending type. For thick and thin bending types, bilinear, drilling and incompatible modes membrane types are used.

The following table presents the results from LARSA 4D and results from MacNeal and Harder 1985 that are used as an independent source for comparison. Both load cases give exactly the same results, thus only one table is provided for both of them.

Vertical Displacement at Central Section							
	U _{y43} (ft)	U _{y44} (ft)	U _{y45} (ft)	U _{y46} (ft)	U _{y47} (ft)	U _{y48} (ft)	U _{y49} (ft)
Independent	4.80E-02	2.80E-02	-1.50E-02	-8.00E-02	-1.57E-01	-2.40E-01	-3.15E-01
Thick - Bilinear	4.28E-02	2.85E-02	-1.24E-02	-7.33E-02	-1.45E-01	-2.18E-01	-2.86E-01
Thick - Drilling	4.54E-02	3.00E-02	-1.35E-02	-7.81E-02	-1.54E-01	-2.31E-01	-3.02E-01
Thick - Incompatible	4.56E-02	3.03E-02	-1.34E-02	-7.83E-02	-1.54E-01	-2.31E-01	-3.02E-01
Thin - Bilinear	4.29E-02	2.86E-02	-1.24E-02	-7.34E-02	-1.45E-01	-2.18E-01	-2.86E-01
Thin-Drilling	4.57E-02	3.03E-02	-1.34E-02	-7.83E-02	-1.54E-01	-2.31E-01	-3.02E-01
Thin - Incompatible	4.55E-02	3.02E-02	-1.34E-02	-7.82E-02	-1.54E-01	-2.31E-01	-3.03E-01
Classical - Classical	4.62E-02	3.07E-02	-1.32E-02	-7.87E-02	-1.55E-01	-2.33E-01	-3.05E-01

The following table presents the deviation of LARSA 4D results from the independent source. The percent differences are computed using the maximum independent value, 0.315.

Percent Differences Between LARSA 4D Results and the Independent Source: Vertical Displacement at Central Section

	U _y 43	U _y 44	U _y 45	U _y 46	U _y 47	U _y 48	U _y 49
Thick - Bilinear	-1.6%	0.1%	0.8%	2.1%	3.8%	6.9%	9.1%
Thick - Drilling	-0.8%	0.6%	0.5%	0.6%	1.0%	3.0%	4.1%
Thick - Incompatible	-0.7%	0.7%	0.5%	0.5%	0.9%	2.8%	4.0%
Thin - Bilinear	-1.6%	0.2%	0.8%	2.1%	3.7%	6.9%	9.2%
Thin- Drilling	-0.7%	0.7%	0.5%	0.5%	0.8%	2.8%	4.0%
Thin - Incompatible	-0.8%	0.7%	0.5%	0.6%	0.9%	2.8%	3.9%
Classical - Classical	-0.6%	0.9%	0.6%	0.4%	0.5%	2.2%	3.3%

All element types give results in close proximity to the independent solutions. Note that bilinear thin and thick shell elements give significantly worse results compared to other element types. This can be considered normal as the bilinear membrane type is the simplest membrane type in LARSA 4D.

Twisting Moments at Support

Here, twisting moments at joints at support section of the model (joints 1, 2, 3, 4, 5, 6, 7) are computed and compared to the solutions from the independent source. The model is analyzed using classical bending and membrane types, the thick bending type and the thin bending type. For thick and thin bending types, bilinear, drilling and incompatible modes membrane types are used.

The following table presents the results from LARSA 4D and results from Zienkiewicz 1977 that are used as an independent source for comparison. Note that some results had to be interpolated from published graphs. Both load cases give exactly the same results, thus only one table is provided for both of them.

Twisting Moments at Support

	M _{xy} 1 (lb-ft/ft)	M _{xy} 2 (lb-ft/ft)	M _{xy} 3 (lb-ft/ft)	M _{xy} 4 (lb-ft/ft)	M _{xy} 5 (lb-ft/ft)	M _{xy} 6 (lb-ft/ft)	M _{xy} 7 (lb-ft/ft)
Independent	0	-370	-700	-990	-1210	-1310	-1280
Thick - Bilinear	-83	-333	-648	-915	-1247	-1172	-1159

	M_{xy1} (lb-ft/ft)	M_{xy2} (lb-ft/ft)	M_{xy3} (lb-ft/ft)	M_{xy4} (lb-ft/ft)	M_{xy5} (lb-ft/ft)	M_{xy6} (lb-ft/ft)	M_{xy7} (lb-ft/ft)
Thick - Drilling	-90	-358	-695	-980	-1172	-1236	-1223
Thick - Incompatible	-90	-356	-691	-973	-1158	-1216	-1201
Thin - Bilinear	-84	-333	-647	-913	-1091	-1153	-1143
Thin - Drilling	-90	-357	-693	-977	-1167	-1227	-1210
Thin - Incompatible	-89	-356	-692	-976	-1167	-1231	-1219
Classic - Classic	-2	-357	-695	-986	-1181	-1229	-1172

The following table presents the deviation of LARSA 4D results from the independent source. The percent differences are computed using the maximum independent value, 1310.

Percent Differences Between LARSA 4D Results and the Independent Source: Twisting Moments at Support

	M_{xy1}	M_{xy2}	M_{xy3}	M_{xy4}	M_{xy5}	M_{xy6}	M_{xy7}
Thick - Bilinear	6.3%	-2.8%	-4.0%	-5.7%	2.8%	-10.5%	-9.2%
Thick - Drilling	6.9%	-0.9%	-0.4%	-0.8%	-2.9%	-5.6%	-4.4%
Thick - Incompatible	6.9%	-1.1%	-0.7%	-1.3%	-4.0%	-7.2%	-6.0%
Thin - Bilinear	6.4%	-2.8%	-4.0%	-5.9%	-9.1%	-12.0%	-10.5%
Thin - Drilling	6.9%	-1.0%	-0.5%	-1.0%	-3.3%	-6.4%	-5.3%
Thin - Incompatible	6.8%	-1.0%	-0.6%	-1.0%	-3.3%	-6.0%	-4.7%
Classic - Classic	0.1%	-1.0%	-0.4%	-0.3%	-2.2%	-6.2%	-8.2%

All element types give results in close proximity to the independent solutions, considering results from the independent source have to be interpolated for some of the joints. Note that bilinear thin and thick shell elements give significantly worse results compared to other element types. This can be considered normal as the bilinear membrane type is the simplest membrane type in LARSA 4D.

Transverse Moments at Central Section

Here, transverse moments at joints at the central section of the model (joints 43, 44, 45, 46, 47, 48, 49) are computed and compared to the solutions from the independent source. The model is analyzed using classical bending and membrane types, the thick bending type and the thin bending type. For thick and thin bending types, bilinear, drilling and incompatible modes membrane types are used.

The following table presents the results from LARSA 4D and results from Zienkiewicz 1977 that are used as an independent source for comparison. Note that some results had to be interpolated from published graphs. Both load cases give exactly the same results, thus only one table is provided for both of them.

Transverse Moments at Central Section

	M_{xx43} (lb-ft/ ft)	M_{xx44} (lb-ft/ ft)	M_{xx45} (lb-ft/ ft)	M_{xx46} (lb-ft/ ft)	M_{xx47} (lb-ft/ ft)	M_{xx48} (lb-ft/ ft)	M_{xx49} (lb-ft/ ft)
Independent	-2080	-1980	-1580	-1000	-400	70	-40
Thick - Bilinear	-1916	-1803	-1473	-967	-416	-47	58
Thick - Drilling	-2045	-1918	-1549	-999	-416	-38	66
Thick - Incompatible	-2093	-1968	-1593	-1012	-367	83	51
Thin - Bilinear	-1955	-1845	-1512	-980	-372	68	51
Thin - Drilling	-2094	-1968	-1593	-1012	-367	83	51
Thin - Incompatible	-2048	-1921	-1553	-1002	-418	-39	66
Classic - Classic	-2115	-1989	-1614	-1029	-374	88	148

The following table presents the deviation of LARSA 4D results from the independent source. The percent differences are computed using the maximum independent value, 2080.

Percent Differences Between LARSA 4D Results and the Independent Source: Transverse Moments at Central Section

	M_{xx43}	M_{xx44}	M_{xx45}	M_{xx46}	M_{xx47}	M_{xx48}	M_{xx49}
Thick - Bilinear	7.9%	8.5%	5.2%	1.6%	-0.8%	-5.6%	4.7%
Thick - Drilling	1.7%	3.0%	1.5%	0.1%	-0.8%	-5.2%	5.1%

	M_{xx}43	M_{xx}44	M_{xx}45	M_{xx}46	M_{xx}47	M_{xx}48	M_{xx}49
Thick - Incompatible	-0.6%	0.6%	-0.6%	-0.6%	1.6%	0.6%	4.4%
Thin - Bilinear	6.0%	6.5%	3.3%	0.9%	1.4%	-0.1%	4.4%
Thin - Drilling	-0.7%	0.6%	-0.6%	-0.6%	1.6%	0.6%	4.4%
Thin - Incompatible	1.5%	2.8%	1.3%	-0.1%	-0.9%	-5.2%	5.1%
Classic - Classic	-1.7%	-0.5%	-1.6%	-1.4%	1.3%	0.9%	9.0%

All element types give results in close proximity to the independent solutions, considering results from the independent source have to be interpolated for some of the joints. Note that bilinear thin and thick shell elements give significantly worse results compared to other element types. This can be considered normal as the bilinear membrane type is the simplest membrane type in LARSA 4D.

Longitudinal Moments at Central Section

Here, longitudinal moments at joints at the central section of the model (joints 43, 44, 45, 46, 47, 48, 49) are computed and compared to the solutions from the independent source. The model is analyzed using classical bending and membrane types, the thick bending type and the thin bending type. For thick and thin bending types, bilinear, drilling and incompatible modes membrane types are used.

The following table presents the results from LARSA 4D and results from Zienkiewicz 1977 that are used as an independent source for comparison. Note that some results had to be interpolated from published graphs. Both load cases give exactly the same results, thus only one table is provided for both of them.

Longitudinal Moments at Central Section

	M_{yy}43 (lb-ft/ ft)	M_{yy}44 (lb-ft/ ft)	M_{yy}45 (lb-ft/ ft)	M_{yy}46 (lb-ft/ ft)	M_{yy}47 (lb-ft/ ft)	M_{yy}48 (lb-ft/ ft)	M_{yy}49 (lb-ft/ ft)
Independent	-100	-90	10	140	300	490	700
Thick - Bilinear	-92	-59	34	166	317	470	624
Thick - Drilling	-97	-61	36	176	334	494	655
Thick - Incompatible	-98	-62	37	178	337	497	659
Thin - Bilinear	-93	-59	34	168	319	473	628

	M_{yy43} (lb-ft/ ft)	M_{yy44} (lb-ft/ ft)	M_{yy45} (lb-ft/ ft)	M_{yy46} (lb-ft/ ft)	M_{yy47} (lb-ft/ ft)	M_{yy48} (lb-ft/ ft)	M_{yy49} (lb-ft/ ft)
Thin - Drilling	-97	-61	38	178	337	497	658
Thin - Incompatible	-97	-61	36	176	335	495	656
Classic - Classic	-121	-83	21	171	344	518	658

The following table presents the deviation of LARSA 4D results from the independent source. The percent differences are computed using the maximum independent value, 700.

**Percent Differences Between LARSA 4D Results and the
Independent Source: Longitudinal Moments at Central Section**

	M_{yy43}	M_{yy44}	M_{yy45}	M_{yy46}	M_{yy47}	M_{yy48}	M_{yy49}
Thick - Bilinear	1.2%	4.5%	3.4%	3.7%	2.5%	-2.8%	-10.9%
Thick - Drilling	0.5%	4.1%	3.8%	5.1%	4.8%	0.6%	-6.4%
Thick - Incompatible	0.3%	4.0%	3.8%	5.4%	5.3%	1.0%	-5.8%
Thin - Bilinear	1.0%	4.4%	3.4%	4.0%	2.8%	-2.5%	-10.3%
Thin - Drilling	0.4%	4.1%	3.9%	5.5%	5.3%	1.0%	-5.9%
Thin - Incompatible	0.5%	4.1%	3.8%	5.2%	4.9%	0.7%	-6.3%
Classic - Classic	-2.9%	1.0%	1.5%	4.5%	6.3%	4.0%	-6.0%

All element types give results in close proximity to the independent solutions, considering results from the independent source have to be interpolated for some of the joints. Note that bilinear thin and thick shell elements give significantly worse results compared to other element types. This can be considered normal as the bilinear membrane type is the simplest membrane type in LARSA 4D.

Sources:

- MacNeal, R.H. and Harder, R.L., "A Proposed Standard Set of Problems to Test Finite Element Accuracy," *Finite Elements Analysis and Design 1* (1985).
- SAP 2000, CSI Software Verification Example 2-006, "Shell-Scordelis-Lo Roof with Static Loads."
- Zienkiewicz, "The Finite Element Method" 1977, pp. 350, Figure 13.11c.

For More Information, please refer to the following documentation.

- For help on linear static analysis, see Linear Static Analysis in *LARSA 4D Reference Manual*.

L27: Thermal Stresses in a Plate

A square plate with clamped edges is subjected to a temperature gradient through its thickness. The variation of temperature through the thickness of the plate follows a linear law having T_i as the inner surface temperature and T_o as the outer surface temperature. Bending moment per unit length of the clamped edge to prevent the plate from bending and the corresponding maximum bending stress σ are inspected.

Example Project: The example described here can be found in the Linear Elastic Static folder of your LARSA 4D Samples directory (generally My Documents\LARSA Projects\Samples) in the file L27_Thin_Drilling.

Problem Description

The plate geometry and temperature loading are given in the first following figure. Joint locations and sign convention for the axes are given in the latter figure.

Model Diagram

Finite Element Model

Material properties

$$E = 30 \times 10^6 \text{ psi}$$

$$\alpha = 7 \times 10^{-6} \text{ in/in-}^\circ\text{F}$$

$$\nu = 0.3$$

Solution Comparison

The geometry is modeled by using quadrilateral (A) and triangular (B) shaped plate elements.

The problem is solved using plates with the Classic element behavior, the Thin and Thick Plate bending behavior combined with the Drilling membrane behavior, and the MITC4 element behavior.

Quadrilateral Elements

Result	Theoretical	LARSA 4D <i>Classic</i>	LARSA 4D <i>MITC4</i>	LARSA 4D <i>Thin Plate</i>	LARSA 4D <i>Thick Plate</i>	ANSYS
M (in-lb/in)	-625	-625	-625	-625	-625	-625
σ_{\max} (psi)	-15,000	-15,000	-15,000	-15,000	-15,000	-15,000

Triangular Elements

Result	Theoretical	LARSA 4D <i>Thin Plate</i>	LARSA 4D <i>Thick Plate</i>	ANSYS
M (in-lb/in)	-625	-625	-625	-625
σ_{\max} (psi)	-15,000	-15,000	-15,000	-15,000

References

- ANSYS, Verification Problem No.23, "Thermal Stresses in a Plate."
- Timoshenko, "Strength of Materials" 1956, pp. 91, Equation 87, (ref.4).

For More Information, please refer to the following documentation.

- For help on linear static analysis, see Linear Static Analysis in *LARSA 4D Reference Manual*.

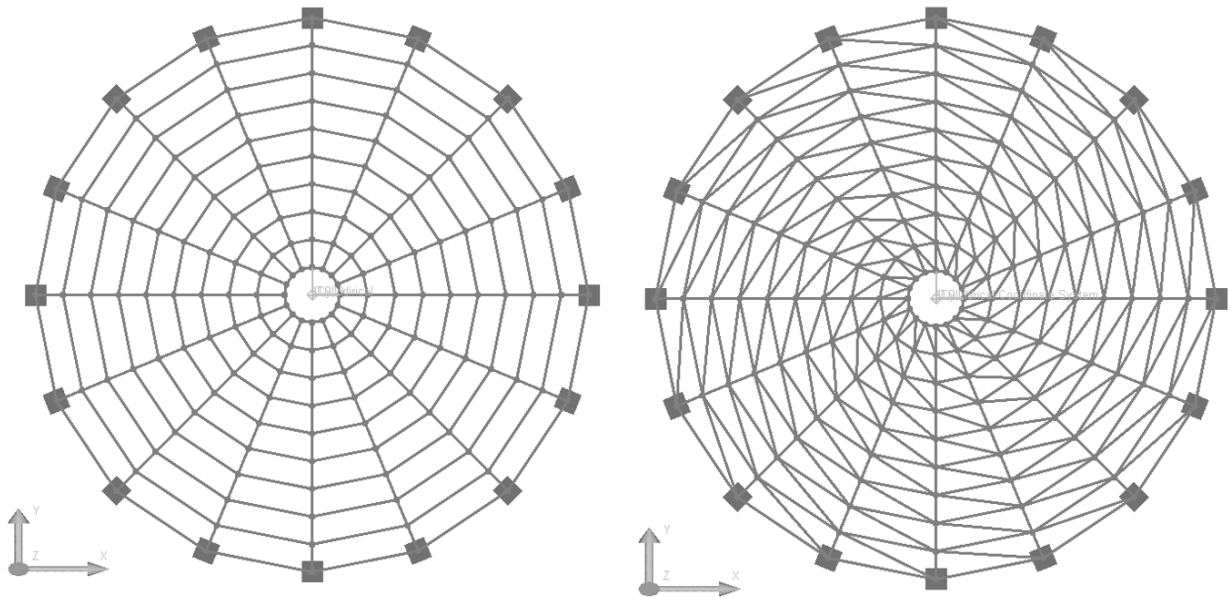
L28: Shell-Temperature Gradient Through Shell Thickness

A flat annular plate is subjected to a linear temperature gradient through its thickness.

Example Project: The example described here can be found in the Linear Elastic Static folder of your LARSA 4D Samples directory (generally My Documents\LARSA Projects\Samples) in the file L28_Thin_Drilling.

Problem Description

The plate has an inner radius of 3 inches and an outer radius of 30 inches. Its thickness is 1 inch. The mesh of this model consists of 144 quad-shaped shell elements, which are distributed in a structured manner in which 9 radial and 16 angular sections divide the shell elements (Model A). The same model is repeated by using triangular shell elements also (Model B). The resulting mesh models are given in following the figure.



Mesh with Quad Shells (A) (left), Mesh with Triangular Shells (B) (right)

The local axes of all shell elements are oriented in such a way that the local x-axis is radial and the local y-axis is tangential. The local axes are defined in this manner so that the desired results are constant along the perimeters. The local axis that points to the radial direction is named as 1 and the tangential local axis is named as 2 in the results.

Loading and boundary conditions

The applied temperature gradient is 100 °F per inch with linear variation through plate thickness. The bottom is warmer than the top of the plate. Linear static analysis is performed with only this load case.

The joints at the outer edge are clamped in all degrees of freedom.

Material properties

$$E = 29,000 \text{ ksi}$$

$$\alpha = 6.5 \times 10^{-6} \text{ in/in-}^\circ\text{F}$$

$$\nu = 0.3$$

Results

Displacement, rotation and moment results are compared with hand calculations based on formulas presented in Roark and Young 1975 as well as the results documented in SAP2000's manuals.

The problem is solved using plates with Thin and Thick Plate bending behavior and the MITC4 element behavior.

The percentage difference from independent results are given next to the results in parentheses.

In the LARSA 4D project file for this problem, U_z values are taken from joint 2 U_z displacement; R_2 values are taken from joint 2 R_y displacement since in this joint, y direction is coinciding with the tangential vector. For Model A, M_{11} results are taken from plate 145's internal reaction at joint 146 in M_{xx} direction and multiplied by -1 since M_{11} is outwards and M_{yy} is inwards; M_{22} results are taken from plate 17's internal reaction at joint 2 in M_{yy} direction and multiplied by -1 since LARSA 4D's sign convention of plates about moments is the opposite of independent results' sign convention. On the other hand, for Model B, M_{xx} and M_{yy} results are taken from the internal moment of plate 24 at joint 17 and plate 160 at joint 1, respectively.

Quadrilateral Thin Plate

Result	Independent	LARSA 4D	SAP2000
U_z @ inner edge (in)	0.01931	0.01905 (-1%)	0.01905 (-1%)
R_2 @ inner edge (rad)	0.00352	0.00347 (-1%)	0.00347 (-1%)
M_{11} @ outer edge (k-in/in)	-2.18100	-2.18209 (0%)	-2.18200 (0%)
M_{22} @ inner edge (k-in/in)	-4.40600	-4.53398 (3%)	-4.01600 (-9%)

Quadrilateral Thick Plate

Result	Independent	LARSA 4D	SAP2000
U_z @ inner edge (in)	0.01931	0.01859 (-4%)	0.01778 (-8%)
R_2 @ inner edge (rad)	0.00352	0.00320 (-9%)	0.00311 (-12%)
M_{11} @ outer edge (k-in/in)	-2.18100	-2.18185 (0%)	-2.18500 (0%)

Result	Independent	LARSA 4D	SAP2000
M_{22} @ inner edge (k-in/in)	-4.40600	-4.31723 (-2%)	-4.47800 (2%)

Quadrilateral MITC4 Plate

Result	Independent	LARSA 4D
U_z @ inner edge (in)	0.01931	0.01859 (-4%)
R_2 @ inner edge (rad)	0.00352	0.00320 (-9%)
M_{11} @ outer edge (k-in/in)	-2.18100	-2.18188 (0%)
M_{22} @ inner edge (k-in/in)	-4.40600	-4.64490 (5%)

Triangular Thin Plate

Result	Independent	LARSA 4D	SAP2000
U_z @ inner edge (in)	0.01931	0.01616 (-16%)	0.01616 (-16%)
R_2 @ inner edge (rad)	0.00352	0.00272 (-23%)	0.00272 (-23%)
M_{11} @ outer edge (k-in/in)	-2.1810	-2.1932 (1%)	-2.1840 (0%)
M_{22} @ inner edge (k-in/in)	-4.4060	-4.3771 (-1%)	-4.3769 (-1%)

Triangular Thick Plate

Result	Independent	LARSA 4D	SAP2000
U_z @ inner edge (in)	0.01931	0.01757 (-9%)	0.01551 (-20%)
R_2 @ inner edge (rad)	0.00352	0.00302 (-14%)	0.00258 (-27%)
M_{11} @ outer edge (k-in/in)	-2.1810	-2.1887 (0%)	-2.1911 (0%)
M_{22} @ inner edge (k-in/in)	-4.4060	-4.6904 (6%)	-4.2930 (-3%)

References

- Roark and Young, "Roark's Formulas for Stress and Strain," 1975, p.361
- SAP 2000, CSI Software Verification Example 2-014, "Shell-Temperature gradient Through Shell Thickness."

For More Information, please refer to the following documentation.

- For help on linear static analysis, see Linear Static Analysis in *LARSA 4D Reference Manual*.

L29: Solid-Straight Beam with Static Loads

A straight cantilever beam, modeled with solid objects, is subjected to unit forces at the tip in the three orthogonal directions and a unit moment at the tip about the three orthogonal directions, each in a different load case.

Problem Description

A straight cantilever beam, modeled with solid objects, is subjected to unit forces at the tip in the three orthogonal directions and a unit moment at the tip about the three orthogonal directions, each in a different load case.

The basic geometry, properties and loading are as described in the publication by MacNeal and Harder 1985. The cantilever beam is 6 inches long, 0.2 inch wide parallel to the z direction and 0.1 inch wide parallel to the Y direction. The three different models are created to each represent a different element shape. Models A, B and C use rectangular-, trapezoidal- and parallelogram-shaped elements, respectively.

Please note that this example is an extreme case presented for testing and verification of the solid object. Solid objects are not in general intended for use in modeling a beam with an $n \times 1 \times 1$ mesh.

Of the six load cases created for each model, load cases 1 through 3 apply unit forces at the cantilever tip in the X, Y and Z directions and load cases 4 through 6 apply unit moments at the cantilever tip about X, Y and Z directions, respectively. The moments are applied as couples.

The independent solution is derived using elementary beam theory that assumes no local Poisson's effect occurs at the support. The beam is modeled in LARSA 4D with all joints fully restrained at the fixed end and with all joints at the free end assigned to a body constraint. Thus, the LARSA 4D model is slightly different from the free hand calculations because in the LARSA 4D model there is a slight local Poisson's effect at the beam ends.

Model Diagrams

Data

$$E = 10,000,000 \text{ lb/in}^2$$

$$\nu = 0.3$$

$$G = 3,846,154 \text{ lb/in}^2$$

Solid object thickness in Y direction = 0.1 in

Loading

Load Case	Load Type	Load
1	P_x Axial Extension	$F_x = +0.25$ lb joints 7, 14, 21 and 28
2	V_z and M_y Shear and bending	$F_z = +0.25$ lb joints 7, 14, 21 and 28
3	V_y and M_z Shear and bending	$F_y = +0.25$ lb joints 7, 14, 21 and 28
4	M_x Twist	$F_y = -2.5$ lb joints 7 and 21 $F_y = +2.5$ lb joints 14 and 28
5	M_y Moment	$F_x = -2.5$ lb joints 7 and 21 $F_x = +2.5$ lb joints 14 and 28
6	M_z Moment	$F_y = +5$ lb joints 7 and 14 $F_y = -5$ lb joints 21 and 28

The following tables summarize the results for Models A-C *with Incompatible Bending* for their Load Case and Type.

Results *WITH* Incompatible Bending Modes for *Load Case 1; P_x Axial Extension*

Load Case; and Type	Model and Element Shape	Mesh	Output Parameter	Theoretical	LARSA4D	SAP2000
Load Case 1; P_x Axial Extension	A- Rectangle	6X1X1	average of joints 7, 14, 21, and 28 in	3.000E-05	---	2.962E-05
Load Case 1; P_x Axial Extension	A- Rectangle	30X1X1	average of joints 7, 14, 21, and 28 in	3.000E-05	---	2.985E-05
Load Case 1; P_x Axial Extension	A- Rectangle	30X4X8	average of joints 7, 14, 21, and 28 in	3.000E-05	---	2.984E-05
Load Case 1; P_x Axial Extension	B- Trapezoid	6X1X1	average of joints 7, 14, 21, and 28 in	3.000E-05	---	2.966E-05
Load Case 1; P_x Axial Extension	B- trapezoid	30X1X1	average of joint 7, 14, 21, and 28 in	3.000E-05	---	2.985E-05
Load Case 1; P_x Axial Extension	B- Trapezoid	30X4X8	average of joints 7, 14, 21, and 28 in	0.1081	---	2.985E-05

Load Case; and Type	Model and Element Shape	Mesh	Output Parameter	Theoretical	LARSA4D	SAP2000
Load Case 1; P _x Axial Extension	C- Parrellelogram	6X1X1	average of joints 7, 14, 21, and 28 in	0.1081	---	2.965E-05
Load Case 1; P _x Axial Extension	C- Parrellelogram	30X1X1	average of joints 7, 14, 21, and 28 in	0.1081	---	2.985E-05
Load Case 1; P _x Axial Extension	C- Parrellelogram	30X4X8	average of joints 7, 14, 21, and 28 in	0.1081	---	2.985E-05

Results *WITH* Incompatible Bending Modes for Load Case 2; V_z and M_y Shear and bending

Load Case; and Type	Model and Element Shape	Mesh	Output Parameter	Theoretical	LARSA4D	SAP2000
Load Case 2; V _z and M _y Shear and Bending	A- Rectangle	6X1X1	average of joint 7, 14, 21, and 28 in	0.1081	---	0.1057
Load Case 2; V _z and M _y Shear and Bending	A- Rectangle	30X1X1	average of joint 7, 14, 21, and 28 in	0.1081	---	0.1.077
Load Case 2; V _z and M _y Shear and Bending	A- Rectangle	30X4X8	average of joint 7, 14, 21, and 28 in	0.1081	---	0.1073
Load Case 2; V _z and M _y Shear and Bending	B- Trapezoid	6X1X1	average of joint 7, 14, 21, and 28 in	0.1081	---	0.0051
Load Case 2; V _z and M _y Shear and Bending	B- Trapezoid	30X1X1	average of joint 7, 14, 21, and 28 in	0.1081	---	0.1071
Load Case 2; V _z and M _y Shear and Bending	B- Trapezoid	30X4X8	average of joint 7, 14, 21, and 28 in	0.1081	---	0.1069

Load Case; and Type	Model and Element Shape	Mesh	Output Parameter	Theoretical	LARSA4D	SAP2000
Load Case 2; V_z and M_y Shear and Bending	C- parallelogram	6X1X1	average of joint 7, 14, 21, and 28 in	0.1081	---	0.0673
Load Case 2; V_z and M_y Shear and Bending	C- parallelogram	30X1X1	average of joint 7, 14, 21, and 28 in	0.1081	---	0.1076
Load Case 2; V_z and M_y Shear and Bending	C- parallelogram	30X4X8	average of joint 7, 14, 21, and 28 in	0.1081	---	0.1072

Results *WITH* Incompatible Bending Modes for Load Case 3; V_y and M_z Shear and bending

Load Case; and Type	Model and Element Shape	Mesh	Output Parameter	Theoretical	LARSA4D	SAP2000
Load Case 3; V_z and M_z Shear and Bending	A- Rectangle	6X1X1	average of joint 7, 14, 21, and 28 in	0.4321	---	0.4203
Load Case 3; V_z and M_z Shear and Bending	A- Rectangle	30X1X1	average of joint 7, 14, 21, and 28 in	0.4321	---	0.4300
Load Case 3; V_z and M_z Shear and Bending	A- Rectangle	30X4X8	average of joint 7, 14, 21, and 28 in	0.4321	---	0.4286
Load Case 3; V_z and M_z Shear and Bending	B- trapezoid	6X1X1	average of joint 7, 14, 21, and 28 in	0.4321	---	0.0129
Load Case 3; V_z and M_z Shear and Bending	B- trapezoid	30X1X1	average of joint 7, 14, 21, and 28 in	0.4321	---	0.4060
Load Case 3; V_z and M_z Shear and Bending	B- trapezoid	30X4X8	average of joint 7, 14, 21, and 28 in	0.4321	---	0.4246

Load Case; and Type	Model and Element Shape	Mesh	Output Parameter	Theoretical	LARSA4D	SAP2000
Shear and Bending						
Load Case 3; V_z and M_z Shear and Bending	C- Parellelogram	6X1X1	average of joint 7, 14, 21, and 28 in	0.4321	---	0.2276
Load Case 3; V_z and M_z Shear and Bending	C- Parellelogram	30X1X1	average of joint 7, 14, 21, and 28 in	0.4321	---	0.4257
Load Case 3; V_z and M_z Shear and Bending	C- Parellelogram	30X4X8	average of joint 7, 14, 21, and 28 in	0.4321	---	0.4280

Results *WITH* Incompatible Bending Modes for Load Case 4; M_x Twist

Load Case; and Type	Model and Element Shape	Mesh	Output Parameter	Theoretical	LARSA4D	SAP2000
Load Case 4; M_x twist	A- Rectangle	6X1X1	average of joint 7, 14, 21, and 28 in	0.00280	---	0.00280
Load Case 4; M_x twist	A- Rectangle	30X1X1	average of joint 7, 14, 21, and 28 in	0.00280	---	0.00289
Load Case 4; M_x twist	A- Rectangle	30X4X8	average of joint 7, 14, 21, and 28 in	0.00280	---	0.00331
Load Case 4; M_x twist	B- Trapezoid	6X1X1	average of joint 7, 14, 21, and 28 in	0.00280	---	0.00172
Load Case 4; M_x twist	B- Trapezoid	30X1X1	average of joint 7, 14, 21, and 28 in	0.00280	---	0.00276
Load Case 4; M_x twist	B- Trapezoid	30X4X8	average of joint 7, 14, 21, and 28 in	0.00280	---	0.00330

Load Case; and Type	Model and Element Shape	Mesh	Output Parameter	Theoretical	LARSA4D	SAP2000
Load Case 4; M_x twist	C- Parellelogram	6X1X1	average of joint 7, 14, 21, and 28 in	0.00280	---	0.00255
Load Case 4; M_x twist	C- Parellelogram	30X1X1	average of joint 7, 14, 21, and 28 in	0.00280	---	0.00288
Load Case 4; M_x twist	C- Parellelogram	30X4X8	average of joint 7, 14, 21, and 28 in	0.00280	---	0.00331

Results *WITH* Incompatible Bending Modes for Load Case 5; M_y Moment

Load Case; and Type	Model and Element Shape	Mesh	Output Parameter	Theoretical	LARSA4D	SAP2000
Load Case 5; M_y Moment	A- Rectangle	6X1X1	average of joint 7, 14, 21, and 28 in	9.00E-04	---	8.906E-04
Load Case 5; M_y Moment	A- Rectangle	30X1X1	average of joint 7, 14, 21, and 28 in	9.00E-04	---	8.981E-04
Load Case 5; M_y Moment	A- Rectangle	30X4X8	average of joint 7, 14, 21, and 28 in	9.00E-04	---	8.955E-04
Load Case 5; M_y Moment	B- Trapezoid	6X1X1	average of joint 7, 14, 21, and 28 in	9.00E-04	---	3.240E-05
Load Case 5; M_y Moment	B- Trapezoid	30X1X1	average of joint 7, 14, 21, and 28 in	9.00E-04	---	8.930E-04
Load Case 5; M_y Moment	B- Trapezoid	30X4X8	average of joint 7, 14, 21, and 28 in	9.00E-04	---	8.921E-04
Load Case 5; M_y Moment	C- Parellelogram	6X1X1	average of joint 7, 14, 21, and 28 in	9.00E-04	---	6.369E-04
Load Case 5; M_y Moment	C- Parellelogram	30X1X1	average of joint 7, 14, 21, and 28 in	9.00E-04	---	8.976E-04

Load Case; and Type	Model and Element Shape	Mesh	Output Parameter	Theoretical	LARSA4D	SAP2000
Load Case 5; M _y Moment	C- Parellelogram	30X4X8	average of joint 7, 14, 21, and 28 in	9.00E-04	---	8.952E-04

Results *WITH* Incompatible Bending Modes for Load Case 6; M_z Moment

Load Case; and Type	Model and Element Shape	Mesh	Output Parameter	Theoretical>	LARSA4D	SAP2000
Load Case 6 M _z Moment	A- Rectangle	6X1X1	average of joint 7, 14, 21, and 28 in	0.00180	---	0.00177
Load Case 6; M _z Moment	A- Rectangle	30X1X1	average of joint 7, 14, 21, and 28 in	0.00180	---	0.00179
Load Case 6; M _z Moment	A- Rectangle	30X4X8	average of joint 7, 14, 21, and 28 in	0.00180	---	0.00179
Load Case 6; M _z Moment	B- Trapezoid	6X1X1	average of joint 7, 14, 21, and 28 in	0.00180	---	0.00004
Load Case 6; M _z Moment	B- Trapezoid	30X1X1	average of joint 7, 14, 21, and 28 in	0.00180	---	0.00169
Load Case 6; M _z Moment	B- Trapezoid	30X4X8	average of joint 7, 14, 21, and 28 in	0.00180	---	0.00177
Load Case 6 M _z Moment	C- Parellelogram	6X1X1	average of joint 7, 14, 21, and 28 in	0.00180	---	0.00112
Load Case 6; M _z Moment	C- Parellelogram	30X1X1	average of joint 7, 14, 21, and 28 in	0.00180	---	0.00178
Load Case 6; M _z Moment	C- Parellelogram	30X4X8	average of joint 7, 14, 21, and 28 in	0.00180	---	0.00179

The tables below summarize the results for Models A-C *WITHOUT* Incompatible Bending for their Load Case and Type.

Load Case; and Type	Model and Element Shape	Mesh	Output Parameter	Theoretical	LARSA4D	SAP2000
Load Case 1; P _x Axial Extension	A- Rectangle	6X1X1	average of joints 7, 14, 21, and 28 in	3.000E-05	---	2.914E-05
Load Case 1; P _x Axial Extension	A- Rectangle	30X1X1	average of joints 7, 14, 21, and 28 in	3.000E-05	---	2.982E-05
Load Case 1; P _x Axial Extension	A- Rectangle	30X4X8	average of joints 7, 14, 21, and 28 in	3.000E-05	---	2.995E-05
Load Case 1; P _x Axial Extension	B- Trapezoid	6X1X1	average of joints 7, 14, 21, and 28 in	3.000E-05	---	2.915E-05
Load Case 1; P _x Axial Extension	B- trapezoid	30X1X1	average of joint 7, 14, 21, and 28 in	3.000E-05	---	2.982E-05
Load Case 1; P _x Axial Extension	B- Trapezoid	30X4X8	average of joints 7, 14, 21, and 28 in	3.000E-05	---	2.995E-05
Load Case 1; P _x Axial Extension	C- Parallelogram	6X1X1	average of joints 7, 14, 21, and 28 in	3.000E-05	---	2.915E-05
Load Case 1; P _x Axial Extension	C- Parallelogram	30X1X1	average of joints 7, 14, 21, and 28 in	3.000E-05	---	2.982E-05
Load Case 1; P _x Axial Extension	C- Parallelogram	30X4X8	average of joints 7, 14, 21, and 28 in	3.000E-05	---	2.995E-05

Results *WITH* Incompatible Bending Modes for Load Case 2; V_z and M_y Shear and bending

Load Case; and Type	Model and Element Shape	Mesh	Output Parameter	Theoretical	LARSA4D	SAP2000
Load Case 2; V _z and M _y Shear and Bending	A- Rectangle	6X1X1	average of joint 7, 14, 21, and 28 in	0.1081	---	0.0100

Load Case; and Type	Model and Element Shape	Mesh	Output Parameter	Theoretical	LARSA4D	SAP2000
Load Case 2; V_z and M_y Shear and Bending	A- Rectangle	30X1X1	average of joint 7, 14, 21, and 28 in	0.1081	---	0.0718
Load Case 2; V_z and M_y Shear and Bending	A- Rectangle	30X4X8	average of joint 7, 14, 21, and 28 in	0.1081	---	0.1070
Load Case 2; V_z and M_y Shear and Bending	B- Trapezoid	6X1X1	average of joint 7, 14, 21, and 28 in	0.1081	---	0.0028
Load Case 2; V_z and M_y Shear and Bending	B- Trapezoid	30X1X1	average of joint 7, 14, 21, and 28 in	0.1081	---	0.0452
Load Case 2; V_z and M_y Shear and Bending	B- Trapezoid	30X4X8	average of joint 7, 14, 21, and 28 in	0.1081	---	0.1047
Load Case 2; V_z and M_y Shear and Bending	C- parallelogram	6X1X1	average of joint 7, 14, 21, and 28 in	0.1081	---	0.0034
Load Case 2; V_z and M_y Shear and Bending	C- parallelogram	30X1X1	average of joint 7, 14, 21, and 28 in	0.1081	---	0.0296
Load Case 2; V_z and M_y Shear and Bending	C- parallelogram	30X4X8	average of joint 7, 14, 21, and 28 in	0.1081	---	0.1016

Results *WITH* Incompatible Bending Modes for Load Case 3; V_y and M_z Shear and bending

Load Case; and Type	Model and Element Shape	Mesh	Output Parameter	Theoretical	LARSA4D	SAP2000
Load Case 3; V_y and M_z	A- Rectangle	6X1X1	average of joint 7, 14, 21, and 28 in	0.4321	---	0.0109

Load Case; and Type	Model and Element Shape	Mesh	Output Parameter	Theoretical	LARSA4D	SAP2000
Shear and Bending						
Load Case 3; V_y and M_z Shear and Bending	A- Rectangle	30X1X1	average of joint 7, 14, 21, and 28 in	0.4321	---	0.1558
Load Case 3; V_y and M_z Shear and Bending	A- Rectangle	30X4X8	average of joint 7, 14, 21, and 28 in	0.4321	---	0.4168
Load Case 3; V_y and M_z Shear and Bending	B- trapezoid	6X1X1	average of joint 7, 14, 21, and 28 in	0.4321	---	0.0045
Load Case 3; V_y and M_z Shear and Bending	B- trapezoid	30X1X1	average of joint 7, 14, 21, and 28 in	0.4321	---	0.1345
Load Case 3; V_y and M_z Shear and Bending	B- trapezoid	30X4X8	average of joint 7, 14, 21, and 28 in	0.4321	---	0.4135
Load Case 3; V_y and M_z Shear and Bending	C- Parellelogram	6X1X1	average of joint 7, 14, 21, and 28 in	0.4321	---	0.0062
Load Case 3; V_y and M_z Shear and Bending	C- Parellelogram	30X1X1	average of joint 7, 14, 21, and 28 in	0.4321	---	0.1169
Load Case 3; V_y and M_z Shear and Bending	C- Parellelogram	30X4X8	average of joint 7, 14, 21, and 28 in	0.4321	---	0.4084

Results *WITH* Incompatible Bending Modes for Load Case 4; M_x Twist

Load Case; and Type	Model and Element Shape	Mesh	Output Parameter	Theoretical	LARSA4D	SAP2000
Load Case 4; M_x Twist	A- Rectangle	6X1X1	average of joint 7, 14, 21, and 28 in	0.00341	---	0.00280
Load Case 4; M_x Twist	A- Rectangle	30X1X1	average of joint 7, 14, 21, and 28 in	0.00341	---	0.00289
Load Case 4; M_x Twist	A- Rectangle	30X4X8	average of joint 7, 14, 21, and 28 in	0.00341	---	0.00331
Load Case 4; M_x Twist	B- Trapezoid	6X1X1	average of joint 7, 14, 21, and 28 in	0.00341	---	0.00159
Load Case 4; M_x Twist	B- Trapezoid	30X1X1	average of joint 7, 14, 21, and 28 in	0.00341	---	0.00183
Load Case 4; M_x Twist	B- Trapezoid	30X4X8	average of joint 7, 14, 21, and 28 in	0.00341	---	0.00322
Load Case 4; M_x Twist	C- Parellelogram	6X1X1	average of joint 7, 14, 21, and 28 in	0.00341	---	0.00108
Load Case 4; M_x Twist	C- Parellelogram	30X1X1	average of joint 7, 14, 21, and 28 in	0.00341	---	0.00320
Load Case 4; M_x Twist	C- Parellelogram	30X4X8	average of joint 7, 14, 21, and 28 in	0.00341	---	0.00310

Results *WITH* Incompatible Bending Modes for Load Case 5; M_y Moment

Load Case; and Type	Model and Element Shape	Mesh	Output Parameter	Theoretical	LARSA4D	SAP2000
Load Case 5; M_y Moment	A- Rectangle	6X1X1	average of joint 7, 14, 21, and 28 in	9.00E-04	---	8.370E-05
Load Case 5; M_y Moment	A- Rectangle	30X1X1	average of joint 7, 14, 21, and 28 in	9.00E-04	---	5.983E-04

Load Case; and Type	Model and Element Shape	Mesh	Output Parameter	Theoretical	LARSA4D	SAP2000
Load Case 5; M _y Moment	A- Rectangle	30X4X8	average of joint 7, 14, 21, and 28 in	9.00E-04	---	8.913E-04
Load Case 5; M _y Moment	B- Trapezoid	6X1X1	average of joint 7, 14, 21, and 28 in	9.00E-04	---	1.880E-05
Load Case 5; M _y Moment	B- Trapezoid	30X1X1	average of joint 7, 14, 21, and 28 in	9.00E-04	---	3.711E-04
Load Case 5; M _y Moment	B- Trapezoid	30X4X8	average of joint 7, 14, 21, and 28 in	9.00E-04	---	8.713E-04
Load Case 5; M _y Moment	C- Parellelogram	6X1X1	average of joint 7, 14, 21, and 28 in	9.00E-04	---	2.520E-05
Load Case 5; M _y Moment	C- Parellelogram	30X1X1	average of joint 7, 14, 21, and 28 in	9.00E-04	---	2.199E-04
Load Case 5; M _y Moment	C- Parellelogram	30X4X8	average of joint 7, 14, 21, and 28 in	9.00E-04	---	8.417E-04

Results *WITH* Incompatible Bending Modes for Load Case 6; M_z Moment

Load Case; and Type	Model and Element Shape	Mesh	Output Parameter	Theoretical	LARSA4D	SAP2000
Load Case 6 M _z Moment	A- Rectangle	6X1X1	average of joint 7, 14, 21, and 28 in	0.00180	---	0.00005
Load Case 6; M _z Moment	A- Rectangle	30X1X1	average of joint 7, 14, 21, and 28 in	0.00180	---	0.00065
Load Case 6; M _z Moment	A- Rectangle	30X4X8	average of joint 7, 14, 21, and 28 in	0.00180	---	0.00174
Load Case 6; M _z Moment	B- Trapezoid	6X1X1	average of joint 7, 14, 21, and 28 in	0.00180	---	0.00002

Load Case; and Type	Model and Element Shape	Mesh	Output Parameter	Theoretical	LARSA4D	SAP2000
Load Case 6; M _z Moment	B- Trapezoid	30X1X1	average of joint 7, 14, 21, and 28 in	0.00180	---	0.00056
Load Case 6; M _z Moment	B- Trapezoid	30X4X8	average of joint 7, 14, 21, and 28 in	0.00180	---	0.00172
Load Case 6 M _z Moment	C- Parellelogram	6X1X1	average of joint 7, 14, 21, and 28 in	0.00180	---	0.00002
Load Case 6; M _z Moment	C- Parellelogram	30X1X1	average of joint 7, 14, 21, and 28 in	0.00180	---	0.00047
Load Case 6; M _z Moment	C- Parellelogram	30X4X8	average of joint 7, 14, 21, and 28 in	0.00180	---	0.00170

Solution Comparison

Sources:

- Cook and Young, "Advanced Mechanics of Materials," 1985, pp. 244.
- SAP 2000, CSI Software Verification Example 5-002, "Solid-Straight Beam with Static Loads."

For More Information, please refer to the following documentation.

- For help on linear static analysis, see Linear Static Analysis in *LARSA 4D Reference Manual*.

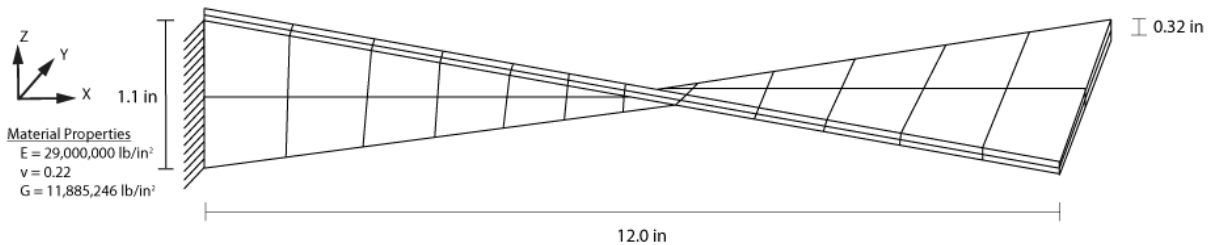
L30: Solid-Twisted Beam with Static Loads

A twisted cantilever beam, modeled with solid elements, is subjected to unit forces at the tip in the in-plane and out-of-plane directions, that is, the Y and Z directions, respectively. The in-plane and out-of-plane loads are applied in different load cases.

Problem Description

A twisted cantilever beam, modeled with solid elements, is subjected to unit forces at the tip in the in-plane and out-of-plane directions, that is, the Y and Z directions, respectively. The in-plane and out-of-plane loads are applied in different load cases.

The geometry, properties and loading are based on the publication by MacNeal and Harder 1985. The cantilever beam is twisted 90° from the root (fixed end) to the tip. It is 12 inches long, 1.1 inches wide and 0.32 inches thick. For modeling in LARSA 4D the twisted beam is meshed $12 \times 2 \times 2$ (48 area objects total) as shown in the figure.



Model Diagrams

Loading

Load Case	Load
IN	$F_y = +1 \text{ lb}$ equally distributed to all joints at free tip of beam
OUT	$F_z = +1 \text{ lb}$ equally distributed to all joints at free tip of beam

Results with incompatible Bending Modes

Load Case; and Type	Output Parameter	Theoretical*	LARSA4D	SAP2000*
Load Case IN; In-Plane	U_y , in average of all joints at tip	0.005429	---	0.005322

Load Case; and Type	Output Parameter	Theoretical*	LARSA4D	SAP2000*
Load Case OUT; Out-of-Plane	U_z , in average of all joints at tip	0.001749	---	0.001719

Solution Comparison

Sources:

- Cook and Young, "Advanced Mechanics of Materials," 1985, pp. 244.
- SAP 2000, CSI Software Verification Example 5-004, "Solid-Twisted Beam with Static Loads."

For More Information, please refer to the following documentation.

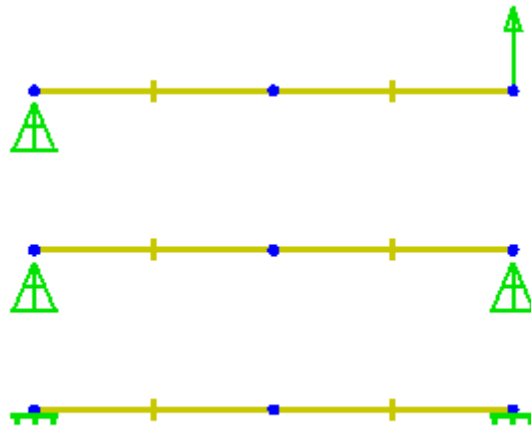
- For help on linear static analysis, see Linear Static Analysis in *LARSA 4D Reference Manual*.

L31: Non-Prismatic Beam with Nonlinear Thermal Load

A tapered beam is subjected to a nonlinear thermal gradient load. The behavior of the beam is examined by considering three different support conditions: pin-roller, pin-pin, and fix-fix.

Problem Description

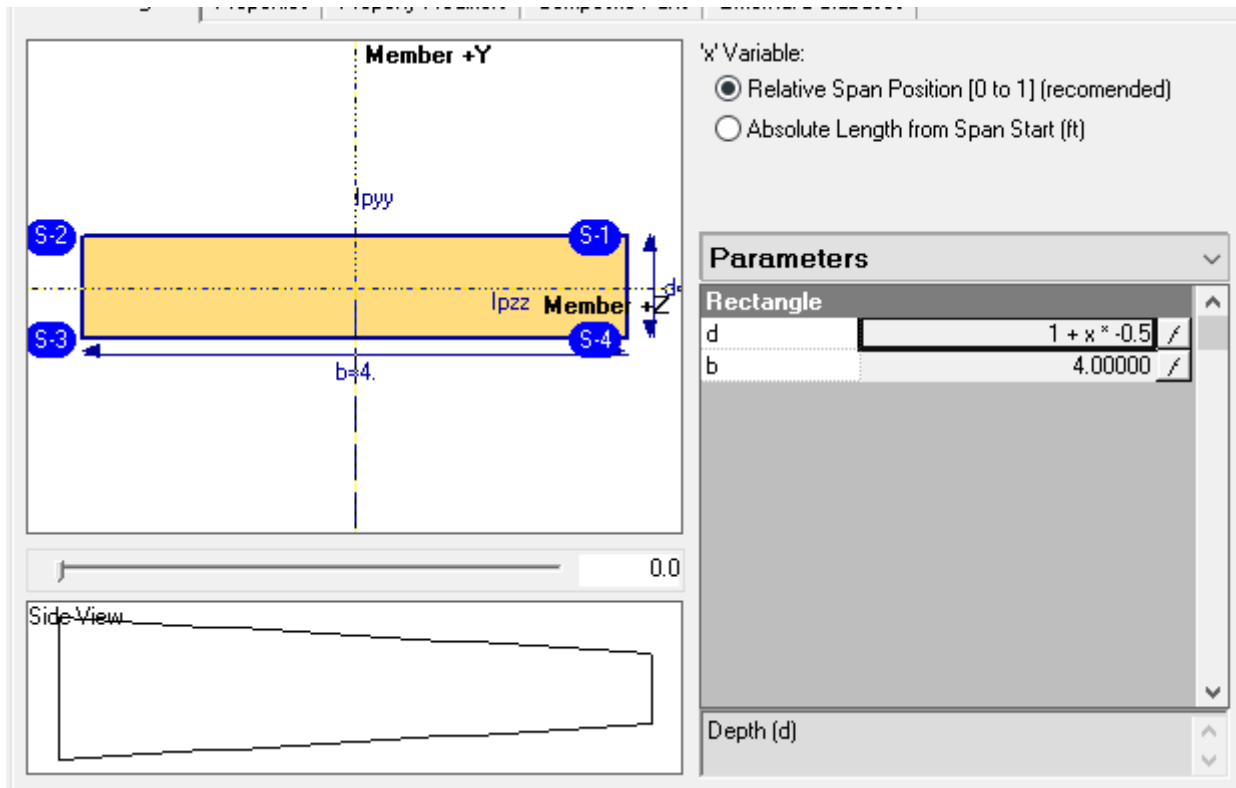
A beam having a non-prismatic cross-section shape, with its depth varying linearly along its length, is subjected to a nonlinear thermal gradient load also along its depth. The beam is 300 ft in length, has a depth that ranges from 1.0 to 0.5 feet, and is divided into two elements of equal length. The behavior of the beam is examined by considering three different support conditions: pin-roller, pin-pin, and fix-fix.



Beam Models

A thermal change is applied through the entire depth of the cross-section with formula $t = y^2$, where y is measured from the lower extreme fiber of the section in feet (y is therefore in the range $[0, 1]$) and t is in $^{\circ}\text{F}$. The temperature change at the top is 1°F . For the purposes of entering the temperature curve into LARSA 4D, it has been discretized into 10 points equally spaced on the section y -axis.

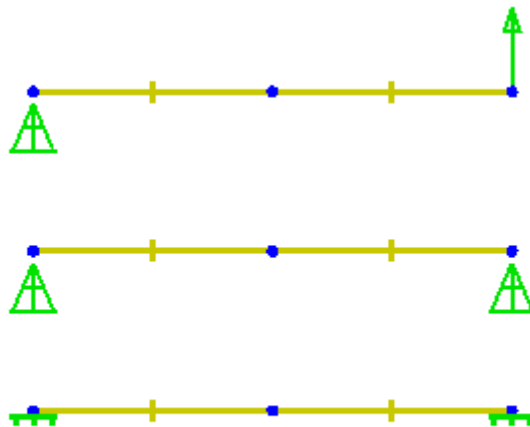
The non-prismatic rectangular cross-section is defined by utilizing the Section Composer tool. The width of the beam is constant and 4 ft. The depth, on the other hand, varies through its length in such a way that it follows the equation $d = 1 - x/2$, where x is the relative span distance (in the range $[0, 1]$) and d is the section depth. The cross-section centroid is aligned with the member reference axis along its length. In LARSA 4D, a span is assigned to the two beam elements to obtain the continuous change in depth throughout the whole beam.



Non-Prismatic Section

The material of the beam is Fc4 concrete.

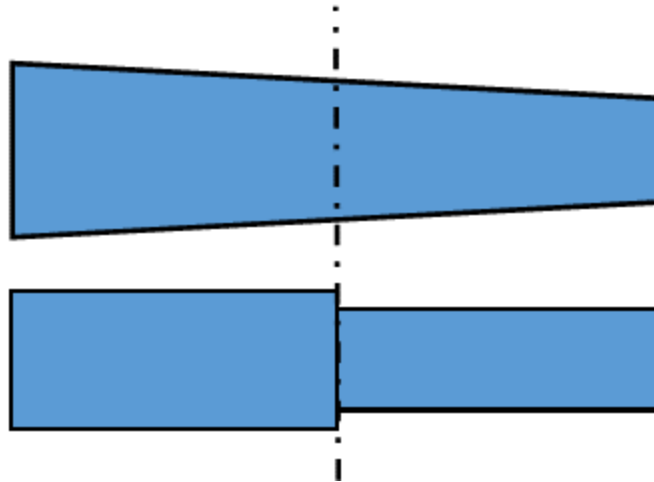
The structure is modeled by considering three different support conditions. In the first one, the beam is supported by a pin on one end and a roller at the other end (**Model A**). Both ends are pinned at the second one (**Model B**). Finally, both ends are fixed for the last one (**Model C**).



Model A (Top), B (Middle), and C (Bottom)

Solution Comparison

LARSA 4D uses averaged cross-section properties for each non-prismatic beam element. The averaged section parameters are listed below.



Non-Prismatic Beam (Top) and Equivalent Section Approach (Bottom)

Averaged Section Parameters (in ft, ft², and ft⁴)

Element	Width (b)	Depth (d)	Area (A)	Inertia (I)
Left	4.0	0.875	3.5	0.24
Right	4.0	0.625	2.5	0.09

Since the section of the beam is not constant through its length, the structure is not symmetric. The section area of the left element is greater than the right one so the external forces due to the temperature change are not the same for both elements. This unbalanced force causes lateral displacement and rotation at the mid-span even for Models B and C where the ends are translationally fixed.

The displacements at mid-span reported by LARSA 4D, and corresponding hand calculations, are:

Displacements. Units are ft.

	Horiz. Disp.		Vert. Disp.	
	Hand Calc.	LARSA 4D	Hand Calc.	LARSA 4D
Model A	2.10e-4	2.12e-4	4.26e-2	4.28e-2
Model B	7.80e-5	7.83e-5	4.26e-2	4.28e-2
Model C	7.80e-5	7.83e-5	-3.50e-3	-3.56e-3

To compute the “external” component of stress at the composite cross-section centroid, the stress at each fiber $E\epsilon_t$ is integrated over the area of the section, i.e.

$$F = \int E\alpha y^2 da$$

$$M = \int E\alpha y^2(y-d/2) da$$

where E and α are the elastic modulus and coefficient of thermal expansion, y is the location of the fiber relative to the lowest fiber of the section, and $d/2$ is the distance from the lowest fiber to the centroid of the composite section.

Computation of “External” Force and Moment. Units are kip, ft and °F.

Member	Average Depth (d_{av})	Width (b)	Elastic Modulus, (E)	α	Force (F)	Moment (M)
Left	0.875	4.0	519,120	5.50e-6	2.55	0.56
Right	0.625	4.0	519,120	5.50e-6	0.93	0.15

External forces on each node are shown below.

Computation of External Nodal Forces. Units are kip and ft

	@ start		@ mid-span		@ end	
	Axial Force	Moment	Axial Force	Moment	Axial Force	Moment
Model A	-	0.554	1.621	-0.409	0.929	-0.145
Model B	-	0.554	1.621	-0.409	-	-0.145
Model C	-	-	1.621	-0.409	-	-

By solving the structure under external nodal forces, we can compute the member end forces as internal forces (P_{int} : Internal axial force, M_{int} : Internal Moment).

Internal Forces. Units are kip and ft

	@ Left Member Start		@ Right Member Start	
	P_{int}	M_{int}	P_{int}	M_{int}
Model A	2.55	0.55	0.93	0.15
Model B	0.95	0.55	-0.68	0.15
Model C	0.95	-0.05	-0.68	-0.18

The total stress in each shape is computed in the following table by adding the “external” stress as given by the total strains above and the “internal” stress based on the value of the nonlinear curve at the fiber. Note that stress recovery point 1 and 3 are at top and bottom fibers, respectively.

Hand Calc. Stress Computation. Units are kip and ft.

Model A	@ Left Member Start		@ Right Member Start	
	Stress Point 1	Stress Point 3	Stress Point 1	Stress Point 3
y	1.0	0.0	0.75	0.0
$(P_{int}/A) + (M_{int}c/I)$	1.47	-0.19	0.70	-0.08
$-E\alpha y^2$	-2.86	0.0	-1.61	0.0
Total Stress:				
Hand Calc	-1.39	-0.19	-0.91	-0.08
LARSA 4D	-1.38	-0.20	-0.91	-0.07

Model B	@ Left Member Start		@ Right Member Start	
	Stress Point 1	Stress Point 3	Stress Point 1	Stress Point 3
y	1.0	0.0	0.75	0.0
$(P_{int}/A) + (M_{int}c/I)$	1.07	-0.60	0.16	-0.62
$-E\alpha y^2$	-2.86	0.0	-1.61	0.0
Total Stress:				
Hand Calc	-1.79	-0.60	-1.45	-0.62
LARSA 4D	-1.78	-0.60	-1.45	-0.61

Model C	@ Left Member Start		@ Right Member Start	
	Stress Point 1	Stress Point 3	Stress Point 1	Stress Point 3
y	1.0	0.0	0.75	0.0
$(P_{int}/A) + (M_{int}c/I)$	0.16	0.32	-0.70	0.25
$-E\alpha y^2$	-2.86	0.0	-1.61	0.0
Total Stress:				
Hand Calc	-2.70	0.32	-2.31	0.25
LARSA 4D	-2.71	0.32	-2.32	0.25

For More Information, please refer to the following documentation.

- Member Thermal Loads in *LARSA 4D Reference Manual*.

L32: Isotropic Plate Cantilever using an Orthotropic Material Definition

A cantilever beam having isotropic material properties is modeled using orthotropic formulation plate elements by giving the the same modulus of elasticity in all loaded directions. The structure is subject to axial extension, in plane shear and bending, out of plane shear and bending, twist, in plane moment and out of plane moment joint loads. The tip joint displacement is compared to a model with isotropic formulation plate elements.

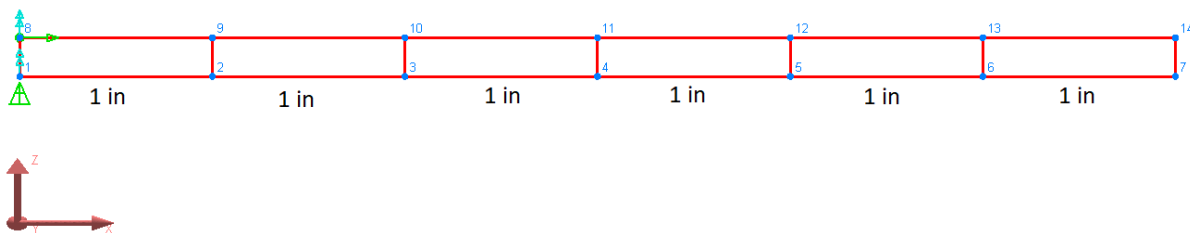
The purpose of this verification problem is to test the orthotropic material formulation for plate elements by comparison with the isotropic plate element formulation. The orthotropic plates are given numerical properties that result in isotropic behavior in the directions loaded.

The tip joint displacements of the cantilever structure modeled with orthotropic material plate formulation elements is compared to an identical model with isotropic material plate elements having the same modulus of elasticity and shear modulus values. This comparison is done for different plate shapes including rectangular, parallelogram, trapezoidal, and triangular and different bending and membrane types, including the thin plate, thick plate, bilinear membrane, and membrane with drilling degrees of freedom. The Material UCS is also varied to create a material angle of 11°, 45°, and 90°.

Test 1 validates orthotropic plate elements with identical material properties in both material axis directions by comparison to plate elements using the isotropic element formulation set to the same material properties. Test 2 validates orthotropic plate elements with non-identical material properties in the two material axis directions but under loading that causes strain in either only the Material 1 axis or only the Material 2 axis, and the isotropic comparison model uses material properties equal to the orthotropic model properties in the material axis under loading.

Problem Description

A cantilever beam 6 inches long, 0.2 inches tall, and 0.1 inches thick is divided into 1-inch plate elements. It is restrained in translation X, Y and Z at bottom-left corner and translation X, Y at top-left corner. Additionally, rotation Z is restrained at these corners. (Rotation Y DOFs of the beams generated with bilinear membrane type plates are also restrained to satisfy stability)



Beam Model

In Test 1, the material has elastic modulus 10,000,000 lb/in² and shear modulus 4,000,000 lb/in². The orthotropic formulation model is created by setting the same elastic modulus and shear modulus values for E_{11} , E_{22} , G_{12} , G_{13} , and

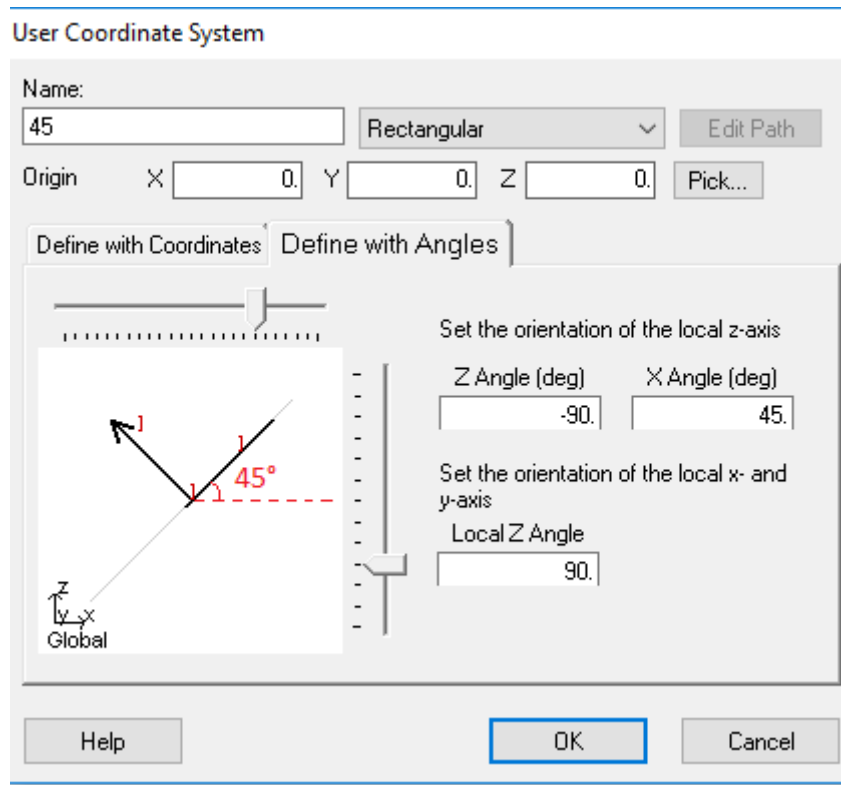
G_{23} . (Poisson's ratio, which can be computed from the elastic modulus and shear modulus but must be entered by the user for orthotropic materials, is 0.25.)

In Test 2, two orthotropic materials are used, each with elastic modulus $10,000,000 \text{ lb/in}^2$ in one direction and $20,000,000 \text{ lb/in}^2$ in the other direction, and other properties as in Test 1. The orthotropic materials are identical except that one has the elastic modulus values in E_{11} and E_{22} , and the other in E_{22} and E_{11} (i.e., reversed).

Properties: Orthotropic Material Properties										
Materials \ Sections \ UCS \ Spring Properties \ Isolator Definitions \ Material Time Effects \ Temperature Curve										
Basic Properties \ More Properties \ Orthotropic Properties										
	Name	Anisotropy	Material UCS	Modulus of Elasticity E11	Modulus of Elasticity E22	Poisson's Ratio m12	Shear Modulus G12	Shear Modulus G13	Shear Modulus G23	Assigned
1	Isotropic	Isotropic	(NONE)							Yes
2	Orthotropic 90	Orthotropic	90	2.0000e7	1.0000e7	0.2500	4.0000e6	4.0000e6	4.0000e6	Yes
3	Orthotropic 0	Orthotropic	0	1.0000e7	2.0000e7	0.2500	4.0000e6	4.0000e6	4.0000e6	Yes
4										

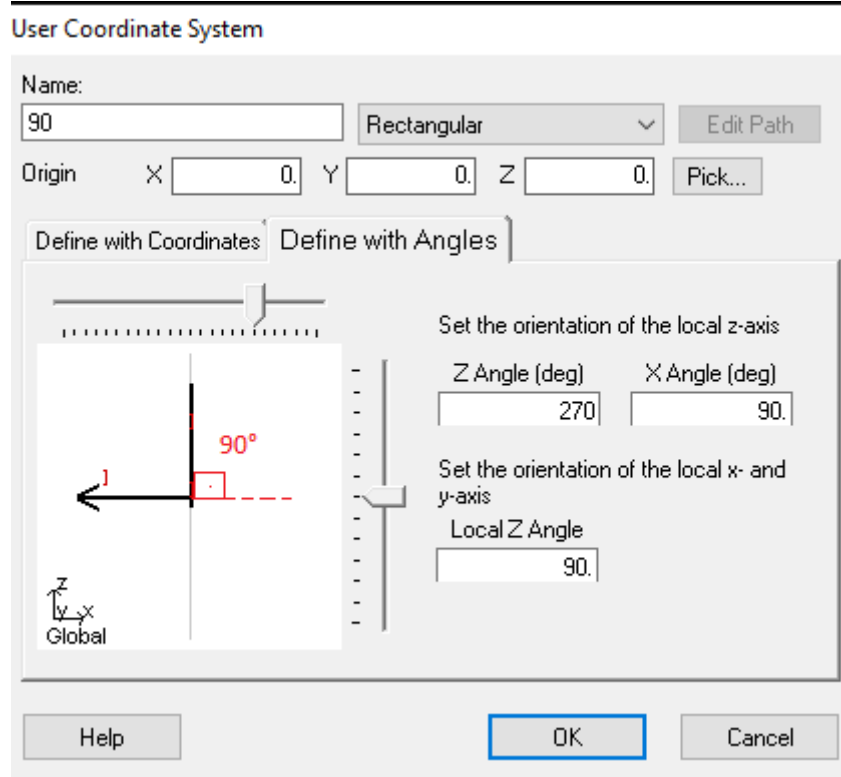
Test 2 Material Definitions

Material axes are configured using the Material UCS parameter of the materials. In Test 1, the orthotropic material is repeated three times, and a different User Coordinate System is assigned to each to achieve material angles of 0° , 45° , and 90° . (Since the material has identical properties in both directions, the results are expected to be identical regardless of the material axes, which is one of the results to be verified here.) To obtain the material axis orientation where $\theta=45^\circ$, a Material UCS can be as given as:



UCS of 45° Material Angle Plate

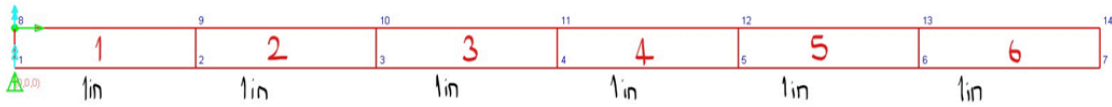
In Test 2, the material whose E_{11} matches the E value of the isotropic material ($10,000,000 \text{ lb/in}^2$) is given a User Coordinate System such that it gives a material angle of 0° , and the orthotropic material whose E_{22} matches the E value of the isotropic material is given a User Coordinate System such that it gives a material angle of 90° , which aligns E_{22} with the applied load. (There is no 45° case in Test 2 because the load would cause strain along both material axes, which could not be compared to an equivalent isotropic model.)



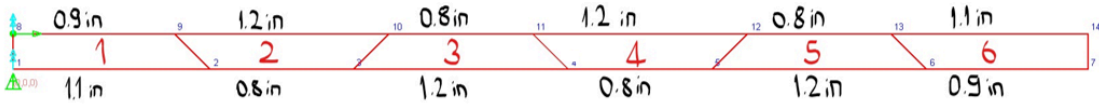
UCS of 90° Material Angle Plate

Four different element shapes are used for comparison: rectangular, trapezoidal, parallelogram and triangular with the geometric properties shown below:

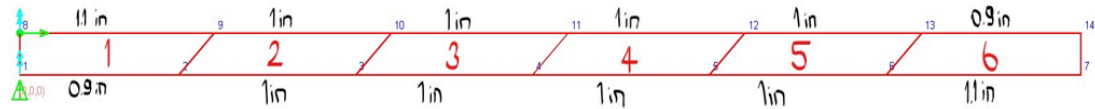
a. Rectangular



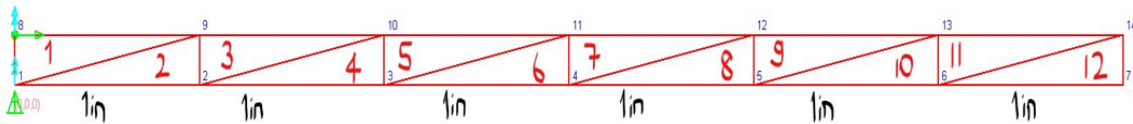
b. Trapezoidal



c. Parallelogram



d. Triangular

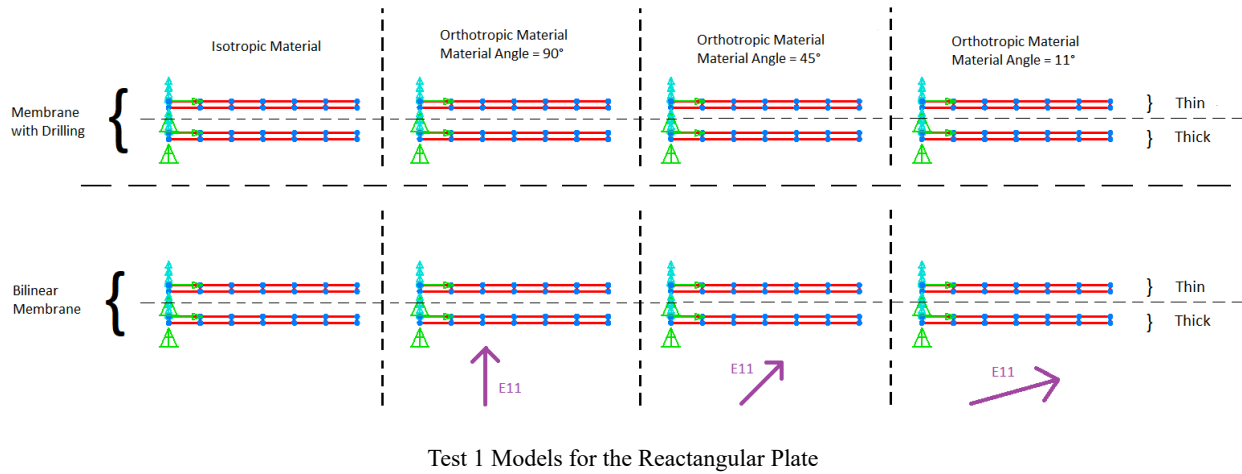


Different Shapes and Their Properties

In Test 1, all four shapes are created. In Test 2, only rectangular elements are created because the second material axis may impact results in the other shapes.

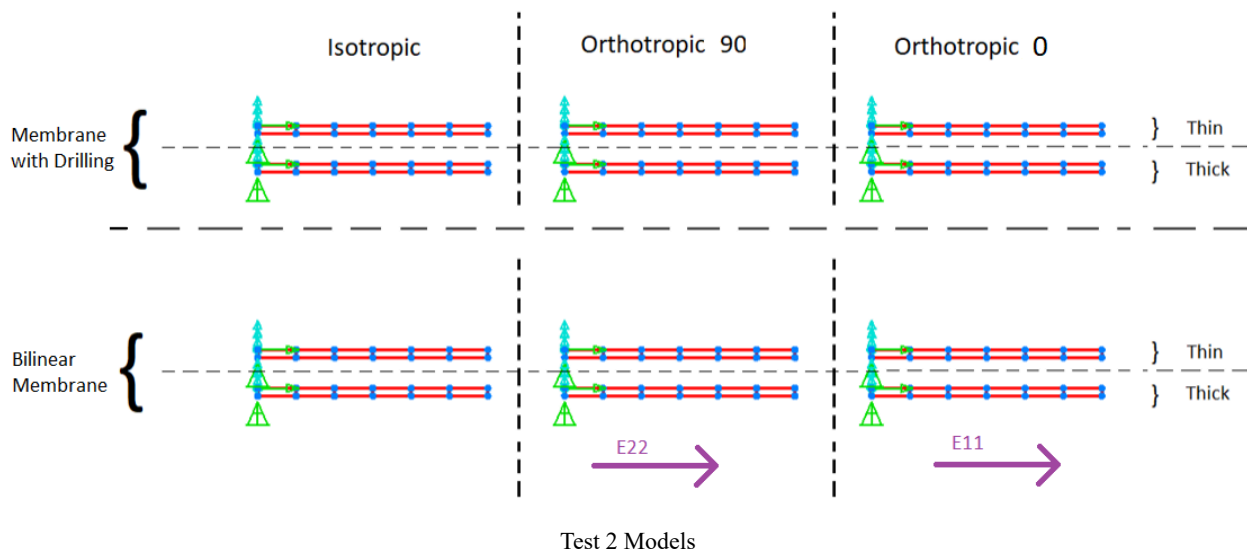
Since the orientation of the material axes are determined only by the Material UCS and not by the geometry of the element, there is no need to make any additional changes to have the material axes of the elements be aligned.

Two bending and two membrane types are also tested for all of the shapes, which making 16 models for each shape. The models for each shape type are stored in a single project file and are arranged as follows for Test 1:

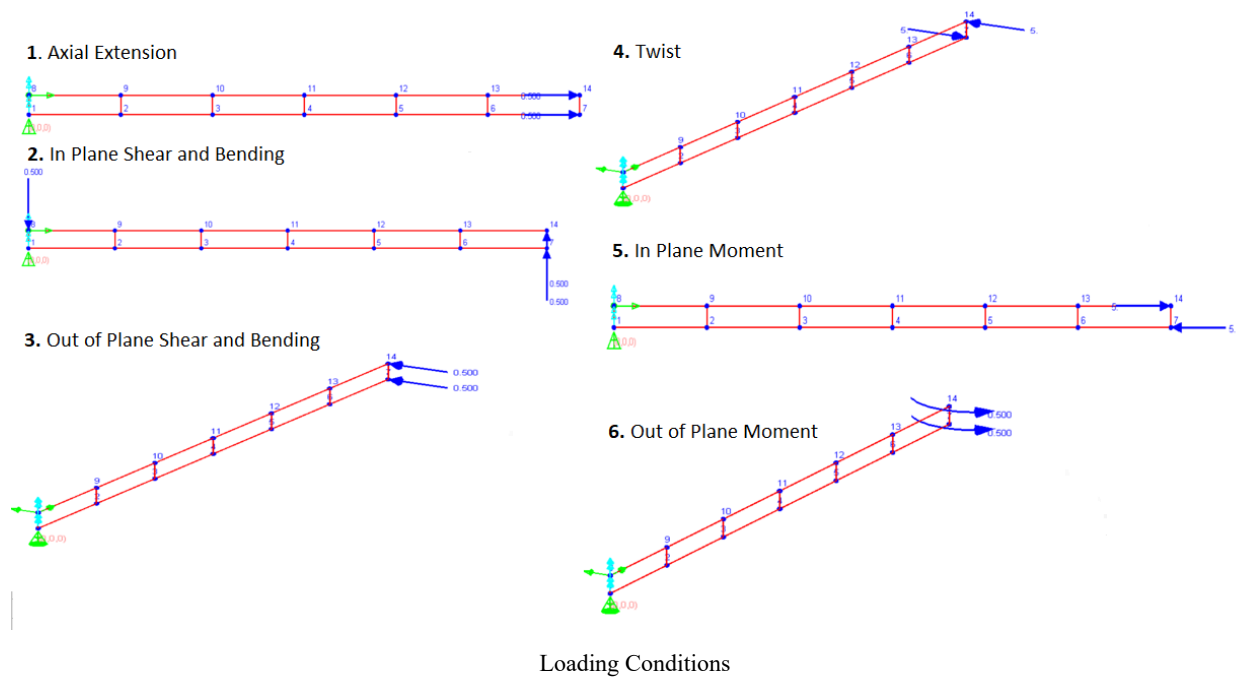


For triangular elements, the Constant Strain Triangle membrane behavior is used in all models.

There are 12 models in Test 2:



The load magnitudes of the axial extension, in plane shear and bending, out of plane shear and bending joint loads are 0.5 lb. Twist and in plane moment loads are 5 lb and out of plane moment is 0.5 lb-in in magnitude. The joint loads are shown below:



In Test 2, load conditions that cause strain in the second material axis are excluded, leaving axial extension, out of plane shear and bending, twist, and out of plane moment joint loads.

Solution Comparison

The tip displacements are compared by taking the average displacements of joint 7 and joint 14, which are the top and bottom joints of the right most plate and percent differences with respect to isotropic case are presented in parenthesis. Example tables of displacements are given below for thin and thick bending type plates, with drilling membrane type.

Test 1

Average Tip Displacements for Rectangular Thick Plates With Drilling Membrane

Load Case	Output Parameter	Isotropic	Orthotropic 90	Orthotropic 45	Orthotropic 11
1. Axial Extension	U1 (in)	3.00E-05	3.00E-05	3.00E-05	3.00E-05
2. In Plane Shear and Bending	U3 (in)	1.06E-01	1.06E-01	1.06E-01	1.06E-01
3. Out of Plane Shear and Bending	U2 (in)	4.32E-01	4.32E-01	4.32E-01	4.32E-01
4. Twist	U2 (in)	2.94E-03	2.94E-03	2.94E-03	2.94E-03

Load Case	Output Parameter	Isotropic	Orthotropic 90	Orthotropic 45	Orthotropic 11
5. In Plane Moment	U1 (in)	8.89E-04	8.8E-04	8.89E-04	8.89E-04
6. Out of Plane Moment	R3 (rad)	3.60E-02	3.60E-02	3.60E-02	3.60E-02

Average Tip Displacements for Rectangular Thin Plates With Drilling Membrane

Load Case	Output Parameter	Isotropic	Orthotropic 90	Orthotropic 45	Orthotropic 11
1. Axial Extension	U1 (in)	3.00E-05	3.00E-05	3.00E-05	3.00E-05
2. In Plane Shear and Bending	U3 (in)	1.06E-01	1.06E-01	1.06E-01	1.06E-01
3. Out of Plane Shear and Bending	U2 (in)	4.32E-01	4.32E-01	4.32E-01	4.32E-01
4. Twist	U2 (in)	2.24E-03	2.24E-03	2.24E-03	2.24E-03
5. In Plane Moment	U1 (in)	8.89E-04	8.89E-04	8.89E-04	8.89E-04
6. Out of Plane Moment	R3 (rad)	3.60E-02	3.60E-02	3.60E-02	3.60E-02

All of the remaining results (parallelogram, triangular for thin and thick plate types and with the drilling and bilinear membrane types) match exactly.

Test 2

Average Tip Displacements for Rectangular Thin Plates With Drilling Membrane

Load Case	Output Parameter	Isotropic	Orthotropic 90	Orthotropic 0
1. Axial Extension	U1 (in)	3.00E-05	3.00E-05	3.00E-05
3. Out of Plane Shear and Bending	U2 (in)	4.32E-01	4.32E-01	4.32E-01
4. Twist	U2 (in)	2.24E-03	2.24E-03	2.24E-03
6. Out of Plane Moment	R3 (rad)	3.6E-02	3.6E-02	3.6E-02

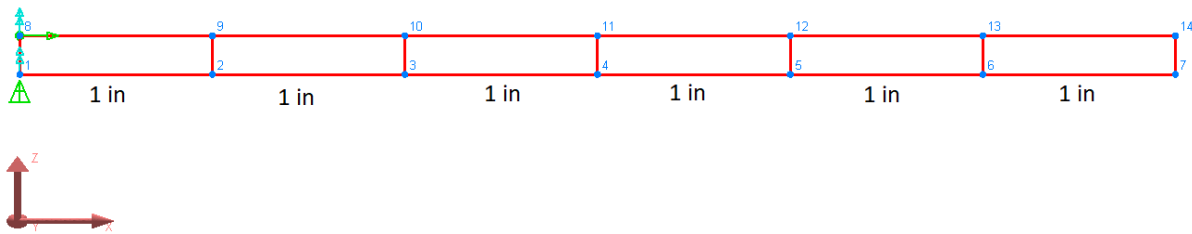
For the thin and thick plane bending type, all the results match (both bilinear and with drilling) except for the twist load case result. There is maximum 0.1% difference with respect to isotropic results in twist case. This difference is due to having greater stiffness in the transverse direction so the orthotropic models become a little bit stiffer than the isotropic ones.

L33: Cantilever with Orthotropic Material

A cantilever structure having orthotropic material properties is subjected to axial extension, in plane shear and bending, out of plane shear and bending, twist, in plane moment and out of plane moment joint loads.

Problem Description

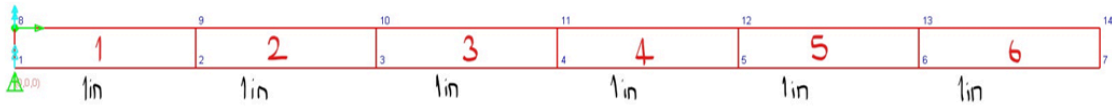
The tip joint displacements of this cantilever structure are evaluated. The analysis is done for different plate shapes including rectangular, parallelogram, trapezoidal, and triangular. Thin and thick bending types and bilinear and drilling membrane types are compared. The problem geometry and support conditions are the same as in Sample L32 (page 137).



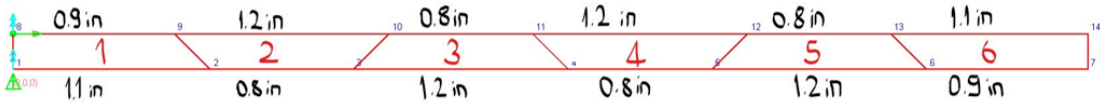
Model Geometry

Four different shapes are used for comparison: rectangular, trapezoidal, parallelogram, and triangular with the geometric properties as:

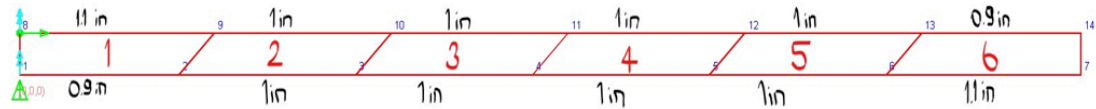
a. Rectangular



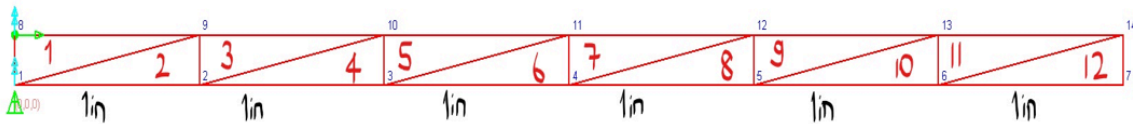
b. Trapezoidal



c. Parallelogram



d. Triangular



Different Shapes and Their Properties

Material properties are:

$$E11 = 30,000 \text{ kip/in}^2$$

$$E22 = 15,000 \text{ kip/in}^2$$

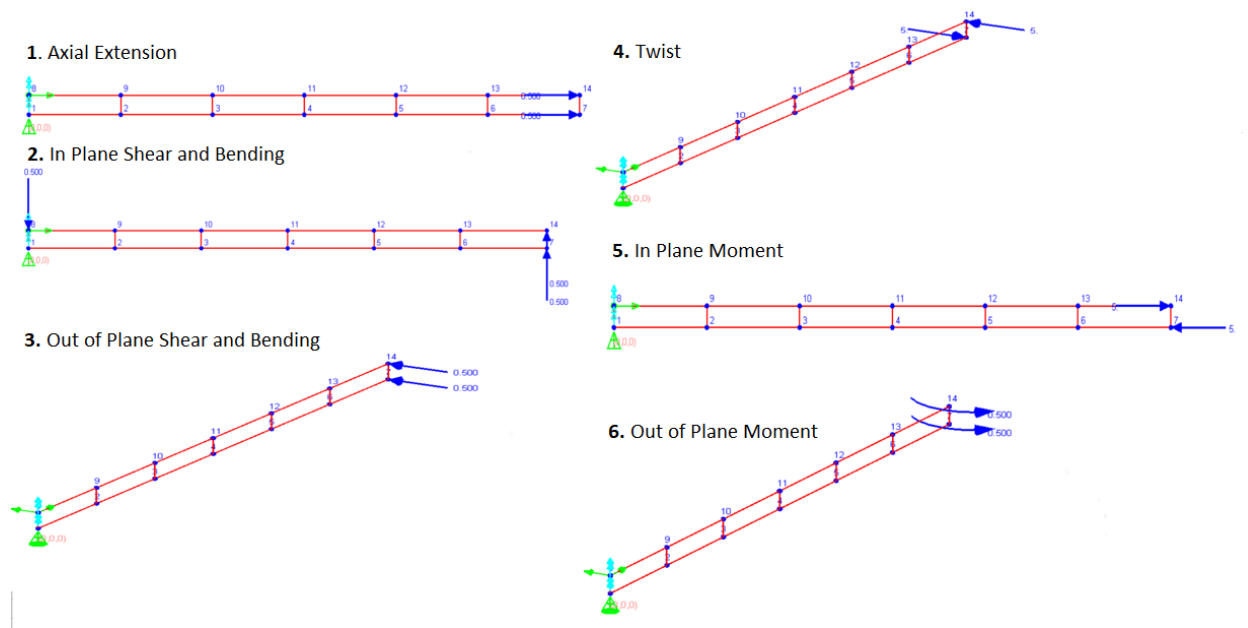
$$G12 = 6,600 \text{ kip/in}^2$$

$$G13 = 11,693 \text{ kip/in}^2$$

$$G22 = 11,693 \text{ kip/in}^2$$

$$\text{Poisson's Ratio } \nu_{12} = 0.2$$

The load magnitudes of the axial extension, in plane shear and bending, out of plane shear and bending joint loads are 0.5 lb. Twist and in plane moment loads are 5 lb and out of plane moment is 0.5 lb-in in magnitude. The joint loads are shown below:



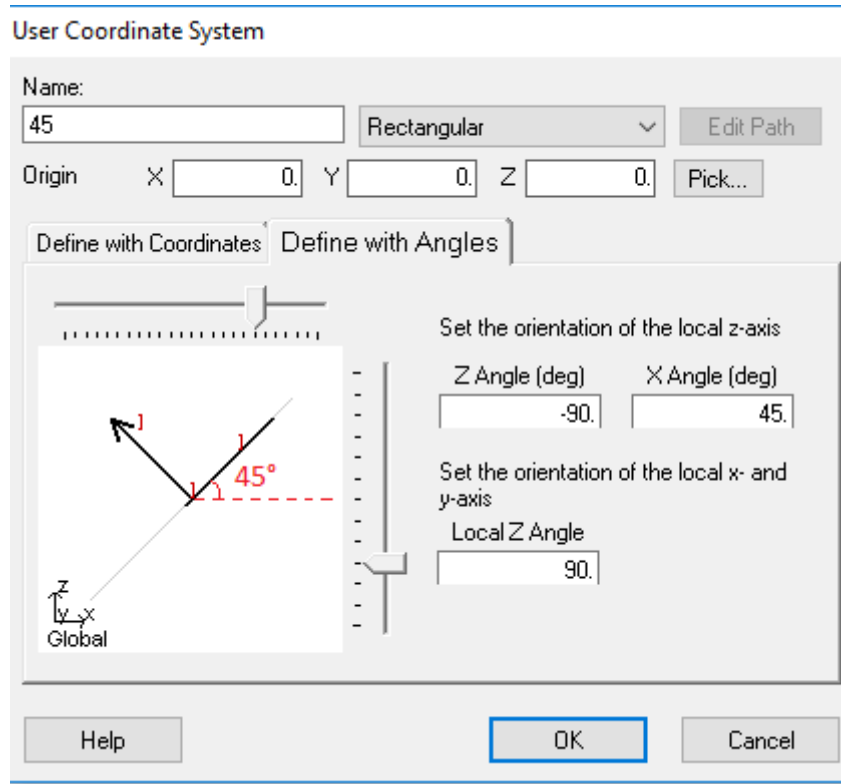
Loading Conditions

Material axes are configured using the Material UCS parameter of the materials, as shown below. Since the orientation of the material axes are determined only by the Material UCS and not by the geometry of the element, there is no need to make any changes to have the material axes of the elements be aligned.

Properties: Orthotropic Material Properties										
Materials \ Sections \ UCS \ Spring Properties \ Isolator Definitions \ Material Time Effects \ Temperature Curve \										
Basic Properties \ More Properties \ Orthotropic Properties										
	Name	Anisotropy	Material UCS	Modulus of Elasticity E11	Modulus of Elasticity E22	Poisson's Ratio m12	Shear Modulus G12	Shear Modulus G13	Shear Modulus G23	Assigned
1	Orthotropic 90	Orthotropic	90	3.0000e7	1.5000e7	0.2000	6.6000e6	1.1693e7	1.1693e7	Yes
2	Orthotropic 45	Orthotropic	45	3.0000e7	1.5000e7	0.2000	6.6000e6	1.1693e7	1.1693e7	Yes
3	Orthotropic 11	Orthotropic	11	3.0000e7	1.5000e7	0.2000	6.6000e6	1.1693e7	1.1693e7	Yes
4										

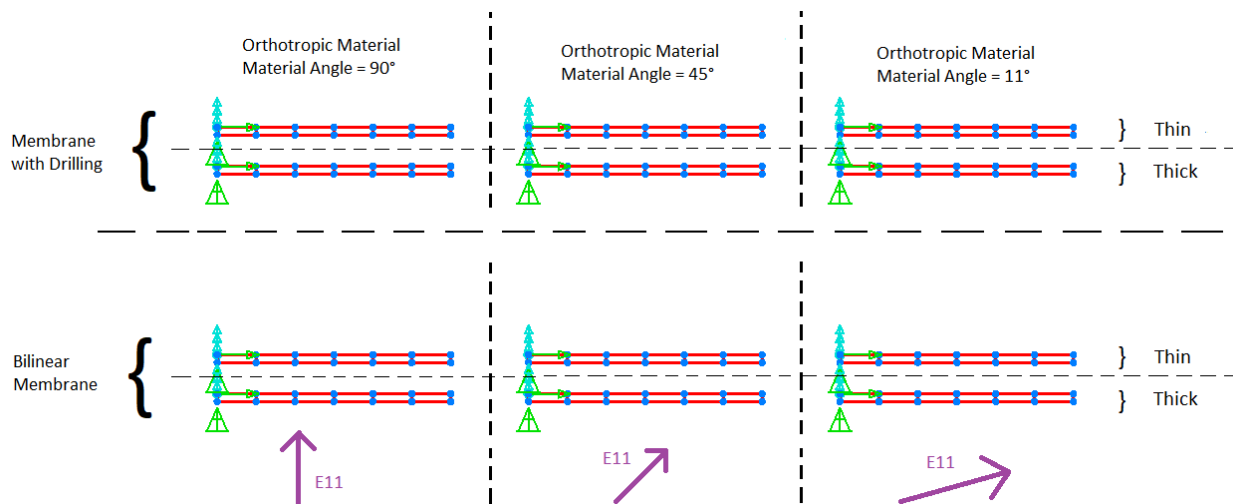
Material Definitions

As an example, to obtain a $\theta=45^\circ$ material angle, the material's local X axis needs to be rotated 45 degrees in counter-clockwise direction. To obtain this material axis orientation, a UCS configuration can be given as:



UCS of 45° Material Angle Plate

Different bending and membrane types are tested for all of the shapes separately, which makes 12 different models for the quadrilateral shapes and 6 different models for the triangular shape, which are laid out as:



Models for the Rectangular Plate

Triangular elements only support the Constant Strain Triangle membrane behavior.

For the in plane load cases axial extension, in plane shear and bending and in plane moment, only the membrane behavior of the plate element is relevant. And for out of plane shear and bending, twist, and out of plane moment, only the plate bending behavior is relevant.

Solution Comparison

The tip displacements are compared to SAP2000 V21 results by taking the average displacements of joint 7 and joint 14, which are the top and bottom joints of the right-most plate.

Example comparison table of displacements can be seen below for 11 degree material angle rectangular plate for thin bending type and bilinear membrane type:

Load Case	Output Parameter	LARSA 4D	SAP2000	Percent Difference
1. Axial Extension	U1 (in)	1.06E-05	1.06E-05	0.0%
2. In Plane Shear and Bending	U3 (in)	5.28E-03	5.28E-03	0.0%
3. Out of Plane Shear and Bending	U2 (in)	1.53E-01	1.53E-01	0.0%
4. Twist	U2 (in)	5.64E-03	5.64E-03	0.0%
5. In Plane Moment	U1 (in)	4.39E-05	4.39E-05	0.0%
6. Out of Plane Moment	R3 (rad)	1.27E-02	1.27E-02	0.0%

Example comparison table of displacements for triangular mesh can be seen below for 11 degree material angle plate for thin bending type and bilinear membrane type:

Load Case	Output Parameter	LARSA 4D	SAP2000	Percent Difference
1. Axial Extension	U1 (in)	1.06E-05	1.06E-05	0.0%
2. In Plane Shear and Bending	U3 (in)	2.03E-03	2.03-03	0.0%
3. Out of Plane Shear and Bending	U2 (in)	1.52E-01	1.52E-01	0.0%
4. Twist	U2 (in)	5.52E-03	5.52E-03	0.0%
5. In Plane Moment	U1 (in)	1.66E-05	1.66E-05	0.0%
6. Out of Plane Moment	R3 (rad)	1.27E-02	1.27E-02	0.0%

LARSA 4D's bilinear membrane behavior matched SAP 2000's plane stress plate element exactly for all shape types, material angles, and in-plane loading conditions. On the other hand, there are up to 35% difference between LARSA 4D's drilling membrane behavior and SAP 2000's shell elements for meshes with trapezoidal and parallelogram

elements. Similar differences can also be observed from the comparison of isotropic material behavior given in L18 (page 63).

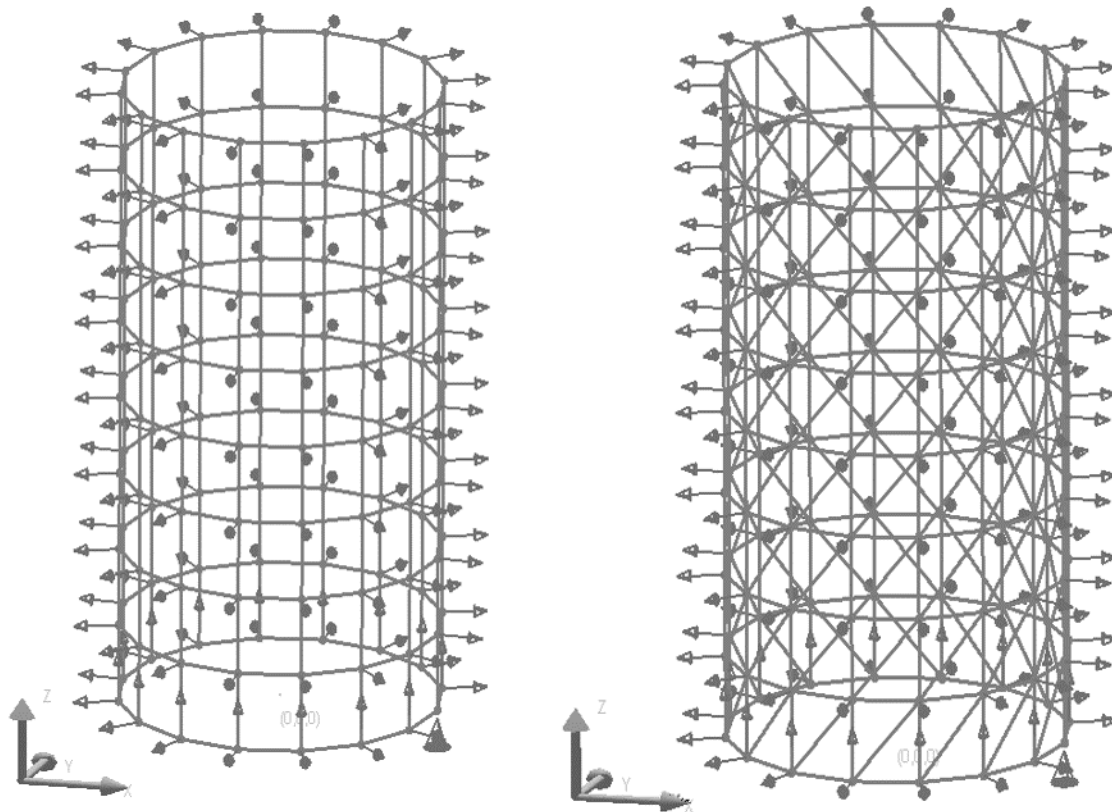
LARSA 4D's thin plate bending behavior matched SAP 2000's thin shell element exactly for all shape types, material angles, and out-of-plane loading conditions. LARSA 4D's thick plate bending behavior matched SAP 2000's thick shell element with insignificant differences (0-1.5%) in out-of-plane shear, bending, and moment (but not twist) for all shape types and material angles. In the thick plate twist cases, significant differences between LARSA 4D and SAP 2000 were found. However, LARSA 4D's thick plate has comparable results to LARSA 4D's thin plate in all twist cases, and in many cases the LARSA 4D results and the SAP 2000 results are believed to be equidistant from the true solution which indicates the current mesh density is not sufficient to represent the deformed shape for twisting.

L35: Plate Initial Strain Load

A cylinder is analyzed for a 25°F uniform temperature load. The same loading is also represented by an equivalent initial strain load applied to the plate elements. Displacements in vertical direction and plate internal forces are compared.

Problem Description

The cylinder is 200 inches tall and has a 60 inch radius. The wall thickness is 1 inch. Geometry of the structure is the same as the 8x16 model discussed in sample L20 (page 75) except the support conditions.



Model Geometry

Material properties are:

$$E = 29,000 \text{ kip/in}^2$$

$$\text{Poisson's Ratio} = 0.0$$

$$G = 14,500 \text{ kip/in}^2$$

$$\text{Thermal Expansion Coef.} = 6.5 \times 10^{-6} \text{ 1/}^\circ\text{F}$$

The displacement directions of all joints are oriented such that axis 1 points radially outward and axis 3 points upward. The joints at the base of the cylinder are restrained against translation in the local 1 and 3 directions but one of them is restrained in local 2 direction also. All the other joints are restrained against translation in the local 1 direction only. The local axes of all the shells are oriented such that axis 3 points radially outward and axis 2 points upward.

The structure is subjected to 25°F uniform temperature change. This temperature change load is also in a separate model represented by an equivalent strain load of 1.625×10^{-4} (computed as the coefficient of thermal expansion times the temperature change) on each plate element in both local x and y directions.

Solution Comparison

Solutions are compared for the Bilinear, Incompatible, and Drilling plate membrane behaviors and the MITC4 behavior for quadrilateral elements and the Bilinear membrane behavior for triangular elements. (Since the loading is related to in plane behavior only, only membrane behavior is considered.) The thermal load and the initial strain load are also compared.

The top displacement and the plate internal forces are compared from any of the joint at top and any of the plate, respectively.

Quadrilateral Bilinear Plate

Parameter	Uniform Temperature	Initial Strain
local U_3 (in)	0.0325	0.0325
F_{11} (lb/in)	-4712.50	-4712.50

Quadrilateral Incompatible Plate

Parameter	Uniform Temperature	Initial Strain
local U_3 (in)	0.0325	0.0325
F_{11} (lb/in)	-4712.50	-4712.50

Quadrilateral Drilling Plate

Parameter	Uniform Temperature	Initial Strain
local U_3 (in)	0.0325	0.0325
F_{11} (lb/in)	-4712.50	-4712.50

Quadrilateral MITC4 Plate

Parameter	Uniform Temperature	Initial Strain
local U_3 (in)	0.0325	0.0325
F_{11} (lb/in)	-4712.50	-4712.50

Triangular Bilinear Plate

Parameter	Uniform Temperature	Initial Strain
local U_3 (in)	0.0325	0.0325
F_{11} (lb/in)	-4712.50	-4712.50

Initial strain case results match with the uniform temperature load case results for all models, perfectly.

The same example is repeated by using staged construction analysis. The total initial strain is applied within two separate stages in such a way that half strain is applied in both stages (i.e. 1/2 in first stage and the remaining 1/2 in the next stage). At the end of the final stage, the same displacements and internal forces are obtained.

Samples for Nonlinear Elastic Static Analysis

These samples provide an overview of the nonlinear elastic static analysis.

N01: Tie Beam with Geometric Stiffening	157
Solution Comparison	158
Reference	158
N02: Cable with Hanging Loads	159
Solution Comparison	159
N03: Beam on an Elastic Soil Foundation	161
Solution Comparison	161
Reference	162
N04: Truss with Misaligned Supports - Nonlinear Static	163
Solution Comparison	163
N05: Nonlinear Analysis of Cable Roof	165
Solution Comparison	165
N06: Diamond Shaped Frame - Geometric Nonlinear	167
Reference	168
Solution Comparison	168
N07: Diamond Shaped Frame - Geometric Nonlinear - Incremental Joint Displacement Loading	169
Reference	170
Solution Comparison	170
N08: A High Arch Structure - Geometric Nonlinear	171
Solution Comparison	172
Reference	172
N09: Thermal Expansion to Close a Gap	173
Solution Comparison	173
N13: Straight Cantilever Girder with Nonlinear Shell Elements in Membrane Action	175
Problem Description	175
Solution Comparison	176
References	177

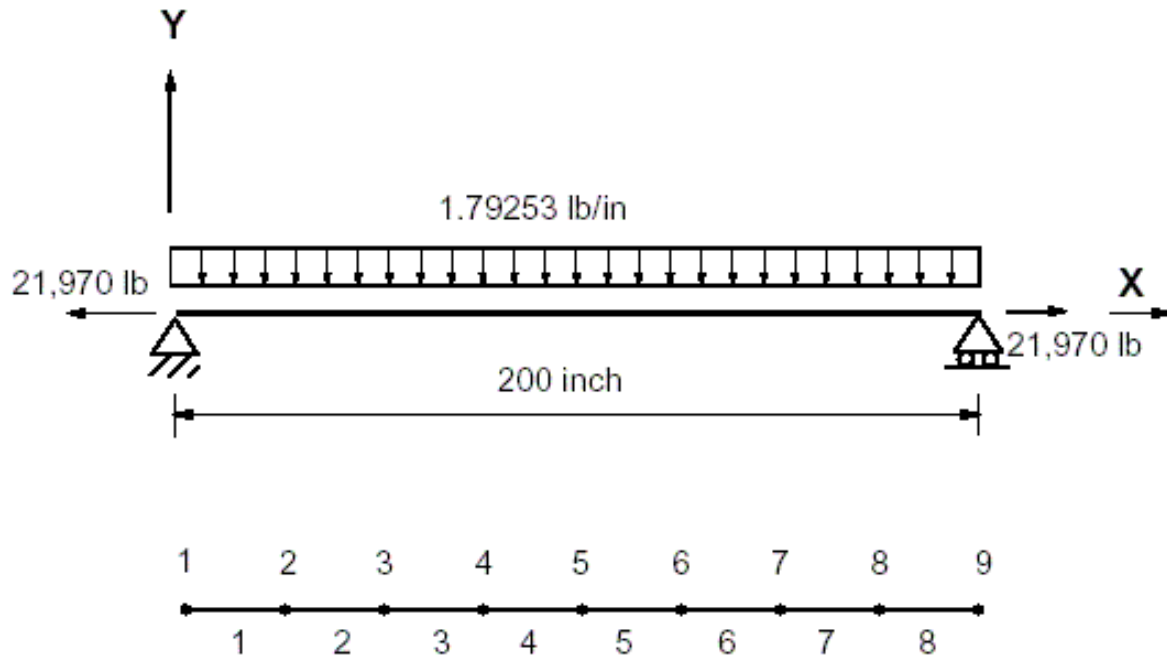
N14: Straight Cantilever Girder with Nonlinear Shell Elements in Plate Action	179
Problem Description	179
Solution Comparison	180
References	181
N15: Slit Annular Plate with Vertical Load	183
Problem Description	183
Solution Comparison	184
References	185
N22: Rail-Structure Interaction (RSI) under thermal loads	187
Background	187
Model	187
Solution and comparison	188
References	190

N01: Tie Beam with Geometric Stiffening

A tie beam is subjected to the action of a tensile force and a uniform lateral load. The tensile force is 21,970 lb and the uniform lateral load is 1.79258 lb/in. The beam is steel and has a square section of 2.5 in by 2.5 in.

Determine the maximum deflection, maximum bending moment and the slope at the lefthand support. In this sample, the effect of geometric stiffening is included by using nonlinear static analysis and compare the results to those in problem 10 where the geometric nonlinearity is ignored. Also, for this sample problem, two different finite models are created to see the behavior of beam element and nonlinear shell element (MITC4), separately.

Example Project: The example described here can be found in the Nonlinear Elastic Static folder of your LARSA 4D Samples directory (generally My Documents\LARSA Projects\Samples) in the file N01.



Sample N01

The first model has 9 joints and 8 beam elements. The second one has 18 joints and 8 shell elements. The tensile force is specified as an external force acting at joint 9 for the first model and joint 17 and joint 18 for the second model. The uniform load is specified as an external beam loading and external plate loading for the first and second model, respectively. For the second model, shells are placed in out of plane action. Also, as plate and membrane type, MITC4 is used to get nonlinear behavior.

Modulus of Elasticity = 30,000,000 lb/in²

Span = 200 inches

A = 6.25 in²

I_{zz} = 3.2552 in⁴

Uniform Load = 1.79253 lb/in

Tensile Force S = 21,970 lb

Nonlinear static analysis is performed using one (1) load step and maximum of 20 iterations.

Solution Comparison

	Timoshenko	Beam	Shell
Vertical Disp @ Node 5 (in)	-0.200	-0.1995	-0.1970
Rotation @ Joint 1(rad)	-0.0032352	-0.003236	-0.003218
Moment @ I-end of Beam 5(in-lb)	-4579.91	-4580.29	-4514.73

The nonlinear static analysis includes the geometric stiffening effect of the beam. For comparison of results to the linear static analysis, refer to the previous problem.

Reference

- Timoshenko, S., "Strength of Materials, Part II", 3rd Edition, D. Van Nostrand Co., Inc., New York, p. 42.

For More Information, please refer to the following documentation.

- For help on Nonlinear Elastic Static analysis, see Nonlinear Static Analysis in *LARSA 4D Reference Manual*.

N02: Cable with Hanging Loads

The cable supports three vertical loads. The area of the cable is 0.1 ft². The elastic modulus of the cable is 200,000 kips/ft².

Determine the reaction forces and the maximum tension in the cable.

Example Project: The example described here can be found in the Nonlinear Elastic Static folder of your LARSA 4D Samples directory (generally My Documents\LARSA Projects\Samples) in the file N02.

The model has 5 joints and 4 cable elements. A small tensile force

Sample 12

is specified as prestress force to give initial stiffness to the cable.

Modulus of Elasticity = 200,000 kips/ft²

A = 0.10 ft²

Initial Tensile Force = .10 kips

Solution Comparison

Sources:

- LARSA 4D
- Beer and Johnston, page 260.

	LARSA	Beer
Reaction Ax (kips)	-17.89	-17.9
Reaction Az (kips)	+5.03	+5.03
Reaction Bz (kips)	16.97	16.97
Max Cable Tension (kips)	24.66	24.70

The tension in the cable varies from 17.9 kips (element # 2) to 24.7 kips (element # 4).

For More Information, please refer to the following documentation.

- For help on Nonlinear Elastic Static analysis, see Nonlinear Static Analysis in *LARSA 4D Reference Manual*.

N03: Beam on an Elastic Soil Foundation

A 30-inch long beam rests on an elastic foundation. The beam is 3 inches wide and 1 inch deep. The soil is active in compression only. The foundation modulus is 5000 lb/cubic inch. A concentrated load of 8000 lbs is applied at the midspan of the beam. For this sample problem, two different finite models are created to see the behavior of beam element and nonlinear shell element (MITC4), separately.

Determine the midspan displacement and the contact length of the beam.

Example Project: The example described here can be found in the Nonlinear Elastic Static folder of your LARSA 4D Samples directory (generally My Documents\LARSA Projects\Samples) in the file N03.

Sample N03

The material and section property data of the beam are:

Modulus of Elasticity = 30,000,000 lb/in²

Poisson's Ratio = 0.00

I_{zz} = 0.25 in⁴

A = 3 in²

There are two models which are modeled with different element types. The first model has **beam and compression-only foundation spring elements**. The second model has **shell and compression-only foundation spring elements**. Due to symmetry, only one half of the structure is modeled.

The beam is divided into 10 equal length beam and shell elements for first and second model, respectively. The foundation is modeled using the compression-only foundation spring elements. The spring constant (K) is taken as foundation modulus times the beam width times the spacing between the springs.

$K = (\text{Foundation Modulus}) \times \text{Contact Area}$

$K = 5000 \times 3 \times 1.5$

$K = 22,500 \text{ lb/in.}$

Solution Comparison

The results for the displacement under the load and the extent of the contact are compared to the exact solution by Heteyni and to the solution from NISA.

The displacement reported is in the direction of the load (-Z direction) at the point of application of the load and the results are in inches.

The contact length is computed by linear interpolation of the vertical displacement over the beam segment in which the deflection changes sign.

	Heteyni	NISA	Beam	Shell
Displacement	0.043480	0.043478	0.043478	0.044193
Half length of contact	10.505	10.546	10.546	10.534

The comparison of the results is excellent.

Reference

- Faten F. Mahmoud, N.J. Slamon and W.R. Marks, "A Direct Automated Procedure for Frictionless Contact Problems", *International Journal of Numerical Methods Eng.*, 18 (1982), pp. 245-257.
- M. Heteyni, "Beams on Elastic Foundation", University of Michigan Press, Ann Arbor, Michigan, 1967.
- NISA, Verification Problems Manual, EMRC, 1990

For More Information, please refer to the following documentation.

- For help on Nonlinear Elastic Static analysis, see Nonlinear Static Analysis in *LARSA 4D Reference Manual*.

N04: Truss with Misaligned Supports - Nonlinear Static

A 1000 inch span truss has six flexible supports. The four interior supports are misaligned. The truss is subjected to four point loads at the lower chord.

Determine the vertical displacements at the joints along the bottom chord of the truss and the final gap widths.

Example Project: The example described here can be found in the Nonlinear Elastic Static folder of your LARSA 4D Samples directory (generally My Documents\LARSA Projects\Samples) in the file N04.

Sample N04

Truss elements of constant cross section are used to model the structure. The material and section property of the truss is:

Modulus of Elasticity = 30,000,000 lb/in²

Poisson's Ratio = 0.00

Area = 10 in²

The misalignments of the interior supports are modeled using compression-only foundation spring with built-in gap element.

K = 1,000,000 lb/in

Gap Distance @ Joint 2= 0.80 inch

Gap Distance @ Joint 3= 0.90 inch

Gap Distance @ Joint 4= 1.20 inch

Gap Distance @ Joint 5= .50 inch

The exterior supports have no misalignment and the gap distance is specified as zero.

K = 1,000,000,000 lb/in

The joint at the top center of the truss is restrained from moving in the horizontal direction. Only the vertical movement is allowed at the center supports.

Concentrated forces of 40,000 lbs each are applied at the interior joints of the bottom chord of the truss.

Solution Comparison

Joint Displacements (inch)

Sources:

- W.R. Marks, "Solution of Frictionless Contact Problems by a Conjugate Gradient Technique," M.Sc. Thesis, University of Wisconsin, Milwaukee (1979).
- EMRC, "NISA II Verification Problems Manual", 1991.

• LARSA 4D

	Marks	EMRC	LARSA
X Displacement			
Node 2	-0.11801		-0.11779
Node 3	-0.03822		-0.03823
Node 4	-0.05359		-0.05361
Node 5	0.12368		0.12340
Z Displacement			
Node 2	-0.59902		-0.59902
Node 3	-0.91924		-0.91926
Node 4	-0.90721		-0.90722
Node 5	-0.53625		-0.53627
Extent of Gap (inch)			
Node 2 InitialGap=0.8	No Contact	No Contact	No Contact
Node 3 InitialGap=0.9	-0.019241	-0.019241	-0.01926
Node 4 InitialGap=1.2	No Contact	No Contact	No Contact
Node 5 InitialGap=0.5	-0.036254	-0.036254	-0.036266
Interior Support Reaction Forces (kips)			
Node 2	0	0	0
Node 3	19.24	19.24	19.26
Node 4	0	0	0
Node 5	36.25	36.25	36.27

For More Information, please refer to the following documentation.

- For help on Nonlinear Elastic Static analysis, see Nonlinear Static Analysis in *LARSA 4D Reference Manual*.

N05: Nonlinear Analysis of Cable Roof

An orthogonal cable network with hyperbolic paraboloid shape is subjected to point loads.

Determine the displacements.

Example Project: The example described here can be found in the Nonlinear Elastic Static folder of your LARSA 4D Samples directory (generally My Documents\LARSA Projects\Samples) in the file N05.

Sample N05

The roof is modeled by a finite element mesh of 80 cable elements and 41 joints. The joints on the outer boundary are fixed.

The material and sectional properties of the cables are:

Modulus of Elasticity = 24,000,000 lb/in²

Area = 1.0 in²

Solution Comparison

Vertical Displacement in negative Z Direction (feet)

Sources:

- LARSA 4D
- G.R. Monforton and N.M. El-Hakim, "Analysis of Truss- Cable Structures", Computers & Structures,
- EMRC, "NISA II Verification Problems Manual", 1991.

	LARSA	Monforton	EMRC
Joint 1	0.440	0.441	0.443
Joint 3	1.370	1.371	1.367
Joint 7	3.752	3.752	3.719
Joint 13	1.669	1.669	1.671
Joint 19	0.961	0.962	0.969
Joint 23	0.559	0.561	0.567
Joint 25	0.223	0.224	0.228
Joint 26	0	0	0
Joint 34	0	0	0

The LARSA results are in excellent agreement with the energy search solution of Ref [1] and they are in good agreement with the NISA computer program results.

For More Information, please refer to the following documentation.

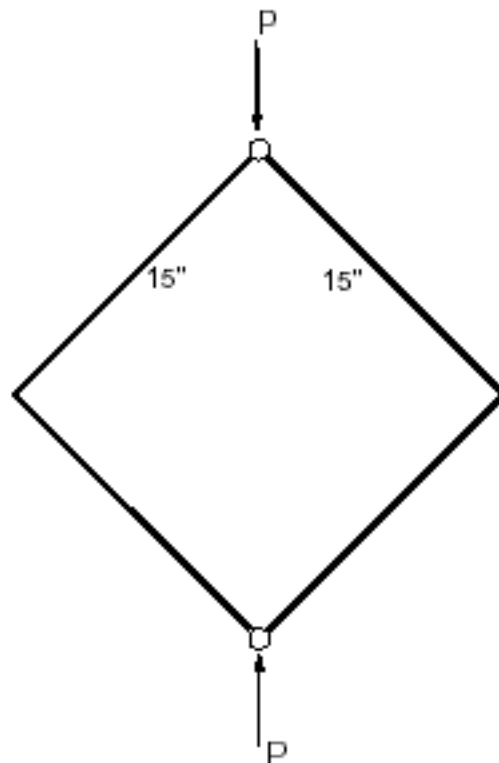
- For help on Nonlinear Elastic Static analysis, see Nonlinear Static Analysis in *LARSA 4D Reference Manual*.

N06: Diamond Shaped Frame - Geometric Nonlinear

A large diamond shape structure with two pin joints and two rigid joints is subjected to a compressive load at the two opposite corners.

Determine the load-displacement curve at the point of load application for applied load up to 40,000 lbs.

Example Project: The example described here can be found in the Nonlinear Elastic Static folder of your LARSA 4D Samples directory (generally My Documents\LARSA Projects\Samples) in the file N06.



Sample N06

The material properties for the frame are:

Modulus of Elasticity = 30,000,000 psi

Poisson's Ratio = 0.0

Shear Modulus = 15,000,000 psi

The section properties for the frame are:

$A_{xx} = 1.0 \text{ in}^2$

$I_{yy} = 0.083333 \text{ m}^4$

$l_{zz} = 0.08333 \text{ m}^4$

In primary load case 1, point loads of 1,000 lbs each are applied at the top and bottom points of the frame.

$F1-Z = -1,000 \text{ lb}$

$F3-Z = +1,000 \text{ lb}$

20 equal load increments are defined for computing the load-deflection behavior of the structure from $P = 2,000$ to $P = 40,000$ lbs. The load-deflection option is used in defining the load combination data.

The finite element model consists of 120 beam elements and 120 joints.

Reference

- T. J. R. Hughes and W. K. Lui, "Nonlinear Finite Element Analysis of Shells - Part II: Two Dimensional Shells", *Comp. Meth. Appl. Mech. Eng.*, 27 (1981), 167-181.
- EMRC, "NISA II Verification Problems Manual", 1991.

Solution Comparison

The load-displacement curves are calculated for the vertical and horizontal displacements of the structure. The vertical displacement is at the top and bottom corners of the structure. The horizontal displacement is at the mid-left and right corners of the structure.

The values computed by LARSA are in excellent agreement with the experimental results of Hughes and with the numerical results from EMRC.

For More Information, please refer to the following documentation.

- N07: Diamond Shaped Frame - Geometric Nonlinear - Incremental Joint Displacement Loading on page 169.
- For help on Nonlinear Elastic Static analysis, see Nonlinear Static Analysis in *LARSA 4D Reference Manual*.

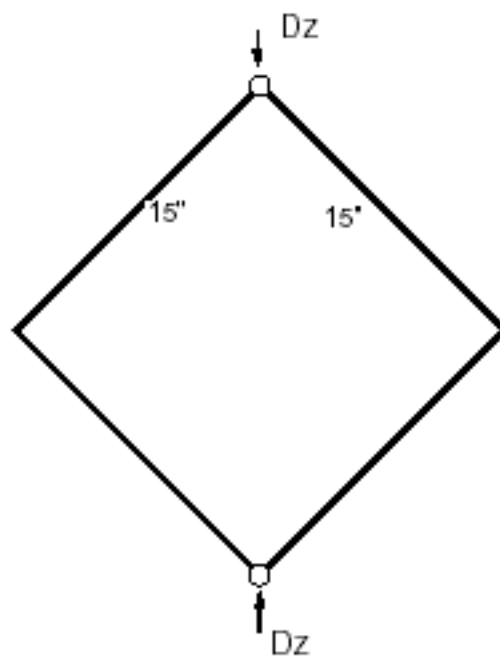
N07: Diamond Shaped Frame - Geometric Nonlinear - Incremental Joint Displacement Loading

A large diamond shape structure with two pin joints and two rigid joints is subjected to a compressive load at the two opposite corners.

Determine the load-displacement curve at the point of load application using incremental joint displacement loading.

Example Project: The example described here can be found in the Nonlinear Elastic Static folder of your LARSA 4D Samples directory (generally My Documents\LARSA Projects\Samples) in the file N07.

In N06: Diamond Shaped Frame - Geometric Nonlinear (page 167), the load-displacement behavior was computed using incremental applied joint loading.



Sample N07

The material properties for the frame are:

Modulus of Elasticity = 30,000,000 psi

Poisson's Ratio = 0.0

Shear Modulus = 15,000,000 psi

The section properties for the frame are:

$A_{xx} = 1.0 \text{ in}^2$

$I_{yy} = 0.08333 \text{ in}^4$

$I_{zz} = 0.08333 \text{ in}^4$

In primary load case 1, joint displacement loads of 1 inch each are applied at the top and bottom points of the frame.

F1-Z = -1 inch

F3-Z = +1 inch

20 equal load increments are defined for computing the load-deflection behavior of the structure. The load-deflection option is used in defining the load combination data.

The finite element model consists of 120 beam elements and 120 joints.

Reference

- T. J. R. Hughes and W. K. Lui, "Nonlinear Finite Element Analysis of Shells - Part II: Two Dimensional Shells", *Comp. Meth. Appl. Mech. Eng.*, 27 (1981), 167-181.
- EMRC, "NISA II Verification Problems Manual", 1991.

Solution Comparison

The load-displacement curves are calculated for the vertical and horizontal displacements of the structure. The vertical displacement is at the top and bottom corners of the structure. The horizontal displacement is at the mid-left and right corners of the structure.

The values computed by LARSA are in excellent agreement with the experimental results of Hughes and with the numerical results from EMRC.

For More Information, please refer to the following documentation.

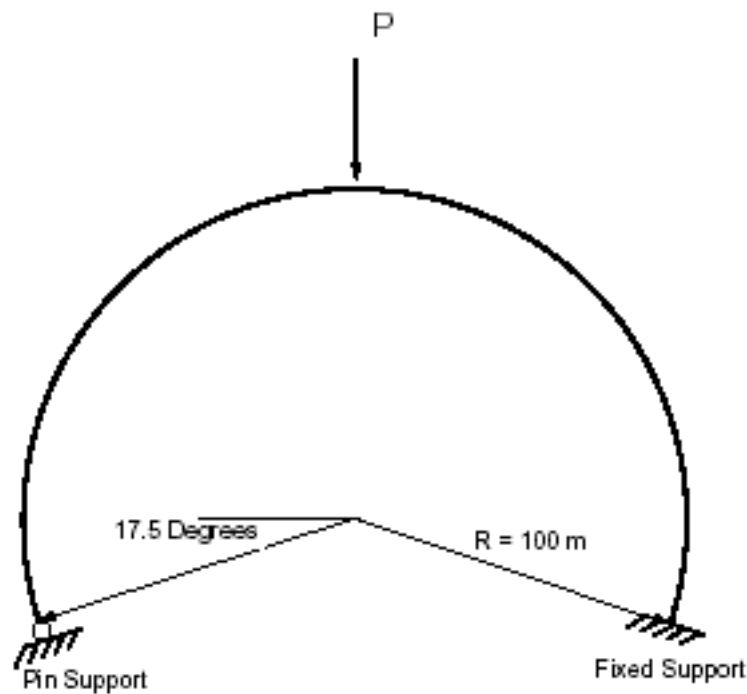
- For help on Nonlinear Elastic Static analysis, see Nonlinear Static Analysis in *LARSA 4D Reference Manual*.
- N06: Diamond Shaped Frame - Geometric Nonlinear on page 167.

N08: A High Arch Structure - Geometric Nonlinear

A high circular arch structure of radius 100 meters is subjected to a concentrated load at its midpoint. One end of the arch is a fixed support and the other end is a pinned support. For this sample problem, two different finite models are created to see the behavior of beam element and nonlinear shell element (MITC4), separately.

Determine the load-displacement behavior at the point of load application using incremental joint displacement loading.

Example Project: The example described here can be found in the Nonlinear Elastic Static folder of your LARSA 4D Samples directory (generally My Documents\LARSA Projects\Samples) in the file N08.



Sample 39

The material properties for the arch are:

Modulus of Elasticity = 12,000,000 Pa

Poisson's Ratio = 0.30

Shear Modulus = 4,603,345 Pa

The section properties for the arch are:

$A_{xx} = 1.0\text{ m}^2$

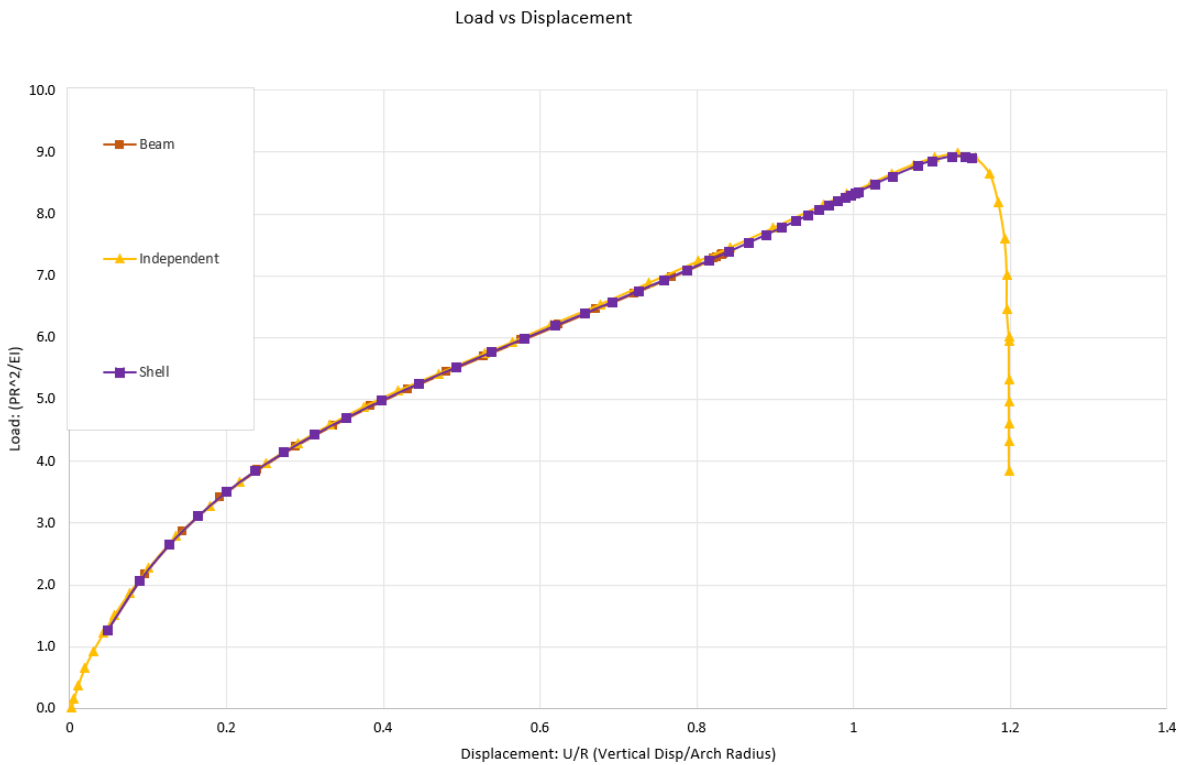
$I_{yy} = 0.08333\text{ m}^4$

$I_{zz} = 0.08333\text{ m}^4$

Two different finite element models, model A and model B are created with beam and shell elements separately. The finite element model A and B consists of 50 beam elements and 51 joints and 50 shell elements and 102 joints, respectively. Nonlinear static analysis has been performed using the load-deflection option for load combinations.

For model B, two sets of joints are used to model the shells for out-of-plane action, and all those joints are restrained in the transverse direction to eliminate the effect of the Poisson's ratio.

Solution Comparison



Load Displacement Curves

The load-displacement curves for the vertical displacements are compared with results from Zienkiewicz and EMRC. The results are in excellent agreement.

Reference

- O.C. Zienkiewicz, "The Finite Element Method", McGraw Hill Book Company, 1977.
- EMRC, "NISA II Verification Problems Manual", 1991.

For More Information, please refer to the following documentation.

- For help on Nonlinear Elastic Static analysis, see Nonlinear Static Analysis in *LARSA 4D Reference Manual*.

N09: Thermal Expansion to Close a Gap

An aluminum-alloy bar is initially at a temperature of 70 degrees F. Calculate the stress in the bar after it has been heated to 170 degrees F. The supports are assumed to be rigid. There is a gap between the support and the end joint of the bar. The gap distance is 0.002 in.

Example Project: The example described here can be found in the Nonlinear Elastic Static folder of your LARSA 4D Samples directory (generally My Documents\LARSA Projects\Samples) in the file N09.

The material properties for the bar are:

Modulus of Elasticity = 10,500,000 psi

Coefficient of Thermal Expansion = 0.0000125

The section property for the bar is:

Axx = 1.0 in²

The finite element model consists of 1 truss element and 1 nonlinear foundation element with built-in gap and spring. The spring stiffness is arbitrarily selected at a high value. Nonlinear static analysis is performed.

To run this model in LARSA 4D with settings compatible with the reference software ANSYS, use Staged Construction Analysis with geometric nonlinearity turned off.

Solution Comparison

Sources:

- LARSA 4D with geometric nonlinearity turned on
- LARSA 4D with geometric nonlinearity turned off
- Swanson Analysis Systems, "ANSYS Verification Problems Manual".

	LARSA-wGN	LARSA-woGN	Swanson
Stress (psi)	-6,1338	-6,125	-6,125

The comparison of the results is excellent.

For More Information, please refer to the following documentation.

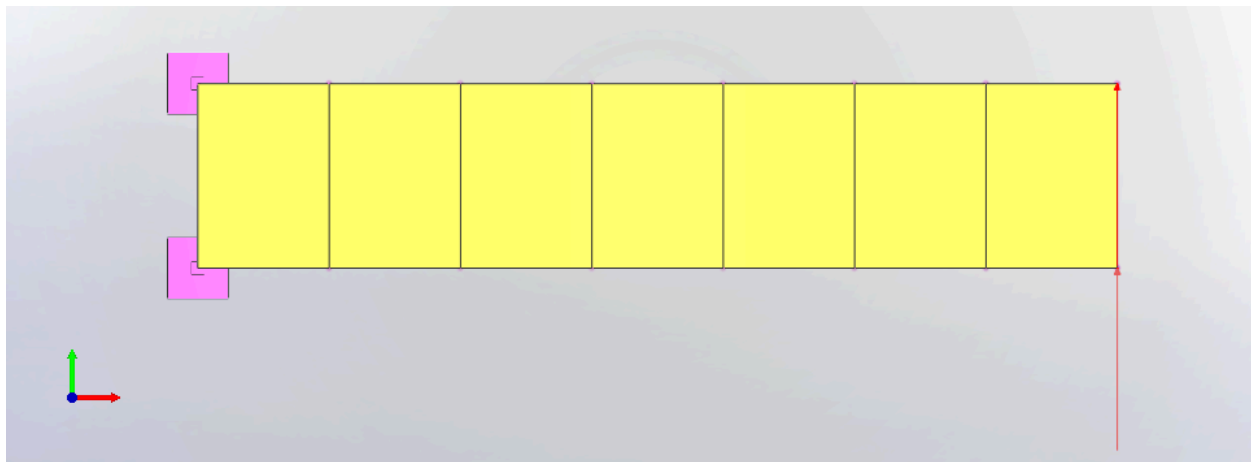
- For help on Nonlinear Elastic Static analysis, see Nonlinear Static Analysis in *LARSA 4D Reference Manual*.

N13: Straight Cantilever Girder with Nonlinear Shell Elements in Membrane Action

A straight cantilever girder described in Louie L. Yaw, 2009 with square cross-section is modeled with nonlinear shell elements. The girder is subjected to tip shearing force to get the behavior of the nonlinear shell element (MITC4) in membrane action (in-plane). Model is analyzed thanks to the large strain assumption by using **Incremental Nonlinear Static Analysis** option.

Example Project: The example described here can be found in the Nonlinear Elastic Static folder of your LARSA 4D Samples directory (generally My Documents\LARSA Projects\Samples) in the file N13.

Problem Description



Cantilever girder with tip shear force

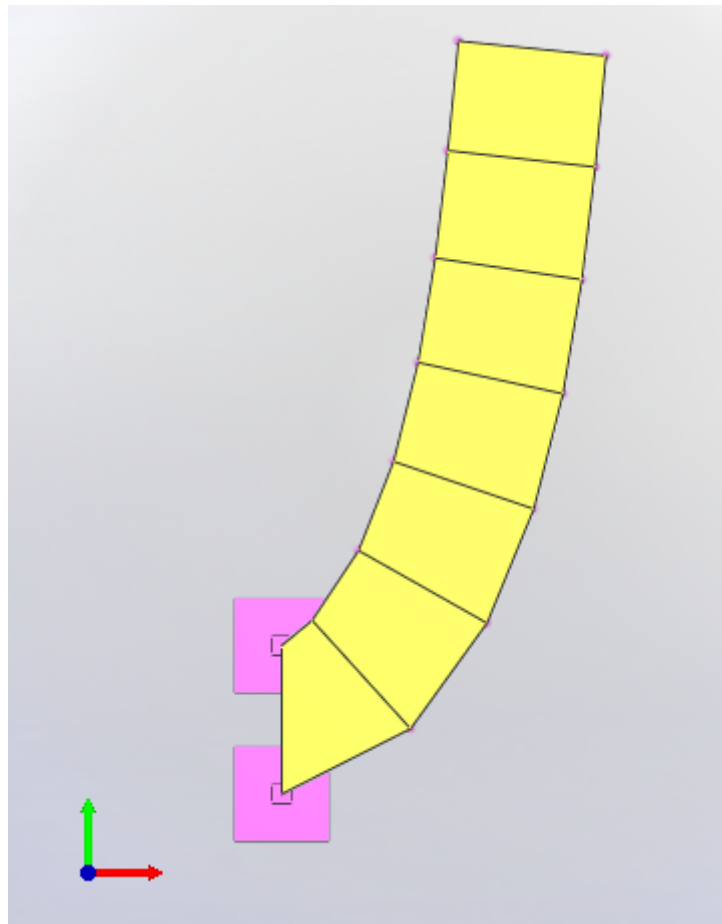
The girder consists of a total of seven nonlinear shell elements. In order to obtain the cantilever behavior; the left end of the section (17th and 25th joints) are restrained for all directions, all other joints are left free for all directions.

The cross-section has 2 ft. width and 2 ft. thickness. The total length of the girder is 10 ft.

Example material has 1800 lb/ft² elastic modulus with 0 Poisson's ratio.

The girder is modeled with shell elements. In order to get nonlinear behavior, MITC4 plate and membrane types are used.

Total 20 lbs load is divided into 40 equal load steps, and those steps are applied incrementally. Loading is applied at right end of the section (24th and 32nd joints) equally.



Deflected Shape

Solution Comparison

As a result, average lateral displacement (U_y) at the tip of the girder is obtained. For the sake of comparison, results which are given by ADINA is listed.

The results of the first 20 steps are listed below. Unit of the results is "feet".

Step	Parameter	LARSA 4D	ADINA	Difference
1	U_y	1.01	1.01	0%
2	U_y	1.96	1.96	0%
3	U_y	2.82	2.82	0%
4	U_y	3.57	3.57	0%
5	U_y	4.22	4.22	0%
6	U_y	4.77	4.77	0%

Step	Parameter	LARSA 4D	ADINA	Difference
7	U _y	5.23	5.23	0%
8	U _y	5.63	5.63	0%
9	U _y	5.97	5.97	0%
10	U _y	6.26	6.26	0%
11	U _y	6.51	6.51	0%
12	U _y	6.73	6.73	0%
13	U _y	6.93	6.93	0%
14	U _y	7.10	7.10	0%
15	U _y	7.26	7.26	0%
16	U _y	7.40	7.40	0%
17	U _y	7.53	7.53	0%
18	U _y	7.64	7.64	0%
19	U _y	7.75	7.75	0%
20	U _y	7.84	7.84	0%

References

- Yaw, L. L. (2009). 1 2D Corotational Beam Formulation.
- ADINA R&D, Inc: ADINA 9.6.0 (April 2020)

For More Information, please refer to the following documentation.

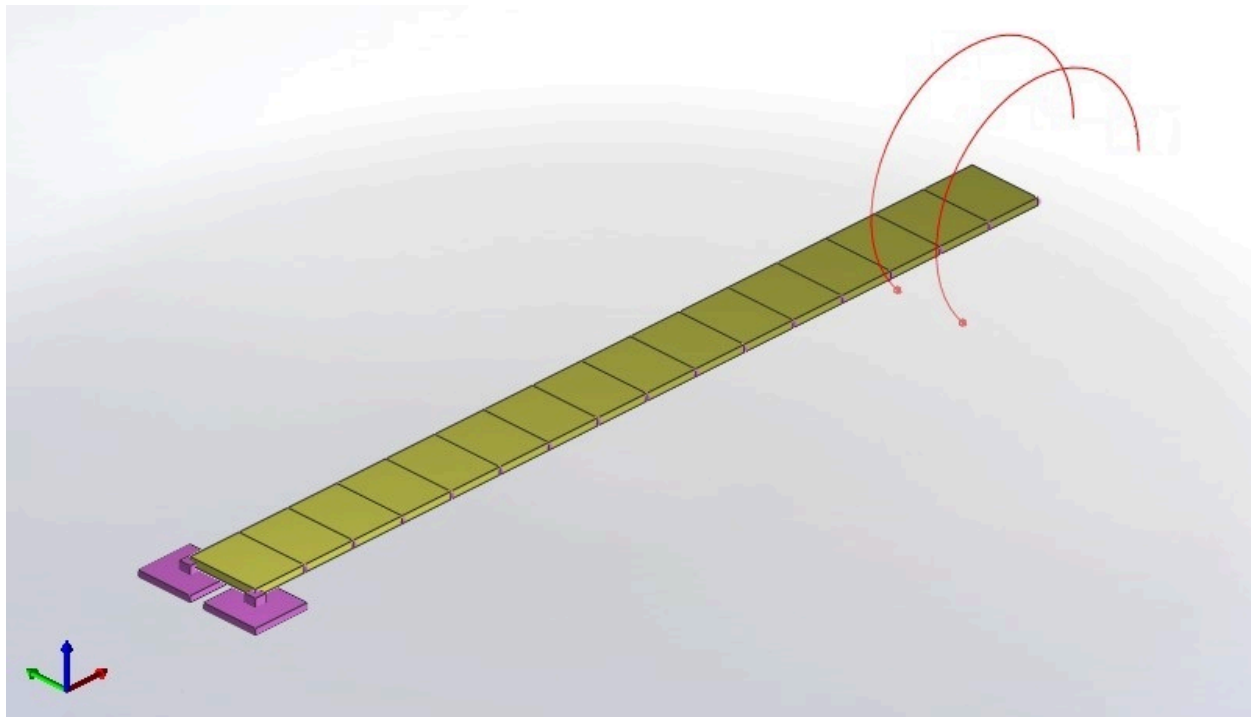
- For help on nonlinear static analysis, see Nonlinear Static Analysis in *LARSA 4D Reference Manual*.
- For help on nonlinear plate elements, see Shells in *LARSA 4D Reference Manual*.

N14: Straight Cantilever Girder with Nonlinear Shell Elements in Plate Action

A straight cantilever girder with a rectangular cross-section is modeled with nonlinear shell elements. The girder is subjected to tip moment force to get the behavior of the nonlinear shell element (MITC4) in plate action (out-of-plane). Model is analyzed thanks to the large strain assumption by using **Incremental Nonlinear Static Analysis** option.

Example Project: The example described here can be found in the Nonlinear Elastic Static folder of your LARSA 4D Samples directory (generally My Documents\LARSA Projects\Samples) in the file N14.

Problem Description



Cantilever girder with tip moment force

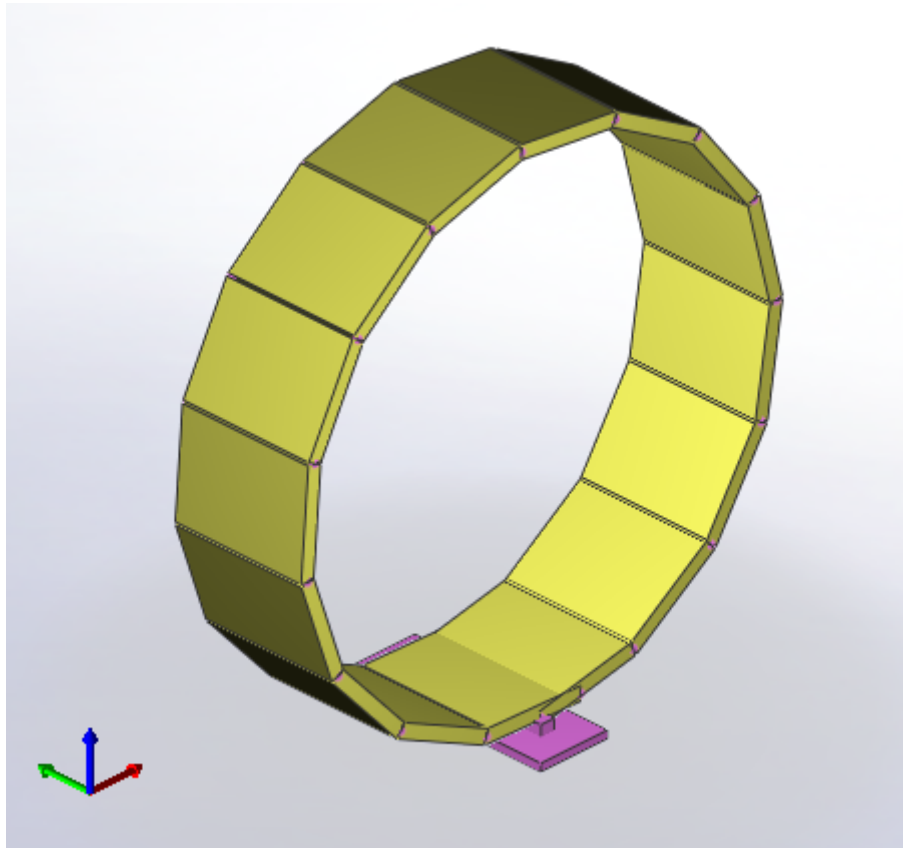
The girder consists of a total of 16 nonlinear shell elements. In order to obtain the cantilever behavior; the left end of the section (1st and 2nd joints) are restrained for all directions. In addition to that, all joints are restrained for drilling motion in the following manner. Since the displacement coordinate system of joints is the global coordinate system, the direction of the drilling degrees of freedom changes under the deformation of the model. Therefore, the model is restrained in both rotational x and z directions.

The cross-section has 1 in. width and 0.1 in. thickness. The total length of the girder is 12 in.

Example material has 1,200,000 lb/in² elastic modulus with 0 Poisson's ratio.

The girder is modeled with shell elements. In order to get nonlinear behavior, MITC4 plate and membrane types are used.

The total 52.36 lb-in load is divided into 20 equal load steps, and those steps are applied incrementally. Loading is applied at the right end of the section (33rd and 34th joints) equally.

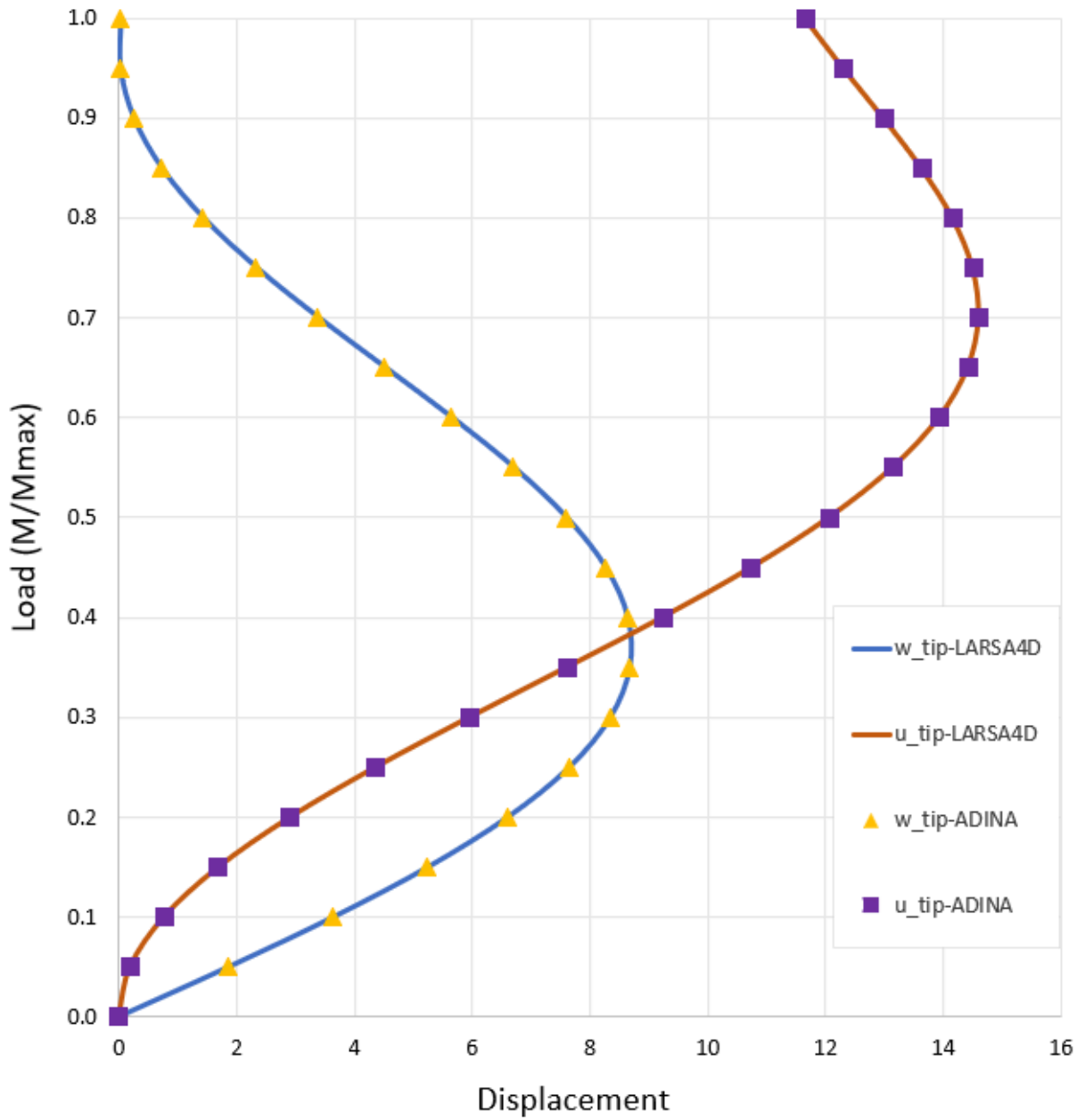


Deflected shape

Solution Comparison

As a result, average axial and vertical displacement (U_x and U_z) at the tip of the girder is obtained. For the sake of comparison, results which are given by ADINA are shown in the figure below.

Results of the 20 steps are shown below. Results are in inches.



Load deflection curves

References

- Ko, Y., Lee, P. S., & Bathe, K. J. (2017). The MITC4+ shell element in geometric nonlinear analysis. Computers & Structures, 185, 1-14.
- ADINA R&D, Inc: ADINA 9.6.0 (April 2020)

For More Information, please refer to the following documentation.

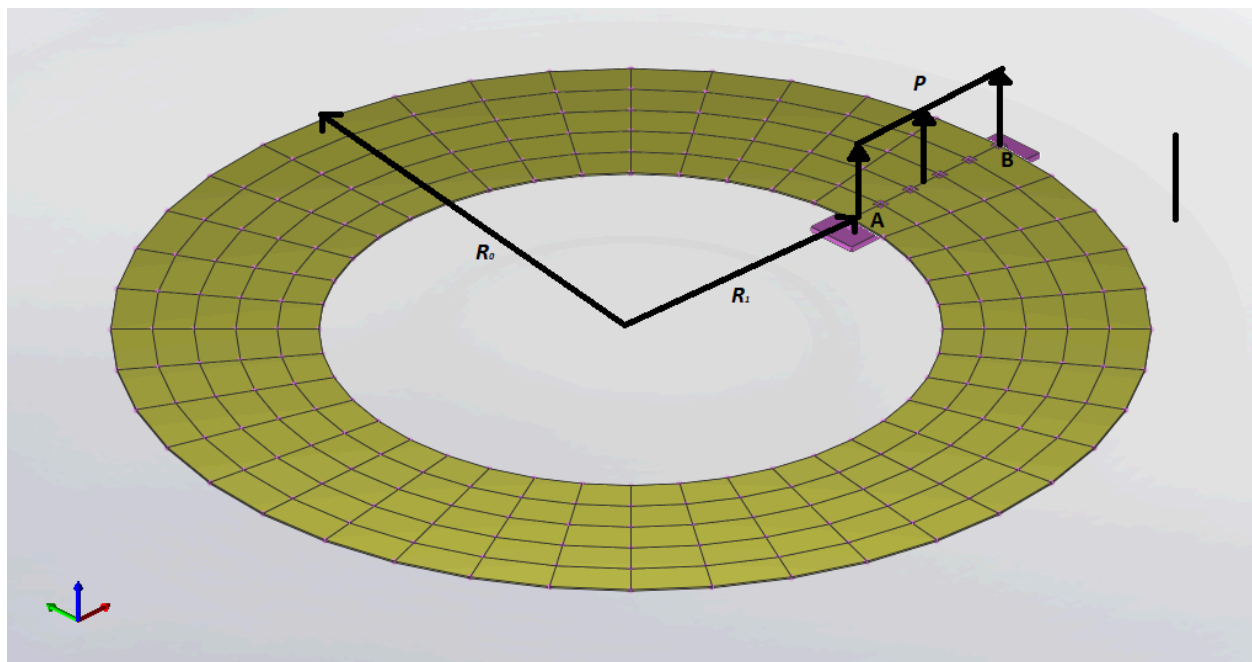
- For help on nonlinear static analysis, see Nonlinear Static Analysis in *LARSA 4D Reference Manual*.
- For help on nonlinear plate elements, see Shells in *LARSA 4D Reference Manual*.

N15: Slit Annular Plate with Vertical Load

A slit annular plate is modeled by nonlinear elements. The annular plate is meshed 5x40 times in polar coordinate. The plate is subjected to tip shearing force. Model is analyzed thanks to the large strain assumption by using **Incremental Nonlinear Static Analysis** option.

Example Project: The example described here can be found in the Nonlinear Elastic Static folder of your LARSA 4D Samples directory (generally My Documents\LARSA Projects\Samples) in the file N15.

Problem Description



Slit Annular Plate with 5*40 mesh

The model consists of total 200 nonlinear shell elements. The boundary condition of the model is as follows ; 1st, 42nd, 83rd, 124th, 165th and 206th joints are restrained for all directions, all other joints are left free for all directions.

Dimensions of the model are as follows;

$$R_0 = 10.0 \text{ ft}$$

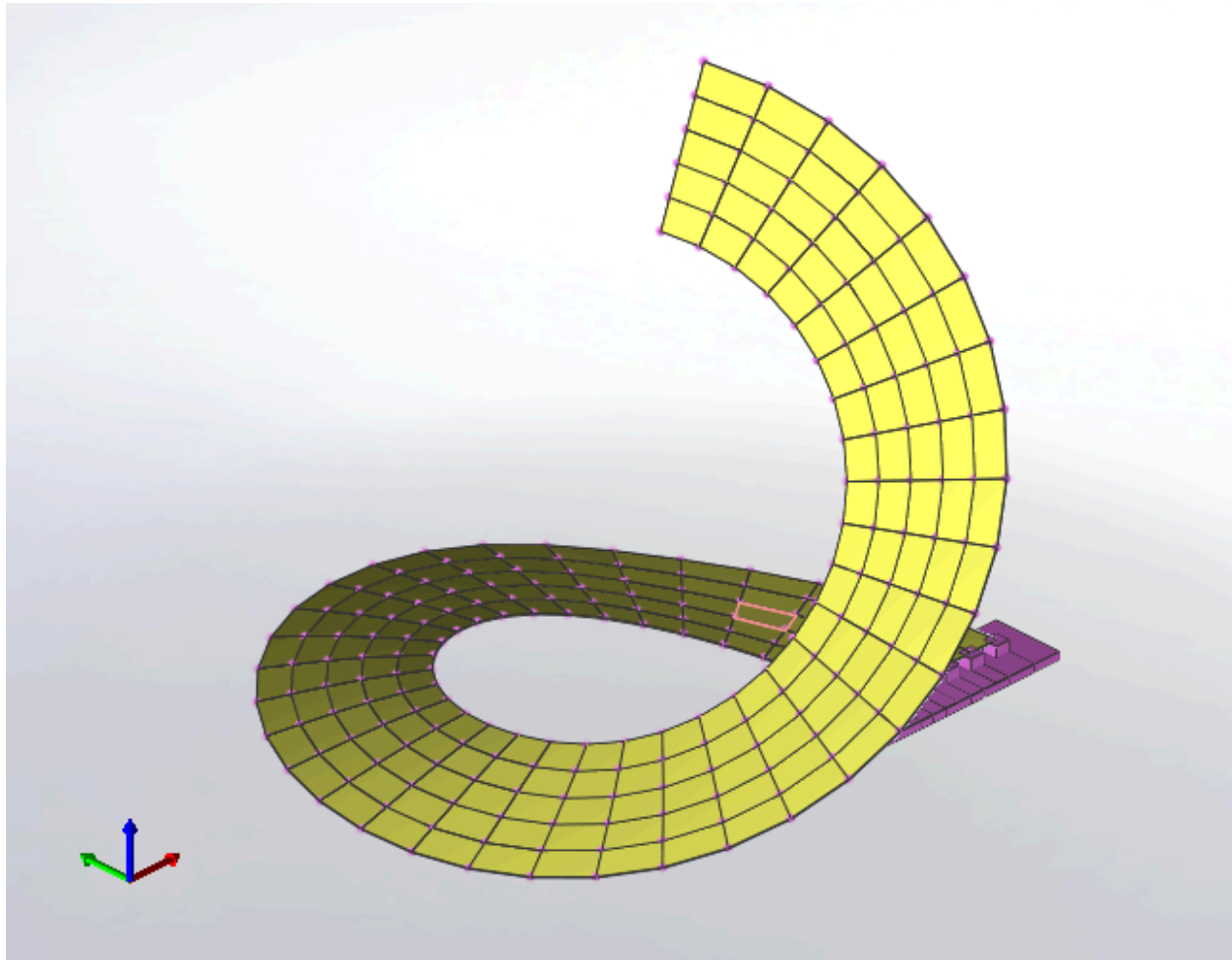
$$R_1 = 6.0 \text{ ft}$$

$$\text{Thickness} = 0.03 \text{ ft}$$

Example material has 21,000,000 kips/ft² elastic modulus with 0 Poisson's ratio.

The girder is modeled with shell elements. In order to get nonlinear behavior, MITC4 plate and membrane types are used.

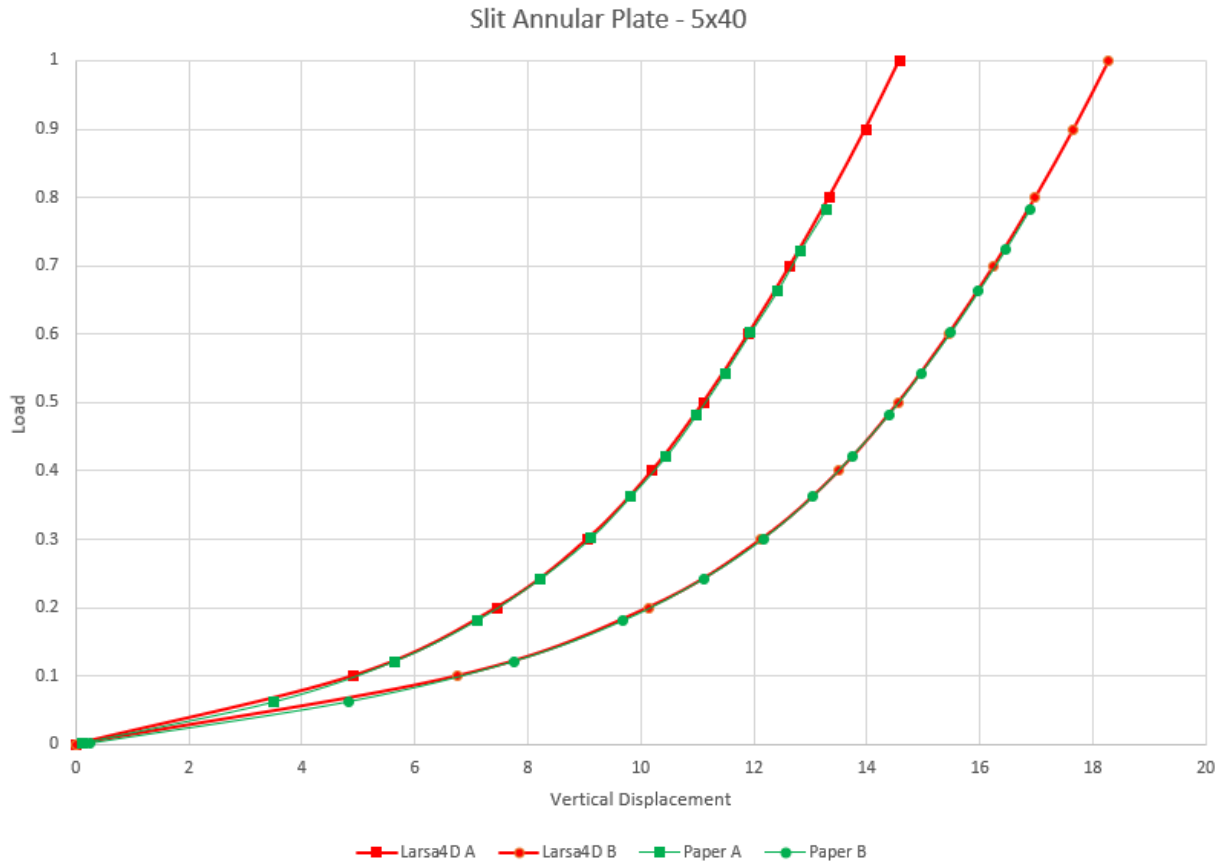
Total 5 kips load is divided into 100 equal load steps and those steps are applied incrementally. Loading is applied at 41st, 82nd, 123rd, 164th, 205th and 246th joints of the section.



Deflected shape

Solution Comparison

The load-displacement curve of model is shown below. The curve contains both results of MITC4 and independent results for comparison.



Results are in excellent agreement with independent results.

References

- Ko, Y., Lee, P. S., & Bathe, K. J. (2017). The MITC4+ shell element in geometric nonlinear analysis. *Computers & Structures*, 185, 1-14.

For More Information, please refer to the following documentation.

- For help on nonlinear static analysis, see Nonlinear Static Analysis in *LARSA 4D Reference Manual*.
- For help on nonlinear plate elements, see Shells in *LARSA 4D Reference Manual*.

N22: Rail-Structure Interaction (RSI) under thermal loads

Perform Rail-Structure Interaction analysis using a simplified model with inelastic rail-deck connection. This example is a part of a validation example "Test-case No. 1" from UIC Code 774-3.

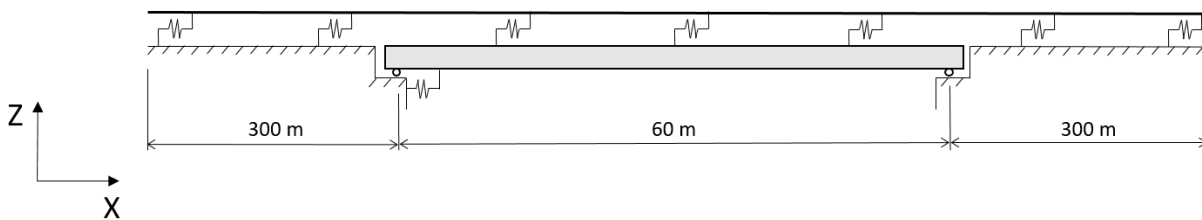
Example Project: The example described here can be found in the Rail Structure Interaction (RSI) analysis folder of your LARSA 4D Samples directory (generally My Documents\LARSA Projects\Samples) in the file N22.

Background

The interaction between a rail and a structure comes from their relative movement with respect to each other. Deformations in the bridge due to temperature variation or applied loads cause additional stresses in the rails. At the same time, forces applied to the track induce additional loads on the bridge. The goal of the RSI analysis is to determine displacements and additional stresses in the rail due to the interaction.

Model

This model is a simplified two-dimensional Rail-Structure Interaction model. The bridge is modeled as a simply-supported beam with a single span of 60 m. The deck and girders properties are combined into an equivalent cross-section with the following properties: $E = 2.1 \times 10^8 \text{ kN/m}^2$, $I_{zz} = 2.59 \text{ m}^4$, $A = 0.74 \text{ m}^2$. The beam's centroid is positioned at 2.64 m from the bridge supports in the positive Z-direction. The centroid offset is modeled using member offsets. The height of the deck is 6 m. The position of the rails is assumed to coincide with the top of the deck. The track consists of two rails combined together and extends 300 m beyond the bridge on each side to model the track on embankment. The track is modeled using beam elements. Track properties are equal to combined properties of two UIC 60 rails and are as follows: $E = 2.1 \times 10^8 \text{ kN/m}^2$, $I_{zz} = 6.08 \times 10^{-5} \text{ m}^4$, $A = 0.0153 \text{ m}^2$.

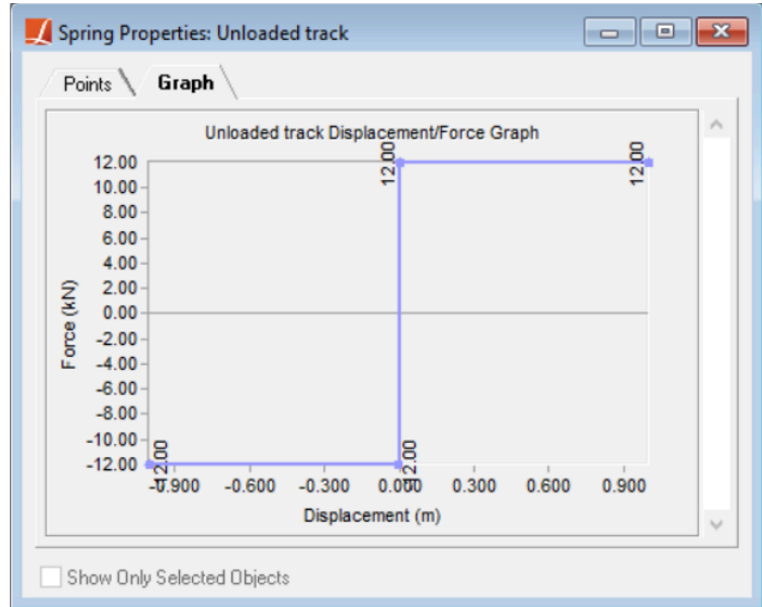


Simplified Rail-Structure Interaction model

The connection between the track and the deck represents ballast-rail fastening system. In order to model this connection, both the track and deck are meshed to have members with the length of 0.6 m, which is assumed to be the distance between the ties (or sleepers). This way each track joint has a corresponding bridge joint and discrete supports can be modeled between these joints. To model the track behavior in the transition zones between embankment and the bridge, additional fixed joints corresponding to the track joints are created beyond the bridge ends. These joints represent the embankment. Discrete supports are modeled next between the corresponding joints of the track and bridge or embankment. In the longitudinal (Global X) direction, these supports are modeled with inelastic springs. The resistance of the track to longitudinal displacement depends on the relative displacement between the track and the

bridge. According to UIC 774-3, the track-deck connection in the longitudinal direction can be approximated using a bilinear function. For the bilinear function, the displacement at the beginning of the plastic zone is taken to be 2 mm. The value of the track's longitudinal restraint depends on the level of vertical load. In this analysis, temperature variation without vertical loading is considered. Therefore, the longitudinal restraint of an unloaded track is used, which is equal to 20 kN per meter of track. Since the track-deck connection is modeled with discrete inelastic springs positioned at 0.6 m, the longitudinal restraint for each spring is 12 kN. These properties are used to construct a bilinear backbone curve that is defined in the *Spring Properties* and shown below. The Polygonal Hysteretic Model is set to bilinear as well. It is assumed that degradation is not modeled. Therefore, parameter Alpha is set to 200, which corresponds to the response without stiffness degradation, and all the other degradation parameters are set to zero.

	Displacement (m)	Force (kN)
1	-1.0000	-12.0000
2	-0.0020	-12.0000
3	0.0020	12.0000
4	1.0000	12.0000
5		



Bilinear force-displacement backbone curve corresponding to the properties of track-deck connection in the longitudinal direction

The connection in the vertical direction is modeled using very stiff linear springs. However, in this analysis, only longitudinal connections are utilized. The connection between the bridge and left abutment is modeled with a linear spring with the stiffness of 6×10^5 kN/m to represent the foundation-abutment-bearing system stiffness.

Two separate thermal variations are considered: $+50^\circ\text{C}$ temperature change for the rail and $+35^\circ\text{C}$ for the deck.

Solution and comparison

The results of the analysis are compared with the UIC 774-3 and listed below.

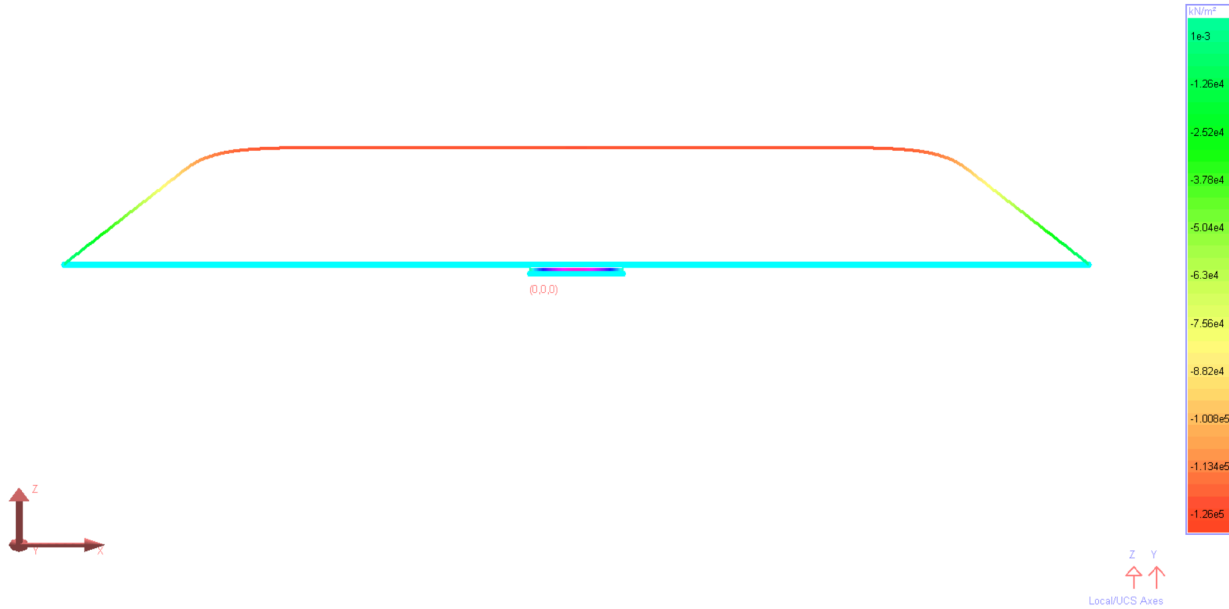
Sources:

- LARSA 4D
- UIC 774-3

	LARSA	UIC
Thermal variation in the rail		
Rail stress, MPa	-126	-126
Thermal variation in the deck		
Rail stress, MPa	-31.10	-30.67

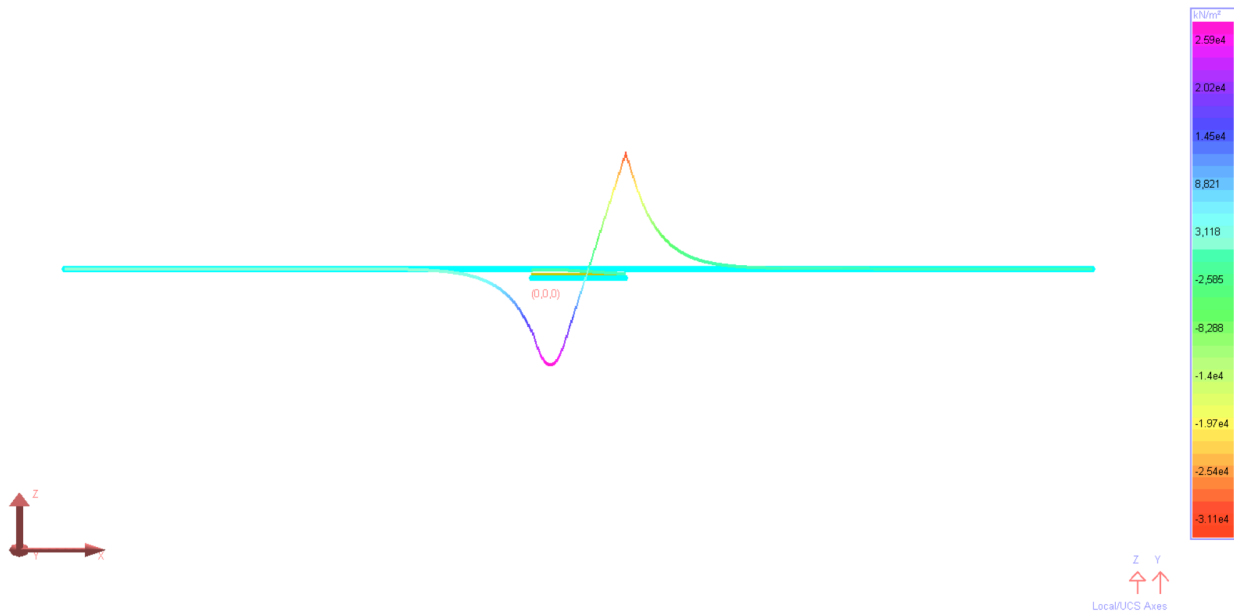
	LARSA	UIC
Absolute displacement of the deck, mm	-1.23	-1.69
Support reaction, kN	735.95	700.12

When temperature variation is applied to the rail, three distinct zones can be seen in the rail response: a central zone with constant stress and without expansion or contraction and two "expansion zones" at the ends with length of about 150 m.



Stresses in the rail due to temperature variations in the rail

When temperature variation is applied to the deck, the maximum rail stress is produced at the right support.



Stresses in the rail due to temperature variations in the deck

References

- UIC Code 774-3. "Track/bridge interaction. Recommendations for calculations", 2nd edition, 2001

For More Information, please refer to the following documentation.

- For help on nonlinear static analysis, see Nonlinear Static Analysis in *LARSA 4D Reference Manual*.
- For help on inelastic springs, see Springs in *LARSA 4D Reference Manual*.

Samples for Eigenvalue Analysis

These samples provide an overview of the eigenvalue analysis.

For More Information, please refer to the following documentation.

- For help on eigenvalue analysis, see Eigenvalue and Stressed Eigenvalue Analysis in *LARSA 4D Reference Manual*.

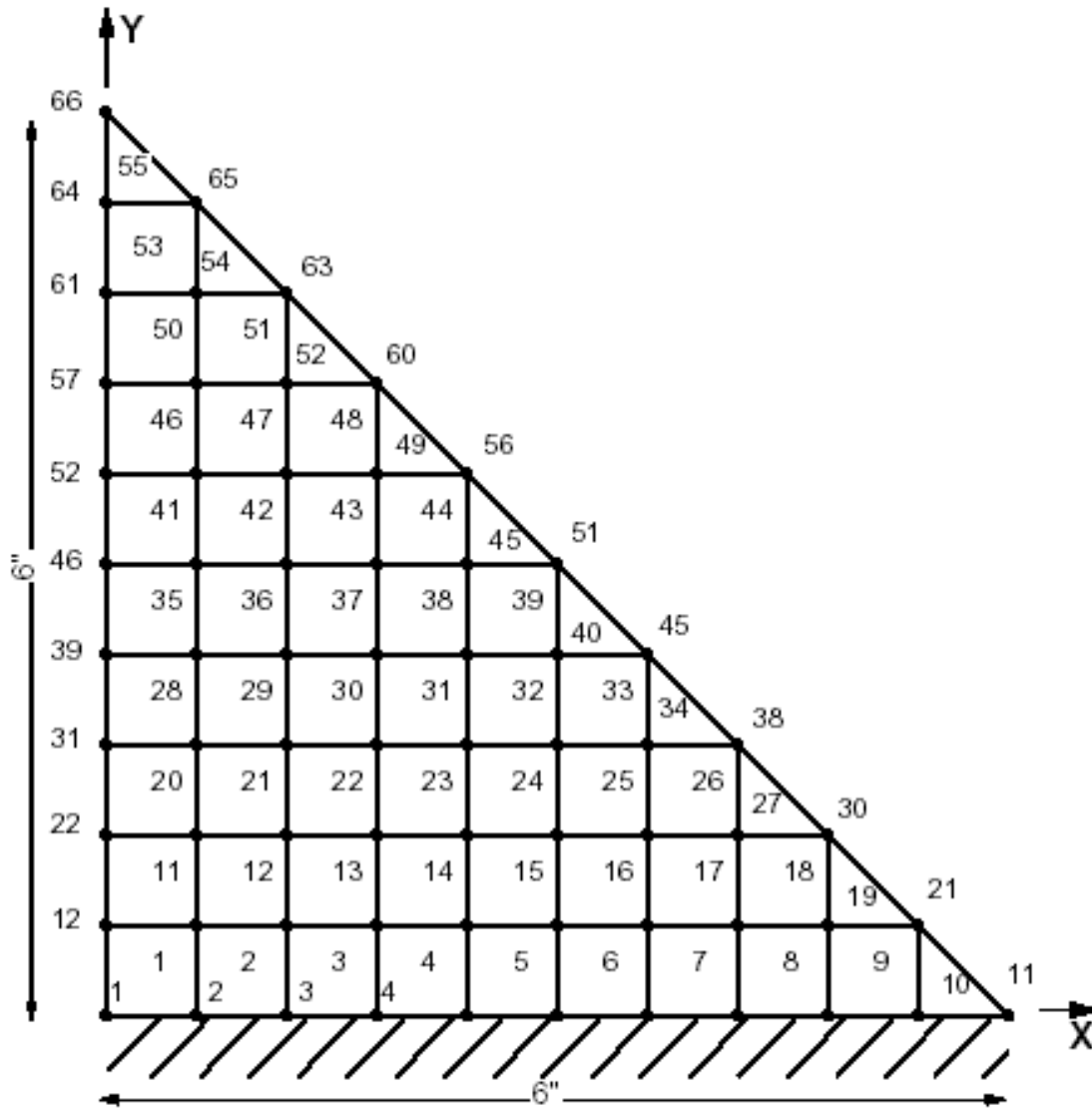
E01: Triangular Cantilever Plate Eigenvalues	193
Solution Comparison	195
Reference	195
E02: Square Cantilever Plate Eigenvalues	197
Solution Comparison	199
E03: Beam Eigenvalues	201
Solution Comparison	201
E04: Cantilever Beam Eigenvalues	203
Solution Comparison	203
E05: Rectangular Cantilever Plate Eigenvalues	205
Solution Comparison	207
E06: Mass Spring Model Eigenvalues	209
Solution Comparison	211
E07: 2D Frame (Wilson & Bathe) Eigenvalues	213
Solution Comparison	214
References	214
E08: ASME Frame Eigenvalues	215
Solution Comparison	216
References	217
E09: Natural Frequencies of a Torsional System	219
Solution Comparison	219

E01: Triangular Cantilever Plate Eigenvalues

A triangular cantilever plate is subjected to its own weight. Compute the lowest three natural frequencies of the plate.

Example Project: The example described here can be found in the Eigenvalue folder of your LARSA 4D Samples directory (generally My Documents\LARSA Projects\Samples) in the file E01.

The plate is 6.0 inches by 6.0 inches and the thickness is 0.034 inches. The weight density is 0.06414 lb/in³. The elastic modulus of the material is 6,500,000 lb/in² and Poisson's ratio is 0.3541.



Sample E01

The model used has 66 joints and 55 plate elements. The joints 1 to 11 are fixed in all six (6) degrees of freedom. Since the plate elements do not have any stiffness about the axis perpendicular to the plane of the plate, the rotation about the global Z-axis for joints 12 to 66 are eliminated.

The joint masses are automatically computed by LARSA. The material and sectional property data of the plate structure are given as:

Modulus of Elasticity = 6,500,000 lb/in²

Poisson Ratio = 0.3541

Shear Modulus = 2,400,118 lb/in²

Height of Triangle = 6.0 inch

Plate Thickness = 0.034 inch

Weight Density = 0.06414 lb/in³ g = 386 in/sec³

Solution Comparison

Sources:

- LARSA 4D
- COSMOS7
- NASTRAN

	LARSA	COSMOS7	NASTRAN
f1 (hz)	55.5	55.6	55.6
f2 (hz)	204.23	206.5	205.5
f3 (hz)	281.33	283.1	283.2

The comparison is based on the results obtained by the computer programs COSMOS7, ANSYS and NASTRAN for the problem in the reference article.

Reference

- "ASME Pressure Vessel and Piping 1972 Computer Programs Verification.", I.S. Tuba and W.B. Wright, ASME publication, I-24, Problem 2.

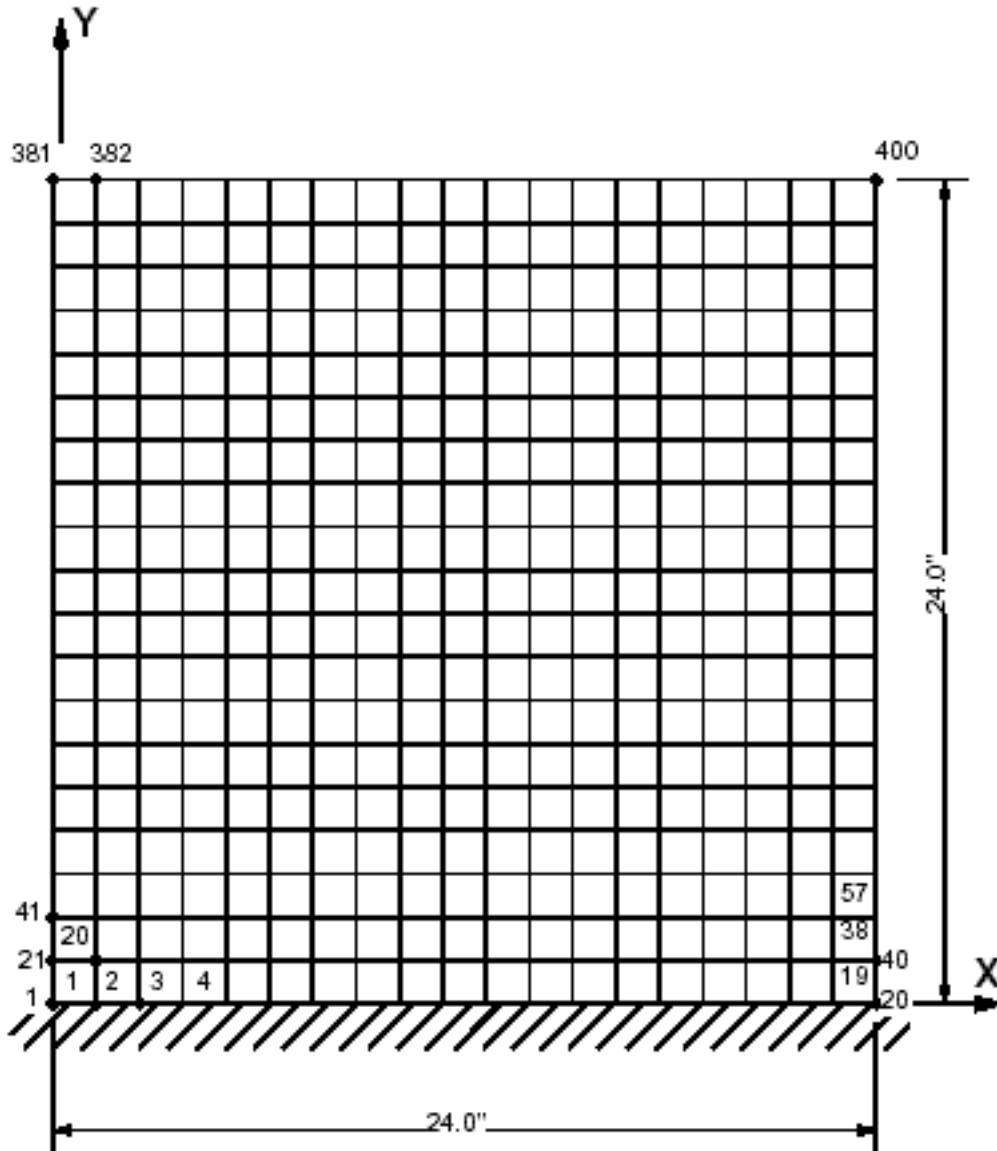
For More Information, please refer to the following documentation.

- For help on eigenvalue analysis, see Eigenvalue and Stressed Eigenvalue Analysis in *LARSA 4D Reference Manual*.

E02: Square Cantilever Plate Eigenvalues

A square cantilever plate of 24 x 24 inches and 1 inch thick has weight density of 0.490 kip/ft³. The plate is fixed at its base. Determine the first five eigenvalues.

Example Project: The example described here can be found in the Eigenvalue folder of your LARSA 4D Samples directory (generally My Documents\LARSA Projects\Samples) in the file E02.



Sample E02

The plate model has 19 x 19 mesh. It consists of 400 joints and 361 plate elements. The in-plane action of the plate is restrained by eliminating X and Y translations and Z rotations for all the joints.

The properties of the plate are:

Plate Size = 24 x 24 inch

Modulus of Elasticity = 29,500 ksi

Poisson Ratio = 0.00

Shear Modulus = 14,750 ksi

Weight Density = 0.000280 kip/in³ g = 386.4 in/sec²

The model is created in LARSA 4D using the Classic and MITC4 plate element behaviors.

Solution Comparison

Result	Harris	SAP90	Classic	MITC4
f ₁ (hz)	56.16	55.866	56.51	56.48
f ₂ (hz)	154.23	136.61	155.18	153.84
f ₃ (hz)	350.88	342.65	352.92	352.26
f ₄ (hz)	449.24	438.60	451.97	448.43
f ₅ (hz)	535.62	497.51	539.16	533.56

Harris results are obtained using the Ritz method with beam mode shapes. All five modes are in good agreement with the results for both LARSA 4D plate behaviors.

The LARSA 4D results also approximately match with SAP90 for the first, third and fourth modes.

Sources:

- Harris, C.M. and Crete, C.E., "Shock and Vibration Handbook," McGraw-Hill, 1976.
- Computers & Structures Inc., "SAP90 Structural Analysis Verification Manual", October, 1990.
- LARSA 4D (Classic, MITC4)

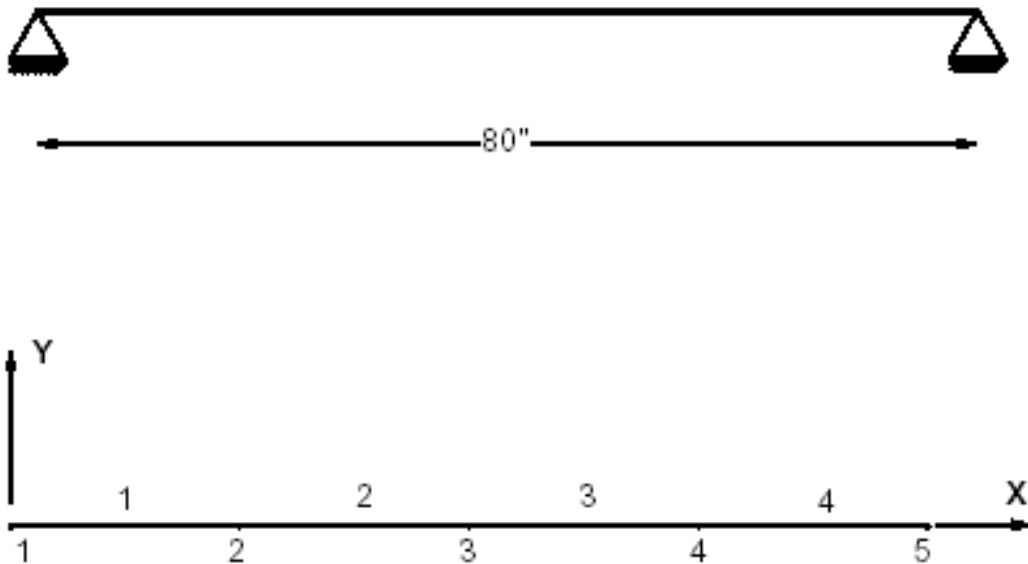
For More Information, please refer to the following documentation.

- For help on eigenvalue analysis, see Eigenvalue and Stressed Eigenvalue Analysis in *LARSA 4D Reference Manual*.

E03: Beam Eigenvalues

A simply supported beam is subjected to its own weight. The span length is 80 inches and the beam is steel with 2 inches square cross section. The mass density of the beam is 0.000728 lb-sec²/in⁴. Determine the fundamental frequency of the beam.

Example Project: The example described here can be found in the Eigenvalue folder of your LARSA 4D Samples directory (generally My Documents\LARSA Projects\Samples) in the file E03.



Sample 16

The model of the beam has 5 joints and 4 beam elements. Joints 1 and 5 are pin supports. The joints 2, 3 and 4 represent the lateral dynamic degrees of freedom.

Modulus of Elasticity = 30,000,000 psi

Span Length = 80 inches

A = 4 in²

I_{zz} = 1.3333 in⁴

Weight Density = 0.281 lb/in² g = 386 in/sec²

Solution Comparison

Sources:

- LARSA 4D
- Thomson, W.T., "Vibration Theory and Application," Prentice-Hall, Inc., Englewood Cliffs, N.Y., 2nd Printing, 1965, p.18.

- Swanson Analysis Systems, Inc., "ANSYS Verification Manual".

	LARSA	Thomson	Swanson
f1 (Hertz)	28.77	28.77	28.77

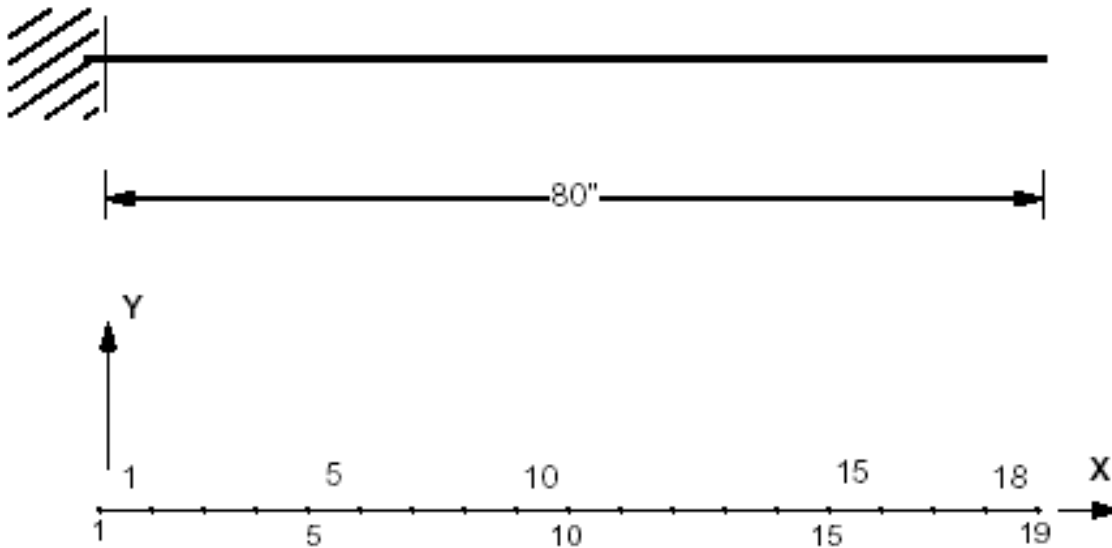
For More Information, please refer to the following documentation.

- For help on eigenvalue analysis, see Eigenvalue and Stressed Eigenvalue Analysis in *LARSA 4D Reference Manual*.

E04: Cantilever Beam Eigenvalues

A cantilever beam is subjected to its own weight. The span length is 80 inches. The steel beam has 2 x 2 inches square cross section. The weight density of the beam is 0.281 lb/in³. Determine the lowest three frequencies of the beam.

Example Project: The example described here can be found in the Eigenvalue folder of your LARSA 4D Samples directory (generally My Documents\LARSA Projects\Samples) in the file E04.



Sample E04

The model used as shown in the figure has 19 joints and 18 beam elements. The beam is fixed at joint 1. The program computes the nodal (joint) masses for the eigenvalue analysis.

The data used for the problem is:

Modulus of Elasticity = 30,000,000 psi

Span Length = 80 inch

$A = 4 \text{ in}^2$

$I = 1.3333 \text{ in}^4$

Weight Density = 0.281 lb/in³ $g = 386 \text{ in/sec}^2$

Solution Comparison

Sources:

- LARSA 4D
- Thomson, W.T., "Vibration Theory and Application," Prentice-Hall, Inc., Englewood Cliffs, N.Y., 2nd Printing, 1965, p. 275.

	LARSA	Thomson
fl (hertz)	10.233	10.247
fl (hertz)	63.907	64.221
fl (hertz)	178.38	179.82

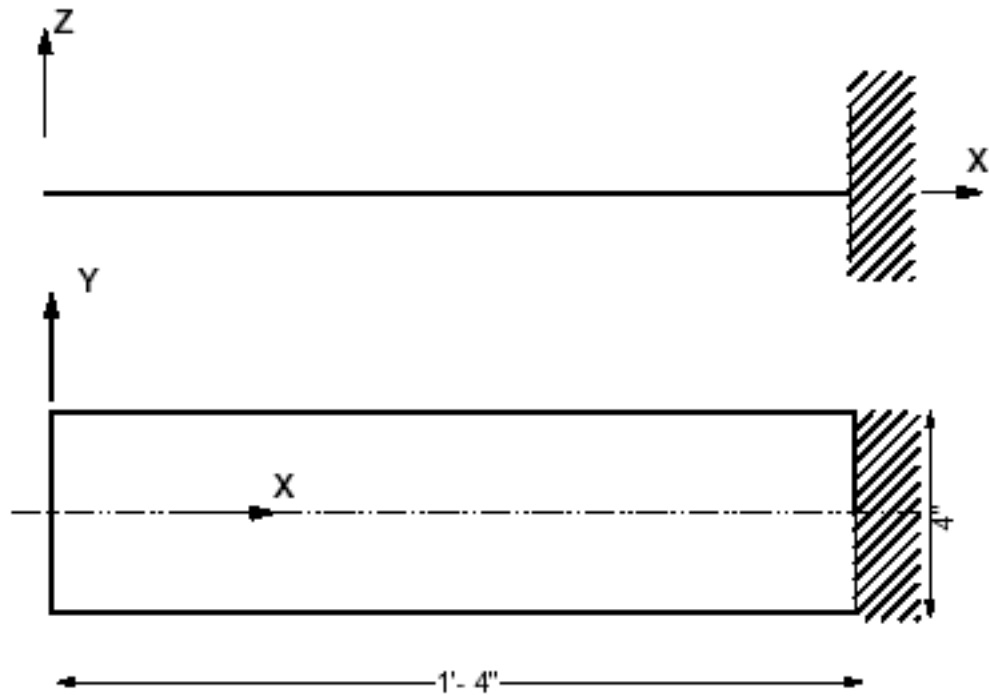
For More Information, please refer to the following documentation.

- For help on eigenvalue analysis, see Eigenvalue and Stressed Eigenvalue Analysis in *LARSA 4D Reference Manual*.

E05: Rectangular Cantilever Plate Eigenvalues

A rectangular cantilever plate of uniform thickness has its own weight as the sole loading. The plate is 16 inches in span and 1 inch thick. The weight density of the plate is 0.281 lb/in^3 . The width of the plate is 4 inches. One four inch wide end of the plate is fixed. Determine the fundamental natural frequency.

Example Project: The example described here can be found in the Eigenvalue folder of your LARSA 4D Samples directory (generally My Documents\LARSA Projects\Samples) in the file E05.



Sample E05

This is a rectangular plate with one edge fixed. The model used has 4 x 2 mesh size and consists of 15 joints and 8 plate elements.

Modulus of Elasticity = 30,000,000 psi

Poisson's Ratio = 0.30

Shear Modulus = 11,538,461 psi

Weight Density = 0.281 lb/in³

Plate Thickness = 1 inch

Plate Width = 4 inches

Span Length = 16 inches $g = 386.4 \text{ in/sec}^2$

The model is created in LARSA 4D using the Classic and MITC4 plate element behaviors.

Solution Comparison

Result	Timoshenko	Classic	MITC4
f_1	128.09	128.11	128.11

Sources:

- Timoshenko, S., and Young, D.H., "Vibration Problems in Engineering", 3rd Edition, D. Van Nostrand Co., Inc., New York, 1955, p. 389.
- LARSA 4D (Classic, MITC4)

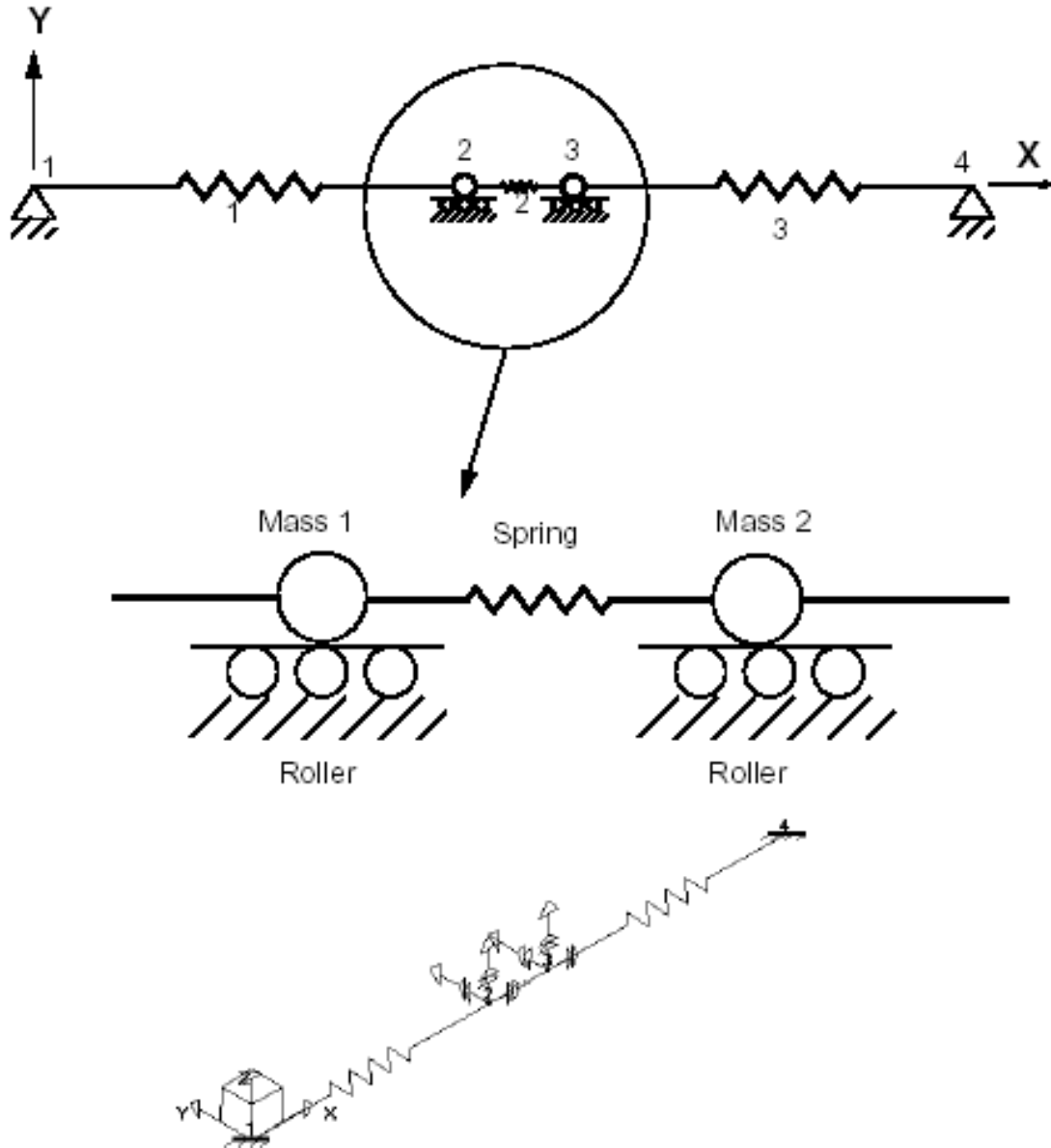
For More Information, please refer to the following documentation.

- For help on eigenvalue analysis, see Eigenvalue and Stressed Eigenvalue Analysis in *LARSA 4D Reference Manual*.

E06: Mass Spring Model Eigenvalues

This is a system with two lumped masses and three springs. Determine the fundamental natural frequency.

Example Project: The example described here can be found in the Eigenvalue folder of your LARSA 4D Samples directory (generally My Documents\LARSA Projects\Samples) in the file E06.



Sample E06

The model has 4 joints, 3 spring elements and 2 joint masses. The dynamic degrees of freedom is selected in the Global X-direction so that it matches with the spring directions.

The joint locations in the X direction are arbitrarily selected since the length has no effect on the stiffness of a spring element. The translational degrees of freedom in X direction at joints 2 and 3 are the degrees of freedom of the model. All other degrees of freedom are eliminated from the model. The values for the lumped masses and spring constants are given as:

$$M1 = 0.5 \text{ lb-sec}^2/\text{in}$$

$$M2 = 1.0 \text{ lb-sec}^2/\text{in}$$

K1 = 200 lb/in

K2 = 800 lb/in

K3 = 200 lb/in

Solution Comparison

Sources:

- Thomson, W.T., "Vibration Theory and Applications," Prentice- Hall, Inc., Englewood Cliffs, N.Y., 2nd Edition, 1965, P. 163.
- LARSA 4D

	Thomson	LARSA
fl (hz)	2.5814	2.5814
fl (hz)	8.3263	8.3263

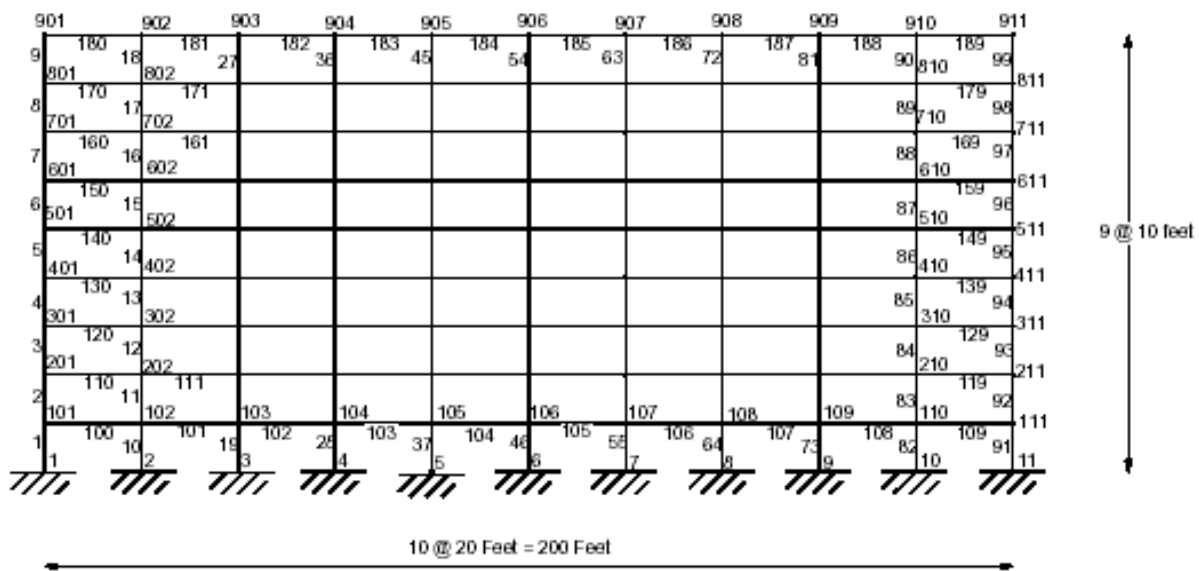
For More Information, please refer to the following documentation.

- For help on eigenvalue analysis, see Eigenvalue and Stressed Eigenvalue Analysis in *LARSA 4D Reference Manual*.

E07: 2D Frame (Wilson & Bathe) Eigenvalues

This 2D frame structure has 10 equal bays and 9 stories. The bottom ends of the base columns are fixed. All members have the same section properties. Determine the frame's three lowest natural frequencies.

Example Project: The example described here can be found in the Eigenvalue folder of your LARSA 4D Samples directory (generally My Documents\LARSA Projects\Samples) in the file E07.



Sample E07

The material properties of the beams and columns are:

Modulus of Elasticity = 432,000 kip/ft²

Weight Density = 1 kip/ft³

The sectional properties of the beams and columns are:

A = 3.00 ft²

I_{zz} = 1.00 ft⁴

The geometry of the structure is based on:

Column Height = 10 feet

Column Spacing = 20 feet

The frame is modeled in the global XZ plane with Z as the vertical direction. The joints are numbered such that the footing level is 1 to 11. First level joints are from 101-111, second level joints are from 201-211, etc. The joints along

the base are completely fixed. Columns are numbered 1 to 99 from bottom to top and left to right. The beams are numbered 100-189. The local z-axis of all beams and columns is normal to the plane of the frame.

This is a plane (2D) model, the degrees of freedom for the out-of-plane translational displacement (in Y) and in-plane rotations (about X and Z) are removed from the analysis. The joints can move in Global X and Z directions and rotate about the Global Yaxis.

Solution Comparison

Sources:

- LARSA 4D
- Bathe,K.J., Wilson,E.L., "Large Eigenvalue Problems in Dynamic Analysis", Journal of the Eng.Mech.Div., ASCE, Vol.98, No. EM6, Proc.Paper 9433, Dec 1972.
- Computers & Structures Inc., "SAP90 Structural Analysis Verification Manual", October 1990, 2-1.

	LARSA	Bathe	SAP90
f1 (hertz)	0.122202	0.122202	0.122202
f2 (hertz)	0.374165	0.374165	0.374165
f3 (hertz)	0.648210	0.648210	0.648210

The comparison of the frequencies for all three modes are good between LARSA and the references.

References

- Ref [3] - Peterson, F.E., "EASE2, Elastic Analysis of Structural Engineering, Example Problem Manual," Engineering Analysis Corporation, Berkeley, California, 1981.

For More Information, please refer to the following documentation.

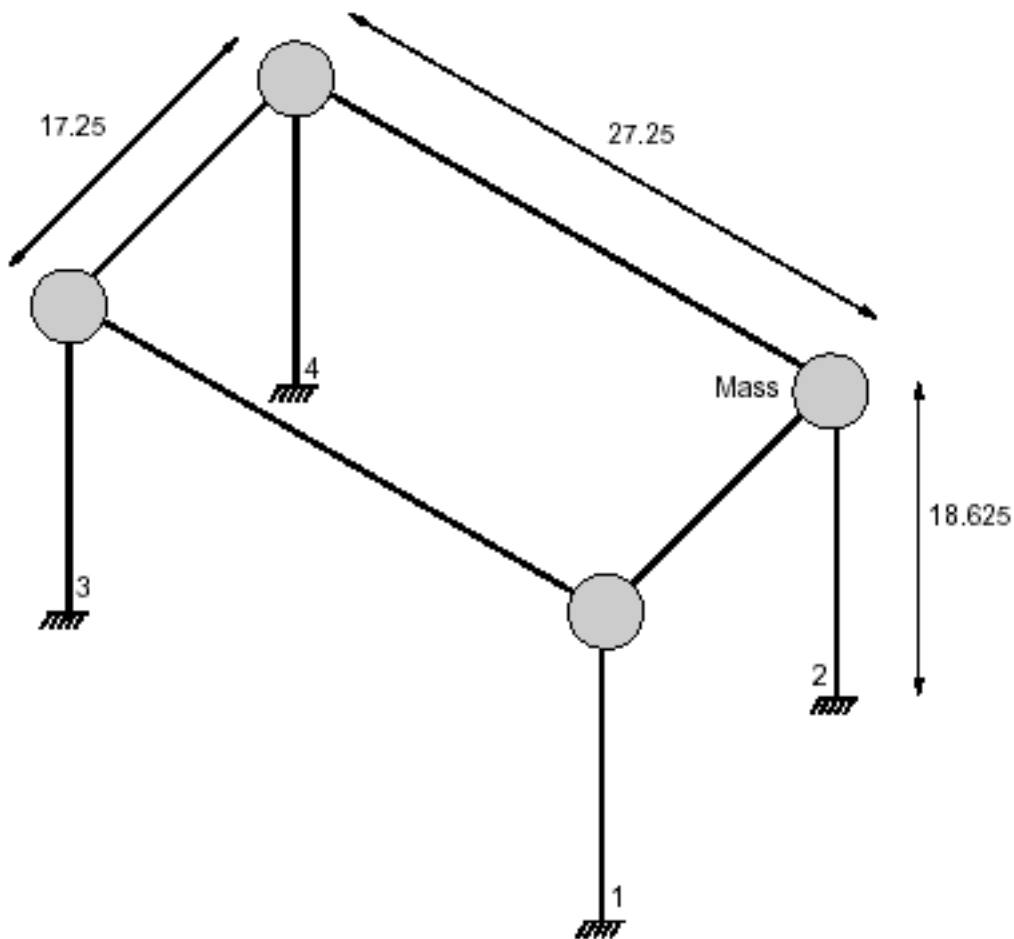
- For help on eigenvalue analysis, see Eigenvalue and Stressed Eigenvalue Analysis in *LARSA 4D Reference Manual*.

E08: ASME Frame Eigenvalues

This frame is from ASME 1972 Program Verification and Qualification Library. It is a single story 3D frame with a single bay in each direction. The frame is made of 2-inch steel pipe segments welded to 2.75-inch steel cubes. The legs are welded to a heavy base plate to assure full restraint.

Example Project: The example described here can be found in the Eigenvalue folder of your LARSA 4D Samples directory (generally My Documents\LARSA Projects\Samples) in the file E08.

Determine the lowest 24 natural frequencies and mode shapes of the 3D structure considering the shear deformations.



Sample 31

The material properties of the pipes are:

Modulus of Elasticity = 27,900,000 lb/in²

Poisson's Ratio = 0.30

Shear Modulus = 10,730,769 lb/in²

The pipe section is constant throughout with 2.375 in. outer diameter and 0.154 in. wall thickness. The section properties for the pipes are:

$A_{xx} = 1.0745 \text{ in}^2$

$A_{yy} = 0.5037 \text{ in}^2$

$A_{zz} = 0.5037 \text{ in}^2$

$I_{xx} = 1.3314 \text{ in}^4$

$I_{yy} = 0.6657 \text{ in}^4$

$I_{zz} = 0.6657 \text{ in}^4$

The self weight of the structure is represented by mass elements at the joints. The steel cubes are modeled as mass elements at the corner joints of the frame.

The mass elements at the corner joints including the weight of 2.75 inch steel cubes are:

$M_{xt} = 0.0253816 \text{ lb-sec}^2/\text{in}$

$M_{yt} = 0.0253816 \text{ lb-sec}^2/\text{in}$

$M_{zt} = 0.0253816 \text{ lb-sec}^2/\text{in}$

The mass elements at all other joints are specified as:

$M_{xt} = 0.00894223 \text{ lb-sec}^2/\text{in}$

$M_{yt} = 0.00894223 \text{ lb-sec}^2/\text{in}$

$M_{zt} = 0.00894223 \text{ lb-sec}^2/\text{in}$

Solution Comparison

Natural Frequencies (Hertz)

Sources:

- ANSYS, Engineering Analysis System, Examples Manual, Swanson Analysis Systems, Inc., Elizabeth, PA, 1977.
- EASE2, Elastic Analysis for Structural Engineering, Example Problem Manual, Engineering Analysis Corporation,
- COSMOS, Finite Element Analysis Program
- LARSA 4D

	ANSYS	EASE2	COSMOS	LARSA
Mode 1	111.52	111.53	111.2	111.21
Mode 2	115.95	115.96	115.8	115.77
Mode 3	137.60	137.61	137.1	137.13
Mode 4	218.02	218.03	215.7	215.74
Mode 5	404.23	404.23	404.1	404.16
Mode 6	422.70	422.72		422.50
Mode 7	451.72	451.75		451.45
Mode 8	553.99	554.07		548.80
Mode 9	735.70	735.81		733.29

	ANSYS	EASE2	COSMOS	LARSA
Mode 10	762.32	762.44		758.26
Mode 11	852.57	852.72		850.98
Mode 12	894.08	894.26		891.85

The natural frequencies computed by LARSA are in good agreement with the values obtained by ANSYS and EASE2 programs. LARSA and COSMOS results are identical. In ANSYS and EASE2 solutions, 24 eigenvalues are computed using the Guyan reduction method retaining only 24 mass degrees of freedom, whereas in LARSA and COSMOS, the eigenvalue problem has been solved using all degrees of freedom.

References

- Program Verification and Qualification Library, ASME Pressure Vessel and Piping Division, Committee on Computer Technology, 1972.

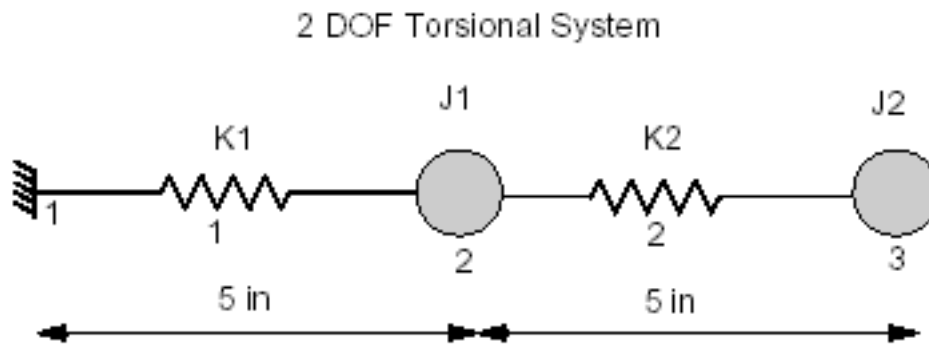
For More Information, please refer to the following documentation.

- For help on eigenvalue analysis, see Eigenvalue and Stressed Eigenvalue Analysis in *LARSA 4D Reference Manual*.

E09: Natural Frequencies of a Torsional System

A simple torsional system has two torsional springs with stiffness $K = 100.0$ lb-in/rad and two mass elements with rotary inertia of 1.0 lb-in-sec². Determine the lowest two natural frequencies and mode shapes of the system.

Example Project: The example described here can be found in the Eigenvalue folder of your LARSA 4D Samples directory (generally My Documents\LARSA Projects\Samples) in the file E09.



Sample E09

The system is modeled using 2-node torsional spring elements and mass elements. Joint 1 is fixed and all degrees of freedom except rotation about the Global X are restrained at joints 2 and 3.

Solution Comparison

Natural Frequencies (rad/sec)

Sources:

- W.T. Thomson, "Theory of Vibration with Applications", Prentice-Hall Inc., Englewood Cliffs, NJ, 2nd Edition (1981).
- EMRC, "NISA II Verification Problems Manual", 1991.
- LARSA 4D

	Thomson	EMRC	LARSA
Mode 1 $f=0.9836$ (hertz)	6.18	6.18	6.18
Mode 2 $f=2.5752$ (hertz)	16.18	16.18	16.18

For More Information, please refer to the following documentation.

- For help on eigenvalue analysis, see Eigenvalue and Stressed Eigenvalue Analysis in *LARSA 4D Reference Manual*.

Samples for Stressed Eigenvalue Analysis

These samples provide an overview of the stressed eigenvalue analysis.

For More Information, please refer to the following documentation.

- For help on stressed eigenvalue analysis, see Eigenvalue and Stressed Eigenvalue Analysis in *LARSA 4D Reference Manual*.

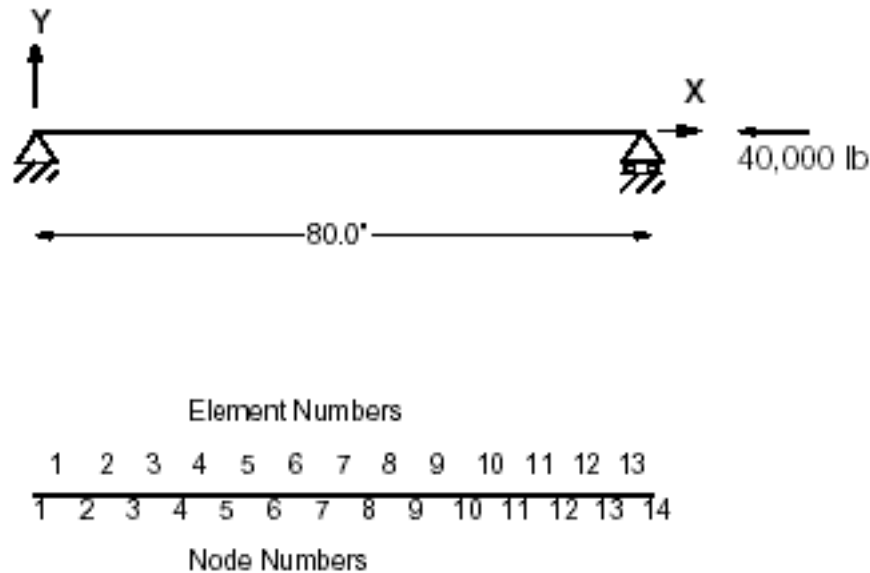
ES01: Vibrations of Axially Loaded Beam - Nonlinear	223
Solution Comparison	224

ES01: Vibrations of Axially Loaded Beam - Nonlinear

A beam is subjected to the action of self-weight and an axial compressive force P . The beam is 80 inches long and pinned at both ends. The magnitude of the axial compressive load is 40,000 lbs. The weight of the beam is considered and the weight density is 0.281 lb/in³. The beam has a square cross-section of 2 x 2 inches.

Example Project: The example described here can be found in the Stressed Eigenvalue folder of your LARSA 4D Samples directory (generally My Documents\LARSA Projects\Samples) in the file ES01.

Determine the axial deflection and maximum stress under static loading. Use the results to determine the first three natural frequencies of the structure and the slope at the left-hand support. Eigenvalue analysis uses the stiffness matrix of the deformed and stressed structure.



Sample ES01

The model is selected with enough elements to characterize the dynamic behavior.

Modulus of Elasticity = 30,000,000 lb/in²

Span Length = 80 inches

$A = 4 \text{ in}^2$

$I = 1.3333 \text{ in}^4$

Weight Density = 0.281 lb/in³

Axial Load = 40,000 lb (compression)

The axial load is applied at joint 14 in the negative X direction.

Solution Comparison

Sources:

- LARSA 4D
- Timoshenko, S., and Young, D.H., "Vibration Problems in Engineering", 3rd Edition, D. Van Nostrand Co., Inc., New York, 1955, p. 374.

	LARSA	Timoshenko
f1 (hz)	17.073	17.055
f2 (hz)	105.37	105.32
f3 (hz)	249.46	249.39
Horizontal Displacement (U14)	-0.0267 in	-0.0267
Axial Force (Compression)	40000. lb	40000.

If the stress stiffening (geometric nonlinearity) is ignored, the natural frequency of the structure would be 28.76 hz instead of the 17.07 hz.

For More Information, please refer to the following documentation.

- For help on stressed eigenvalue analysis, see Eigenvalue and Stressed Eigenvalue Analysis in *LARSA 4D Reference Manual*.

Samples for Response Spectra Analysis

These samples provide an overview of the response spectra analysis.

For More Information, please refer to the following documentation.

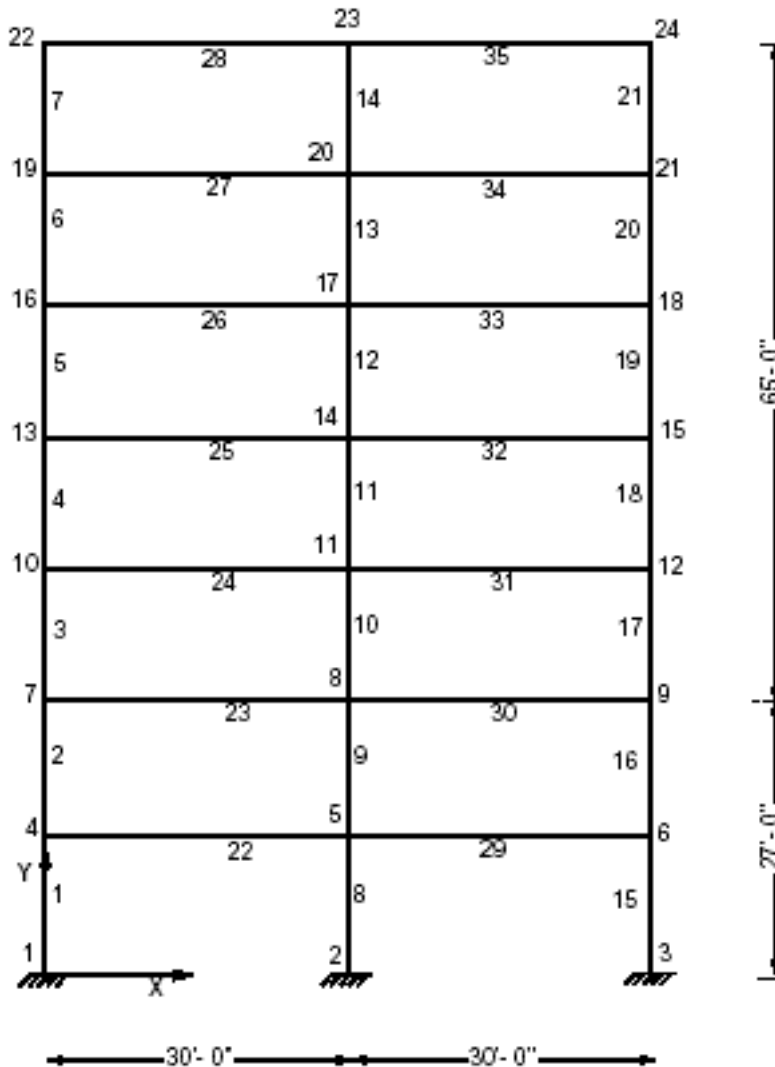
- For help on response spectra analysis, see Response Spectra Analysis in *LARSA 4D Reference Manual*.

RSA01: 2D Frame with Static and Seismic Loads	227
Solution Comparison	230
References	233

RSA01: 2D Frame with Static and Seismic Loads

A seven-story 2D frame structure is subjected to static lateral loads, static vertical loads and dynamic (seismic) lateral loads. The dynamic loads are represented by a response spectrum. The analysis is performed for two independent static load cases and one dynamic load case. Load combinations are generated to combine the static load cases with the dynamic load condition.

Example Project: The example described here can be found in the Response Spectra folder of your LARSA 4D Samples directory (generally My Documents\LARSA Projects\Samples) in the file RSA01.



Sample RSA01

Determine the displacements and element forces for all static and dynamic load conditions. Also, determine the mode shapes and natural frequencies of the structure.

The 2-D model consists of 24 joints and 35 beam elements. This is plane frame problem. The translational displacement in Global Z-direction and rotations about Global X and Y-directions are deleted from the model. The joints 1, 2 and 3 are fixed supports.

The material property data is given:

Modulus of Elasticity = 29,500 ksi

and sectional property data:

Area = 51.17 in² Izz = 2150 in⁴ Designation = S1

Area = 62.10 in² Izz = 2670 in⁴ Designation = S2

Area = 72.30 in² Izz = 3230 in⁴ Designation = S3

Area = 84.40 in² Izz = 3910 in⁴ Designation = S4

Area = 50.00 in² Izz = 3330 in⁴ Designation = S5

Area = 50.00 in² Izz = 4020 in⁴ Designation = S6

Area = 50.00 in² Izz = 5120 in⁴ Designation = S7

In the reference, to reduce the size of the system of equations, the lateral (X) displacements of the exterior columns have been constrained to the lateral (X) displacements of the middle column at each corresponding level. This eliminates all axial deformations in the beams. A DOF Constraint is used to produce a model similar to Ref [2] for the comparison of the results.

The load cases and Response Spectra Analysis result case (see Response Spectra Analysis [see “Response Spectra Analysis” in *LARSA 4D Reference Manual*] for more details) are defined as:

LoadCase	Type	Load Case Definition
1	STATIC	STATIC VERTICAL LOADS
2	STATIC	STATIC LATERAL LOADS
3	RSA	LATERAL DYNAMIC LOADS

The combined (factored) load cases are:

Comb Case	(Primary Load Case x Contribution Factor)
1	(Case 1 x 1.00) + (Case 2 x 1.00)
2	(Case 1 x 1.00) + (Case 3 x 1.00)
3	(Case 1 x 1.00) + (Case 3 x -1.00)

The first combination case is created using load combinations. Since the RSA result case will be added to a new Response Spectra group at the bottom of the Analysis Results Explorer, second and third cases are created using **Results** → **Linear Combination...**

The load combination 1 combines the static vertical and lateral loads. The load combination 2 combines the static vertical load condition with the dynamic load condition. The load combination case 3 combines the static vertical load case with the dynamic load case with the signs reversed.

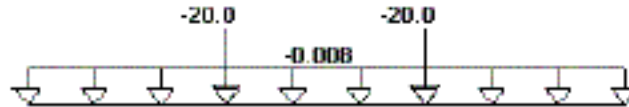
Load Case 1 (Static Vertical Loads):

The static vertical load is applied on all horizontal beam elements 22 to 35 and it consists of:

Uniform Load $W = 0.1$ kip/ft (0.008333 kip/in)

Point Load $P = 20$ kips @ 10 ft from the I-end of the beam

Point Load $P = 20$ kips @ 20 ft from the I-end of the beam



Sample 3a

Load Case 2 (Static Lateral Loads):

In load case 2, the static horizontal loads are applied at each level as joint loads. The joint loads are entered for joints 4, 7, 10, 13, 16, 19 and 22 acting in the X-direction.

$F_x = 2.5$ kips @ joint 4

$F_x = 5.0$ kips @ joint 7

$F_x = 7.5$ kips @ joint 10

$F_x = 10$ kips @ joint 13

$F_x = 12.5$ kips @ joint 16

$F_x = 15$ kips @ joint 19

$F_x = 20$ kips @ joint 22

Load Case 3 (Seismic Loads):

This load case is defined for RSA (Response Spectra Analysis). It is defined using Response Spectra Analysis result case tool which can be reached from **Results** → **Response Spectra Case...**. The complete quadratic combination (CQC) method of modal combination is selected. The seismic response spectrum table is applied in X-direction with a factor of 1.00. The critical damping ratio of 0.05 is used. The spectrum table is defined using frequency versus acceleration normalized with respect to g

In the Reference, a typical story mass of 0.49 kip-sec²/in has been used in the lateral direction (X) and each floor mass has been assigned to the joints on the exterior columns. To obtain similar effect, we will apply 0.49 kip-sec²/in as the mass in the horizontal direction (X) at joints 4, 7, 10, 13, 16, 19, 22.

Seismic Response Spectrum Data are given as Frequency versus Acceleration and normalized in Gravitation g (386.4):

0.5000	0.160189	0.7855	0.258617	1.0000	0.482251
1.5000	0.641750	2.0000	1.046620	2.3186	0.921167
2.5000	.882996	3.0000	0.880624	3.5000	0.718264
4.0000	0.798052	4.1322	0.704753	4.5000	0.746135
0.5000	0.160189	0.7855	0.258617	1.0000	0.482251
5.5000	0.943909	6.0000	0.787220	6.2422	0.804605

6.5000	0.905796	7.0000	0.636531	7.5000	0.665413
8.0000	0.627807	8.4034	0.588211	8.5000	0.572438
9.0000	0.523663	9.5000	0.564412	10.000	0.581609
10.500	0.530631	10.515	0.527825	11.000	0.477599
11.500	0.493366	12.000	0.518093	12.500	0.520045
12.579	0.519598	13.000	0.505311		

Procedure for Analysis:

First the analysis is performed for the static load cases using the **Linear Static Analysis** option of LARSA. For the static analysis, the program automatically considers only the static load cases.

The next step is to return to the preprocessor and request **Unstressed Eigenvalue Analysis** for 7 mode shapes. You must select **Keep Previous Results** option from the **Run** dialog box to keep the results from static analysis run.

After eigenvalue analysis, RSA (Response Spectra Analysis) result case is generated using Response Spectra result case tool which can be reached from **Results** → **Response Spectra Case...**. The spectrum table for this problem is provided in a file with filename RSA01.drs Use this file as the file for response spectrum data.

All the results from static, eigenvalue and response spectra analysis can be seen in Analysis Results Explorer.

Solution Comparison

The results for static, dynamic and for load combinations as computed in LARSA are identical to the results in the Reference.

The sign for the participation and amplitude factors are different in LARSA and SAP90 because of using a different plane of analysis. However, keeping the sign is important for CQC method of modal combination to obtain correct results.

The modal amplitude factors and spectral accelerations, velocities and displacements, CQC modal correlation factors are tabulated in the LARSA output file with extension LI3.

Sources:

- "SAP90, A Series of Computer Programs for the Finite Element Analysis of Structures. Verification Manual", Computers & Structures, 1992.
- LARSA 4D

	SAP90	LARSA
Static Analysis Results (Load Case 2)		
X Disp @ Joint 22 (inch)	1.079	1.450764
Axial Force - Member 1 (kip)	69.99 (Tension)	-69.99
Moment - Member 1 (kip-in)	2324.68	2324.68
Eigenvalue Analysis Results		
Frequency = f1 (hz)	0.7854	0.7854
Frequency = f2 (hz)	2.3187	2.3187

	SAP90	LARSA
Frequency =f3 (hz)	4.1315	4.1315
Frequency =f4 (hz)	6.2430	6.2430
Frequency =f5 (hz)	8.4041	8.4041
Frequency = f6 (hz)	10.519	10.519
Frequency = f7 (hz)	12.576	12.576
Participation Factors for X-Direction		
Mode=1 Frequency=0.7854	1.66	-1.656
Mode=2 Frequency=2.3187	0.624	-0.624
Mode=3 Frequency=4.1315	-0.379	0.379
Mode=4 Frequency=6.2430	-0.269	0.269
Mode=5 Frequency=8.4041	0.220	-0.220
Mode=6 Frequency=10.519	0.153	-0.153
Mode=7 Frequency=12.576	0.103	0.103
Modal Amplitude Factors in X-Direction		
Mode=1 Frequency=0.7554	6.7948	-6.7948
Mode=2 Frequency=2.3187	1.0457	-1.0457
Mode=3 Frequency=4.1315	-0.1532	0.1532
Mode=4 Frequency=6.2430	-0.0544	0.0544
Mode=5 Frequency=8.4041	0.01795	-0.01795
Mode=6 Frequency=10.519	0.007124	-0.007124
Mode=7 Frequency=12.576	0.003319	0.003319
Spectral Acceleration in X-Direction		
Mode=1 Frequency=0.79	99.92	99.92
Mode=2 Frequency=2.32	355.93	355.93
Mode=3 Frequency=4.13	272.52	272.52
Mode=4 Frequency=6.24	311.02	311.02
Mode=5 Frequency=8.40	227.24	227.24
Mode=6 Frequency=10.52	203.79	203.79
Mode=7 Frequency=12.58	200.78	200.78
Velocity in X-Direction		
Mode=1 Frequency=0.79	20.25	20.25
Mode=2 Frequency=2.32	24.43	24.43
Mode=3 Frequency=4.13	10.50	10.50
Mode=4 Frequency=6.24	7.93	7.93
Mode=5 Frequency=8.40	4.30	4.30

	SAP90	LARSA
Mode=6 Frequency=10.52	3.08	3.08
Mode=7 Frequency=12.58	2.54	2.54
Displacement in X-Direction		
Mode=1 Frequency=0.79	4.10	4.10
Mode=2 Frequency=2.32	1.68	1.68
Mode=3 Frequency=4.13	0.40	0.40
Mode=4 Frequency=6.24	0.20	0.20
Mode=5 Frequency=8.40	0.08	0.08
Mode=6 Frequency=10.52	0.05	0.05
Mode=7 Frequency=12.58	0.03	0.03
Displacements and Member Forces		
Horizontal Displacement @ Joint 22	5.4313	5.4313
Axial Force in Member 1	261.5	261.5
Moment in Member 1	9916	9916
Load Combination Horizontal Displacements		
Joint=1	0.00000	0.00000
Joint=4	0.702191	0.702201
Joint=7	1.727692	1.727689
Joint=10	2.662273	2.662265
Joint=13	3.554482	3.554485
Joint=16	4.331373	4.331372
Joint=19	5.004939	5.004927
Joint=22	5.413500	5.431349
Load Combination Vertical Displacements		
Joint=1	0.00000	0.00000
Joint=4	0.008850	0.008853
Joint=7	0.015564	0.015570
Joint=10	0.019761	0.019769
Joint=13	0.022620	0.022630
Joint=16	0.023609	0.023621
Joint=19	0.023333	0.023346
Joint=22	0.022588	0.022602
Load Combination Horizontal Reaction Forces		

	SAP90	LARSA
Joint=1	94.50	94.50
Joint=2	133.8	133.8
Joint=3	84.07	84.07
Load Combination Vertical Reaction Forces		
Joint=1	406.52	406.52
Joint=4	312.0	312.0
Joint=7	406.5	406.5
Load Combination Vertical Reaction Moments		
Joint=1	9634.23	9434.23
Joint=4	13390	13394
Joint=7	10200	10197

Modal Correlation Factors in CQC:

Mode	1	2	3	4	5	6	7
1	1.00	0.01					
2	0.01	1.00	0.03	0.01			
3		0.03	1.00	0.05	0.02	0.01	0.01
4		0.01	0.05	1.00	0.10	0.03	0.02
5			0.02	0.10	1.00	0.16	0.06
6			0.01	0.03	0.16	1.00	0.24
7			0.01	0.02	0.06	0.24	1.00

References

- "Static and Dynamic Analysis of Multistory Frame Structure Using DYNAMIC/EASE2," Engineering Analysis Corporation and Computers/Structures International.

For More Information, please refer to the following documentation.

- For help on response spectra analysis, see Response Spectra Analysis in *LARSA 4D Reference Manual*.

Samples for Time History Analysis

These samples provide an overview of the linear and nonlinear time history analysis and the linear dynamic rolling stock analysis.

For More Information, please refer to the following documentation.

- For help on time history analysis, see Linear Time History Analysis in *LARSA 4D Reference Manual*.

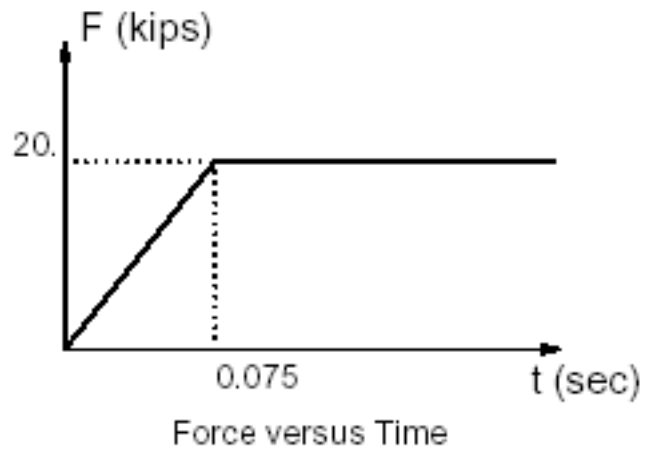
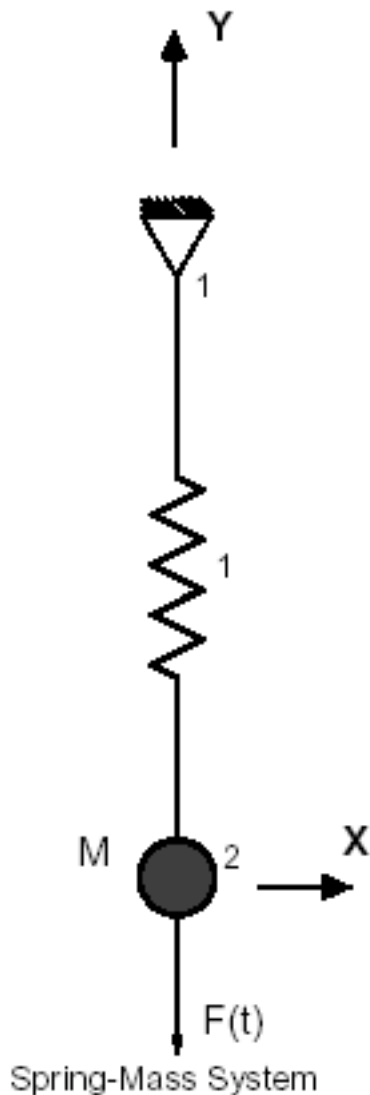
TH01: Spring Mass System Time History Analysis	237
Solution Comparison	238
TH02: Beam with Concentrated Mass & Dynamic Load	239
Solution Comparison	240
TH03: Cantilever Beam Time History Analysis	243
Solution Comparison	245
References	246
TH04: Dynamic Analysis of a Bridge	247
Solution Comparison	248
References	248
TH05: Two Dimensional Frame with Linear Viscous Damper	249
Background	249
Problem Description	249
Nonlinear Dashpots	253
Limitations	255
References	255
TH15: Rolling Stock Analysis	257
Model Setup	257
Rolling Stock Analysis	260
Moving Load Analysis	262
Comparison of Results	263
Dynamic Effect	264
TH18: Hysteretic Spring Time History Analysis	267
Modeling	269
Case 1: Hysteretic spring with bilinear backbone curve and without stiffness and strength degradation	269

Case 2: Hysteretic spring with bilinear backbone curve and stiffness degradation	271
Case 3: Hysteretic spring with bilinear backbone curve and ductility-based strength degradation	271
Case 4: Hysteretic spring with bilinear backbone curve and energy based strength degradation	272
Case 5: Hysteretic spring with trilinear backbone curve and vertex-oriented polygonal hysteretic model (PHM)	272
Case 6: Hysteretic spring with trilinear backbone curve and yield-oriented PHM	273
Case 7: Hysteretic spring with trilinear backbone curve, yield-oriented PHM, and slip	274
References	274
TH19: Simple frame with friction damper	277
Background	277
Model	277
Solution and Comparison	279
References	282
TH20: Vehicle-Track-Structure Interaction Analysis	285
Background	285
Model	285
VTSI Analysis	286
Rolling Stock Analysis	288
Moving Load Analysis	289
Solution and comparison	289
References	291

TH01: Spring Mass System Time History Analysis

A spring is supporting concentrated mass and subjected to a dynamic load with a rise time and a maximum value. Determine the maximum deflection and time of maximum response.

Example Project: The example described here can be found in the Time History folder of your LARSA 4D Samples directory (generally My Documents\LARSA Projects\Samples) in the file TH01.



Sample TH01

The model consists of 2 joints, 1 spring element and 1 mass element. The joint locations are selected arbitrarily. The stiffness of a spring element is defined as the force per unit displacement. The length of the spring has no effect on the solution. The structural model has one degree of freedom in the direction of the spring where the mass is attached.

In LARSA 4D, mass is entered in force units. However, in this verification problem, mass is given in kips-sec²/in (a unit related to the slug). In order to convert it to force units, it should be multiplied by gravitational acceleration (386.0886 in/sec²).

The integration time step of 0.004 seconds is used with total of 40 time steps. The results are reported for all time steps.

$$M = 0.0259067 \text{ kips-sec}^2/\text{in}$$

$$g = 386.0886 \text{ in/sec}^2$$

$$M = 0.0259067 * 386.0886 = 10 \text{ kips}$$

$$k = 83.4 \text{ kips/in}$$

$$\text{Force} = 20 \text{ kips after } 0.075 \text{ rise time}$$

The time history database file for this problem is in a DTH file.

Solution Comparison

Maximum Deflection and Time of Maximum Response

	LARSA 4D	Biggs	Swanson
Displacement (in)	0.3356	0.331	0.335
Time (sec)	0.092	0.092	0.092

Sources

- Biggs, J.M., "Introduction to Structural Dynamics," McGraw-Hill Book Co., New York, 1964, p 50.
- Swanson Analysis Systems, Inc., "ANSYS Verification Manual".

For More Information, please refer to the following documentation.

- For help on time history analysis, see Linear Time History Analysis in *LARSA 4D Reference Manual*.

TH02: Beam with Concentrated Mass & Dynamic Load

A steel beam supporting a concentrated mass is subjected to a dynamic load with a rise time and a maximum value. The weight of the beam is considered negligible. The beam is 20 feet in span and the moment of inertia in the plane of bending is 800.6 in^4 . The rise time of the applied dynamic load (from zero to 20 kips) is 0.075 seconds and the load on the beam stays as 20 kips after 0.075 seconds. Determine the maximum deflection, maximum bending moment (stress) and the time of the maximum response.

Example Project: The example described here can be found in the Time History folder of your LARSA 4D Samples directory (generally My Documents\LARSA Projects\Samples) in the file TH02.

The model consists of 3 joints, 2 beam elements and a lumped mass.

In LARSA 4D, mass is entered in force units. However, in this verification problem, mass is given in $\text{kips}\cdot\text{sec}^2/\text{in}$ (a unit related to the slug). In order to convert it to force units, it should be multiplied by gravitational acceleration ($386.0886 \text{ in}/\text{sec}^2$).

The integration time step chosen is 0.004 seconds.

Modulus of Elasticity = 30,000 ksi

Span = 20 feet $I_{zz} = 800.6 \text{ in}^4$

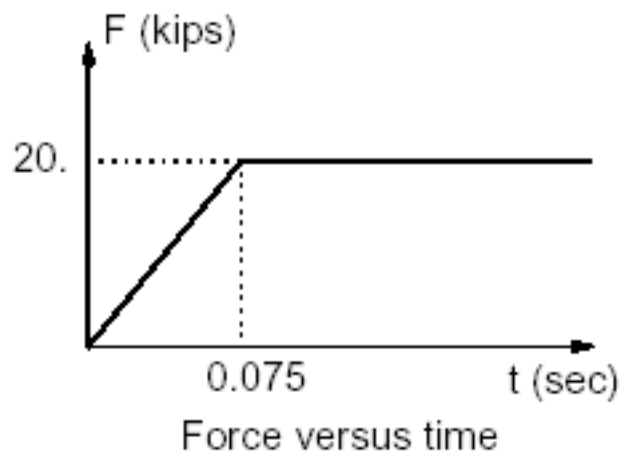
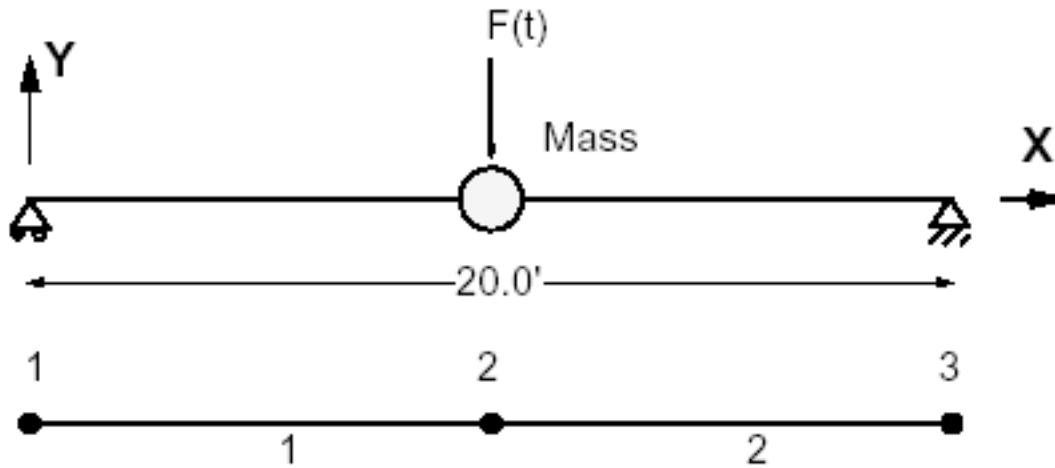
Force = 20 kips with rise time of 0.075 seconds

Mass = $0.0259067 \text{ kips}\cdot\text{sec}^2/\text{in}$

$g = 386.0886 \text{ in}/\text{sec}^2$

$M = 0.0259067 * 386.0886 = 10 \text{ kips}$

The time history database file for this problem is in a DTH file.



Sample TH02

Solution Comparison

Maximum Deflection, Time of Maximum Response and Maximum Bending Moment

	LARSA 4D	Biggs	Swanson
Displacement (in)	0.3356	0.331	0.335
Time (sec)	0.092	0.092	0.092
Moment (kip-in)	-1679	-1654	-1673

Sources:

- Biggs, J. M., "Introduction to Structural Dynamics," McGraw-Hill Book Co., New York, 1964, p 50.

- Swanson Analysis Systems Inc., "ANSYS Verification Manual"

For More Information, please refer to the following documentation.

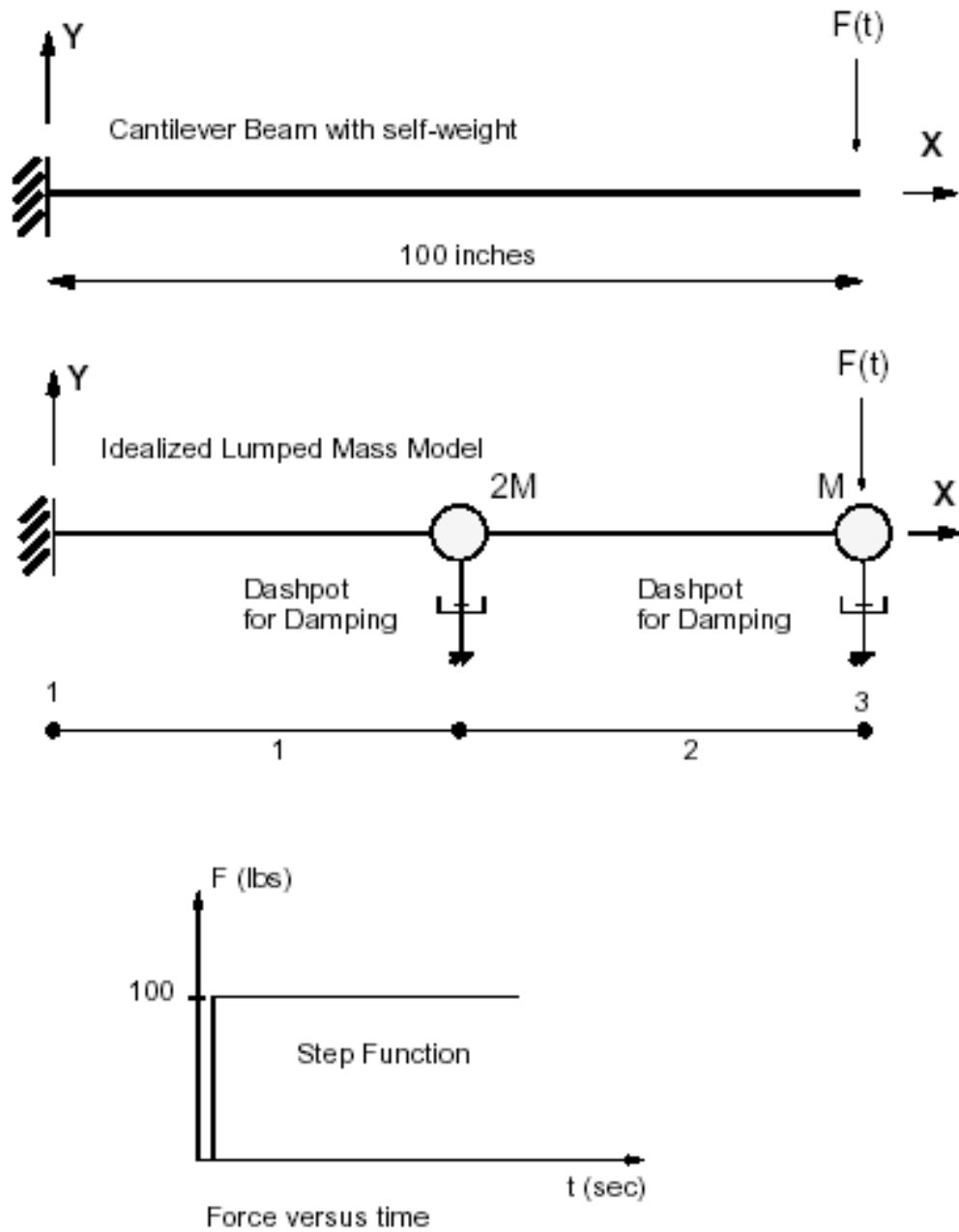
- For help on time history analysis, see Linear Time History Analysis in *LARSA 4D Reference Manual*.

TH03: Cantilever Beam Time History Analysis

A vertical load P is applied instantaneously at time zero on the free end of a cantilever beam. The beam is initially at rest. The load stays constant after time zero. The structure has two lumped masses. The damping is considered to be proportional to the mass. The beam is 100 inches in span with moment of inertia of 4 in^4 .

Determine the vertical displacement at the tip and the mid point of the beam as function of time.

Example Project: The example described here can be found in the Time History folder of your LARSA 4D Samples directory (generally My Documents\LARSA Projects\Samples) in the file TH03.



Sample TH03

The response is calculated by direct integration of the equations of motion. The structure is idealized as a 3 joint and 2 beam element model with 2 lumped masses. The damping is specified as Rayleigh damping:

$$[C] = a [M] + b [K]$$

In this problem, the damping is given as mass proportional damping with;

$$a = 0.6312465$$

$$b = 0.$$

The material and sectional properties of the beam are:

Modulus of Elasticity = 1,000,000 lb/in²

Shear Modulus = 500,000 lb/in²

$I_{zz} = 4 \text{ in}^4$

In LARSA 4D, mass is entered in force units. However, in this verification problem, mass is given in lb-sec²/in (a unit related to the slug). In order to convert it to force units, it should be multiplied by gravitational acceleration (386 in/sec²). The nodal (joint) mass elements are specified in the global Ydirection:

$M2 = 2 \text{ lb-sec}^2/\text{in}$

$M3 = 1 \text{ lb-sec}^2/\text{in}$

$g = 386 \text{ in/sec}^2$

$M2 = 2 * 386 = 772 \text{ lb}$

$M3 = 1 * 386 = 386 \text{ lb}$

The load P versus time is entered using the Time History tool:

t (sec)	P (lb)
0.0000	0.0
0.0099	0.0
0.0100	100.0
100.00	100.0

These data are saved in a DTH file.

The linear time history analysis option of LARSA is executed using 80 time steps with an integration time step of 0.02 seconds. This time step is about 1/20th of the period of the second mode and the errors in the predicted response by direct integration will be very small. LARSA uses Newmark integration.

Solution Comparison

Vertical Displacement (in inches) at the Tip (Joint 3)

	LARSA 4D	EASE2	Theory
t = 0.00	0.0000	0.0000	0.0000
t = 0.08	0.2396	0.2396	0.3059
t = 0.16	0.9972	0.9970	1.1187
t = 0.24	2.1086	2.1082	2.2640
t = 0.32	3.4793	3.4787	3.6658

	LARSA 4D	EASE2	Theory
t = 0.40	5.1037	5.1027	5.3245
t = 0.48	6.9266	6.9252	7.1666
t = 0.56	8.7694	8.7679	8.9956
t = 0.64	10.4320	10.4305	10.6215
t = 0.72	11.8275	11.8260	11.9830
t = 0.80	12.9677	12.9664	13.0979
t = 0.88	13.8344	13.8333	13.9282
t = 0.96	14.3276	14.3270	14.3614
t = 1.04	14.3654	14.3654	14.3334
t = 1.12	13.9868	13.9874	13.9106
t = 1.20	13.3123	13.3135	13.2143

The results presented under the “Theory” column are computed manually by solving the two-by-two system for eigenvectors and superimposing the responses contributed by each mode. The damping ratio for each mode is calculated from the two-by-two mass-proportional damping matrix. Numerical results from LARSA 4D compares well to results from EASE2 and manual computation.

References

- Peterson, F.E., “EASE2 - Example Problem Manual”, 1981, Problem 3.02 & 4.02.

For More Information, please refer to the following documentation.

- For help on time history analysis, see Linear Time History Analysis in *LARSA 4D Reference Manual*.

TH04: Dynamic Analysis of a Bridge

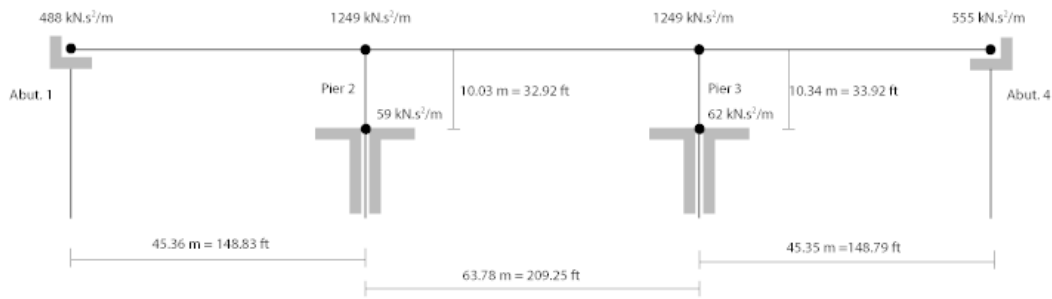
A three-span reinforced-concrete bridge is subjected to the three-dimensional ground displacement records of the 1994 Northridge earthquake.

Example Project: The example described here can be found in the Time History folder of your LARSA 4D Samples directory (generally My Documents\LARSA Projects\Samples) in the file TH04.

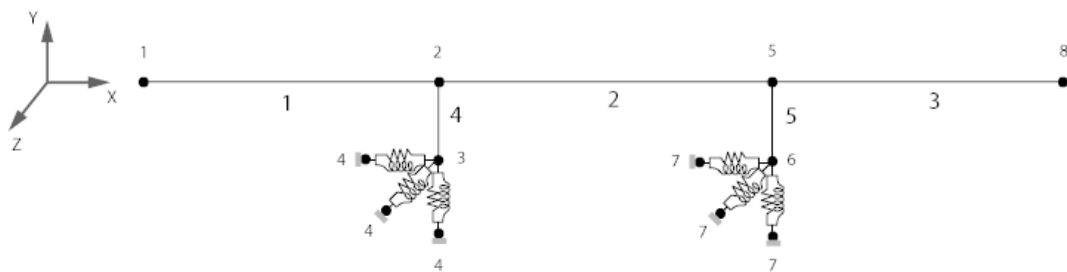
The structure is identical to the collapsed first frame of the SR14/15 southbound separation and overhead bridge located 25 miles north of downtown Los Angeles. The ground motion is believed to have varied in space during actual event due to wave passage and loss of coherence effects, as well as different local soil conditions at the supports.

Determine the response of the structure to spatially varying support displacements by direct integration of the equations of motion with a time step of $\Delta T = 0.02\text{sec}$.

Assume the analysis height of the piers to be equal to the distance from the grade level to the center of gravity of the deck, and account for soil-structure interaction by using foundation springs. Use classical Rayleigh damping (Mass-Proportional = 0.52367 and Stiffness-Proportional = 0.00236) with 5% damping ratios for the first and fifth modes of vibration.



Model Diagram



TH04 Sample

Deck	Pier 2	Foundation Springs @ Pier 2	Pier 3	Foundation Springs @ Pier 3
$E = 23.2 \times 10^6 \text{ kN/m}^2$	$E = 24.3 \times 10^6 \text{ kN/m}^2$	$k_x = 2.7 \times 10^5 \text{ kN/m}$	$E = 24.3 \times 10^6 \text{ kN/m}^2$	$k_x = 3.1 \times 10^5 \text{ kN/m}$
$G = 9.28 \times 10^6 \text{ kN/m}^2$	$G = 9.72 \times 10^6 \text{ kN/m}^2$	$k_y = 12.0 \times 10^5 \text{ kN/m}$	$G = 9.72 \times 10^6 \text{ kN/m}^2$	$k_y = 15.0 \times 10^5 \text{ kN/m}$
$A = 8.800 \text{ m}^2$	$A = 4.207 \text{ m}^2$	$k_z = 5.1 \times 10^5 \text{ kN/m}$	$A = 4.207 \text{ m}^2$	$k_z = 6.2 \times 10^5 \text{ kN/m}$
$I_{yy} = 16.299 \text{ m}^4$	$I_{yy} = 1.746 \text{ m}^4$	$k_{\theta_x} = 290.0 \times 10^3 \text{ kNm/rad}$	$I_{yy} = 1.746 \text{ m}^4$	$k_{\theta_x} = 306.0 \times 10^3 \text{ kNm/rad}$
$I_{zz} = 188.566 \text{ m}^4$	$I_{zz} = 4.770 \text{ m}^4$	$k_{\theta_y} = 1.0 \times 10^6 \text{ kNm/rad}$	$I_{zz} = 4.752 \text{ m}^4$	$k_{\theta_y} = 1.0 \times 10^6 \text{ kNm/rad}$
$I_{yz} = 5.854 \text{ m}^4$	$I_{yz} = 0.682 \text{ m}^4$	$k_{\theta_z} = 49.9 \times 10^3 \text{ kNm/rad}$	$I_{yz} = 0.680 \text{ m}^4$	$k_{\theta_z} = 54.0 \times 10^3 \text{ kNm/rad}$

Solution Comparison

Natural Periods of Vibration

	LARSA 4D	ANSYS	IDARC
T1 (sec)	1.003	1.002	1.002
T2 (sec)	0.352	0.352	0.352
T3 (sec)	0.218	0.217	0.217
T4 (sec)	0.207	0.207	0.207
T5 (sec)	0.198	0.197	0.197

Maximum Total Displacements of Nodes 2 and 5

	LARSA 4D	ANSYS	IDARC
U_{x,2} (m)	0.503E+00, -0.425E+00	0.503E+00, -0.425E+00	0.503E+00, -0.425E+00
U_{z,2} (m)	0.324E+00, -0.220E+00	0.324E+00, -0.220E+00	0.324E+00, -0.220E+00
U_{x,5} (m)	0.503E+00, -0.425E+00	0.503E+00, -0.425E+00	0.503E+00, -0.425E+00
U_{z,5} (m)	0.320E+00, -0.227E+00	0.320E+00, -0.227E+00	0.320E+00, -0.227E+00

References

- A.M. Reinhorn, V. Simeonov, G. Mylonakis, and Y. Reichman, "IDARC-BRIDGE: A Computational Platform for Seismic Damage Assessment of Bridge Structures.", 1998, p.113-126. The Department of Civil, Structural and Environmental Engineering at the University of Buffalo, State University of Buffalo New York.

For More Information, please refer to the following documentation.

- For help on time history analysis, see Linear Time History Analysis in *LARSA 4D Reference Manual*.

TH05: Two Dimensional Frame with Linear Viscous Damper

A two-dimensional three-story steel frame with linear viscous dampers at each story.

Example Project: The example described here can be found in the Time History folder of your LARSA 4D Samples directory (generally My Documents\LARSA Projects\Samples) in the file TH05N.

Background

Viscous dashpot damping devices are widely used as structural protective systems for extreme loading (wind and earthquake) cases. Due to their combined benefits in terms of overall displacement reduction and energy dissipation, dampers are considered to be one of the most effective structural protective systems.

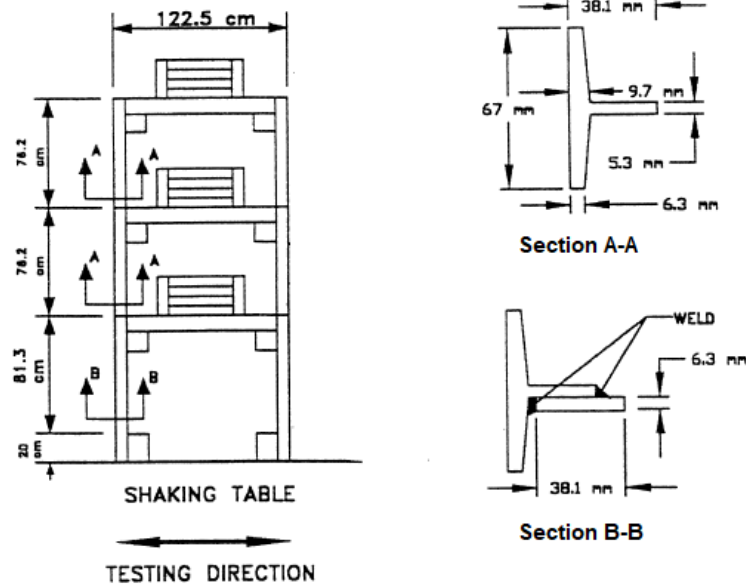
The dashpot isolator element in LARSA 4D is suitable for modeling the behavior of fluid viscous dampers or other devices displaying viscous behavior.

Fluid dampers which operate on the principle of fluid orificing, produce an output force which is proportional to a power of the velocity, i.e. Cv^n , where C is a damping coefficient, v is the velocity across the dashpot, and n is an integer power typically between 0.5 and 2.0 (1.0 implies linear behavior.)

Problem Description

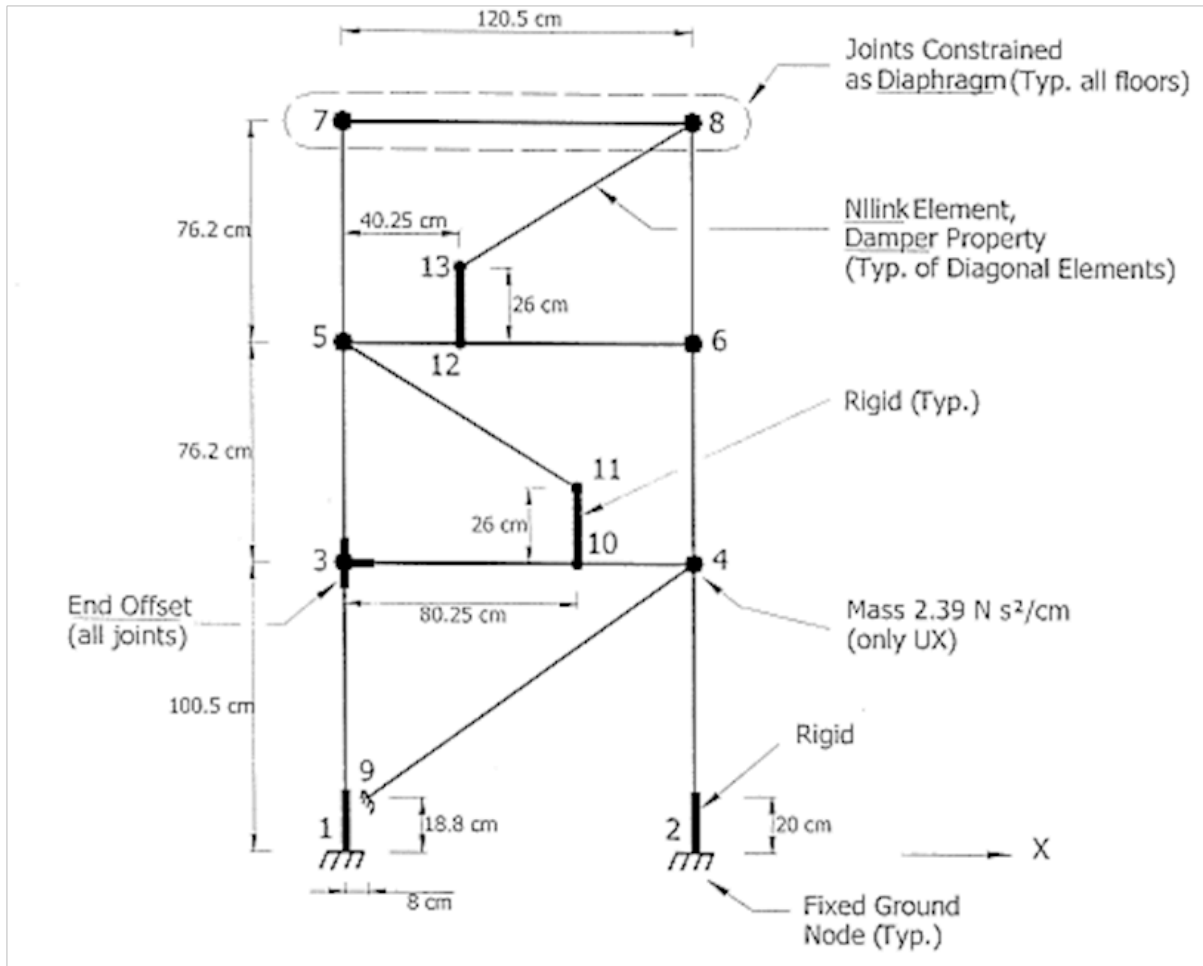
This example comes from Section 5 of Scheller and Constantinou (1999). It is a two-dimensional, three story frame building with diagonal viscous dampers that have linear force versus velocity behavior. The model is subjected to horizontal seismic excitation using a scaled version of the S00E component of the 1940 El Centro record. The LARSA 4D results for modal periods and story drift curves are compared with experimental results obtained using shake table tests.

The test setup and the sections used in the actual shake table test are represented in the figure below.



Shake Table Test (adapted from Scheller and Constantinou (1999))

The two-dimensional three-story experimental steel frame with linear viscous dashpots at each story is modeled in LARSA 4D, as shown in the figure below. The dimensions and properties of the frame elements (fabricated primarily with ST 2X3.85 cut with depth = 1.5 inches) and mass assignments are adopted from Scheller and Constantinou (1999).



Three Dimensional Building (adapted from Scheller and Constantinou (1999))

The member end offsets of the elements are modeled in order to simulate the stiffening effects of the floor weights (steel plates).

The dashpots have coefficient of damping as $C = 160 \text{ N-s/cm}$ and velocity exponent (n) = 1. See below for a comparison of linear ($n=1$) and nonlinear ($n<1$) dashpots.

The model is analyzed with the Nonlinear Time History Analysis in LARSA 4D with the S00E component of the El Centro 1940 earthquake ($p_{ga} = 0.343g$).

Solution and Comparison

Model Periods

First, an eigenvalue analysis is done on the model. The periods of the first three modes are computed and presented in the following table. Computed period values by eigenvalue analysis are in close proximity to those obtained from shake table tests.

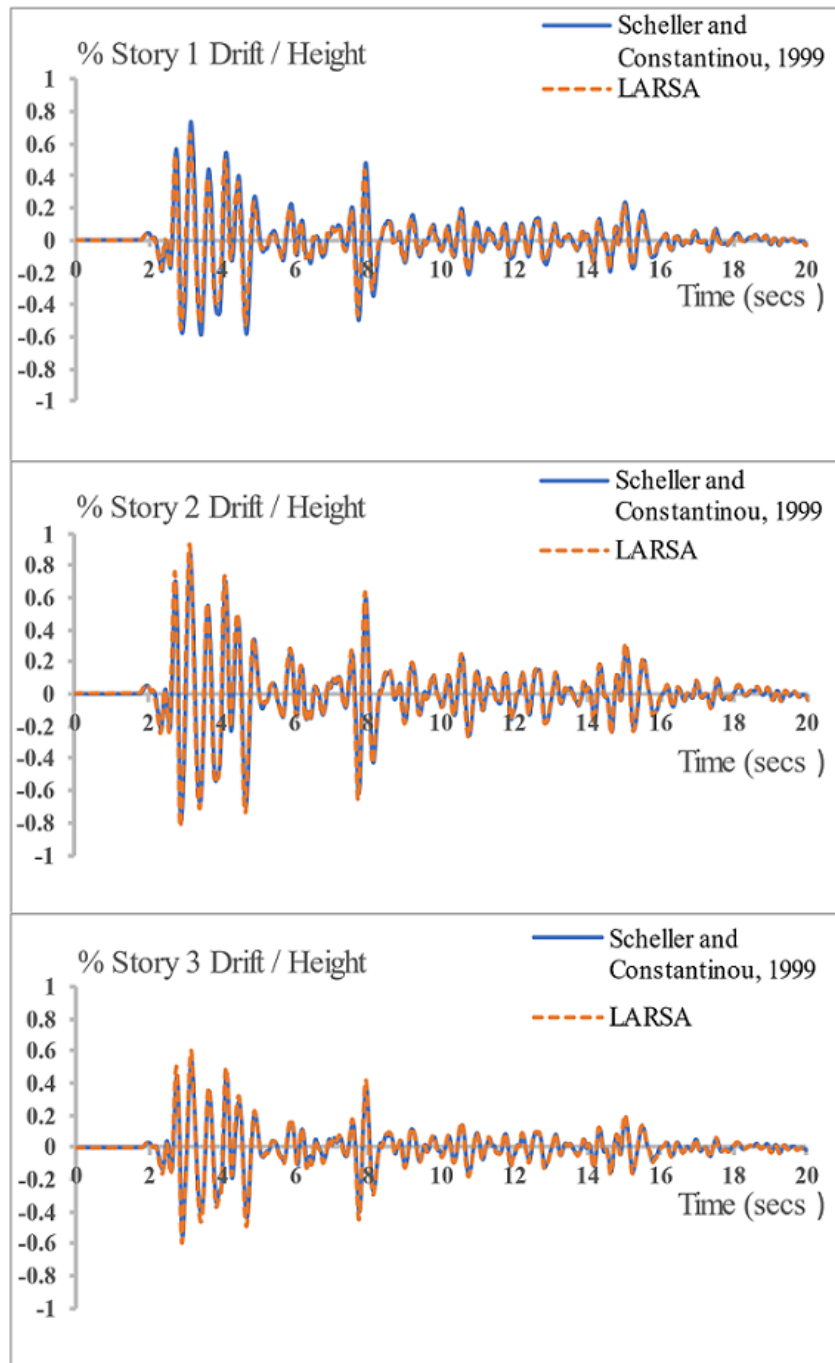
Mode	Experiment Period (sec)	LARSA 4D Period (sec)
1	0.439	0.448
2	0.133	0.132
3	0.070	0.067

Story Drifts

Some representative displacement magnitudes of the 1st story of the frame from the Nonlinear Time History Analysis are:

Time (sec)	Displacement (mm)
1	0.0015
5	-0.2576
10	0.4950

The history of percent-normalized story drifts ($100 \times \text{drift} / \text{story height}$) obtained from LARSA 4D are compared with the corresponding results from Scheller and Constantinou (1999):

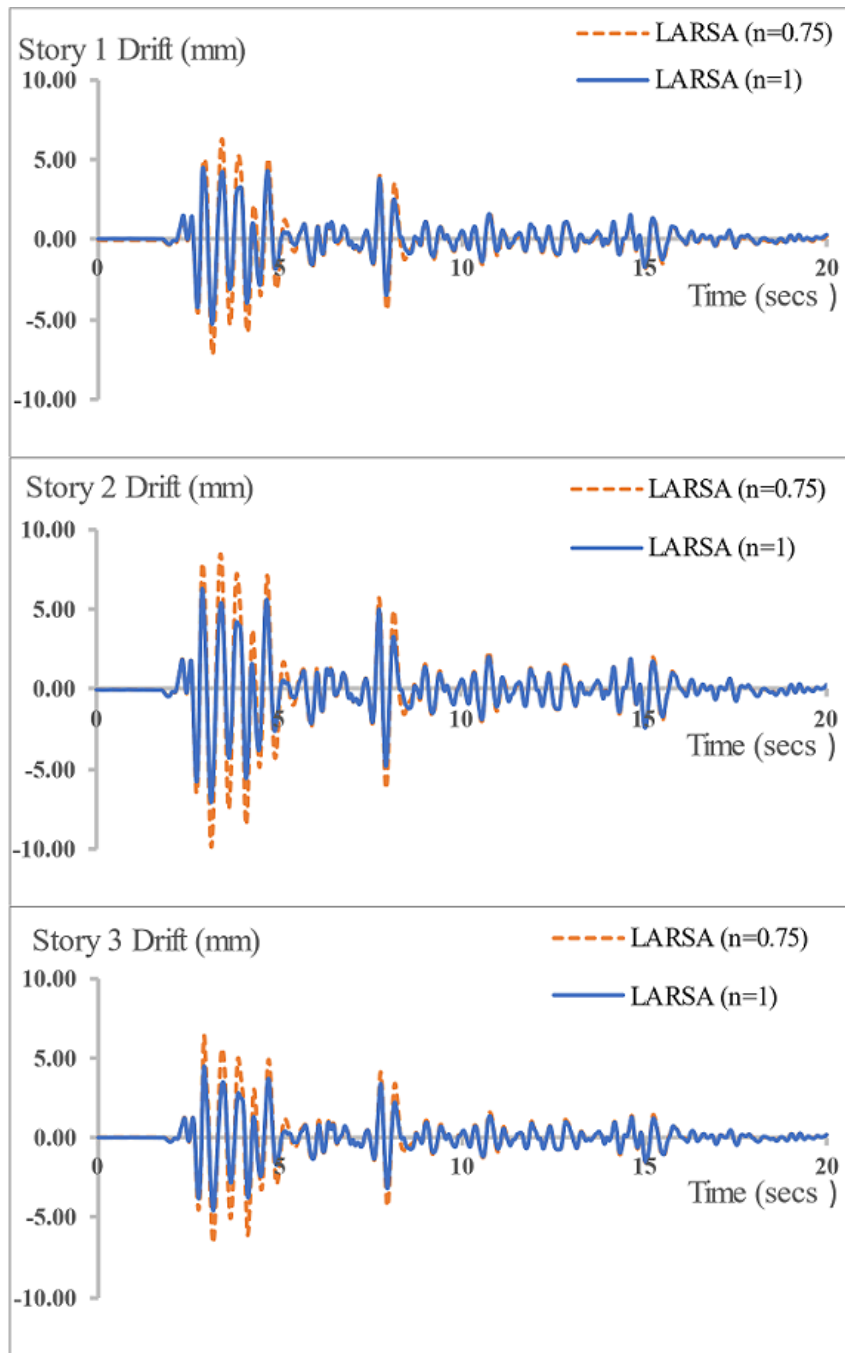


Comparisons for the dynamic responses of the 2D frame

The comparisons indicate that the LARSA is capable of modeling linear dampers with appreciable accuracy.

Nonlinear Dashpots

This problem can also be run with a nonlinear dashpot, that is, with the velocity power n set to 0.75. The figure below shows a comparison of story drifts for a linear ($n=1$) and nonlinear ($n=0.75$) dashpot.



Comparisons of story drifts for linear ($n=1$) and nonlinear ($n=0.75$) dampers

It should be noted that when the velocity exponent n is not 1.0, then the damping coefficient and velocity power must be chosen with respect to a particular choice of units. In the present example C is assumed to have unit as N-s/mm and v as mm/sec. Care should be taken for units of C and v when using nonlinear damping properties.

Limitations

LARSA 4D cannot model the traditional Maxwell or Kelvin elements with dashpots directly. However, those can be modeled in LARSA 4D by combining the damping element with brace elements.

References

- Scheller, J., and Constantinou, M. C. (1999). "Response History Analysis of Structures with Seismic Isolation and Energy Dissipation Systems: Verification Examples for Program SAP2000." Technical Report MCEER-99-0002. University of Buffalo, State University of New York.
- Seleemah, A A, and Constantinou, M C (1997). "Investigation of Seismic Response of Buildings with Linear and Nonlinear Fluid Viscous Dampers." Technical Report NCEER-97-0004, SUNY, University at Buffalo.

For More Information, please refer to the following documentation.

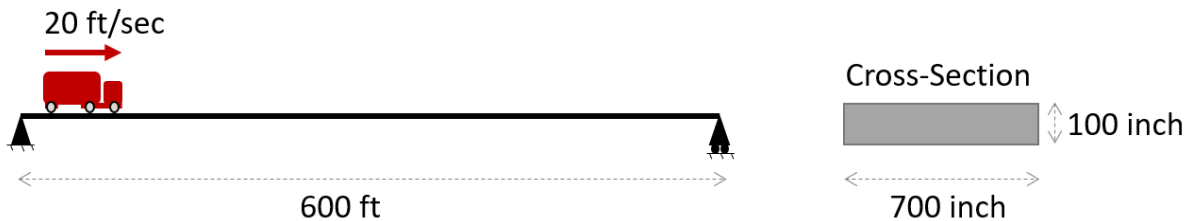
- For help on time history analysis, see Linear Time History Analysis in *LARSA 4D Reference Manual*.

TH15: Rolling Stock Analysis

Rolling Stock Analysis is a linear Time History Analysis using moving load patterns. The mass of the vehicle is not considered.

A single vehicle is moving on a simply supported bridge deck with a constant speed. Determine the mid-span displacements with respect to time and also the maximum bending moment when the vehicle is 140 ft away from the deck end. The results of a Rolling Stock Analysis (RoSA) are compared with the results of a Moving Load Analysis, which is a linear elastic static analysis.

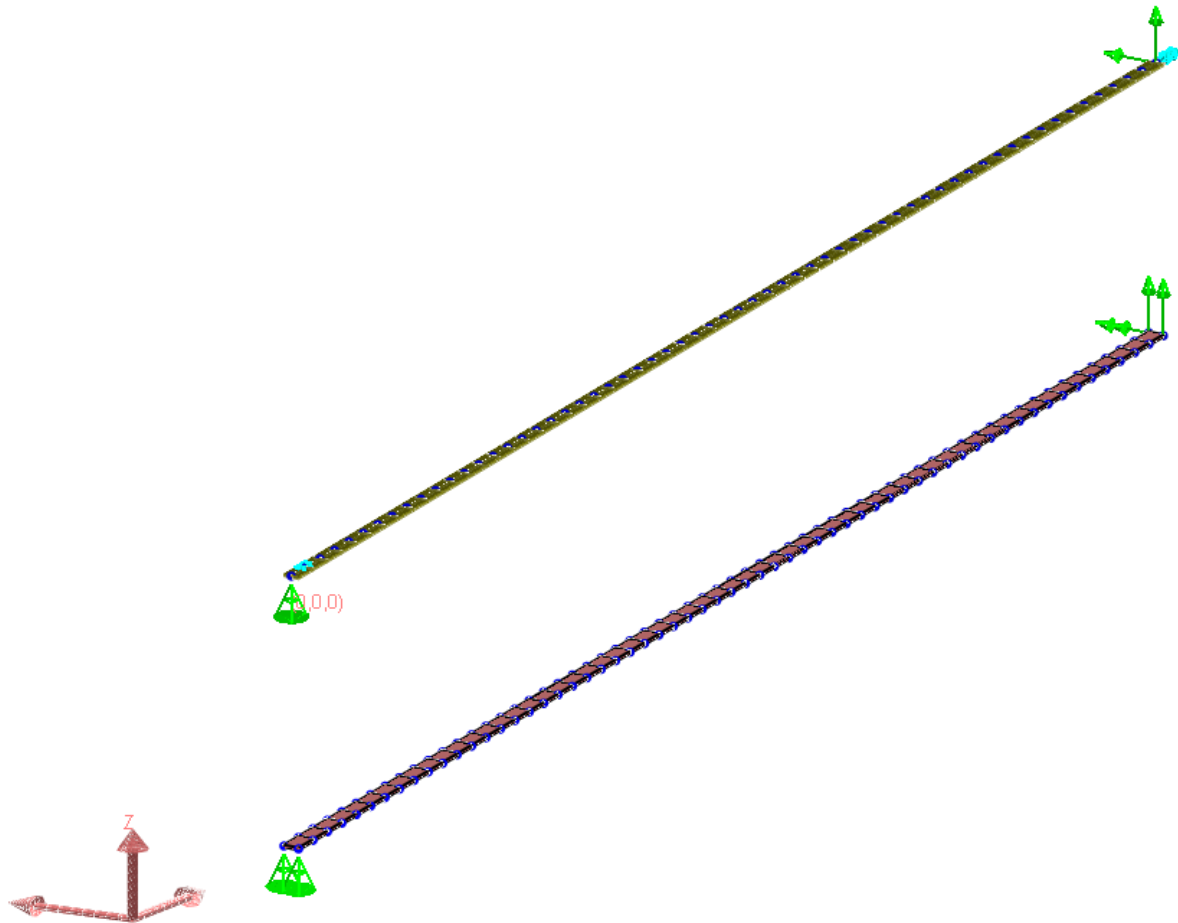
Example Project: The example described here can be found in the TimeHistory folder of your LARSA 4D Samples directory (generally My Documents\LARSA Projects\Samples) in the file TH15.



Sample TH15

Model Setup

A 600 ft long deck 700 inch wide is modeled with two different modeling approaches: girder with 60 beam elements and girder as 60-by-1 plate mesh. The joints along the start of the decks are supported in all translation directions, and the joints along the end of the deck are supported in y and z-translation. Both ends are also supported in x-rotation for the model with beam elements (For plate model, no need to restrain rotation x).



Model View

A36 steel is assigned to the elements. Properties of A36 steel are:

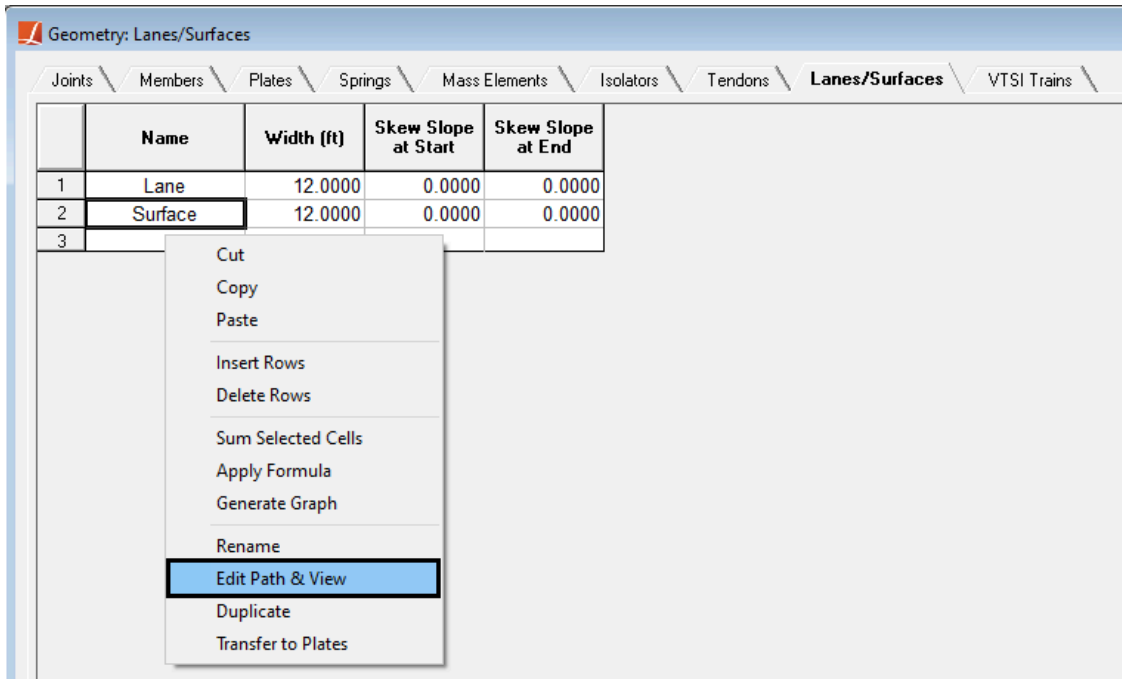
$$E = 2.9E07 \text{ lb/in}^2$$

$$G = 1.12E07 \text{ lb/in}^2$$

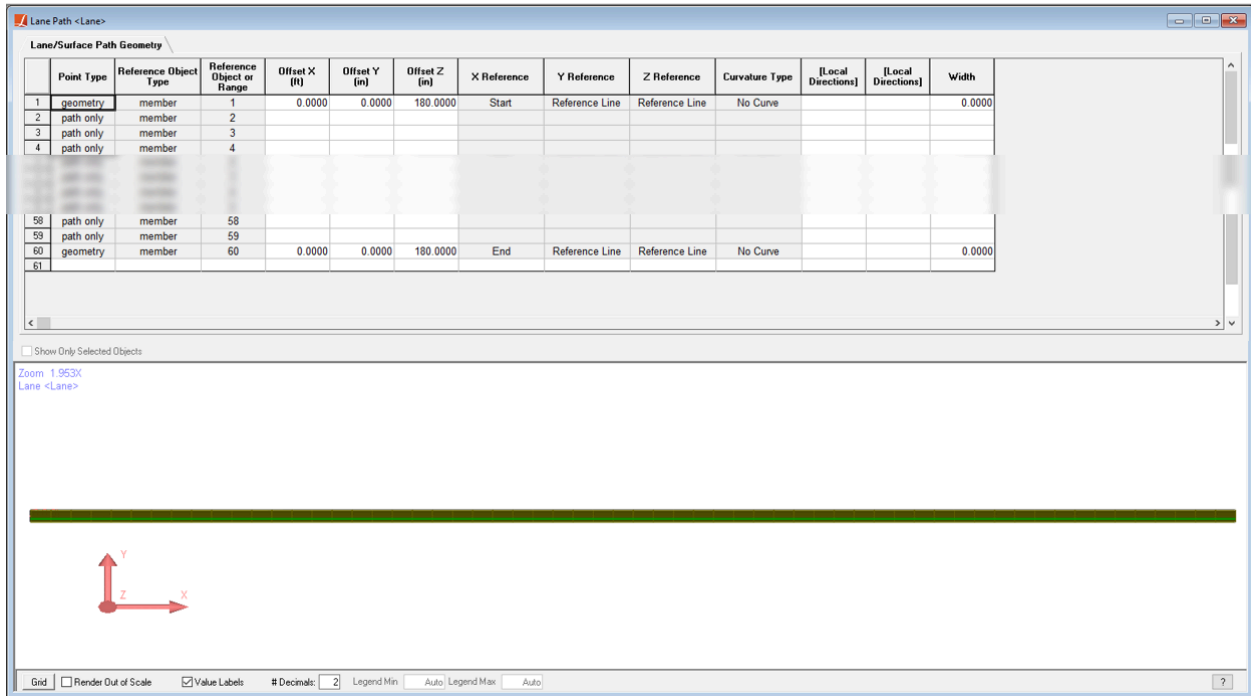
$$\text{Unit Weight} = 0.2836 \text{ lb/in}^3$$

However, for the purposes of making a verification comparison to a static moving load analysis, set the **unit weight** of the material as small as $1.0E-05 \text{ lb/inch}^3$ to remove the effect of the mass of the structure from the dynamic results.

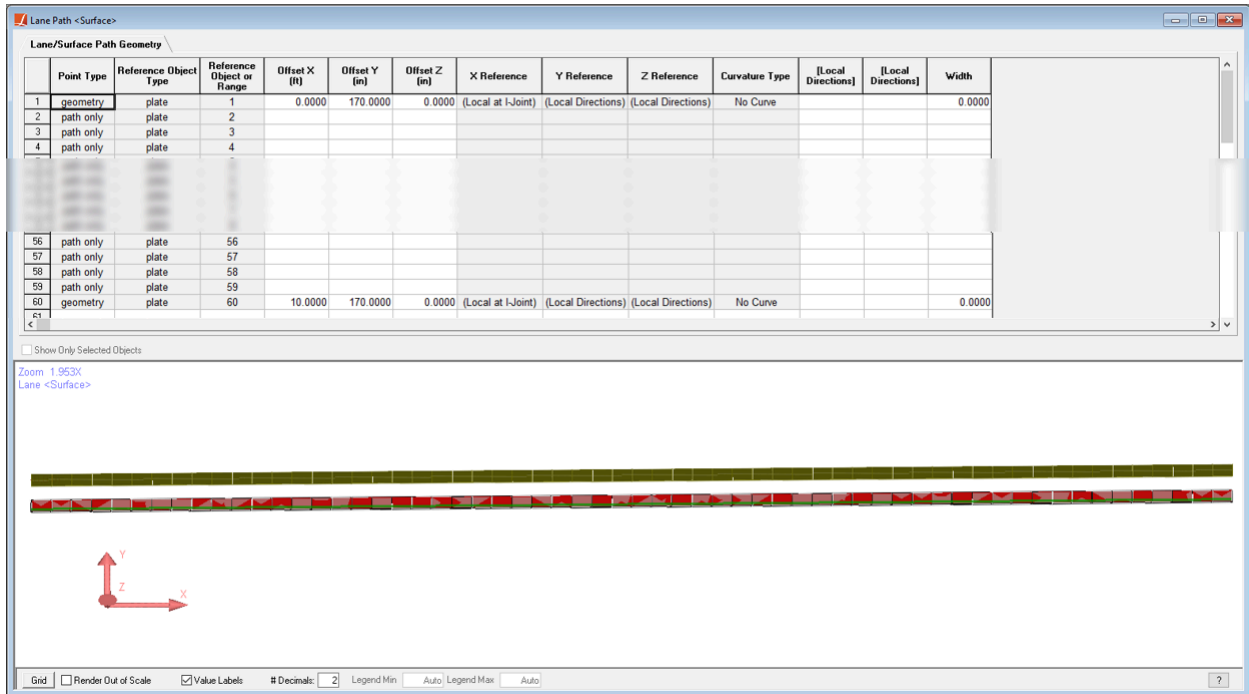
A single lane whose width is 12 feet is defined on the deck surface. It is defined from **Input Data** → **Geometry** → **Lanes/Surfaces**. The path of the lane is defined along the deck and it is offset 180 inch from the center of the deck in the transverse direction. Right click on defined lane or surface and select **Edit Path and View** to view corresponding lane's or surface's definition.



Lane/Surface Geometry



Lane Path Definition

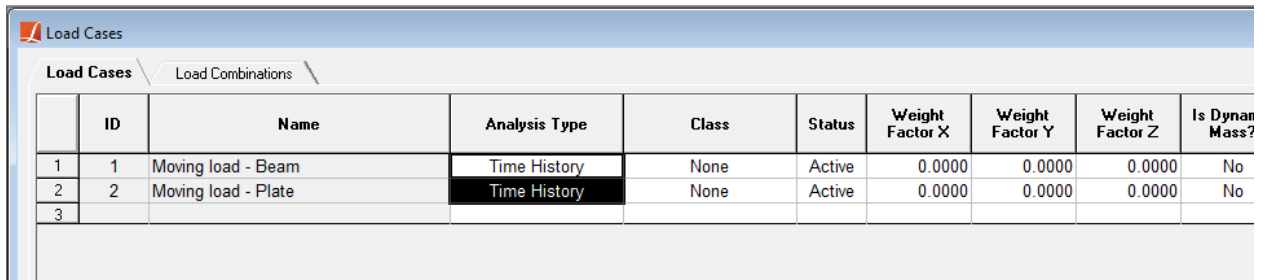


Surface Path Definition

In this example, "HS20-44" vehicle that exists in "movedata" database file, is moving on the defined lane/surface from the start of the deck to its end with a velocity of 200.0 ft/sec. So connect the "movedata.dml" database to the project.

Rolling Stock Analysis

In this example, define two load cases, one is for the model with beams and the other for the model with plate elements. Select **Time History** for their Analysis Type.



Load Cases for Rolling Stock Analysis

Then, apply moving loads from **Moving Loads** → **Basic Moving Loads**.

Select the lane that the load is moving on it and the vehicle, "HS20-44", as load pattern. Enter the vehicle speed as 200 ft/sec.

"Forward" travel direction means the vehicle is moving from the start of the lane definition to the end and "Backward" is the vice versa. Start Position is the distance between the front of the vehicle in the first time step and the start point of the lane definition.

	Lane Loaded	Load Pattern	Applied Load Direction	Load Factor	Direction of Travel	Vehicle Speed (ft/sec)	Start Position (ft)
1	Lane	HS20-44	Global -Z	1.0000	Forward	200.0000	0.0000
2							

Moving Load Definition for Rolling Stock Analysis

Go to **Analysis** → **Moving Load Analysis (Static/Dynamic)** → **Dynamic Rolling Stock**. Select 100 time steps by entering 0.1 sec for the step size and 10 sec for the ending time of the analysis.

Run Moving Load Analysis

Select Analysis Type

- Static Moving Load/Influence
- Dynamic Rolling Stock**
- Vehicle-Track-Structure Interaction

Keep Previous Results
 Perform Quick Integrity Check

Description:
 Performs a linear dynamic rolling stock analysis on time history load cases with moving load patterns.

Time History Options

Rayleigh Damping Constants Other Options

Time step size: 0.1 Ending time interval: 10

Time units are in seconds

Save results every 1 step

Integration Method

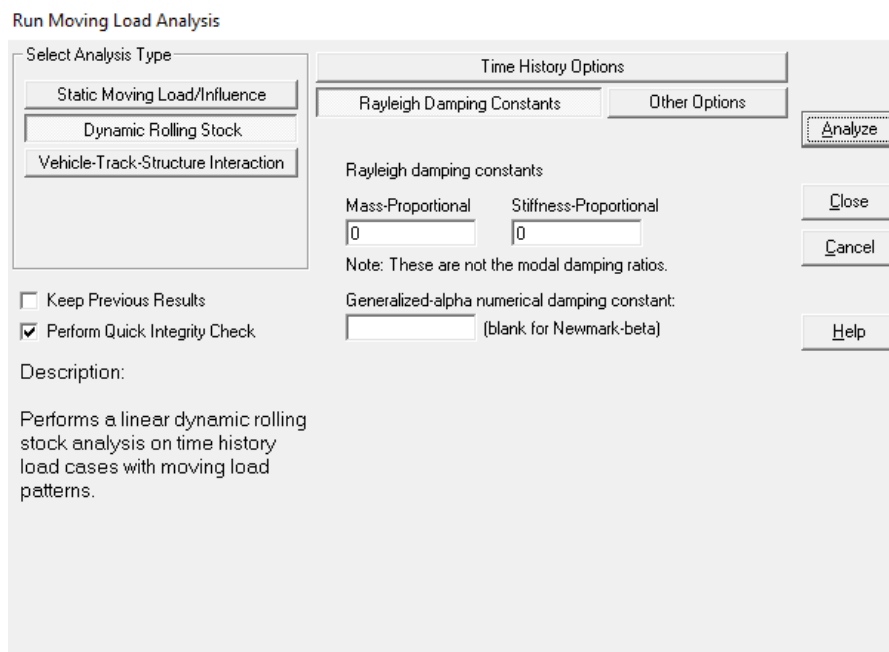
- Constant Step**
- Adaptive Step (uniform base acceleration only)

Step size range: Min 0.0001 Max 1

Analyze Close Cancel Help

Linear Time History Analysis Parameters

For the purposes of making a verification comparison to a static moving load analysis, set the damping of the system to zero by setting the Rayleigh Damping Constants to zero.



Rayleigh Damping Constants

Click **Analyze** to start the analysis.

Moving Load Analysis

The same problem is solved by a Moving Load Analysis to verify the Rolling Stock Analysis results. Similarly, define two load cases for the beam and plate models but this time, **Analysis Type** should be set as **Moving (Static)**.

Load Cases		Load Combinations	
ID	Name	Analysis Type	
1	7	Moving Load - Beam	Moving (Static)
2	8	Moving Load - Plate	Moving (Static)
3			Static
			Moving (Static)
			Response Spectrum
			Time History
			Pushover

Load Cases for Moving Load Analysis

Define the moving load in a same way with the Rolling Stock Analysis. But this time, **Position Increment** should be set instead of **Vehicle Speed** since it is a linear elastic analysis. By entering 20.0 feet to this parameter, vehicle position will be identical for the both analyses' solution steps.

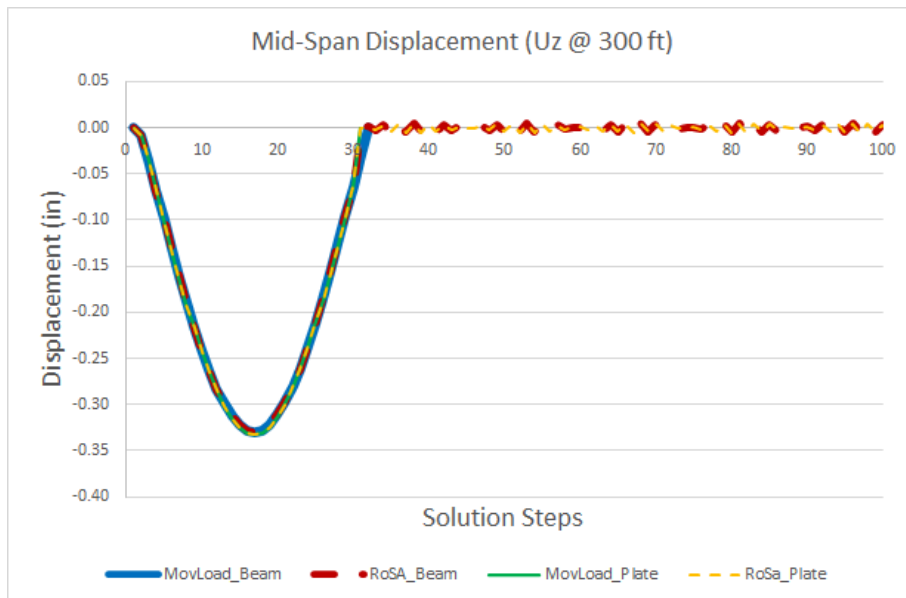
Moving Load - Beam: Basic Moving Loads							
Joint Loads \ Support Disp \ Member Loads \ Plate Loads \ Moving Loads \ Time History \ RSA Loads \							
Basic Moving Loads Influence Loads							
	Lane Loaded	Load Pattern	Applied Load Direction	Load Factor	Direction of Travel	Position Increment (ft)	Start Position (ft)
1	Lane	HS20-44	Global -Z	1.0000	Forward	20.0000	0.0000
2							

Moving Load Definition for Moving Load Analysis

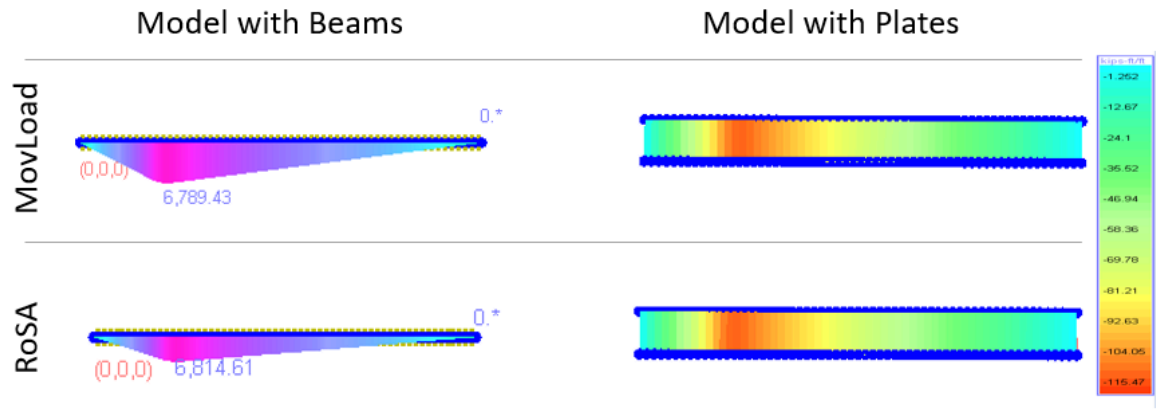
Then, run **Moving Load Analysis**.

Comparison of Results

Displacement histories at mid-span (i.e. @300 feet) and maximum bending moments when the vehicle at 140 feet from the start of both beam and plate structures obtained from Rolling Stock Analysis (RoSA) and Moving Load Analysis (MovLoad) are compared to each other. Vehicle leaves the system at the end of 30th step in both Rolling Stock and Moving Load Analyses.



Mid-Span Displacements



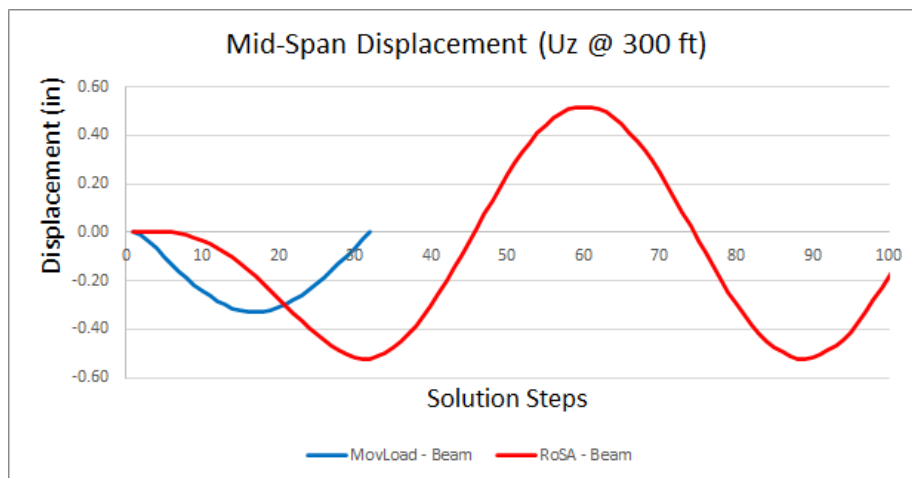
Moment Diagrams when the Vehicle @ 140 ft

Max. Bending Moments on Deck when the Vehicle @ 140 ft (without Mass)

Model	Max. Mz (kips-ft)	Model	Max. Mxx (kips-ft/ft)
MovLoad - Beam	6789.43	MovLoad - Plate	115.38
RoSA - Beam	6814.61	RoSA - Plate	115.47

Dynamic Effect

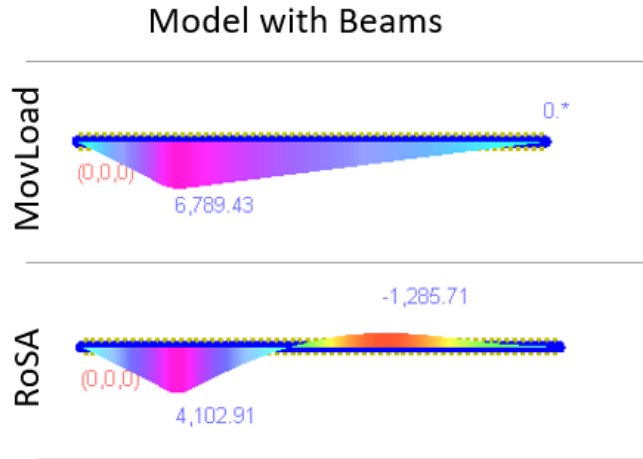
When real unit weight of the material, 0.2836 lb/in^3 , is assigned to the system, mid-span displacement graph obtained from Rolling Stock Analysis magnifies and shifts forward with respect to Moving Load Analysis' plot. Also it oscillates around 0.



Mid-Span Displacements

Similarly moment diagrams when the vehicle at 140 feet from the start point do not overlap anymore. at this point, although Rolling Stock Analysis gives smaller moments than the Moving Load Analysis, the envelope moments, which

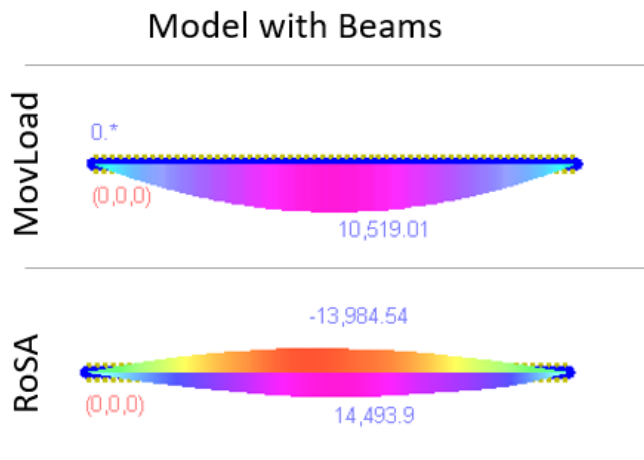
the structure is subjected to throughout the entire solution, are higher for the Rolling Stock Analysis due to the inertial effects. Moreover, it is subjected to both positive and negative moments.



Moment Diagrams when the Vehicle @ 140 ft

Max. Bending Moments on Deck when the Vehicle @ 140 ft (with Mass)

Model	Max. Mz (kips-ft)
MovLoad - Beam	6789.43
RoSA - Beam	4102.91



Moment Diagrams (Envelope)

Envelope Bending Moments on Deck (with Mass)

Model	Max. Mz (kips-ft)	Min. Mz (kips-ft)
MovLoad - Beam	10,519.01	0.0
RoSA - Beam	14,493.90	-13,984.54

For More Information, please refer to the following documentation.

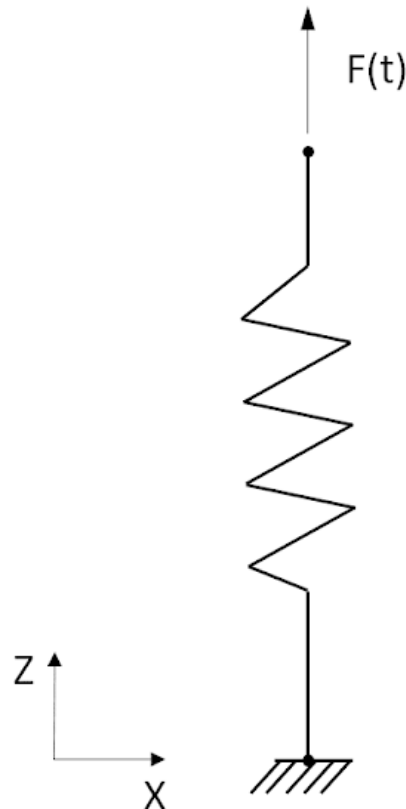
- For help on rolling stock analysis, see Linear Static Moving Load Analysis and Dynamic Rolling Stock Analysis in *LARSA 4D Reference Manual*.
- For help on time history analysis, see Linear Time History Analysis in *LARSA 4D Reference Manual*.

TH18: Hysteretic Spring Time History Analysis

This example demonstrates a response of a single hysteretic (inelastic) spring subjected to a cyclic dynamic load.

Example Project: The example described here can be found in the TimeHistory folder of your LARSA 4D Samples directory (generally My Documents\LARSA Projects\Samples) in the file TH18.

Fifteen springs are considered corresponding to one of the analysis cases or sub-cases described below. The locations of springs' joints are selected arbitrarily. The lengths of the springs have no effect on the solution. The structural model has one degree of freedom per spring in the direction of the spring.



A single hysteretic (inelastic) spring

In order to demonstrate the hysteretic spring parameters available in LARSA 4D, seven different cases are considered in this example:

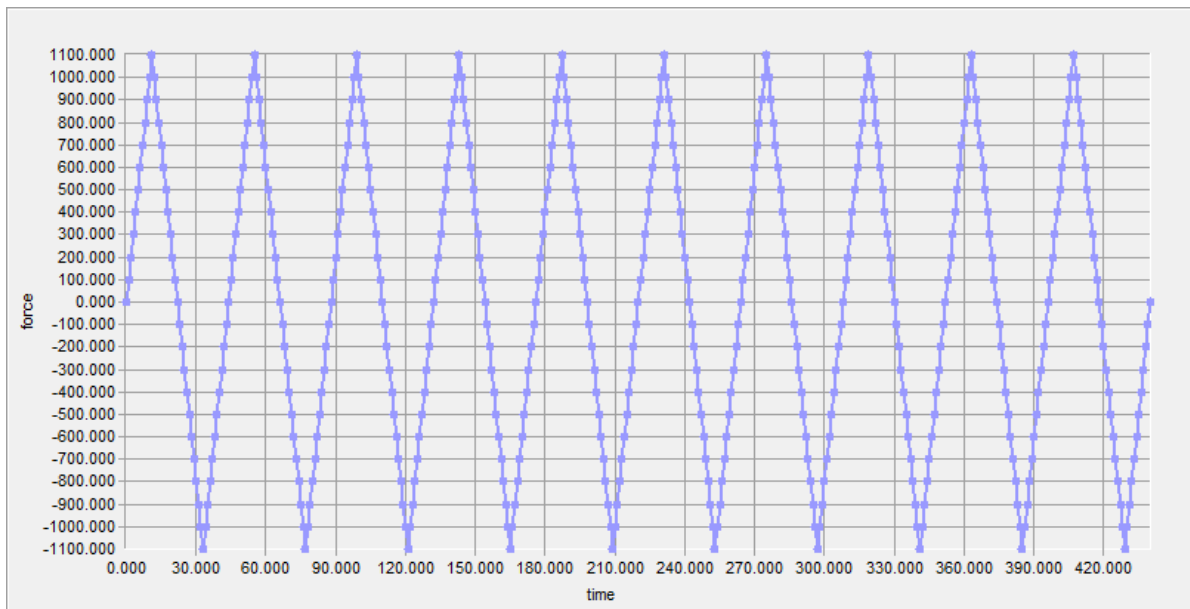
1. Hysteretic spring with bilinear backbone curve and without stiffness and strength degradation
2. Hysteretic spring with bilinear backbone curve and stiffness degradation
3. Hysteretic spring with bilinear backbone curve and ductility-based strength degradation

4. Hysteretic spring with bilinear backbone curve and energy based strength degradation
5. Hysteretic spring with trilinear backbone curve and vertex oriented polygonal hysteretic model (PHM)
6. Hysteretic spring with trilinear backbone curve and yield-oriented PHM
7. Hysteretic spring with trilinear backbone curve, yield-oriented PHM, and slip

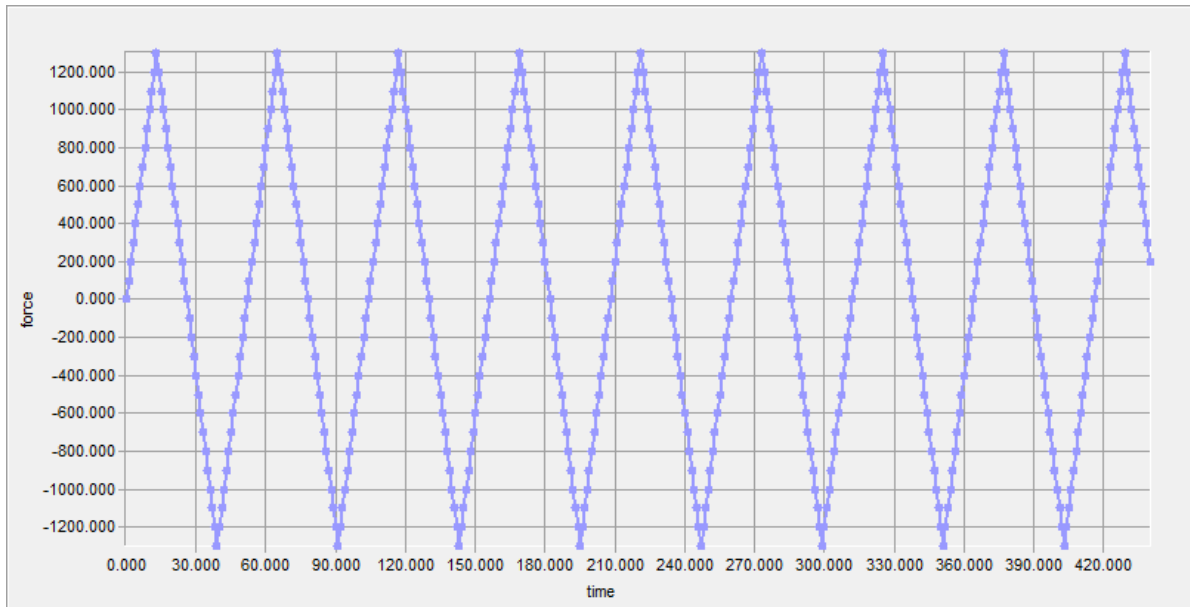
The backbone curve determines the spring's force-deformation relationship. In this example, a bilinear backbone curve specified for cases 1 to 4 and a trilinear backbone curve is chosen for cases 5 to 7.

The Polygonal Hysteretic Model (PHM) is a piecewise linear (multi-linear) hysteretic model that dictates the movement along the hysteresis loops. For a spring with a bilinear backbone curve (cases 1 to 4), only bilinear PHM is available. In this case, the spring's response simply follows a hysteresis loop outlined by the bilinear backbone curve. For a spring with trilinear backbone curve (cases 5 to 7), PHM can be either vertex-oriented or yield-oriented. In the model with vertex-oriented PHM, the response curve "shoots" for the backbone vertexes. Yield-oriented PHM corresponds to response curve "shooting" for the backbone curve's yield points. Various degradation and slip parameters are available for hysteretic springs and are used in cases 2 to 4 and 6 to 7. These parameters are demonstrated and discussed in the corresponding cases.

Time history load is applied to the spring in the Translation-Z direction. Two different time history loads are considered for cases 1 to 4 and 5 to 7.



Cyclic load applied in Cases 1 to 4



Cyclic load applied in Cases 5 to 7

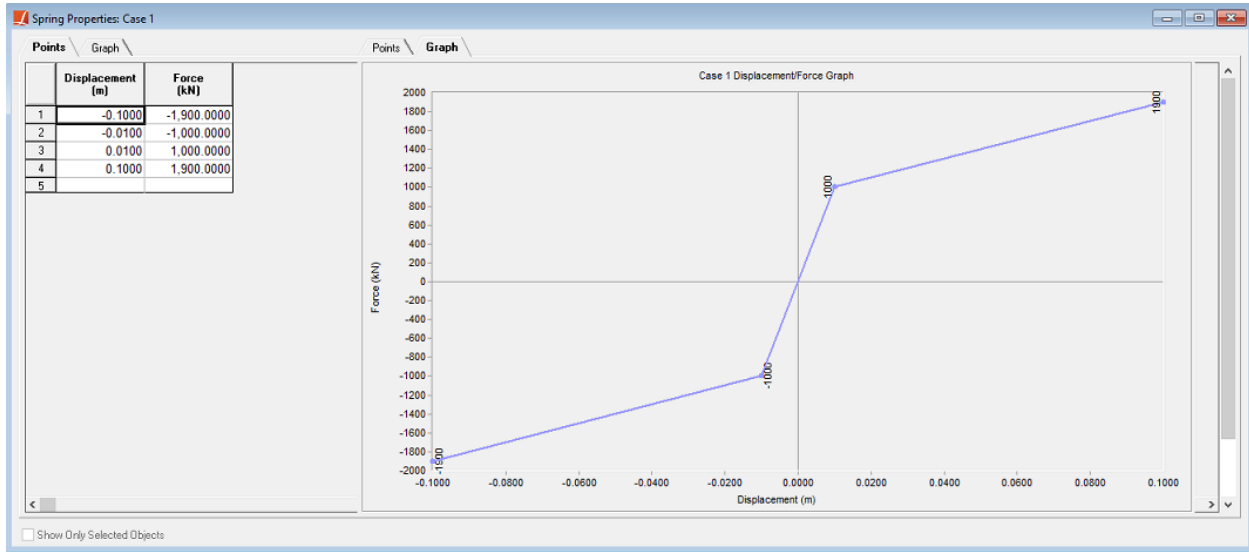
Modeling

The spring is defined from **Input Data** → **Geometry** → **Springs**. The type of the spring should be set to Hysteretic. In this example, the direction in which the spring is acting is local axial. Hysteretic spring properties have to be set in Properties Definition. The spring can also be added to a Structure/Construction Group if needed. All the other properties are used only for linear springs and ignored for hysteretic springs.

Hysteretic spring properties can be defined from **Input Data** → **Properties** → **Spring Properties**. The type of the spring property for this example is chosen as **Hysteretic - Translational** (similarly, **Hysteretic - Rotational** should be chosen if a rotational hysteretic spring is used). All other hysteretic spring parameters are described later in the example as they are encountered.

Case 1: Hysteretic spring with bilinear backbone curve and without stiffness and strength degradation

Create a new hysteretic spring property following the menu as described above and set the appropriate spring property type. An important step in modeling of the hysteretic spring is specifying a force-displacement backbone curve. This can be done by right-clicking the created spring property and selecting **Edit Curve**. For a bilinear curve (cases 1 to 4), four backbone points should be entered in a tabular format. Point (0,0) should not be entered as an input. However, the resulting curve should pass through point (0,0). Meaning that the compressive and tensile stiffnesses must be equal in the pre-yield range. After entering the curve points, the resulting curve can be viewed by selecting the tab Graph.



Bilinear force-displacement backbone curve for Cases 1 to 4 in tabular format and as a graph

In this case, stiffness and strength degradation are not modeled. Therefore, the stiffness degradation parameter Alpha is set to a large value (namely 200) to avoid stiffness degradation. The strength degradation parameters Beta 1 and Beta 2 are set to zero to avoid strength degradation. Slip parameter Gamma is not applicable for a bilinear model and is ignored as an input. After all the parameters are entered, the spring properties window should look as shown below.

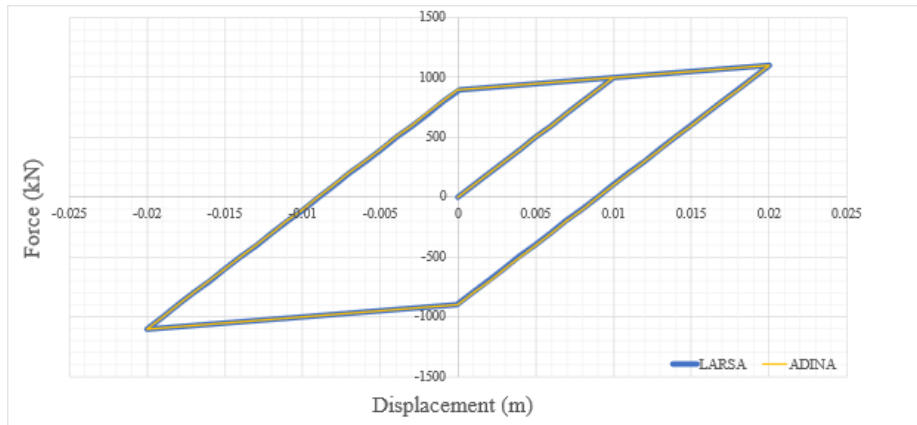
The screenshot shows the 'Properties: Spring Properties' window. It contains a table with the following data:

	Name	Type	Backbone	Polygonal Hysteretic Model	Alpha	Beta 1	Beta 2	Gamma	Mu	Assigned	Number of Points
1	Hysteretic Spring Curve	Hysteretic: Translational	Bilinear	Bilinear	200.0000	0.0000	0.0000	0.0000	0.0000	Yes	4
2											

Hysteretic spring properties

Comparison of Results

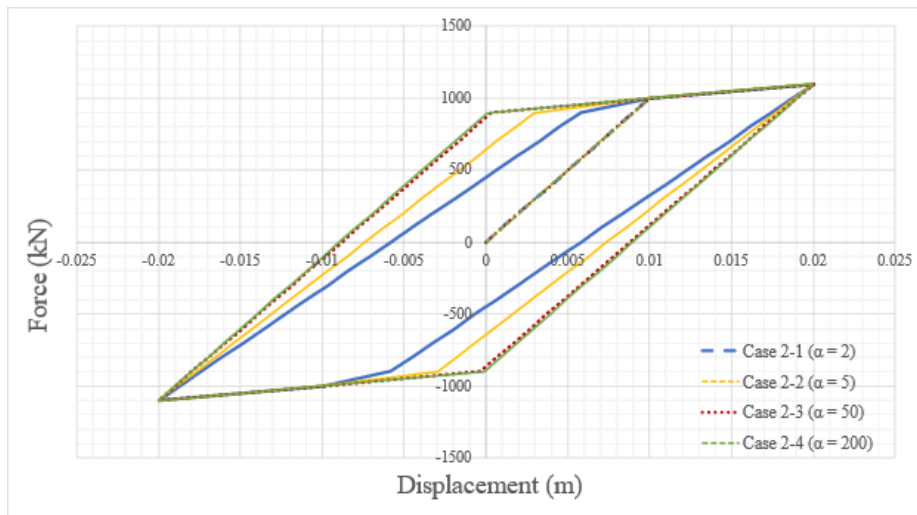
The results of this case are compared with ADINA. The hysteretic spring is modeled in ADINA using a truss element with plastic-bilinear material.



Case 1. The resulting force-displacement relationship and comparison with ADINA

Case 2: Hysteretic spring with bilinear backbone curve and stiffness degradation

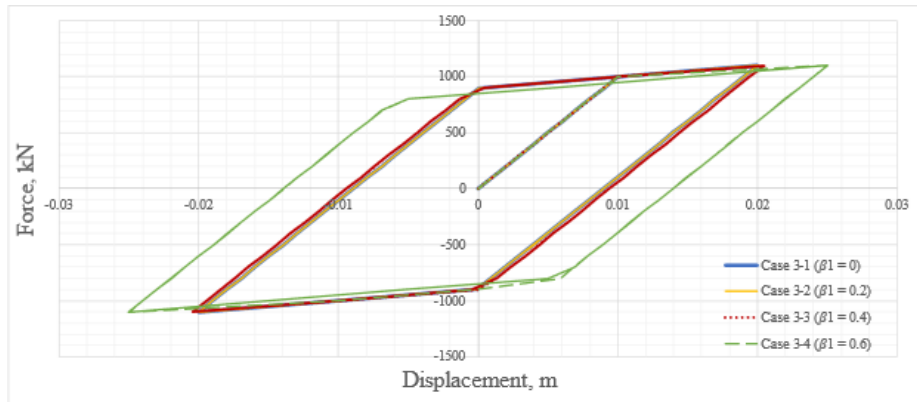
In this case, we introduce the stiffness degradation parameter Alpha. Cases 2-1 to 2-3 correspond to the hysteretic springs with the parameter Alpha varying from 2 to 200. As can be seen from the analysis results, values of Alpha smaller than 200 cause stiffness degradation of the spring.



Case 2. The resulting force-displacement relationship

Case 3: Hysteretic spring with bilinear backbone curve and ductility-based strength degradation

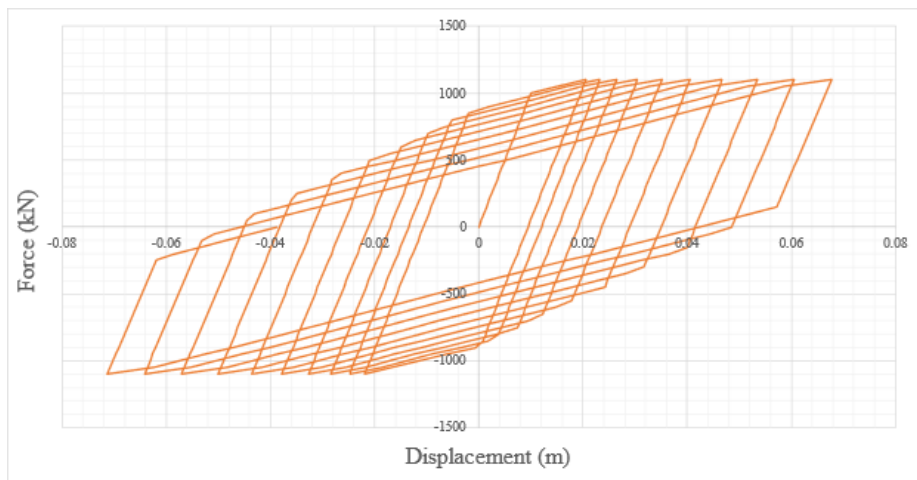
Strength degradation is modeled by reducing the capacity of the backbone curve. This is achieved by introducing two strength degradation parameters: ductility-based strength degradation parameter β_1 and energy-based strength degradation parameter β_2 . Cases 3-1 to 3-4 correspond to the hysteretic springs with the parameter β_1 varying from 0 to 0.6. Parameter β_2 is discussed in the next section.



Case 3. The resulting force-displacement relationship

Case 4: Hysteretic spring with bilinear backbone curve and energy based strength degradation

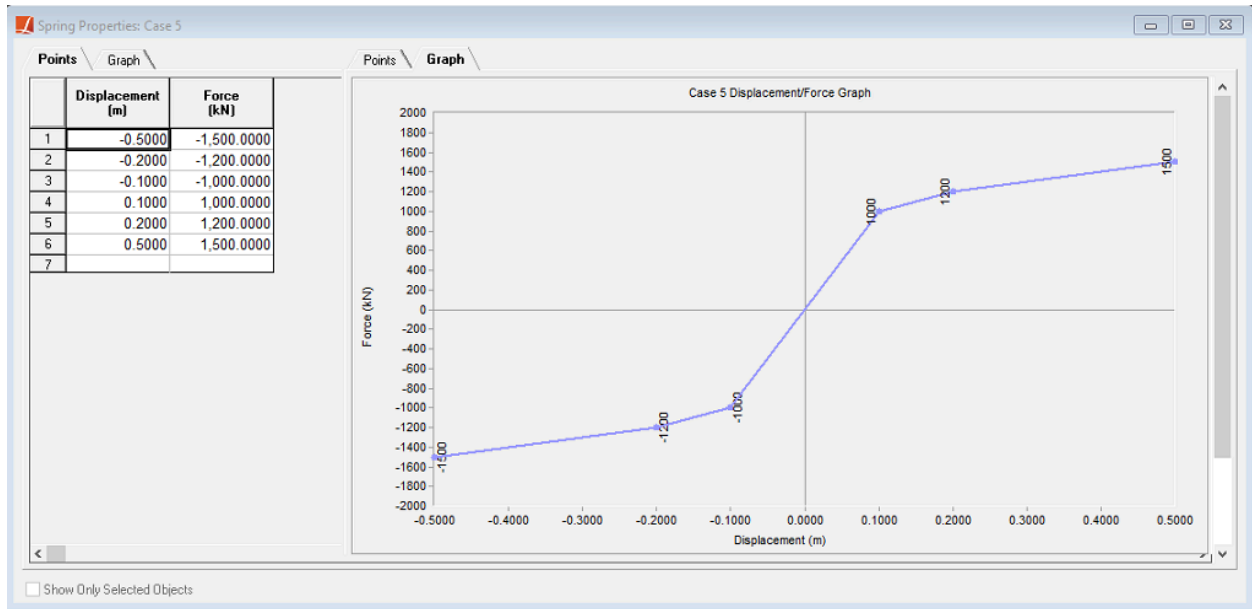
Energy-based strength degradation parameter β_2 is introduced in this section.



Case 4. The resulting force-displacement relationship

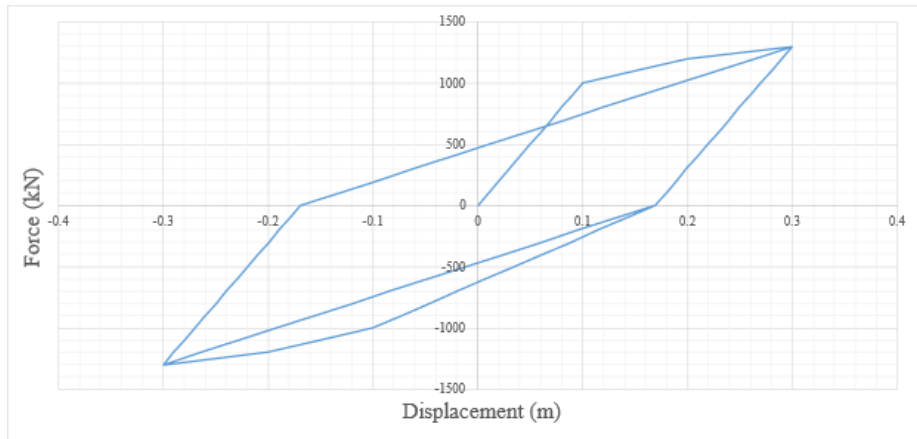
Case 5: Hysteretic spring with trilinear backbone curve and vertex-oriented polygonal hysteretic model (PHM)

For a trilinear backbone curve (cases 5 to 7), six backbone points should be entered in a tabular format. Point (0,0) should not be entered as an input. However, the resulting curve should pass through point (0,0). Meaning that the compressive and tensile stiffnesses must be equal in the pre-yield range. After entering the curve points, the resulting curve can be viewed by selecting the tab Graph.



Trilinear force-displacement backbone curve for Cases 5 to 7 in tabular format and as a graph

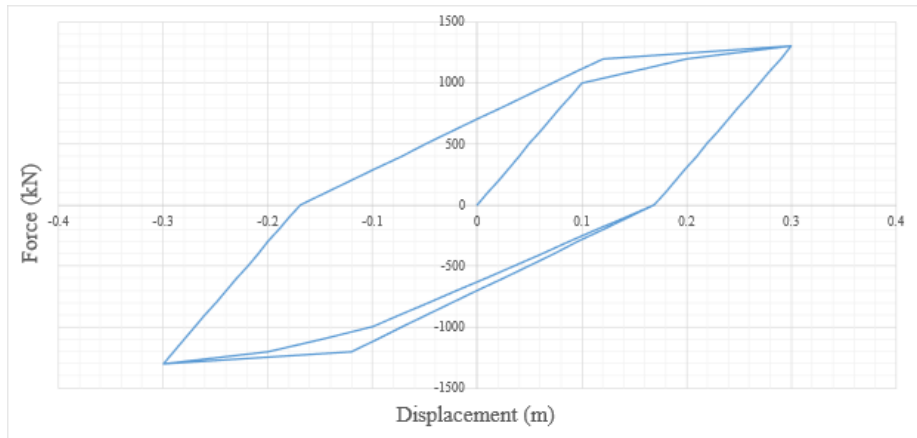
In this hysteretic model, loading and unloading follows the vertex-oriented PHM.



Case 5. The resulting force-displacement relationship

Case 6: Hysteretic spring with trilinear backbone curve and yield-oriented PHM

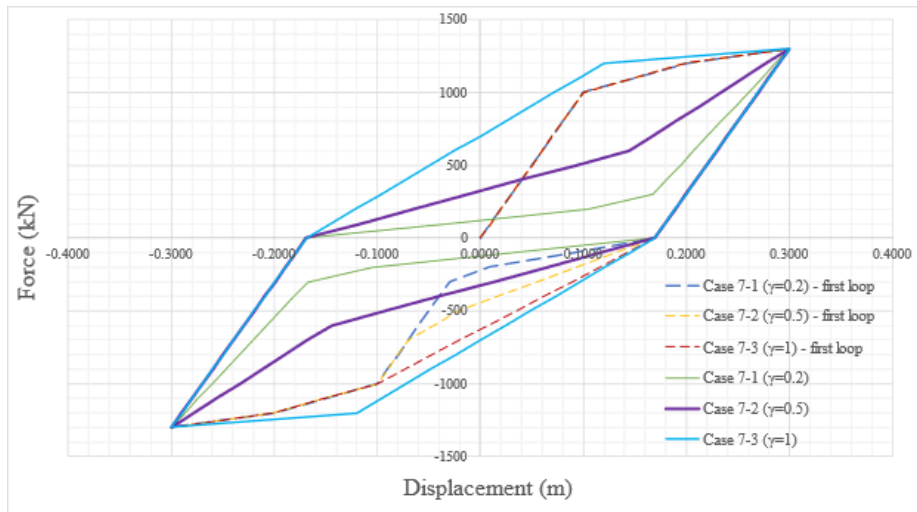
In this hysteretic model, loading and unloading follows the yield-oriented PHM.



Case 6. The resulting force-displacement relationship

Case 7: Hysteretic spring with trilinear backbone curve, yield-oriented PHM, and slip

Slip parameter Gamma is introduced in this case. This parameter controls the amount of pinching of hysteresis loops. Pinching of hysteresis loops is the reduction of their area (and the amount of dissipated energy). When the slip parameter is close to zero, the stiffness is nearly zero. Consequently, the area of the hysteretic loop and the amount of dissipated energy are significantly reduced. When the slip parameter is equal to 1, no pinching is observed. The analysis results below demonstrate the response of the spring with parameter Gamma varying between 0.2 and 1.



Case 7. The resulting force-displacement relationship

References

ADINA (version 9.7.1) by ADINA R&D, Inc.

For More Information, please refer to the following documentation.

- For help on hysteretic springs, see Springs in *LARSA 4D Reference Manual*.
- For help on time history analysis, see Nonlinear Time History Analysis in *LARSA 4D Reference Manual*.

TH19: Simple frame with friction damper

A frame is strengthened with a friction damper-brace assembly. Determine the response of the frame with and without this assembly when subjected to the ground acceleration record of the 1952 Taft, CA, earthquake. This example is from the "Fundamental Concepts of Earthquake Engineering" by R. Villaverde.

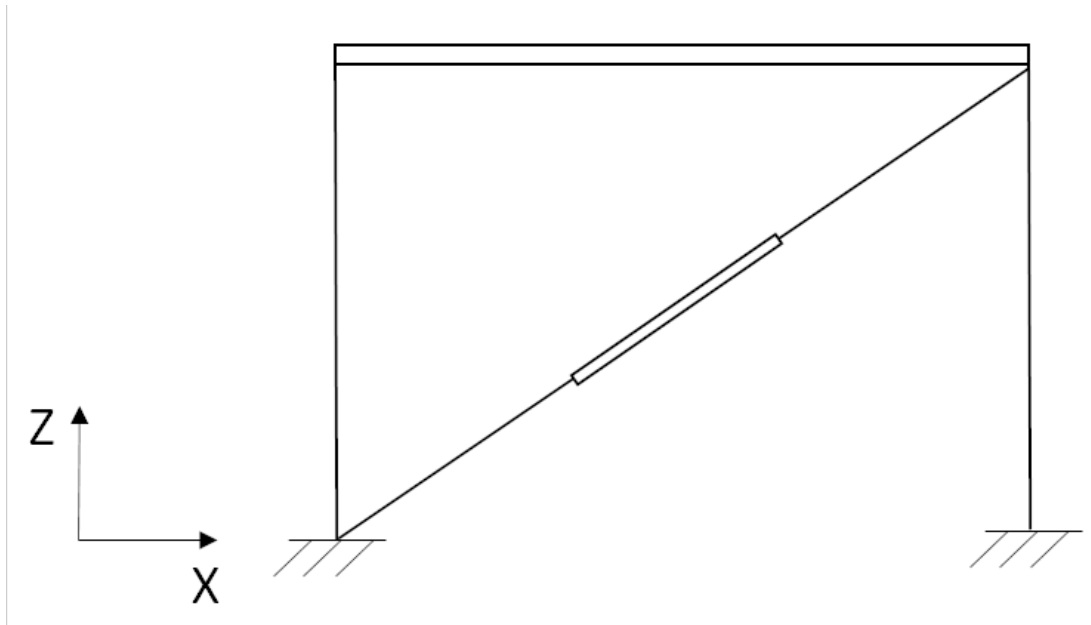
Example Project: The example described here can be found in the TimeHistory folder of your LARSA 4D Samples directory (generally My Documents\LARSA Projects\Samples) in the file TH19.

Background

Hysteretic spring element can be used to model a range of energy dissipating devices. These devices are used to dissipate energy input into a structure due to an earthquake ground motion or wind loading. The amount of dissipated energy is equal to the area under hysteresis loops in the device's resulting force-deformation curve. The device used in this example is a friction damper. This damper is composed of metal plates and the energy is dissipated through sliding of the plates with respect to each other. Once the applied load exceeds the slip force, a slip between the plates occurs. (Another type of damper that can be modeled using the hysteretic spring is a yielding metallic damper. An example of such a device is the unbonded brace (buckling-restrained brace). This device consists of a yielding steel core and concrete-filled steel case that prevents buckling.)

Model

In this example, a frame is strengthened with a friction damper-brace assembly. The frame has one translational degree of freedom in the direction of the applied ground motion. Once a cyclic load is applied and the magnitude of the load acting on the damper is higher than the slip force, the response of the damper can be visualized with force-deformation hysteresis loops. The hysteresis loops form due to the fact that the damper's plates do not return to the original position after the load direction is reversed. Consequently, this behavior can be modeled with the inelastic spring capable of capturing the hysteretic behavior. The damper's behavior is rigid-plastic, meaning that the damper provides rigid connection before it slips and has zero stiffness after that. The rigid-plastic behavior by itself can be modeled using the hysteretic spring element by defining the stiffness to be very large in the elastic range and to be zero in the post-yield range. When combined with a brace, however, the total assembly stiffness is equal to the brace stiffness before the slip and zero stiffness after the slip.



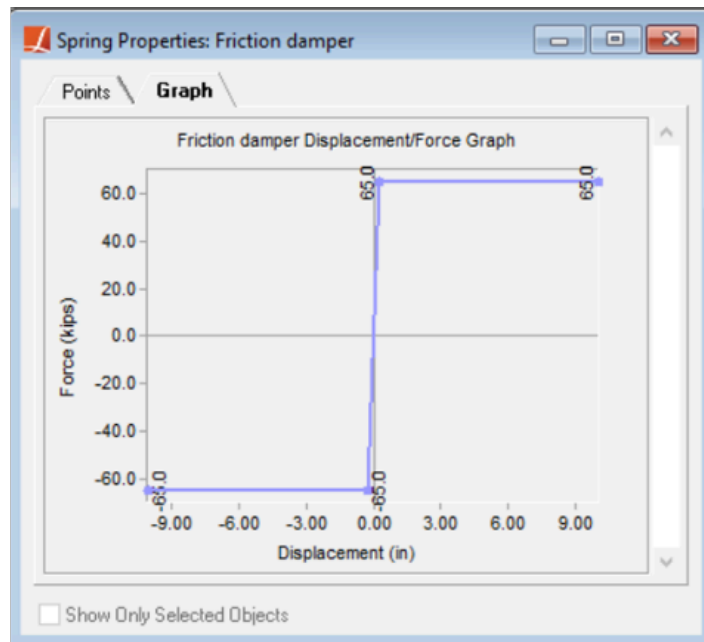
Frame with a friction damper

The frame without the damper has the lateral stiffness equal to 356 kips/in. The beam is assumed to be rigid. The mass of the system is equal to 1 kip-s²/in and assigned to the beam. This results in the undamped natural period of 0.333 s. The damping ratio is 2%. The damper's slip load is 65 kips. The brace has stiffness of 278.1 kips/in. Therefore, the deformation at which the damper slips can be found as $65/278.1 = 0.234$ in. The values of the slip deformation and slip load are used to define the hysteretic spring curve.

Spring Properties: Friction damper

Points \ Graph \

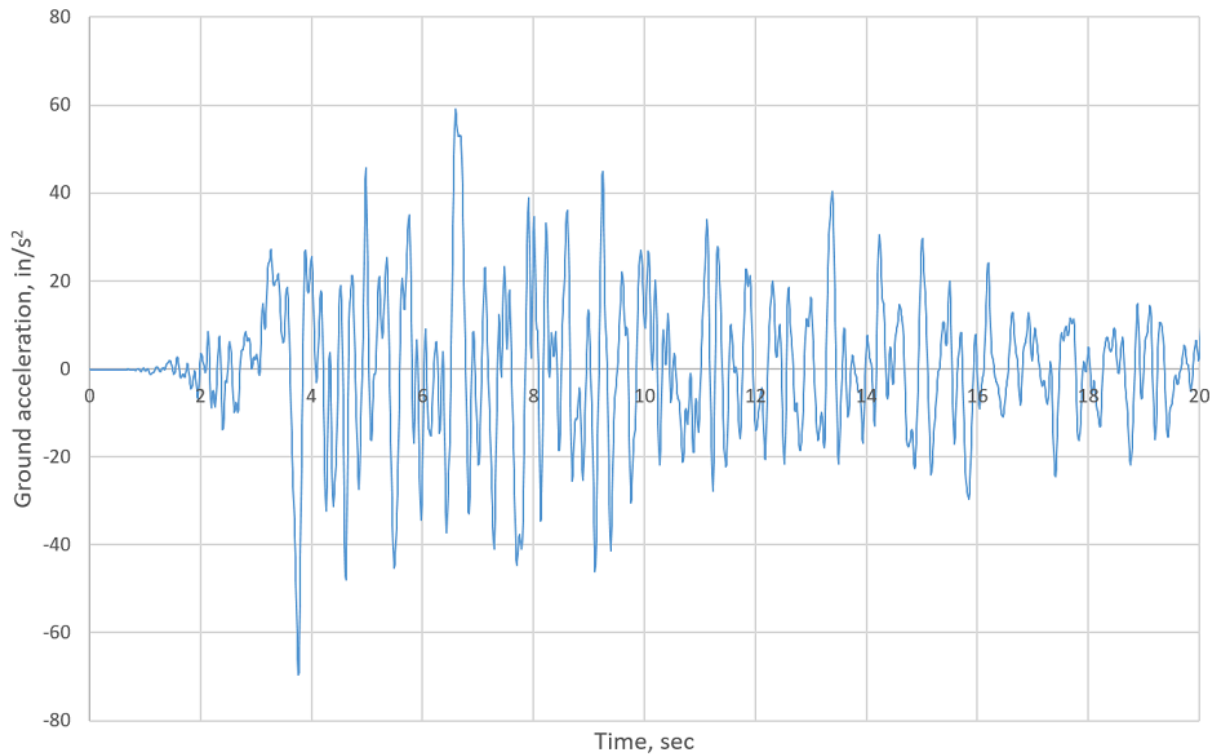
	Displacement (in)	Force (kips)
1	-10.0000	-65.0000
2	-0.2340	-65.0000
3	0.2340	65.0000
4	10.0000	65.0000
5		



Force-displacement backbone curve corresponding to the damper properties

Similarly, if a yielding metallic damper is being modeled, the yield deformation and yield force are used instead of the slip deformation and slip force.

The frame is subjected to the S69E component of the ground acceleration record of the 1952 Taft, CA, earthquake.



S69E component of the ground acceleration record of the 1952 Taft, CA, earthquake

In order to analyze the frame with and without the damper, Construction Stages are defined in this example. In the first stage, the frame is constructed and subjected to the ground motion. In the second stage, a brace is added and time history analysis is performed again. In the third stage, the brace is deconstructed and the hysteretic spring is added instead. This spring represents the friction damper-brace assembly and has the properties described above. Nonlinear time history analysis is performed in this stage to obtain the response of the strengthened frame.

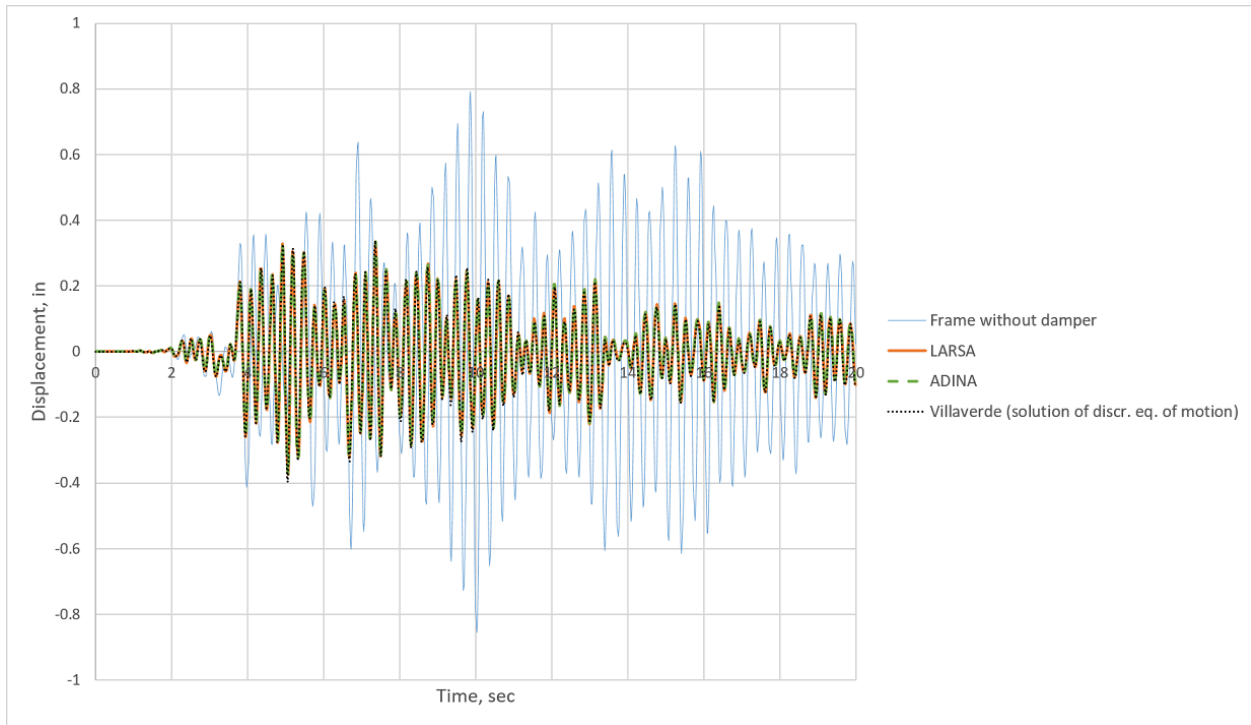
Solution and Comparison

The results of the analysis are compared with ADINA, the results provided in Villaverde, and the solution of discretized equations of motion derived for the frame with damper in Villaverde. The peak values of frame responses are listed below. It should be noted, that based on the value of the frame's peak displacement provided in Villaverde, the damper does not slip, since the maximum deformation of the damper in this case is equal to $0.25 \cdot 0.848 = 0.212$ in, which is less than the slip displacement. This would mean that the damper is not being utilized. To verify the table data provided in Villaverde, the response of the frame was computed using the provided in Villaverde discretized equations of motion and their solutions. The obtained values are listed in the table below and differ from the provided table data.

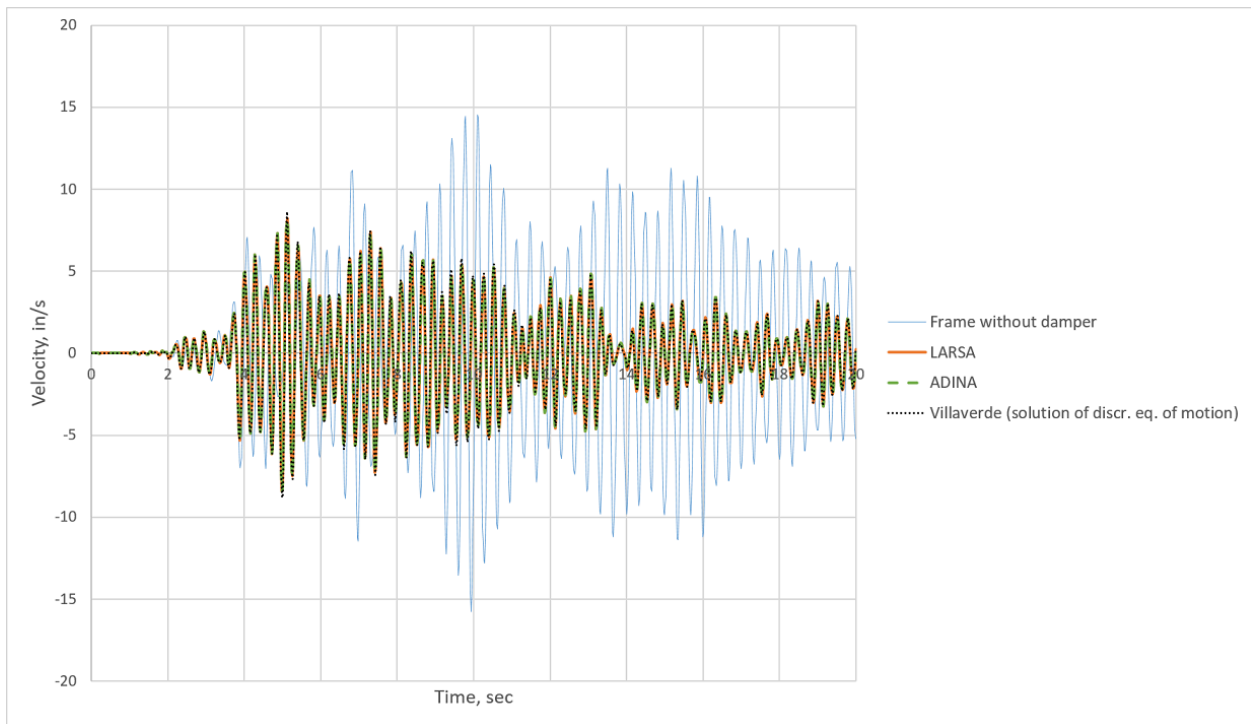
In order to compare the results with ADINA, the hysteretic spring is modeled in ADINA using a truss element with plastic-bilinear material. The obtained results are in good agreement.

Peak displacement, in	LARSA 4D	Villaverde (table data)	Villaverde (solution of provided discr. eq. of motion)	ADINA
Without damper	0.857	0.85		
With brace	0.433	0.44		
With brace and damper	0.375	0.25	0.398	0.375
Peak velocity, in/s	LARSA 4D	Villaverde (table data)	Villaverde (solution of provided discr. eq. of motion)	ADINA
Without damper	15.748	15.5		
With brace	10.59	9.96		
With brace and damper	8.412	5.02	8.82	8.410
Peak abs. acceleration, in/s²	LARSA 4D	Villaverde (table data)	Villaverde (solution of provided discr. eq. of motion)	ADINA
Without damper	292.689	302.4		
With brace	245.735	244.7		
With brace and damper	203.617	111.5	211.881	204.00

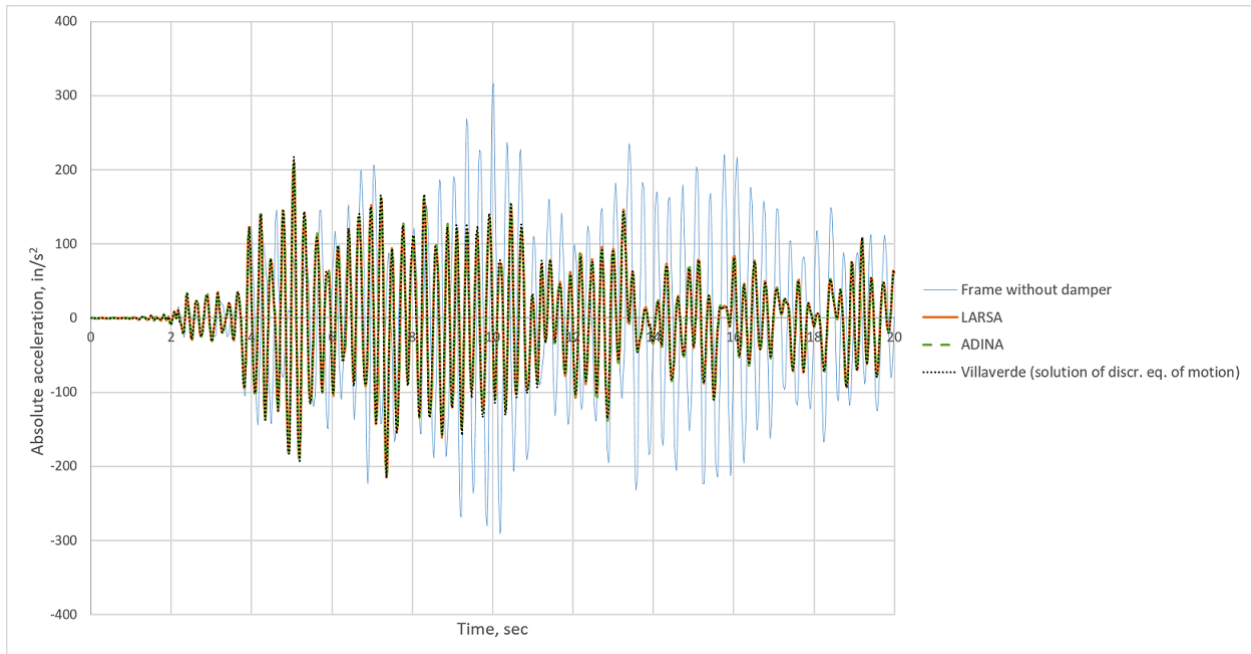
Time history responses for the frame with and without the damper are provided below. For the frame with the damper, the plots include the results obtained from ADINA and computed as the solution of discretized equations of motion provided in Villaverde. The response obtained in LARSA matches ADINA's response well, while slight differences with the computed results based on the equations in Villaverde can be observed. This can be due to the fact that the solution of equations from Villaverde is computed without iterations within a time step. The transitions between different response stages (such as elastic, yielding, unloading) are determined by the value of the frame displacement.



Displacement of the frame

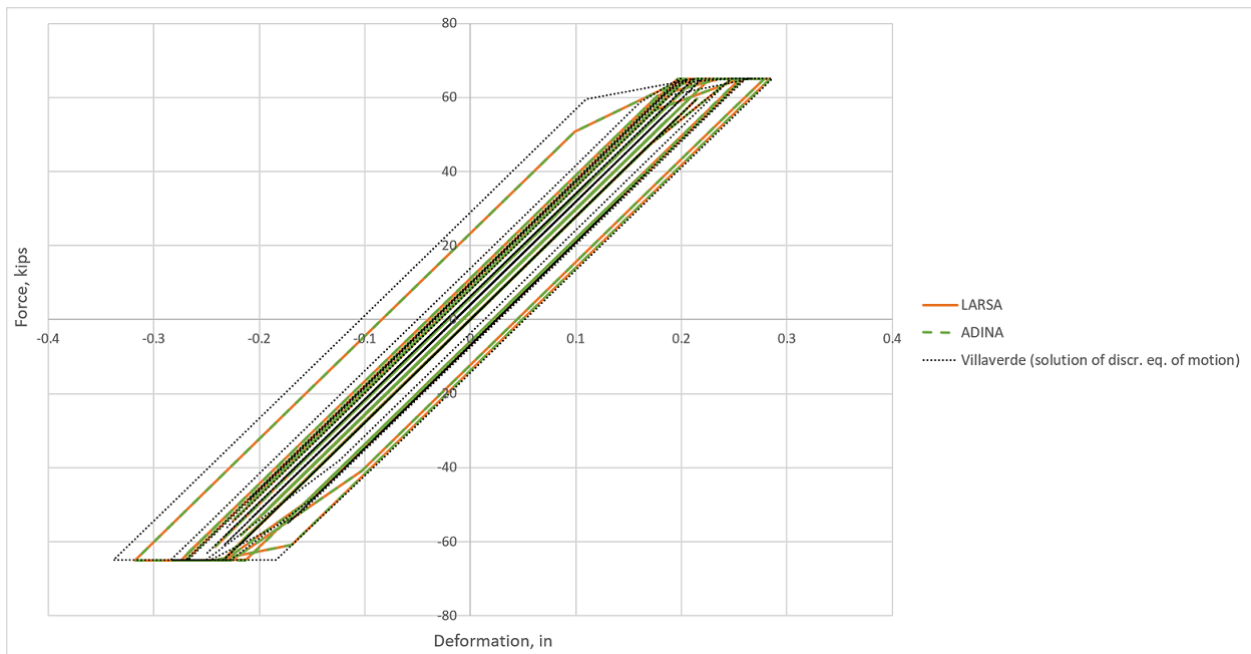


Velocity of the frame



Acceleration of the frame

Force-deformation behavior of the friction damper is shown below.



Force-deformation behavior of the friction damper

References

1. Villaverde, R., "Fundamental Concepts of Earthquake Engineering", CRC Press, 2009

2. PEER Ground Motion Database <https://ngawest2.berkeley.edu/site>
3. ADINA (version 9.7.1) by ADINA R&D, Inc.

For More Information, please refer to the following documentation.

- For help on hysteretic springs, see Springs in *LARSA 4D Reference Manual*.
- For help on time history analysis, see Nonlinear Time History Analysis in *LARSA 4D Reference Manual*.
- For help on stage construction analysis, see Staged Construction Analysis in *LARSA 4D Reference Manual*.

TH20: Vehicle-Track-Structure Interaction Analysis

A single span bridge is subjected to loads from a moving one-car train. The interaction between the vehicle, track, and bridge is taken into account by means of the Vehicle-Track-Structure Interaction (VTSI) analysis. Determine vertical displacements and accelerations of the bridge at the midspan as well as the vehicle's car accelerations. Compare the results of the VTSI analysis with Rolling Stock and Moving Load analyses. This example is adapted from Yang (2004).

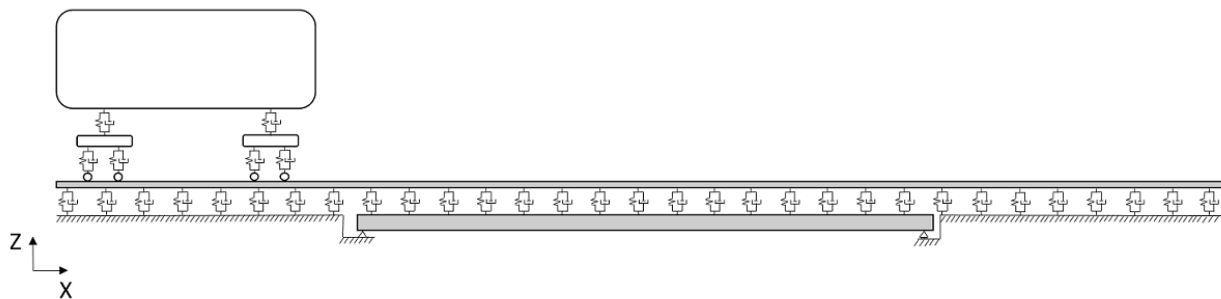
Background

VTSI analysis is a linear time history analysis of coupled vehicle, track, and structure systems. As opposed to the rolling stock analysis, VTSI accounts for the dynamic properties of vehicles. VTSI analysis is necessary when the response of the vehicle has to be evaluated in addition to the response of the structure. This is typically the case in the design of high-speed railways. In this context, the passenger comfort is evaluated based on the vehicle cars' accelerations. The risk of derailment is evaluated using the computed contact forces between the wheels and the track.

Model

The model consists of a simply-supported single-track bridge, a one-car vehicle, rails, ballast and embankment. The total length of the track is 108 m and the length of the bridge is 30 m. The vehicle speed is 100 m/s. The track is extended beyond the bridge to model the transition from the embankment to the bridge. The length of the track on the right side of the bridge is chosen to accommodate the comparison of the solution with Yang (2004) and to evaluate the response of the bridge after the train has passed.

The structure supporting the track is straight. In general, any 3D structure is permitted in VTSI analysis, as long as the track is straight and supported by member elements.



Vehicle-Track-Structure Interaction model

The bridge is modeled with member elements representing a single girder below the rails. An equivalent bridge cross-section has the following properties: $E = 2.83 \times 10^7 \text{ kN/m}^2$, $I_{zz} = 7.84 \text{ m}^4$, $A = 7.73 \text{ m}^2$, and unit weight 52.97 kN/m^3 . The damping ratio is not specified in Yang (2004). However, the response amplitude decay can be observed in the plots from Yang (2004). Therefore, the damping ratio of 0.025 was included in the model to obtain comparable response.

The track consists of two rails and ballast and extends 15 m before the bridge and 63 m after the bridge to model the track on embankment. The rails are modeled with member elements. The UIC 60 rails have the following properties: $E = 2.1 \times 10^8 \text{ kN/m}^2$, $I_{zz} = 3.04 \times 10^{-5} \text{ m}^4$, $A = 0.00765 \text{ m}^2$. The weight of the track is 587 kg per unit length and includes the weight of the sleepers. The unit weight assigned to the material "Rail" (see below) is then 373.93 kN/m^3 . The stiffness and damping of the ballast in the vertical direction are 71,994 kN/m and 17,630 kN-s/m correspondingly, per element.

Two lanes, "Right rail" and "Left rail", are defined with reference to the rail elements. The ballast elements can then be created between the bridge and rail elements. In this example, only vertical interaction is considered. Therefore, rotation about the longitudinal axis is restrained by means of Universal Restraints (Input Data → Universal Restraints) to avoid restraining this degree of freedom at each joint.

In this example, the vehicle consists of a single car, two bogies, and four wheelsets (two per each bogie). A wheelset consists of two rigidly connected wheels, one of which is positioned on the left rail and another is on the right rail. The vehicle properties are as follows: car weight is 409.57 kN, mass moment of inertia of car body around Y axis is entered as 20,404.8 kN-m² and obtained by multiplying the value of 2,080 kg-m² by $g=9.81 \text{ m/s}^2$, longitudinal distance between two bogies is 17.5 m, weight of the bogie is 29.82 kN, bogie mass moment of inertia around X and Y axes are entered as 15.5 kN-m² and 38.55 kN-m² and obtained by multiplying the values of 1.58 kg-m² and 3.93 kg-m² by g , correspondingly, stiffness and damping of the secondary suspension are 530 kN/m and 90.2 kN-s/m correspondingly, wheelset width is 1.5 m and equal to the gauge of the rails, wheel diameter is 0.91 m, wheelset weight is 17.46 kN, longitudinal distance between two wheelsets is 2.5 m, wheelset mass moment of inertia around X axis is entered as 11.18 kN-m² and obtained by multiplying the value of 1.14 kg-m² by g , stiffness and damping of the primary suspension are 590 kN/m and 19.6 kN-s/m correspondingly.

The vehicle is defined using the spreadsheet at Input Data → Geometry → VTSI Trains. In addition to the vehicle properties listed above, geometrical dimensions of the vehicle are added for visualization purposes. A User Coordinate System (UCS) is created to indicate the position of the "ghost" vehicle. The ghost vehicle is added for the purposes of results reporting and visualization. It does not move forward while animating the results (see Vehicle-Track-Structure Interaction Analysis [in LARSA 4D Reference Manual]). This UCS has to be set as Virtual Location in the VTSI Trains spreadsheet. Once all the inputs are entered, right-click the created row and choose Create Train Model.

Name	Virtual Location	Number of Cars	Car Body Length (m)	Car Body Width (m)	Car Body Height (m)	Number of Bogies per Car	Coupler Offset from Car Centroid	Bogie Offset from Car Centroid	Wheel Offset from Bogie	Bogie Spacing (m)	Car Weight (kN)	Car Mass Moment of Inertia Y	Bogie Length (m)	Bogie Width (m)	Bogie Height (m)	Number of Wheels per Bogie	Wheel Spacing (m)	
1	Train	Train UCS	1	25.0000	1.5000	2.0000	2	0.5000	1.1700	0.2000	17.5000	409.5700	2.0800000	2.6000	1.5000	0.3000	2	2.5000
2	Cut																	

Bogie Weight (kN)	Bogie Mass Moment of Inertia X	Bogie Mass Moment of Inertia Y	Secondary Suspension Stiffness	Secondary Suspension Damping	Wheelset Width (m)	Wheel Diameter (m)	Wheelset Weight (kN)	Wheelset Mass Moment of Inertia	Primary Suspension Stiffness	Primary Suspension Damping	Car Coupler Length (m)
29.8200	1.5800	3.9300	530.0000	90.2000	1.5000	0.9100	17.4600	1.1400	590.0000	19.6000	1.0000

VTSI train definition

VTSI Analysis

Create a new load case and set its type to Time History. In the Moving Loads → Basic Moving Loads tab, create a new load. Leave the Lane Loaded field as "None". LARSA 4D determines lanes for the VTSI model based on the predetermined lane names ("Right Rail" and "Left Rail"). The Load Pattern corresponds to the new train created. The Vehicle Speed is set to 100 m/s in this example. The start position must be set to 0. The train will start moving from the beginning of the defined lanes, regardless of the position of the train UCS. When all the parameters are entered, the Moving Loads window should look as below.

	Lane Loaded	Load Pattern	Applied Load Direction	Load Factor	Direction of Travel	Vehicle Speed (m/sec)	Start Position (m)
1	(None)	VTSI: Train	Global -Z	1.0000	Forward	100.0000	0.0000
2							

VTSI load definition

The total analysis time is 1.1 seconds, which corresponds to the time required for the vehicle to start moving from the left embankment, cross the bridge, and reach the end of the modeled part of the right embankment. The time step is set to a small value of 0.001 seconds due to the high speed of the vehicle to be able to capture the dynamics of the vehicle and the response of the track and bridge. With results being saved at every time step, the total of 1,101 time steps are produced (including the initial time step at time 0s).

The Generalized- α integration scheme is used to solve VTSI equations of motion in time. In the analysis settings, **Analysis** → **Advanced Vehicle-Track Structure Interaction Analysis**, set the Generalized- α parameter ρ_∞ to 0.0 to obtain numerical damping (value of 0 corresponds to maximum damping and value of 1 to no damping).

Run Advanced Vehicle-Track-Structure-Interaction Analysis

Select Analysis Type

Vehicle-Track-Structure Interaction

Time History Options

Rayleigh Damping Constants Other Options

Rayleigh damping constants

Mass-Proportional 1.0103 Stiffness-Proportional 3.9593E-04

Note: These are not the modal damping ratios.

Generalized-alpha numerical damping constant: 0 (blank for Newmark-beta)

Keep Previous Results

Perform Quick Integrity Check

Description:

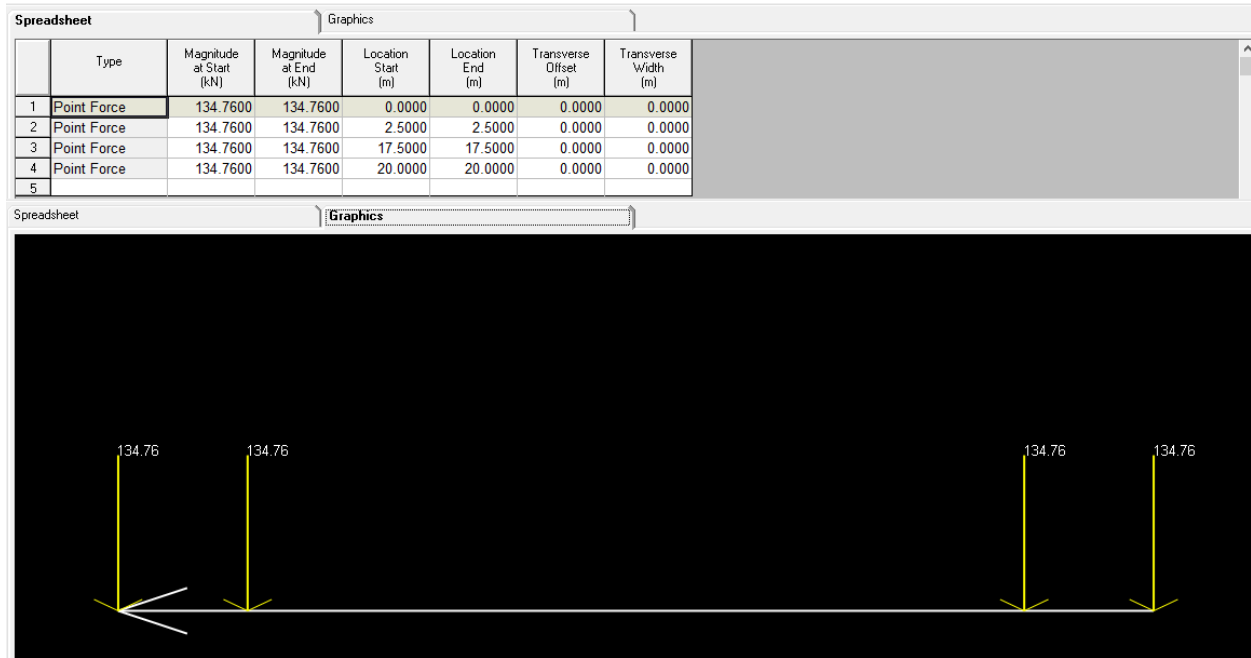
Performs an Advanced Vehicle-Track-Structure Interaction Analysis on time history load cases with moving load patterns.

Analyze Close Cancel Help

Setting numerical damping for VTSI

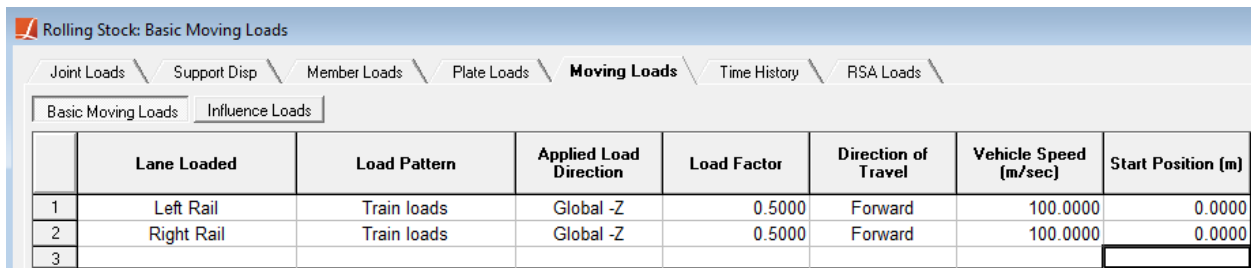
Rolling Stock Analysis

In this example, we will compare VTSI results with the Rolling Stock analysis results. Create a new load case and set its type to Time History. In the Moving Loads tab, create two new loads corresponding to the Left Rail and the Right Rail lanes. Use a load pattern provided with the example and shown below. The total weight of the vehicle is a sum of the weights of the car (409.57 kN), two bogies (29.82 kN each), and four wheelsets (17.46 kN each) and is equal to 539.05 kN. This weight is distributed between the four wheelsets to form the load pattern shown below.



Rolling Stock load pattern

The vehicle weight is then distributed equally between the Left Rail and Right Rail by setting the Load Factor to be 0.5 for both created loads. When all the parameters are entered, the Moving Loads window should look as below.



Rolling Stock load definition

The analysis settings (including Generalized- α integration scheme settings) are the same as for the VTSI analysis. The rolling stock analysis is performed from **Analysis** → **Dynamic Rolling Stock Analysis**.

Moving Load Analysis

For the linear static Moving Load analysis, create a new load case and set its type to Moving (Static). In the Moving Loads tab, create the same loads as for the Rolling Stock analysis. Instead of the vehicle speed, specify the position increment of 1 m. When all the parameters are entered, the Moving Loads window should look as below.

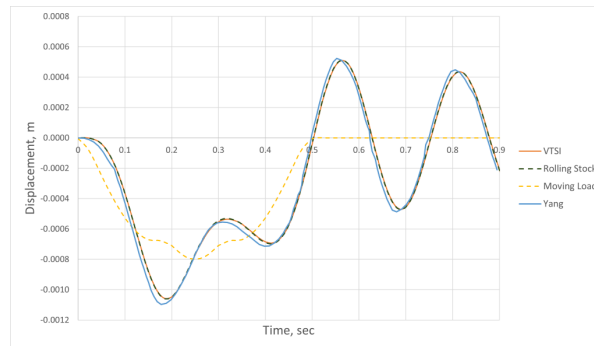
	Lane Loaded	Load Pattern	Applied Load Direction	Load Factor	Direction of Travel	Position Increment (m)	Start Position (m)
1	Left Rail	Train loads	Global -Z	0.5000	Forward	1.0000	0.0000
2	Right Rail	Train loads	Global -Z	0.5000	Forward	1.0000	0.0000
3							

Moving Load definition

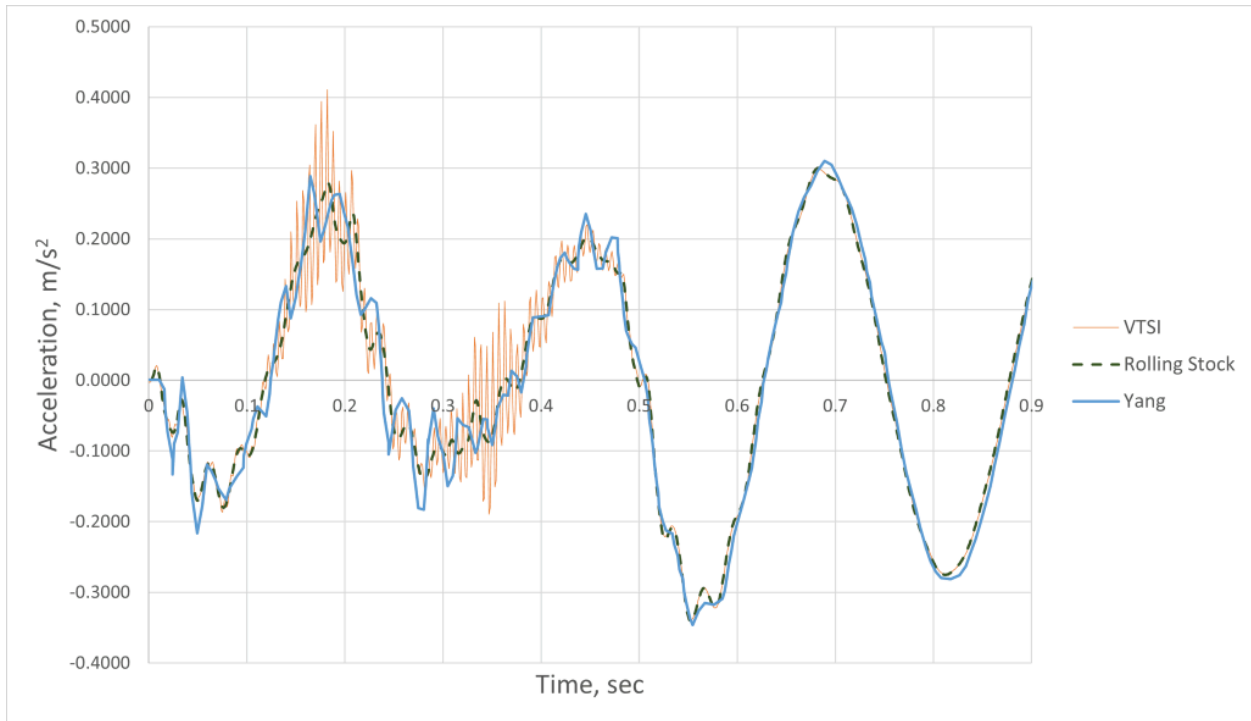
The moving load analysis is performed from **Analysis** → **Static Moving Load Analysis**.

Solution and comparison

The results of the VTSI, Rolling Stock, and Moving Loads analyses are plotted below and compared with the plots provided in Yang (2004). To accommodate the comparison, the results are plotted from the moment when the train enters the bridge ($t = 0.15$ sec), since the analysis in Yang (2004) starts at this point. For the moving load analysis results, time is computed based on the vehicle position and speed.

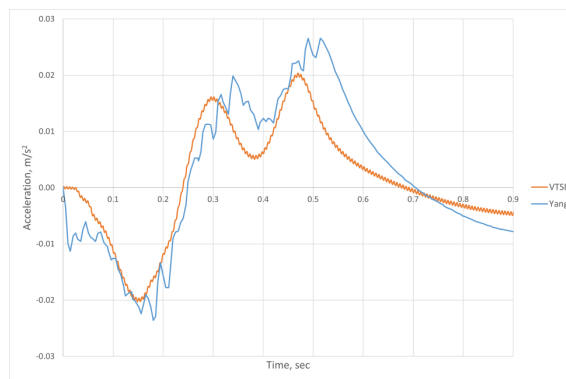


Midspan vertical displacement of the bridge



Midspan vertical acceleration of the bridge

Vehicle car body accelerations are compared next. This value is used to evaluate the passenger comfort. As opposed to the VTSI analysis, the Rolling Stock analysis does not produce the car body acceleration since the vehicle is not modeled explicitly in this case and represented instead as a load pattern calculated from the vehicle weight and wheelsets positions.



Vertical acceleration of the car body

The bridge displacements obtained from the VTSI analysis compare well with the displacements from the Rolling Stock analysis. The differences with the plots reported in Yang (2004) could be due to uncertainties in the amount of bridge damping.

References

1. Yang, Y.B., "Vehicle-Bridge Interaction Dynamics With Applications to High-Speed Railways", World Scientific, 2004

For More Information, please refer to the following documentation.

- For help on Vehicle-Track-Structure Interaction analysis, see Vehicle-Track-Structure Interaction Analysis in *LARSA 4D Reference Manual*.
- For help on time history analysis, see Linear Time History Analysis in *LARSA 4D Reference Manual*.

Samples for Staged Construction Analysis

These samples provide an overview of staged construction analysis.

S01: Creep Effects - Simple Span Concrete Beam	295
S02: Creep and Shrinkage - Cantilevers Loaded at Different Times	297
S03: Creep and Shrinkage - Use CEB-FIP model code 1990 in S02	299
S04: Creep and Shrinkage - Connect Aging Cantilevers	301
S05: Creep and Shrinkage - Use CEB-FIP model code 1990 in sample S04	303
S06: 3-Span Post-Tension Deck	305
S07: Composite I-Girder with Time-Dependent Effects	311
Cross-Section Definition	311
Model Geometry	311
Construction Sequence	311
Verification of Cross-Section Properties	312
Verification of Self-Weight Loading	312
Verification of the Time Effect on Elastic Modulus	314
Verification of Shrinkage	315
S08: Time-Dependent Material Properties Effects	317
Problem Definition	317
Modeling	318
Construction Sequence	321
Verification of Creep	321
Verification of Shrinkage	328
S08b: Time-Dependent Material Properties Effects	333
Problem Definition	333
Modeling	334
Construction Sequence	339
Verification of Creep	339
Verification of Shrinkage	341
S08c: Time-Dependent Material Properties Effects	345
Problem Definition	345

Modeling	346
Verification of Creep	347
S08d: Time-Dependent Material Properties Effects	351
Problem Definition	351
Modeling	352
Construction Sequence	353
Verification of Elastic Modulus	354
S09: Shells with Time-Dependent Material Effects	359
Problem Definition	359
Modeling	360
Verification of Creep	362
Verification of Shrinkage	362
Verification of Elastic Modulus Change	363
S09b: Shells with Time-Dependent Material Effects (Orthotropic Material)	365
Problem Definition	365
Modeling	366
Verification of Creep	367
Verification of Shrinkage	368
Verification of Elastic Modulus Change	368

S01: Creep Effects - Simple Span Concrete Beam

This sample problem demonstrates how to model time-dependent creep effect for a simple span concrete beam.

Example Project: The example described here can be found in the Staged Construction folder of your LARSA 4D Samples directory (generally My Documents\LARSA Projects\Samples) in the file S01.

The formwork supporting wet concrete is removed 10 days after pouring the concrete. On day 50, beam is subjected to additional superimposed load. The stage analysis can be summarized as:

CONSTRUCTION SCHEDULE

Concrete Cast at Day = 0

Remove Forms at Day = 10

Add Superimposed Dead Load at Day = 50

The model has 11 joints and 10 beam elements. Compute maximum vertical deflection and compare the results to those by hand-calculations and by BD2 program.

Modulus of Elasticity = 661,305 lb/ft²

Span = 100 feet

A = 12.0 ft²

I_{zz} = 36.0 ft⁴

Concrete f_{c28} = 6,500 psi

Relative Humidity = 70%

Temperature = 64 Fahrenheit

Time dependent stage analysis is performed using 11 construction stages and steps and maximum of 10 iterations will be performed in each construction step.

S02: Creep and Shrinkage - Cantilevers Loaded at Different Times

This problem involves 2 independent cantilevers, with loads applied at different times. One of the two cantilevers has two separate loads applied to it, but at different times. This sample demonstrates how different two cantilevers respond to time-dependent creep effect when loaded at different times.

Example Project: The example described here can be found in the Staged Construction folder of your LARSA 4D Samples directory (generally My Documents\LARSA Projects\Samples) in the file S02.

Use CEB-FIP model code 1978 with user-defined time dependent material curves in this sample.

CONSTRUCTION SCHEDULE

Concrete Cast at Day = 0

Remove Forms at Day = 28

Apply Load only to Left Cantilever at Day = 28

Apply Additional Loads to both Cantilevers at Day = 100

The model has 22 joints and 20 beam elements. Compare the results to those by hand-calculations and BC program.

Time dependent stage analysis is performed for all construction stages and maximum of 10 iterations is performed in each construction step.

S03: Creep and Shrinkage - Use CEB-FIP model code 1990 in S02

This problem involves 2 independent cantilevers, with loads applied at different times. One of the two cantilevers has two separate loads applied to it, but at different times. This sample demonstrates how different two cantilevers respond to time-dependent creep effect when loaded at different times.

Example Project: The example described here can be found in the Staged Construction folder of your LARSA 4D Samples directory (generally My Documents\LARSA Projects\Samples) in the file S03.

Use CEB-FIP model code 1990 with user-defined time dependent material curves in this sample.

CONSTRUCTION SCHEDULE

Concrete Cast at Day = 0

Remove Forms at Day = 28

Apply Load only to Left Cantilever at Day = 28

Apply Additional Loads to both Cantilevers at Day = 100

The model has 22 joints and 20 beam elements. Compare the results to those by hand-calculations and BC program.

Time dependent stage analysis is performed for all construction stages and maximum of 10 iterations is performed in each construction step.

S04: Creep and Shrinkage - Connect Aging Cantilevers

This is a simple stage analysis. The 2 cantilevers are first assembled at day 28 and allowed to age to day 50. At that point, they are made fully connected at the free ends and allowed to age to day 4000. This sample allows us to see how internal forces related to creep displacements are developing over time.

Example Project: The example described here can be found in the Staged Construction folder of your LARSA 4D Samples directory (generally My Documents\LARSA Projects\Samples) in the file S04.

Use CEB-FIP model code 1978 with user-defined time dependent material curves in this sample.

Time dependent stage analysis is performed for all construction stages using maximum of 10 iterations for construction stage.

S05: Creep and Shrinkage - Use CEB-FIP model code 1990 in sample S04

This is a simple staged construction analysis. The 2 cantilevers are first assembled at day 28 and allowed to age to day 50. At that point, they are made fully connected at the free ends and allowed to age to day 4000. This sample allows us to see how internal forces related to creep displacements are developing over time.

Example Project: The example described here can be found in the Staged Construction folder of your LARSA 4D Samples directory (generally My Documents\LARSA Projects\Samples) in the file S05.

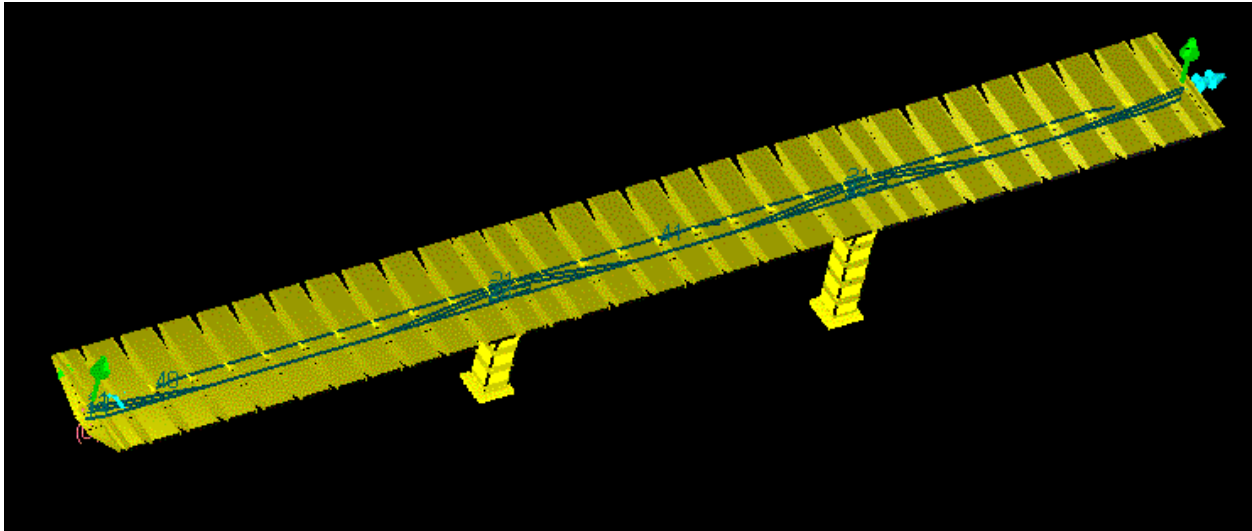
Use CEB-FIP model code 1990 in this sample.

Time dependent stage analysis is performed for all construction stages using maximum of 10 iterations for construction stage.

S06: 3-Span Post-Tension Deck

This sample problem (courtesy of International Bridge Technologies, San Diego) is for time-dependent construction analysis for a transit crossing which has post-tension concrete deck supported by two concrete piers. The structure has 3 spans and 2 concrete piers. Each span has 3 bottom tendons. There are also 2 top slab continuity tendons.

Example Project: The example described here can be found in the Staged Construction folder of your LARSA 4D Samples directory (generally My Documents\LARSA Projects\Samples) in the file S06.



Sample S06

The deck concrete properties are:

$f'_c = 6500$ psi
Poisson ratio = 0.2
Mean T = 64 Farhenheit
Density = 0.155 kip/ft³
 $s = 0.25$ (see CEB FIP 2.1.6.1)
RH = 70% (relative humidity)
 $h = 0.762$ ft (notional thickness)
 $bsc = 5$ (shrinkage coeff, see ceb fip 90)

The pier concrete properties are:

$f'_c = 5000$ psi
Poisson ratio = 0.2
Mean T = 64 Farhenheit
Density = 0.155 kip/ft³
 $s = 0.25$ (see CEB FIP 2.1.6.1)
RH = 70% (relative humidity)

LARSA 4D Sample and Verification Problems

$h = 2.545$ ft (notional thickness)

$bsc = 5$ (shrinkage coeff, see ceb fip 90)

The tendon properties are:

STRAND AREA = 0.00151

ANCHOR-SET = 0.03125

FRICITION = 0.25

WOBBLE = 0.0002

Tendon Layouts

Tendon layouts are defined using the bottom of segments as reference. In this example, we will be using several reference points defined from the bottom of the reference segment : at 5.330 feet (1), at 0.500 ft (2), at 5.833 ft (3), at 3.833 ft (4), at 4.330 (5), at 1.670 (6), at 3.000 ft (7), at 6.500 ft (8).

Span 1 Bottom Tendon Layouts (PI is for POINT OF INTERSECTION)

TENDON ID 11

38 STRANDS

LEFT ANCHOR AT 1.208 FT FROM START OF SEGMENT 100 AND 5.330 FT OFFSET FROM BOTTOM

RIGHT ANCHOR AT 1.46 FT FROM END OF SEGMENT 114 and 5.833 FT OFFSET FROM BOTTOM

(PI) AT 7.25 FROM START OF SEGM 104 AND 5.833 FT OFFSET FROM BOTTOM WITH RADIUS 20 FT

(PI) AT 3.25 FROM START OF SEGM 109 AND 0.500 FT OFFSET FROM BOTTOM WITH RADIUS 20 FT

(PI) AT 3.50 FROM START OF SEGM 113 AND 5.833 FT OFFSET FROM BOTTOM WITH RADIUS 20 FT

TENDON ID 12

38 STRANDS

LEFT ANCHOR AT 1.208 FT FROM START OF SEGMENT 100 AND 3.833 FT FROM BOTTOM

RIGHT ANCHOR AT 1.46 FT FROM END OF SEGMENT 114 and 3.000 FT FROM BOTTOM

(PI) AT 7.25 FROM START OF SEGM 103 AND 0.500 FT FROM BOTTOM WITH RADIUS 20 FT

(PI) AT 3.25 FROM START OF SEGM 110 AND 0.500 FT FROM BOTTOM WITH RADIUS 20 FT

(PI) AT 3.50 FROM START OF SEGM 113 AND 4.330FT FROM BOTTOM WITH RADIUS 20 FT

TENDON ID 13

38 STRANDS

LEFT ANCHOR AT 1.208 FT FROM START OF SEGMENT 100 AND 1.670 FT OFFSET FROM BOTTOM

RIGHT ANCHOR IS AT 1.46 FT FROM END OF SEGMENT 114 AND 1.670 FT OFFSET FROM BOTTOM

(PI) AT 3.625 FT FROM START OF SEGMENT 101 AND 0.500 FT OFFSET FROM BOTTOM WITH RADIUS 20 FT

(PI) AT 3.500 FT FROM START OF SEGMENT 113 AND 0.500 FT OFFSET FROM BOTTOM WITH RADIUS 20 FT

(SPAN 2 BOTTOM TENDONS)

TENDON ID 21

30 STRANDS

LEFT ANCHOR AT 1.46 FT FROM START OF SEGMENT 113 WITH OFFSET 5.833 FT

RIGHT ANCHOR AT 1.46 FT FROM END OF SEGMENT 211 WITH OFFSET 5.833 FT

(PI) AT 3.625 FT FROM START OF SEGMENT 114 AND 5.833 FT FT OFFSET FROM BOTTOM WITH RADIUS 20 FT

LARSA 4D Sample and Verification Problems

(PI) AT 7.250 FT FROM START OF SEGMENT 203 LEVEL 0.500 FT RADIUS 20 FT

(PI) AT 3.250 FT FROM START OF SEGMENT 206 LEVEL 0.500 FT RADIUS 20 FT

(PI) AT 3.500 FT FROM START OF SEGMENT 210 LEVEL 5.833 FT RADIUS 20 FT

TENDON ID 22

30 STRANDS

LEFT ANCHOR SEGM 113 RECESS 1.46 OFFSET ELEV 3.000 FT

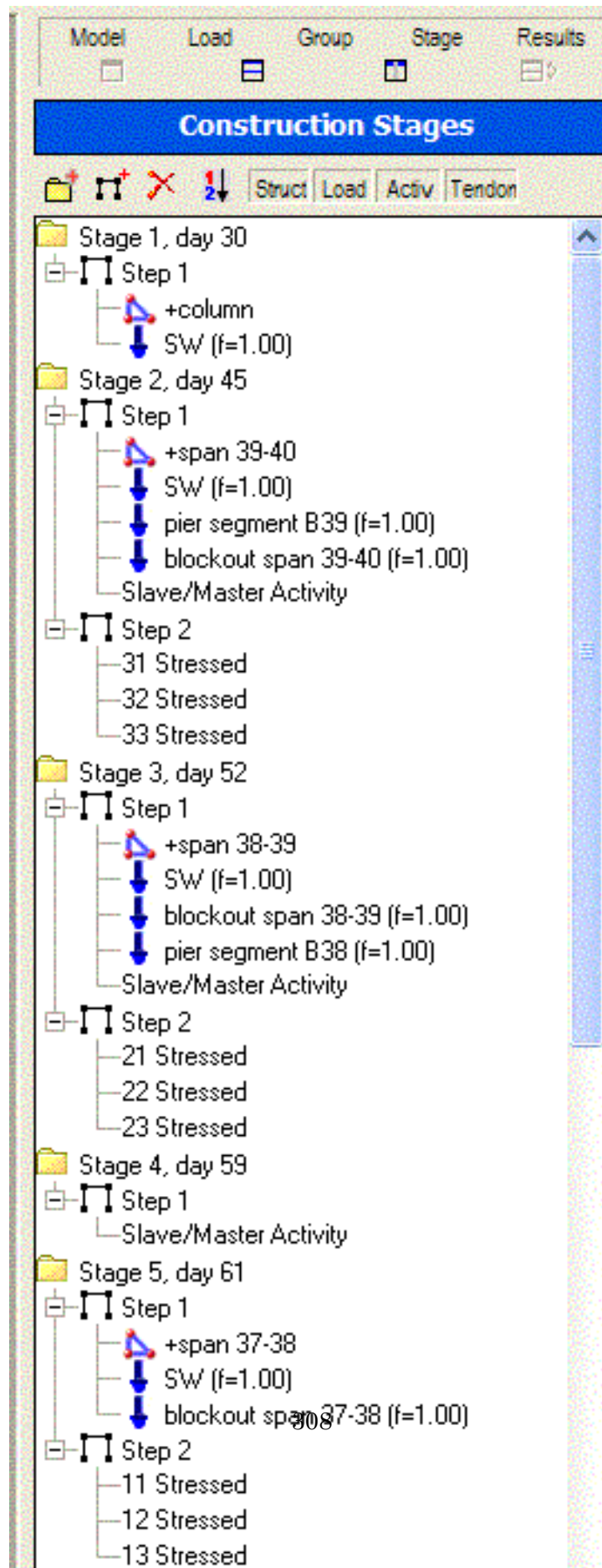
RIGHT ANCHOR SEGMENT 211 RECESS 1.46 OFFSET ELEV 3.000 FT

(PI) AT 3.625 FT FROM START OF SEGMENT 114 LEVEL 4.330 RADIUS 20 FT

(PI) AT 7.250 FT FROM START OF SEGMENT 202 LEVEL 0.500 FT RADIUS 20 FT

(PI) AT 3.250 FT FROM START OF SEGMENT 207 LEVEL 0.500 FT RADIUS 20 FT

(PI) AT 3.500 FT FROM START OF SEGMENT 210 LEVEL 4.330 RADIUS 20 FT



LARSA 4D Sample and Verification Problems

TENDON ID 23

30 STRANDS

ANCHOR LEFT SEGM 113 RECESS 1.46 OFFSET ELEV 1.670

RIGHT SEGM 211 RECESS 1.46 OFFSET ELEV 1.670

(PI) AT 3.625 SEGM 114 LEVEL 0.500 RADIUS 20

(PI) AT 3.5 SEGM 210 LEVEL 0.500 RADIUS 20

(SPAN 3 BOTTOM TENDONS) (LEVEL ELEV BOTTOM 5.33 0.5 5.833 3.833 4.33 1.67 3.0)

TENDON ID 31

18 STRANDS

ANCHOR LEFT SEGM 210 RECESS 1.46 OFFSET ELEV 3

RIGHT SEGM 309 RECESS 1.208 OFFSET ELEV 1

(PI) AT 3.625 SEGM 211 LEVEL 3 RADIUS 20

(PI) AT 7.25 SEGM 303 LEVEL 2 RADIUS 20

(PI) AT 3.25 SEGM 305 LEVEL 2 RADIUS 20

DEFINE 32

AREA 0.0453 STRAND 30 JACK 1 DUCT 1 TYPE 1

ANCHOR LEFT SEGM 210 RECESS 1.46 OFFSET ELEV 7

RIGHT SEGM 309 RECESS 1.208 OFFSET ELEV 4

(PI) AT 3.625 SEGM 211 LEVEL 5 RADIUS 20

(PI) AT 7.250 SEGM 302 LEVEL 2 RADIUS 20

(PI) AT 3.250 SEGM 306 LEVEL 2 RADIUS 20

DEFINE 33

AREA 0.0453 STRAND 30 JACK 1 DUCT 1 TYPE 1

ANCHOR LEFT SEGM 210 RECESS 1.46 OFFSET ELEV 6

RIGHT SEGM 309 RECESS 1.208 OFFSET ELEV 6

(PI) AT 3.625 FT FROM START OF SEGMENT 211 LEVEL 2 RADIUS 20

(PI) AT 1.500 FT FROM START OF SEGMENT 308 LEVEL 2 RADIUS 20

(TOP SLAB CONTINUITY TENDONS)

DEFINE 40

24 STRANDS

ANCHOR LEFT SEGM 103 RECESS 2 OFFSET ELEV 1

RIGHT SEGM 205 RECESS 2 OFFSET ELEV 1

(PI) AT 7.500 FT FROM START OF SEGMENT 103 LEVEL 6.5 FT OFFSET FROM BOTTOM WITH RADIUS 20

(PI) AT 2.500 FT FROM START OF SEGMENT 205 LEVEL 6.5 FT OFFSET FROM BOTTOM WITH RADIUS 20

DEFINE 41

24 STRANDS

ANCHOR LEFT SEGM 204 RECESS 2 OFFSET ELEV 1

ANCHOR RIGHT SEGM 306 RECESS 2 OFFSET ELEV 1

LARSA 4D Sample and Verification Problems

(PI) AT 7.500 FT FROM START OF SEGMENT 204 LEVEL 6.5 FT OFFSET FROM BOTTOM WITH RADIUS 20

(PI) AT 2.500 FT FROM START OF SEGMENT 306 LEVEL 6.5 FT OFFSET FROM BOTTOM WITH RADIUS 20

The model has 53 joints and 50 beam elements. Five (5) structure groups and seven (7) load cases are used. Time dependent stage analysis is performed starting from Stage 1 (day 30) to Stage 24 (day 6000).

S07: Composite I-Girder with Time-Dependent Effects

This sample problem verifies shrinkage on a single-span composite beam containing a steel I shape and a concrete slab on top.

Example Project: The example described here can be found in the Staged Construction folder of your LARSA 4D Samples directory (generally My Documents\LARSA Projects\Samples) in the file S07.

Cross-Section Definition

The cross-section used in this problem is composed of a steel I-shape and a concrete slab on top. The dimensions are as follows. I-shape: 5 ft deep; 2 ft wide; 0.2 ft flange and web thickness. Rectangle shape: 0.8 ft deep; 4 ft wide. A36 and Fc_4 materials are used (Fc_4 is also chosen as the reference material). The shapes are placed such that the reference axes of the cross-section are located at the centroid of the concrete rectangular slab.

Stress Recovery Points are set on the section at this point to determine where LARSA 4D will report stresses later. This example includes six Stress Recovery Points: 1-4 clockwise around the I-shape, and 5 & 6 at the upper-right and upper-left of the concrete slab, respectively.

Model Geometry

The girder and deck system is supported by a pin on one end and a roller at the other (the supports are level with the centroid of the deck). The length of the span is 300 ft. The span is divided into 10 segments. The girder is along the x-axis with the z-axis parallel to the web. The members have an orientation angle of 90 degrees. (This is a 2D problem: TY, RX, and RZ are fixed as universal restraints.)

The member elements are not assigned a material because their materials are set in the Section Composer section. It has no member end offsets.

Because the reference axes are placed at a different location from the centroid, the composite centroid is shifted down from the joint-to-joint line automatically.

Construction Sequence

The composite beam will be constructed in two phases. The steel part will be constructed first. After the steel part deforms due to self-weight, the concrete slab will be added.

The cross-section is defined in LARSA Section Composer with a construction sequence state (State A) in which only the steel I-shape is active.

Verification of Cross-Section Properties

Centroid

The distance from the reference axis to the composite centroid is computed by taking the weighted average of the centroid locations of the two shapes (relative to the reference axis), each weighted by the corresponding E^*A :

Shape	cy (ft)	E (kip/ft ²)	A (ft ²)	E*A	cy*E*A
I	-2.9	4.176x10 ⁶	1.72	7.182x10 ⁶	-20.8x10 ⁶
Rectangle	0	5.1912x10 ⁵	3.20	1.638x10 ⁶	0
Total				8.821x10 ⁶	-20.8x10 ⁶
Composite	-2.36				

LARSA Section Composer's computation of the centroid location matches exactly.

Area and Izz

Hand calculations to verify A and Izz follow. When computing properties of composite sections, the area and moment of inertia properties of each shape are factored by the ratio of the modulus elasticity of the shape to the modulus of elasticity of the reference material (which in this example is the material of the rectangle). The total cross-sectional area is the sum of the factored areas of the two shapes. For computing the moment of inertia in z (Izz), the moment of inertia of each shape individually (as given from standard formulas) is transformed by adding the shape's area times the square of the distance from the shape's centroid to the section centroid. Each shape's contribution to Izz is then factored by the ratio of its modulus of elasticity to that of the reference material, and the two contributions are summed.

Shape	A (ft ²)	A*E/E_ref	Izz (ft ⁴)	Izz+Ac ²	(Izz+Ac ²)*E/ E_ref
I	1.72	13.8	6.23	6.74	54.2
Rectangle	3.20	3.20	0.171	17.9	17.9
Composite		17.0			72.2

LARSA Section Composer's computations of the composite A and Izz match exactly.

Verification of Self-Weight Loading

Reactions

The weight of the two shapes and the total weight of the composite beam is computed in the following table:

Shape	Area (ft ²)	Length (ft)	Density (kip/ft ³)	Weight (kip)
I	1.72	300	0.49	253

Shape	Area (ft ²)	Length (ft)	Density (kip/ft ³)	Weight (kip)
Rectangle	3.20	300	0.15	144
Composite				397

This model is constructed in two stages. In the first stage, the I shape is constructed alone and self-weight is applied. In the second stage, the rectangle shape is constructed, making a composite section, and the additional self-weight from this shape is applied. The total Z reaction reported in LARSA 4D matches the total weight hand calculation above for the incremental reactions in each stage (corresponding to the weight of each piece alone) and the cumulative reaction at the end of the second stage.

Displacements

The maximum deflection at mid-span is given by $d=5/384*(W*L^3)/(EI)$, where $L = 300$ ft. The two incremental deflections and the cumulative deflection are given in the table below:

Stage	W (kip)	E (kip/ft ²)	I (ft ⁴)	d (ft)
One (I alone)	253	4.176x10 ⁶	6.23	3.42
Two (rectangle added)	144	5.1912x10 ⁵	72.2	1.35
Cumulative				4.77

The two incremental displacements and the cumulative displacement computed by LARSA 4D match exactly.

Stresses

There is no strain at the compound centroid in a model with loading and restraints such as in this problem. Stresses are due entirely to the bending stress. Further, at the pin supports there is no bending stress.

The stress at mid-span can be computed by first computing the rotational strain (the slope of the strain curve along the member's y-axis) which is given by $r=M/(E*I)$, where $M = WL/8$. Because of the composite assembly of this structure, only the I shape takes the load of its self-weight, while both parts of the composite section take the load of the rectangle.

Stage	W (kip)	M (kip-ft)	E (kip/ft ²)	I (ft ⁴)	r (1/ft)
One (I alone)	253	9490	4.176x10 ⁶	6.23	3.65x10 ⁻⁴
Two (rectangle added)	144	5400	5.1912x10 ⁵	72.2	1.44x10 ⁻⁴

The rotational strain is converted into a stress at a fiber by multiplying it by the modulus of elasticity at the fiber and the distance from the fiber to the section centroid.

In the first stage, when the section is composed of the I shape alone, note that the beam centroid is at the I shape centroid, and thus stress point 3 is located at 2.5 ft from the section centroid. In the second stage, the fiber locations are relative to the composite centroid. The incremental stresses are reported below:

Stage	Stress Point	Fiber Location (ft)	E (kip/ft ²)	Stress (kip/ft ²)
One	Point 3 @ Mid-Span	-2.5	4.176x10 ⁶	3800
Two	Point 3 @ Mid-Span	-3.044	4.176x10 ⁶	-1,830
Two	Point 5 @ Mid-Span	2.756	5.1912x10 ⁵	206

The stresses in LARSA 4D match up to rounding.

Verification of the Time Effect on Elastic Modulus

In a time-dependent analysis, the concrete slab will be affected by the time effect on elastic modulus while the steel part will remain unchanged. This necessitates a recomputation of the composite member properties. In this example we will assume the self-weight loading occurs 15 days after casting.

The effect of time is modeled by multiplying E by $f = \text{sqrt}(\text{age}/(4.0+0.857 \times \text{age}))$ where age is in days and is no greater than 28. The concrete E is multiplied by $f = 0.943$. As above, the location of the composite centroid relative to the reference line is determined by the following table:

Shape	cy (ft)	f*E (kip/ft ²)	A (ft ²)	f*E*A	cy*f*E*A
I	-2.9	4.176x10 ⁶	1.72	7.182x10 ⁶	-20.8x10 ⁶
Rectangle	0	4.895x10 ⁵	3.20	1.545x10 ⁶	0
Total				8.73x10 ⁶	-20.8x10 ⁶
Composite	-2.38				

Hand calculations for A and Izz follow as described above, except this time we treat the reference material as the time-adjusted concrete.

Shape	A (ft ²)	A*E/E_ref	Izz (ft ⁴)	Izz+Ac ²	(Izz+Ac ²)*E/E_ref
I	1.72	14.7	6.23	6.69	57.0
Rectangle	3.20	3.20	0.171	18.3	18.3
Composite		17.9			75.4

LARSA 4D does not report time-adjusted cross-sectional properties.

In LARSA 4D, a Material Time Effect record (with default settings) is applied to the Fc_4 material. The casting day of the composite member is set to day 0. Self-weight loading is applied on day 15. The CEB-FIP 90 analysis code is chosen, the time effect on elastic modulus is turned on (all other time effects are turned off), and a Time-Dependent Staged Construction Analysis is run.

The results in the first stage are unchanged.

Displacements

The maximum deflection at mid-span is given by $5/384*(W*L^3)/(EI)$. W and L are as before. E is from the reference material, now the time-adjusted concrete property. The revised computation for incremental displacement in the second stage is:

Stage	W (kip)	E (kip/ft ²)	I (ft ⁴)	d (ft)
Two (rectangle added)	144	4.895x10 ⁵	75.4	1.37

Stresses

The revised stresses are:

Stage	W (kip)	M (kip-ft)	E (kip/ft ²)	I (ft ⁴)	r (1/ft)
Two (rectangle added)	144	5400	4.895x10 ⁵	75.4	1.46x10 ⁻⁴

The rotational strain is converted into a stress at a fiber by multiplying it by the modulus of elasticity at the fiber and the distance from the fiber to the section centroid.

In the first stage, when the section is composed of the I shape alone, note that the beam centroid is at the I shape centroid, and thus stress point 3 is located at 2.5 ft from the section centroid. In the second stage, the fiber locations are relative to the composite centroid. The incremental stresses are reported below:

Stage	Stress Point	Fiber Location (ft)	E (kip/ft ²)	Stress (kip/ft ²)
Two	Point 3 @ Mid-Span	-3.044	4.176x10 ⁶	-1,860
Two	Point 5 @ Mid-Span	2.756	4.895x10 ⁵	197

The results in LARSA 4D are correct up to rounding.

Verification of Shrinkage

To verify shrinkage, we will look at the total effect of shrinkage between days 15 and 400. Shrinkage, ϵ_S as given below according to CEB-FIP 90, is an additional strain added into the cross-section accumulated from time t_0 to time t_1 . In this part, the time effect on elastic modulus is not included.

$$\epsilon_S(t_0, t_1) = E_c S_0 * [\text{BetaS}(t_1) - \text{BetaS}(t_0)]$$

$$E_c S_0 = (160 + 10 * \text{BetaSC} * (9 - F_c_{28}/10)) / 1000000 * (-1.55 * (1.0 - (RH/100.)^3))$$

$$\text{BetaS}(t) = \text{sqrt}((t - TS) / (350 * ((H/100)^2 + (t - TS))))$$

where $TS = 3$, $\text{BetaSC} = 5$, $H = 2 * \text{Area}/\text{Perimeter}$ converted to millimeters, RH is the relative humidity (80%), and t_0 , t_1 are the ages of the section in days. $F_c_{28} = 27.6 \text{ MN/m}^2$ (576 kip/ft²).

Shrinkage in the composite section is due only to the effect of shrinkage in the concrete part. The area of the rectangle is 3.2 ft² and the perimeter for this example is treated as 9.6 ft (which includes the unexposed perimeter at the interface

of the shapes in order to match the perimeter used by LARSA 4D). $H = 203.2$ mm. Substituting these values into the formula gives $\epsilon S(15,400) = -1.33 \times 10^{-4}$.

Because the two shapes that make up the cross-section are connected and governed by the assumption that plane sections remain plane, shrinkage will create self-equilibrating stress (also known as eigenstresses) in both the concrete and steel parts of the section.

The computation of self-equilibrating stress due to shrinkage involves combining two equal-and-opposite strains. The first component is the “external” component with magnitude ϵS in the concrete part (and zero in the steel part), and it is integrated across the fibers that make up the cross-section area to determine an equivalent force $F = \epsilon S * E * A$ and moment $M = F * c_y$ imposed at the beam end at the composite centroid. This force and moment determines the actual deformation of the beam. In Ghali, Favre, and Elbadry (2002) example 5.2, the external component corresponds to the forces and moments that undo the artificial restraint on shrinkage.

Using the E and A values of the concrete part and the distance from the beam centroid to the centroid of the concrete part (the same as the offset of the beam centroid from the beam reference axis given in the first table), $F = -222$ kip, $M = -522$ kip-ft. The corresponding strain for the composite beam is -2.51×10^{-5} pure strain and -1.39×10^{-5} 1/ft bending strain.

The second or “internal” component has magnitude $-\epsilon S$ at any fiber in the concrete part and zero at any fiber in the steel part, but it does not cause deformation. It corresponds to Ghali, Favre, and Elbadry’s strain in the section when shrinkage is restrained.

Self-equilibrating stress at a fiber is the modulus of elasticity at the fiber multiplied by the sum of the strain due to the external component (a linear stress profile across the entire cross-section) and the strain due to the internal component at the fiber (a step function with value $-\epsilon S$ in the concrete part and 0 in the steel part).

There are no continuity stresses in a model such as this. Stress is constant along the length of the beam.

The computation of total stress is given in the following table:

Stress Point	Fiber Location (ft)	E (kip/ft ²)	Stress (kip/ft ²)
Point 3	-3.044	4.176×10^6	72.5
Point 5	2.756	5.1912×10^5	36.2

The results in LARSA 4D match up to rounding.

S08: Time-Dependent Material Properties Effects

This sample problem verifies creep and shrinkage strain calculations a wide column modeled using beam and shell elements with dimensions $1.0 \times 1.2 \text{ m} \times 0.4 \text{ m}$ under vertical loading.

Example Project: The example described here can be found in the Staged Construction folder of your LARSA 4D Samples directory (generally My Documents\LARSA Projects\Samples) in the file S08.

Problem Definition

A very wide column is subjected to a point load in the gravitational direction. Determine the vertical displacements due to creep and shrinkage separately, and compare the values obtained in CEB-FIP 78, CEB-FIP 90, CEB-FIP 2010, EN1992/Eurocode 2004, AASHTO LRFD v6, AASHTO LRFD v7/8, AS3600, and IRC-112 2020 codes.

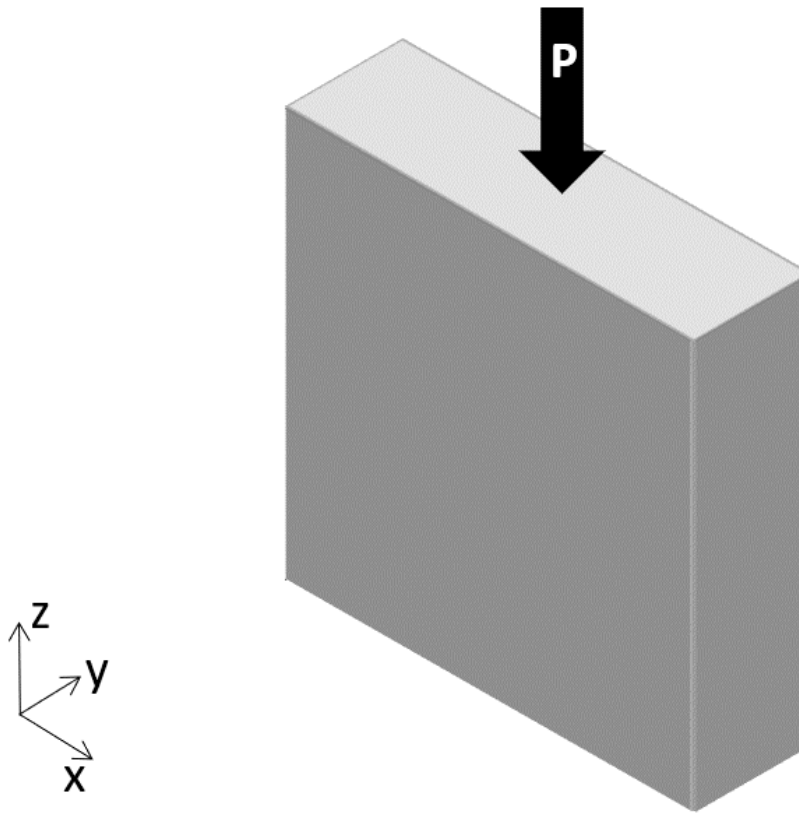


Figure 1: Problem Definition

Modeling

In LARSA 4D, the same object is created in two different ways, by using a frame element and a shell element for modeling. The dimensions of both the frame and the shell are 1.0×1.2 m and their thickness is 0.4 m. The equivalent loadings are also identical. The point load P is 10,000 kN in magnitude.

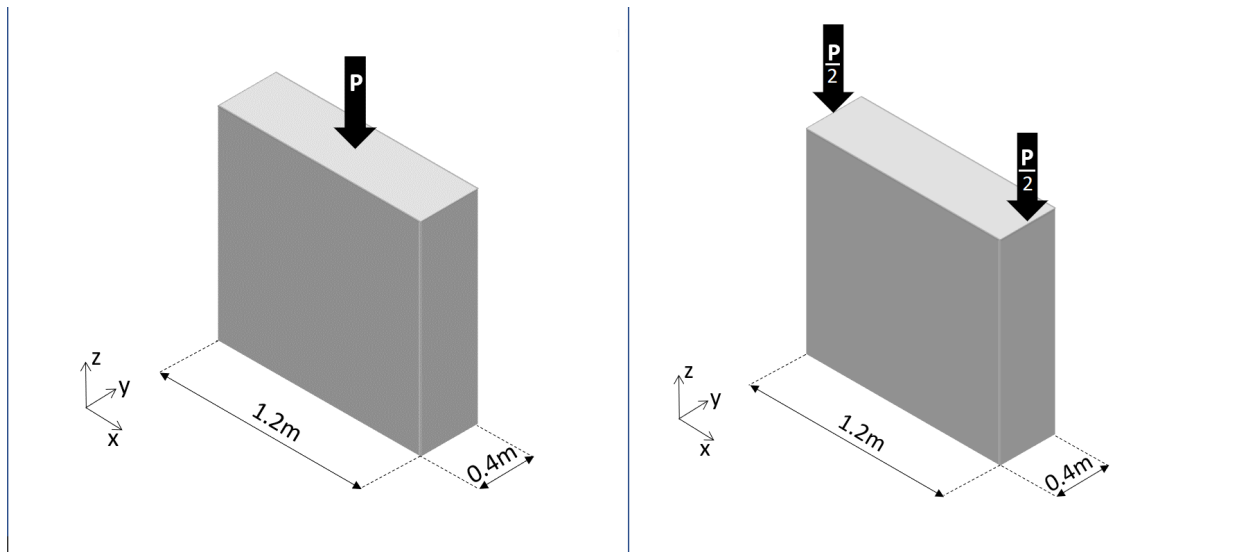


Figure 2: Problem Definition: the Frame Element (left) and the shell (right).

The frame is supported by a fixed support at the bottom end and the orientation of the member is along the Z-axis. The shell is supported by a fixed support at the bottom left end (Joint 3) as can be seen in Figure 3. Translation of Joint 4, on the other hand, is left free in the direction of x . Additionally, to hinder out of plane deformations, top joints (Joints, 5 and 6) are restrained the translation in the direction of Y.

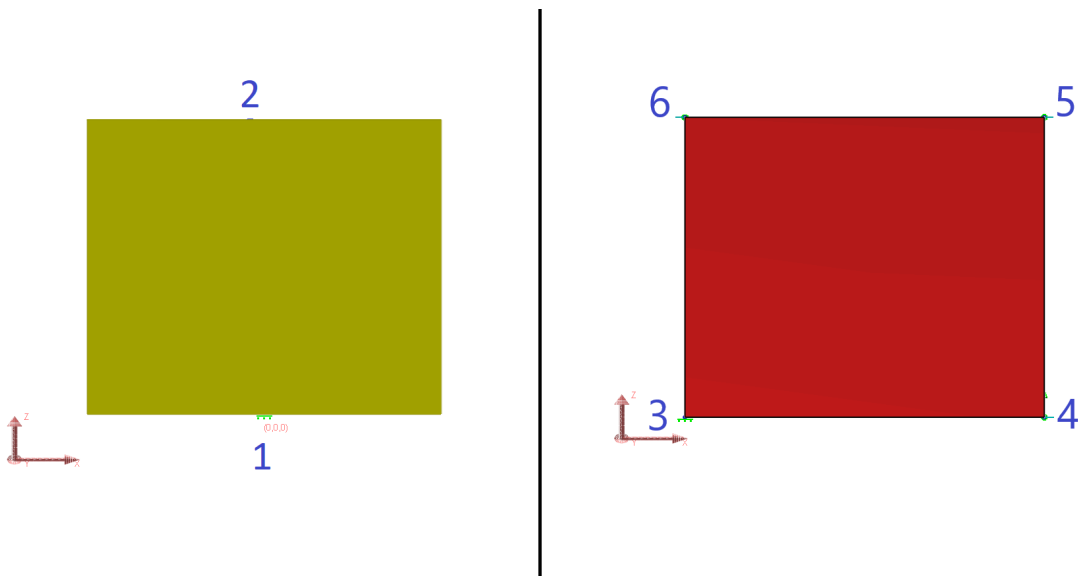


Figure 3: Joints of the Frame (left) and the shell (right) from the Front Plane

Material properties of concrete such as Modulus of Elasticity (E), Poisson Ratio, Shear Modulus (G), F_{ck} , Concrete Cement Hardening Type and Material Time-Effect should be entered manually for the both models as shown in Figure 4, Figure 5 and Figure 6.

	Name	Modulus of Elasticity (N/mm ²)	Poisson Ratio	Shear Modulus (N/mm ²)	Unit Weight (N/mm ³)	Thermal Expansion (1/°C *10 ⁻⁶)	Assigned
1	Concrete	35,000.00	0.2000	14,583.33	0.0000	0.000000	Yes
2	Concrete Rectangular Plate	35,000.00	0.2000	14,583.33	0.0000	0.000000	Yes
3							

Figure 4: Material Properties.

Additional properties for the material under the **More Properties** segment are given in Figure 5. **Material Time Effect** has to be set to take the time dependent material properties for the solution. However, before defining **Material Time Effects**, the design code which will be used for the time-effects calculations should be selected from **Analysis** → **Time Dependent Analysis Options** → **Code For Creep and Shrinkage**. In this example, check both **Include Creep** and **Include Shrinkage** options. Time effect on elastic modulus is not included.

	Name	Yield Stress (N/mm ²)	Post-yield to Initial Slope Ratio	Concrete Strength Specimen	Concrete Fck or Steel Fu (N/mm ²)	Concrete Cement Hardening Type	Tendon GUTS (N/mm ²)	Material Time-Effect	Assigned
1	Concrete	0.00	0.020	Cylinder	32.00	Normal	0.00	Concrete Time	Yes
2	Concrete Rectangular Plate	0.00	0.020	Cylinder	32.00	Normal	0.00	Concrete Time_RectangularPlate	Yes
3									

Figure 5: More Properties

When performing verification for CEB-FIP 78, from the **Material Time Effects** tab, parameters required for the selected code should be defined for the plate and the frame.

	Name	Notional Thickness Coefficient	Creep Coefficient (Environment)	Creep Coefficient (Notional Thickness)	Shrinkage Coef (Environment)	Shrinkage Coef (Notional Thickness)	Delayed Modulus of Elasticity Coef	Creep Factor	Shrinkage Factor	Relaxation Factor	Assigned
1	Concrete Time	1.5000	2.3500	1.3702	-0.0004	0.7847	0.4000	1.0000	1.0000	1.0000	Yes
2	Concrete Time_RectangularPla	1.5000	2.3500	1.3095	-0.0004	0.7507	0.4000	1.0000	1.0000	1.0000	Yes
3											

Figure 6: Material Time Effects for CEB-FIP78

Construction Sequence

Two different construction sequences are considered, Case A and Case B. In both cases, all elements are cast on the 10th day. Case A models a cast-in-place segment. In Case A, the elements are constructed on the 11th day (i.e. their stiffness is considered beginning at the age of 1). In Case B a pre-cast model is considered where the elements are constructed on the 25th day (i.e. their stiffness is considered beginning at the age of 15, what happened before than is ignored).

At the age of 16th day of concrete, elements are subjected to external sustained load (construction day 26). In order to represent that events in the model and get results for the desired ages such as 40th and 100th days, construction stages should be defined for those times (50 and 110 days).

Ambient temperature is taken as 20°C during the whole construction sequence.

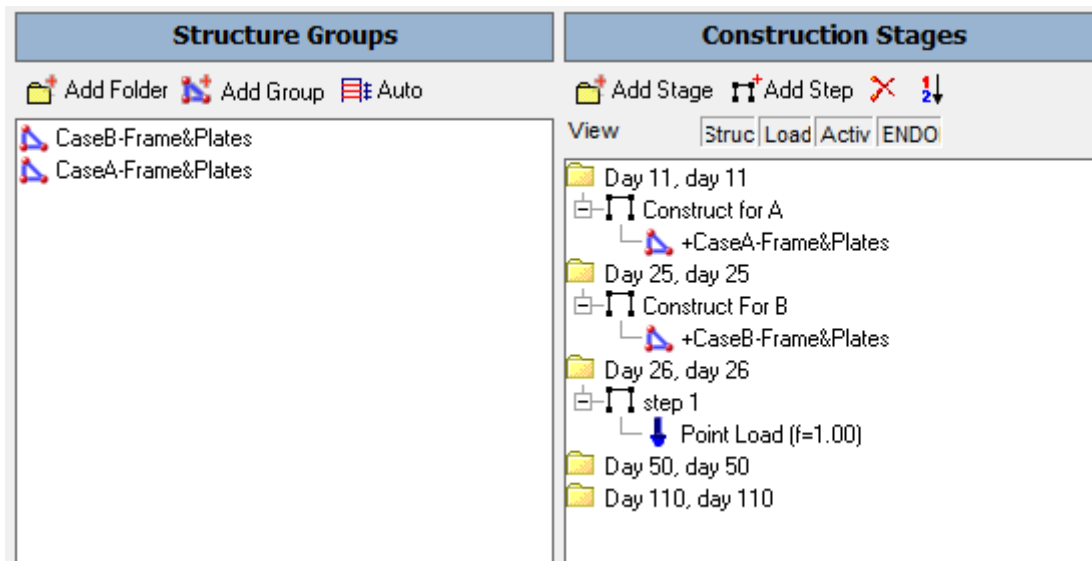


Figure 7: Construction Stages

Verification of Creep

The creep and shrinkage displacements can be observed independently. For example, right clicking on the **Day 110: Creep** in the Analysis Results and selecting the joint displacements will show the cumulative displacements of all the previous stages, plus the creep displacement of the Day 110 stage, as in Figure 8.

	Joint	Result Case	Translation X (mm)	Translation Y (mm)	Translation Z (mm)	Rotation X (rad)	Rotation Y (rad)	Rotation Z (rad)
1	1	Day 110: Creep	0.0000	0.0000	0.0000	0.0000	0.0000	0.0000
2	2	Day 110: Creep	0.0000	0.0000	-0.7826	0.0000	0.0000	0.0000
3	3	Day 110: Creep	0.0000	0.0000	0.0000	0.0000	0.0000	0.0000
4	4	Day 110: Creep	0.0000	0.0000	0.0000	0.0000	0.0000	0.0000
5	5	Day 110: Creep	0.0000	0.0000	-0.7826	0.0000	0.0000	0.0000
6	6	Day 110: Creep	0.0000	0.0000	-0.7826	0.0000	0.0000	0.0000

Figure 8: Joint Displacements

To get the joint displacements due to creep of the Day 110 stage only, select **Extract Creep** from the drop down menu.

	Joint	Result Case	Translation X (mm)	Translation Y (mm)	Translation Z (mm)	Rotation X (rad)	Rotation Y (rad)	Rotation Z (rad)
1	1	Day 110: Creep	0.0000	0.0000	0.0000	0.0000	0.0000	0.0000
2	2	Day 110: Creep	0.0000	0.0000	-0.7826	0.0000	0.0000	0.0000
3	3	Day 110: Creep	0.0000	0.0000	0.0000	0.0000	0.0000	0.0000
4	4	Day 110: Creep	0.0000	0.0000	0.0000	0.0000	0.0000	0.0000
5	5	Day 110: Creep	0.0000	0.0000	-0.7826	0.0000	0.0000	0.0000
6	6	Day 110: Creep	0.0000	0.0000	-0.7826	0.0000	0.0000	0.0000

Figure 9: Joint Displacements due to Creep Deformation in Day 110

Creep formulas provided by each design code are given below. Hand calculations are performed based on these formulas and the obtained results are compared with the LARSA 4D results.

Parameters

RH = 60 (ambient relative humidity, %)

f_{ck} = 32 (characteristic compressive strength of concrete at the age of 28 days, MPa)

t = 100 (age of concrete in days at the moment considered)

t_0 = 16 (age of concrete at loading, days)

k_4 = 0.6 (environment variable, for AS3600)

$\phi_{cc,b}$ = 0 (basic creep coefficient which can be input manually or is calculated automatically if it is set as 0, for AS3600)

λ = 1.5 (coefficient depending on the ambient environment, for CEB-FIP 78)

Assumptions

In LARSA 4D, **frame** elements are considered as column elements, i.e. the perimeter of the cross-section are subjected to atmosphere. Therefore the V/S ratio and notional thickness become:

$$V/S = (\text{width} \times \text{thickness} \times \text{length}) / (2(\text{width} \times \text{length} + \text{thickness} \times \text{length})) = \text{width} \times \text{thickness} / (2 \times (\text{width} + \text{thickness}))$$

$$h = 2(V/S) = \text{width} \times \text{thickness} / (\text{width} + \text{thickness})$$

Notional thickness for frame element is calculated as **300 mm**.

On the other hand, **shell** elements are considered as slab elements, accordingly the edges in the direction of thickness are not subjected to atmosphere.

$$V/S = (\text{width} \times \text{thickness} \times \text{length}) / (2 \times \text{width} \times \text{length}) = \text{thickness} / 2$$

$$h = 2(V/S) = \text{thickness}$$

Notional thickness for shell element is calculated as **400 mm**.

Creep Strain Calculation

Creep strain is calculated by multiplying the strain which is not time-dependent with the creep coefficient.

$$\epsilon_c(t, t_0) = \sigma / E_c \times \phi(t, t_0)$$

where,

σ is constant stress on the member

E_c is elastic modulus of concrete

$\phi(t, t_0)$ is creep coefficient

Creep Coefficients

CEB-FIP 78

$$\phi(t, t_0) = \beta_a(t_0) + \phi_d \times \beta_d(t - t_0) + \phi_f \times [\beta_f(t) - \beta_f(t_0)]$$

where,

β_a is the part which is developed during the first few days after the load had been imposed (It is 0 in LARSA 4D.)

ϕ_d is delayed modulus of elasticity coefficient

β_d should be input to LARSA 4D as a time-dependent curve

ϕ_f is flow coefficient obtained from $\phi_{f1} \times \phi_{f2}$ (ϕ_{f1} depends on the ambient environment and ϕ_{f2} depends on the notional thickness.)

β_f should be input to LARSA 4D as a time-dependent curve

Effect of cement and curing temperature:

$$t_{0,adj} = (\alpha/30) \times \sum_0^{t_m} [(T(t_m) + 10) \times \Delta t_m]$$

α is cement type coefficient (1 for normal and slowly hardening cements (NR, SL), 2 for rapid hardening cements (RA), and 3 for rapid hardening high strength cements (RS).)

T is the mean daily temperature of concrete (It is assumed 20°C for the CEB-FIP 78 code.)

Δt_m is the number of days when the mean daily temperature has assumed the value T.

CEB-FIP 90

$$\phi(t, t_0) = \phi_0 \times \beta_c(t - t_0)$$

where,

$$\phi_0 = \phi_{RH} \times \beta(f_{cm}) \times \beta(t_0)$$

$$\phi_{RH} = 1 + (1 - (RH/100)) / (0.46 \times (h/100)^{1/3})$$

$$\beta(f_{cm}) = 5.3 / (f_{cm}/10)^{0.5}$$

$$\beta(t_0) = 1 / (0.1 + t_{0,adj})^{0.2}$$

$$\beta_c(t - t_0) = [(t - t_{0,adj}) / (\beta_H + t - t_{0,adj})]^{0.3}$$

$$\beta_H = 150 \times \{1 + (1.2 \times RH/100)^{18}\} \times (h/100) + 250 \leq 1500$$

f_{cm} is mean characteristic compressive strength of concrete at the age of 28 days ($f_{ck} + 8\text{MPa}$)

Effect of cement and curing temperature:

$$t_{0,adj} = t_{0,T} \times [(9 / (2 + t_{0,T}^{1.2})) + 1]^\alpha \geq 0.5 (\text{days})$$

α is cement type coefficient (-1 for slowly hardening cement (SL), 0 for normal and rapid hardening cements (NR and RA), and 1 for rapid hardening high strength cements (RS).)

$t_{0,T}$ is temperature adjusted concrete age calculated based on Eqn. 2.1-72 (LARSA 4D takes concrete age at loading if the temperature adjusted time is off.)

CEB-FIP 2010

$$\phi(t, t_0) = \phi_{bc}(t, t_0) + \phi_{dc}(t, t_0)$$

where,

The basic creep coefficient may be estimated from:

$$\phi_{bc}(t, t_0) = \beta_{bc}(f_{cm}) \times \beta_{bc}(t, t_0)$$

$$\beta_{bc}(f_{cm}) = 1.8 / (f_{cm})^{0.7}$$

$$\beta_{bc}(t, t_0) = \ln((30 / t_{0,adj}) + 0.035)^2 \times (t - t_0) + 1$$

The drying creep coefficient may be estimated from:

$$\phi_{dc}(t, t_0) = \beta_{dc}(f_{cm}) \times \beta(RH) \times \beta_{dc}(t_0) \times \beta_{dc}(t, t_0)$$

$$\beta_{dc}(f_{cm}) = 412 / (f_{cm})^{1.4}$$

$$\beta(RH) = (1 - RH/100) / (0.1 \times h/100)^{1/3}$$

$$\beta_{dc}(t_0) = 1 / (0.1 + (t_{0,adj})^{0.2})$$

$$\beta_{dc}(t, t_0) = [(t - t_0) / (\beta_h + t - t_0)]^{\nu(t_0)}$$

$$\beta_h = 1.5 \times h + 250 \times \alpha_{f_{cm}} \leq 1500 \times \alpha_{f_{cm}}$$

$$\alpha_{f_{cm}} = (35 / f_{cm})^{0.5}$$

$$\nu(t_0) = 1 / [2.3 + (3.5 / (t_{0,adj})^{0.5})]$$

f_{cm} is mean characteristic compressive strength of concrete at the age of 28 days ($f_{ck} + 8\text{MPa}$)

Effect of cement and curing temperature:

LARSA 4D Sample and Verification Problems

$$t_{0,adj} = t_{0,T} \times \left[\left(\frac{9}{2+t_{0,T}^{1.2}} \right) + 1 \right]^\alpha \geq 0.5 (\text{days})$$

α is cement type coefficient (-1 for slowly hardening cement (SL), 0 for normal hardening cements (NR), and 1 for rapid hardening and rapid hardening high strength cements (RA and RS).)

$t_{0,T}$ is temperature adjusted concrete age calculated based on Eqn. 5.1-85 (LARSA 4D takes concrete age at loading if the temperature adjusted time is off.)

EN1992/EuroCode 2004

$$\phi(t, t_0) = \phi_0 \times \beta_c(t, t_0)$$

where,

$$\phi_0 = \phi_{RH} \times \beta(f_{cm}) \times \beta(t_0)$$

$$\phi_{RH} = 1 + \left((1 - RH/100) / (0.1 \times h^{1/3}) \right) \text{ for } f_{cm} \leq 35 \text{ MPa}$$

$$\phi_{RH} = 1 + \left((1 - RH/100) / (0.1 \times h^{1/3}) \right) \times \alpha_1 \times \alpha_2 \text{ for } f_{cm} > 35 \text{ MPa}$$

$$\beta(f_{cm}) = 16.8 / (f_{cm})^{0.5}$$

$$\beta(t_0) = 1 / (0.1 + t_{0,adj}^{0.2})$$

$$\beta_c(t, t_0) = \left[(t - t_0) / (\beta_H + t - t_0) \right]^{0.3}$$

$$\beta_H = 1.5 \times [1 + (0.012 \times RH)^{18}] \times h + 250 \leq 1500 \text{ for } f_{cm} \leq 35 \text{ MPa}$$

$$\beta_H = 1.5 \times [1 + (0.012 \times RH)^{18}] \times h + 250 \times \alpha_3 \leq 1500 \times \alpha_3 \text{ for } f_{cm} > 35 \text{ MPa}$$

$$\alpha_1 = [35 / f_{cm}]^{0.7}$$

$$\alpha_2 = [35 / f_{cm}]^{0.2}$$

$$\alpha_3 = [35 / f_{cm}]^{0.5}$$

f_{cm} is mean characteristic compressive strength of concrete at the age of 28 days ($f_{ck} + 8\text{MPa}$)

Effect of cement and curing temperature:

$$t_{0,adj} = t_{0,T} \times \left[\left(\frac{9}{2+t_{0,T}^{1.2}} \right) + 1 \right]^\alpha \geq 0.5 (\text{days})$$

α is cement type coefficient (-1 for slowly hardening cement (SL), 0 for normal hardening cements (NR), and 1 for rapid hardening and rapid hardening high strength cements (RA and RS).)

$t_{0,T}$ is temperature adjusted concrete age calculated based on Eqn. 5.1-85 (LARSA 4D takes concrete age at loading if the temperature adjusted time is off.)

AASHTO LRFD v6

$$\phi(t, t_0) = 1.9 \times k_s \times k_{hc} \times k_f \times k_{td} \times t_0^{-0.118}$$

where,

$$k_s = 1.45 - 0.13(V/S) \geq 1.0 \text{ (V/S in inch)}$$

$$k_{hc} = 1.56 - 0.008 \times RH$$

$$k_f = 5 / (1 + f'_{ci})$$

$$k_{td} = (t - t_0) / (61 - 4 \times f'_{ci} + t - t_0)$$

$$f'_{ci} = 0.80 \times f'_c \text{ (ksi)}$$

f'_c is characteristic compressive strength of concrete at age of 28 days.

AASHTO LRFD v7/8

$$\phi(t, t_0) = 1.9 \times k_s \times k_{hc} \times k_f \times k_{td} \times t_0^{-0.118}$$

where,

$$k_s = 1.45 - 0.13(V/S) \geq 1.0 \text{ (V/S in inch)}$$

$$k_{hc} = 1.56 - 0.008 \times RH$$

$$k_f = 5 / (1 + f'_{ci})$$

$$k_{td} = (t - t_0) / [12 \times (100 - 4 \times f'_{ci}) / (f'_{ci} + 20) + t - t_0]$$

$$f'_{ci} = 0.80 \times f'_c \text{ (ksi)}$$

f'_c is characteristic compressive strength of concrete at age of 28 days.

IRC-112 2020

$$\phi(t, t_0) = \phi_0 \times \beta_c(t, t_0)$$

where,

$$\phi_0 = \phi_{RH} \times \beta(f_{cm}) \times \beta(t_0)$$

$$\phi_{RH} = 1 + ((1 - RH/100) / (0.1 \times h^{3/2})) \text{ for } f_{cm} \leq 45 \text{ MPa}$$

$$\phi_{RH} = [1 + ((1 - RH/100) / (0.1 \times h^{3/2})) \times \alpha_1] \times \alpha_2 \text{ for } f_{cm} > 45 \text{ MPa}$$

$$\beta(f_{cm}) = 18.78 / (f_{cm})^{0.5}$$

$$\beta(t_0) = 1 / (0.1 + t_{0,adj}^{0.2})$$

$$\beta_c(t, t_0) = [(t - t_0) / (\beta_H + (t - t_0))]^{0.3}$$

$$\beta_H = 1.5 \times [1 + (0.012 \times RH)^{18}] \times h + 250 \leq 1500 \text{ for } f_{cm} \leq 45 \text{ MPa}$$

$$\beta_H = 1.5 \times [1 + (0.012 \times RH)^{18}] \times h + 250 \times \alpha_3 \leq 1500 \times \alpha_3 \text{ for } f_{cm} > 45 \text{ MPa}$$

$$\alpha_1 = (43.75 / f_{cm})^{0.7}$$

$$\alpha_2 = (43.75 / f_{cm})^{0.2}$$

$$\alpha_3 = (43.75 / f_{cm})^{0.5}$$

f_{cm} is mean characteristic compressive strength of concrete at the age of 28 days ($f_{ck} + 10 \text{ MPa}$)

Effect of cement and curing temperature:

$$t_{0,adj} = t_{0,T} \times [(9 / (2 + t_{0,T}^{1.2})) + 1]^\alpha \geq 0.5 \text{ (days)}$$

α is cement type coefficient (-1 for slowly hardening cement (SL), 0 for normal hardening cements (NR), and 1 for rapid hardening and rapid hardening high strength cements (RA and RS).)

$t_{0,T}$ is temperature adjusted concrete age calculated based on Eqn. A2-13 (LARSA 4D takes concrete age at loading if the temperature adjusted time is off.)

AS-3600 2009

$$\phi_{cc}(t, t_0) = k_2 \times k_3 \times k_4 \times k_5 \times \phi_{cc,b}$$

where,

$$k_2 = \alpha_2 \times t^{0.8} / (t^{0.8} + 0.15 \times t_h)$$

LARSA 4D Sample and Verification Problems

$$\alpha_2 = 1 + 1.12 \times e^{-0.008 \times t_h}$$

$$k_3 = 1.75 + (t_0 - 7) \times (1.1 - 1.75) / (28 - 7) \text{ for } t_0 \leq 28$$

$$k_3 = 1.1 + (t_0 - 28) \times (0.9 - 1.1) / (365 - 28) \text{ for } 28 < t_0 \leq 365$$

$$k_3 = 0.9 \text{ for } t_0 > 365$$

$$k_5 = 1 \text{ for } f'_c \leq 50$$

$$k_5 = 2 - \alpha_3 - 0.02 \times (1 - \alpha_3) \times f'_c \text{ for } 50 < f'_c \leq 100$$

$$\alpha_3 = 0.7 / (k_4 \times \alpha_2)$$

$\phi_{cc,b}$ is basic creep coefficient

k_4 is environment variable

f'_c is characteristic compressive strength of concrete at age of 28 days.

Both cases (Case A and Case B) gives the same results for the creep calculation since they are loaded at the same age which is later than the construction of both groups.

Creep Displacements of Frame Elements (Units are in mm)

Code	Hand Calc.	LARSA 4D	Error (%)
CEB-FIP 78	-0.555	-0.555	0.0
CEB-FIP 90	-0.702	-0.703	0.0
CEB-FIP 2010	-0.691	-0.691	0.0
EN1992/Eurocode 2004	-0.664	-0.664	0.0
AASHTO LRFD v6	-0.603	-0.603	0.0
AASHTO LRFD v7/8	-0.617	-0.617	0.0
IRC-112 2020	-0.784	-0.784	0.0
AS-3600 2009	-0.856	-0.855	0.0

Creep Displacements of Shell Elements (Units are in mm)

Code	Hand Calc.	LARSA 4D	Error (%)
CEB-FIP 78	-0.507	-0.507	0.0
CEB-FIP 90	-0.644	-0.644	0.0
CEB-FIP 2010	-0.659	-0.659	0.0
EN1992/Eurocode 2004	-0.610	-0.610	0.0
AASHTO LRFD v6	-0.603	-0.603	0.0
AASHTO LRFD v7/8	-0.617	-0.617	0.0
IRC-112 2020	-0.719	-0.719	0.0

Code	Hand Calc.	LARSA 4D	Error (%)
AS-3600 2009	-0.684	-0.684	0.0

LARSA 4D's creep computations match exactly with hand calculations.

Verification of Shrinkage

For the shrinkage displacements of Day 110 stage only, follow the same procedure as before, this time by right clicking **Day 110: Shrinkage** and extracting the results for shrinkage.

Unlike in the case of creep, Case A and Case B do not undergo the same shrinkage. So the results are presented in different tables for each case.

Joint	Result Case	Translation X (mm)	Translation Y (mm)	Translation Z (mm)	Rotation X (rad)	Rotation Y (rad)	Rotation Z (rad)
1	Day 110: Shrinkage	0.0000	0.0000	0.0000	0.0000	0.0000	0.0000
2	Day 110: Shrinkage	0.0000	0.0000	-0.0736	0.0000	0.0000	0.0000
3	Day 110: Shrinkage	0.0000	0.0000	0.0000	0.0000	0.0000	0.0000
4	Day 110: Shrinkage	-0.0667	0.0000	0.0000	0.0000	0.0000	0.0000
5	Day 110: Shrinkage	-0.0667	0.0000	-0.0556	0.0000	0.0000	0.0000
6	Day 110: Shrinkage	0.0000	0.0000	-0.0556	0.0000	0.0000	0.0000

Figure 11: Joint Displacements due to Shrinkage Deformation in 110 days

Shrinkage formulas provided by each design code are given below. Hand calculations are performed based on these formulas and the obtained results are compared with the LARSA 4D results.

Parameters

$RH = 60$ (ambient relative humidity, %)

$f_{ck} = 32$ (characteristic compressive strength of concrete at the age of 28 days, MPa)

$t = 100$ (age of concrete in days at the moment considered)

$k_4 = 0.6$ (environment variable - for AS3600)

$\epsilon_{csd,b}^* = 0.0008$ (drying basic shrinkage strain - for AS3600)

Assumptions

Age of concrete at the beginning of shrinkage or swelling, t_s (days) is

$t_s = 3$ days for CEB-FIP 90, CEB-FIP 2010, and IRC2020

$t_s = 14$ days for EN1992/Eurocode 2004

$t_s = 0$ day for AASHTO LRFD v6, AASHTO v7/8, and AS3600

Any t_s value greater than 0 can be used by defining the input parameters required for CEB-FIP 78 code.

The assumption for notional thickness calculation discussed in creep section is also valid for the shrinkage calculations.

In LARSA 4D, shrinkage occurs only in the time interval between the construction day and time of the moment considered. Shrinkage induced displacement before the construction day, accordingly, is ignored.

Shrinkage Strain Calculation

CEB-FIP 78

$$\epsilon_{sh}(t, t_s) = \epsilon_{s0}[\beta_s(t) - \beta_s(t_s)]$$

where,

ϵ_{s0} is shrinkage coefficient obtained from $\epsilon_{s1} \times \epsilon_{s2}$ (ϵ_{s1} is environment shrinkage coefficient and ϵ_{s2} is the notional thickness shrinkage coefficient)

β_s should be input to LARSA 4D as a curve

CEB-FIP 90

$$\epsilon_{sh}(t, t_s) = \epsilon_{cs0} \times \beta_s(t - t_s)$$

where,

$$\epsilon_{cs0} = \epsilon_s(f_{cm}) \times \beta_{RH}$$

$$\epsilon_s(f_{cm}) = [160 + 10 \times \beta_{sc} \times (9 - f_{cm}/10)] \times 10^{-6}$$

β_{sc} is a coefficient which depends on the type of cement (4 for slowly hardening cements SL, 5 for normal or rapid hardening cements N and R, and 8 for rapid hardening high strength cements RS)

$$\beta_{RH} = -1.55 \times \beta_{sRH} \text{ for } 40\% \leq RH \leq 99\%$$

$$\beta_{RH} = 0.25 \text{ for } RH \geq 99\%$$

$$\beta_{sRH} = 1 - (RH / 100)^3$$

$$\beta_s(t - t_s) = [(t - t_s) / (350 \times (h/100)^2 + t - t_s)]^{0.5}$$

f_{cm} is mean characteristic compressive strength of concrete at the age of 28 days ($f_{ck} + 8\text{MPa}$)

CEB-FIP 2010

$$\epsilon_{sh}(t, t_s) = \epsilon_{cas}(t) + \epsilon_{cds}(t, t_s)$$

where,

$$\epsilon_{cas}(t) = \epsilon_{cas0}(f_{cm}) \times \beta_{as}(t)$$

$$\epsilon_{cds}(t, t_s) = \epsilon_{cds0}(f_{cm}) \times \beta_{RH}(RH) \times \beta_{ds}(t - t_s)$$

$$\epsilon_{cas0}(f_{cm}) = -\alpha_{as}((f_{cm}/10)/(6 + f_{cm}/10))^{2.5} \times 10^{-6}$$

$$\beta_{as}(t) = 1 - \exp(-0.2 \times t^{0.5})$$

LARSA 4D Sample and Verification Problems

$$\epsilon_{cds0}(f_{cm}) = [(220 + 110 \times \alpha_{ds1}) \times \exp(-\alpha_{ds2} \times f_{cm})] \times 10^{-6}$$

$$\beta_{RH} = -1.55 \times [1 - (RH/100)^3] \text{ for } 40 \leq RH \leq 99\% \times \beta_{s1}$$

$$\beta_{RH} = 0.25 \text{ for } RH \geq 99\% \times \beta_{s1}$$

$$\beta_{ds}(t-t_s) = [(t-t_s)/(0.035 \times h^2 + (t-t_s))]^{0.5}$$

$$\beta_{s1} = (35/f_{cm})^{0.1} \leq 1.0$$

α_{as} , α_{ds1} and α_{ds2} are the coefficients dependent on the type of cement

f_{cm} is mean characteristic compressive strength of concrete at the age of 28 days ($f_{ck} + 8\text{MPa}$)

EN1992/EuroCode 2004

$$\epsilon_{sh} = \epsilon_{cd} + \epsilon_{ca}$$

where,

The development of the drying shrinkage strain in time follows from:

$$\epsilon_{cd}(t) = \beta_{ds}(t, t_s) \times k_h \times \epsilon_{cd,0}$$

k_h is a coefficient depending on the notional size h

$$\beta_{ds}(t, t_s) = (t-t_s)/((t-t_s)+0.04 \times h^{3/2})$$

$\epsilon_{cd,0}$ is taken from Table 3.2 in code.

The autogenous shrinkage strain follows from:

$$\epsilon_{ca}(t) = \beta_{as}(t) \times \epsilon_{ca}(\infty)$$

$$\epsilon_{ca}(\infty) = 2.5 \times (f_{ck} - 10) \times 10^{-6}$$

$$\beta_{as}(t) = 1 - \exp(-0.2t^{0.5})$$

f_{cm} is mean characteristic compressive strength of concrete at the age of 28 days ($f_{ck} + 8\text{MPa}$)

AASHTO LRFD v6

$$\epsilon_{sh} = k_s \times k_{hs} \times k_f \times k_{td} \times 0.48 \times 10^{-3}$$

where,

$$k_{hs} = (2.00 - 0.014 \times RH)$$

$$k_{td} = (t - t_s)/(61 - 4 \times f'_{ci} + t - t_s)$$

The other constants are obtained the same way as in the creep specification.

AASHTO LRFD v7/8

$$\epsilon_{sh} = k_s \times k_{hs} \times k_f \times k_{td} \times 0.48 \times 10^{-3}$$

where,

$$k_{hs} = (2.00 - 0.014 \times RH)$$

$$k_{td} = (t - t_s)/(12 \times (100 - 4 \times f'_{ci})/(f'_{ci} + 20) + t - t_s)$$

The other constants are obtained the same way as in the creep specification.

IRC-112 2020

$$\epsilon_{sh}(t,t_s) = \epsilon_{cd}(t) + \epsilon_{ca}(t,t_s)$$

where,

$$\epsilon_{cd}(t) = \beta_{ds}(t,t_s) \times k_h \times \epsilon_{cd}$$

$$\beta_{ds}(t,t_s) = (t - t_s) / [(t - t_s) + 0.04 \times h^{3/2}]$$

$$\epsilon_{cd} = 0.85[(220 + 110 \times \alpha_{ds1}) \times \exp(-\alpha_{ds2} \times f_{cm} / 12.5)] \times 10^{-6} \times \beta_{RH}$$

$$\beta_{RH} = 1.55 \times [1 - (RH/100)^3]$$

$$\epsilon_{ca}(t) = \beta_{as}(t) \times \epsilon_{ca}$$

$$\beta_{as}(t) = 1 - e^{-0.2 \times t^{0.5}}$$

ϵ_{ca} is taken from Table 6.6

α_{ds1} and α_{ds2} are coefficients dependent on the type of cement

f_{cm} is mean characteristic compressive strength of concrete at the age of 28 days ($f_{ck} + 10\text{MPa}$)

AS-3600 2009

$$\epsilon_{sh}(t,t_s) = \epsilon_{cse} + \epsilon_{csd}$$

where,

$$\epsilon_{cse} = \epsilon_{cse}^* \times (1 - e^{-0.1 \times t})$$

$$\epsilon_{cse}^* = (0.06 \times f'_c - 1) \times 50 \times 10^{-6}$$

$$\epsilon_{csd} = k_1 \times k_4 \times \epsilon_{csd,b}$$

$$k_1 = \alpha_1 \times t^{0.8} / (t^{0.8} + 0.15 \times t_h)$$

$$\alpha_1 = 0.8 + 1.2 \times e^{-0.005 \times t_h}$$

$$\epsilon_{csd,b} = (1 - 0.008 \times f'_c) \times \epsilon_{csd,b}^*$$

$\epsilon_{csd,b}^*$ is drying basic shrinkage strain

k_4 is environment variable

f'_c is characteristic compressive strength of concrete at age of 28 days.

Shrinkage Displacements of Frame Elements in Group A (Units are in mm)

Code	Hand Calc.	LARSA 4D	Error (%)
CEB-FIP 78	-0.053	-0.053	0.0
CEB-FIP 90	-0.086	-0.086	0.0
CEB-FIP 2010	-0.134	-0.134	0.0
EN1992/Eurocode 2004	-0.130	-0.130	0.0
AASHTO LRFD v6	-0.392	-0.392	0.0
AASHTO LRFD v7/8	-0.396	-0.396	0.0

Code	Hand Calc.	LARSA 4D	Error (%)
IRC-112 2020	-0.135	-0.135	0.0
AS-3600 2009	-0.212	-0.212	0.0

Shrinkage Displacements of Shell Elements in Group A (Units are in mm)

Code	Hand Calc.	LARSA 4D	Error (%)
CEB-FIP 78	-0.035	-0.035	0.0
CEB-FIP 90	-0.065	-0.065	0.0
CEB-FIP 2010	-0.113	-0.113	0.0
EN1992/Eurocode 2004	-0.102	-0.102	0.0
AASHTO LRFD v6	-0.392	-0.392	0.0
AASHTO LRFD v7/8	-0.396	-0.396	0.0
IRC-112 2020	-0.102	-0.102	0.0
AS-3600 2009	-0.173	-0.173	0.0

Shrinkage Displacements of Frame Elements in Group B (Units are in mm)

Code	Hand Calc.	LARSA 4D	Error (%)
CEB-FIP 78	-0.043	-0.043	0.0
CEB-FIP 90	-0.055	-0.055	0.0
CEB-FIP 2010	-0.078	-0.078	0.0
EN1992/Eurocode 2004	-0.109	-0.109	0.0
AASHTO LRFD v6	-0.259	-0.259	0.0
AASHTO LRFD v7/8	-0.259	-0.259	0.0
IRC-112 2020	-0.103	-0.103	0.0
AS-3600 2009	-0.127	-0.127	0.0

LARSA 4D's shrinkage computations match exactly with the hand calculations.

S08b: Time-Dependent Material Properties Effects

This sample problem verifies creep and shrinkage strain calculations a wide column modeled using a shell element with dimensions 0.4 x 1.0 m x 0.1 m with loading in the gravitational and lateral directions.

Example Project: The example described here can be found in the Staged Construction folder of your LARSA 4D Samples directory (generally My Documents\LARSA Projects\Samples) in the file S08.

Problem Definition

A column modeled with a shell element is subjected to two point loads of 10,000 kN magnitude in the gravitational and lateral directions, as shown in Figure 1. Determine the vertical displacements and also the horizontal displacements in the direction of x due to creep and shrinkage separately, and compare the values obtained in CEB-FIP 78, CEB-FIP 90, CEB-FIP 2010, EN1992/Eurocode 2004, AASHTO LRFD v6, AASHTO LRFD v7/8, AS3600, and IRC-112 2020 codes.

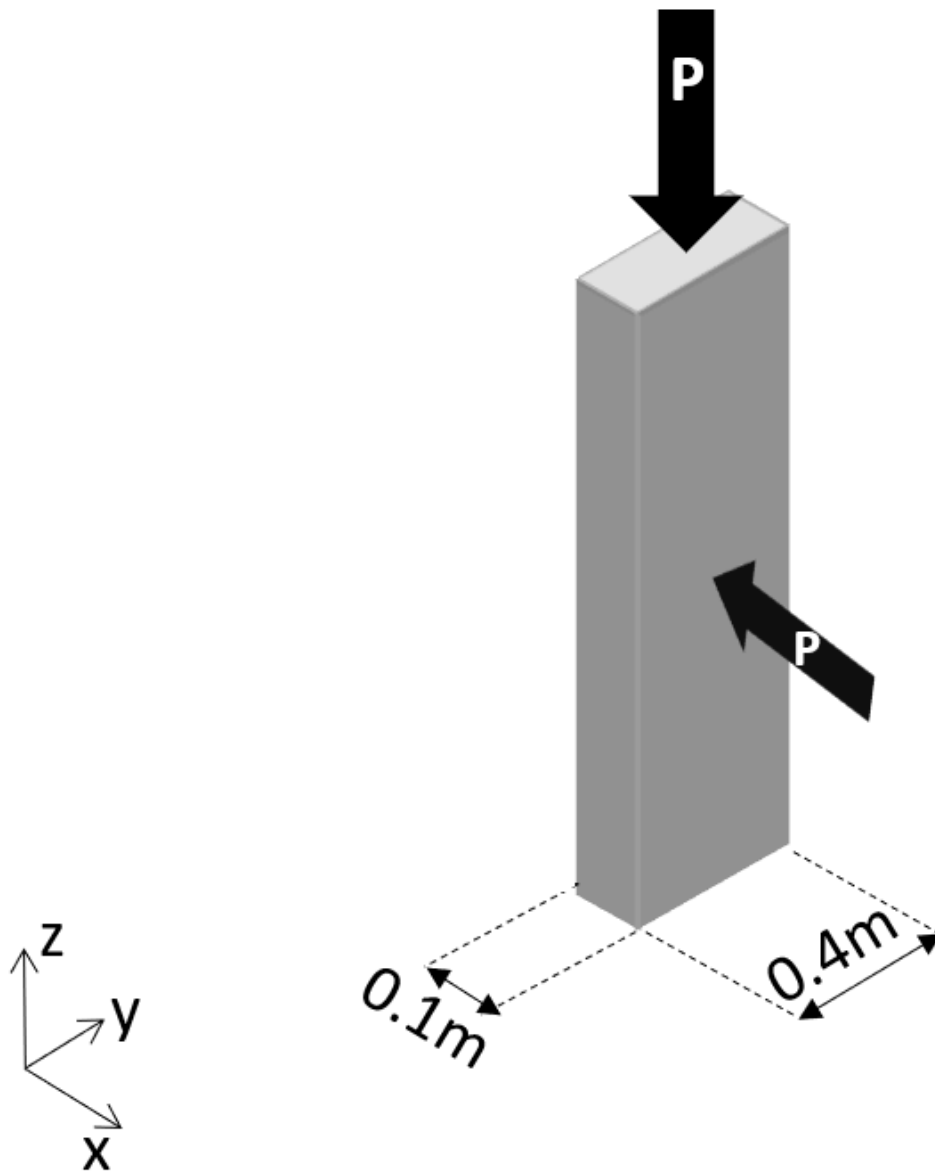


Figure 1: Problem Definition

Modeling

The column is modeled in LARSA 4D as a shell. The shell dimensions are 0.4 x 1.0 m and the thickness is 0.1 m.

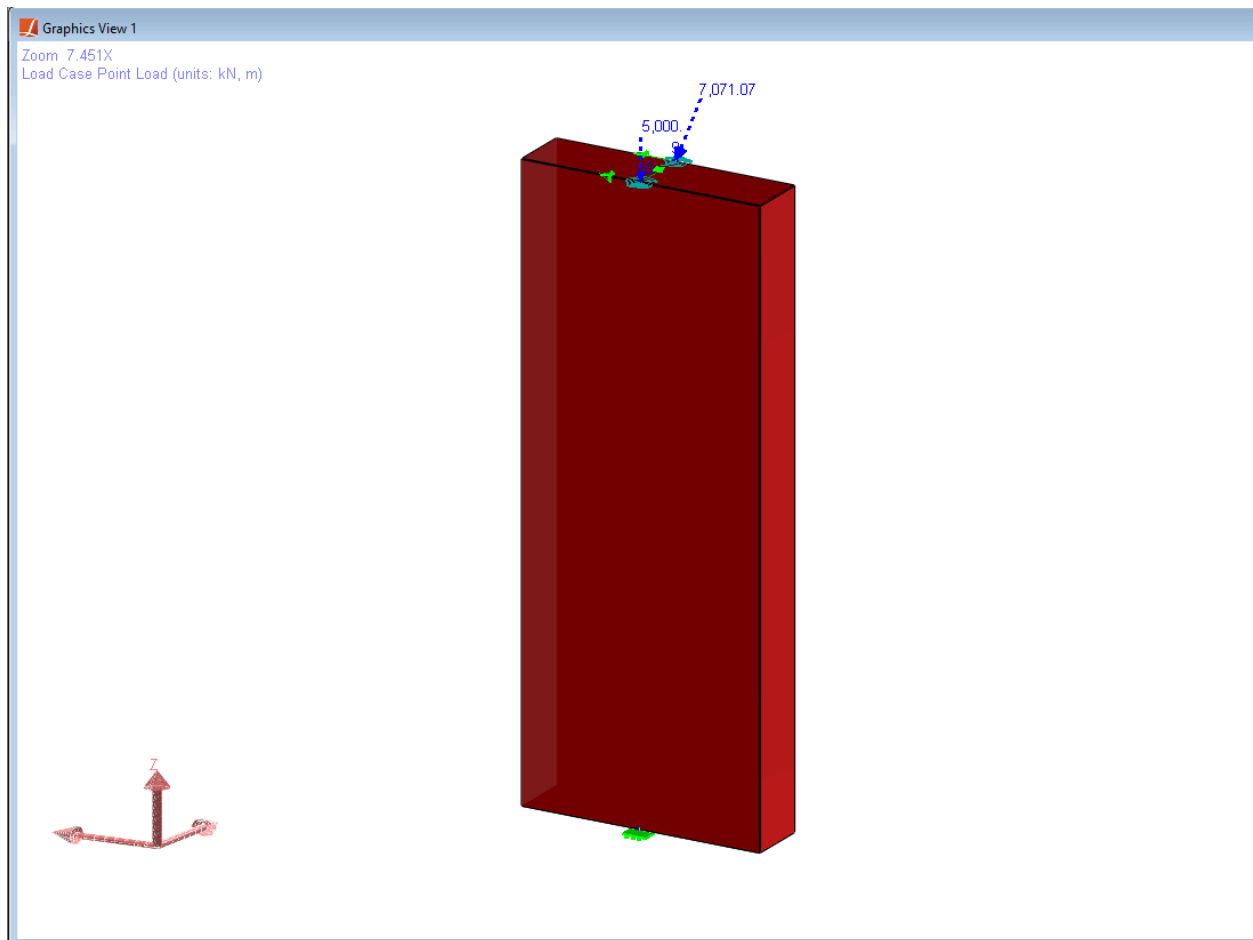


Figure 2: the Model

Joints of the shell can be seen in figure 2 below. Joint 7 is a fixed support. Joint 8 is free in Translation-X, joint 10 is free in Translation-Z and joint 9 is free in the Translation-X and Translation-Z directions. The orientation of the member is along the Z-axis.

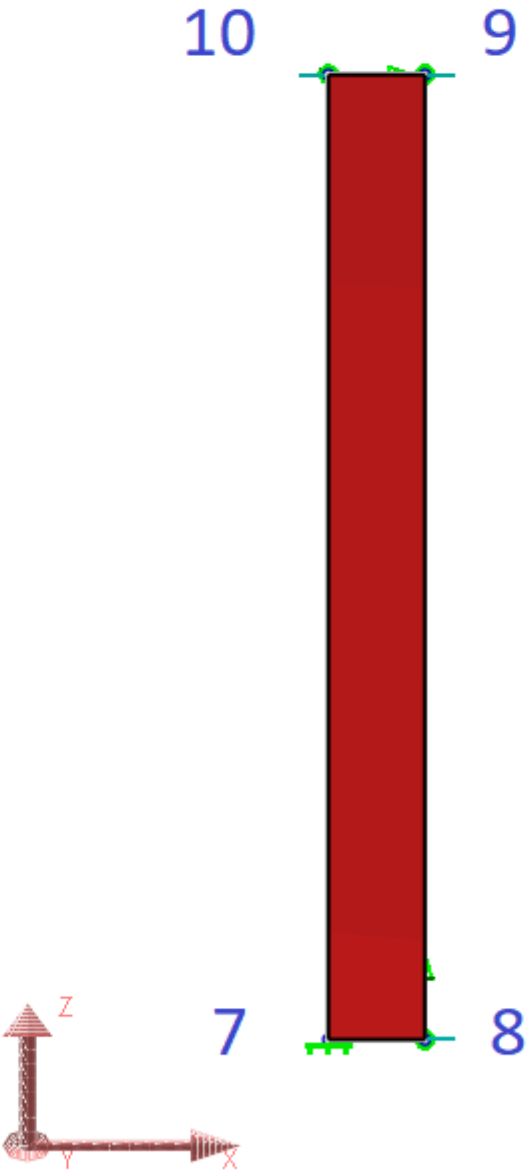


Figure 3: Joints from the Front Plane

The material properties of concrete were entered manually as shown in Figure 4.

	Name	Yield Stress (N/mm ²)	Post-yield to Initial Slope Ratio	Concrete Strength Specimen	Concrete Fck or Steel Fu (N/mm ²)	Concrete Cement Hardening Type	Tendon GUTS (N/mm ²)	Material Time-Effect	Assigned
1	Concrete Rectangular Plate	0.00	0.020	Cylinder	32.00	Normal	0.00	Concrete Time	Yes
2									

Figure 4: Material Properties.

Additional properties for the material under the **More Properties** segment are given in Figure 5.

	Name	Yield Stress (N/mm ²)	Post-yield to Initial Slope Ratio	Concrete Strength Specimen	Concrete Fck or Steel Fu (N/mm ²)	Concrete Cement Hardening Type	Tendon GUTS (N/mm ²)	Material Time-Effect	Assigned
1	Concrete Rectangular Plate	0.00	0.020	Cylinder	32.00	Normal	0.00	Concrete Time	Yes
2									

Figure 5: More Properties

The loadings on the column is divided to joints on both sides. Graphics View shows the resultant of two 5,000 kN point loads applied on the joint 9.

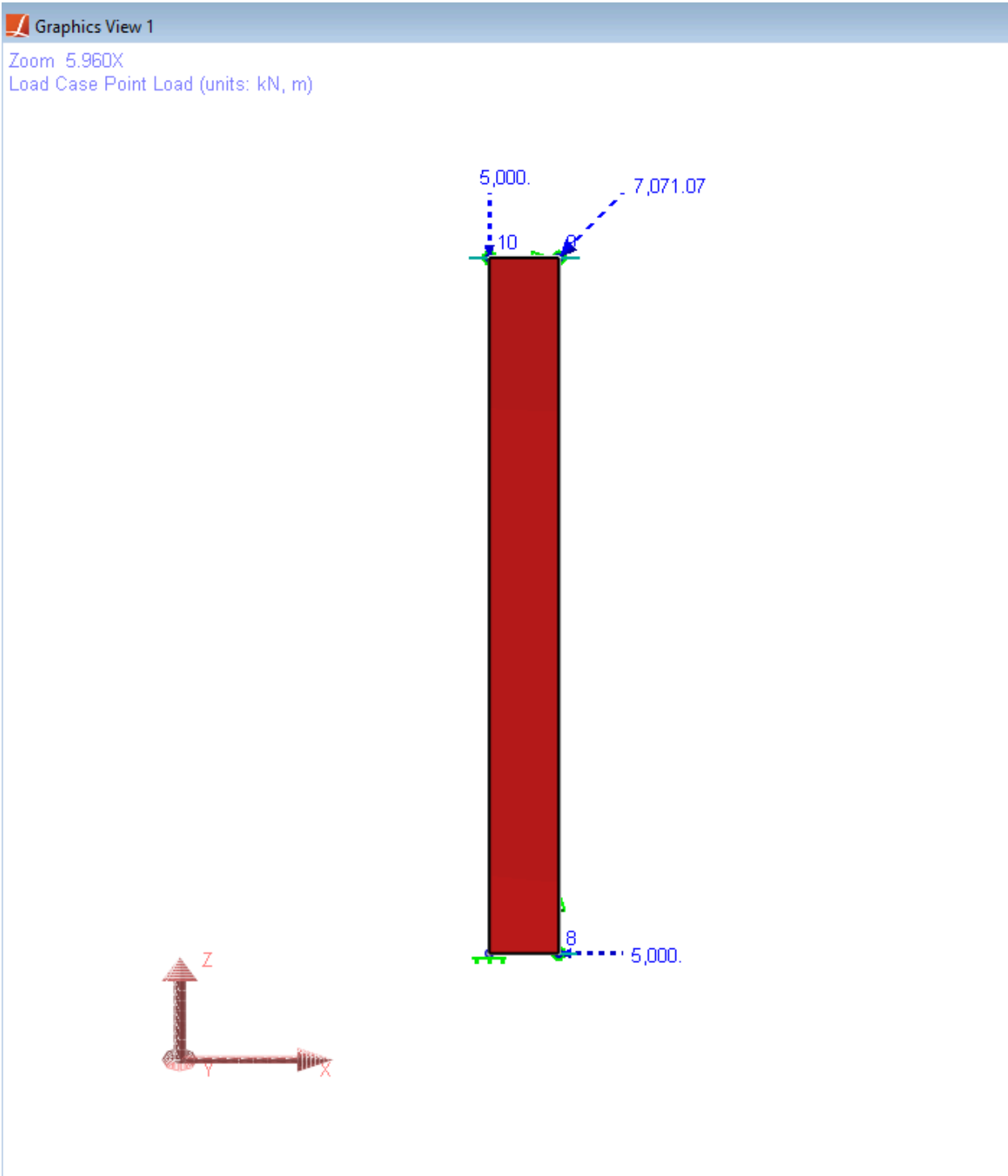


Figure 6: Loading

Construction Sequence

Construction sequence is completely same with the Case A group stated in example S08. The column will be cast in 10th day and constructed at 11th day. They are loaded at age of 16 days of concrete which is the 26th day of the construction. Creep and shrinkage displacements at 110th day will be focused on.

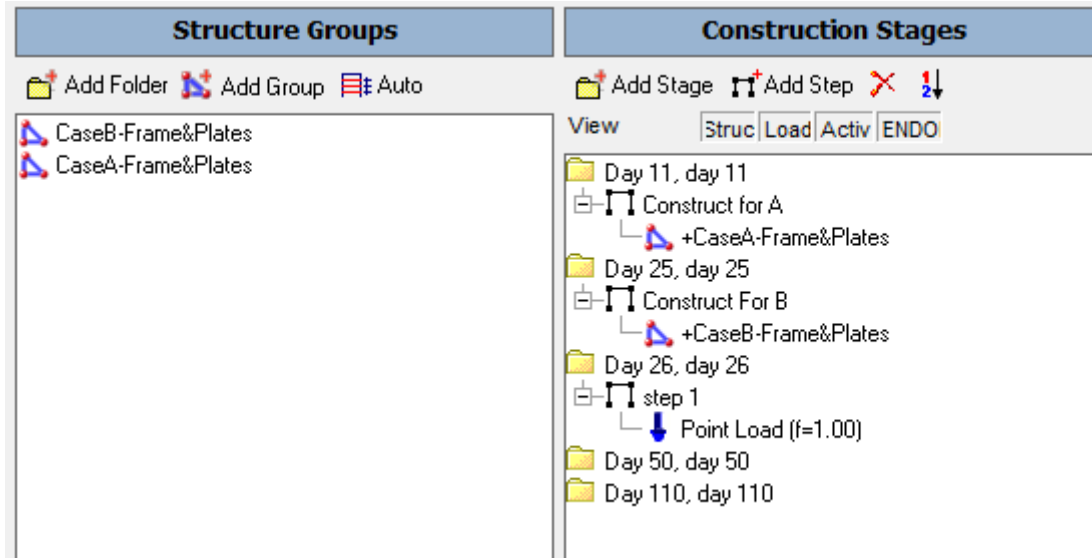


Figure 7: Construction Stages

Verification of Creep

The creep and shrinkage displacements can be observed independently. For example, right clicking on the **Day 110: Creep** in the Analysis Results and selecting the joint displacements will show the cumulative displacements of all the previous stages, plus the creep displacement of the Day 110 stage, as in Figure 6. The locations of the joints 7, 8, 9, 10 can be seen in the Figure 6.

	Joint	Result Case	Translation X (mm)	Translation Y (mm)	Translation Z (mm)	Rotation X (rad)	Rotation Y (rad)	Rotation Z (rad)
1	7	Day 110: Creep	0.0000	0.0000	0.0000	0.0000	0.0000	0.0000
2	8	Day 110: Creep	-0.0144	0.0000	0.0000	0.0000	0.0000	0.0000
3	9	Day 110: Creep	-0.0144	0.0000	-15.5651	0.0000	0.0000	0.0000
4	10	Day 110: Creep	0.0000	0.0000	-15.5651	0.0000	0.0000	0.0000

Figure 6: Joint Displacements

To get the joint displacements due to creep of the Day 110 stage only, select **Extract Creep** from the drop down menu.

	Joint	Result Case	Translation X (mm)	Translation Y (mm)	Translation Z (mm)	Rotation X (rad)	Rotation Y (rad)	Rotation Z (rad)
1	7	Day 110: Creep	0.0000	0.0000	0.0000	0.0000	0.0000	0.0000
2	8	Day 110: Creep	-0.0856	0.0000	0.0000	0.0000	0.0000	0.0000
3	9	Day 110: Creep	-0.0856	0.0000	-8.5634	0.0000	0.0000	0.0000
4	10	Day 110: Creep	0.0000	0.0000	-8.5634	0.0000	0.0000	0.0000

Figure 7: Joint Displacements due to Creep Deformation in 110 days

Hand calculations are performed based on these formulas and the obtained results are compared with the LARSA 4D results.

Parameters

RH = 60 (ambient relative humidity, %)

f_{ck} = 32 (characteristic compressive strength of concrete at the age of 28 days, MPa)

t = 100 (age of concrete in days at the moment considered)

t_0 = 16 (age of concrete at loading, days)

Construction Day = 1 (after casting)

k_4 = 0.6 (environment variable, for AS3600)

$\phi_{cc,b} = 0$ (basic creep coefficient which can be input manually or is calculated automatically if it is set as 0, for AS3600)

$\lambda = 1.5$ (coefficient depending on the ambient environment, for CEB-FIP 78)

Assumptions

In LARSA 4D, **shell** elements are considered as slab elements accordingly the edges in the direction of thickness are not subjected to atmosphere.

$V/S = (\text{width} \times \text{thickness} \times \text{length}) / (2 \times \text{width} \times \text{length}) = \text{thickness} / 2$

$h = 2(V/S) = \text{thickness}$

Notional thickness for shell element is calculated as **400 mm**.

Creep Displacements (Units are in mm)

Code	Hand Calc. X	Displacement X	Error (%)	Hand Calc. Z	Displacement Z	Error (%)
CEB-FIP 78	-0.061	-0.061	0.0	-6.079	-6.087	0.1
CEB-FIP 90	-0.077	-0.077	0.0	-7.722	-7.723	0.0
CEB-FIP 2010	-0.079	-0.079	0.0	-7.904	-7.904	0.0
EN1992/ Eurocode 2004	-0.073	-0.073	0.0	-7.314	-7.314	0.0
AASHTO LRFD v6	-0.072	-0.072	0.0	-7.236	-7.235	0.0
AASHTO LRFD v7/8	-0.074	-0.074	0.0	-7.410	-7.409	0.0
IRC-112 2020	-0.086	-0.086	0.0	-8.625	-8.625	0.0
AS-3600 2009	-0.082	-0.082	0.0	-8.204	-8.204	0.0

LARSA 4D's creep computations match exactly.

Verification of Shrinkage

For the shrinkage displacements of Day 110 stage only, follow the same procedure as before, this time by right clicking **Day 110: Shrinkage** and extracting the results for shrinkage.

LARSA 4D reports only the shrinkage deformations after the construction day and in the exmple construction day (1) is less than the t_s except for AASHTO LRFD v6.

Joint Displacements

Min/Max for: None Incremental Results Report In Local UCS Extract Shrinkage

	Joint	Result Case	Translation X (mm)	Translation Y (mm)	Translation Z (mm)	Rotation X (rad)	Rotation Y (rad)	Rotation Z (rad)
1	7	Day 110: Shrinkage	0.0000	0.0000	0.0000	0.0000	0.0000	0.0000
2	8	Day 110: Shrinkage	-0.0035	0.0000	0.0000	0.0000	0.0000	0.0000
3	9	Day 110: Shrinkage	-0.0035	0.0000	-0.0345	0.0000	0.0000	0.0000
4	10	Day 110: Shrinkage	0.0000	0.0000	-0.0345	0.0000	0.0000	0.0000

Figure 7: Joint Displacements due to Shrinkage Deformation in 110 days

Hand calculations are performed based on these formulas and the obtained results are compared with the LARSA 4D results.

Parameters

$RH = 60$ (ambient relative humidity, %)

$f_{ck} = 32$ (characteristic compressive strength of concrete at the age of 28 days, MPa)

$t = 100$ (age of concrete in days at the moment considered)

Construction Day = 1 (after casting)

$k_4 = 0.6$ (environment variable - for AS3600)

$\epsilon_{csd,b}^* = 0.0008$ (drying basic shrinkage strain - for AS3600)

Assumptions

Age of concrete at the beginning of shrinkage or swelling, t_s (days) is

$t_s = 3$ days for CEB-FIP 90 and CEB-FIP 2010

$t_s = 14$ days for EN1992/Eurocode 2004

$t_s = 0$ day for AASHTO LRFD v6

Any t_s value greater than 0 can be used by defining the input parameters required for CEB-FIP 78 code.

The assumption for notional thickness calculation discussed in creep section is also valid for the shrinkage calculations.

In LARSA 4D, shrinkage occurs during the time interval between the construction day and time of the moment considered. Shrinkage induced displacement before the construction day, accordingly, is ignored.

Shrinkage Displacements (Units are in mm)

Code	Hand Calc. X	Displacement X	Error (%)	Hand Calc. Z	Displacement Z	Error (%)
CEB-FIP 78	-0.0035	-0.0035	0.0	-0.0354	-0.0354	0.0
CEB-FIP 90	-0.0065	-0.0065	0.0	-0.0650	-0.0650	0.0
CEB-FIP 2010	-0.0113	-0.0113	0.0	-0.1130	-0.1130	0.0
EN1992/ Eurocode 2004	-0.0102	-0.0102	0.0	-0.1020	-0.1020	0.0
AASHTO LRFD v6	-0.0392	-0.0392	0.0	-0.3920	-0.3920	0.0
AASHTO LRFD v7/8	-0.0396	-0.0396	0.0	-0.3956	-0.3955	0.0
IRC-112 2020	-0.0102	-0.0102	0.0	-0.1022	-0.1022	0.0
AS-3600 2009	-0.0173	-0.0173	0.0	-0.1731	-0.1731	0.0

LARSA 4D's shrinkage computations match exactly with the hand calculations for both directions.

S08c: Time-Dependent Material Properties Effects

This sample problem verifies concrete cement hardening type and temperature adjusted time in creep strain calculations a wide column modeled using beam and shell elements with dimensions $1.0 \times 1.2 \text{ m} \times 0.4 \text{ m}$ under vertical loading.

Example Project: The example described here can be found in the Staged Construction folder of your LARSA 4D Samples directory (generally My Documents\LARSA Projects\Samples) in the file S08c.

Problem Definition

Determine the creep vertical displacements of the wide column, which is described in S08, due to creep with adjusted time for various cement hardening types and compare the values obtained in CEB-FIP 78, CEB-FIP 90, CEB-FIP 2010, EN1992/Eurocode 2004 and IRC-112 2020 codes (temperature adjusted time option for CEB-FIP 78 code is not available).

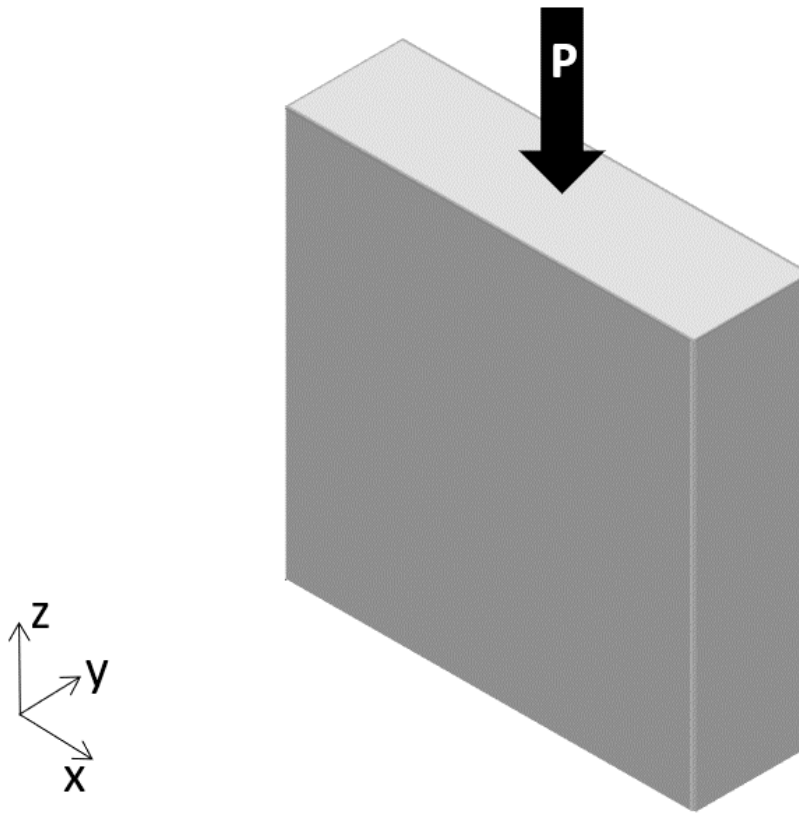


Figure 1: Problem Definition

Modeling

The same modeling approach and construction sequence described in S08 are used except altering the concrete cement hardening type under the **More Properties** segment (Figure 2) and activating temperature adjusted time shown in **Time-Dependent Material Properties** sheet (Figure 3).

	Name	Yield Stress (N/mm ²)	Post-yield to Initial Slope Ratio	Concrete Strength Specimen	Concrete Fck or Steel Fu (N/mm ²)	Concrete Cement Hardening Type	Tendon GUTS (N/mm ²)	Material Time-Effect	Assigned
1	Concrete	0.00	0.020	Cylinder	32.00	Normal	0.00	Concrete Time	Yes
2									

Figure 2: Concrete Cement Hardening Type.

	Name	Creep Factor	Shrinkage Factor	Relaxation Factor	Exponent of Creep Development Eqn.	Constant in Shrinkage Development Eqn.	Temp. Adjusted Concrete Age
1	Concrete Time	1.0000	1.0000	1.0000	0.3000	350.0000	Yes
2							

Figure 3: Temperature Adjusted Time

Finally, ambient temperature is set 35°C for each step in order to examine the temperature adjustment effect clearly (Figure 3).

	Name	Construction Day	Temperature (*C)	Humidity (%)
1	Day 11	11	35.0000	60.0000
2	Day 25	25	35.0000	60.0000
3	Day 26	26	35.0000	60.0000
4	Day 50	50	35.0000	60.0000
5	Day 110	110	35.0000	60.0000
6				

Figure 3: Ambient Temperature of Stages

Verification of Creep

Hand calculations are performed based on these formulas given in S08 and the obtained results for the frame elements are compared with the LARSA 4D results.

Both cases (Case A and Case B) gives the same results for the creep calculation since they are loaded at the same age which is later than the construction of both groups.

Creep Displacements without temperature adjusted time (Units are in mm)

Code	Hardening Type	Hand Calc.	LARSA 4D	Error (%)
CEB-FIP 78	Slow	-0.555	-0.555	0.0

Code	Hardening Type	Hand Calc.	LARSA 4D	Error (%)
CEB-FIP 78	Normal	-0.555	-0.555	0.0
CEB-FIP 78	Rapid	-0.647	-0.647	0.0
CEB-FIP 78	Rapid High Str.	-0.695	-0.695	0.1
CEB-FIP 90	Slow	-0.747	-0.747	0.0
CEB-FIP 90	Normal	-0.702	-0.702	0.0
CEB-FIP 90	Rapid	-0.702	-0.702	0.0
CEB-FIP 90	Rapid High Str.	-0.658	-0.658	0.0
CEB-FIP 2010	Slow	-0.750	-0.750	0.0
CEB-FIP 2010	Normal	-0.691	-0.691	0.0
CEB-FIP 2010	Rapid	-0.633	-0.633	0.0
CEB-FIP 2010	Rapid High Str.	-0.633	-0.633	0.0
EN1992/Eurocode 2004	Slow	-0.698	-0.698	0.0
EN1992/Eurocode 2004	Normal	-0.664	-0.664	0.0
EN1992/Eurocode 2004	Rapid	-0.632	-0.632	0.0
EN1992/Eurocode 2004	Rapid High Str.	-0.632	-0.632	0.0
IRC-112 2020	Slow	-0.824	-0.824	0.0
IRC-112 2020	Normal	-0.784	-0.784	0.0
IRC-112 2020	Rapid	-0.746	-0.746	0.0
IRC-112 2020	Rapid High Str.	-0.746	-0.746	0.0

Creep Displacements with temperature adjusted time (Units are in mm)

Code	Hardening Type	Hand Calc.	LARSA 4D	Error (%)
CEB-FIP 90	Slow	-0.611	-0.611	0.0
CEB-FIP 90	Normal	-0.587	-0.587	0.0

Code	Hardening Type	Hand Calc.	LARSA 4D	Error (%)
CEB-FIP 90	Rapid	-0.587	-0.587	0.0
CEB-FIP 90	Rapid High Str.	-0.562	-0.562	0.0
CEB-FIP 2010	Slow	-0.576	-0.576	0.0
CEB-FIP 2010	Normal	-0.549	-0.549	0.0
CEB-FIP 2010	Rapid	-0.522	-0.522	0.0
CEB-FIP 2010	Rapid High Str.	-0.522	-0.522	0.0
EN1992/Eurocode 2004	Slow	-0.601	-0.601	0.0
EN1992/Eurocode 2004	Normal	-0.586	-0.586	0.0
EN1992/Eurocode 2004	Rapid	-0.571	-0.571	0.0
EN1992/Eurocode 2004	Rapid High Str.	-0.571	-0.571	0.0
IRC-112 2020	Slow	-0.709	-0.709	0.0
IRC-112 2020	Normal	-0.692	-0.692	0.0
IRC-112 2020	Rapid	-0.674	-0.674	0.0
IRC-112 2020	Rapid High Str.	-0.674	-0.674	0.0

LARSA 4D's creep computations match exactly with hand calculations.

S08d: Time-Dependent Material Properties Effects

This sample problem verifies time dependent elastic modulus calculations a wide column modeled using frame elements with dimensions $1.0 \times 1.2 \text{ m} \times 0.4 \text{ m}$ under vertical loading.

Example Project: The example described here can be found in the Staged Construction folder of your LARSA 4D Samples directory (generally My Documents\LARSA Projects\Samples) in the file S08d.

Problem Definition

Determine the vertical displacements of the wide column with time dependent modulus at several concrete ages and compare the values obtained in CEB-FIP 78, CEB-FIP 90, CEB-FIP 2010, EN1992/Eurocode 2004 and IRC-112 2020 codes.

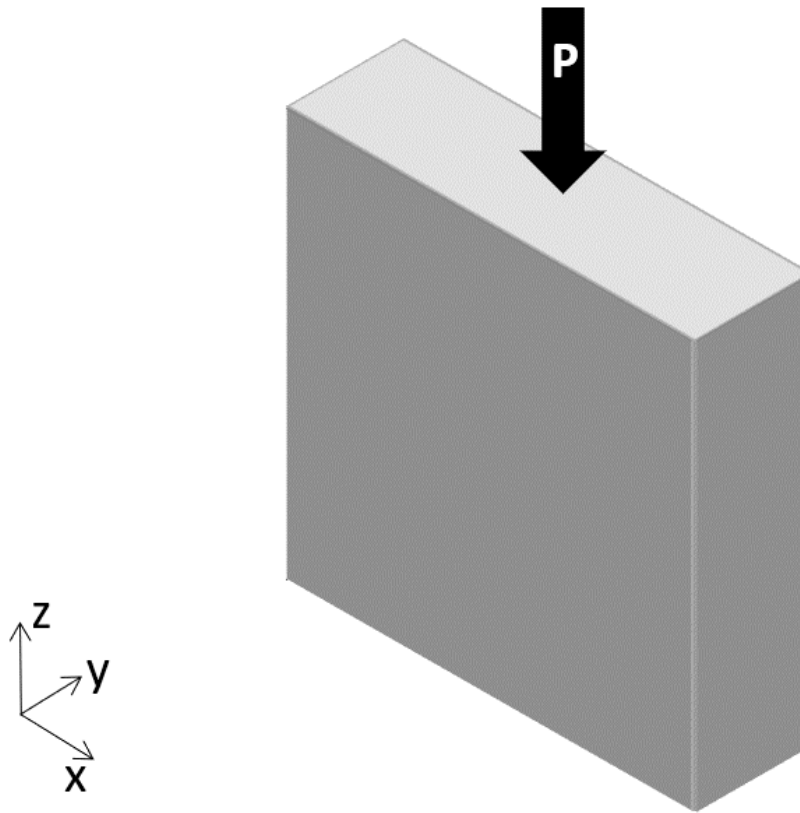


Figure 1: Problem Definition

Modeling

The same modeling approach described in S08c is used but this time, time dependent modulus is turned on and creep is off in **Analysis** → **Time Dependent Analysis Options** (Figure 2). When the **Use Legacy Elastic Modulus Curve** option is activated, LARSA 4D will use the built in curve given in Time Effect on Modulus of Elasticity section (Unless user defined curve is entered). If it is unchecked and no user-defined curve is entered, time dependent modulus curve of the selected design code will be used (for CEB-FIP 78, CEB-FIP90, CEB-FIP2010, EN1992/EuroCode 2004, and IRC-112 2020). For the other design codes, the built-in curve is taken even if **Legacy Elastic Modulus** is unchecked.

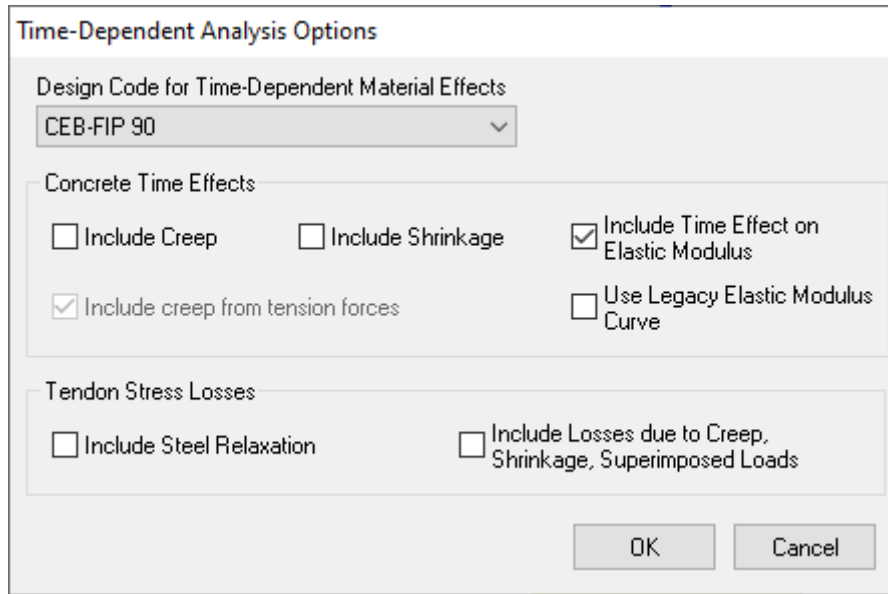


Figure 2: Time Dependent Analysis Options.

Construction Sequence

The same construction sequence with the previous example is acted and one more stage (Day 10,000) is added. The load that has been already applied at Day 26 is applied at Day 110 and Day 10,000 once more.

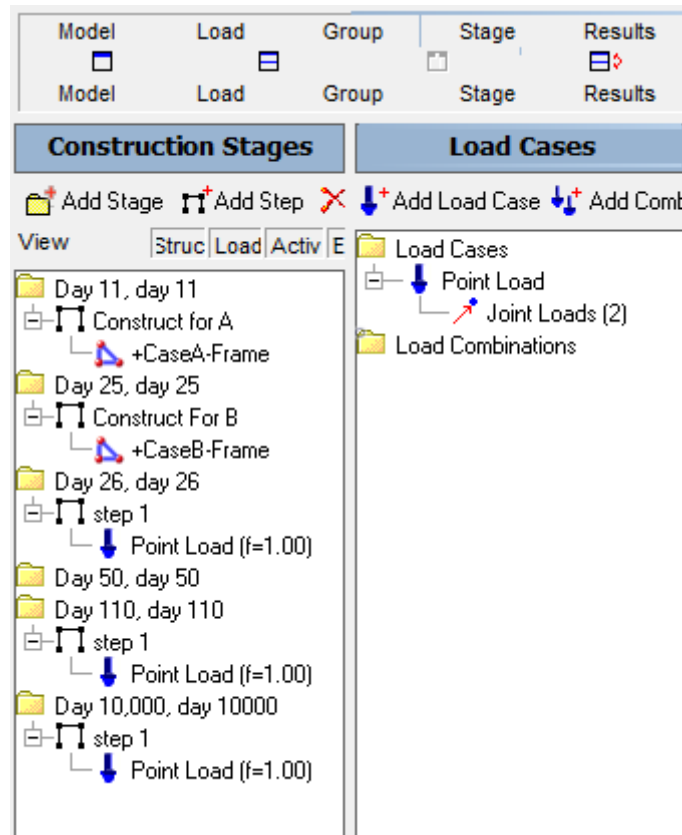


Figure 2: Construction Sequence.

Verification of Elastic Modulus

Time dependent modulus formulas provided by each design code are given below. Hand calculations are performed based on these formulas and the obtained results for the frame elements are compared with the LARSA 4D results. Comparisons for the cases in which temperature adjusted time is on and off are provided separately for the codes except CEB-FIP 78 (Temperature adjusted time option is not available for the CEB-FIP 78 code). Axial displacements at particular ages are calculated from the modulus at that time obtained from LARSA 4D by utilizing the following formula.

$$U_2 = P \times L / (E(t) \times A)$$

where,

P is axial load applied

L is length of the column

A is cross-section area

E(t) is modulus at time t.

U_2 is incremental axial displacement

Elastic Modulus

CEB-FIP 78

$$E_c(t) = 1.25 \times E_{cm}$$

$$E_{cm} = 9.5 \times (f_{cm}(t))^{1/3}$$

$f_{cm}(t)$ is strength of the concrete at time t .

CEB-FIP 90

$$E_{ci}(t) = \beta_E(t) \times E_{ci}$$

$$\beta_E(t) = (\beta_{cc}(t))^{0.5}$$

$$\beta_{cc}(t) = \exp[s \times (1 - (28/t)^{0.5})]$$

s is a coefficient which depends on the type of cement (0.38 for slowly hardening cements SL, 0.25 for normal or rapid hardening cements N and R, and 0.20 for rapid hardening high strength cements RS)

E_{ci} is the modulus of elasticity at an age 28 days

CEB-FIP 2010

$$E_{ci}(t) = \beta_E(t) \times E_{ci}$$

$$\beta_E(t) = (\beta_{cc}(t))^{0.5}$$

$$\beta_{cc}(t) = \exp[s \times (1 - (28/t)^{0.5})]$$

s is a coefficient which depends on the type of cement (0.38 for slowly hardening cements SL (32.5N), 0.25 for normal hardening cements N (32.5R, 42.5N), 0.20 for rapid and rapid hardening high strength cements R and RS (42.5R, 52.5N, 52.5R), and 0.20 for $f_{cm} > 60\text{MPa}$)

E_{ci} is the modulus of elasticity at an age 28 days

EN1992/EuroCode 2004 and IRC-112 2020

$$E_{ci}(t) = (f_{cm}(t)/f_{cm})^{0.3} \times E_{ci}$$

$$f_{cm}(t) = \beta_{cc}(t) \times f_{cm}$$

$$\beta_{cc}(t) = \exp[s \times (1 - (28/t)^{0.5})]$$

s is a coefficient which depends on the type of cement (0.38 for slowly hardening cements SL (32.5N), 0.25 for normal hardening cements N (32.5R, 42.5N), and 0.20 for rapid and rapid hardening high strength cements R and RS (42.5R, 52.5N, 52.5R))

f_{cm} is mean compressive strength at age 28 days.

E_{ci} is the modulus of elasticity at an age 28 days

For the comparison, axial displacements (U_z) at the concrete age of 16th (Day 26), 100th (Day 110), and 9,990th (Day 10,000) when the columns are loaded are selected.

Both cases (Case A and Case B) gives the same results since they are loaded at the same age which is later than the construction of both groups.

Incremental axial displacements without temperature adjusted time (Units are in mm)

LARSA 4D Sample and Verification Problems

Code	Hardening Type	Hand Calc. (U_{z,26})	LARSA 4D (U_{z,26})	Hand Calc. (U_{z,110})	LARSA 4D (U_{z,110})	Hand Calc. (E_{z, 10,000})	LARSA 4D (U_{z, 10,000})
Legacy	-	-0.626	-0.626 (0%)	-0.595	-0.595 (0%)	-0.595	-0.595 (0%)
CEB-FIP 78	Slow	-0.627	-0.627 (0%)	-0.549	-0.549 (0%)	-0.521	-0.521 (0%)
CEB-FIP 78	Normal	-0.627	-0.627 (0%)	-0.549	-0.549 (0%)	-0.521	-0.521 (0%)
CEB-FIP 78	Rapid	-0.589	-0.589 (0%)	-0.536	-0.536 (0%)	-0.521	-0.521 (0%)
CEB-FIP 78	Rapid High Str.	-0.571	-0.571 (0%)	-0.531	-0.531 (0%)	-0.521	-0.521 (0%)
CEB-FIP 90	Slow	-0.633	-0.633 (0%)	-0.544	-0.544 (0%)	-0.497	-0.497 (0%)
CEB-FIP 90	Normal	-0.620	-0.620 (0%)	-0.561	-0.561 (0%)	-0.529	-0.529 (0%)
CEB-FIP 90	Rapid	-0.620	-0.620 (0%)	-0.561	-0.561 (0%)	-0.529	-0.529 (0%)
CEB-FIP 90	Rapid High Str.	-0.615	-0.615 (0%)	-0.568	-0.568 (0%)	-0.541	-0.541 (0%)
CEB-FIP 2010	Slow	-0.633	0.633 (0%)	-0.544	-0.544 (0%)	-0.497	-0.497 (0%)
CEB-FIP 2010	Normal	-0.620	0.620 (0%)	-0.561	-0.561 (0%)	-0.529	-0.529 (0%)
CEB-FIP 2010	Rapid	-0.615	0.615 (0%)	-0.568	-0.568 (0%)	-0.541	-0.541 (0%)
CEB-FIP 2010	Rapid High Str.	-0.615	0.615 (0%)	-0.568	-0.568 (0%)	-0.541	-0.541 (0%)
EN1992/ Eurocode 2004	Slow	-0.618	-0.618 (0%)	-0.564	-0.564 (0%)	-0.534	-0.534 (0%)
EN1992/ Eurocode 2004	Normal	-0.610	-0.610 (0%)	-0.575	-0.575 (0%)	-0.554	-0.554 (0%)

Code	Hardening Type	Hand Calc. (U _{z,26})	LARSA 4D (U _{z,26})	Hand Calc. (U _{z,110})	LARSA 4D (U _{z,110})	Hand Calc. (E _{z, 10,000})	LARSA 4D (U _{z, 10,000})
EN1992/ Eurocode 2004	Rapid	-0.607	-0.607 (0%)	-0.579	-0.579 (0%)	-0.562	-0.562 (0%)
EN1992/ Eurocode 2004	Rapid High Str.	-0.607	-0.607 (0%)	-0.579	-0.579 (0%)	-0.562	-0.562 (0%)
IRC-112 2020	Slow	-0.618	-0.618 (0%)	-0.564	-0.564 (0%)	-0.534	-0.534 (0%)
IRC-112 2020	Normal	-0.610	-0.610 (0%)	-0.575	-0.575 (0%)	-0.554	-0.554 (0%)
IRC-112 2020	Rapid	-0.607	-0.607 (0%)	-0.579	-0.579 (0%)	-0.562	-0.562 (0%)
IRC-112 2020	Rapid High Str.	-0.607	-0.607 (0%)	-0.579	-0.579 (0%)	-0.562	-0.562 (0%)

Incremental axial displacements with temperature adjusted time (Units are in mm)

Code	Hardening Type	Hand Calc. (U _{z,26})	LARSA 4D (U _{z,26})	Hand Calc. (U _{z,110})	LARSA 4D (U _{z,110})	Hand Calc. (E _{z, 10,000})	LARSA 4D (U _{z, 10,000})
CEB-FIP 90	Slow	-0.590	-0.590 (0%)	-0.529	-0.529 (0%)	-0.496	-0.496 (0%)
CEB-FIP 90	Normal	-0.592	-0.592 (0%)	-0.551	-0.551 (0%)	-0.528	-0.528 (0%)
CEB-FIP 90	Rapid	-0.592	-0.592 (0%)	-0.551	-0.551 (0%)	-0.528	-0.528 (0%)
CEB-FIP 90	Rapid High Str.	-0.592	-0.592 (0%)	-0.559	-0.559 (0%)	-0.541	-0.541 (0%)
CEB-FIP 2010	Slow	-0.590	-0.590 (0%)	-0.529	-0.529 (0%)	-0.496	-0.496 (0%)
CEB-FIP 2010	Normal	-0.592	-0.592 (0%)	-0.551	-0.551 (0%)	-0.528	-0.528 (0%)
CEB-FIP 2010	Rapid	-0.592	-0.592 (0%)	-0.559	-0.559 (0%)	-0.541	-0.541 (0%)
CEB-FIP 2010	Rapid High Str.	-0.592	-0.592 (0%)	-0.559	-0.559 (0%)	-0.541	-0.541 (0%)

Code	Hardening Type	Hand Calc. (U_{z,26})	LARSA 4D (U_{z,26})	Hand Calc. (U_{z,110})	LARSA 4D (U_{z,110})	Hand Calc. (E_{z, 10,000})	LARSA 4D (U_{z, 10,000})
EN1992/ Eurocode 2004	Slow	-0.592	-0.592 (0%)	-0.555	-0.555 (0%)	-0.533	-0.533 (0%)
EN1992/ Eurocode 2004	Normal	-0.593	-0.593 (0%)	-0.568	-0.568 (0%)	-0.554	-0.554 (0%)
EN1992/ Eurocode 2004	Rapid	-0.593	-0.593 (0%)	-0.573	-0.573 (0%)	-0.562	-0.562 (0%)
EN1992/ Eurocode 2004	Rapid High Str.	-0.593	-0.593 (0%)	-0.573	-0.573 (0%)	-0.562	-0.562 (0%)
IRC-112 2020	Slow	-0.592	-0.592 (0%)	-0.555	-0.555 (0%)	-0.533	-0.533 (0%)
IRC-112 2020	Normal	-0.593	-0.593 (0%)	-0.568	-0.568 (0%)	-0.554	-0.554 (0%)
IRC-112 2020	Rapid	-0.593	-0.593 (0%)	-0.573	-0.573 (0%)	-0.562	-0.562 (0%)
IRC-112 2020	Rapid High Str.	-0.593	-0.593 (0%)	-0.573	-0.573 (0%)	-0.562	-0.562 (0%)

LARSA 4D's displacements due to time dependent elastic modulus computations match exactly with hand calculations.

S09: Shells with Time-Dependent Material Effects

This sample problem verifies time dependent elastic modulus change, creep and shrinkage strain calculations a wide column discussed in S08 sample modeled using quadrilateral and triangular shell elements under vertical loading.

Example Project: The example described here can be found in the Staged Construction folder of your LARSA 4D Samples directory (generally My Documents\LARSA Projects\Samples) in the file S09_CEBFIP90_CreepShrinkage_AxialForce.

Problem Definition

A very wide column is subjected to a point load in the gravitational direction. Determine the vertical displacements due to creep and shrinkage separately, and compare the values obtained in CEB-FIP 90 code.

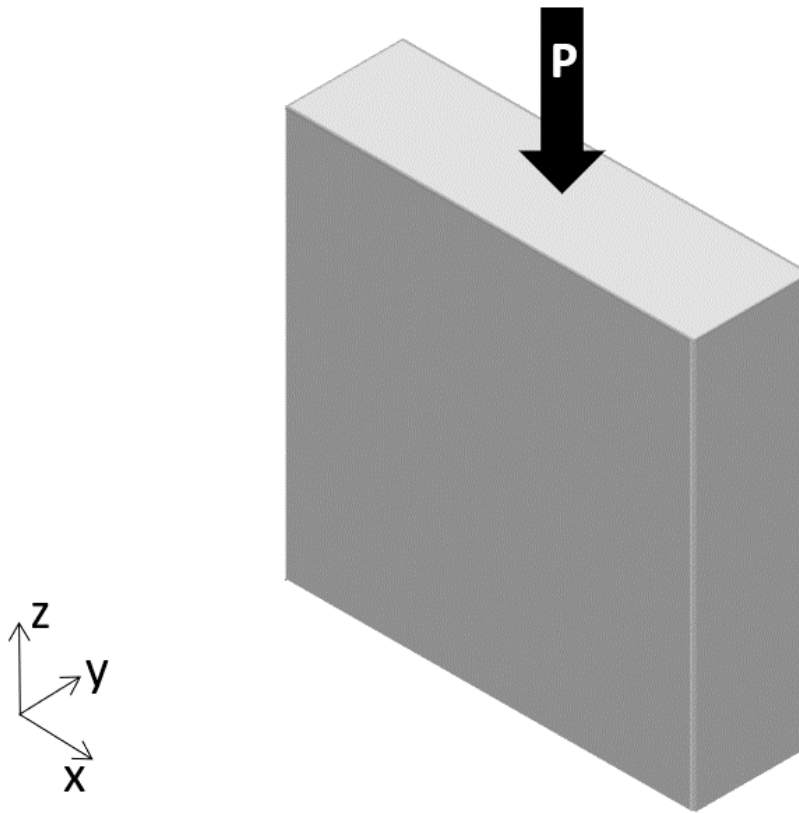


Figure 1: Problem Definition

Modeling

In LARSA 4D, the same object is created in two different ways, by using quadrilateral and triangular shell elements for modeling. The column is subjected to uniform compression load so the point load, P (10,000 kN in magnitude), is distributed to each top node based on the corresponding tributary areas.

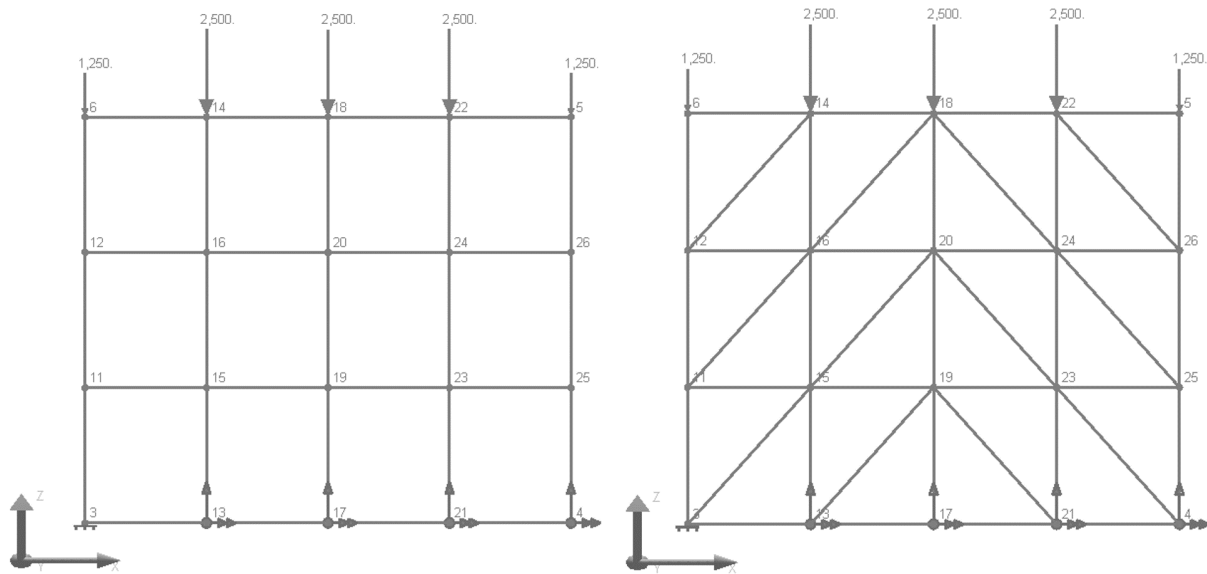


Figure 2: Problem Definition: the Quad Mesh (left) and the Triangle Mesh (right).

The models are supported by a fixed support at the bottom left end (Joint 3) as can be seen in Figure 2. Translation of Joints 4, 13, 17, and 21, on the other hand, is left free in the direction of x . Additionally, to provide stiffness for the out of plane direction, bottom nodes are restrained the rotation about direction of x .

Material properties of concrete such as Modulus of Elasticity (E), Poisson Ratio, Shear Modulus (G), F_{ck} , Concrete Cement Hardening Type and Material Time-Effect are same with the CEB-FIP90 case of the previous example. In addition, time dependent elastic modulus curve is defined (Figure 3).

Time VS Modulus of Elasticity: Concrete Time		
Coefficients		Graph
	Age (Days)	Modulus of Elasticity (N/mm ²)
1	1.0000	35,000.0000
2	25.0000	35,000.0000
3	26.0000	45,000.0000
4	150.0000	45,000.0000
5		

Figure 3: Time vs Elastic Modulus.

The same construction sequence with the previous example is acted and one more stage (Day 111) is added in which the axial force is acted one more time.

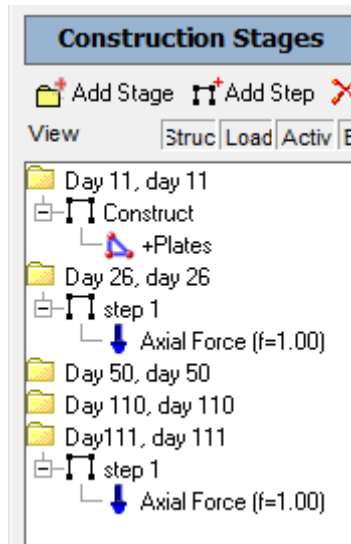


Figure 4: Construction Sequence

Verification of Creep

The creep and shrinkage displacements can be observed independently. For example, right clicking on the **Day 110: Creep** in the Analysis Results and selecting the joint displacements will show the cumulative displacements of all the previous stages, plus the creep displacement of the Day 110 stage.

Creep Displacements (Units are in mm)

Output Parameter	Hand Calc.	LARSA 4D Quad-Bilinear	LARSA 4D Quad-Incomp.	LARSA 4D Quad-Drilling	LARSA 4D Quad-MITC4	LARSA 4D Triangle-Bilinear
Average of Jt. 5,6,14,18,22	-0.644	-0.644 (0%)	-0.644 (0%)	-0.644 (0%)	-0.644 (0%)	-0.644 (0%)

LARSA 4D's creep computations match exactly with hand calculations.

Verification of Shrinkage

For the shrinkage displacements of Day 110 stage only, follow the same procedure as before, this time by right clicking **Day 110: Shrinkage** and extracting the results for shrinkage.

Shrinkage Displacements (Units are in mm)

Output Parameter	Hand Calc.	LARSA 4D Quad-Bilinear	LARSA 4D Quad-Incomp.	LARSA 4D Quad-Drilling	LARSA 4D Quad-MITC4	LARSA 4D Triangle-Bilinear
Average of Jt. 5,6,14,18,22	-0.065	-0.065 (0%)	-0.065 (0%)	-0.065 (0%)	-0.065 (0%)	-0.065 (0%)

LARSA's shrinkage computations match exactly with the hand calculations.

Verification of Elastic Modulus Change

For the elastic modulus change verification, incremental displacement ratio at Day 26 and Day 111 stages ($U_{z_{26}} / U_{z_{111}}$) are inversely proportional with the ratio of elastic modulus at corresponding stages (E_{111} / E_{26}), this time by right clicking **Day 111: Step 1** and checking the Incremental Results.

Vertical Displacement Ratios ($U_{z@Day 26} / U_{z@Day 111}$) (Units are in mm)

Output Parameter	Elastic Modulus Ratio (E_{111} / E_{26})	LARSA 4D Quad-Bilinear	LARSA 4D Quad-Incomp.	LARSA 4D Quad-Drilling	LARSA 4D Quad-MITC4	LARSA 4D Triangle-Bilinear
Average of Jt. 5,6,14,18,22	1.29	1.29 (0%)	1.29 (0%)	1.29 (0%)	1.29 (0%)	1.29 (0%)

S09b: Shells with Time-Dependent Material Effects (Orthotropic Material)

This sample problem verifies time dependent elastic modulus change, creep and shrinkage strain calculations a wide column discussed in S08 sample modeled using quadrilateral and triangular shell elements with orthotropic materials under vertical loading.

Example Project: The example described here can be found in the Staged Construction folder of your LARSA 4D Samples directory (generally My Documents\LARSA Projects\Samples) in the file S09b_CEBFIP90_CreepShrinkageVarE_AxialForce.

Problem Definition

A very wide column is subjected to a point load in the gravitational direction. Determine the vertical displacements due to varying elastic modulus, creep and shrinkage separately, and compare the values obtained in CEB-FIP 90 code.

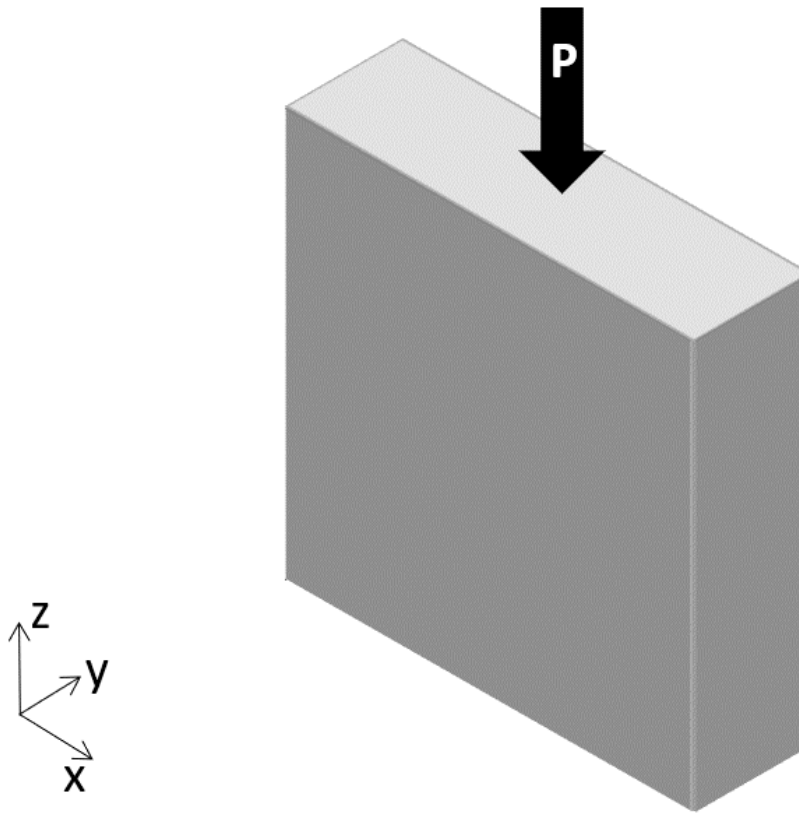


Figure 1: Problem Definition

Modeling

The models used for S09 are regenerated by assigning orthotropic material with the same isotropic material properties. The column is subjected to uniform compression load so the point load, P (10,000 kN in magnitude), is distributed to each top node based on the corresponding tributary areas.

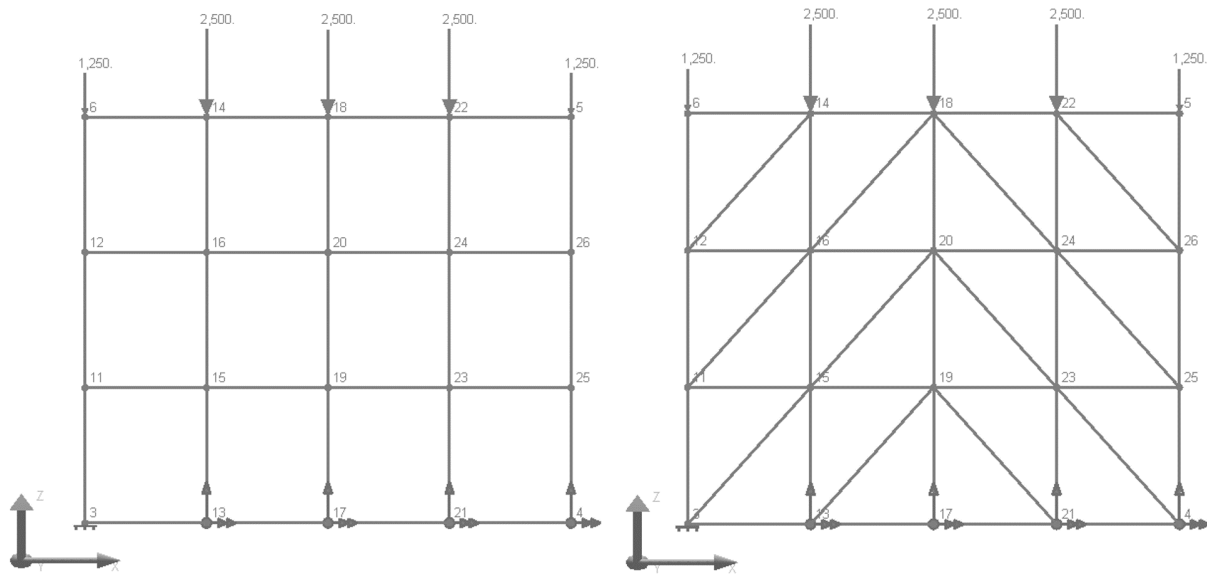


Figure 2: Problem Definition: the Quad Mesh (left) and the Triangle Mesh (right).

Material properties of concrete (also Material Time Effects) are completely the same with the previous example. But this time, those properties are assigned to an orthotropic material.

Properties: Orthotropic Material Properties

Materials / Sections / UCS / Spring Properties / Isolator Definitions / Material Time Effects / Temperature Curve

Basic Properties / More Properties / Orthotropic Properties

	Name	Anisotropy	Material UCS	Modulus of Elasticity E11	Modulus of Elasticity E22	Poisson's Ratio m12	Shear Modulus G12	Shear Modulus G13	Shear Modulus G23	Assigned
1	Concrete ORT	Orthotropic	(NONE)	35,000.0000	35,000.0000	0.2000	14,583.3333	14,583.3333	14,583.3333	Yes
2										

Figure 3: Orthotropic Material Properties

The models are supported by a fixed support at the bottom left end (Joint 3) as can be seen in Figure 2. Translation of Joints 4, 13, 17, and 21, on the other hand, is left free in the direction of X. Additionally, to provide stiffness for the out of plane direction, bottom nodes are restrained the rotation about direction of X.

Verification of Creep

The creep and shrinkage displacements can be observed independently. For example, right clicking on the **Day 110: Creep** in the Analysis Results and selecting the joint displacements will show the cumulative displacements of all the previous stages, plus the creep displacement of the Day 110 stage.

Creep Displacements (Units are in mm)

Output Parameter	Hand Calc.	LARSA 4D Quad-Bilinear	LARSA 4D Quad-Incomp.	LARSA 4D Quad-Drilling	LARSA 4D Triangle-Bilinear
Average of Jt. 5,6,14,18,22	-0.644	-0.644 (0%)	-0.644 (0%)	-0.644 (0%)	-0.644 (0%)

LARSA 4D's creep computations match exactly with hand calculations.

Verification of Shrinkage

For the shrinkage displacements of Day 110 stage only, follow the same procedure as before, this time by right clicking **Day 110: Shrinkage** and extracting the results for shrinkage.

Shrinkage Displacements (Units are in mm)

Output Parameter	Hand Calc.	LARSA 4D Quad-Bilinear	LARSA 4D Quad-Incomp.	LARSA 4D Quad-Drilling	LARSA 4D Triangle-Bilinear
Average of Jt. 5,6,14,18,22	-0.065	-0.065 (0%)	-0.065 (0%)	-0.065 (0%)	-0.065 (0%)

LARSA's shrinkage computations match exactly with the hand calculations.

Verification of Elastic Modulus Change

For the elastic modulus change verification, incremental displacement ratio at Day 26 and Day 111 stages ($U_{z_{26}} / U_{z_{111}}$) are inversely proportional with the ratio of elastic modulus at corresponding stages (E_{111} / E_{26}), this time by right clicking **Day 111: Step 1** and checking the Incremental Results.

Vertical Displacement Ratios ($U_{z@ \text{Day } 26} / U_{z@ \text{Day } 111}$) (Units are in mm)

Output Parameter	Elastic Modulus Ratio (E_{111} / E_{26})	LARSA 4D Quad-Bilinear	LARSA 4D Quad-Incomp.	LARSA 4D Quad-Drilling	LARSA 4D Triangle-Bilinear
Average of Jt. 5,6,14,18,22	1.29	1.29 (0%)	1.29 (0%)	1.29 (0%)	1.29 (0%)

Samples for Influence-Based Analysis

These samples provide an overview of the influence line and surface analysis.

For More Information, please refer to the following documentation.

- For help on influence line and surface analysis, see Influence Line & Surface Analysis in *LARSA 4D Reference Manual*.

INF01: AASHTO LFD Simple Span	371
Model Setup	371
Result Case Setup	372
Accessing Results	373
Solution Comparison	375
INF02: AASHTO LFD Three Span	377
Model Setup	377
Span Break Markers	379
Result Case Setup	380
Accessing Results	382
INF10: Influence Surface	385
Model Setup	385
Result Case Setup	385
Accessing Results	385

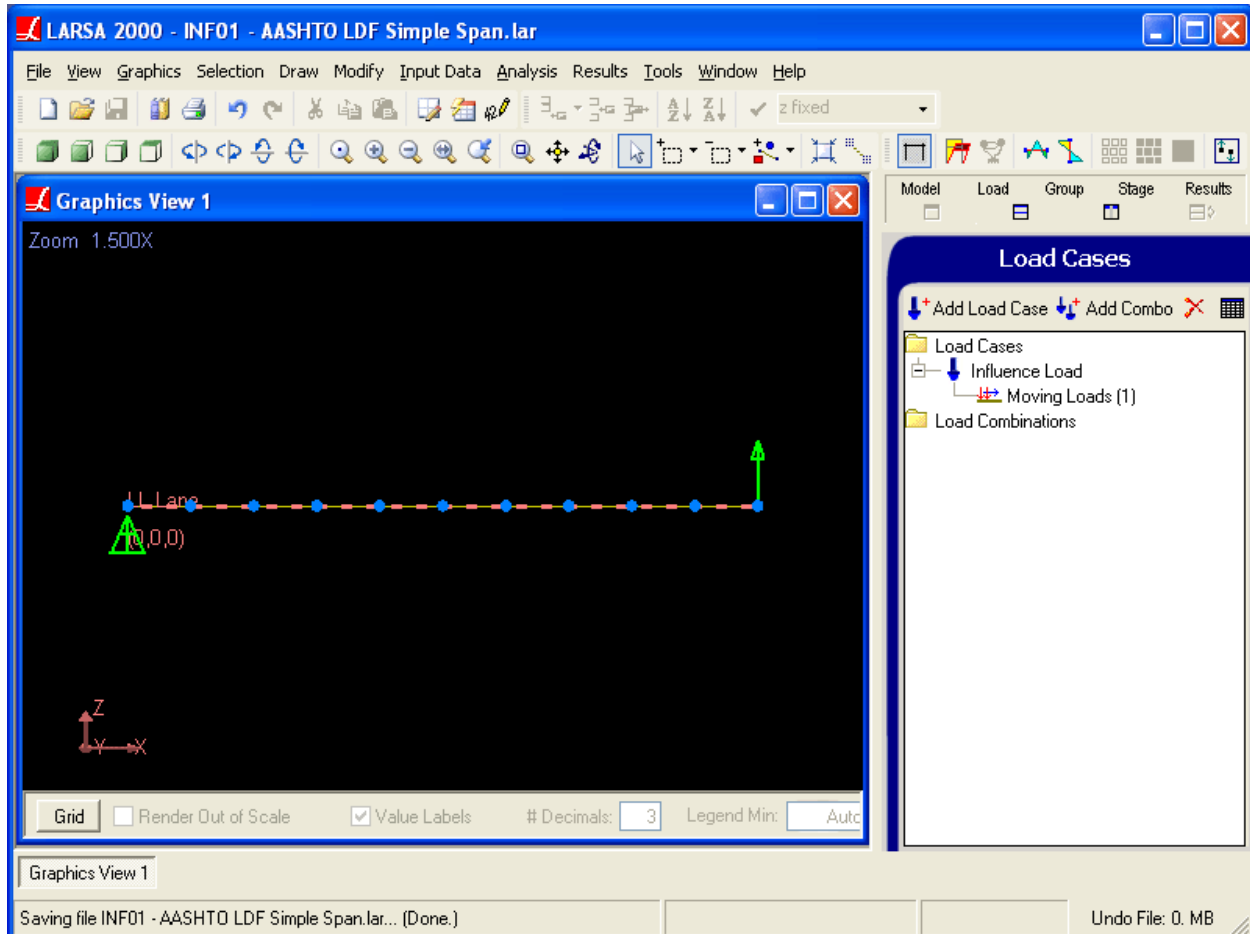
INF01: AASHTO LFD Simple Span

A single simply-supported span is loaded according to AASHTO LFD's live load specifications using influence lines.

Example Project: The example described here can be found in the Influence folder of your LARSA 4D Samples directory (generally My Documents\LARSA Projects\Samples) in the file INF01.

Model Setup

This model consists of a single 200-foot span divided into 10 members of equal length. The left end at (0,0,0) is fully supported in translation and left free in rotation. The right end at (200,0,0) is supported in z-translation only. Universal Restraints [in *LARSA 4D User's Manual*] are used to support all joints in y-translation and x- and z-rotation, reducing the model to two dimensions in the X-Z plane.



Sample INF01

A lane [see “Lanes” in *LARSA 4D Reference Manual*], named "LL Lane," is created along the length of the span. A unit load will march along the lane to generate the influence line coefficients. To create the lane, you can use the **Draw > From Selected Members > Lane** command.

The standard moving load database is connected to the project [see “Connecting Databases” in *LARSA 4D User’s Manual*].

To create the influence line coefficients, a moving load case must be set up. In the Load Cases Explorer [in *LARSA 4D User’s Manual*] a load case named "Influence Load" is created. In the case, a single moving load is applied with the following specification:

Lane Loaded	Load Pattern	Applied Load Direction	Load Factor	Direction of Travel
LL Lane	INFLUENCELOAD	Global -Z	1.00	Forward

The Linear Moving Load/Influence analysis is run on the model.

Result Case Setup

After the analysis, influence-based cases are created for the different types of AASHTO LFD loading. Using **Results > Influence Line/Surface Case** command three times, separate cases are created:

LL Lane/HL-93 Design Truck

This case specifies the loading of a HL-93 Design Truck, which is the HS20-44 truck with the rear axle variably positioned between 14 and 30 feet behind the previous axle. The vehicle is defined in the standard moving load database and so is available because the database was connected earlier.

LL Lane/HL-93 Design Truck

LL Lane/AASHTO Point 18kip (moment)/Lane Load

This case specifies the loading of a 18 kip point load, which is to be used for evaluating moments, as well as a 0.64 kip/ft lane load.

Load Patterns	Factor	Max #
1. AASHTO Point 18kip (moment)	1	1
2. (no pattern used)	1	1
3. (no pattern used)	1	1

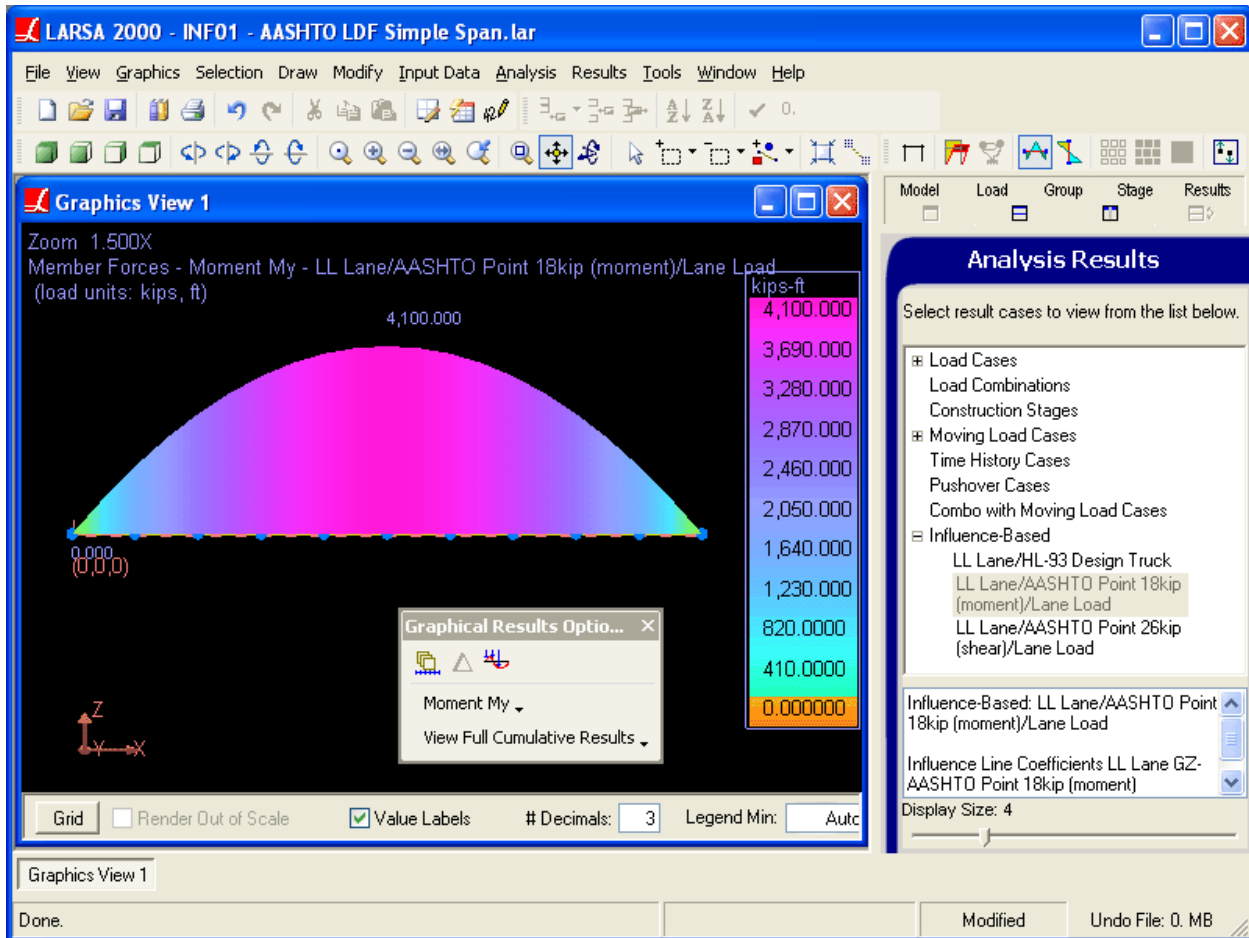
LL Lane/AASHTO Point 18kip (moment)/Lane Load

LL Lane/AASHTO Point 26kip (shear)/Lane Load

This case specifies the loading of a 26 kip point load, which is to be used for evaluating shears, as well as a 0.64 kip/ft lane load.

Accessing Results

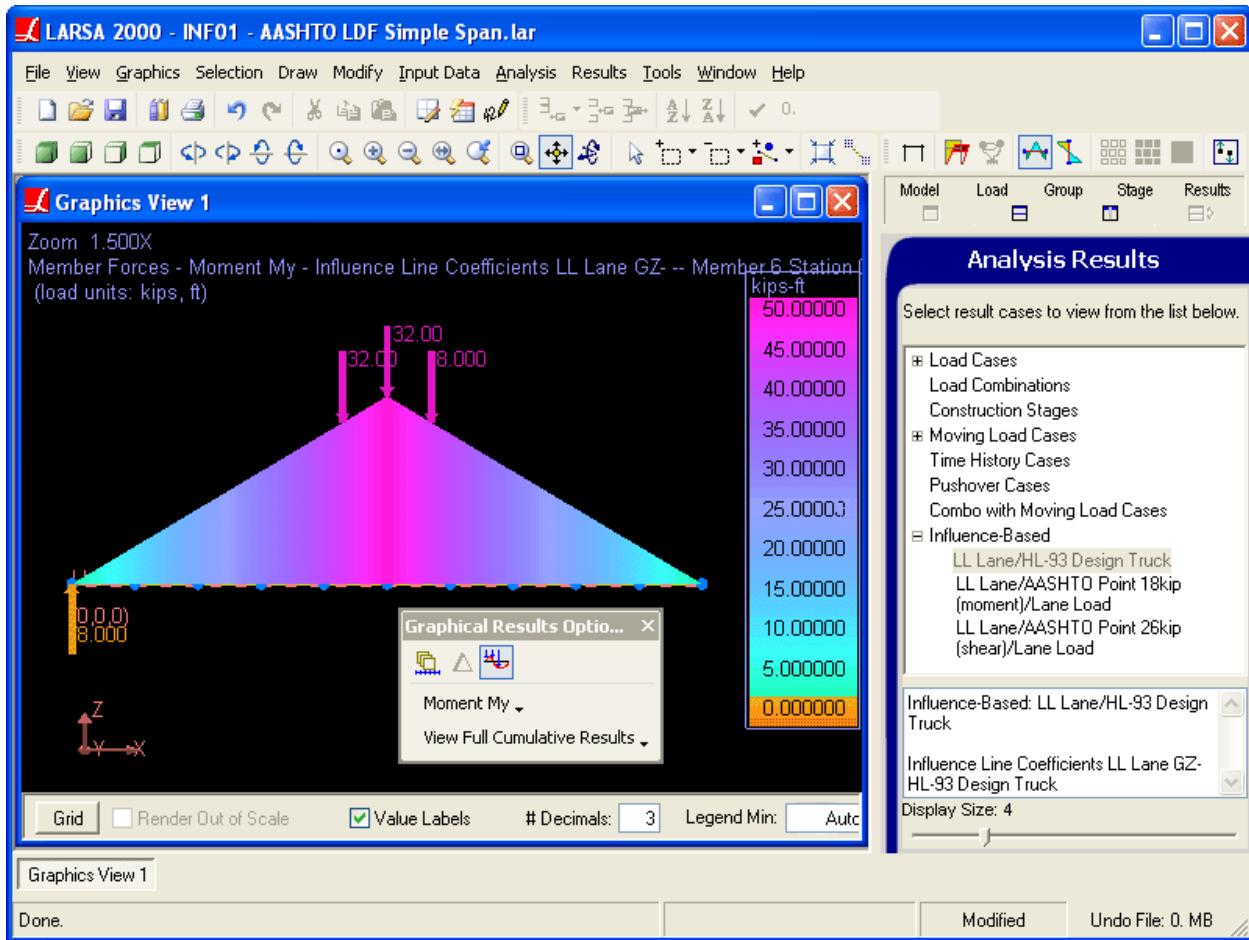
The three result cases show up in the Analysis Results Explorer. To access results, click the name of the case and use graphical or spreadsheet results. Moments for the second case are shown in the figure below.



Moments from Concentrated + Lane Load

LARSA will not automatically switch between the 18 and 26 kip loads depending on whether you are investigating shears or moments. The engineer is responsible for using the appropriate result case for each investigation.

You may check where LARSA decided to place the truck and point loads to produce the maximum effect for any point on the structure using the graphical influence coefficient view [see “Influence Coefficients Graphical View” in *LARSA 4D User’s Manual*]. An image of that is shown below. Arrows indicate the locations of the axles of the HL-93 Design Truck to produce the maximum moment at the first station of the sixth member.



Influence Coefficients and Load Placement

Solution Comparison

For a 200 foot span, LARSA yields expected results:

Sources:

- LARSA 4D
- Theoretical

	LARSA	Theoretical
Maximum Moment (kip-ft)	4100	4100
Maximum Shear (kip)	90.32	90.00

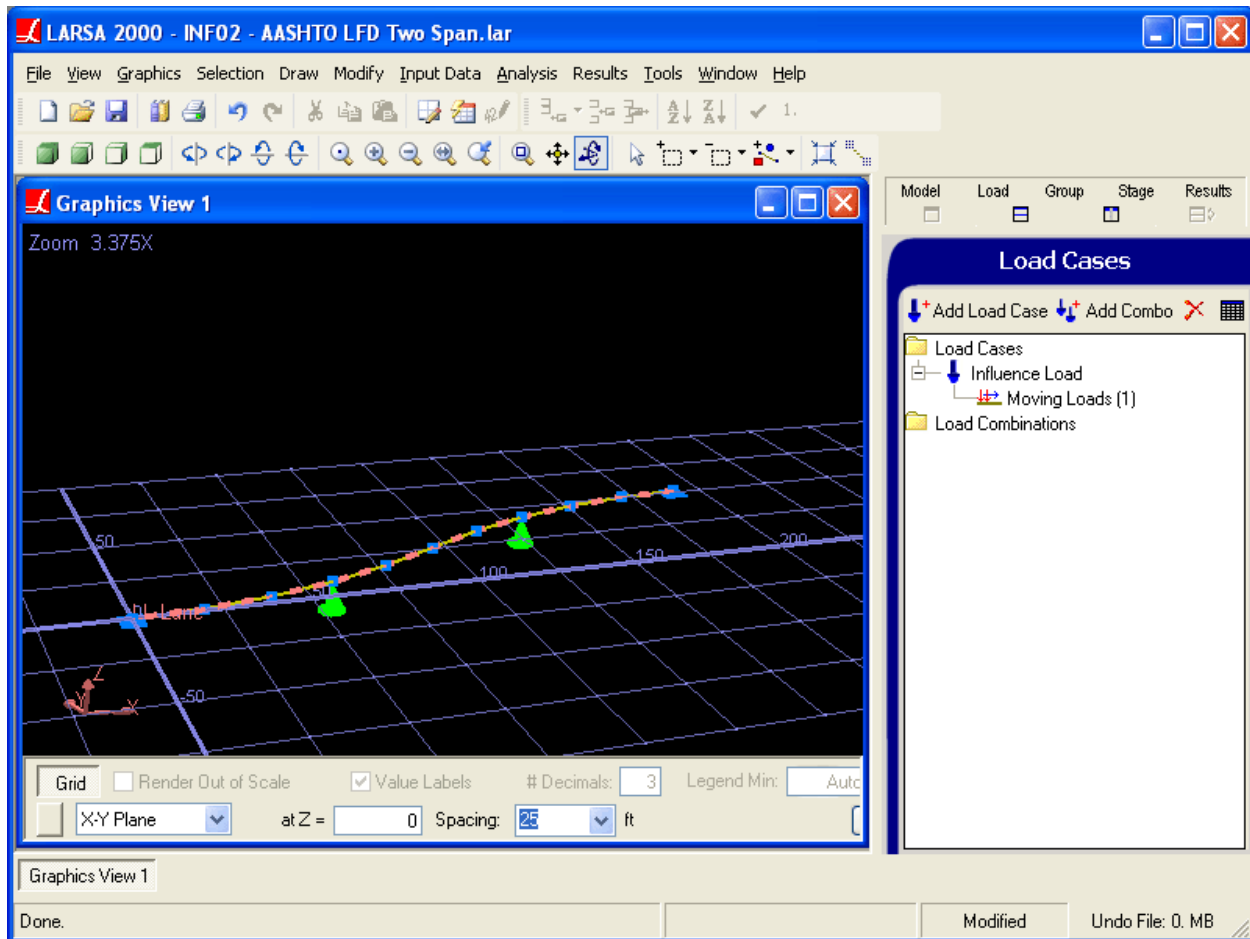
For More Information, please refer to the following documentation.

- For help on influence line and surface analysis, see Influence Line & Surface Analysis in *LARSA 4D Reference Manual*.

INF02: AASHTO LFD Three Span

A three-span curved bridge is loaded according to AASHTO LFD's live load specifications using influence lines. This example illustrates the use of bridge paths and span break makers.

Example Project: The example described here can be found in the Influence folder of your LARSA 4D Samples directory (generally My Documents\LARSA Projects\Samples) in the file INF02.

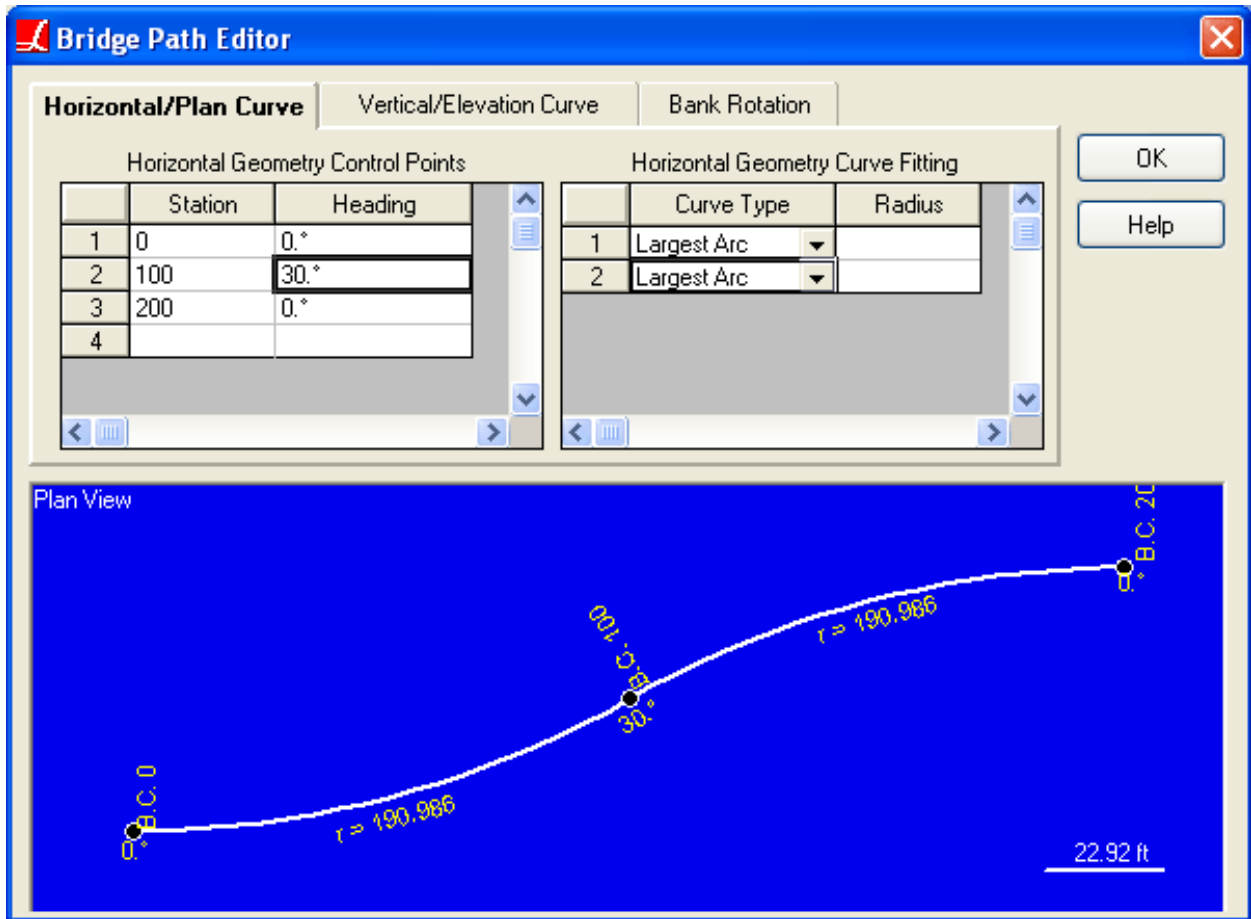


Sample INF02

Model Setup

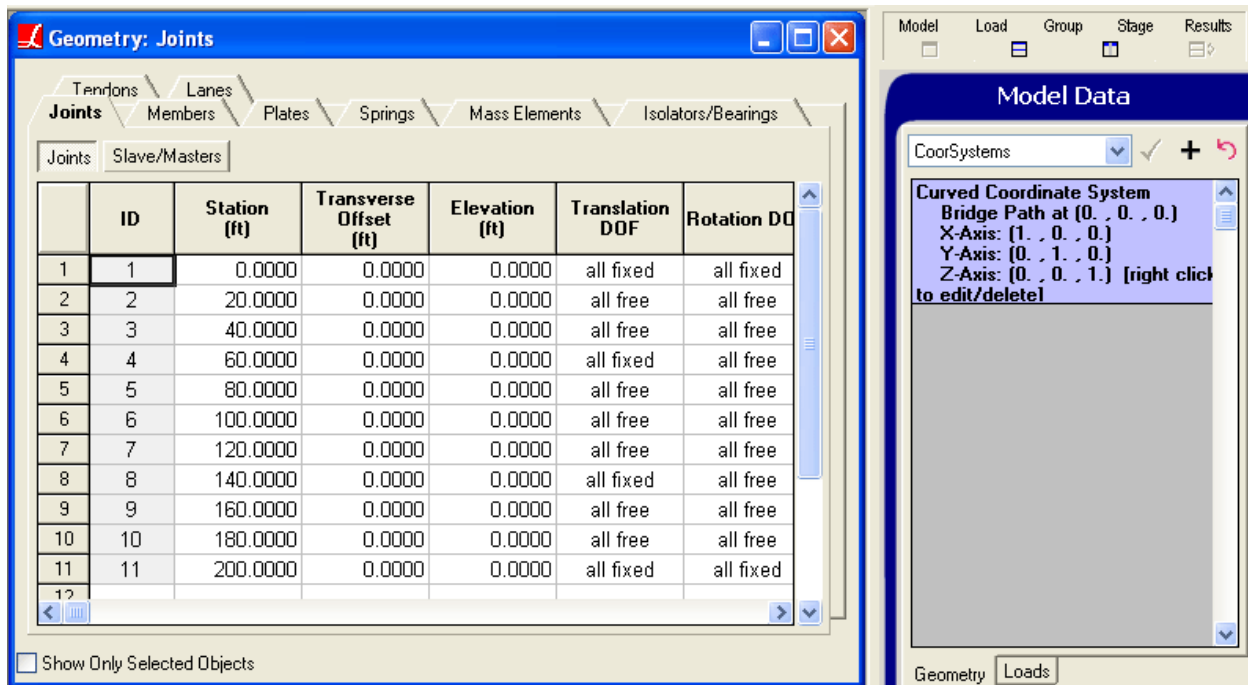
This model consists of a 200-foot bridge in three spans of length 60, 80, and 60 feet. The bridge is divided into members of 20 feet each (span 1: members 1-3; span 2: members 4-7; span 3: members 8-10). The end joints are fully supported. The intermediate supports are simply supported, supported in translation but not rotation.

The bridge is curved using Bridge Paths [in *LARSA 4D Reference Manual*]. A bridge path coordinate system is defined as follows:



Bridge Path

With the bridge coordinate system set as the active coordinate system, the coordinates of the joints are simply spaced 20-feet along the station axis.



Joint coordinates with the bridge path coordinate system active

The lane and moving load case setup are identical as in the previous sample: INF01: AASHTO LFD Simple Span (page 371).

Span Break Markers

AASHTO LFD Section 3.11.3 provides that for the determination of maximum negative moments, two concentrated loads on different spans must be considered. It is possible to specify that two point loads be applied using influence lines, but a special feature has been added that ensures 1) that a second load is only considered for negative moments, and 2) that the second concentrated load is applied on a different span than the first concentrated load.

LARSA cannot automatically determine where one span ends and another span begins. In complex bridge models, the locations of supports at spans are not located near the deck where the influence lines are considered but at the base of piers. So LARSA needs to be informed where one span ends and another begins on the lane path definition.

The lane path definition is amended by inserting *Span Break* markers after the last geometry point of each span. In this example, the first span ends after the third member, member 3. However, the last geometry point on the span is the geometry point at the *start* of member 4. A span break marker goes after this row to indicate that the first span contains member 3. If a marker were placed after the geometry point at the start of member 3, the first span would go only as far as the beginning of member 3, not to its end.

The second span break marker is placed four rows later, after the row for the geometry point at the start of member 8. This makes the middle span contain members 4, 5, 6, and 7.

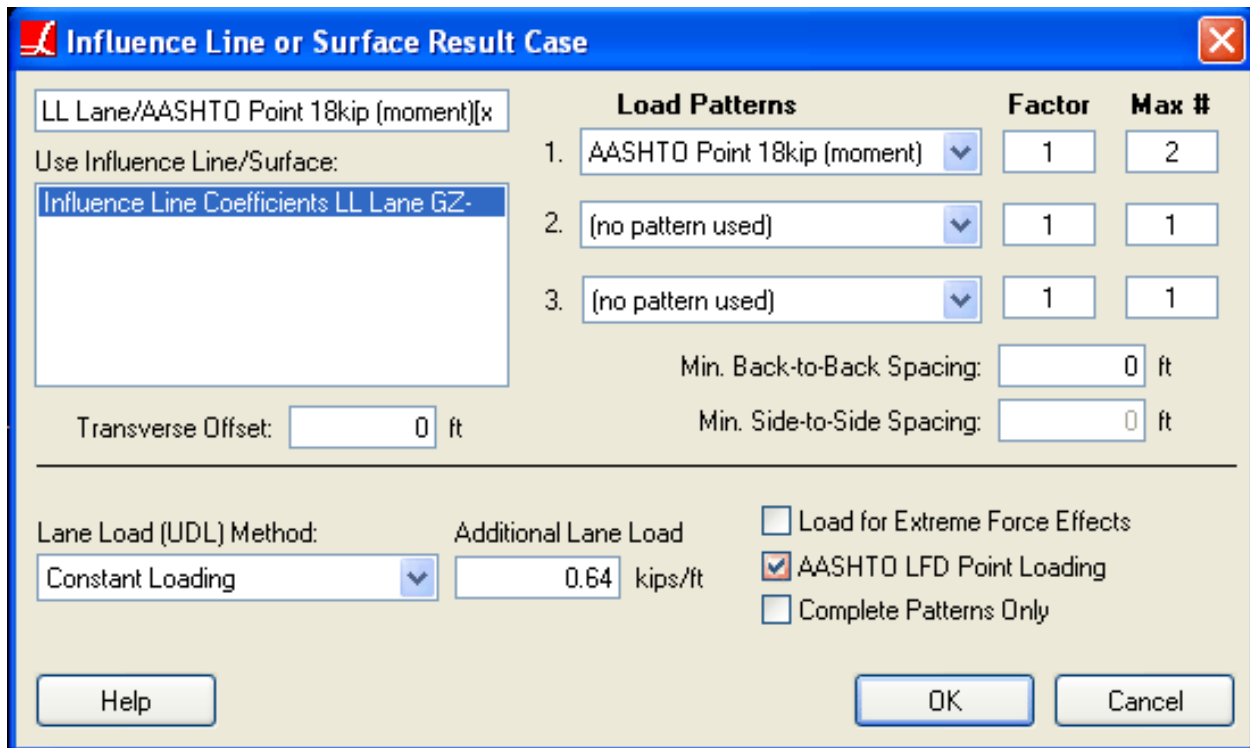
	Point Type	Reference Object Type	Reference Object or Range	Offset X (ft)	Offset Y (in)	Offset Z (in)	X Reference
1	geometry	member	1	0.0000	0.0000	0.0000	Start
2	geometry	member	2	0.0000	0.0000	0.0000	Start
3	geometry	member	3	0.0000	0.0000	0.0000	Start
4	geometry	member	4	0.0000	0.0000	0.0000	Start
5	span mark						
6	geometry	member	5	0.0000	0.0000	0.0000	Start
7	geometry	member	6	0.0000	0.0000	0.0000	Start
8	geometry	member	7	0.0000	0.0000	0.0000	Start
9	geometry	member	8	0.0000	0.0000	0.0000	Start
10	span mark ▾						
11	geometry	member	9	0.0000	0.0000	0.0000	Start
12	geometry	member	10	0.0000	0.0000	0.0000	Start
13	geometry	member	10	0.0000	0.0000	0.0000	End
14							

Span break markers added to the lane path definition

Result Case Setup

The result case setup for the vehicle load pattern and the 26 kip concentrated load for shear using influence-based results is identical to the previous sample: INF01: AASHTO LFD Simple Span (page 371).

The setup for the 18 kip concentrated load for negative moment is slightly different. The load is set with *Max #* to 2, since there can be at most two loads applied. In addition, the *AASHTO LFD Point Loading* option is checked.



Concentrated Loads for Negative Moment

The *AASHTO LFD Point Loading* option has two effects. The first is to ensure that the two concentrated loads are placed in separate spans. The other effect is to ensure that the second load is only applied in certain circumstances. But, LARSA cannot simply apply the load only when the engineer is investigating envelope minimums for member forces. "Negative moments" as intended by the AASHTO LFD specification may not mean negatively-signed moments as outputted by LARSA. The orientation of the model and LARSA's sign conventions may result in positively-signed moments being the ones intended to be considered "negative" for the purposes of AASHTO LFD.

The second concentrated load is applied when enveloping member end forces or member sectional forces for local y or z moments. It is applied in either the y or z direction, and either for enveloped minimums (negatives) or enveloped maximums (positives), depending on the orientation angle of the member. The following table indicates when the second concentrated load will be applied. It is dependent on the sign convention for the results. Member sectional forces, stresses, and member end forces *at the end joint* have the same sign convention. This is also the sign convention used in graphical diagrams of member forces and stresses. Member end forces *at the start joint* has the opposite sign convention.

Orientation Angle	Sectional Forces (and End Forces at End)	End Forces at Start at End)
0° (-45 to 45)	positive y moments	negative y moments
90° (45 to 135)	negative z moments	positive z moments
180° (135 to 225)	negative y moments	positive y moments
270° (225 to 315)	positive z moments	negative z moments

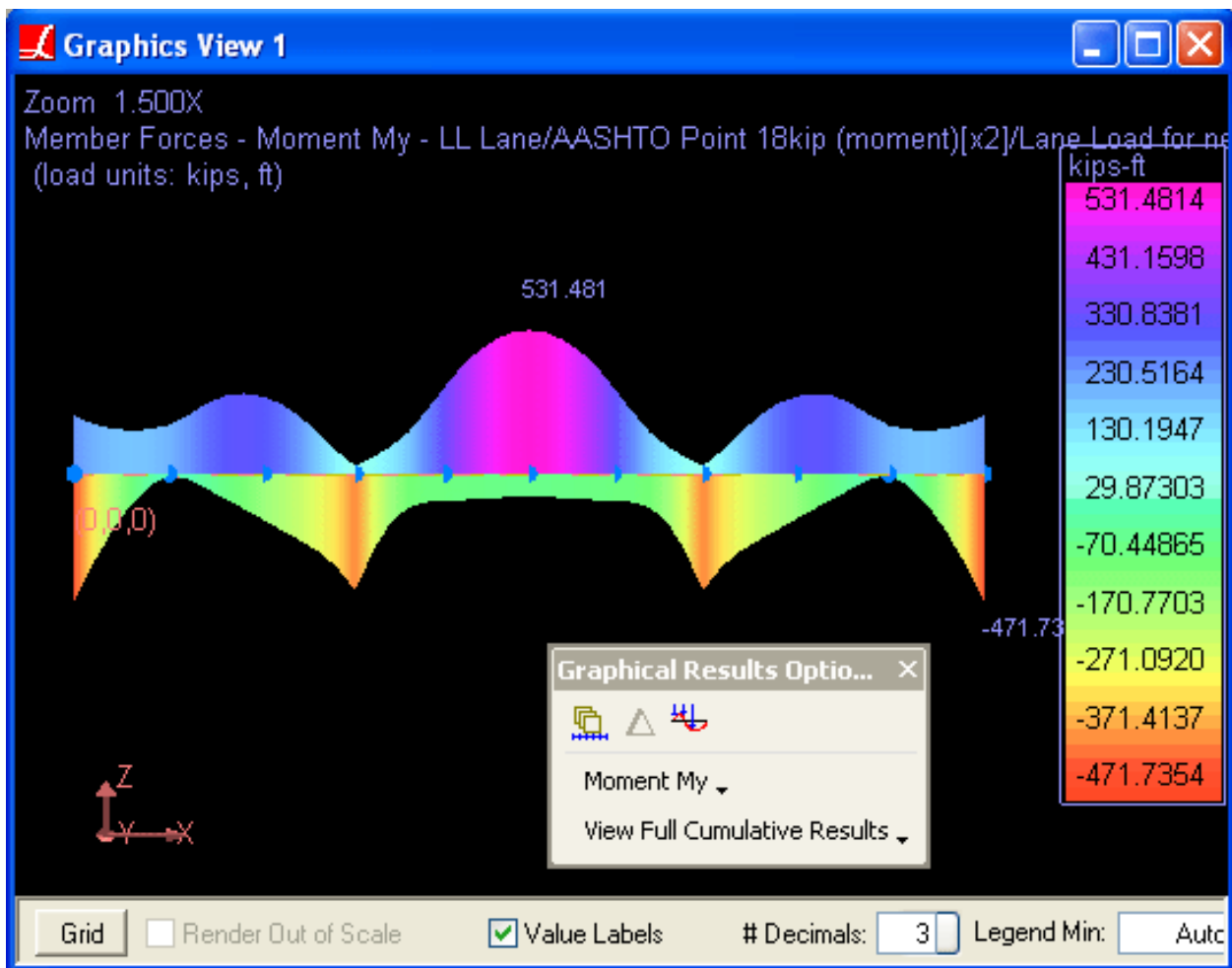
The engineer should confirm that the conditions in which the second concentrated load is applied corresponds with the intentions of the specification for each model.

The AASHTO LFD Point Loading option should only be used when the elevation axis is the global z-axis.

Accessing Results

See the previous sample (INF01: AASHTO LFD Simple Span (page 371)) for an overview of accessing influence line results.

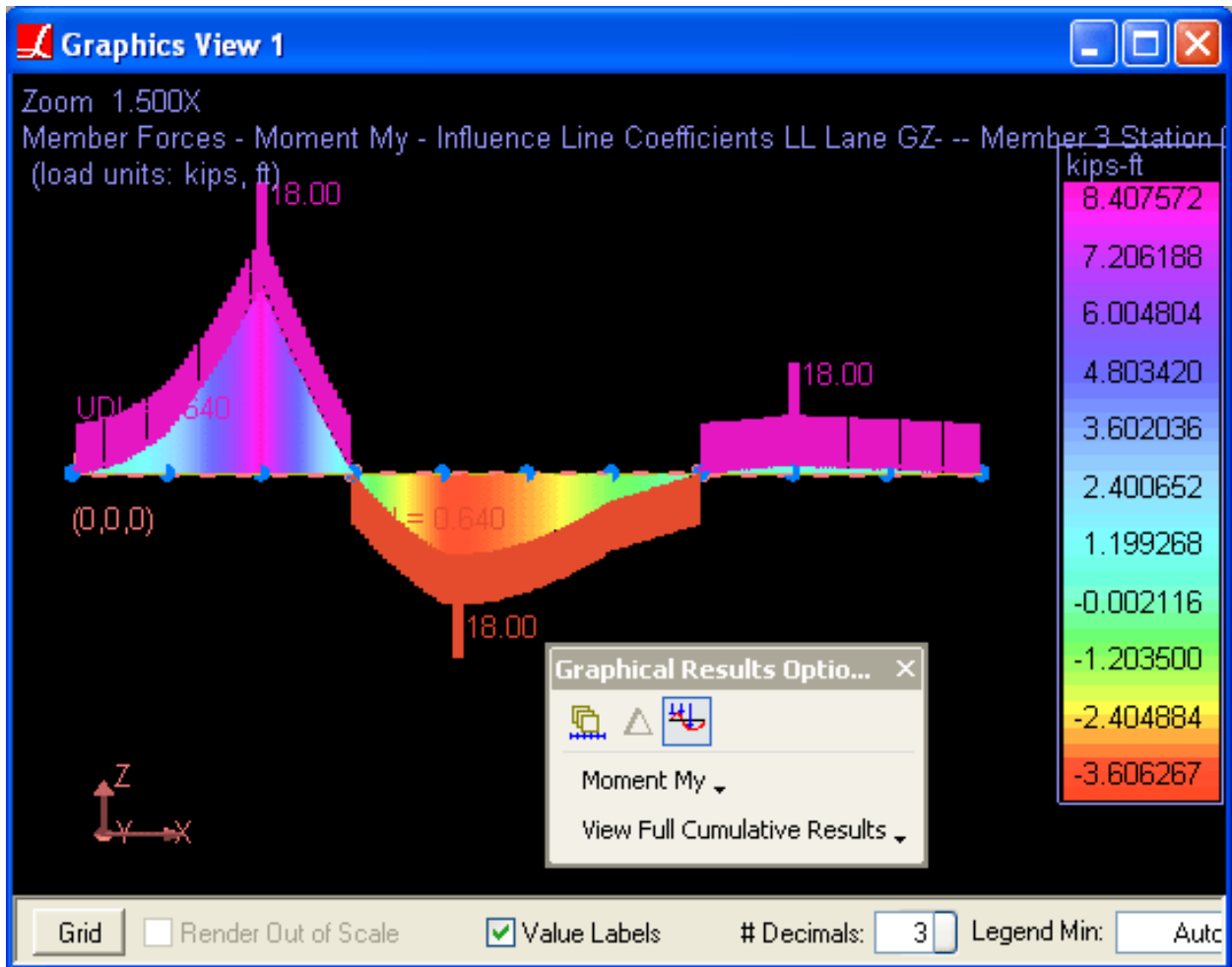
To verify the application of the second concentrated load for moments, select the *LL Lane/AASHTO Point 18kip (moment)[x2]/Lane Load for negative moments only* case in the Analysis Results Explorer. Then turn on graphical moment diagrams and select the direction *Moment My*.



Moment Diagram for Three-Span Bridge

Next activate graphical influence coefficient view [see “Influence Coefficients Graphical View” in *LARSA 4D User’s Manual*]. Using the pointer tool, click member 3 and when prompted enter station 0. LARSA will display the influence line coefficients with the locations of the two concentrated loads applied. In this model, the members were created

with orientation angle 0. As a result, the concentrated loads are applied for positive y moments in sectional forces and in graphical diagrams. This is shown below:



Influence Coefficients and Load Placement

Influence coefficients view always shows two diagrams: above the bridge are positive moments, below the bridge are negative moments. Two concentrated loads were applied for positive moments, and, appropriately, one concentrated load for negative moments, following the sign convention of LARSA. The solid bars above and below represent the application of the uniform lane load.

This diagram shows that the first concentrated load was placed directly above member 3's start, where it produced the maximum positive y-moment at the start of member 3. The second concentrated load was placed in the third span, at the next worst position for positive y moments.

For More Information, please refer to the following documentation.

- For help on influence line and surface analysis, see Influence Line & Surface Analysis in *LARSA 4D Reference Manual*.

INF10: Influence Surface

Influence surfaces are used for a vehicular live load analysis of a bridge deck. Influence surfaces are used for live load analysis for decks modeled as a surface of shell elements.

Example Project: The example described here can be found in the Influence folder of your LARSA 4D Samples directory (generally My Documents\LARSA Projects\Samples) in the file INF10.

Sample INF10

Model Setup

In this model, a 200 ft long deck 40 feet wide is modeled as a 10-by-4 shell mesh. The joints along the start of the deck are supported in translation, and the joints along the end of the deck are supported in z-translation only.

A lane is defined on the deck surface. The lane is given a width of 40 feet in **Input Data > Geometry > Lanes**. The path of the lane is defined along the edge of the strip of shells down the center of the deck.

The influence surface coefficients are set up in the same way as for influence lines. A load case is given a moving load with the *INFLUENCELOAD* load pattern. But because many more coefficients are generated for surfaces, a position increment of 2 feet rather than the default 1 foot is used.

The moving load analysis is used to generate the influence surface coefficients.

Result Case Setup

Following the analysis, an influence-based result case is created to simulate the application of a HL-93 Design Truck. With influence surfaces, it is possible to use new two-dimensional load patterns that model vehicles with actual width. Each wheel, rather than each axle, is modeled as a separate load. The load pattern *HL-93 Design Truck T/C* in the standard load pattern database models the truck as 6 feet wide, with six wheels, following the AASHTO code.

Accessing Results

See the earlier sample INF01: AASHTO LFD Simple Span (page 371) for an overview of accessing influence-based results.

Using graphical influence coefficients view, the position of the vehicle that leads to the most extreme effects can be viewed. The figure below shows the position of the two-dimensional vehicle on the deck.

A two-dimensional load pattern over the influence coefficients

For More Information, please refer to the following documentation.

- For help on influence line and surface analysis, see Influence Line & Surface Analysis in *LARSA 4D Reference Manual*.

Samples for Steel Bridge Design and Rating

These samples provide an overview for steel bridge analysis design and load rating.

SBD06: Straight Steel Plate Girder Bridge with 90 Degree Skew (LFD)	389
Problem Details	389
Dead Load	392
Live Load	392
Model Generation	394
Compound Element Result Extraction	398
Non-Composite and Composite Dead Load Analysis Results	399
2) Influence Surface Based Live Load Analysis	404
SBD07: Curved Steel Plate Girder Bridge With 60 Degree Skew (LFD)	417
Problem Details	417
Dead Load	420
Live Load	420
Model Generation	422
Compound Element Result Extraction	426
Non-Composite and Composite Dead Load Analysis Results	427
2) Influence Surface Based Live Load Analysis	433
SBD08: Three-Span Continuous Horizontally Curved Composite Steel Tub-Girder Bridge	445
Problem Details	445
Dead Load	452
Live Load	452
Load Combinations	452
Modeling and Code Check in LARSA 4D - Steel Bridge Module (SBM)	453
References	498

SBD06: Straight Steel Plate Girder Bridge with 90 Degree Skew (LFD)

The bridge chosen for this example is a straight two-lane steel plate girder bridge with a 90-degree skew and with identical four-girder cross-sections. The bridge is three-span continuous over span lengths of 80, 100 and 80 feet along the control centerline. The live load results are reported for HS25-44 and lane loading using influence surface analysis.

Example Project: The example described here can be found in the Steel Bridge Module folder of your LARSA 4D Samples directory (generally My Documents\LARSA Projects\Samples) in the file SBD06.

Problem Details

The bridge layout is shown in Figure 1.

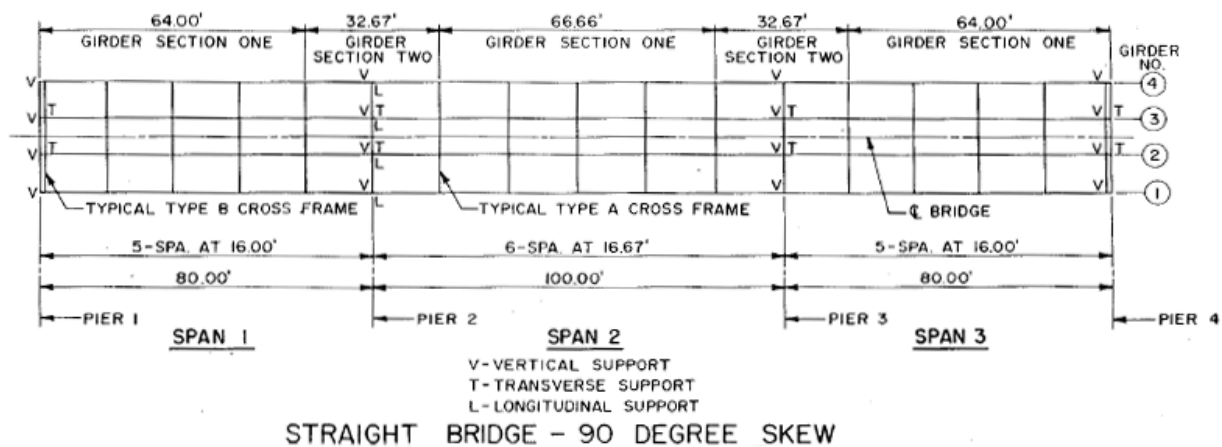


Figure 1: Plan View

The materials used in this model are:

Steel

$E_s = 29,000$ ksi

Weight Density = 490 pcf

Steel Girders = Type A572 Steel

Cross-Frames = Type A36 Steel

Concrete

$E_c = 3,820$ ksi

Weight Density = 150 pcf (which includes allowance for steel reinforcement)

$f_c' = 4.5$ ksi

$n = 8$

The deck slab thickness is 9 inches, as shown in Figure 2, including the 1/2-inch non-structural wearing surface. The parapet dimensions and deck overhang details are given in Figure 3.

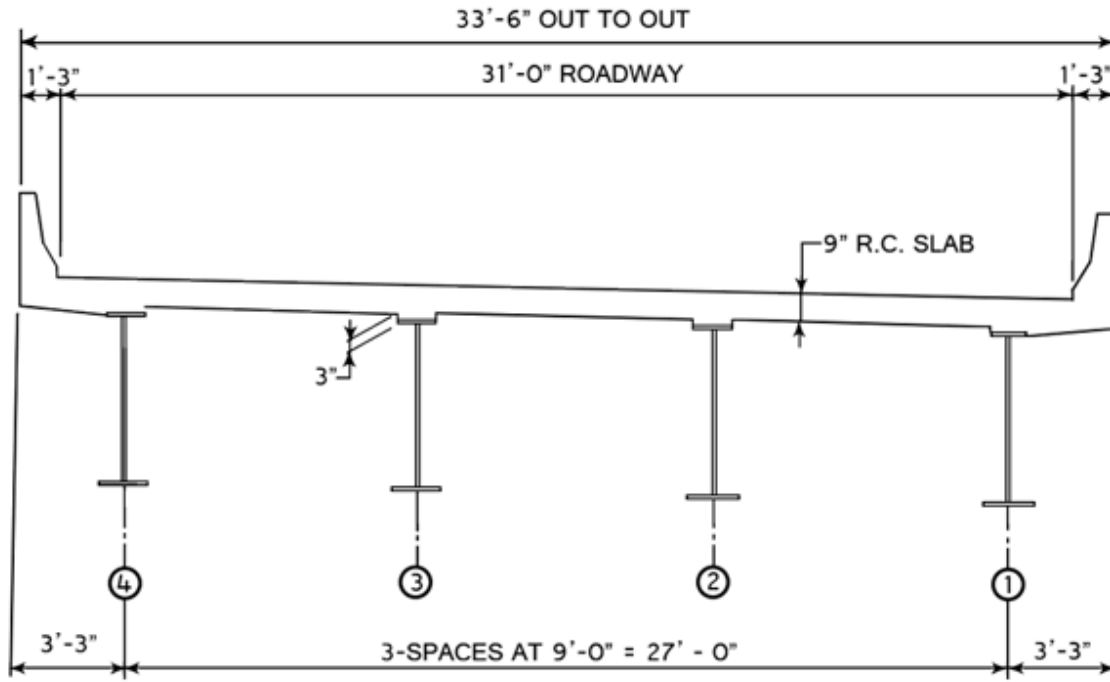


Figure 2: Typical Cross-Section

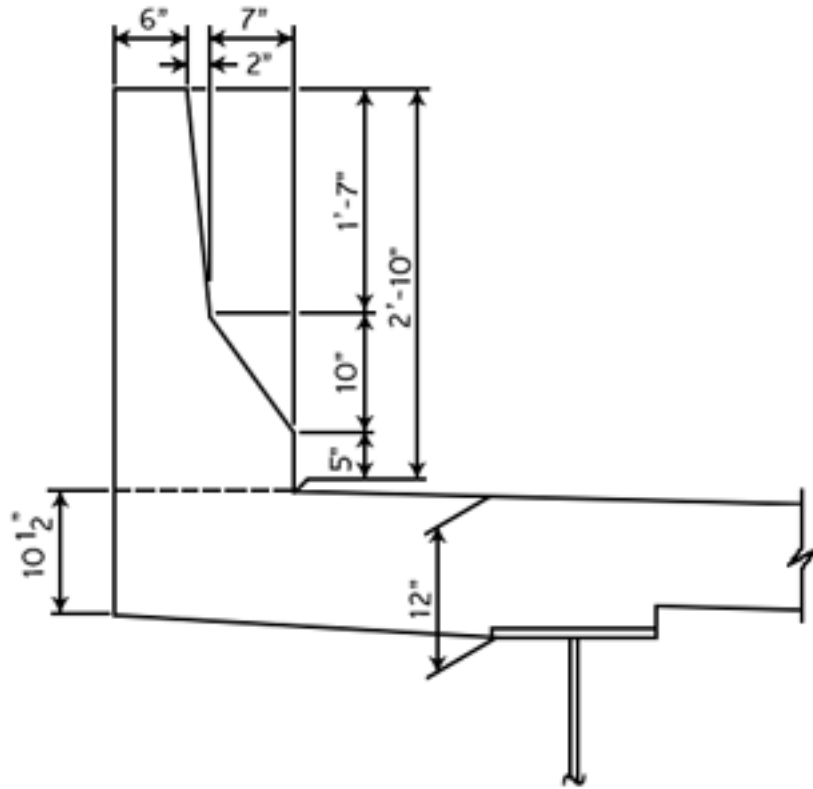


Figure 3: Parapet and Deck Overhang Detail

The plate sizes for Girder Sections One and Two are given in the table below. The locations of these girder sections are shown in Figure 1.

	Section One	Section Two
Web Plate	7/16" x 60"	7/16" x 60"
Top Flange	7/8" x 14"	1 3/4" x 14"
Bottom Flange	1" x 18"	2" x 18"

There are two types of cross-frames used in this example, as seen in Figure 4. Typical intermediate cross-frames are Type A, and the cross-frames at piers 1 and 4 are Type B. Member sizes for the cross frames are given in Figure 4.

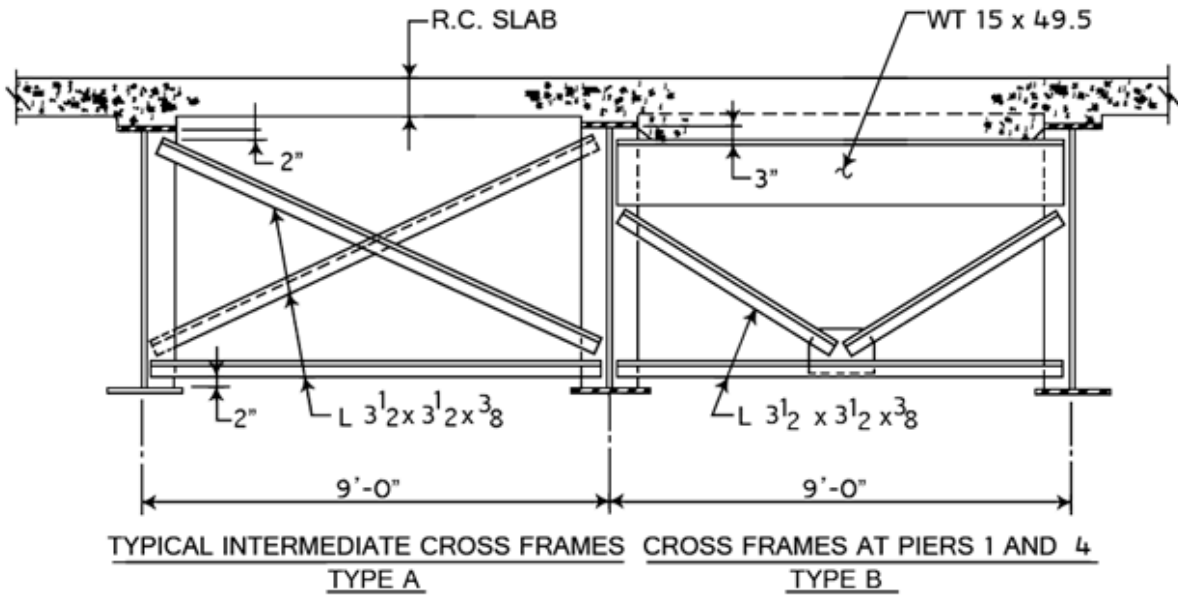


Figure 4: Cross-Frames

Dead Load

The non-composite dead load consists of all of the dead loads, except the weight of the parapet and future wearing surface. The composite dead load includes all of the dead loads.

The stay-in-place forms are 15 psf and are used between the girders, but not on the overhangs.

The future wearing surface is 30 psf and placed between the parapets.

Live Load

The live load consists of a HS25-44 truck, as shown in the figure below, and distributed lane loading.

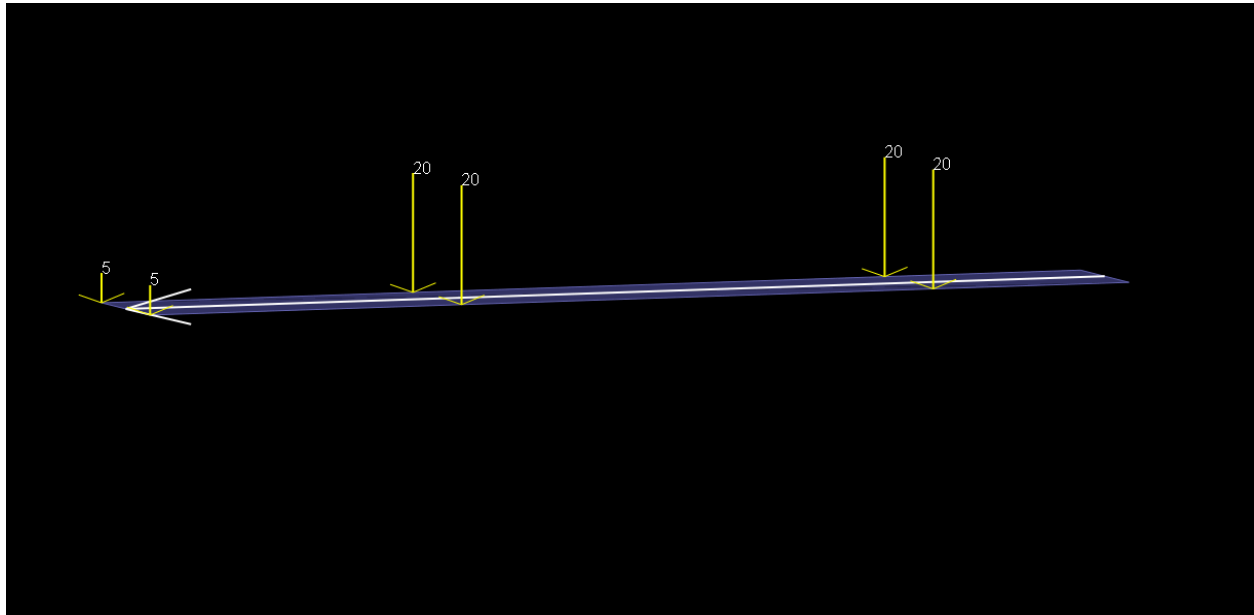


Figure 6: HS25-44 (2D)

HS25-44 (2D)

Magnitude (kips)	Location (ft)	Transverse Offset (ft)
5	0	3
5	0	-3
20	14	3
20	14	-3
20	Varies 28 - 44	3
20	Varies 28 - 44	-3

☛ The live load pattern HS25-44 has been added to the moving load database and to review live load patterns select from the menu **Input Data** → **Edit Database**.

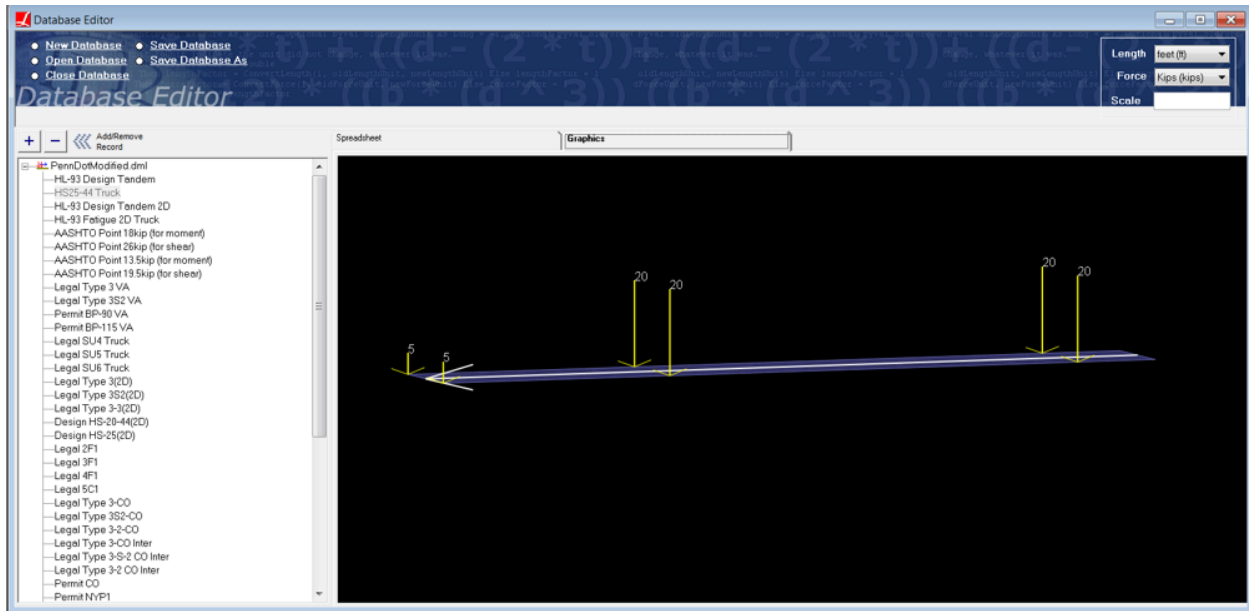


Figure 7: Moving Load Database

Model Generation

The model is created using the Steel Bridge Module within LARSA 4D BRIDGE. While this model could have been created using the graphical generation tools of LARSA 4D, the Steel Bridge Module provides a parametric approach for fast-track generation of LARSA 4D models for I, box, and tub girder steel bridges and for performing AASHTO LRFD code check and load rating on these bridges. The module is specifically developed for the special needs of skewed and/or curved bridges and bridge structures with complex geometry.

Steel I-girder sections can be represented as a single beam element or as multi-element section where the flanges are represented as beam elements and the web as shell elements. In this example, we will have I-girders modeled using a combination of member and shell elements. This modeling type allows easier extraction of lateral bending moments of the flanges. The top flange of the girder will be connected to the deck with rigid elements. The bridge deck is modeled using shell elements.

The model generated is for staged construction analysis where non-composite and composite states and the deck pouring sequence are handled with ease.

The finite element model generated is displayed below.

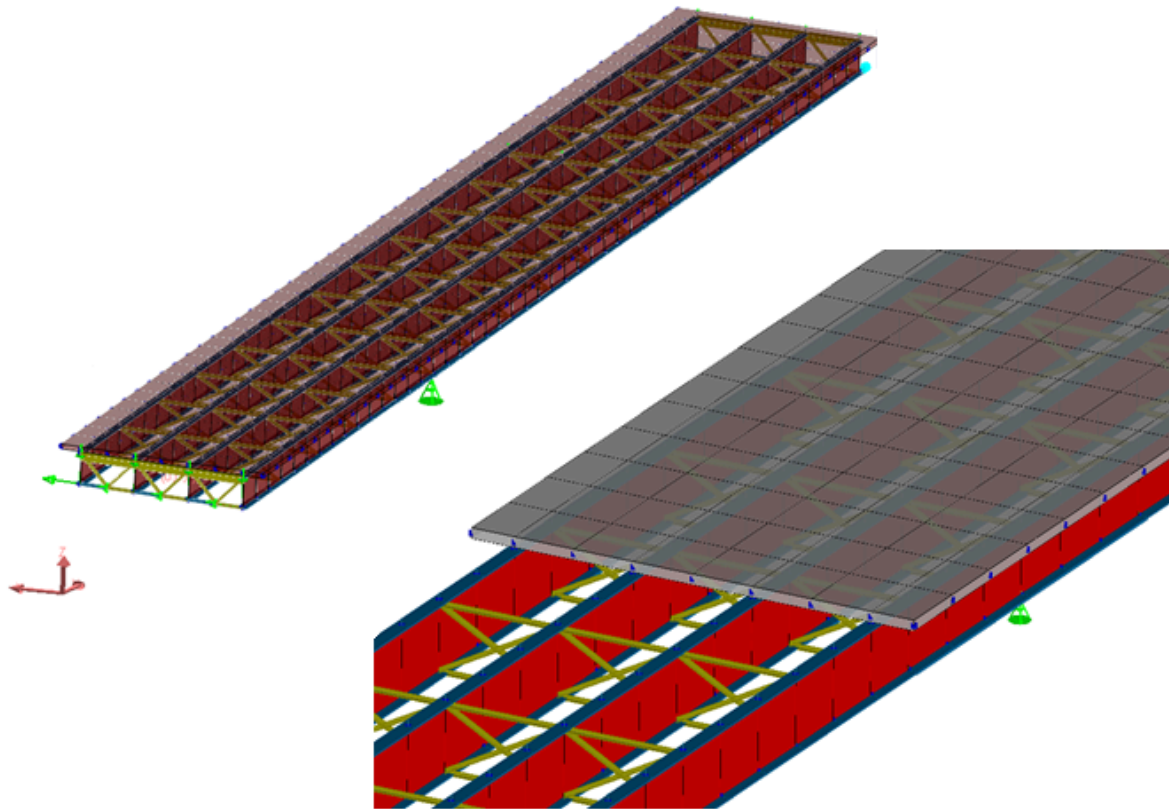


Figure 8: LARSA 4D Finite Element Model

In the first stage, girders and cross frames are constructed as seen in Figure 9.

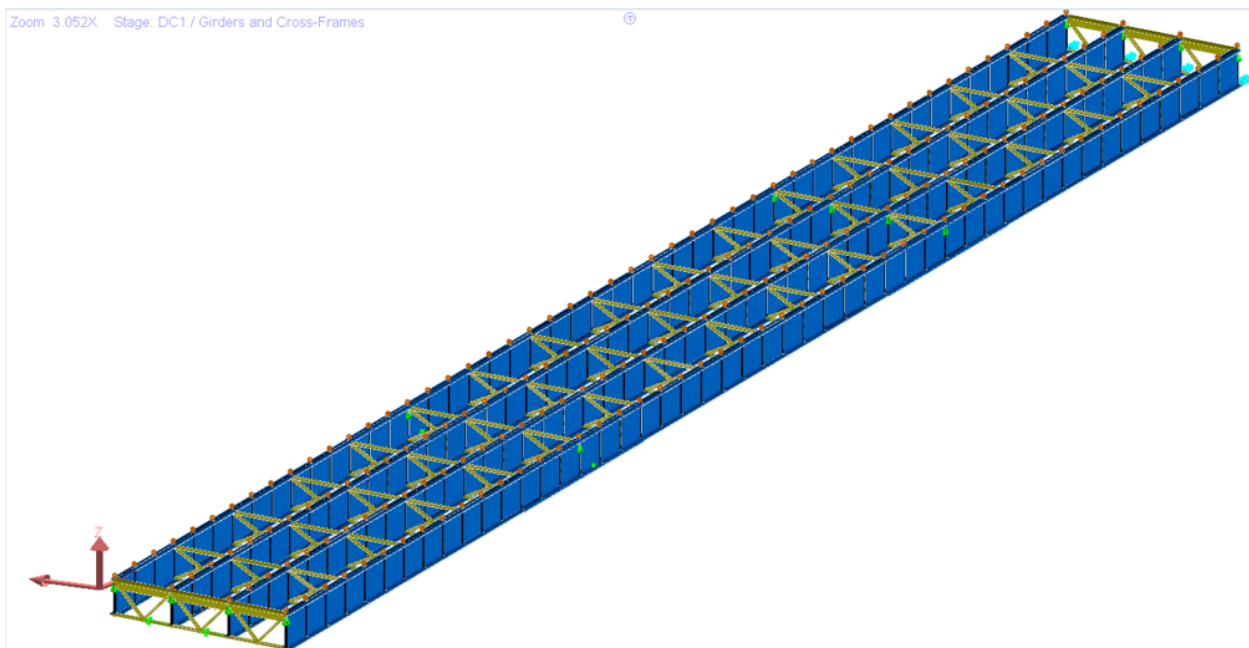


Figure 9: Stage 1-Girders and Cross Frames

In the second stage, stay-in-place form loads are applied to the girders as seen in Figure 10.

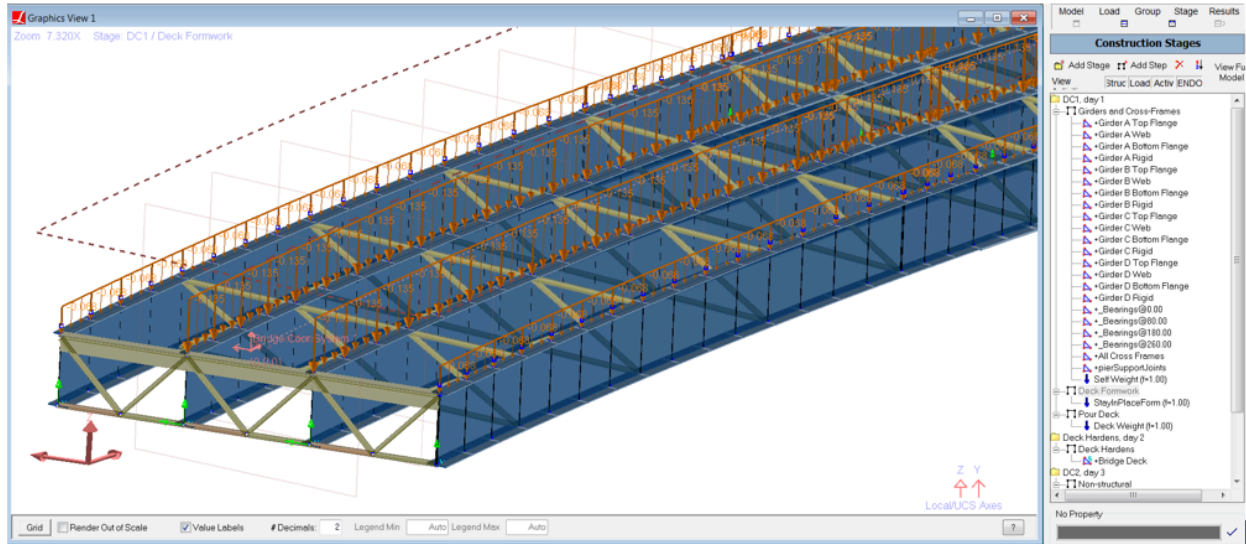


Figure 10: Stage 2-Stay in place form loads

In the third stage, the deck is poured and wet concrete loading is applied to the girders as seen in Figure 11.

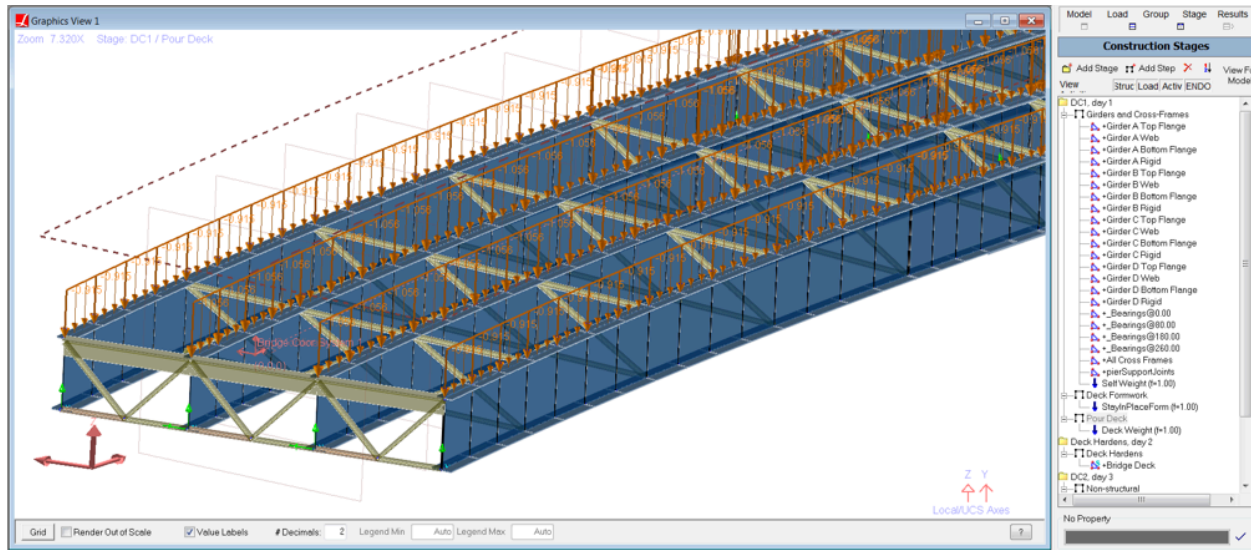


Figure 11: Stage 3-Deck Pouring

In the fourth stage, the deck gained its stiffness and deck elements are constructed with LARSA 4D's stiffness only option.

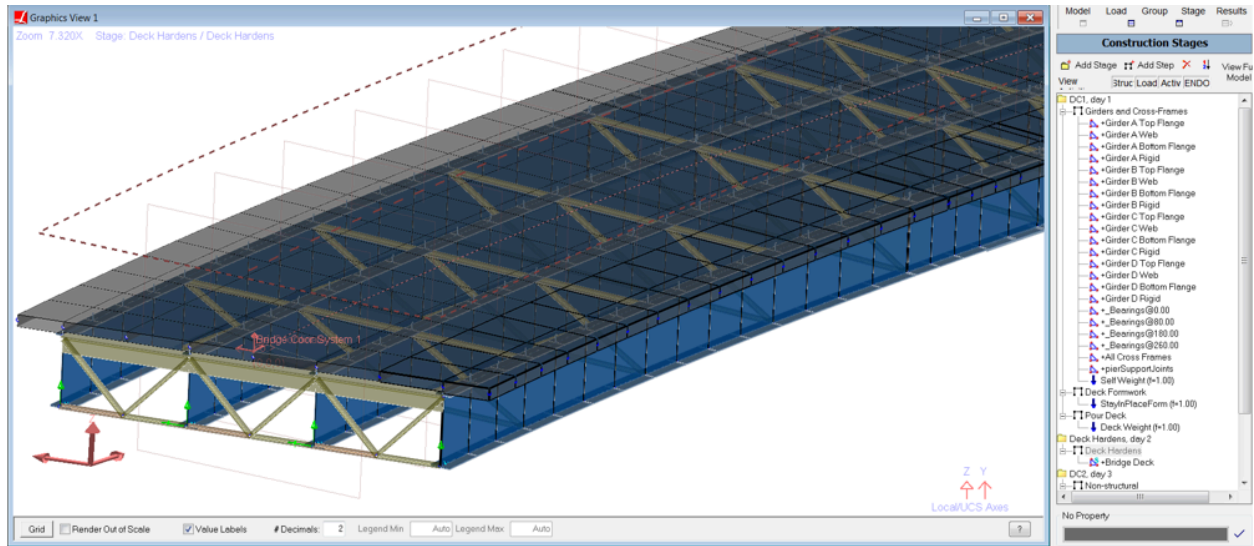


Figure 12: Stage 4-Deck Gains Stiffness

In the fifth stage, parapet loads are applied to the overhang plate elements as uniform plate load as seen in Figure 13.

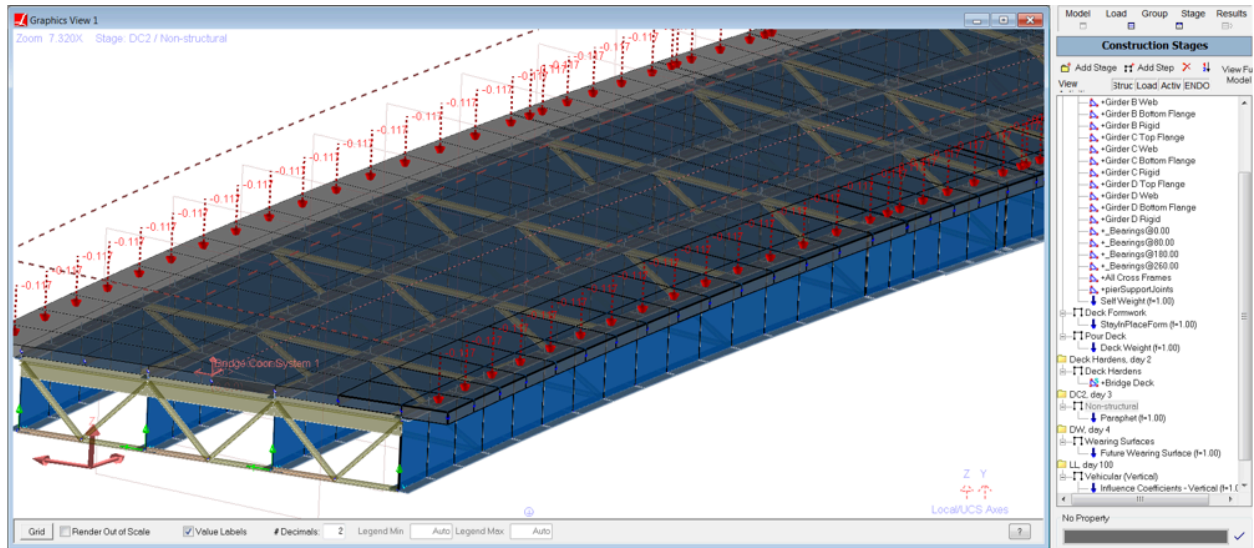


Figure 13: Stage 5-parapet

In the sixth stage, future wearing surface loads are applied to deck plate elements as seen in Figure 14.

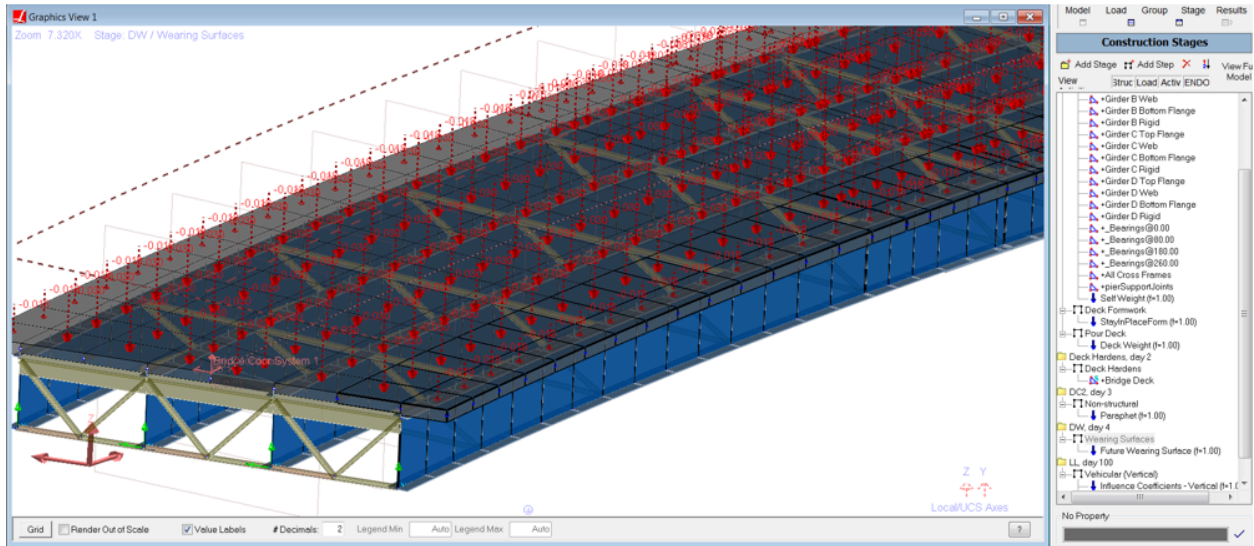


Figure 14: Stage 6-Future Wearing Surface

Modular ratio values of "n" and "3n" will be used by defining a material time effect as seen in Figure 15. In the seventh stage, the stiffness of the deck will be modified for the analysis of live load.

Properties: CEB-FIP 90

Materials / Sections / UCS / Spring Properties / Isolator Definitions / **Material Time Effects**

	Name	Creep Factor	Shrinkage Factor	Relaxation Factor	Steel Relaxation Type	Assigned
1	LRFD-3n	1.0000	1.0000	1.0000	Custom	Yes
2						

Time VS Modulus of Elasticity: LRFD-3n

Coefficients / Graph

	Time (Days)	Modulus of Elasticity (kips/ft ²)
1	1.0000	1.8336e5
2	99.0000	1.8336e5
3	100.0000	5.5008e5
4	200.0000	5.5008e5
5		

LL, day 100

- [-] Vehicular (Vertical)
 - [-] Influence Coefficients - Vertical (f=1.00)
 - [-] Run Linear Moving Load/Influence Analysis

No Property

Figure 15: Stage 7-Influence Surface Analysis

Compound Element Result Extraction

In order to determine the forces in a girder modeled not as a single beam but as multiple elements, the compound element forces feature of LARSA 4D shall be used. Compound Element Forces reports the combined forces and moments of a group of elements about their combined centroid.

Non-Composite and Composite Dead Load Analysis Results

The non-composite dead load consists of all of the dead loads, except the weight of parapet and future wearing surface. The composite dead load includes all dead loads.

Deck weight is applied to the exterior girders as uniform member loads with a magnitude of 1.007 kips/ft.

Deck weight is applied to the interior girders as uniform member loads with a magnitude of 1.056 kips/ft.

Stay-in-place form loading is applied to the exterior girders as uniform member loads with a magnitude of 0.0675 kips/ft.

Stay-in-place form loading is applied to the interior girders as uniform member loads with a magnitude of 0.135 kips/ft.

Follow the instructions below to review the loads.

- ☛ To see load spreadsheets, click the **Loads** button above the explorers, right-click the **StayInPlaceForm** load case and choose **Edit loads**.
- ☛ To see loads graphically, choose from the menu **Graphics** → **Show** and turn on **Input Loads**. Click the **Loads** button above the explorers, then click the **StayInPlaceForm** load case.

The non-composite dead load analysis results for the Girder 3 can be seen in Figure 16. Follow the steps below in order to see the results for Girder 3.

- ☛ Select the structure group: Click the **Group** button above the explorers. Click **Composite 2**. Click **Select (Unselect Everything Else)**.
- ☛ Select the result case: Click the **Results** above the explorers. Right click the **NonComposite** result case. Choose **Compound Element Forces**.

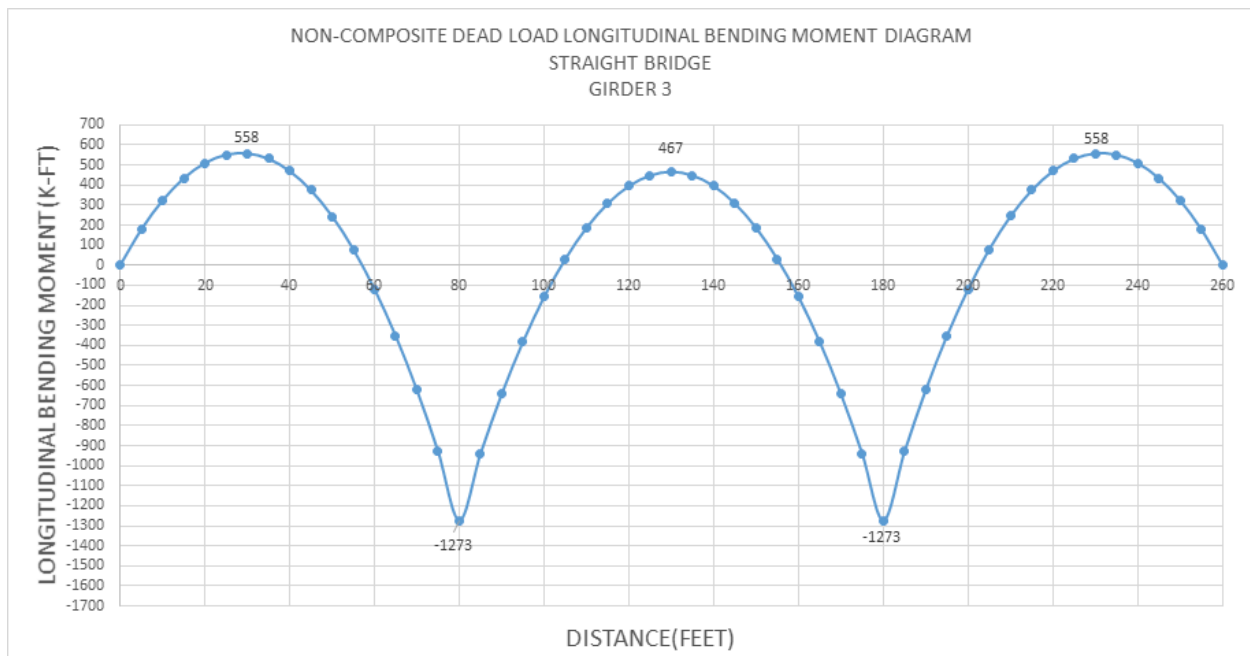


Figure 16: Girder 3 Non-composite Dead Load Bending Moment

The non-composite dead load analysis results for the Girder 4 can be seen in Figure 17. Follow the steps below in order to see the results for Girder 4.

- ☛ Select the structure group: Click the **Group** button above the explorers. Click **Composite 1**. Click **Select (Unselect Everything Else)**.
- ☛ Select the result case: Click the **Results** above the explorers. Right click the **NonComposite** result case. Choose **Compound Element Forces**.

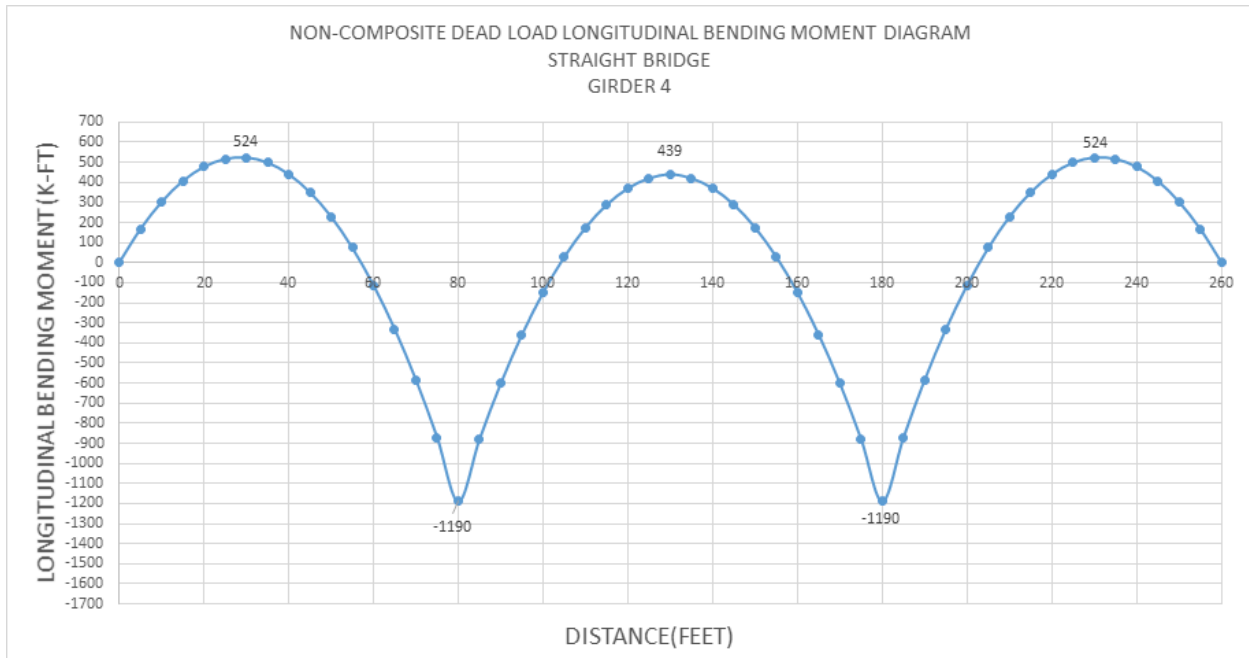


Figure 17: Girder 4 Non-composite Dead Load Bending Moment

Follow the steps below in order to see reactions.

- ☛ Select the structure group: Click the **Group** button above the explorers. Click **Bearing@0.00**. Click **Select (Unselect Everything Else)**.
- ☛ Select the result case: Click the **Results** above the explorers. Right click the **NonComposite** result case. Choose **Joint Reactions**.
- ☛ Select the structure group: Click the **Group** button above the explorers. Click **Bearing@80.00**. Click **Select (Unselect Everything Else)**.
- ☛ Select the structure group: Click the **Group** button above the explorers. Click **Bearing@180.00**. Click **Select (Unselect Everything Else)**.
- ☛ Select the structure group: Click the **Group** button above the explorers. Click **Bearing@260.00**. Click **Select (Unselect Everything Else)**.

The reactions can be seen below.

Reactions for Non-Composite Dead Load (kips)

Girder 1	Girder 2	Girder 3	Girder 4	Pier Total
----------	----------	----------	----------	------------

Pier 1	37.14	40.09	40.11	37.13	154.48
Pier 2	134.42	143.34	143.34	134.42	555.51
Pier 3	134.41	143.33	143.33	134.41	555.49
Pier 4	37.14	40.1	40.11	37.14	154.48
Girder Total	343.11	366.86	366.9	343.1	
				Bridge Total	1419.96

- ☛ Select the structure group: Click the **Group** button above the explorers. Click **Composite 1**. Click **Select (Unselect Everything Else)**.
- ☛ Select the result case: Click the **Results** above the explorers. Right click the **NonComposite** result case. Choose **Joint Displacements**.
- ☛ Select the structure group: Click the **Group** button above the explorers. Click **Composite 2**. Click **Select (Unselect Everything Else)**.

The deflections of 0.4 PT of Span 1 and the centerline of Span 2 can be seen below.

Vertical Deflections for Dead Load Non-Composite (in)

	0.4 PT of Span 1	Centerline of Span 2
Girder 3	0.49	0.51
Girder 4	0.46	0.48

The composite dead load consists of the future wearing surface and parapet load.

30 psf future wearing surface load is applied to deck plate elements as a uniform load. parapet load is calculated from the dimensions given in figure 3 and it is applied to overhang plates as uniform load with a magnitude of 10.4 psf.

- ☛ To see load spreadsheets, click the **Loads** button above the explorers. Right click the **parapet** load case and choose **Edit Loads**.
- ☛ To see loads graphically, in the menu choose **Graphics** → **Show** and turn on **Input Loads**. Then click the **Loads** button above the explorers and click the **parapet** load case.
- ☛ Select the structure group: Click the **Group** button above the explorers. Click **Composite 2**. Click **Select (Unselect Everything Else)**.
- ☛ Select the results case, click **Results**. Right click **Composite**. Click **Compound Element Forces**

The composite dead load analysis results for the Girder 3 can be seen in figure 18.

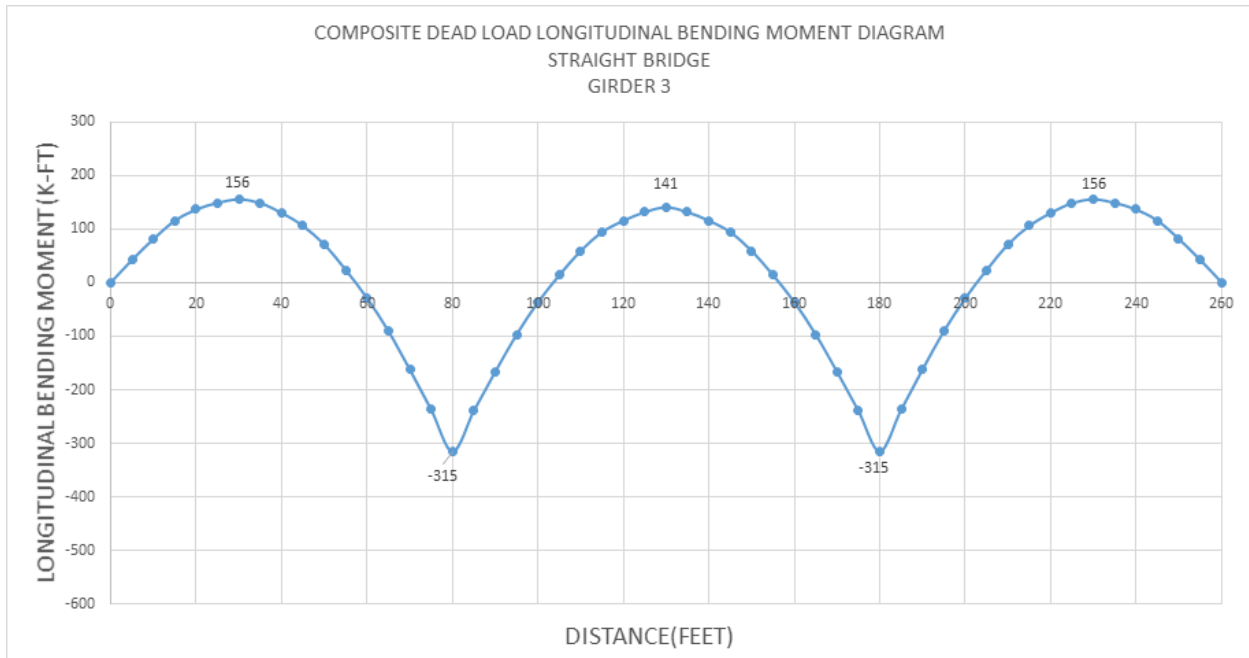


Figure 18: Girder 3 Composite Dead Load Bending Moment

- Select the structure group: Click the **Group** button above the explorers. Click **Composite 1**. Click **Select (Unselect Everything Else)**.
- Select the result case: Click the **Results** above the explorers. Right click the **Composite** result case. Choose **Compound Element Forces**.

The composite dead load analysis results for the Girder 4 can be seen in figure 19.

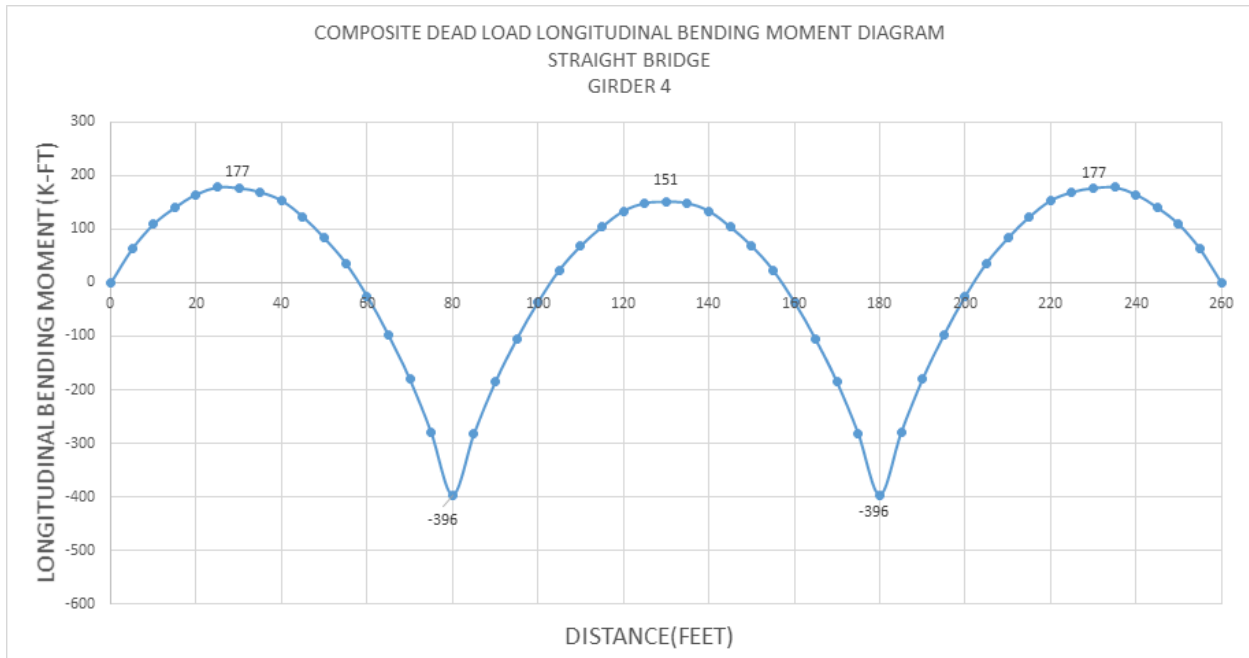


Figure 19: Girder 4 Composite Dead Load Bending Moment

The reactions can be seen below.

- ☛ Select the structure group: Click the **Group** button above the explorers. Click **Bearing@0.00**. Click **Select (Unselect Everything Else)**.
- ☛ Select the result case: Click the **Results** above the explorers. Right click the **Composite** result case. Choose **Joint Reactions**.
- ☛ Select the structure group: Click the **Group** button above the explorers. Click **Bearing@80.00**. Click **Select (Unselect Everything Else)**.
- ☛ Select the structure group: Click the **Group** button above the explorers. Click **Bearing@180.00**. Click **Select (Unselect Everything Else)**.
- ☛ Select the structure group: Click the **Group** button above the explorers. Click **Bearing@260.00**. Click **Select (Unselect Everything Else)**.

Vertical Reactions Composite Dead Load (kips)

	Girder 1	Girder 2	Girder 3	Girder 4	Pier Total
Pier 1	14.17	9.06	9.04	14.18	46.45
Pier 2	48.47	32.7	32.7	48.46	162.33
Pier 3	48.47	32.7	32.7	48.46	162.33
Pier 4	14.17	9.06	9.04	14.18	46.45
Girder Total	125.27	83.52	83.49	125.28	
				Bridge Total	417.56

The deflections of 0.4 PT of Span 1 and the centerline of Span 2 can be seen below

- ☛ Select the structure group: Click the **Group** button above the explorers. Click **Composite 1**. Click **Select (Unselect Everything Else)**.
- ☛ Select the result case: Click the **Results** above the explorers. Right click the **Composite** result case. Choose **Joint Displacements**.
- ☛ Select the structure group: Click the **Group** button above the explorers. Click **Composite 2**. Click **Select (Unselect Everything Else)**.

Vertical Deflections Composite Dead Load (in)

	0.4 PT of Span 1	Centerline of Span 2
Girder 3	0.069	0.083
Girder 4	0.086	0.099

2) Influence Surface Based Live Load Analysis

2.1) Live Load Definitions

HS25-44 truck and lane loading will be applied according to AASHTO LFD. We will use the influence surface based result cases in LARSA 4D for simulating following conditions.

- 1 - HS25-44 Truck Only
- 2 - For Positive Moment: Concentrated Load (22.5 Kips) + Lane (0.8 kips/ft)
- 3 - For Negative Moment: Concentrated Load Pair (2 x 22.5 Kips) + Lane (0.8 kips/ft)
- 4 - For Shear: Concentrated Load (32.5 Kips) + Lane (0.8 kips/ft)

LARSA4D will find the worst case live load positioning for the result cases using the conditions above.

2.2) Influence Surface Result Case Settings

Influence based result case definition consists of general loading parameters, vehicular loading options and uniform/patch loading options.

General loading parameters include design lane width, overall factor and multiple presence factors along with other options. The overall factor defined on General Options parameters tab applies to both vehicular and lane loading. However the factor defined in vehicular tab applies to vehicle loads only.

General options for influence surface result cases will be defined as shown in figure 21.

The design lane width is 12 feet.

Multiple presence factors are 1.00 for 1 lane and 2 lanes loaded, 0.90 for 3 lanes loaded, and 0.75 for 4 or more lanes loaded.

Overall factor is entered as 1.232 and detailed explanation is below.

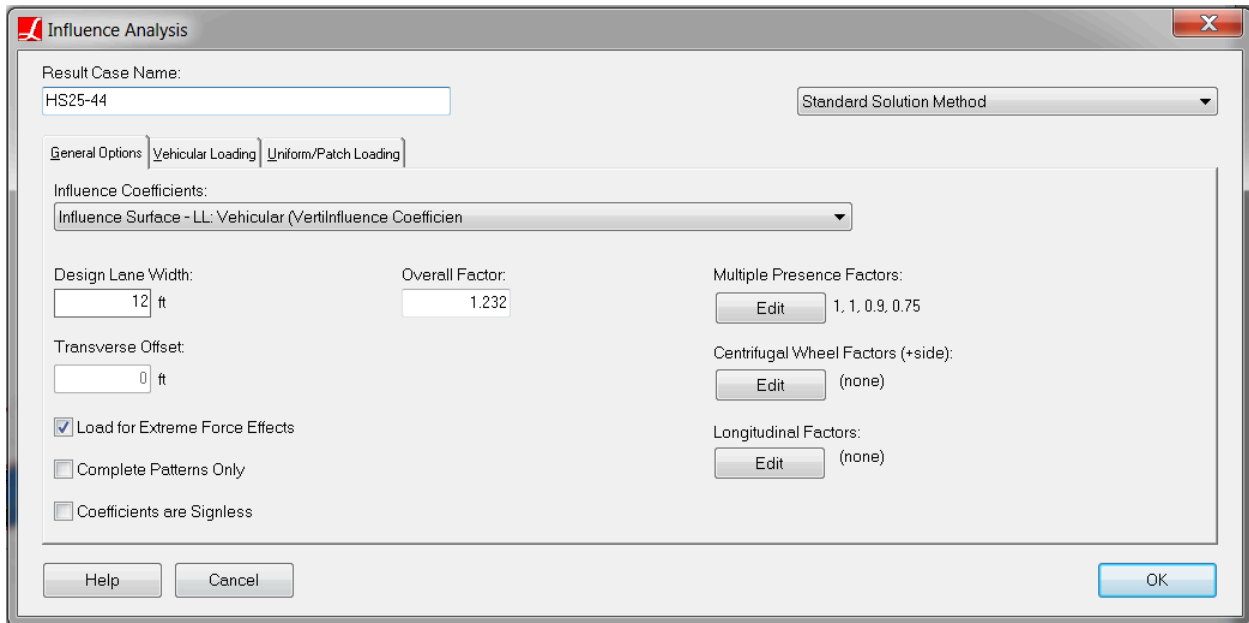


Figure 21: General Settings of Influence Surface Result Case

LARSA 4D provides the ability for the user to enter different impact factors for every span as longitudinal factors. In our example for 80 feet span, the impact factor is calculated as $0.244 = 50 / (L + 125)$ where $L = 80$ feet (span length) and for 100 feet span, impact factor is calculated as $0.222 = 50 / (L + 125)$ where $L = 100$ feet (span length). These factors can be entered as the longitudinal factors using the stations along the control centerline as in figure 22.

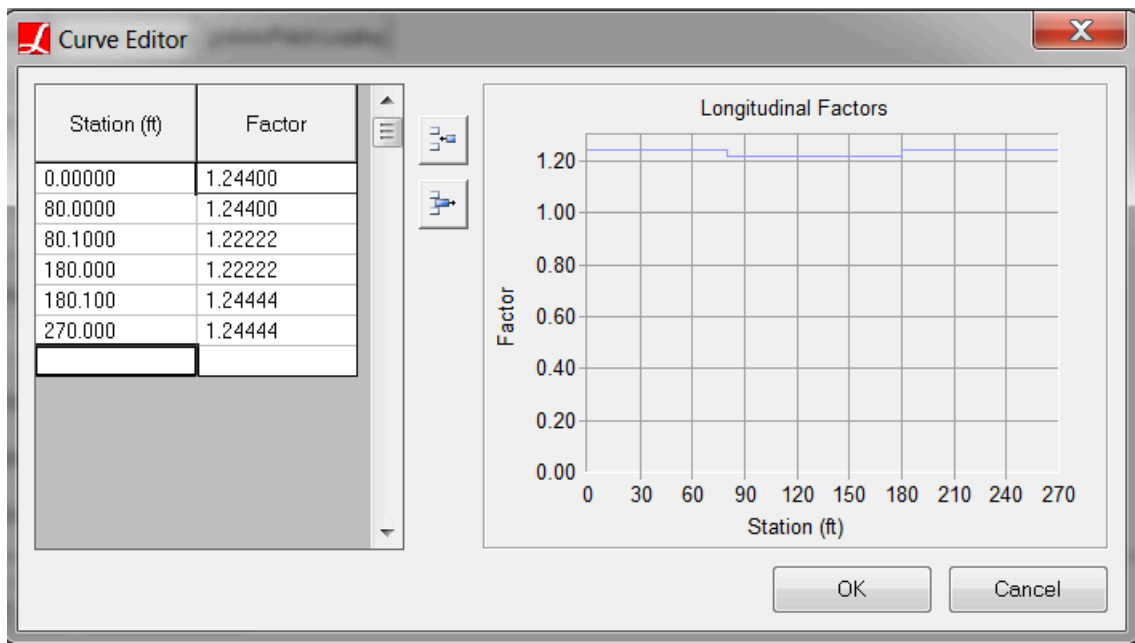


Figure 22: Impact factors as longitudinal factors

In this example the variation of impact factors is less than 1% and for simplicity it will be ignored. An average 90 feet span length is used in impact factor calculation and it is calculated as 0.232. Overall factor is entered as 1.232 (1.00 + Impact factor) for all influence surface cases as seen in figure 21.

In LFD, the impact factor is applied to the entire live load. In LRFD, dynamic load allowance is applied only to the design truck and design tandem. For this reason LARSA4D has options for entering different live load factors for vehicles and lane loading. The overall factor entered in General Options tab is for entire live load and suitable for LFD loading. Factor entered in Vehicular Loading tab is applied to the vehicle only (doesn't effect the lane loading), and it is suitable for LRFD loading.

Vehicle loading factor is entered as 1.00 for all 4 cases. UDL factor is entered as 0.00 for HS25-44 truck only case since the AASHTO LFD doesn't require the lane loading and truck loading together. For the remaining 3 cases, UDL factor is entered as 1.

The design lane vehicle margin is entered as 2 feet.

Vehicular Loading tabs for all 4 cases can be seen in Figure 23.

LARSA 4D Sample and Verification Problems

Influence Analysis

Result Case Name: HS25-44 Standard Solution Method

General Options | Vehicular Loading | Uniform/Patch Loading

Add Lane Type | Add Vehicle | X

Lane Type, UDL Factor: 0
HS25-44 Truck (Factor: 1.23255814)

Vehicle Load Pattern: HS25-44 Truck

Factor: 1.23255 Max #:

One Load Pattern Per Span

Min. Back-to-Front Spacing: ft
Design Lane Vehicle Margin: ft
Min. Side-to-Side Spacing: ft
Vehicle Direction: Any

Lane Options: Max Lanes: No Limit UDL Factor: 0

Lane Transverse Constraints: Min: ft Max: ft

Help Cancel OK

Influence Analysis

Result Case Name: Concentrated Load(22.5 Kips) + Lane(0.8 kips/ft) Standard Solution Method

General Options | Vehicular Loading | Uniform/Patch Loading

Add Lane Type | Add Vehicle | X

Lane Type
AASHTO Point 22.5kip (for moment) (Factor: 1.23255814)

Vehicle Load Pattern: AASHTO Point 22.5kip (for moment)

Factor: 1.23255 Max #:

One Load Pattern Per Span

Min. Back-to-Front Spacing: ft
Design Lane Vehicle Margin: ft
Min. Side-to-Side Spacing: ft
Vehicle Direction: Any

Lane Options: Max Lanes: No Limit UDL Factor: 1

Lane Transverse Constraints: Min: ft Max: ft

Help Cancel OK

Influence Analysis

Result Case Name: Concentrated Load(32.5 Kips) + Lane(0.8 kips/ft) Standard Solution Method

General Options | Vehicular Loading | Uniform/Patch Loading

Add Lane Type | Add Vehicle | X

Lane Type
AASHTO Point 32.5kip (for shear) (Factor: 1.23255814)

Vehicle Load Pattern: AASHTO Point 32.5kip (for shear)

Factor: 1.23255 Max #:

One Load Pattern Per Span

Min. Back-to-Front Spacing: ft
Design Lane Vehicle Margin: ft
Min. Side-to-Side Spacing: ft
Vehicle Direction: Any

Lane Options: Max Lanes: 407 UDL Factor: 1

Lane Transverse Constraints: Min: ft Max: ft

Help Cancel OK

Influence Analysis

UDL load magnitude is entered as 0.8 kip/ft along with UDL width per design lane as 10 ft according to AASHTO LFD and a screenshot from LARSA 4D can be seen in the figure 24.

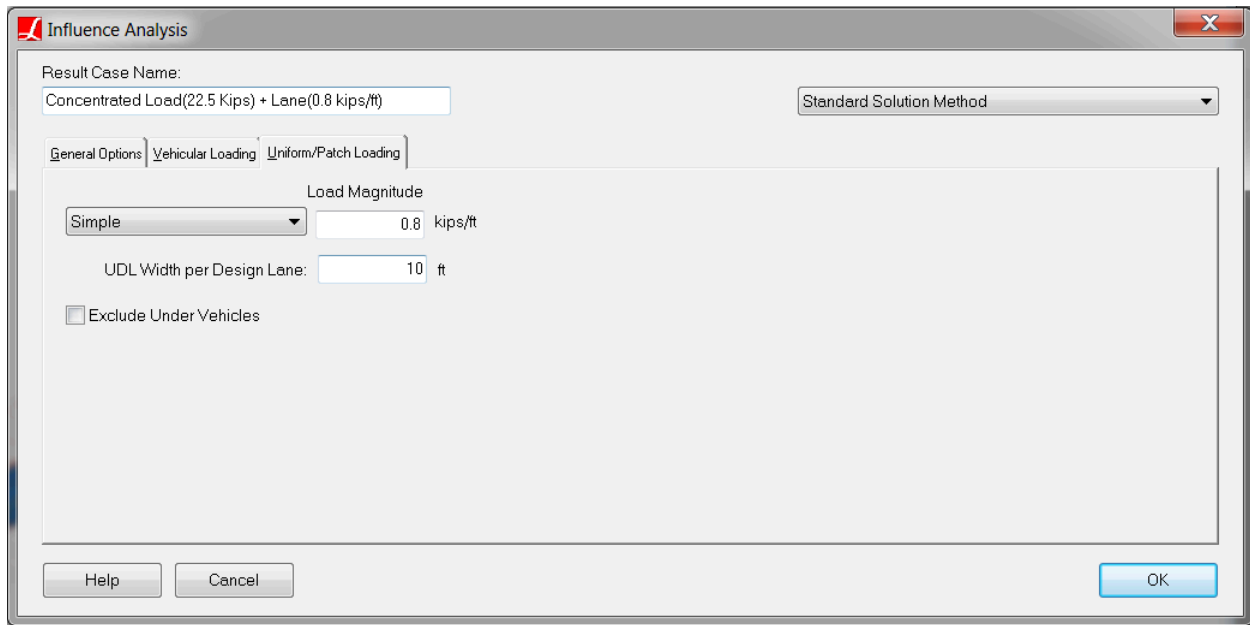


Figure 24: Lane Load Settings of Influence Surface Result Case

Follow the steps below in order to view influence surface result case settings shown above.

- ☛ Select the result case: Click the **Results** above the explorers. Right click the **HS25-44** result case. Choose **Properties**.
- ☛ Select the result case: Click the **Results** above the explorers. Right click the **Concentrated Load (22.5 Kips)** result case. Choose **Properties**.
- ☛ Select the result case: Click the **Results** above the explorers. Right click the **Concentrated Load (32.5 Kips) + Lane (0.8 kips/ft)** result case. Choose **Properties**.
- ☛ Select the result case: Click the **Results** above the explorers. Right click the **Concentrated Load Pair (22.5 Kips) + Lane (0.8 kips/ft)** result case. Choose **Properties**.

2.3) Live Load Analysis Results

In order to see the force effect on each girder, LARSA 4D's compound element force tool will be used. Compound element forces report the combined forces and moments of a group of elements regards to their combined centroid. These results are used to determine the forces in a girder modeled not as a single beam but as a group of elements. Since our deck is modeled with plate elements and the girder with beam and plate elements, the compound element forces tool will be used to find the forces for composite section. With the help of this tool, the user can see the force effects on each girder directly.

Thus AASHTO Section 3, Part C, Distribution of Loads is not applicable for this type of refined modelling therefore the results reported do not require girder distribution factors to be used.

In this example, we will be using extreme effect groups to extract envelope of forces. Extreme effect groups represent the worst-case scenario from a set of result cases, similar to envelopes, but are saved as new result cases. For positive

moment, extreme effect group named 'Positive Moment' is created and includes result cases corresponding truck alone (HS25-44) and lane load for positive moment (Concentrated Load (22.5 Kips) + Lane).

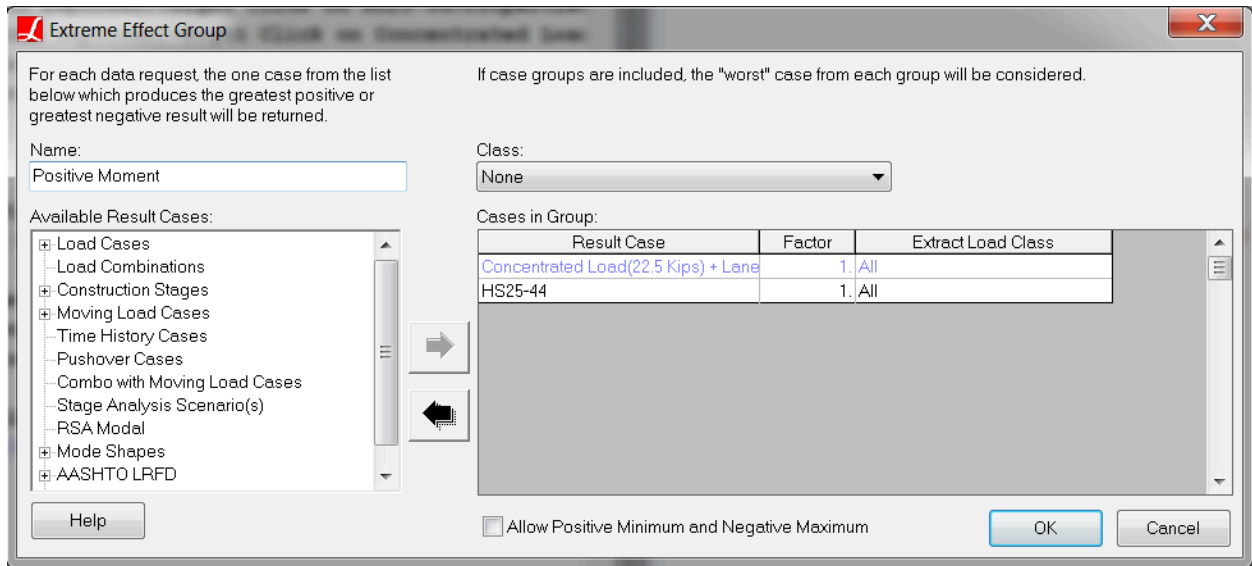


Figure 25: Extreme Effect Group For Positive Moment

For negative moment, extreme effect group named "Negative Moment" is created and includes result cases corresponding truck alone (HS25-44) and lane load for negative moment (Concentrated Load Pair (22.5 Kips) + Lane).

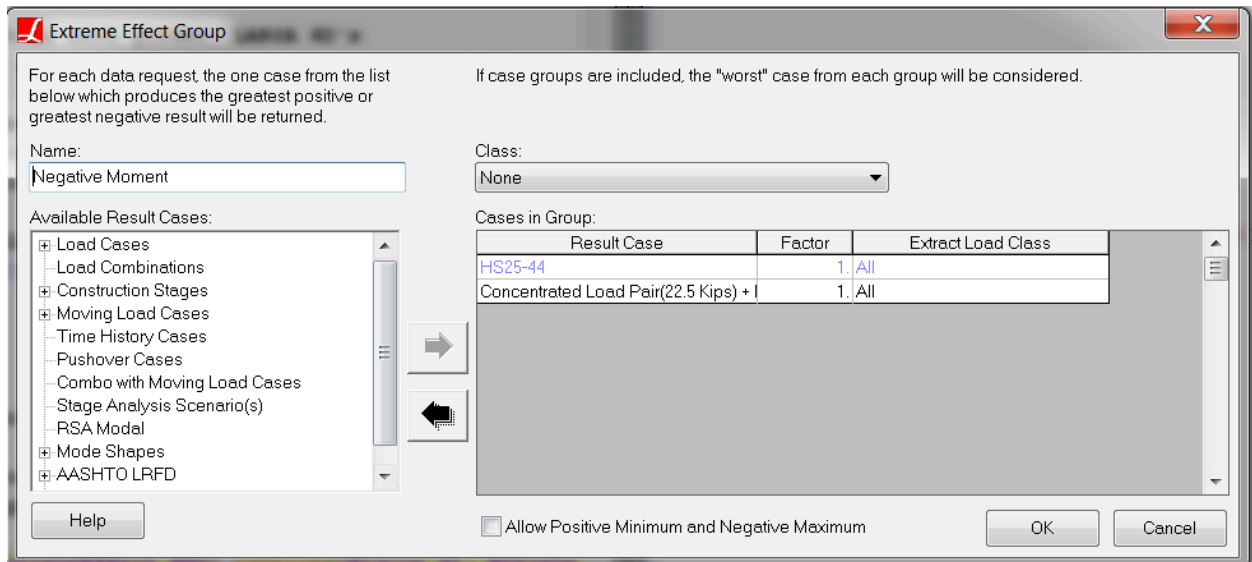


Figure 26: Extreme Effect Group For Negative Moment

For shear , extreme effect group named "Shear" is created and includes result cases corresponding truck alone (HS25-44) and lane load for shear (Concentrated Load (32.5 Kips) + Lane).

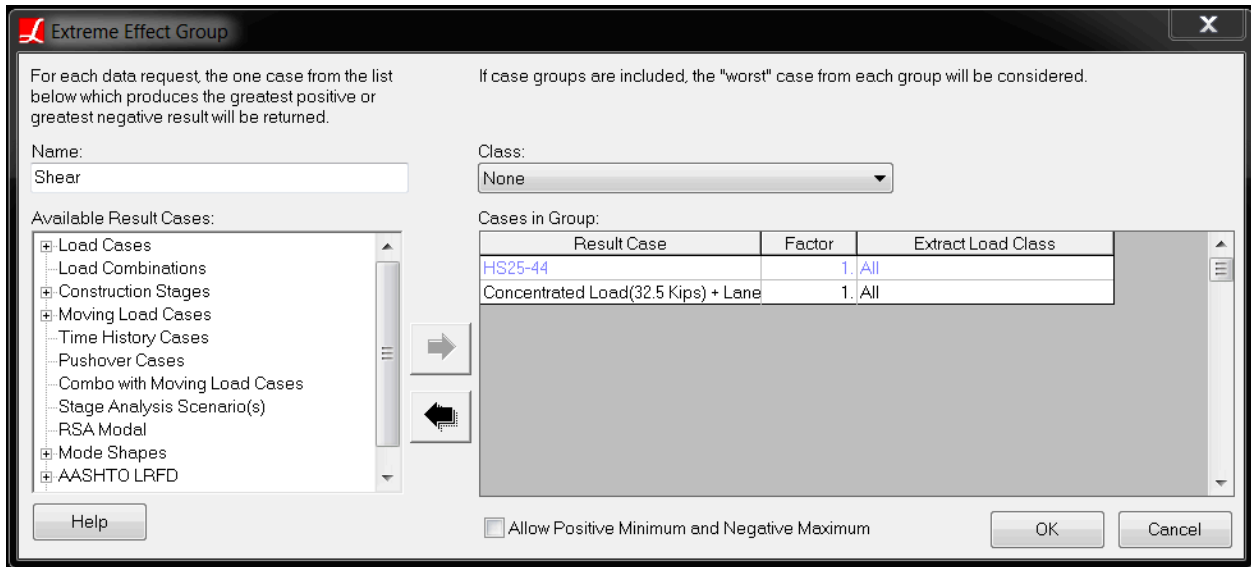


Figure 27: Extreme Effect Group For Shear

Bending moment results for girder 3 is shown in figure 28.

Follow the steps below in order to see bending moment results for Girder 3.

- Select the structure group: Click the **Group** button above the explorers. Click **Composite 2**. click **Select (Unselect Everything Else)**.
- Select the result case: Click the **Results** above the explorers. Right click the **Positive Moment** result case. Choose **Compound Element Forces**.
- Select Envelope Max My
- Select the result case: Click the **Results** above the explorers. Right click the **Negative Moment** result case. Choose **Compound Element Forces**.
- Select Envelope Min My

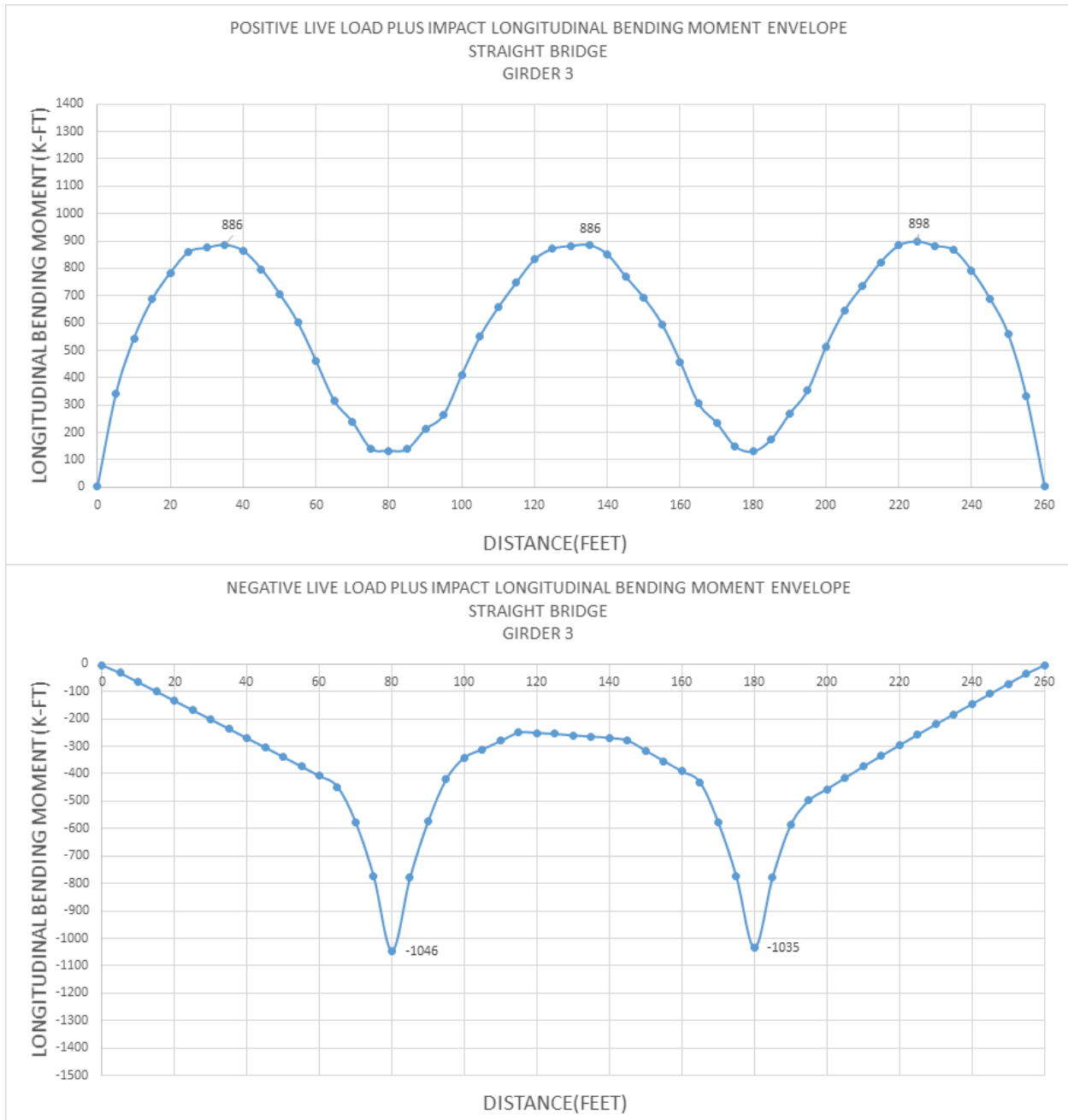


Figure 28: Girder 3 Bending Moment

Bending moment results for girder 4 is shown in figure 29. Follow the steps below in order to see bending moment results for Girder 4.

- ☛ Select the structure group: Click the **Group** button above the explorers. Click **Composite 1**. click **Select (Unselect Everything Else)**.
- ☛ Select the result case: Click the **Results** above the explorers. Right click the **Positive Moment** result case. Choose **Compound Element Forces**.
- ☛ Select Envelope Max My

☛ Select the result case: Click the **Results** above the explorers. Right click the **Negative Moment** result case. Choose **Compound Element Forces**.

☛ Select Envelope Min My

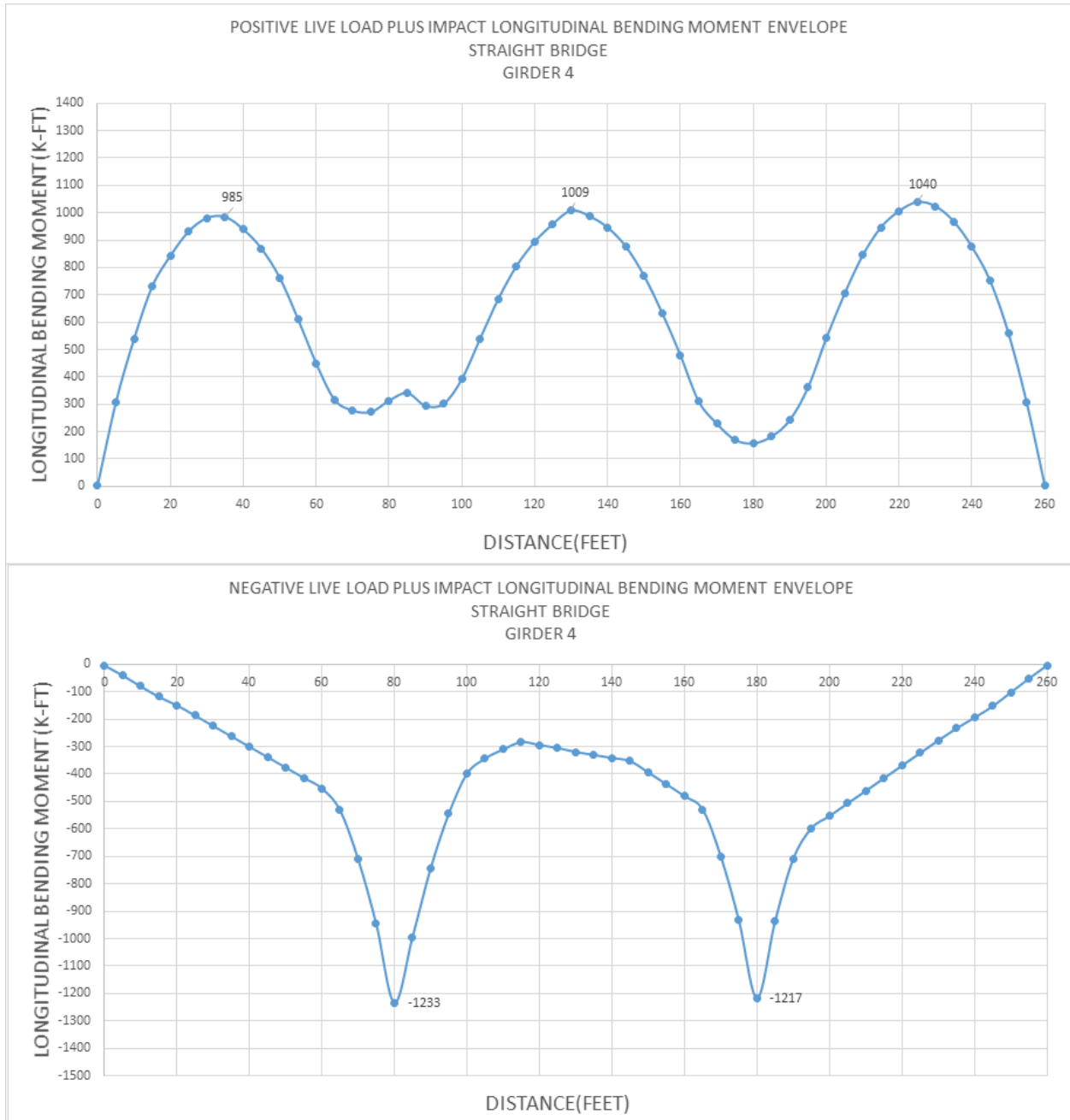


Figure 29: Girder 4 Bending Moment

Critical reactions at supports are tabulated below. Follow the steps below in order to display live load reaction forces.

☛ Select the structure group: Click the **Group** button above the explorers. Click **Bearing@0.00**, click **Select (Unselect Everything Else)**.

- ☛ Select the result case: Click the **Results** above the explorers. Right click the **Shear** result case. Choose **Joint Reactions**.
- ☛ Select Envelope Max Fz
- ☛ Select the structure group: Click the **Group** button above the explorers. Click **Bearing@80.00**. click **Select (Unselect Everything Else)**.
- ☛ Select the structure group: Click the **Group** button above the explorers. Click **Bearing@180.00**. click **Select (Unselect Everything Else)**.
- ☛ Select the structure group: Click the **Group** button above the explorers. Click **Bearing@260.00**. click **Select (Unselect Everything Else)**.

Live Load Vertical Reactions (kips)

	Girder 1	Girder 2	Girder 3	Girder 4
Pier 1	68.29	86.51	86.51	68.08
Pier 2	118.91	138.53	138.41	118.42
Pier 3	115.54	137.98	137.87	114.99
Pier 4	68.32	84.36	84.20	68.03

The maximum tensile and compressive forces for the cross-frames at the center of span 2 between girder 2 and 3 are tabulated below.

Follow the steps below in order to see axial force for live load.

- ☛ Select the structure group: Click the **Group** button above the explorers. Click **_Cross-frame G3-G2@130**. click **Select (Unselect Everything Else)**.
- ☛ Select all 3 result cases: Click the **Results** above the explorers. Right click the **Positive Moment** result case. Choose **Member Sectional Forces**. Press **CTRL** on the keyboard and click **Negative Moment**, **Shear** result cases.
- ☛ Select Envelope Fx

Cross Frame Axial Force At Center Of Span 2 Between Girder 2-3 Due to Live Load (kips)

	Bottom Chord	Diagonals
Tension	7.57	16.49
Compression	-5.51	-11.29

Bottom flange lateral moments for girder 3 and 4 can be seen below.

Bottom Flange Lateral Moment Due to Live Load (kips.ft)

	Pier 2	Center of Span 2
Girder 3	3.39	1.71
Girder 4	3.97	2.21

- ☛ Select the structure group: Click the **Group** button above the explorers. Click **Girder B Bottom Flange**. Click **Select (Unselect Everything Else)**.
- ☛ Select all 3 result cases: Click the **Results** above the explorers. Right click the **Positive Moment** result case. Choose **Member Sectional Forces**. Press **CTRL** on the keyboard and click **Negative Moment**, **Shear** result cases.
- ☛ Select Envelope My

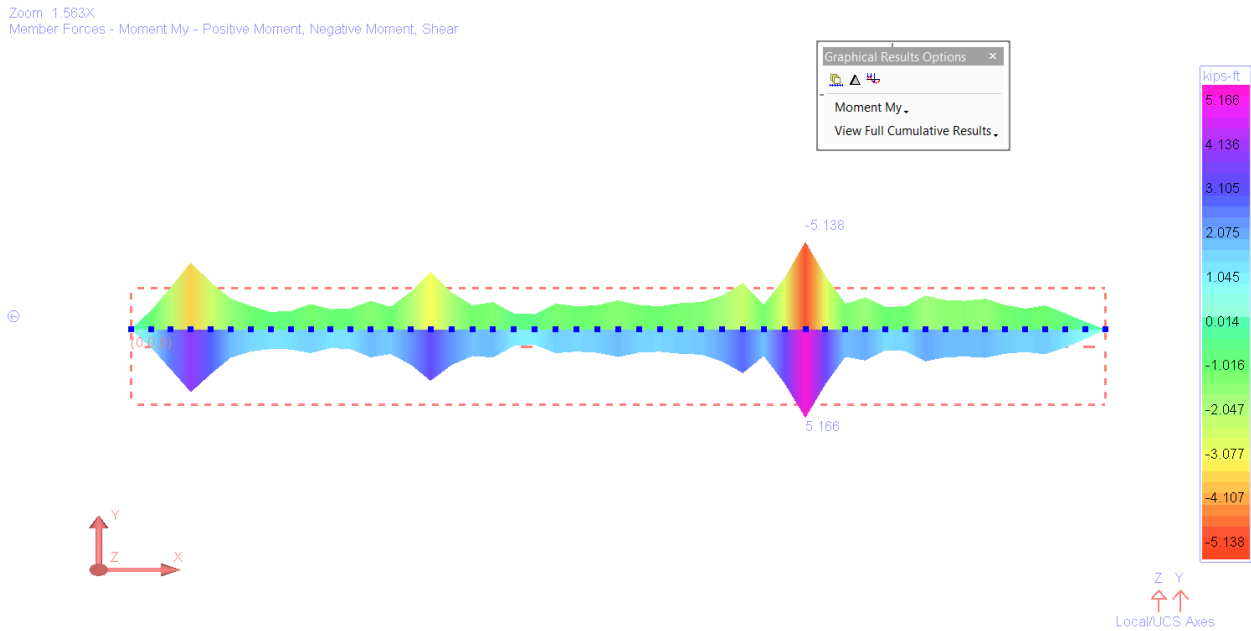


Figure 30: Girder 3 Bottom Flange Lateral Moments

- ☛ Select the structure group: Click the **Group** button above the explorers. Click **Girder A Bottom Flange**. Click **Select (Unselect Everything Else)**.
- ☛ Select all 3 result cases: Click the **Results** above the explorers. Right click the **Positive Moment** result case. Choose **Member Sectional Forces**. Press **CTRL** on the keyboard and click **Negative Moment**, **Shear** result cases.
- ☛ Select Envelope My

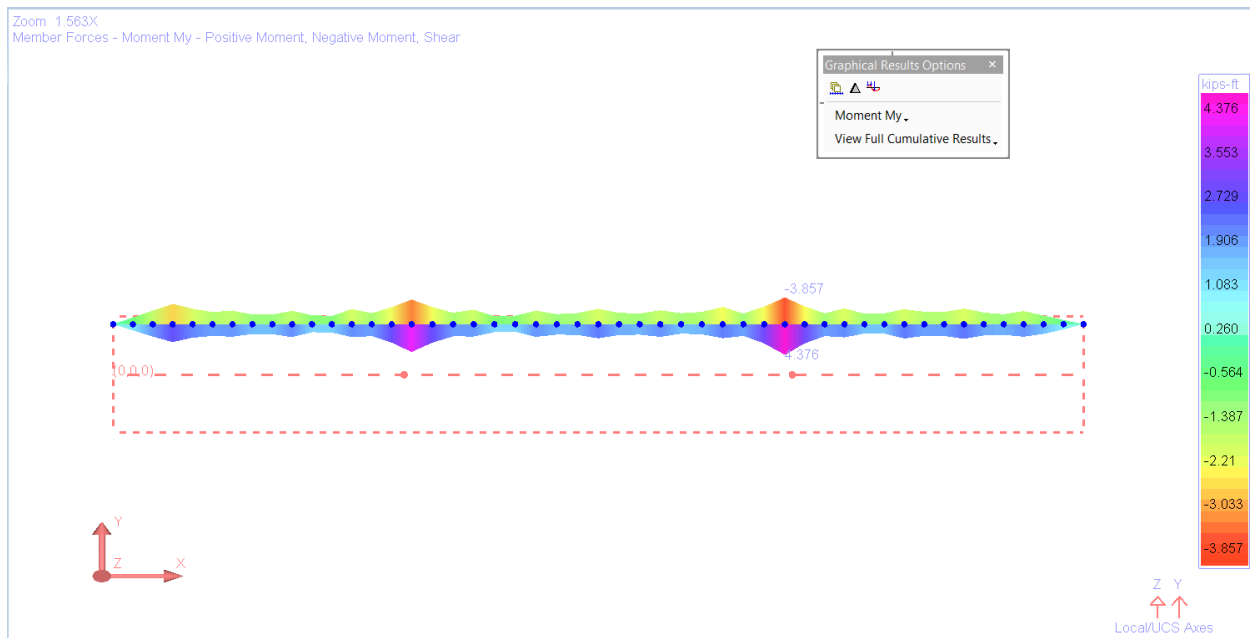


Figure 31: Girder 4 Bottom Flange Lateral Moments

SBD07: Curved Steel Plate Girder Bridge With 60 Degree Skew (LFD)

Featuring a 60 degree skew, the bridge chosen for this example is a two-lane steel plate girder bridge with identical four-girder cross-sections. This curved bridge, featuring a 500 feet radius, is three-span continuous over span lengths of 80, 100, and 80 feet, along the control centerline. The live load results are reported for HS25-44 and lane loading using influence surface analysis.

Example Project: The example described here can be found in the Steel Bridge Module folder of your LARSA 4D Samples directory (generally My Documents\LARSA Projects\Samples) in the file SBD07.

Problem Details

The bridge layout is shown in Figure 1.

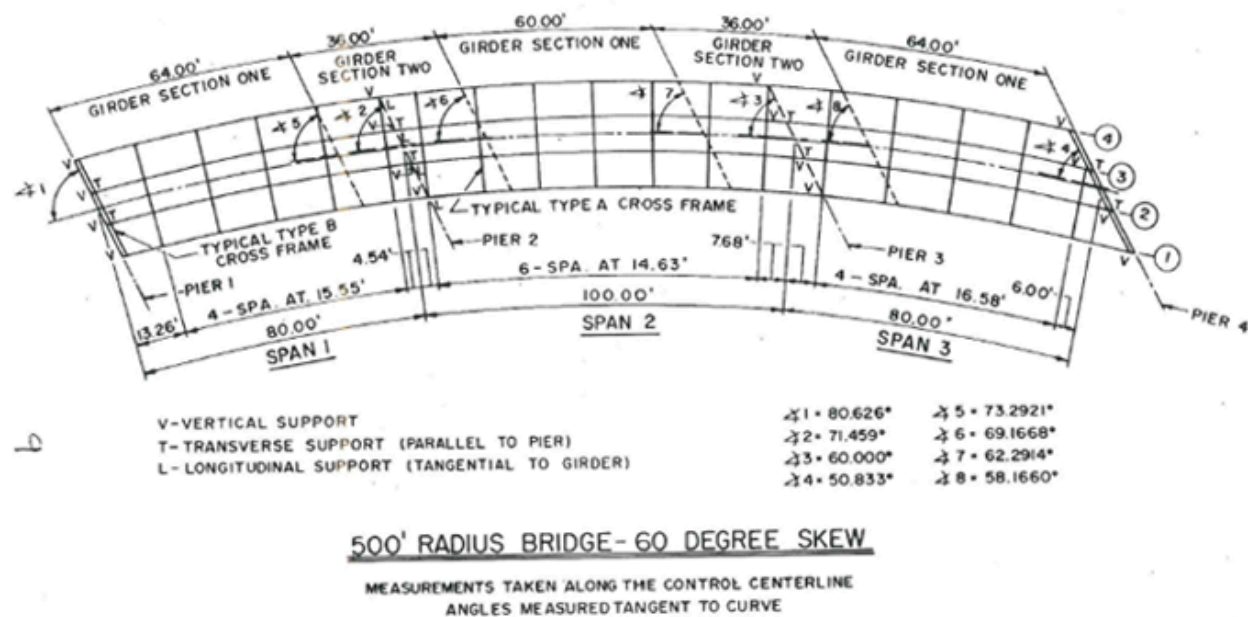


Figure 1: Plan View

The materials used in this model are:

Steel

$E_s = 29,000$ ksi

Weight Density = 490 pcf

Steel Girders = Type A572 Steel

Cross-Frames = Type A36 Steel

Concrete

$E_c = 3,820$ ksi

Weight Density = 150 pcf (which includes allowance for steel reinforcement)

$f_c' = 4.5$ ksi

$n = 8$

The deck slab thickness is 9 inches, as shown in Figure 2, including the 1/2-inch non-structural wearing surface. The parapet dimensions and deck overhang details are given in Figure 3.

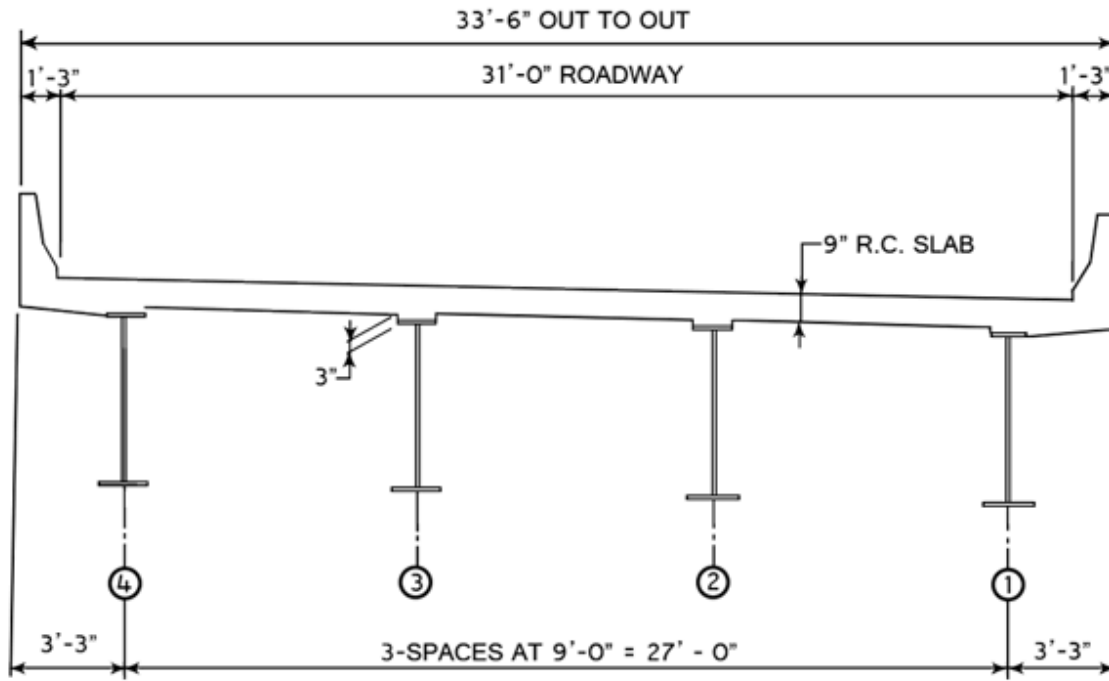


Figure 2: Typical Cross-Section

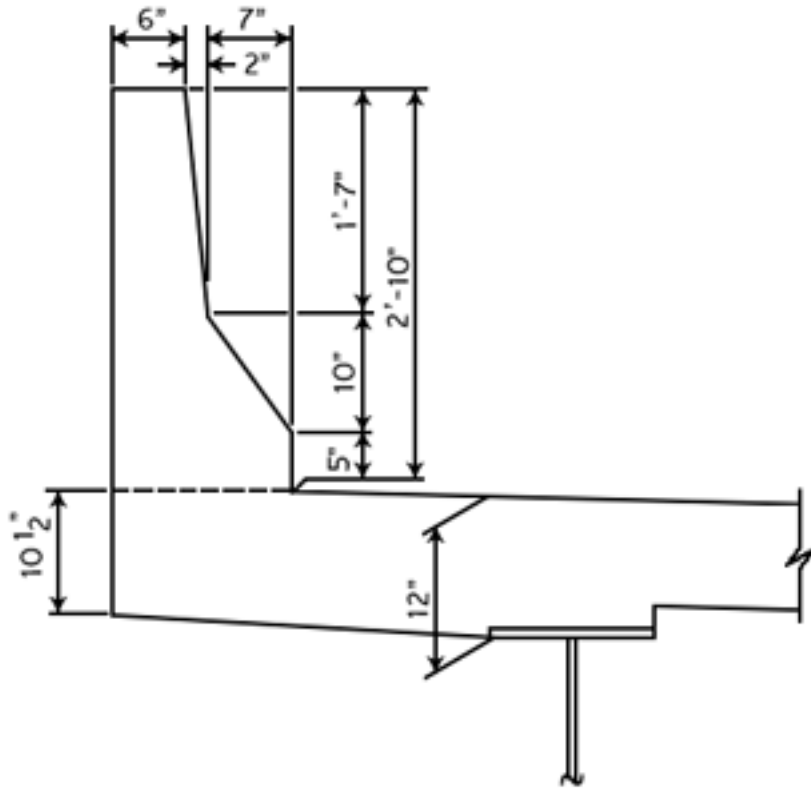


Figure 3: Parapet and Deck Overhang Detail

The plate sizes for Girder Sections One and Two are given in the table below. The locations of these girder sections are shown in Figure 1.

	Section One	Section Two
Web Plate	7/16" x 60"	7/16" x 60"
Top Flange	7/8" x 14"	1 3/4" x 14"
Bottom Flange	1" x 18"	2" x 18"

There are two types of cross-frames used in this example, as seen in Figure 4. Typical intermediate cross-frames are Type A, and the cross-frames at piers 1 and 4 are Type B. Member sizes for the cross frames are given in Figure 4.

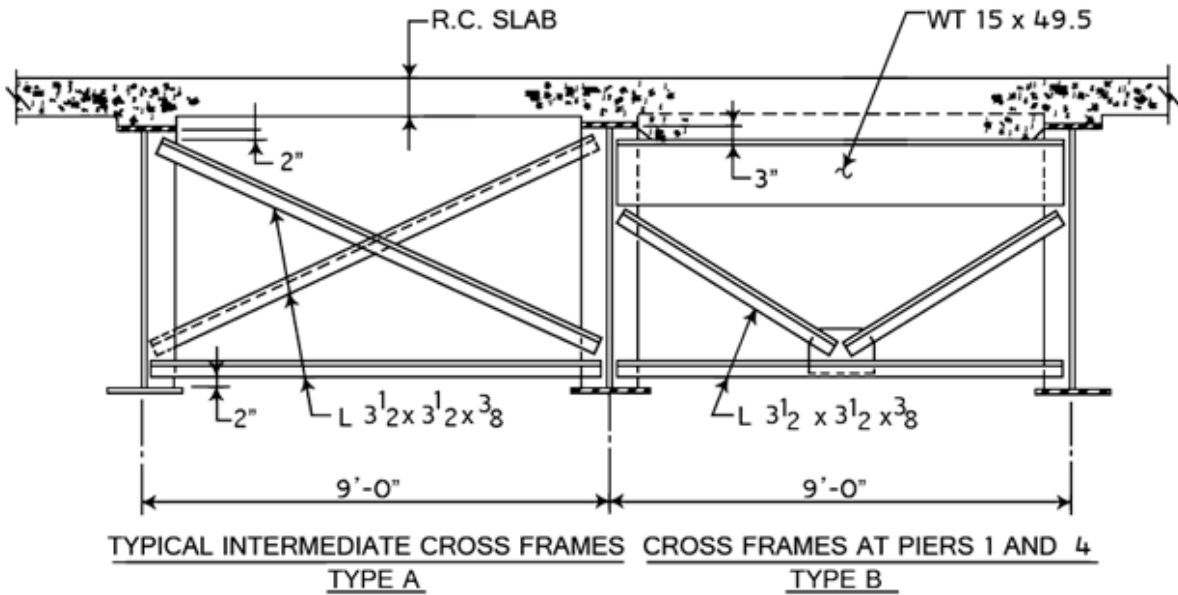


Figure 4: Cross-Frames

Dead Load

The non-composite dead load consists of all of the dead loads, except the weight of the parapet and future wearing surface. The composite dead load includes all of the dead loads.

The stay-in-place forms are 15 psf and are used between the girders, but not on the overhangs.

The future wearing surface is 30 psf and placed between the parapets.

Live Load

The live load consists of a HS25-44 truck, as shown in the figure below, and distributed lane loading.

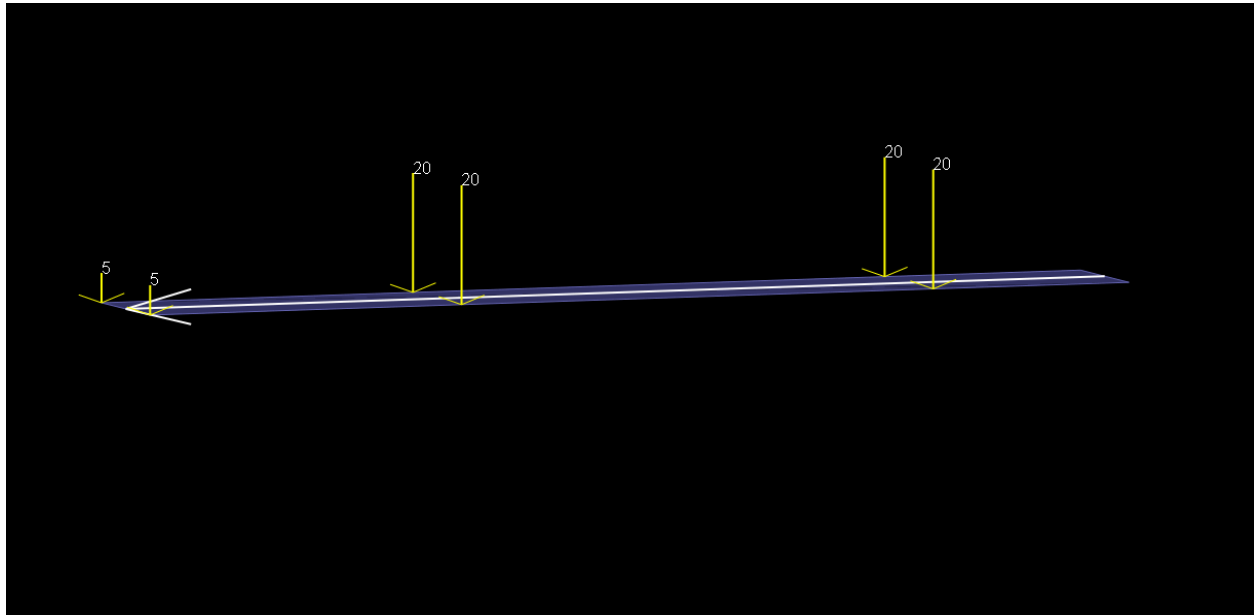


Figure 6: HS25-44 (2D)

HS25-44 (2D)		
Magnitude (kips)	Location (ft)	Transverse Offset (ft)
5	0	3
5	0	-3
20	14	3
20	14	-3
20	Varies 28 - 44	3
20	Varies 28 - 44	-3

☛ The live load pattern HS25-44 has been added to the moving load database and to review live load patterns select from the menu **Input Data** → **Edit Database**.

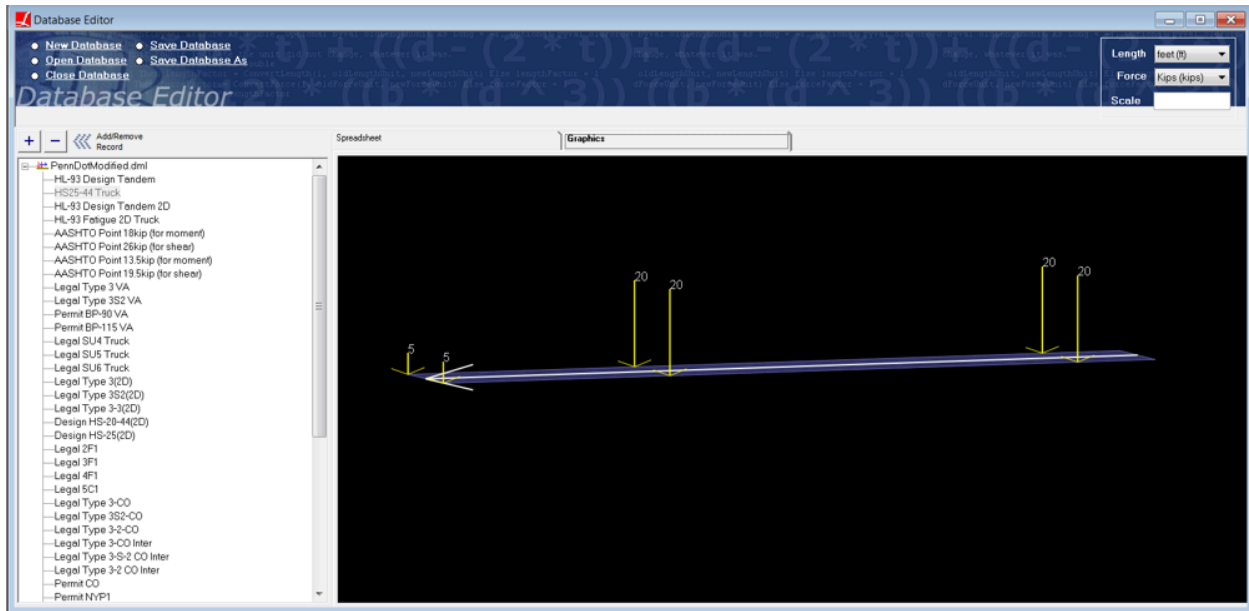


Figure 7: Moving Load Database

Model Generation

The model is created using the Steel Bridge Module within LARSA 4D BRIDGE. While this model could have been created using the graphical generation tools of LARSA 4D, the Steel Bridge Module provides a parametric approach for fast-track generation of LARSA 4D models for I, box, and tub girder steel bridges and for performing AASHTO LRFD code check and load rating on these bridges. The module is specifically developed for the special needs of skewed and/or curved bridges and bridge structures with complex geometry.

Steel I-girder sections can be represented as a single beam element or as multi-element section where the flanges are represented as beam elements and the web as shell elements. In this example, we will have I-girders modeled using a combination of member and shell elements. This modeling type allows easier extraction of lateral bending moments of the flanges. The top flange of the girder will be connected to the deck with rigid elements. The bridge deck is modeled using shell elements.

The model generated is for staged construction analysis where non-composite and composite states, deck pouring sequences are handled with ease.

The finite element model generated is displayed below.

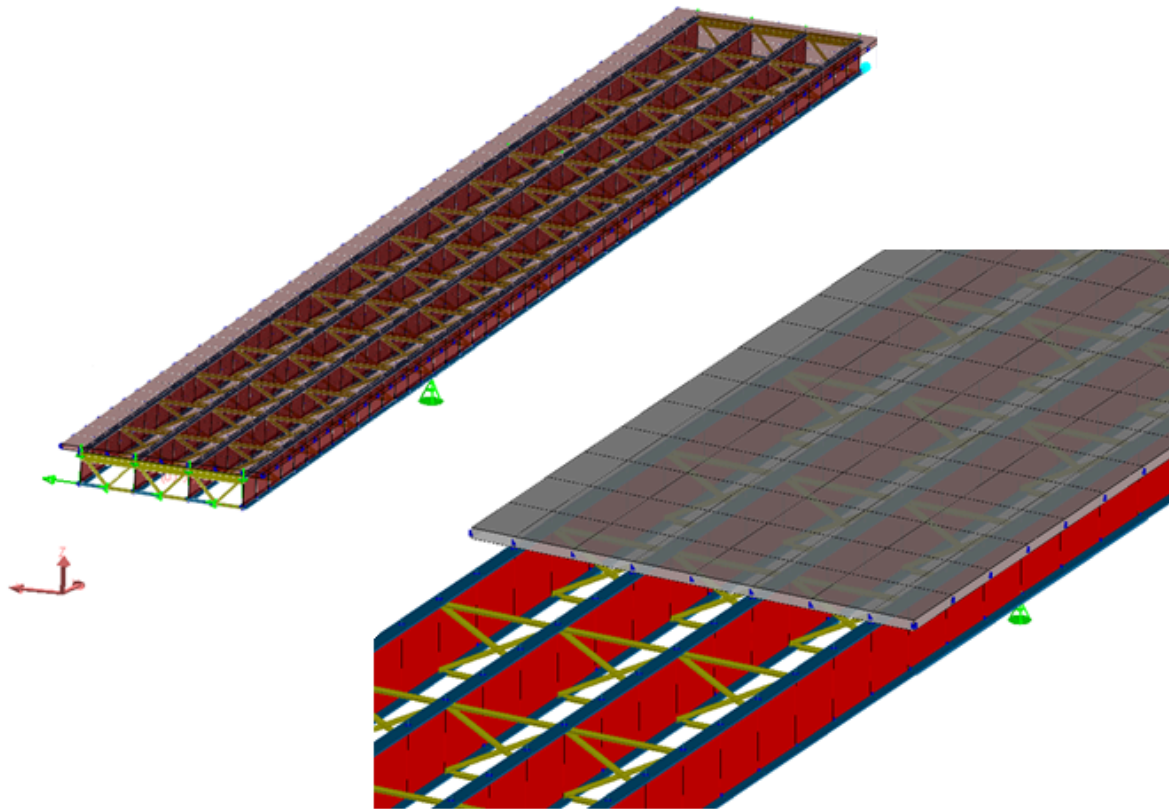


Figure 8: LARSA 4D Finite Element Model

In the first stage, girders and cross frames are constructed as seen in Figure 9.

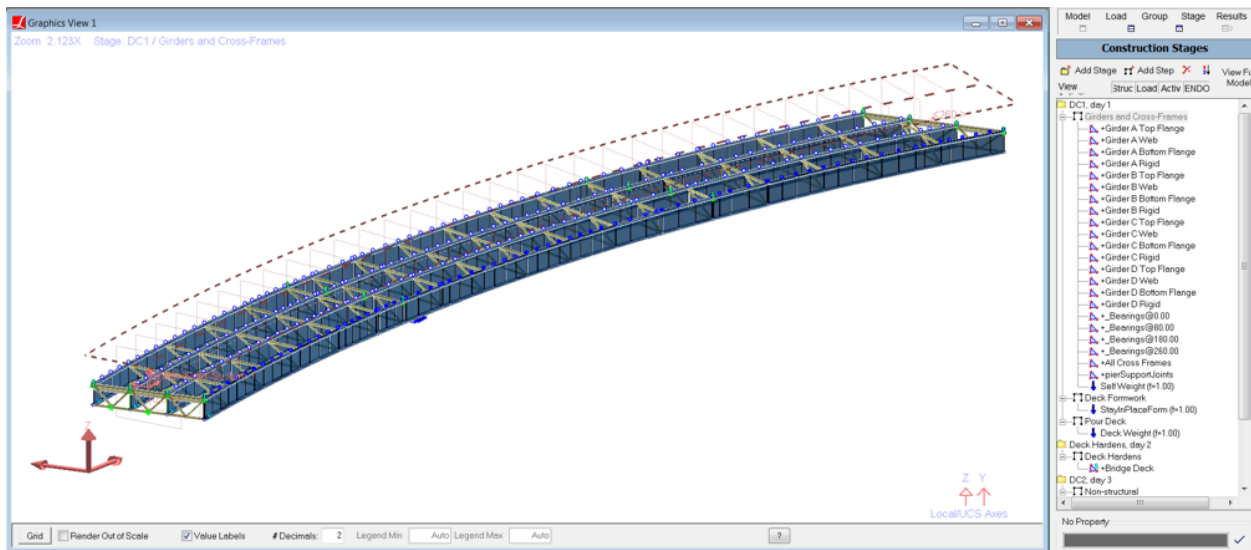


Figure 9: Stage 1-Girders and Cross Frames

In the second stage, stay-in-place form loads are applied to the girders as seen in Figure 10.

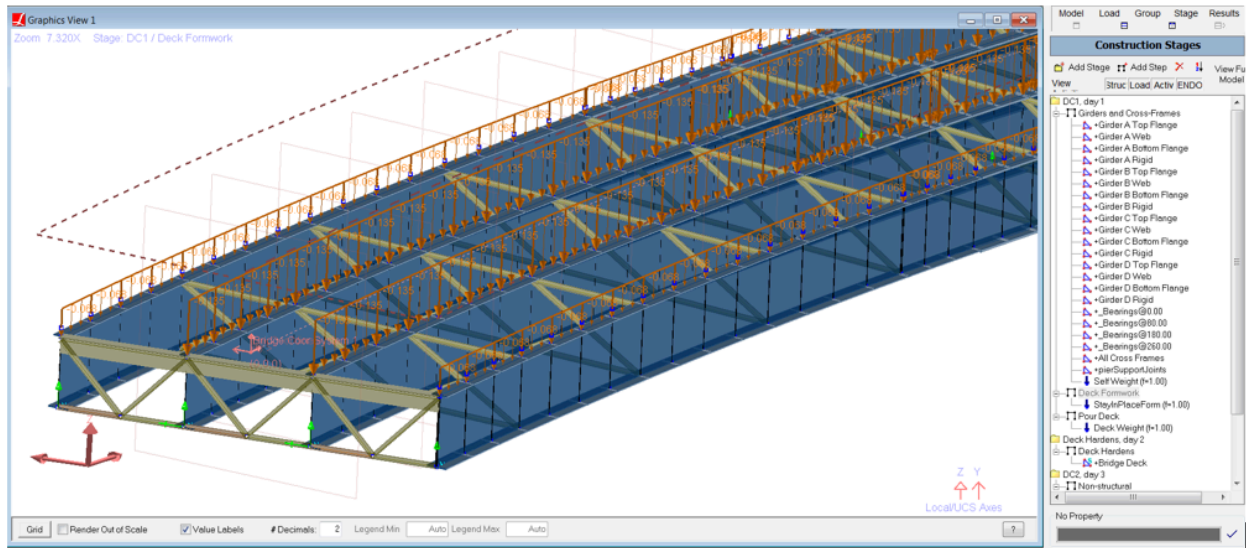


Figure 10: Stage 2-Stay in place form loads

In the third stage, the deck is poured and wet concrete loading is applied to the girders as seen in Figure 11.

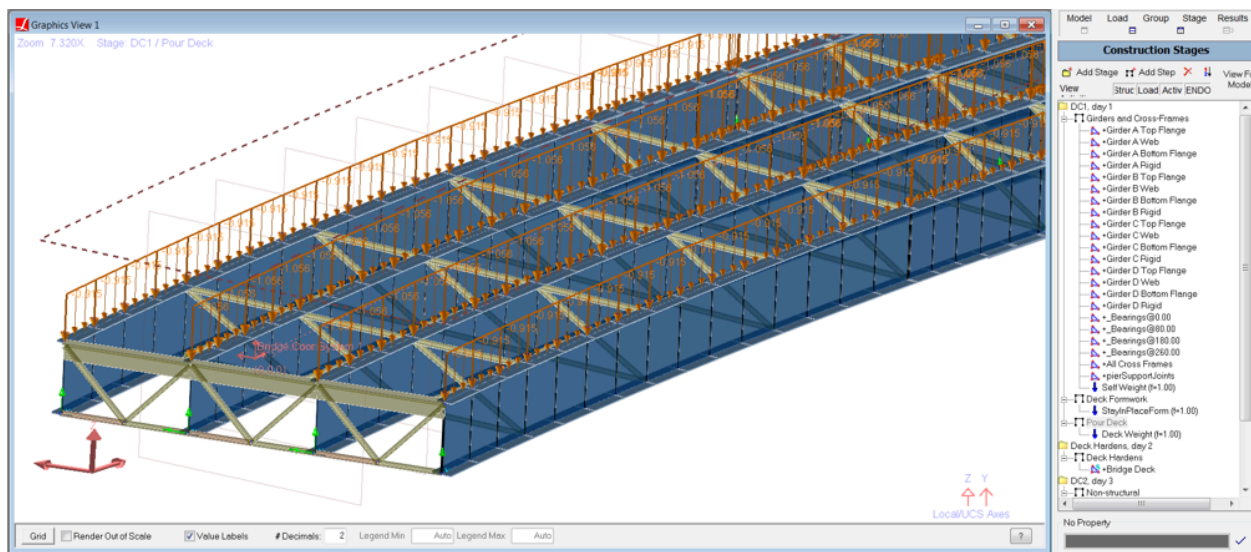


Figure 11: Stage 3-Deck Pouring

In the fourth stage, the deck gained its stiffness and deck elements are constructed with LARSA 4D's stiffness only option.

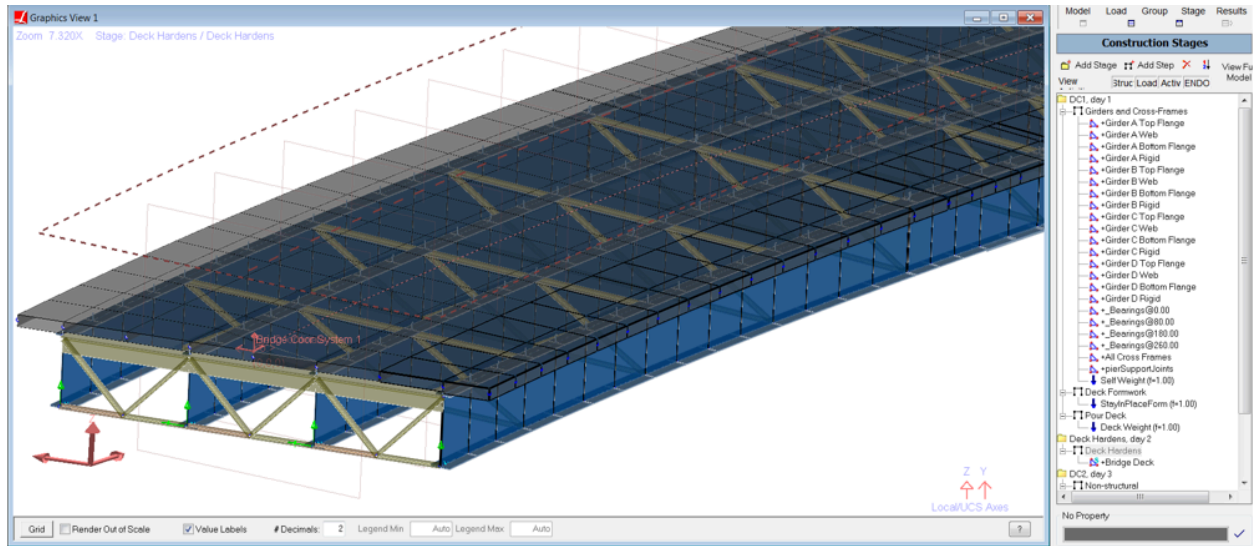


Figure 12: Stage 4-Deck Gains Stiffness

In the fifth stage, parapet loads are applied to the overhang plate elements as uniform plate load as seen in Figure 13.

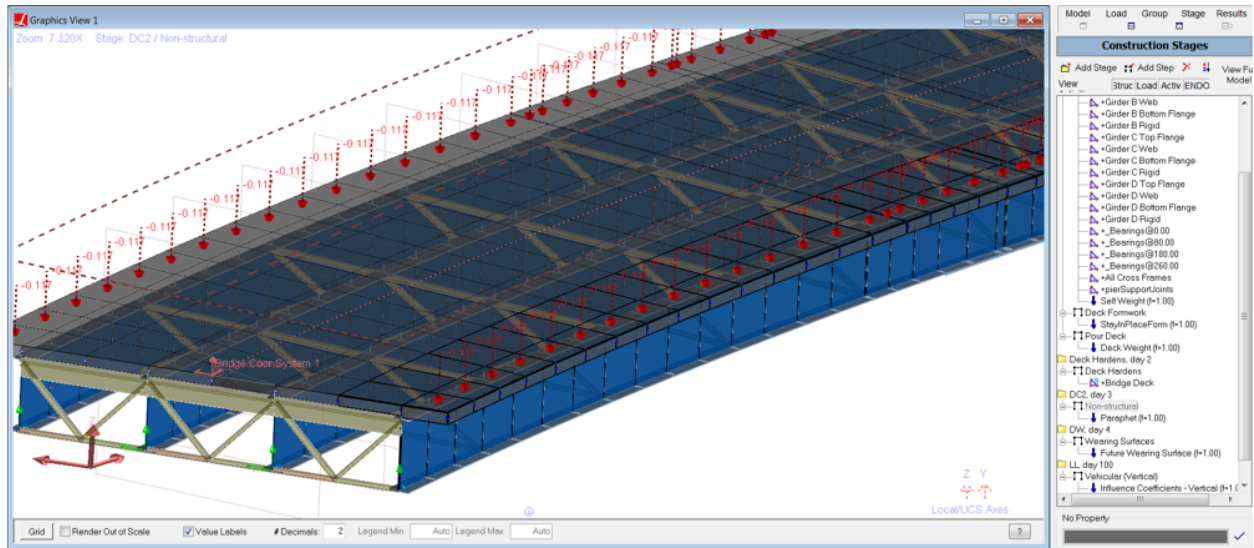


Figure 13: Stage 5-parapet

In the sixth stage, future wearing surface loads are applied to deck plate elements as seen in Figure 14.

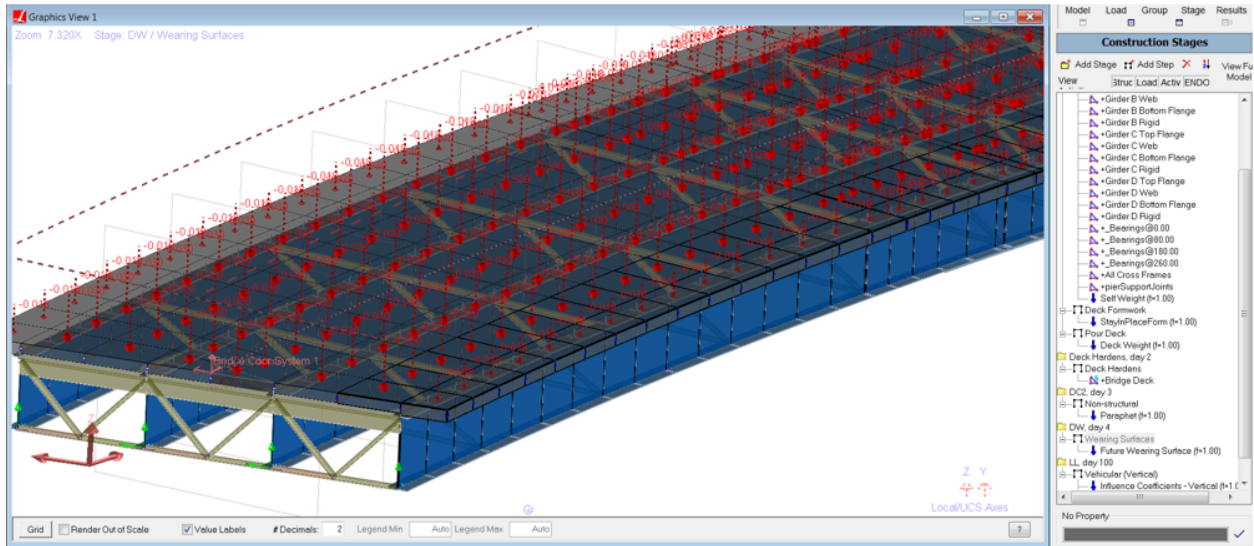


Figure 14: Stage 6-Future Wearing Surface

Modular ratio values of "n" and "3n" will be used by defining a material time effect as seen in Figure 15. In the seventh stage, the stiffness of the deck will be modified for the analysis of live load.

Properties: CEB-FIP 90

Materials / Sections / UCS / Spring Properties / Isolator Definitions / **Material Time Effects**

	Name	Creep Factor	Shrinkage Factor	Relaxation Factor	Steel Relaxation Type	Assigned
1	LRFD-3n	1.0000	1.0000	1.0000	Custom	Yes
2						

Time VS Modulus of Elasticity: LRFD-3n

Coefficients / Graph

	Time (Days)	Modulus of Elasticity (kips/ft ²)
1	1.0000	1.8336e5
2	99.0000	1.8336e5
3	100.0000	5.5008e5
4	200.0000	5.5008e5
5		

LL, day 100
 Vehicular (Vertical)
 Influence Coefficients - Vertical (f=1.00)
 Run Linear Moving Load/Influence Analysis

No Property

Figure 15: Stage 7-Influence Surface Analysis

Compound Element Result Extraction

In order to determine the forces in a girder modeled not as a single beam but as multiple elements, the compound element forces feature of LARSA 4D shall be used. Compound Element Forces reports the combined forces and moments of a group of elements about their combined centroid.

Non-Composite and Composite Dead Load Analysis Results

The non-composite dead load consists of all of the dead loads, except the weight of parapet and future wearing surface. The composite dead load includes all dead loads.

Deck weight is applied to the exterior girders as uniform member loads with a magnitude of 1.007 kips/ft.

Deck weight is applied to the interior girders as uniform member loads with a magnitude of 1.056 kips/ft.

Stay-in-place form loading is applied to the exterior girders as uniform member loads with a magnitude of 0.0675 kips/ft.

Stay-in-place form loading is applied to the interior girders as uniform member loads with a magnitude of 0.135 kips/ft.

Follow the instructions below to review the loads.

- ☛ To see load spreadsheets, click the **Loads** button above the explorers, right-click the **StayInPlaceForm** load case and choose **Edit loads**.
- ☛ To see loads graphically, choose from the menu **Graphics** → **Show** and turn on **Input Loads**. click the **Loads** button above the explorers, then click the **StayInPlaceForm** load case.

The non-composite dead load analysis results for the Girder 3 can be seen in Figure 16.

Follow the steps below in order to see the results for Girder 3.

- ☛ Select the structure group: Click the **Group** button above the explorers. Click **Composite 2**. Click **Select (Unselect Everything Else)**.
- ☛ Select the result case: Click the **Results** above the explorers. Right click the **NonComposite** result case. Choose **Compound Element Forces**.

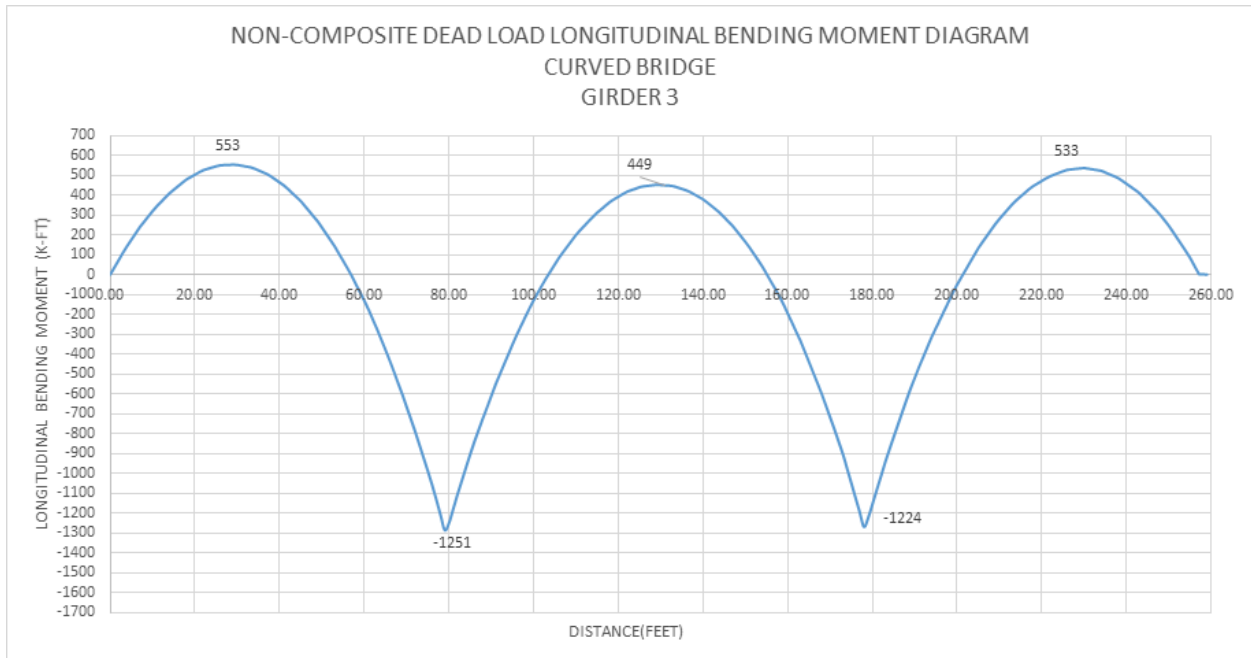


Figure 16: Girder 3 Non-composite Dead Load Bending Moment

The non-composite dead load analysis results for the Girder 4 can be seen in Figure 17. Follow the steps below in order to see the results for Girder 4.

- ☛ Select the structure group: Click the **Group** button above the explorers. Click **Composite 1**. Click **Select (Unselect Everything Else)**.
- ☛ Select the result case: Click the **Results** above the explorers. Right click the **NonComposite** result case. Choose **Compound Element Forces**.

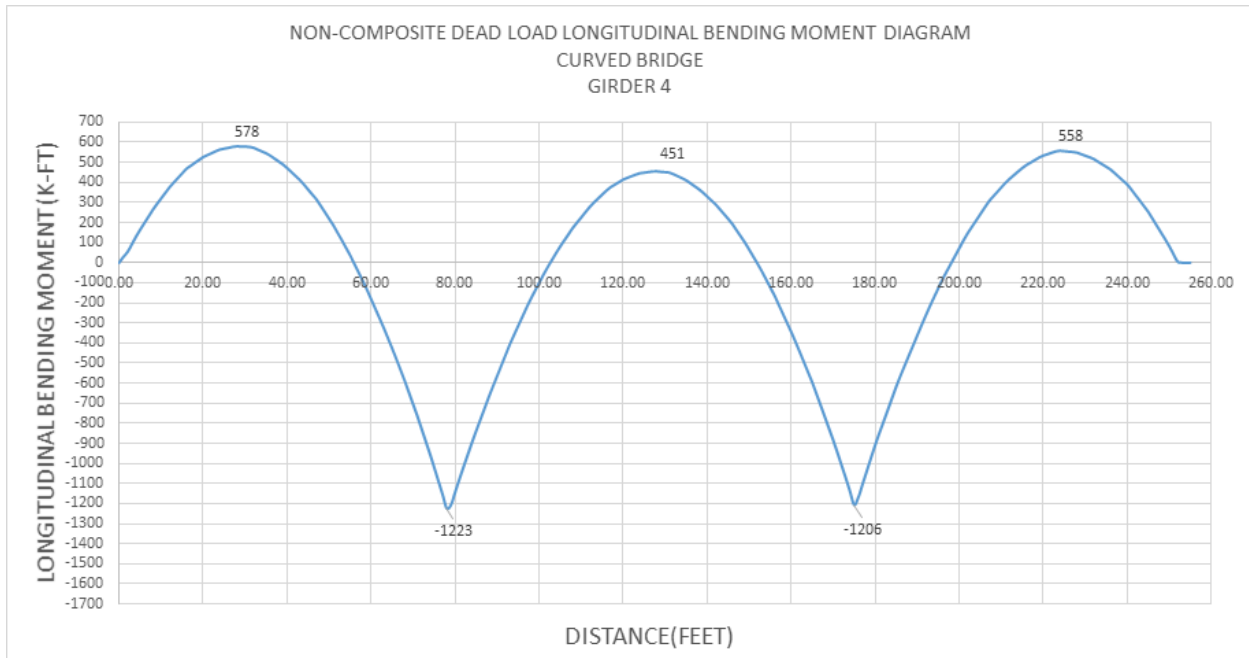


Figure 17: Girder 4 Non-composite Dead Load Bending Moment

Follow the steps below in order to see reactions.

- Select the structure group: Click the **Group** button above the explorers. Click **Bearing@0.00**. Click **Select (Unselect Everything Else)**.
- Select the result case: Click the **Results** above the explorers. Right click the **NonComposite** result case. Choose **Joint Reactions**.
- Select the structure group: Click the **Group** button above the explorers. Click **Bearing@80.00**. Click **Select (Unselect Everything Else)**.
- Select the structure group: Click the **Group** button above the explorers. Click **Bearing@180.00**. Click **Select (Unselect Everything Else)**.
- Select the structure group: Click the **Group** button above the explorers. Click **Bearing@260.00**. Click **Select (Unselect Everything Else)**.

The reactions can be seen below.

Reactions for Non-Composite Dead Load (kips)

	Girder 1	Girder 2	Girder 3	Girder 4	Pier Total
Pier 1	33.76	40.29	39.28	40.05	153.38
Pier 2	140.22	138.36	151.63	129.67	559.88
Pier 3	139.98	138.32	149.82	127.83	555.95
Pier 4	35.15	39.70	40.86	39.57	155.28

Girder Total	349.12	356.67	381.59	337.11	
					Bridge Total
					1424.49

Follow the steps below in order to see joint displacements for Girder 3 and 4.

- ☛ Select the structure group: Click the **Group** button above the explorers. Click **Composite 1**. Click **Select (Unselect Everything Else)**.
- ☛ Select the result case: Click the **Results** above the explorers. Right click the **NonComposite** result case. Choose **Joint Displacements**.
- ☛ Select the structure group: Click the **Group** button above the explorers. Click **Composite 2**. Click **Select (Unselect Everything Else)**.

The deflections of 0.4 PT of Span 1 and the centerline of Span 2 can be seen below.

Vertical Deflections for Dead Load Non-Composite (in)

	0.4 PT of Span 1	Centerline of Span 2
Girder 3	0.49	0.50
Girder 4	0.51	0.49

The composite dead load consists of the future wearing surface and parapet load.

30 psf future wearing surface load is applied to deck plate elements as a uniform load. parapet load is calculated from the dimensions given in figure 3 and it is applied to overhang plates as uniform load with a magnitude of 10.4 psf.

- ☛ To see load spreadsheets, click the **Loads** button above the explorers. Right click the **parapet** load case and choose **Edit Loads**.
- ☛ To see loads graphically, in the menu choose **Graphics** → **Show** and turn on **Input Loads**. Then click the **Loads** button above the explorers and click the **parapet** load case.

Follow the steps below in order to see results for Girder 3.

- ☛ Select the structure group: Click the **Group** button above the explorers. Click **Composite 2**. Click **Select (Unselect Everything Else)**.
- ☛ Select the results case, click **Results**. Right click **Composite**. Click **Compound Element Forces**

The composite dead load analysis results for the Girder 3 can be seen in figure 18.

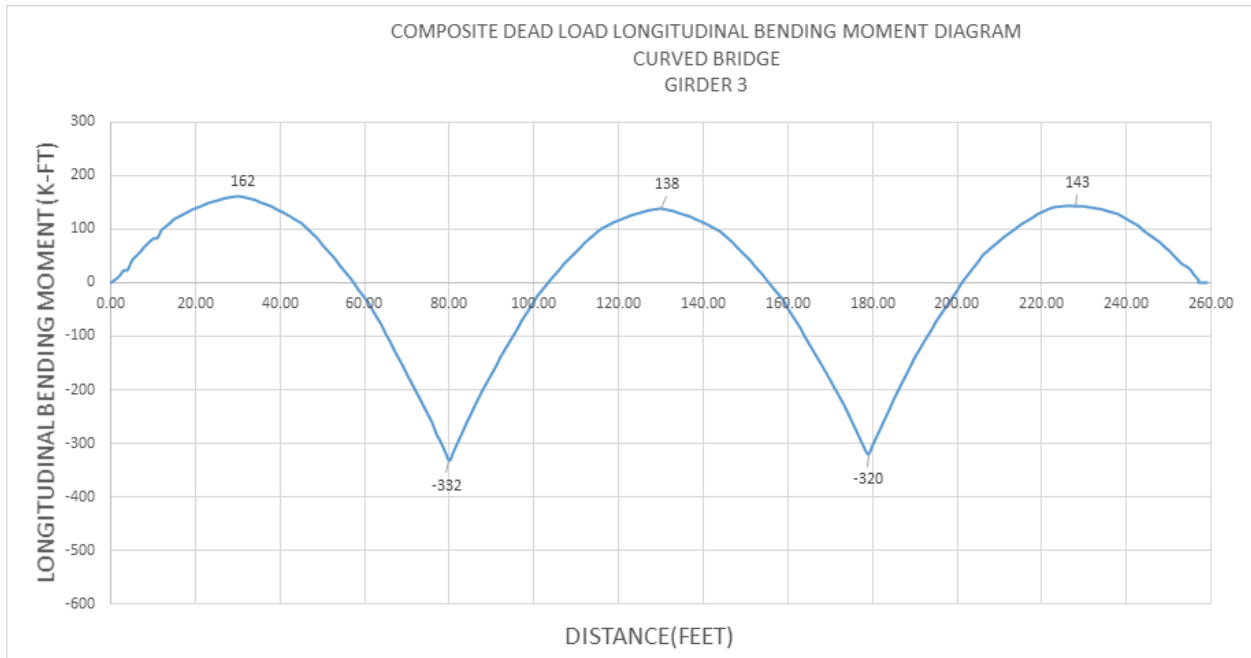


Figure 18: Girder 3 Composite Dead Load Bending Moment

Follow the steps below in order to see results for Girder 4.

- ☛ Select the structure group: Click the **Group** button above the explorers. Click **Composite 1**. Click **Select (Unselect Everything Else)**.
- ☛ Select the result case: Click the **Results** above the explorers. Right click the **Composite** result case. Choose **Compound Element Forces**.

The composite dead load analysis results for the Girder 4 can be seen in figure 19.

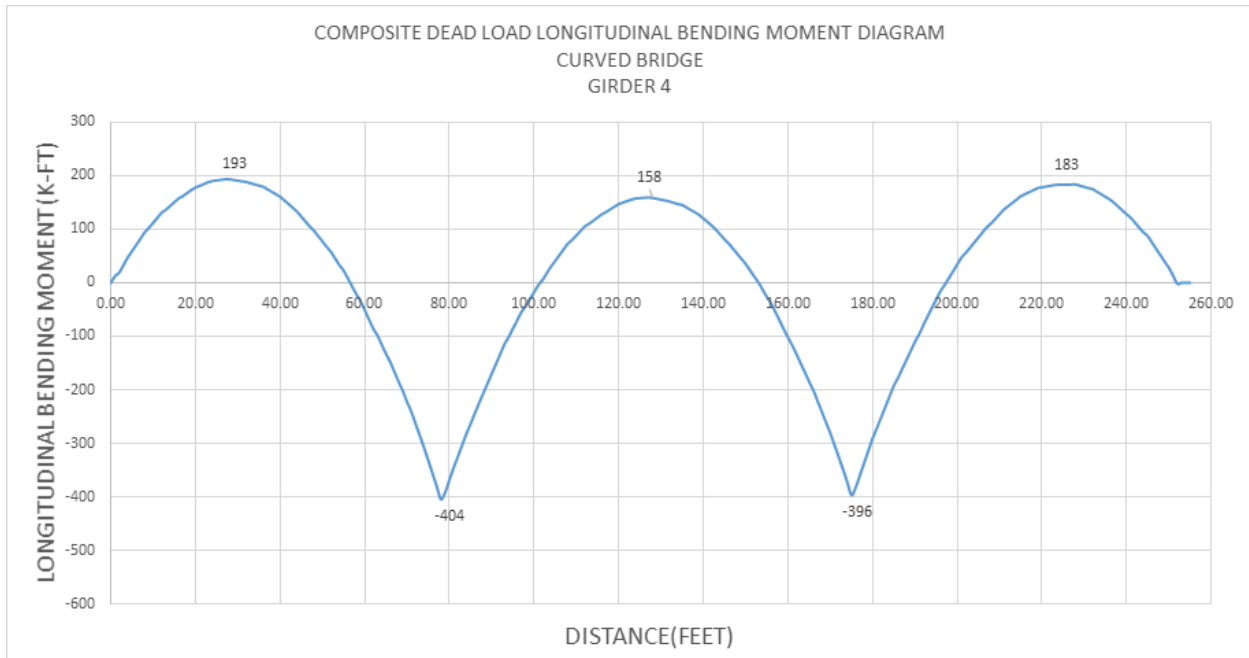


Figure 19: Girder 4 Composite Dead Load Bending Moment

The reactions can be seen below.

Follow the steps below in order to see reactions.

- Select the structure group: Click the **Group** button above the explorers. Click **Bearing@0.00**. Click **Select (Unselect Everything Else)**.
- Select the result case: Click the **Results** above the explorers. Right click the **Composite** result case. Choose **Joint Reactions**.
- Select the structure group: Click the **Group** button above the explorers. Click **Bearing@80.00**. Click **Select (Unselect Everything Else)**.
- Select the structure group: Click the **Group** button above the explorers. Click **Bearing@180.00**. Click **Select (Unselect Everything Else)**.
- Select the structure group: Click the **Group** button above the explorers. Click **Bearing@260.00**. Click **Select (Unselect Everything Else)**.

Vertical Reactions Composite Dead Load (kips)

	Girder 1	Girder 2	Girder 3	Girder 4	Pier Total
Pier 1	12.89	9.19	9.26	14.84	46.19
Pier 2	46.98	33.80	35.06	46.92	162.76
Pier 3	47.85	33.97	34.66	45.68	162.15
Pier 4	14.49	9.80	8.05	14.17	46.52
Girder Total	122.20	86.77	87.03	121.61	

Bridge Total 417.62

The deflections of 0.4 PT of Span 1 and the centerline of Span 2 can be seen below
Follow the steps below in order to see joint displacements for Girder 3 and 4.

- ☛ Select the structure group: Click the **Group** button above the explorers. Click **Composite 1**. Click **Select (Unselect Everything Else)**.
- ☛ Select the result case: Click the **Results** above the explorers. Right click the **Composite** result case. Choose **Joint Displacements**.
- ☛ Select the structure group: Click the **Group** button above the explorers. Click **Composite 2**. Click **Select (Unselect Everything Else)**.

Vertical Deflections Composite Dead Load (in)

	0.4 PT of Span 1	Centerline of Span 2
Girder 3	0.073	0.084
Girder 4	0.094	0.104

2) Influence Surface Based Live Load Analysis

2.1) Live Load Definitions

HS25-44 truck and lane loading will be applied according to AASHTO LFD. We will use the influence surface based result cases in LARSA 4D for simulating following conditions.

- 1 - HS25-44 Truck Only
- 2 - For Positive Moment: Concentrated Load (22.5 Kips) + Lane (0.8 kips/ft)
- 3 - For Negative Moment: Concentrated Load Pair (2 x 22.5 Kips) + Lane (0.8 kips/ft)
- 4 - For Shear: Concentrated Load (32.5 Kips) + Lane (0.8 kips/ft)

LARSA4D will find the worst case live load positioning for the result cases using the conditions above.

2.2) Influence Surface Result Case Settings

Influence based result case definition consists of general loading parameters, vehicular loading options and uniform/patch loading options.

General loading parameters include design lane width, overall factor and multiple presence factors along with other options. The overall factor defined on General Options parameters tab applies to both vehicular and lane loading. However the factor defined in vehicular tab applies to vehicle loads only.

General options for influence surface result cases will be defined as shown in figure 21.

The design lane width is 12 feet.

Multiple presence factors are 1.00 for 1 lane and 2 lanes loaded, 0.90 for 3 lanes loaded, and 0.75 for 4 or more lanes loaded.

Overall factor is entered as 1.232 and detailed explanation is below.

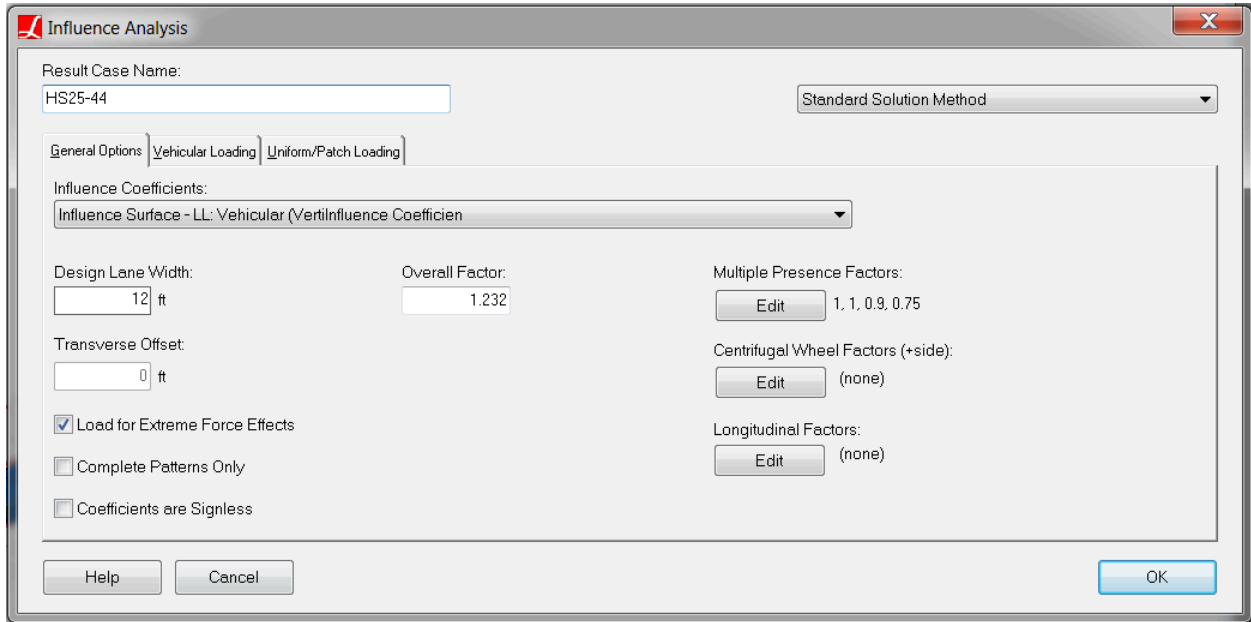


Figure 21: General Settings of Influence Surface Result Case

LARSA 4D provides the ability for the user to enter different impact factors for every span as longitudinal factors. In our example for 80 feet span, the impact factor is calculated as $0.244 = 50 / (L + 125)$ where $L = 80$ feet (span length) and for 100 feet span, impact factor is calculated as $0.222 = 50 / (L + 125)$ where $L = 100$ feet (span length). These factors can be entered as the longitudinal factors using the stations along the control centerline as in figure 22.

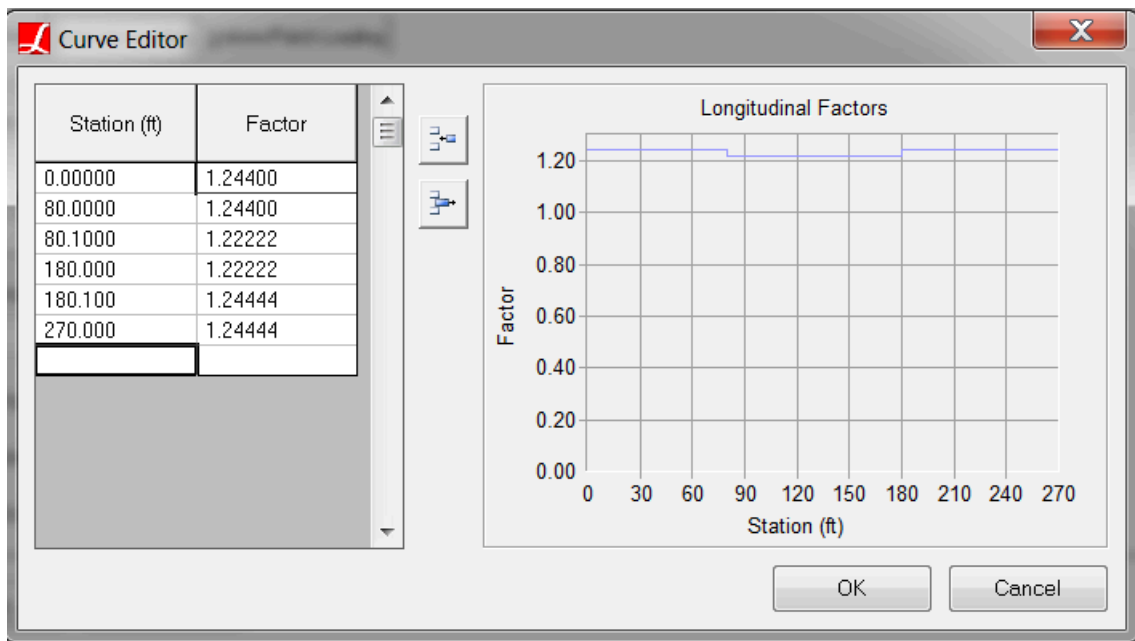


Figure 22: Impact factors as longitudinal factors

In this example the variation of impact factors is less than 1% and for simplicity it will be ignored. An average 90 feet span length is used in impact factor calculation and it is calculated as 0.232. Overall factor is entered as 1.232 (1.00 + Impact factor) for all influence surface cases as seen in figure 21.

In LFD, the impact factor is applied to the entire live load. In LRFD, dynamic load allowance is applied only to the design truck and design tandem. For this reason LARSA4D has options for entering different live load factors for vehicles and lane loading. The overall factor entered in General Options tab is for entire live load and suitable for LFD loading. Factor entered in Vehicular Loading tab is applied to the vehicle only (doesn't effect the lane loading), and it is suitable for LRFD loading.

Vehicle loading factor is entered as 1.00 for all 4 cases. UDL factor is entered as 0.00 for HS25-44 truck only case since the AASHTO LFD doesn't require the lane loading and truck loading together. For the remaining 3 cases, UDL factor is entered as 1.

The design lane vehicle margin is entered as 2 feet.

Vehicular Loading tabs for all 4 cases can be seen in Figure 23.

LARSA 4D Sample and Verification Problems

Influence Analysis

Result Case Name: HS25-44 Standard Solution Method

General Options | Vehicular Loading | Uniform/Patch Loading

Add Lane Type | Add Vehicle | X

Lane Type, UDL Factor: 0
HS25-44 Truck (Factor: 1.23255814)

Vehicle Load Pattern: HS25-44 Truck
 Factor: 1.23255 Max #:
 One Load Pattern Per Span
 Vehicle Direction: Any

Min. Back-to-Front Spacing: ft
 Design Lane Vehicle Margin: ft
 Min. Side-to-Side Spacing: ft

Lane Options: Max Lanes: No Limit UDL Factor: 0
 Lane Transverse Constraints: Min: ft Max: ft

Help Cancel OK

Influence Analysis

Result Case Name: Concentrated Load(22.5 Kips) + Lane(0.8 kips/ft) Standard Solution Method

General Options | Vehicular Loading | Uniform/Patch Loading

Add Lane Type | Add Vehicle | X

Lane Type
AASHTO Point 22.5kip (for moment) (Factor: 1.23255814)

Vehicle Load Pattern: AASHTO Point 22.5kip (for moment)
 Factor: 1.23255 Max #:
 One Load Pattern Per Span
 Vehicle Direction: Any

Min. Back-to-Front Spacing: ft
 Design Lane Vehicle Margin: ft
 Min. Side-to-Side Spacing: ft

Lane Options: Max Lanes: No Limit UDL Factor: 1
 Lane Transverse Constraints: Min: ft Max: ft

Help Cancel OK

Influence Analysis

Result Case Name: Concentrated Load(32.5 Kips) + Lane(0.8 kips/ft) Standard Solution Method

General Options | Vehicular Loading | Uniform/Patch Loading

Add Lane Type | Add Vehicle | X

Lane Type
AASHTO Point 32.5kip (for shear) (Factor: 1.23255814)

Vehicle Load Pattern: AASHTO Point 32.5kip (for shear)
 Factor: 1.23255 Max #:
 One Load Pattern Per Span
 Vehicle Direction: Any

Min. Back-to-Front Spacing: ft
 Design Lane Vehicle Margin: ft
 Min. Side-to-Side Spacing: ft

Lane Options: Max Lanes: 436 UDL Factor: 1
 Lane Transverse Constraints: Min: ft Max: ft

Help Cancel OK

Influence Analysis

UDL load magnitude is entered as 0.8 kip/ft along with UDL width per design lane as 10 ft according to AASHTO LFD and a screenshot from LARSA 4D can be seen in the figure 24.

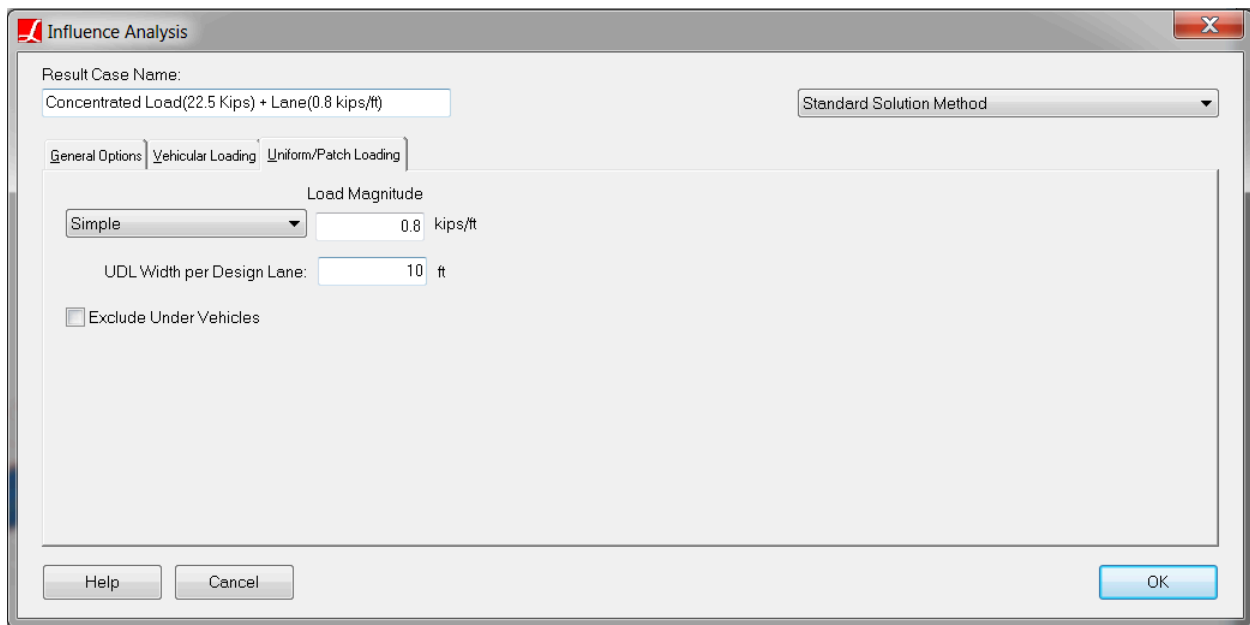


Figure 24: Lane Load Settings of Influence Surface Result Case

Follow the steps below in order to view influence surface result case settings shown above.

- ☛ Select the result case: Click the **Results** above the explorers. Right click the **HS25-44** result case. Choose **Properties**.
- ☛ Select the result case: Click the **Results** above the explorers. Right click the **Concentrated Load (22.5 Kips)** result case. Choose **Properties**.
- ☛ Select the result case: Click the **Results** above the explorers. Right click the **Concentrated Load (32.5 Kips) + Lane (0.8 kips/ft)** result case. Choose **Properties**.
- ☛ Select the result case: Click the **Results** above the explorers. Right click the **Concentrated Load Pair (22.5 Kips) + Lane (0.8 kips/ft)** result case. Choose **Properties**.

2.3) Live Load Analysis Results

In order to see the force effect on each girder, LARSA 4D's compound element force tool will be used. Compound element forces report the combined forces and moments of a group of elements regards to their combined centroid. These results are used to determine the forces in a girder modeled not as a single beam but as a group of elements. Since our deck is modeled with plate elements and the girder with beam and plate elements, the compound element forces tool will be used to find the forces for composite section. With the help of this tool, the user can see the force effects on each girder directly.

Thus AASHTO Section 3, Part C, Distribution of Loads is not applicable for this type of refined modelling therefore the results reported do not require girder distribution factors to be used.

In this example, we will be using extreme effect groups to extract envelope of forces. Extreme effect groups represent the worst-case scenario from a set of result cases, similar to envelopes, but are saved as new result cases. For positive

moment, extreme effect group named 'Positive Moment' is created and includes result cases corresponding truck alone (HS25-44) and lane load for positive moment (Concentrated Load (22.5 Kips) + Lane).

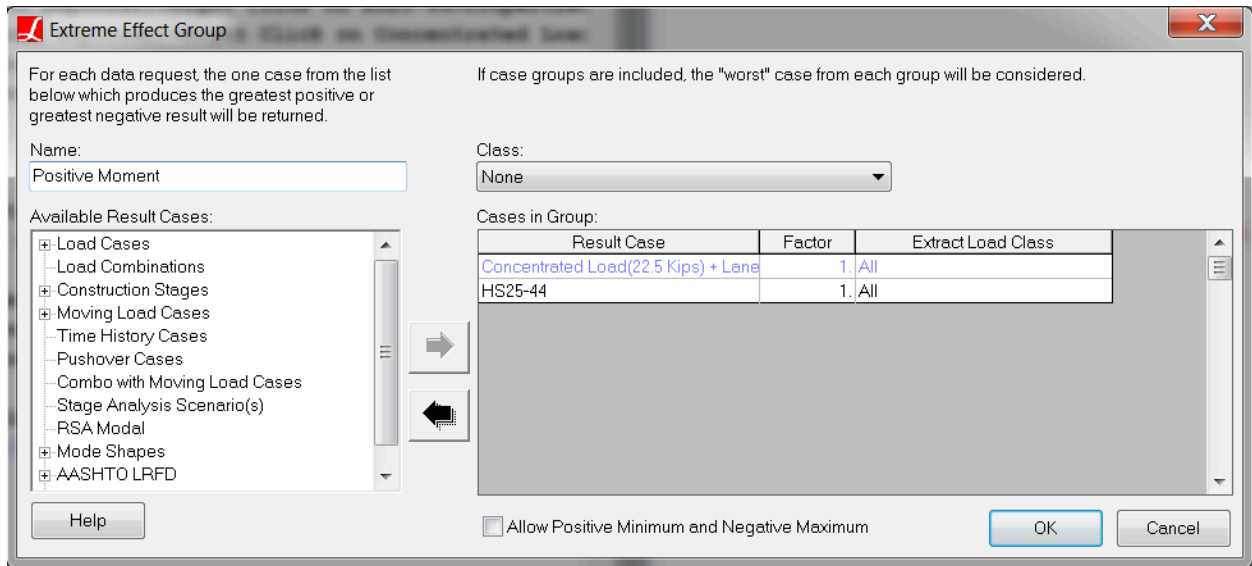


Figure 25: Extreme Effect Group For Positive Moment

For negative moment, extreme effect group named "Negative Moment" is created and includes result cases corresponding truck alone (HS25-44) and lane load for negative moment (Concentrated Load Pair (22.5 Kips) + Lane).

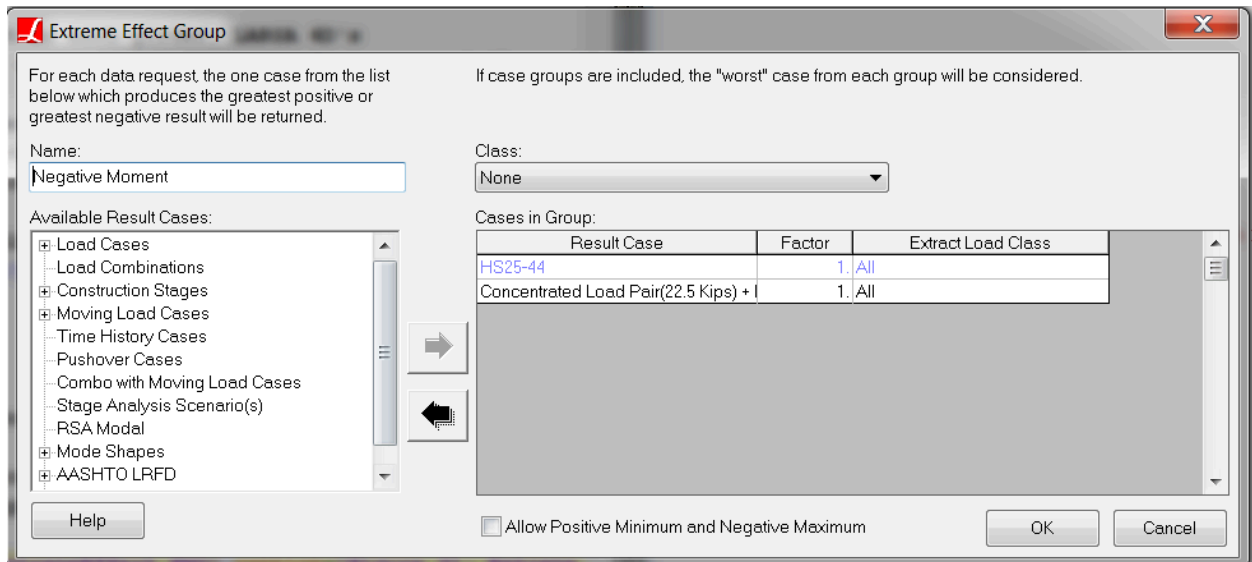


Figure 26: Extreme Effect Group For Negative Moment

For shear, extreme effect group named "Shear" is created and includes result cases corresponding truck alone (HS25-44) and lane load for shear (Concentrated Load (32.5 Kips) + Lane).

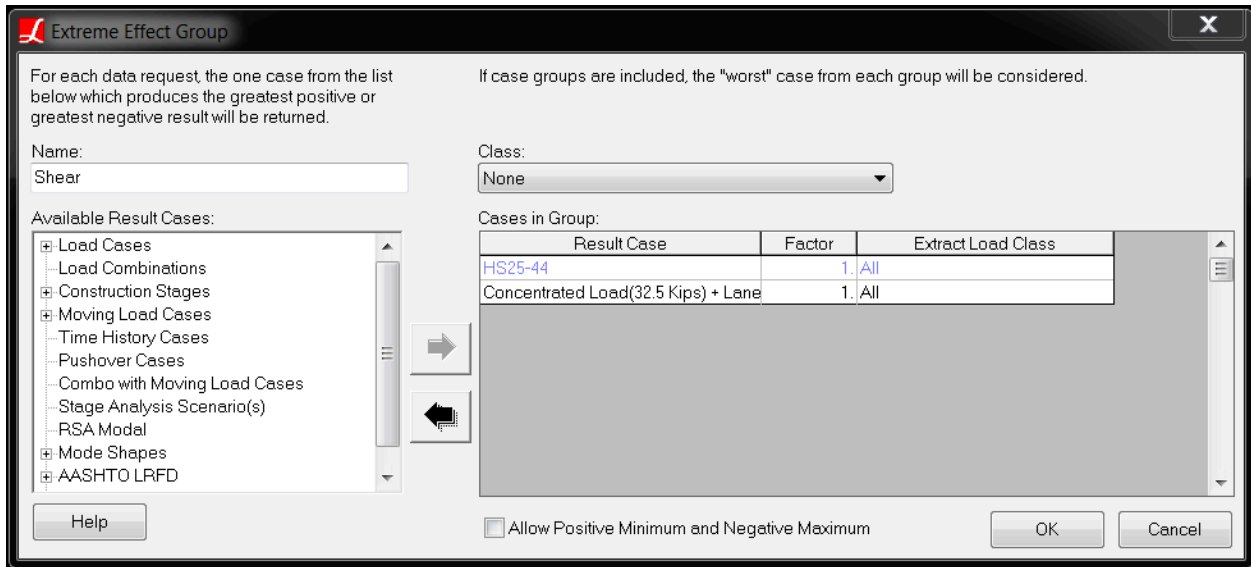


Figure 27: Extreme Effect Group For Shear

Bending moment results for girder 3 is shown in figure 28.

Follow the steps below in order to see bending moment results for Girder 3.

- Select the structure group: Click the **Group** button above the explorers. Click **Composite 2**. click **Select (Unselect Everything Else)**.
- Select the result case: Click the **Results** above the explorers. Right click the **Positive Moment** result case. Choose **Compound Element Forces**.
- Select Envelope Max My
- Select the result case: Click the **Results** above the explorers. Right click the **Negative Moment** result case. Choose **Compound Element Forces**.
- Select Envelope Min My

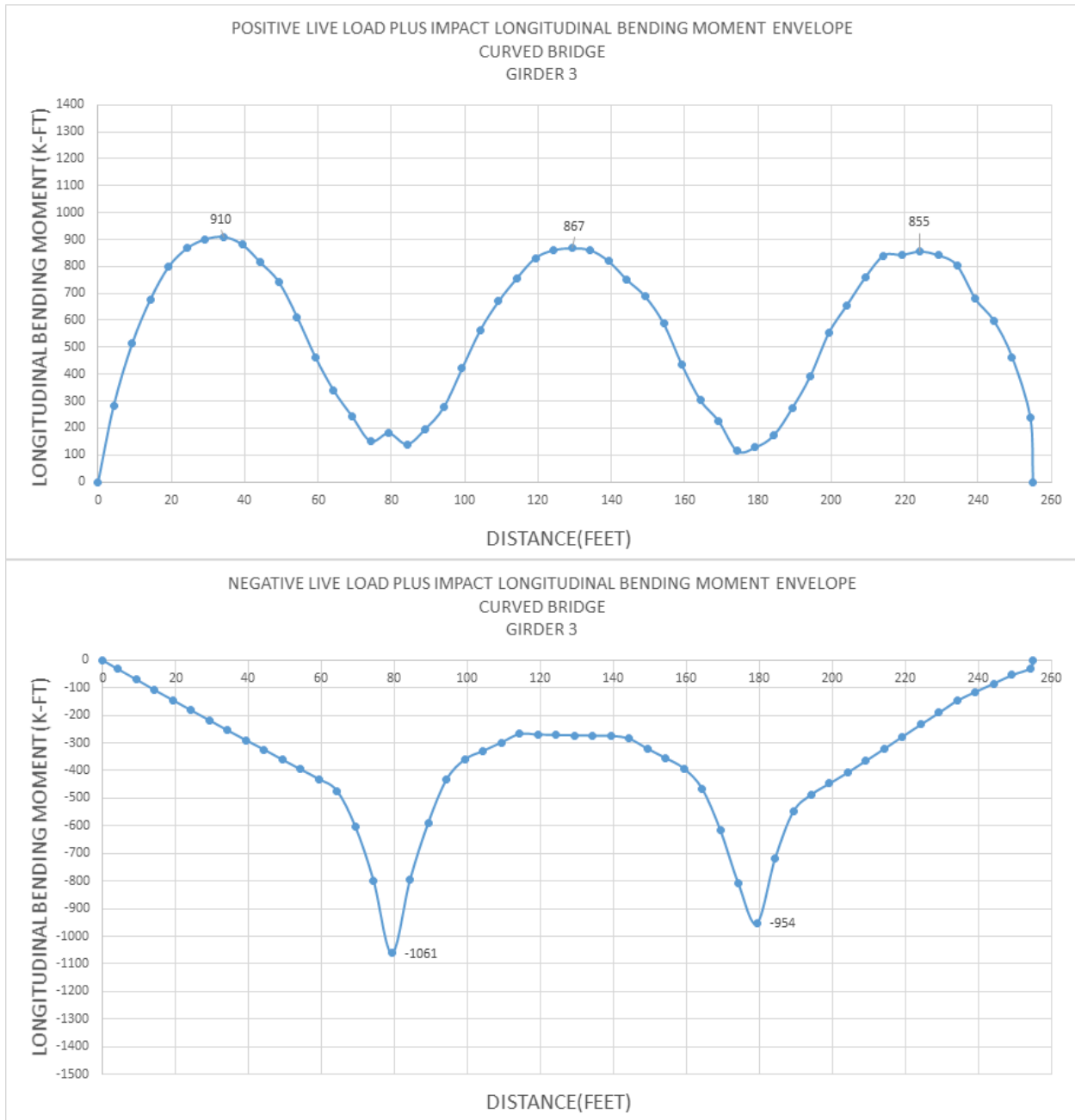


Figure 28: Girder 3 Bending Moment

Bending moment results for girder 4 is shown in figure 29. Follow the steps below in order to see bending moment results for Girder 4.

- Select the structure group: Click the **Group** button above the explorers. Click **Composite 1**. click **Select (Unselect Everything Else)**.
- Select the result case: Click the **Results** above the explorers. Right click the **Positive Moment** result case. Choose **Compound Element Forces**.
- Select Envelope Max My

- ☛ Select the result case: Click the **Results** above the explorers. Right click the **Negative Moment** result case. Choose **Compound Element Forces**.
- ☛ Select Envelope Min My

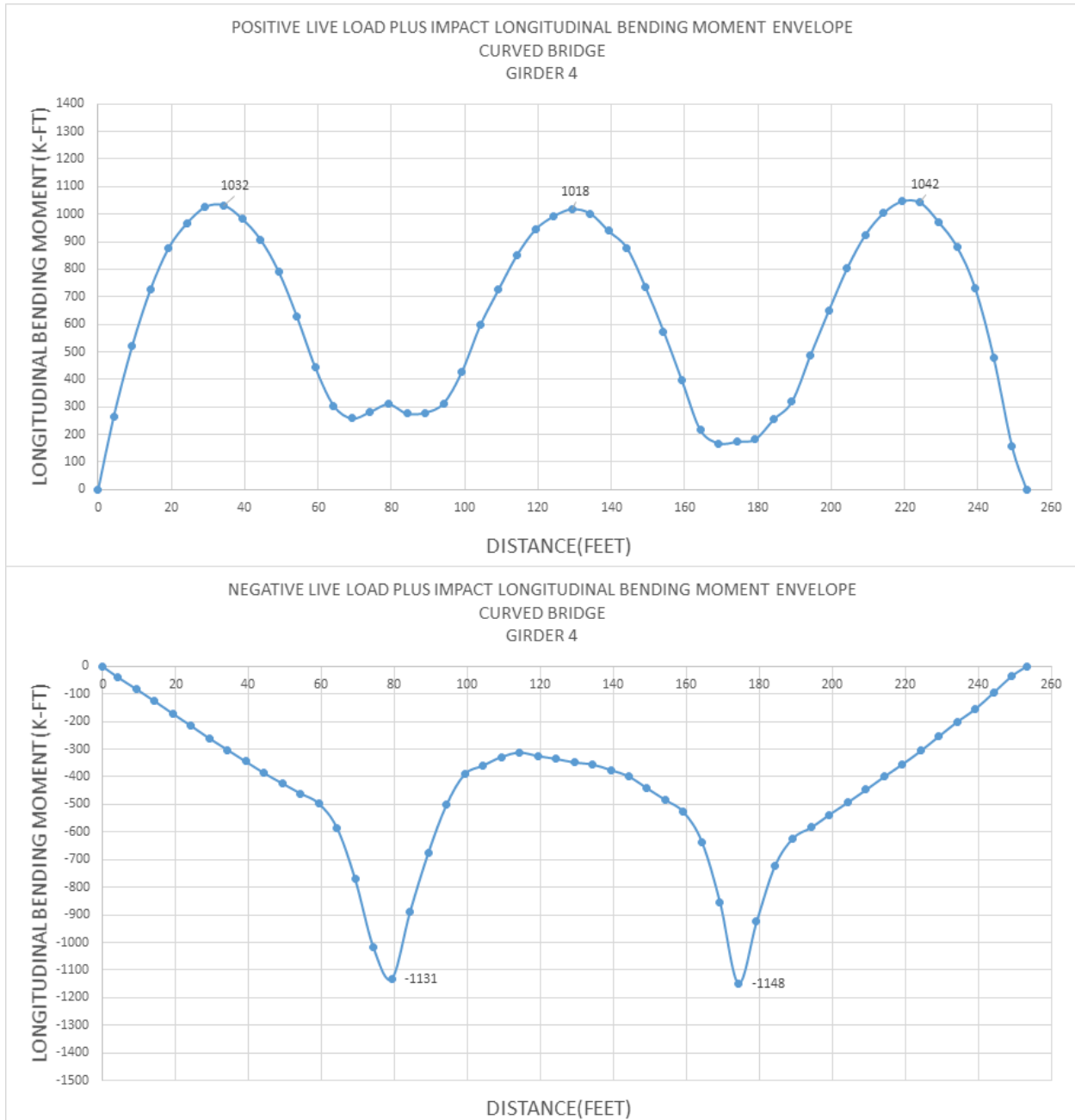


Figure 29: Girder 4 Bending Moment

Critical reactions at supports are tabulated below. Follow the steps below in order to display live load reaction forces.

- ☛ Select the structure group: Click the **Group** button above the explorers. Click **Bearing@0.00**. click **Select (Unselect Everything Else)**.

- ☛ Select the result case: Click the **Results** above the explorers. Right click the **Shear** result case. Choose **Joint Reactions**.
- ☛ Select Envelope Max Fz
- ☛ Select the structure group: Click the **Group** button above the explorers. Click **Bearing@80.00**. click **Select (Unselect Everything Else)**.
- ☛ Select the structure group: Click the **Group** button above the explorers. Click **Bearing@180.00**. click **Select (Unselect Everything Else)**.
- ☛ Select the structure group: Click the **Group** button above the explorers. Click **Bearing@260.00**. click **Select (Unselect Everything Else)**.

Live Load Vertical Reactions (kips)

	Girder 1	Girder 2	Girder 3	Girder 4
Pier 1	66.24	82.51	80.56	65.93
Pier 2	142.69	154.45	155.72	132.58
Pier 3	138.04	159.17	156.81	131.54
Pier 4	63.48	80.69	86.03	76.36

The maximum tensile and compressive forces for the cross-frames at the center of span 2 between girder 2 and 3 are tabulated below.

Follow the steps below in order to see axial force for live load.

- ☛ Select the structure group: Click the **Group** button above the explorers. Click **_Cross-frame G3-G2@130**. click **Select (Unselect Everything Else)**.
- ☛ Select all 3 result cases: Click the **Results** above the explorers. Right click the **Positive Moment** result case. Choose **Member Sectional Forces**. Press **CTRL** on the keyboard and click **Negative Moment**, **Shear** result cases.
- ☛ Select Envelope Fx

Cross Frame Axial Force At Center Of Span 2 Between Girder 2-3 Due to Live Load (kips)

	Bottom Chord	Diagonals
Tension	7.73	16.89
Compression	5.98	11.37

Bottom flange lateral moments for girder 3 and 4 can be seen below.

Bottom Flange Lateral Moment Due to Live Load (kips.ft)

	Pier 2	Center of Span 2
Girder 3	14.15	4.82
Girder 4	3.4	5.48

- ☛ Select the structure group: Click the **Group** button above the explorers. Click **Girder B Bottom Flange**. Click **Select (Unselect Everything Else)**.
- ☛ Select all 3 result cases: Click the **Results** above the explorers. Right click the **Positive Moment** result case. Choose **Member Sectional Forces**. Press **CTRL** on the keyboard and click **Negative Moment**, **Shear** result cases.
- ☛ Select Envelope My

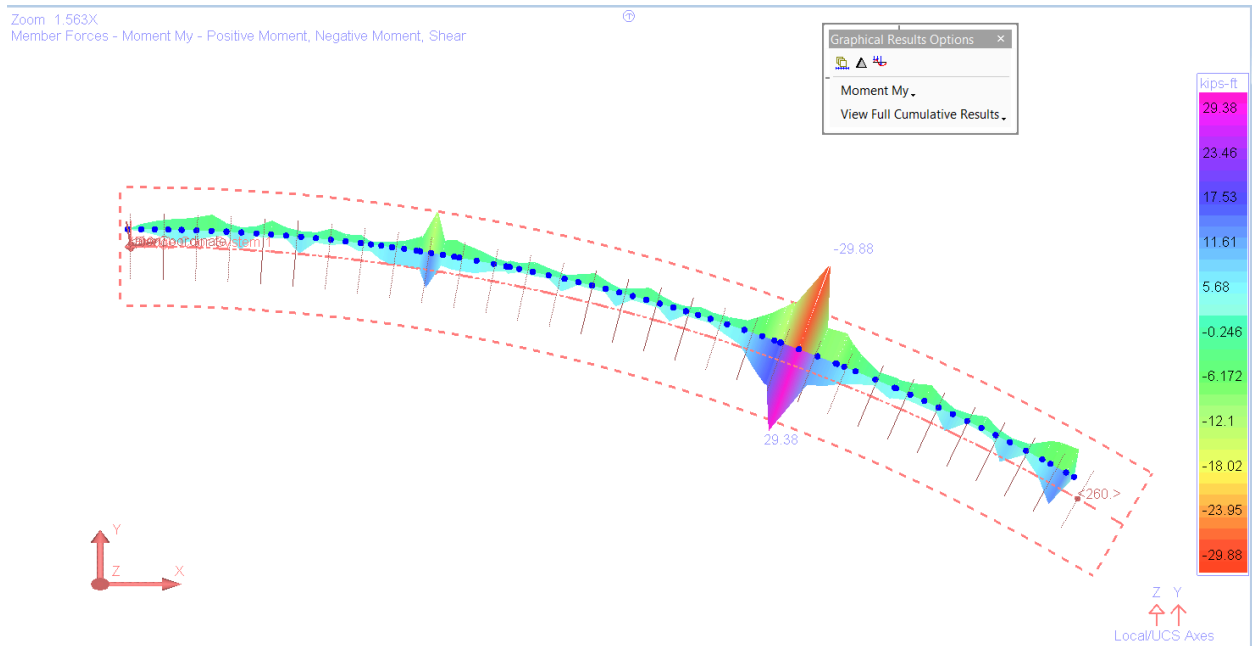


Figure 30: Girder 3 Bottom Flange Lateral Moments

- ☛ Select the structure group: Click the **Group** button above the explorers. Click **Girder A Bottom Flange**. Click **Select (Unselect Everything Else)**.
- ☛ Select all 3 result cases: Click the **Results** above the explorers. Right click the **Positive Moment** result case. Choose **Member Sectional Forces**. Press **CTRL** on the keyboard and click **Negative Moment**, **Shear** result cases.
- ☛ Select Envelope My

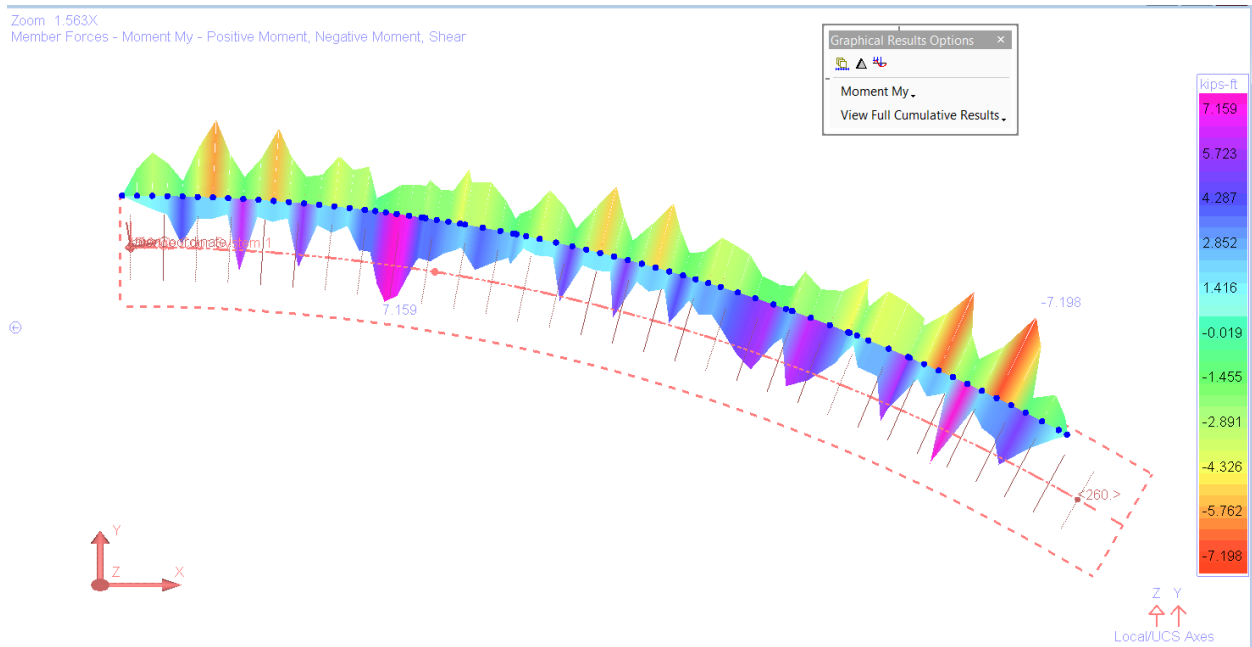


Figure 31: Girder 4 Bottom Flange Lateral Moments

SBD08: Three-Span Continuous Horizontally Curved Composite Steel Tub-Girder Bridge

This example problem is created to demonstrate the modeling and steel bridge code check features of LARSA 4D by taking the design example provided by the Federal Highway Administration as a reference. The design example complies with the provisions of AASHTO LRFD Bridge Design Specifications (7th Edition, 2014)

Example Project: The example described here can be found in the Steel Bridge Module folder of your LARSA 4D Samples directory (generally My Documents\LARSA Projects\Samples) in the file SBD08.

Problem Details

The bridge is three-span continuous horizontally curved tub-girder bridge. Spans are 160'-210'-160' along the centerline and the radius of curvature is 700ft at the centerline. The cross-section of the bridge consists of two open-top trapezoidal tub girders and 4' overhangs for a deck width of 40'-6". The distance between the top flanges of each girder is 10' and the distance between top flanges of adjacent girders is 12'-6".

The deck is cast-in-place (CIP) concrete, structural deck thickness is 9.5in, there is no integral wearing surface. Sequential deck placement is considered for constructability limit state.

Stay-in-place deck forms are between the top flanges of each girder and between the top flanges of adjacent girders.

The deck haunch thickness is 4" from top of the web to the bottom of the deck and it is constant.

Shear connectors are provided along the entire length of each top flange, so tub girders are composite throughout the bridge.

Future wearing surface and parapets are included in the loading.

The materials used in this model are:

Steel

$E_s = 29,000$ ksi

Weight Density = 490 pcf

Type = ASTM A709, Grade 50W Steel

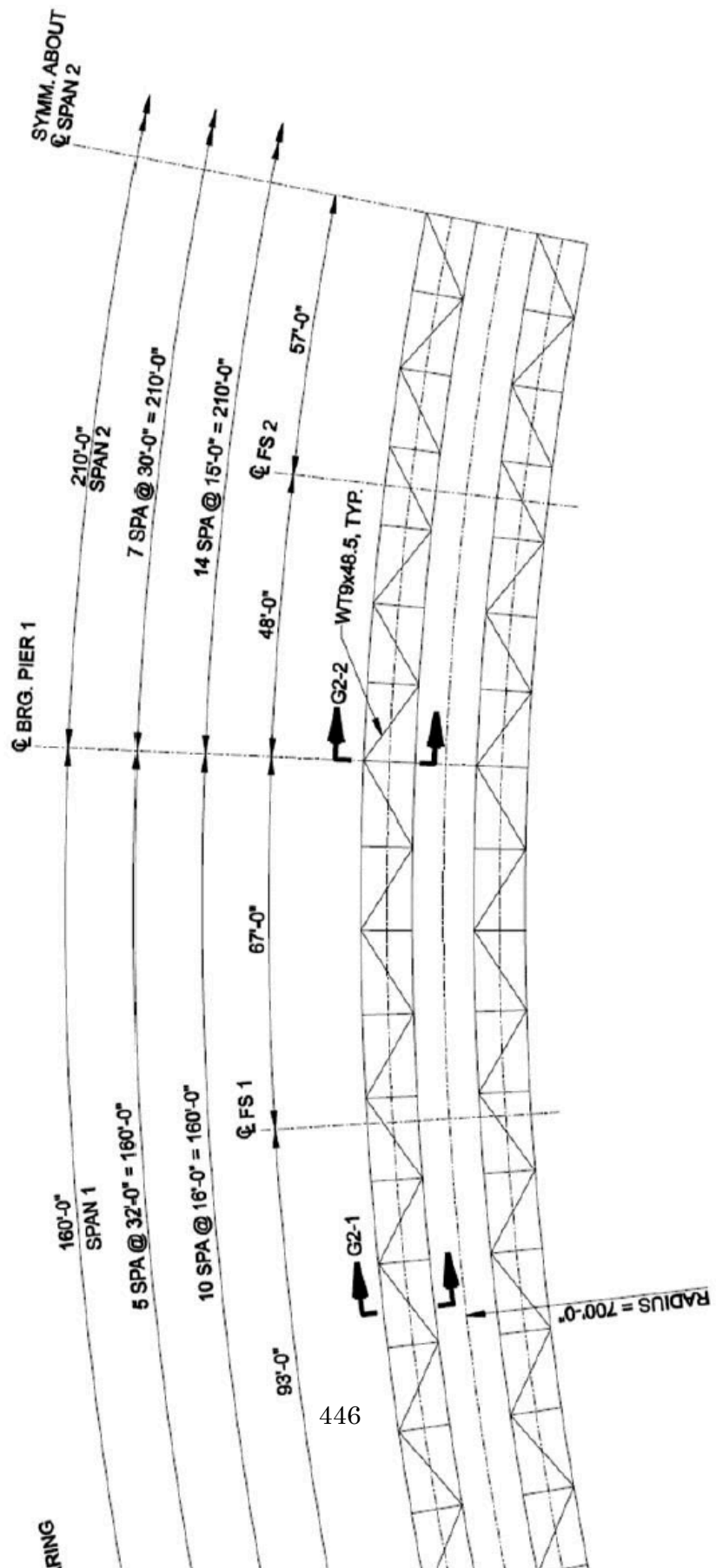
Concrete

$E_c = 3,834$ ksi

Weight Density = 150 pcf

$f_c' = 4$ ksi

Bridge Layout



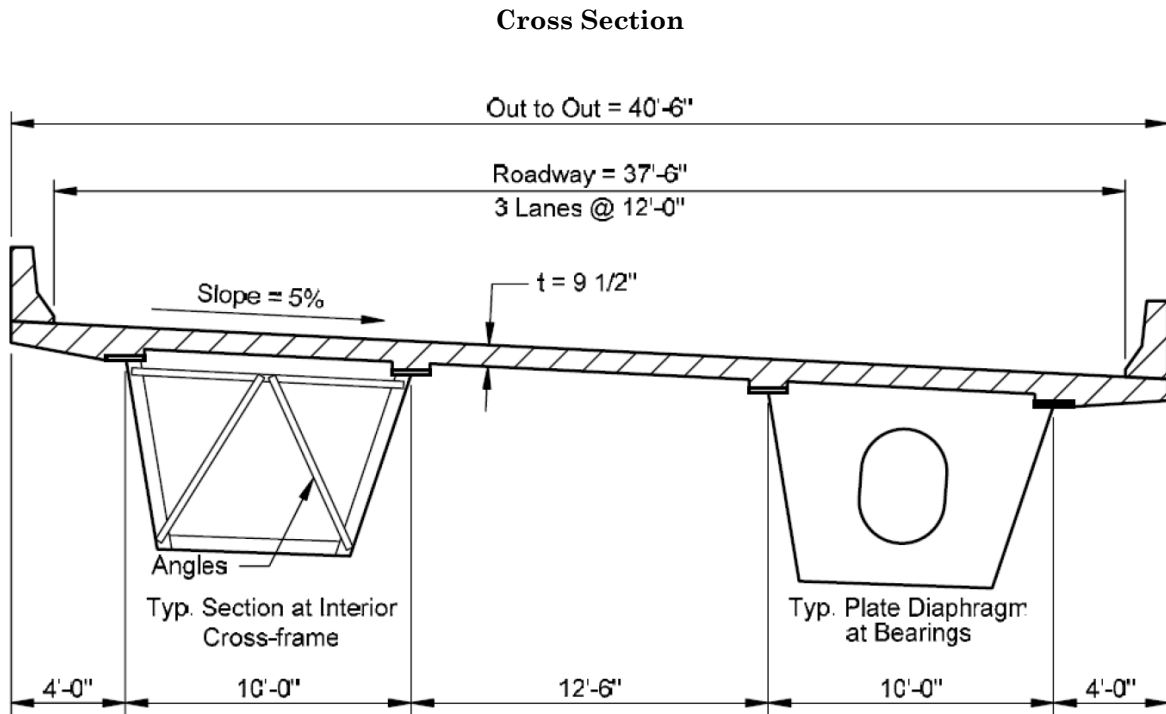


Figure 2: Typical Cross-Section

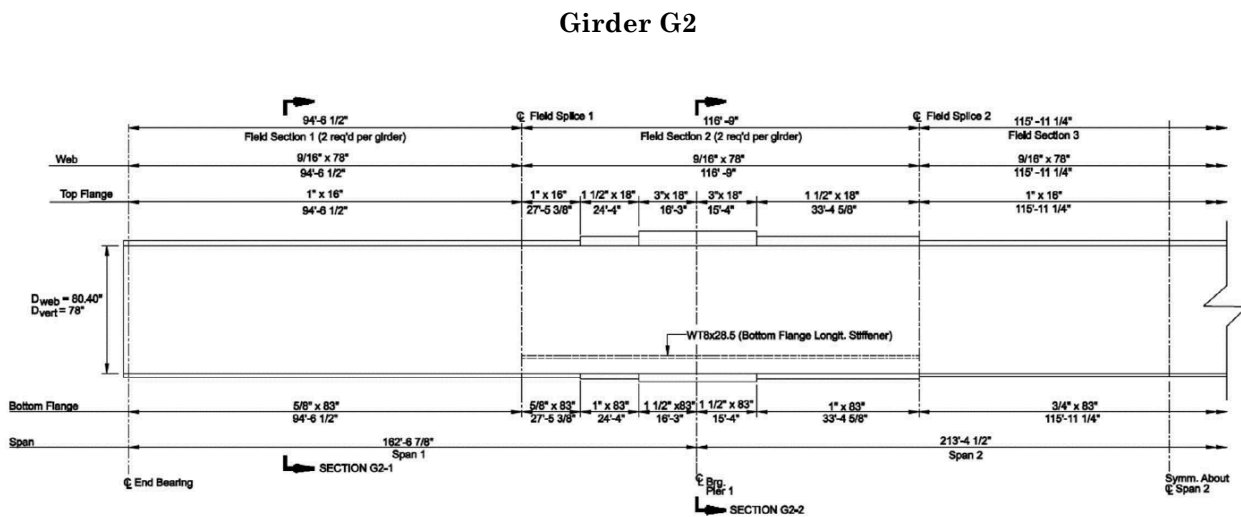


Figure 3: Girder G2 Elevation View

Girder Section G2-1

Section G2-1 is approximately 57ft from the centerline of the bearing at abutment 1.

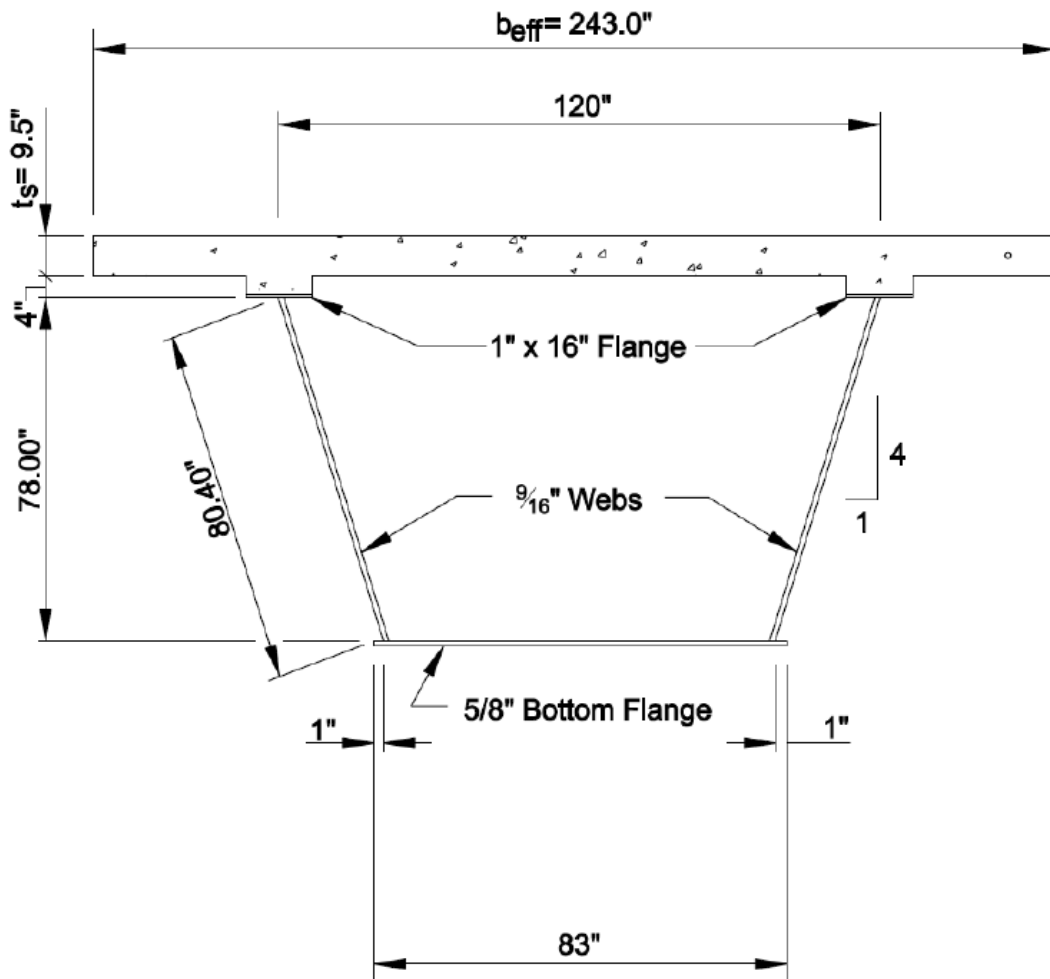


Figure 4: Girder G2 Cross Section at 57ft

Girder Section G2-2

For G2 alignment, G2-2 is at station 162.57 ft. For Bridge Path, G2-2 is at station 160.0 ft.

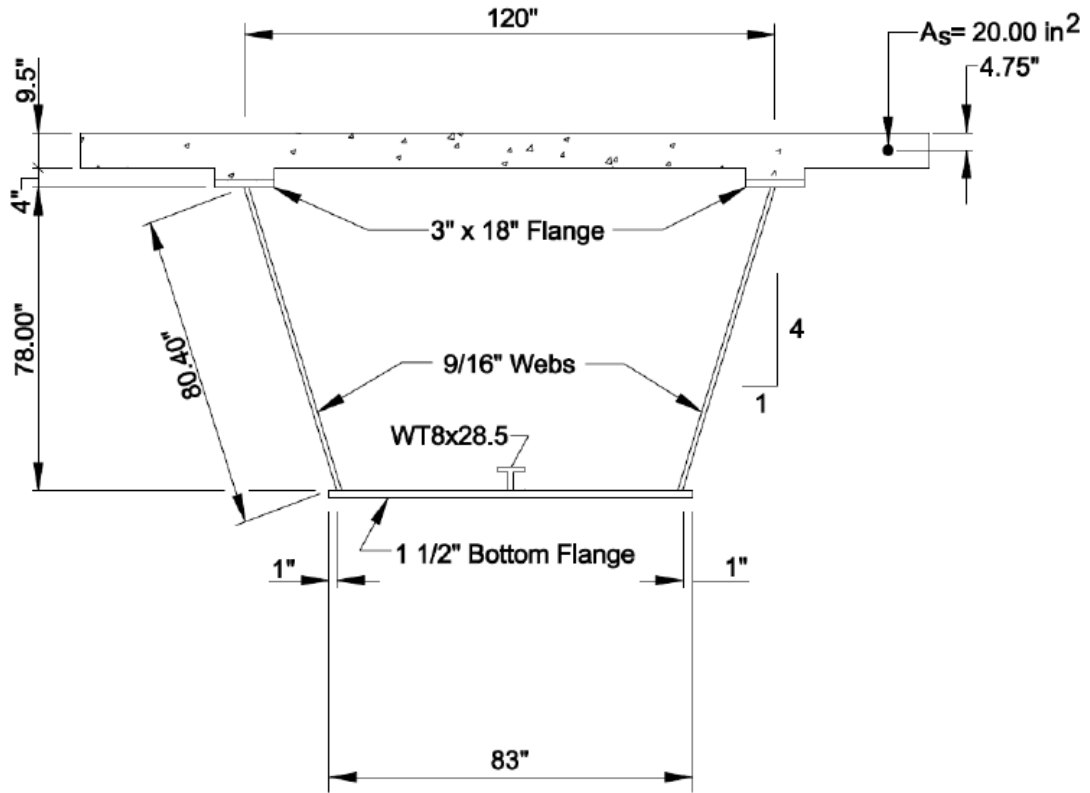
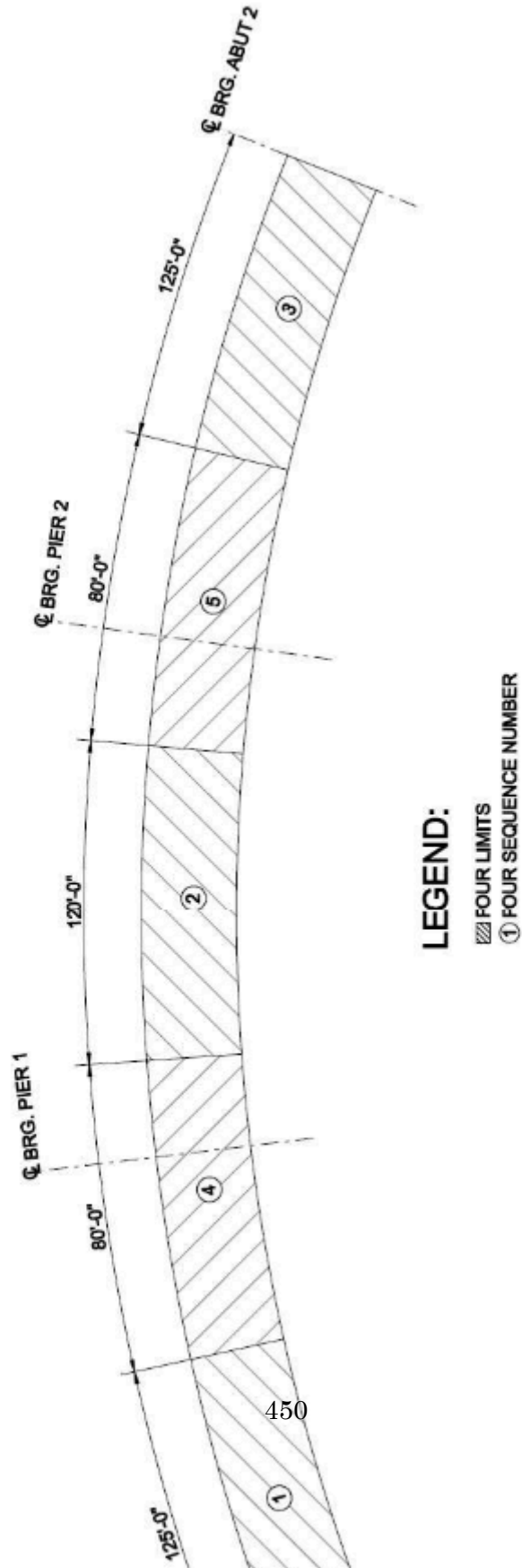


Figure 5: Girder G2 Cross Section at 160ft

Deck Pouring Sequence for Constructability



Bearings

There are abutments and two piers, Pier 1 is at 160ft and Pier 2 is at 370ft. All supports are radial to the roadway.

There are two bearings at each girder support location. The centerline of each bearing is located 28.5” from the girder centerline at the support. The bearings at Pier 1 are fixed against translation in both the radial and longitudinal directions - Fixed Bearings. The bearings at abutments and at Pier 2 are fixed against radial movement, but free in the longitudinal direction – Guided Bearings.

Intermediate Cross Frames

The tub girders are braced internally at intermediate locations with K-type cross frames, where the diagonals intersect the top strut at the top flange level.

Cross frame spacing is uniform, 16ft in end spans and 15ft in the center span.

Cross frame members have a cross sectional area of 5.0 square inches.

There is no external cross frame.

Diaphragms at the Supports

Internal diaphragms at supports, are full-depth plates with a top flange.

External diaphragms at supports, are full-depth plates with top and bottom flanges.

The web plates have a thickness of 0.5 inches.

Each flange has an area of 8.0 square inches.

Top Flange Lateral Bracing

Warren-type truss lateral bracing system is used.

The bracing is directly connected to the flanges at each internal cross frame and internal top strut.

Top flange lateral bracing members have an area of 8.0 square inches.

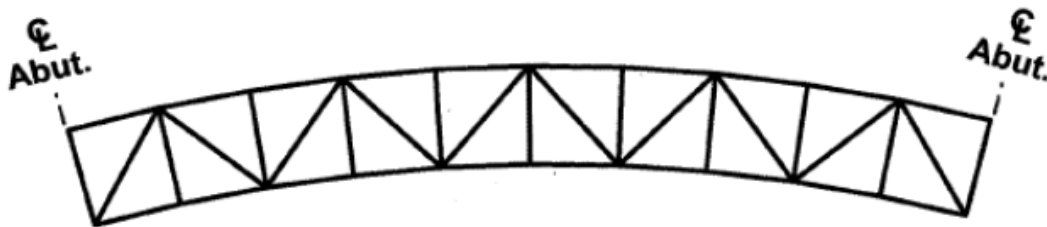


Figure 7: Top Flange Lateral Bracing

Dead Load

The non-composite dead load (DC1): Permanent load before the concrete deck has hardened. The self-weight of steel girders, cross-frames, diaphragms, lateral bracing and the concrete deck weight, haunch weight, stay-in-place metal deck form are considered as non-composite dead loads.

Steel unit weight = 490 pcf

Concrete unit weight = 150 pcf

Permanent deck form = 15 lb/ft²

The composite dead load (DC2): Superimposed dead load of parapets. The parapet weight is applied as line loads along the edges of deck elements.

The parapet load = 495 lb/ft

The component dead load (DW): Superimposed dead load of future wearing surface.

The future wearing surface = 30 lb/ft² (per square foot of roadway)

Live Load

HL-93 vehicular live load and a fatigue load, with the appropriate dynamic load allowance and centrifugal force effects included.

Highway design speed = 35 mph for centrifugal force computations

Load Combinations

Strength I load combination is used for the strength limit state

Strength I: $\eta[1.25(DC) + 1.5(DW) + 1.75((LL+IM) + CE + BR) + 1.2(TU)]$

$\eta=1$ and $BR=TU=0$ for this example, resulting load combination:

$1.25(DC1+DC2) + 1.5(DW) + 1.75((LL+IM) + CE)$

For constructability checks: $\eta[1.25(D) + 1.5(C) + 1.2(WC)]$

$\eta=1$ and $WC=0$ for this example, resulting load combination:

$1.25(D) + 1.5(C)$

where,

η = Load modifier

DC = Dead load: components and attachments

DW = Dead load: wearing surface and utilities

LL = Vehicular live load

IM = Vehicular dynamic load allowance

CE = Vehicular centrifugal force

WS = Wind load on structure

WL = Wind on live load

TU = Uniform temperature

BR = Vehicular braking force

D = Dead load

C = Construction loads

WC = Wind load for construction conditions from an assumed critical direction.

Modeling and Code Check in LARSA 4D - Steel Bridge Module (SBM)

Step A – Generate a new steel girder model

- ☐ Choose the structure type and define the Bridge Path Alignment

Structure

Type:

Alignment:

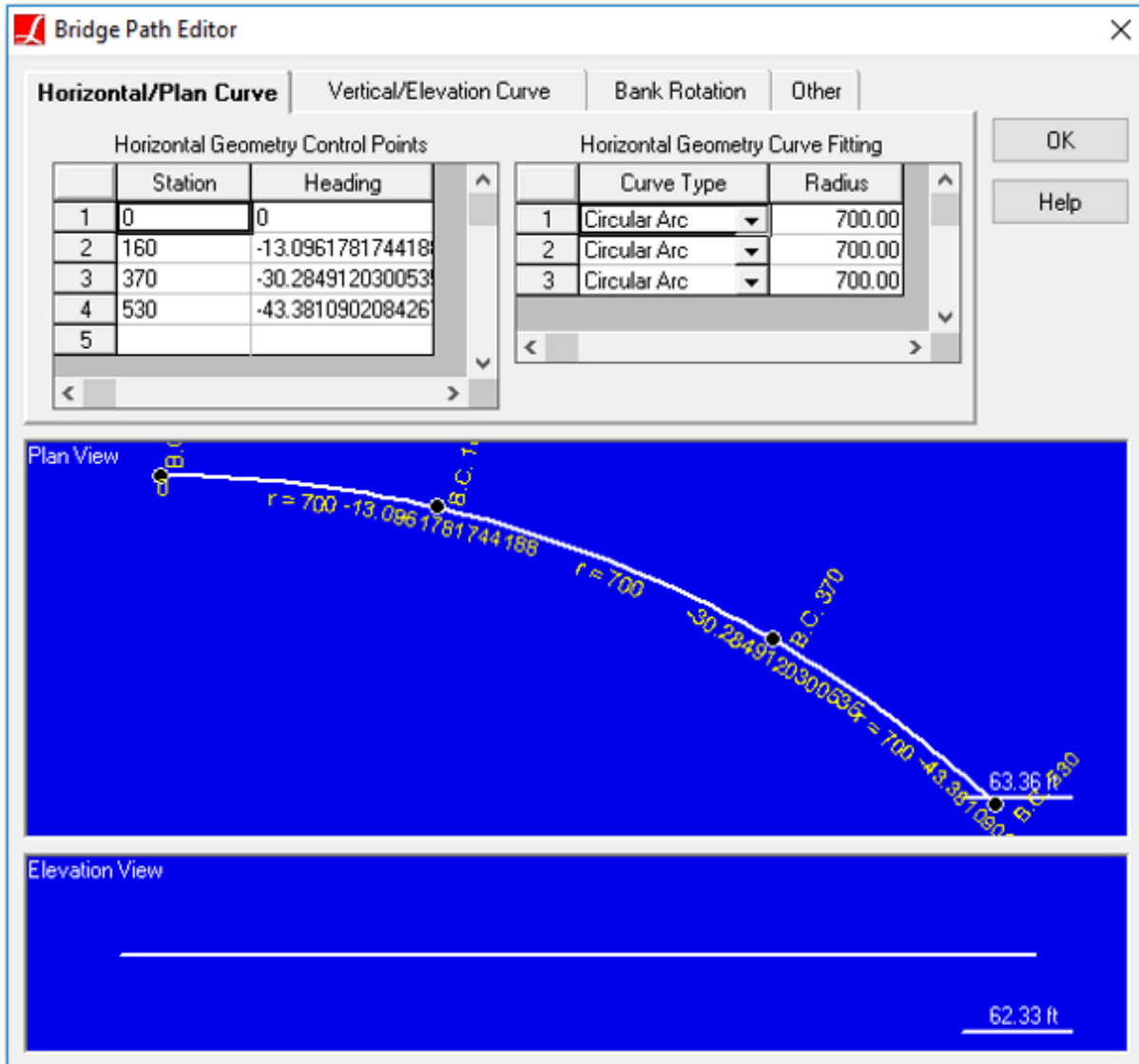


Figure 8: Bridge Path

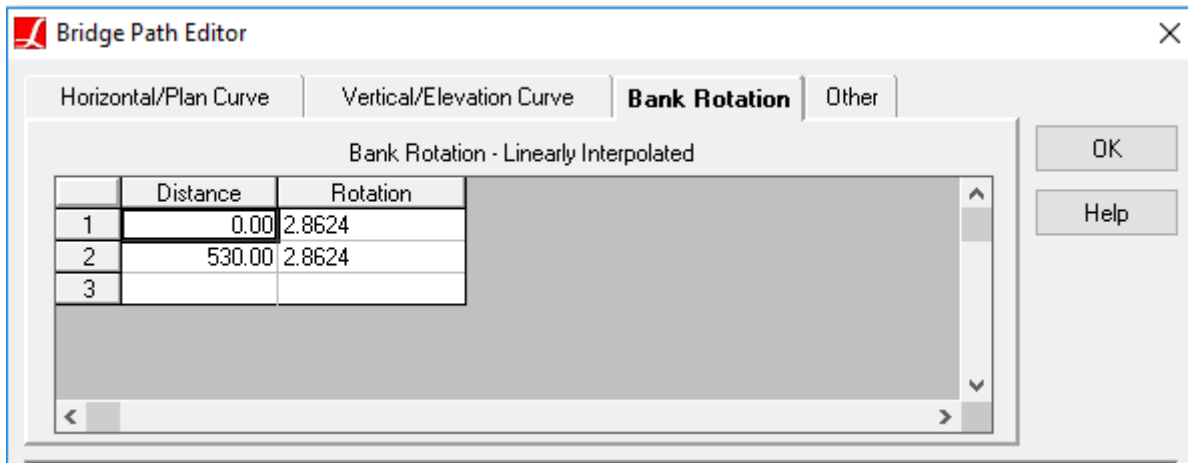


Figure 9: Superelevation

The slope of the roadway (super elevation) is 5%

Bank Rotation: $\tan^{-1}(0.05) = 2.86^\circ$

☛ Edit Abutments and Piers

	Station (ft)	Skew (deg)	Tx Support (lb/in)	Ty Support (lb/in)	Tz Support (lb/in)	Rx Support (lb-in/rad)	Ry Support (lb-in/rad)	Rz Support (lb-in/rad)
1	0.0000	0.0000	free	fixed	fixed	free	free	free
2	160.0000	0.0000	fixed	fixed	fixed	free	free	free
3	370.0000	0.0000	free	fixed	fixed	free	free	free
4	530.0000	0.0000	free	fixed	fixed	free	free	free
5								

Figure 10: Abutments and Piers Spreadsheet

Station 0 ft - Abutment 1 (Guided Bearing)

Station 160 ft - Pier 1 (Fixed Bearing)

Station 370 ft - Pier 2 (Guided Bearing)

Station 530 ft – Abutment 2 (Guided Bearing)

☛ Specify the girder type and material

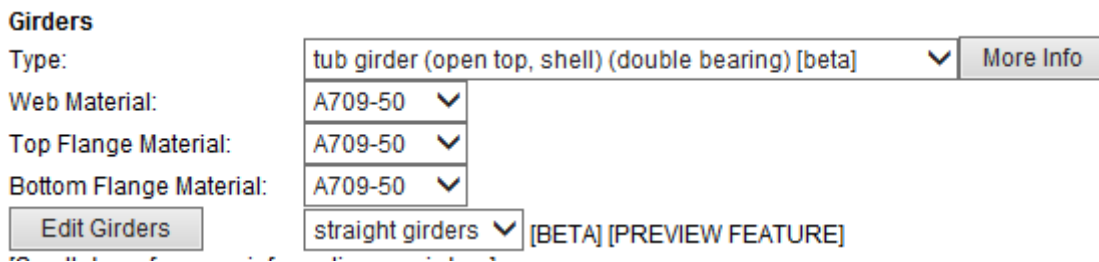


Figure 11: Girder Type and Material

In the finite element analysis used in the example problem, the horizontal curvature of the girders is represented by a series of straight elements connected at nodes. Similarly, straight girders are used in LARSA 4D.

Edit Girders

For the proper deck refinement, transverse offset values in this spreadsheet should be entered from negative to positive or from smaller to larger. For this model, it is -11.25ft to 11.25ft.

It is also possible to enter the transverse offset values in an unordered manner, but the rule is that the smallest transverse offset value corresponds to the smallest number of beams (first beam), the largest transverse offset value corresponds to the largest number of beams (last beam).

Girder	Vertical Offset	Tub Girder	Variation											
Girder Number	Skew Angle	Begin Station (ft)	End Station (ft)	Transverse Offset @ Start (ft)	Transverse Offset @ End (ft)	Haunch Thickness (in)	Web Depth (in)	Web Thickness (in)	Top Flange Width (in)	Bottom Flange Width (in)	Top Flange Thickness (in)	Bottom Flange Thickness (in)	Alignment	
1	1	0.0000	93.0000	-11.2500	-11.2500	4.0000	78.0000	0.5625	16.0000	83.0000	1.0000	0.6250	Default	
2	1	0.0000	120.0000	-11.2500	-11.2500	4.0000	78.0000	0.5625	16.0000	83.0000	1.0000	0.6250	Default	
3	1	0.0000	144.0000	-11.2500	-11.2500	4.0000	78.0000	0.5625	18.0000	83.0000	1.5000	1.0000	Default	
4	1	0.0000	160.0000	-11.2500	-11.2500	4.0000	78.0000	0.5625	18.0000	83.0000	3.0000	1.5000	Default	
5	1	0.0000	175.0000	-11.2500	-11.2500	4.0000	78.0000	0.5625	18.0000	83.0000	3.0000	1.5000	Default	
6	1	0.0000	208.0000	-11.2500	-11.2500	4.0000	78.0000	0.5625	18.0000	83.0000	1.5000	1.0000	Default	
7	1	0.0000	322.0000	-11.2500	-11.2500	4.0000	78.0000	0.5625	16.0000	83.0000	1.0000	0.7500	Default	
8	1	0.0000	355.0000	-11.2500	-11.2500	4.0000	78.0000	0.5625	18.0000	83.0000	1.5000	1.0000	Default	
9	1	0.0000	370.0000	-11.2500	-11.2500	4.0000	78.0000	0.5625	18.0000	83.0000	3.0000	1.5000	Default	
10	1	0.0000	386.0000	-11.2500	-11.2500	4.0000	78.0000	0.5625	18.0000	83.0000	3.0000	1.5000	Default	
11	1	0.0000	410.0000	-11.2500	-11.2500	4.0000	78.0000	0.5625	18.0000	83.0000	1.5000	1.0000	Default	
12	1	0.0000	437.0000	-11.2500	-11.2500	4.0000	78.0000	0.5625	16.0000	83.0000	1.0000	0.6250	Default	
13	1	0.0000	530.0000	-11.2500	-11.2500	4.0000	78.0000	0.5625	16.0000	83.0000	1.0000	0.6250	Default	
14	2	0.0000	93.0000	11.2500	11.2500	4.0000	78.0000	0.5625	16.0000	83.0000	1.0000	0.6250	Default	
15	2	0.0000	120.0000	11.2500	11.2500	4.0000	78.0000	0.5625	16.0000	83.0000	1.0000	0.6250	Default	
16	2	0.0000	144.0000	11.2500	11.2500	4.0000	78.0000	0.5625	18.0000	83.0000	1.5000	1.0000	Default	
17	2	0.0000	160.0000	11.2500	11.2500	4.0000	78.0000	0.5625	18.0000	83.0000	3.0000	1.5000	Default	
18	2	0.0000	175.0000	11.2500	11.2500	4.0000	78.0000	0.5625	18.0000	83.0000	3.0000	1.5000	Default	
19	2	0.0000	208.0000	11.2500	11.2500	4.0000	78.0000	0.5625	18.0000	83.0000	1.5000	1.0000	Default	
20	2	0.0000	322.0000	11.2500	11.2500	4.0000	78.0000	0.5625	16.0000	83.0000	1.0000	0.7500	Default	
21	2	0.0000	355.0000	11.2500	11.2500	4.0000	78.0000	0.5625	18.0000	83.0000	1.5000	1.0000	Default	
22	2	0.0000	370.0000	11.2500	11.2500	4.0000	78.0000	0.5625	18.0000	83.0000	3.0000	1.5000	Default	
23	2	0.0000	386.0000	11.2500	11.2500	4.0000	78.0000	0.5625	18.0000	83.0000	3.0000	1.5000	Default	
24	2	0.0000	410.0000	11.2500	11.2500	4.0000	78.0000	0.5625	18.0000	83.0000	1.5000	1.0000	Default	
25	2	0.0000	437.0000	11.2500	11.2500	4.0000	78.0000	0.5625	16.0000	83.0000	1.0000	0.6250	Default	
26	2	0.0000	530.0000	11.2500	11.2500	4.0000	78.0000	0.5625	16.0000	83.0000	1.0000	0.6250	Default	
27														

Figure 12: Girder Spreadsheet

The last column is the girder alignment and it is the Bridge Path along the centerline, by default.

As you can see, girder stations are entered according to corresponding girder alignment (the Bridge Path).

Web depth in this spreadsheet is the vertical web depth (for inclined webs).

Go to **Tub Girder**

The bottom flange T-stiffener for tub girder is a new feature. In the current version of SBM, if you have a T-stiffener, you should check if it is included in structure groups, construction stages and if its section property is properly assigned after model generation.

Girder		Vertical Offset	Tub Girder		Variation				
	Girder Number	Skew Angle	Begin Station (ft)	End Station (ft)	Theta [for box girders] (deg)	T Stiff. Depth (in)	T Stiff. Flange Width (in)	T Stiff. Flange Thickness (in)	T Stiff. Web Thickness (in)
1	1	0.0000	0.0000	93.0000	14.0362	0.0000	0.0000	0.0000	0.0000
2	1	0.0000	93.0000	120.0000	14.0362	8.2150	7.1200	0.7150	0.4300
3	1	0.0000	120.0000	144.0000	14.0362	8.2150	7.1200	0.7150	0.4300
4	1	0.0000	144.0000	160.0000	14.0362	8.2150	7.1200	0.7150	0.4300
5	1	0.0000	160.0000	175.0000	14.0362	8.2150	7.1200	0.7150	0.4300
6	1	0.0000	175.0000	208.0000	14.0362	8.2150	7.1200	0.7150	0.4300
7	1	0.0000	208.0000	322.0000	14.0362	0.0000	0.0000	0.0000	0.0000
8	1	0.0000	322.0000	355.0000	14.0362	8.2150	7.1200	0.7150	0.4300
9	1	0.0000	355.0000	370.0000	14.0362	8.2150	7.1200	0.7150	0.4300
10	1	0.0000	370.0000	386.0000	14.0362	8.2150	7.1200	0.7150	0.4300
11	1	0.0000	386.0000	410.0000	14.0362	8.2150	7.1200	0.7150	0.4300
12	1	0.0000	410.0000	437.0000	14.0362	8.2150	7.1200	0.7150	0.4300
13	1	0.0000	437.0000	530.0000	14.0362	0.0000	0.0000	0.0000	0.0000
14	2	0.0000	0.0000	93.0000	14.0362	0.0000	0.0000	0.0000	0.0000
15	2	0.0000	93.0000	120.0000	14.0362	8.2150	7.1200	0.7150	0.4300
16	2	0.0000	120.0000	144.0000	14.0362	8.2150	7.1200	0.7150	0.4300
17	2	0.0000	144.0000	160.0000	14.0362	8.2150	7.1200	0.7150	0.4300
18	2	0.0000	160.0000	175.0000	14.0362	8.2150	7.1200	0.7150	0.4300
19	2	0.0000	175.0000	208.0000	14.0362	8.2150	7.1200	0.7150	0.4300
20	2	0.0000	208.0000	322.0000	14.0362	0.0000	0.0000	0.0000	0.0000
21	2	0.0000	322.0000	355.0000	14.0362	8.2150	7.1200	0.7150	0.4300
22	2	0.0000	355.0000	370.0000	14.0362	8.2150	7.1200	0.7150	0.4300
23	2	0.0000	370.0000	386.0000	14.0362	8.2150	7.1200	0.7150	0.4300
24	2	0.0000	386.0000	410.0000	14.0362	8.2150	7.1200	0.7150	0.4300
25	2	0.0000	410.0000	437.0000	14.0362	8.2150	7.1200	0.7150	0.4300
26	2	0.0000	437.0000	530.0000	14.0362	0.0000	0.0000	0.0000	0.0000
27									

Figure 13: Tub Girder Spreadsheet

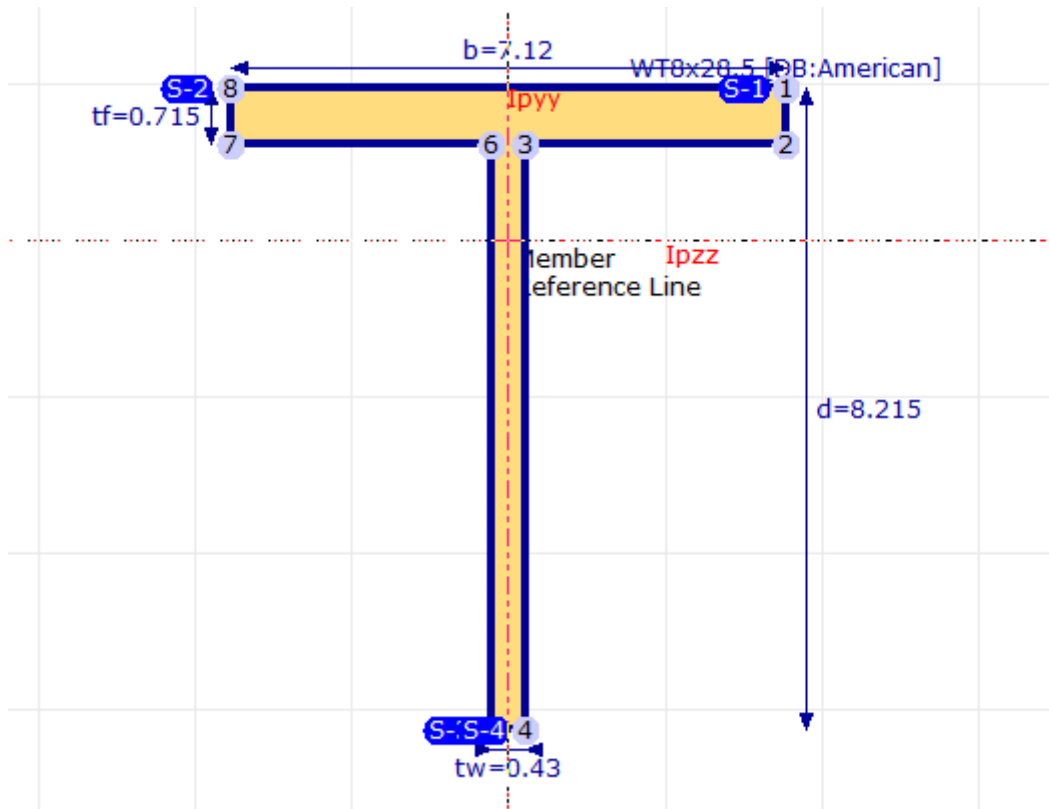


Figure 14: T-Stiffener

Web inclination is 1:4 in the design example. Theta (θ) = $\tan^{-1}(1/4) = 14.036^\circ$

T-stiffener is WT8x28.5

☰ Edit Cross Frames and Splice Points

Supported Cross-frame Types

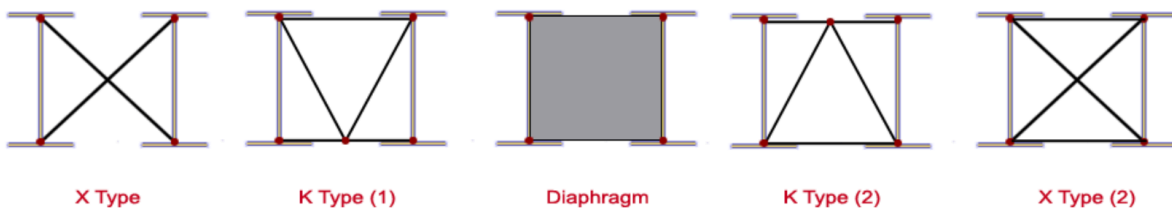


Figure 15: Cross Frames in LARSA4D

Type	Sections	Substringers	Lateral Bracings				
	Station (ft)	Type	Dist. from Bot. of Top Flange (in)	Depth (in)	Skew (deg)	Location	Bays
1	0.0000	Diaphragm with Top Flange	0.0000	0.0000	0.0000	Internal (Tub/Box Only)	ALL
2	0.0000	Diaphragm with Top & Bot. Flange	0.0000	0.0000	0.0000	External	ALL
3	16.0000	K Type (2) (No Bot. Chord)	0.0000	0.0000	0.0000	Internal (Tub/Box Only)	ALL
4	32.0000	K Type (2) (No Bot. Chord)	0.0000	0.0000	0.0000	Internal (Tub/Box Only)	ALL
5	48.0000	K Type (2) (No Bot. Chord)	0.0000	0.0000	0.0000	Internal (Tub/Box Only)	ALL
6	64.0000	K Type (2) (No Bot. Chord)	0.0000	0.0000	0.0000	Internal (Tub/Box Only)	ALL
7	80.0000	K Type (2) (No Bot. Chord)	0.0000	0.0000	0.0000	Internal (Tub/Box Only)	ALL
8	96.0000	K Type (2) (No Bot. Chord)	0.0000	0.0000	0.0000	Internal (Tub/Box Only)	ALL
9	112.0000	K Type (2) (No Bot. Chord)	0.0000	0.0000	0.0000	Internal (Tub/Box Only)	ALL
10	128.0000	K Type (2) (No Bot. Chord)	0.0000	0.0000	0.0000	Internal (Tub/Box Only)	ALL
11	144.0000	K Type (2) (No Bot. Chord)	0.0000	0.0000	0.0000	Internal (Tub/Box Only)	ALL
12	160.0000	Diaphragm with Top Flange	0.0000	0.0000	0.0000	Internal (Tub/Box Only)	ALL
13	160.0000	Diaphragm with Top & Bot. Flange	0.0000	0.0000	0.0000	External	ALL
14	175.0000	K Type (2) (No Bot. Chord)	0.0000	0.0000	0.0000	Internal (Tub/Box Only)	ALL
15	190.0000	K Type (2) (No Bot. Chord)	0.0000	0.0000	0.0000	Internal (Tub/Box Only)	ALL
16	205.0000	K Type (2) (No Bot. Chord)	0.0000	0.0000	0.0000	Internal (Tub/Box Only)	ALL
17	220.0000	K Type (2) (No Bot. Chord)	0.0000	0.0000	0.0000	Internal (Tub/Box Only)	ALL
18	235.0000	K Type (2) (No Bot. Chord)	0.0000	0.0000	0.0000	Internal (Tub/Box Only)	ALL
19	250.0000	K Type (2) (No Bot. Chord)	0.0000	0.0000	0.0000	Internal (Tub/Box Only)	ALL
20	265.0000	K Type (2) (No Bot. Chord)	0.0000	0.0000	0.0000	Internal (Tub/Box Only)	ALL
21	280.0000	K Type (2) (No Bot. Chord)	0.0000	0.0000	0.0000	Internal (Tub/Box Only)	ALL
22	295.0000	K Type (2) (No Bot. Chord)	0.0000	0.0000	0.0000	Internal (Tub/Box Only)	ALL
23	310.0000	K Type (2) (No Bot. Chord)	0.0000	0.0000	0.0000	Internal (Tub/Box Only)	ALL
24	325.0000	K Type (2) (No Bot. Chord)	0.0000	0.0000	0.0000	Internal (Tub/Box Only)	ALL
25	340.0000	K Type (2) (No Bot. Chord)	0.0000	0.0000	0.0000	Internal (Tub/Box Only)	ALL
26	355.0000	K Type (2) (No Bot. Chord)	0.0000	0.0000	0.0000	Internal (Tub/Box Only)	ALL
27	370.0000	Diaphragm with Top Flange	0.0000	0.0000	0.0000	Internal (Tub/Box Only)	ALL
28	370.0000	Diaphragm with Top & Bot. Flange	0.0000	0.0000	0.0000	External	ALL
29	386.0000	K Type (2) (No Bot. Chord)	0.0000	0.0000	0.0000	Internal (Tub/Box Only)	ALL
30	402.0000	K Type (2) (No Bot. Chord)	0.0000	0.0000	0.0000	Internal (Tub/Box Only)	ALL
31	418.0000	K Type (2) (No Bot. Chord)	0.0000	0.0000	0.0000	Internal (Tub/Box Only)	ALL
32	434.0000	K Type (2) (No Bot. Chord)	0.0000	0.0000	0.0000	Internal (Tub/Box Only)	ALL
33	450.0000	K Type (2) (No Bot. Chord)	0.0000	0.0000	0.0000	Internal (Tub/Box Only)	ALL
34	466.0000	K Type (2) (No Bot. Chord)	0.0000	0.0000	0.0000	Internal (Tub/Box Only)	ALL
35	482.0000	K Type (2) (No Bot. Chord)	0.0000	0.0000	0.0000	Internal (Tub/Box Only)	ALL
36	498.0000	K Type (2) (No Bot. Chord)	0.0000	0.0000	0.0000	Internal (Tub/Box Only)	ALL
37	514.0000	K Type (2) (No Bot. Chord)	0.0000	0.0000	0.0000	Internal (Tub/Box Only)	ALL
38	530.0000	Diaphragm with Top Flange	0.0000	0.0000	0.0000	Internal (Tub/Box Only)	ALL
39	530.0000	Diaphragm with Top & Bot. Flange	0.0000	0.0000	0.0000	External	ALL
40							

Figure 16: Cross Frames Spreadsheet

Cross frame type in this problem is K Type (2) with no bottom chord.

Spacing of cross frames is 16' in the end spans and 15' in the midspan.

☰ Go to **Sections**

External and internal diaphragm web plate thickness is given as 0.5in

Cross sectional area of each flange is given as 8square inches. Go to the cell in the spreadsheet that you want to define cross section of the corresponding chord (flanges). In this problem, no standard section is specified for the flanges, so we will select “(Area only)”

Similarly, cross sectional area of cross frame truss members is given as 5square inches

$$8 \text{ in}^2 = 0.05556 \text{ ft}^2$$

$$5 \text{ in}^2 = 0.03472 \text{ ft}^2$$

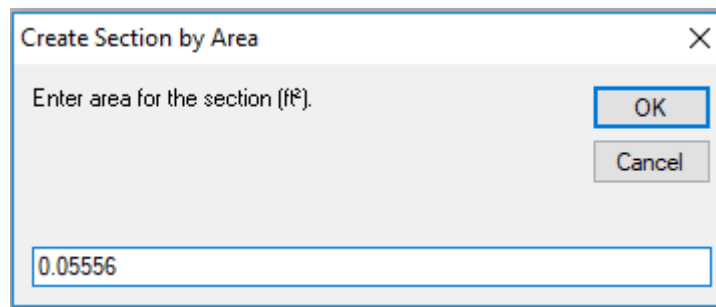


Figure 17: Section by Area

Type	Sections	Substringers	Lateral Bracings		
	Station (ft)	Bracing Top Chord Section	Bracing Bot. Chord Section	Bracing Diagonal Section	Diaphragm Thickness (in)
1	0.0000	Area: .055556	None	None	0.5000
2	0.0000	Area: .055556	Area: .055556	None	0.5000
3	16.0000	Area: .034722	None	Area: .034722	0.0000
4	32.0000	Area: .034722	None	Area: .034722	0.0000
5	48.0000	Area: .034722	None	Area: .034722	0.0000
6	64.0000	Area: .034722	None	Area: .034722	0.0000
7	80.0000	Area: .034722	None	Area: .034722	0.0000
8	96.0000	Area: .034722	None	Area: .034722	0.0000
9	112.0000	Area: .034722	None	Area: .034722	0.0000
10	128.0000	Area: .034722	None	Area: .034722	0.0000
11	144.0000	Area: .034722	None	Area: .034722	0.0000
12	160.0000	Area: .055556	None	None	0.5000
13	160.0000	Area: .055556	Area: .055556	None	0.5000
14	175.0000	Area: .034722	None	Area: .034722	0.0000
15	190.0000	Area: .034722	None	Area: .034722	0.0000
16	205.0000	Area: .034722	None	Area: .034722	0.0000
17	220.0000	Area: .034722	None	Area: .034722	0.0000
18	235.0000	Area: .034722	None	Area: .034722	0.0000
19	250.0000	Area: .034722	None	Area: .034722	0.0000
20	265.0000	Area: .034722	None	Area: .034722	0.0000
21	280.0000	Area: .034722	None	Area: .034722	0.0000
22	295.0000	Area: .034722	None	Area: .034722	0.0000
23	310.0000	Area: .034722	None	Area: .034722	0.0000
24	325.0000	Area: .034722	None	Area: .034722	0.0000
25	340.0000	Area: .034722	None	Area: .034722	0.0000
26	355.0000	Area: .034722	None	Area: .034722	0.0000
27	370.0000	Area: .055556	None	None	0.5000
28	370.0000	Area: .055556	Area: .055556	None	0.5000
29	386.0000	Area: .034722	None	Area: .034722	0.0000
30	402.0000	Area: .034722	None	Area: .034722	0.0000
31	418.0000	Area: .034722	None	Area: .034722	0.0000
32	434.0000	Area: .034722	None	Area: .034722	0.0000
33	450.0000	Area: .034722	None	Area: .034722	0.0000
34	466.0000	Area: .034722	None	Area: .034722	0.0000
35	482.0000	Area: .034722	None	Area: .034722	0.0000
36	498.0000	Area: .034722	None	Area: .034722	0.0000
37	514.0000	Area: .034722	None	Area: .034722	0.0000
38	530.0000	Area: .055556	None	None	0.5000
39	530.0000	Area: .055556	Area: .055556	None	0.5000

Figure 18: Sections Spreadsheet for Cross Frames

Go to **Lateral Bracings**

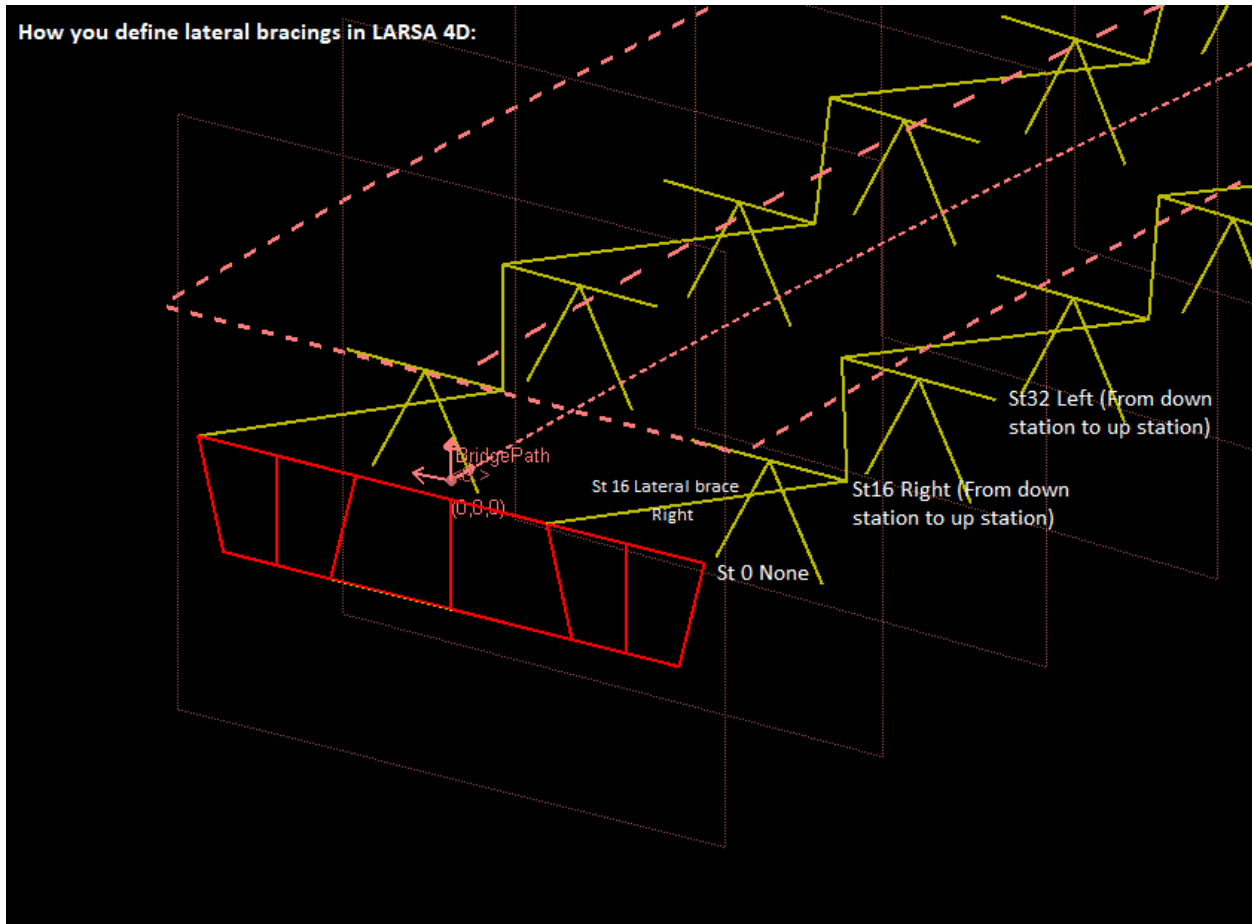


Figure 19: Lateral Bracings in LARSA4D

Top flange lateral bracing members have an area of 8 square inches (0.05556 square feet)

Type	Sections	Substringers	Lateral Bracings
	Station (ft)	Connection @ Web	Section
1	0.0000	Left	None
2	0.0000	Left	None
3	16.0000	Right	Area: .055556
4	32.0000	Left	Area: .055556
5	48.0000	Right	Area: .055556
6	64.0000	Left	Area: .055556
7	80.0000	Right	Area: .055556
8	96.0000	Left	Area: .055556
9	112.0000	Right	Area: .055556
10	128.0000	Left	Area: .055556
11	144.0000	Right	Area: .055556
12	160.0000	Left	Area: .055556
13	160.0000	Left	None
14	175.0000	Right	Area: .055556
15	190.0000	Left	Area: .055556
16	205.0000	Right	Area: .055556
17	220.0000	Left	Area: .055556
18	235.0000	Right	Area: .055556
19	250.0000	Left	Area: .055556
20	265.0000	Right	Area: .055556
21	280.0000	Left	Area: .055556
22	295.0000	Right	Area: .055556
23	310.0000	Left	Area: .055556
24	325.0000	Right	Area: .055556
25	340.0000	Left	Area: .055556
26	355.0000	Right	Area: .055556
27	370.0000	Left	Area: .055556
28	370.0000	Left	None
29	386.0000	Right	Area: .055556

Remember, we have external and internal diaphragms at the supports, so we have two rows with the same station.

Here, lateral brace should be defined using the row of internal diaphragm.

If the lateral brace is defined in the row of external diaphragm by mistake:

9	112.0000	Right	Area: .055556
10	128.0000	Left	Area: .055556
11	144.0000	Right	Area: .055556
12	160.0000	Left	None
13	160.0000	Left	Area: .055556
14	175.0000	Right	Area: .055556
15	190.0000	Left	Area: .055556
16	205.0000	Right	Area: .055556

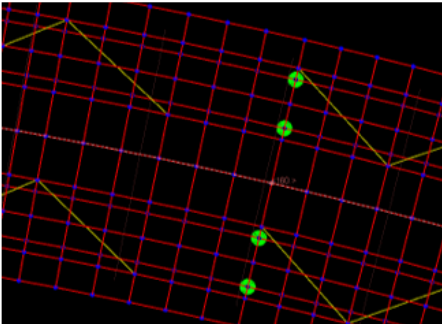


Figure 20: Lateral Bracings Spreadsheet

Enter deck material, deck thickness and the overhang widths

Deck

Material:

Fc_4

Structural Thickness:

9.5 in

Actual Thickness:

9.5 in

Overhang Width (-Y side):

4 ft

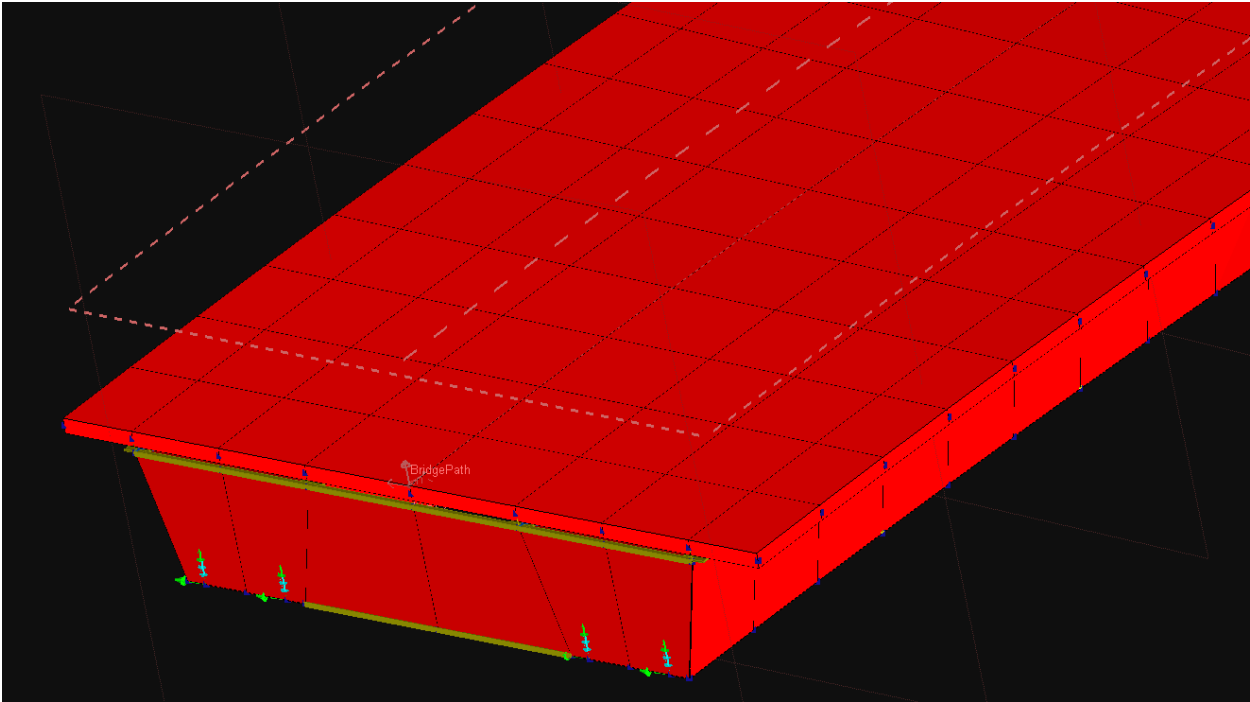
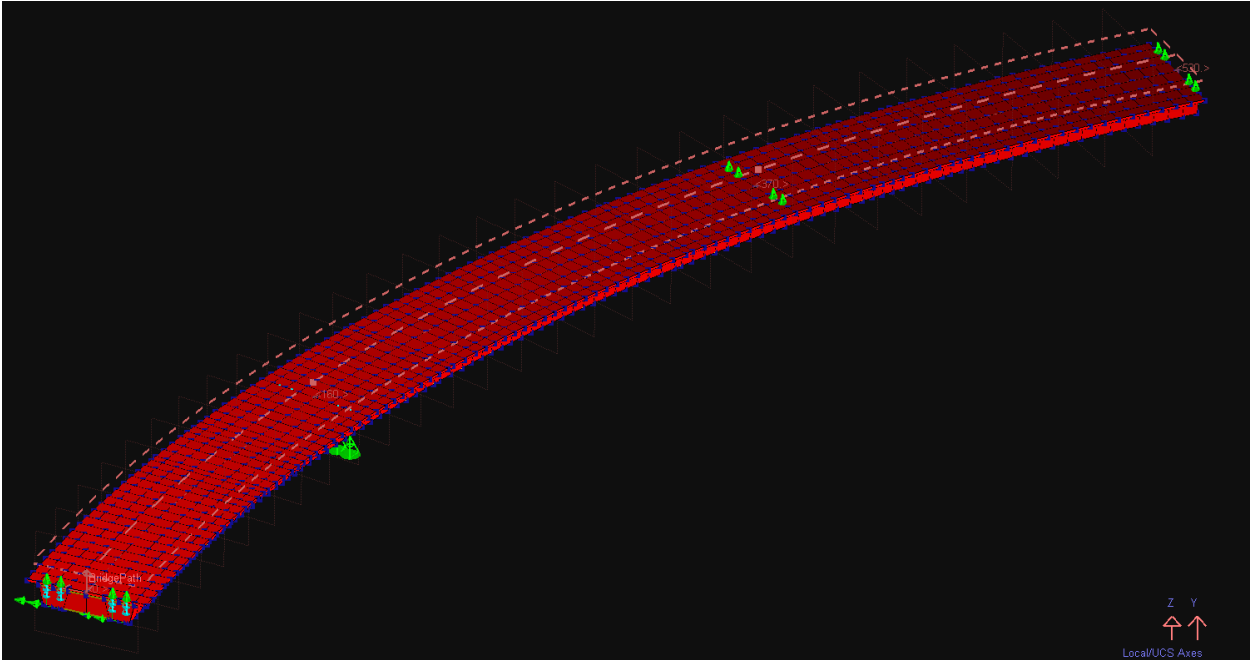
Overhang Width (+Y side):

4 ft

Figure 21: Deck Data

In this problem, the actual thickness is same as the structural thickness and the structural deck thickness is 9.5in

Click **Next** and generate the model



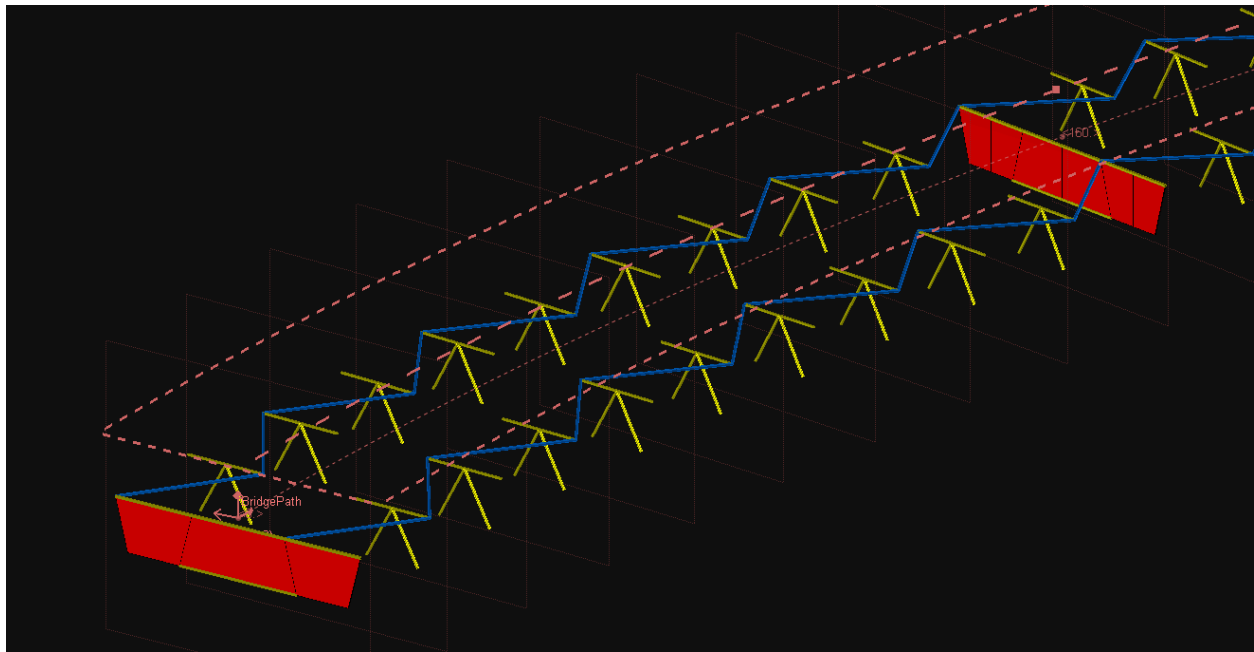


Figure 22: Generated Model

After model generation, you should check your model in detail.

Step B – Create Bridge Loading Data

In the example problem, the concrete deck is assumed to be placed at one time for the Strength Limit State checks. A separate analysis is performed to include deck placement sequence and results are used in constructability checks. Earlier concrete casts are composite for each subsequent cast.

Earlier concrete casts are composite for each subsequent cast.

- ☛ Fill Bridge Loading Table

Bridge Loading Table

Live Load	Vehicular Longitudinal Increment		Centrifugal Longitudinal Increment		Braking Longitudinal Increment	
	5 ft		5 ft <i>Enter zero to ignore centrifugal effect.</i>		0 ft <i>Enter zero to ignore braking effect.</i>	
	Vehicular Transverse Increment		Centrifugal Transverse Increment		Braking Transverse Increment	
	2 ft <i>Entering zero will assume same as longitudinal spacing.</i>		5 ft <i>Entering zero will assume same as longitudinal spacing.</i>		0 ft <i>Entering zero will assume same as longitudinal spacing.</i>	
			Centrifugal Design Velocity			
			35 MPH			
Sidewalk	Sidewalk width+Barrier at +Y edge		Sidewalk width+Barrier at -Y edge		Non-structural sidewalk thickness	
	1.5 ft		1.5 ft		0 kips/ft ² <i>This is the extra thickness assumed on the sidewalks on top of the deck thickness.</i>	
Strength	Wind Load		Railings (+Y)		Railings (-Y)	
	0 kips/ft ²		0.495 kips/ft		0.495 kips/ft	
	Future Wearing Surfaces		Monolithic Wearing Surfaces		Utility Loads [BETA]	
0.03 kips/ft ²		0 kips/ft ²		Utility Loads		
Construction	Screed Weight		Skew Angle of the Screed		Screed Movement	
	0 kips <i>Entering zero for this field will ignore screed loads.</i>		0 deg <i>Enter zero if the screed is not positioned on a skew.</i>		0 ft <i>Enter zero to skip simulation of screed movement.</i>	
	Wind Load		Screed rail position relative to the exterior girder (+Y edge)		Screed rail position relative to the exterior girder (-Y edge)	
	0 kips/ft ²		0 ft <i>Enter zero if the screed is positioned exactly on the exterior girder.</i>		0 ft <i>Enter zero if the screed is positioned exactly on the exterior girder.</i>	
	Deck Formwork Weight		Deck Pouring Sequence			
Stay-in-Place 0.015 kips/ft ² <i>The weight of the deck formwork.</i>		Deck Pouring Sequence Composite as-built				
Load Rating	State: AASHTO <i>Select 'NONE' to skip creating standard live load cases for load rating; otherwise, select the name of the state for which the default design, legal and permit live load cases will be created. Select AASHTO to create standard general live load cases as defined in AASHTO code.</i>					

Figure 23: Bridge Loading Table

Go into Deck Pouring Sequence

	Name	Start Station (ft)	End Station (ft)
1	1	0.0000	125.0000
2	2	205.0000	325.0000
3	3	405.0000	530.0000
4	4	125.0000	205.0000
5	5	325.0000	405.0000

Figure 24: Deck Pouring Data

Click Next

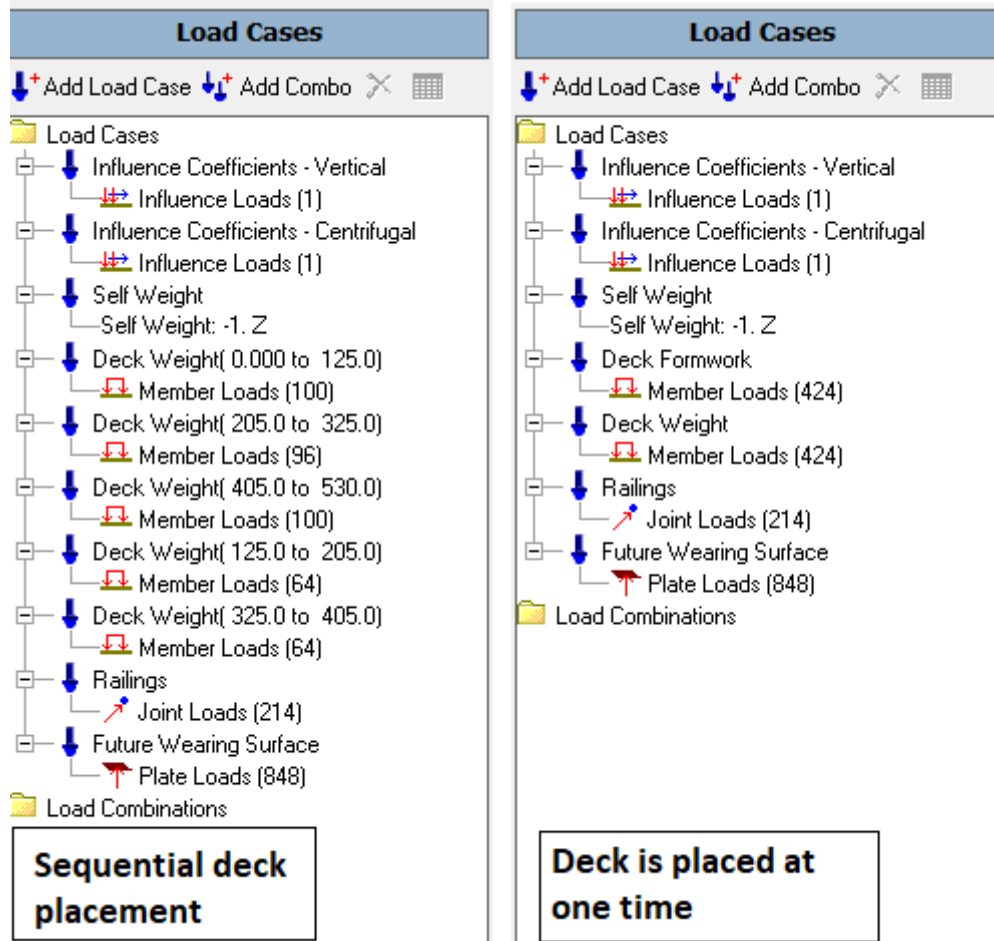


Figure 25: Load Cases

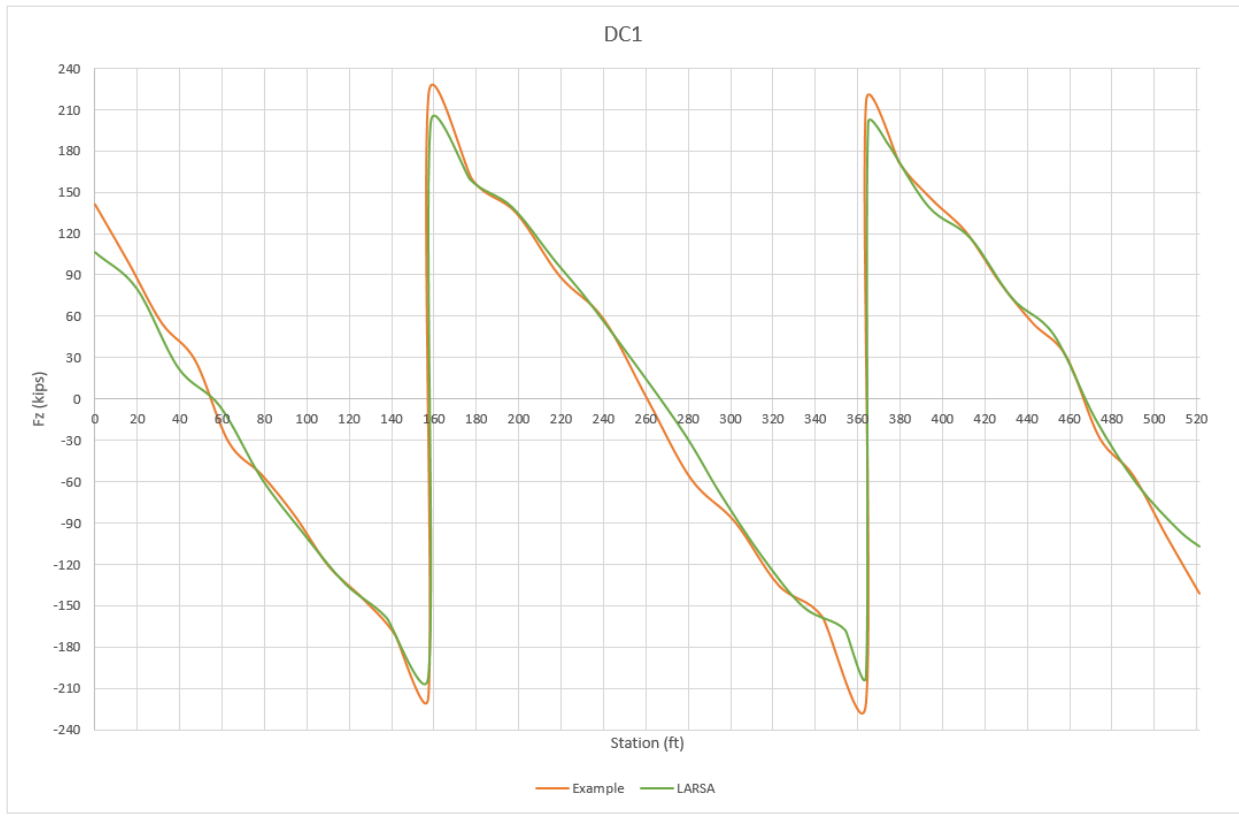
- ◆ Perform the staged construction analysis before the code check

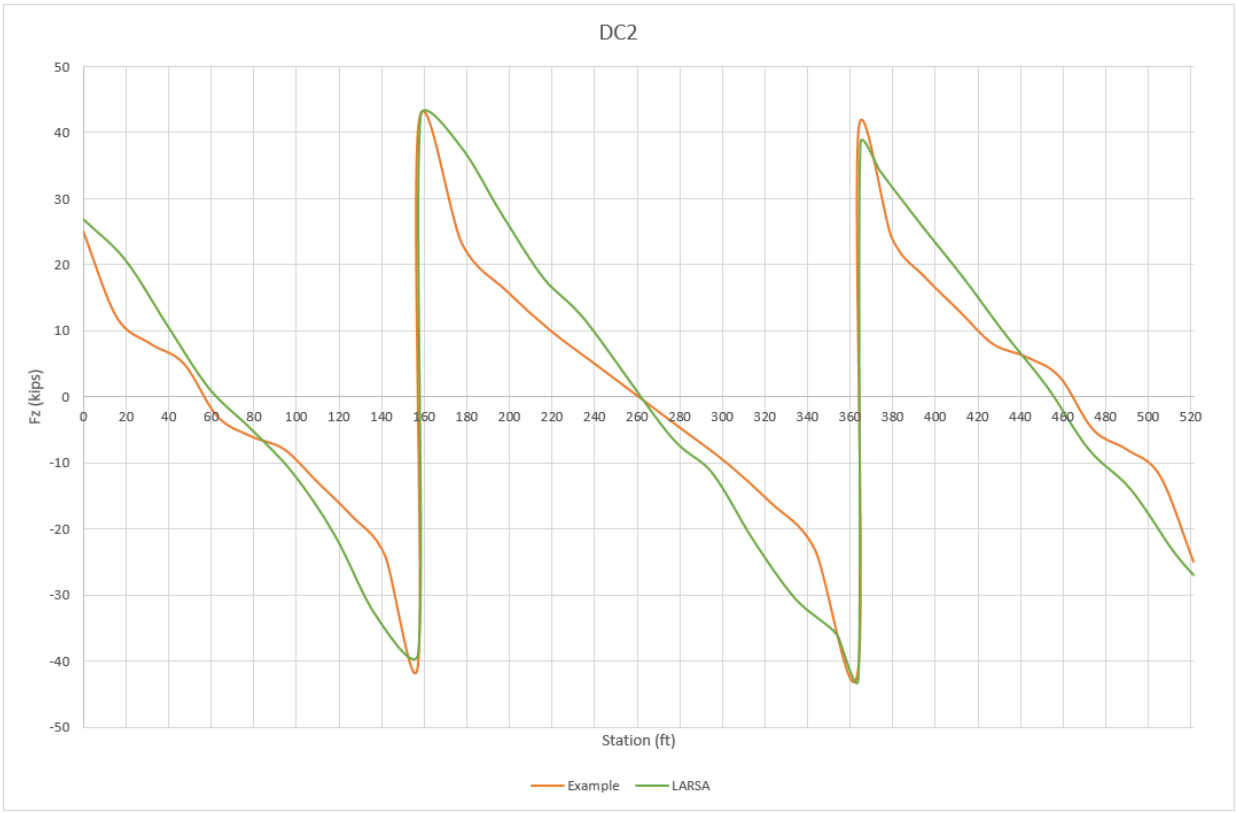
Comparison of the Analysis Results with the Reference Example

- Unfactored shears corresponding to **critical tub girder web** for girder G1 is tabulated as “Table 1 Girder G1 Unfactored Shears” in the reference example. Unfactored shear forces, throughout the bridge, are taken from LARSA 4D by “Compound Element Forces” after the staged construction analysis.

Graphical comparison of the results:

LARSA 4D Sample and Verification Problems





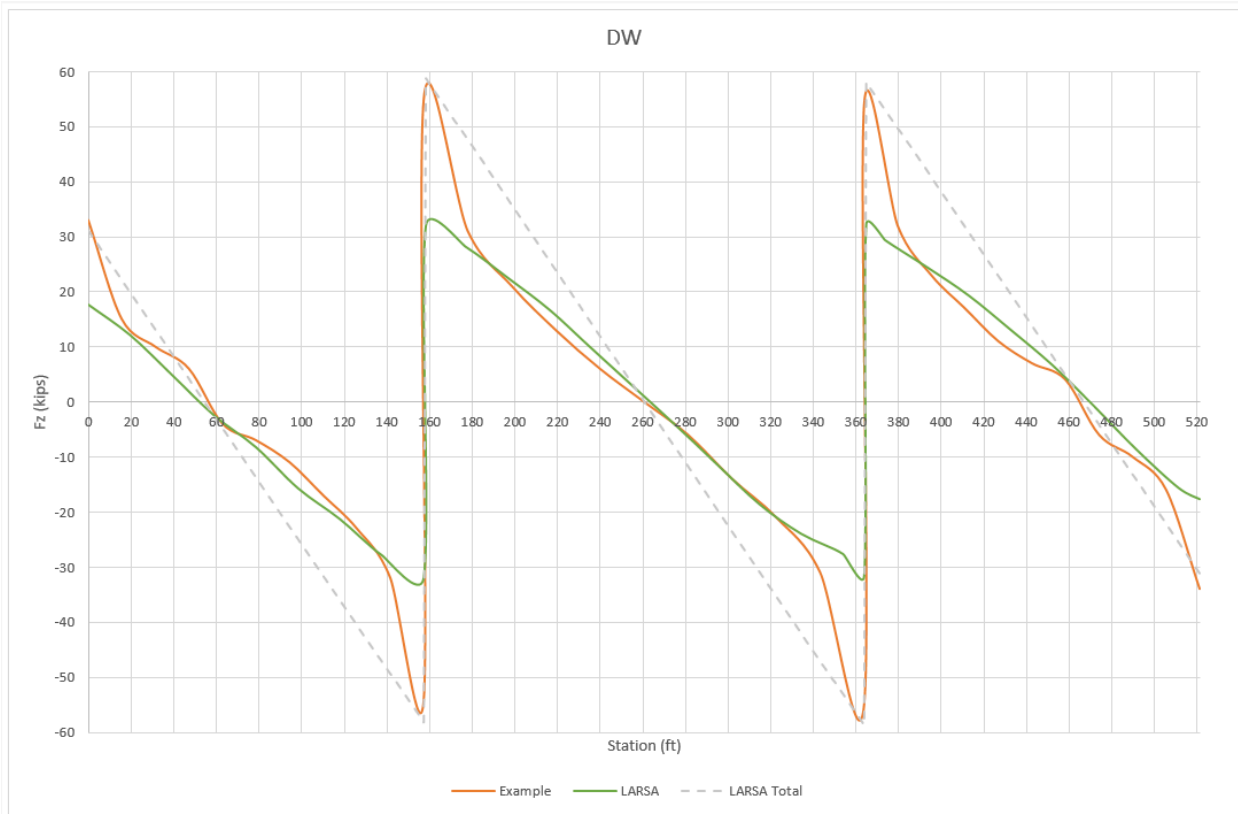
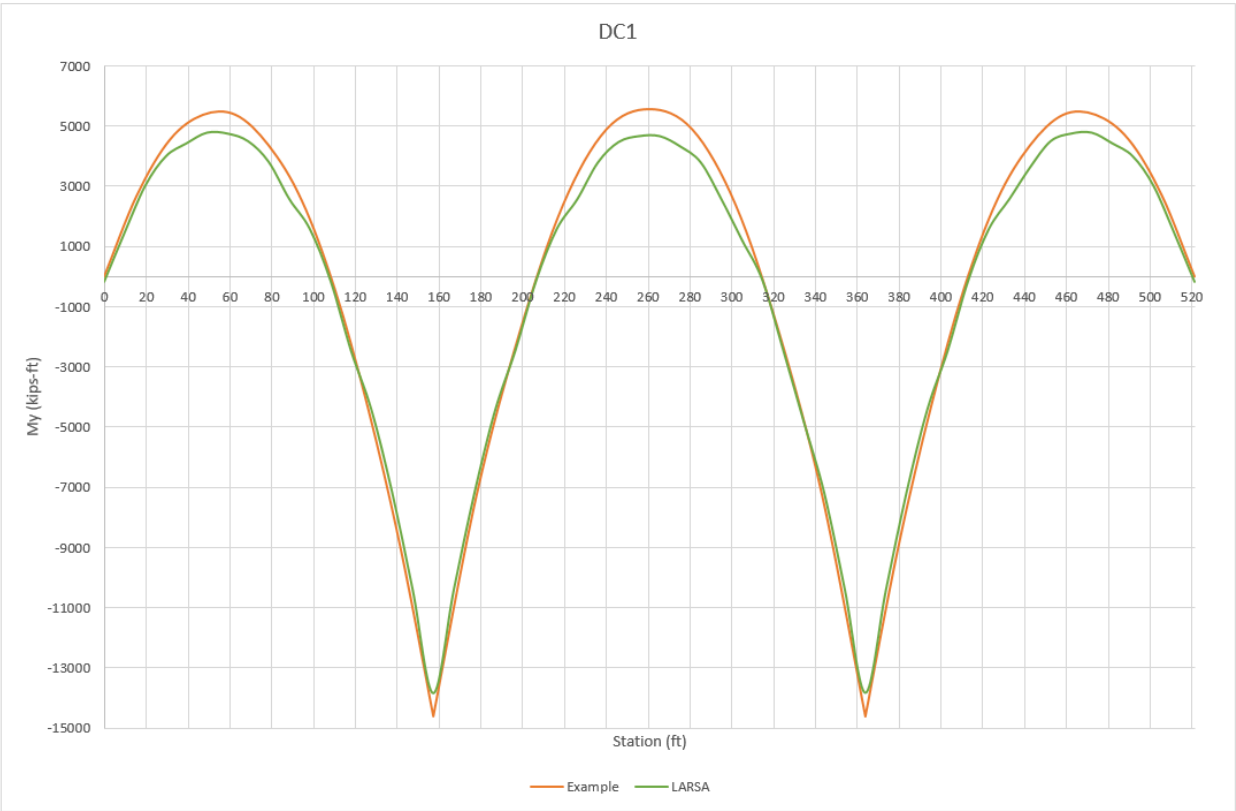
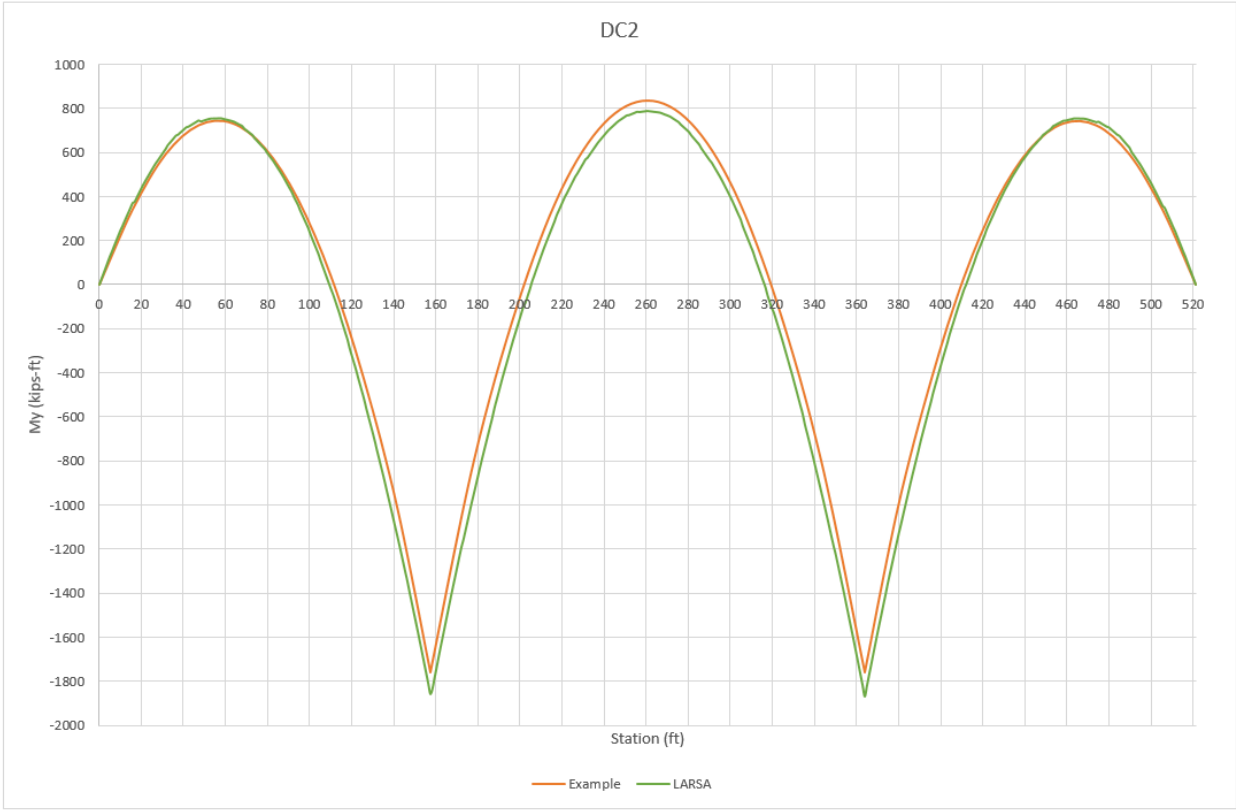


Figure 26: Girder G1 Unfactored Shears

- Unfactored major-axis bending moments for girder G1 is tabulated as “Table 3 Girder G1 Unfactored Major-Axis Bending Moments” in the reference example. Unfactored bending moments, throughout the bridge, are taken from LARSA 4D by “Compound Element Forces” after the staged construction analysis.

Graphical comparison of the results:





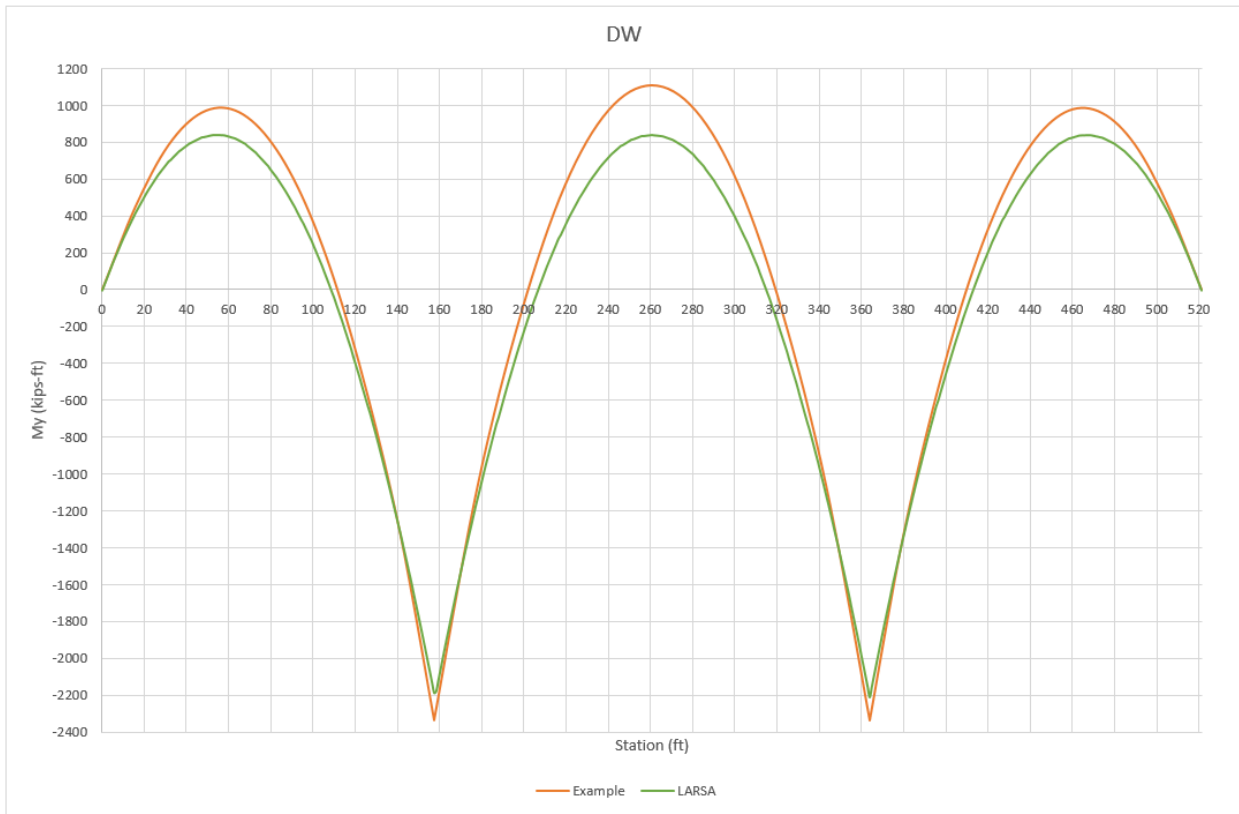
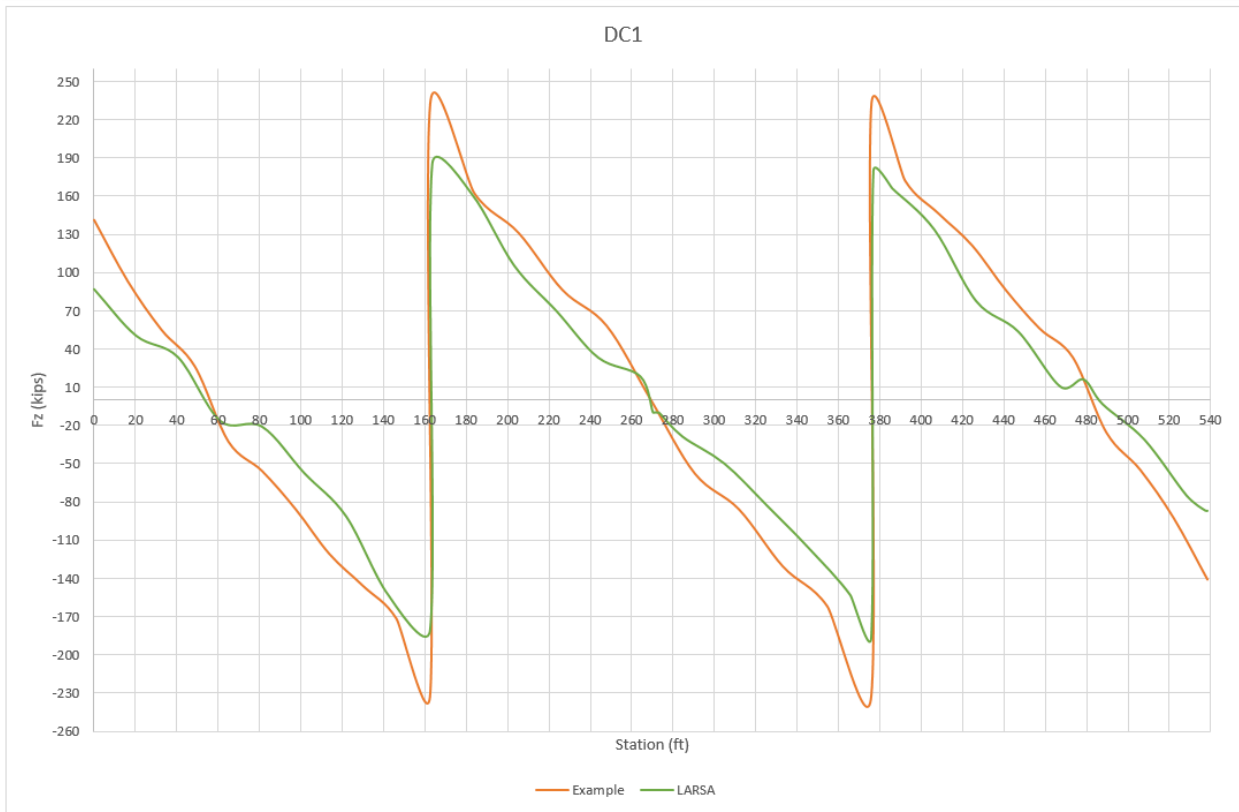


Figure 27: Girder G1 Unfactored Major-Axis Bending Moments

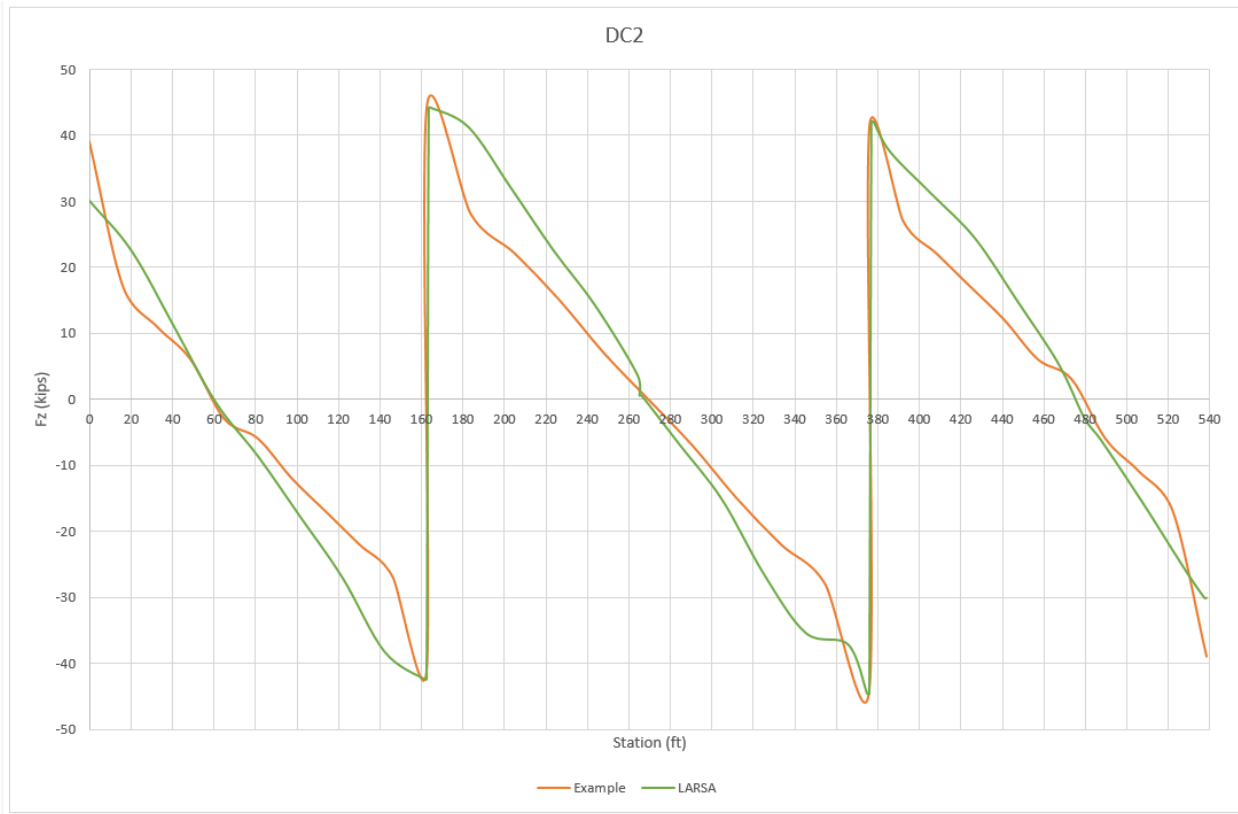
- Unfactored shears corresponding to **critical tub girder web** for girder G1 is tabulated as “Table 2 Girder G2 Unfactored Shears” in the reference example. Unfactored shear forces, throughout the bridge, are taken from LARSA 4D by “Compound Element Forces” after the staged construction analysis.

Graphical comparison of the results:

LARSA 4D Sample and Verification Problems



LARSA 4D Sample and Verification Problems



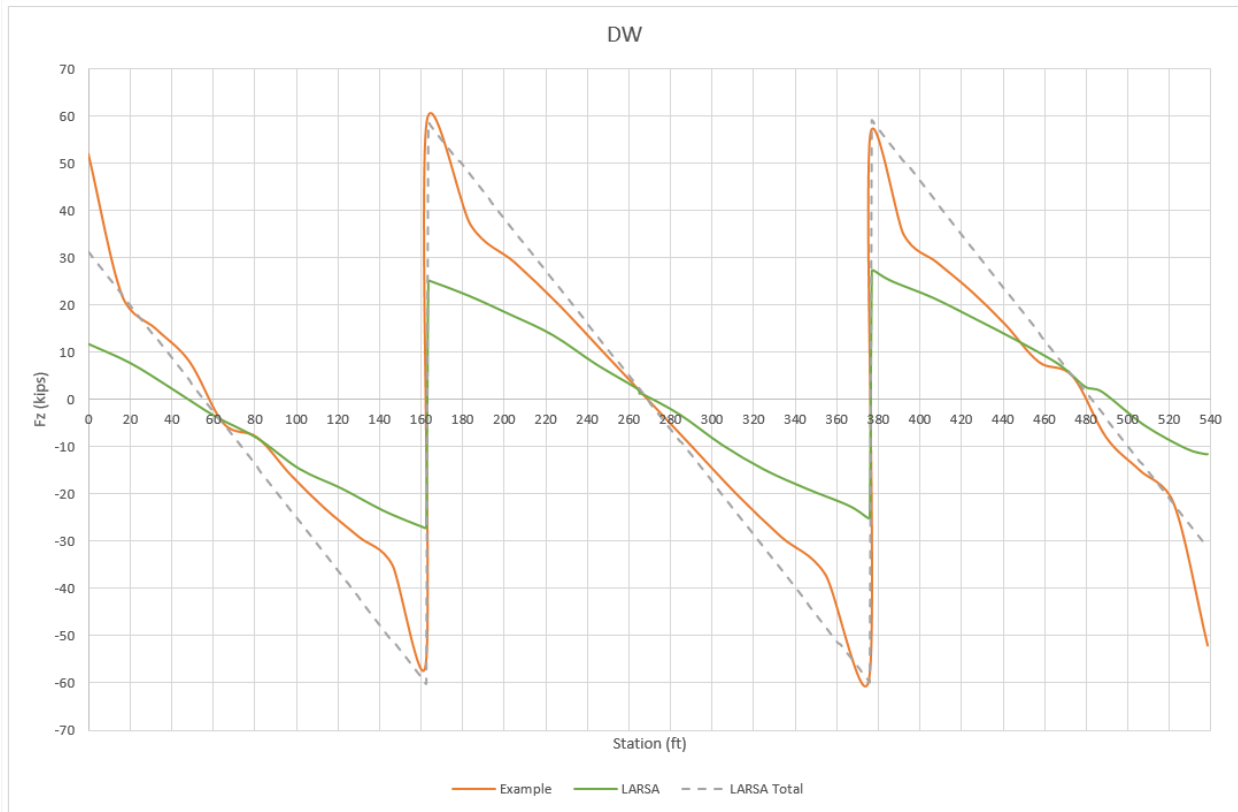
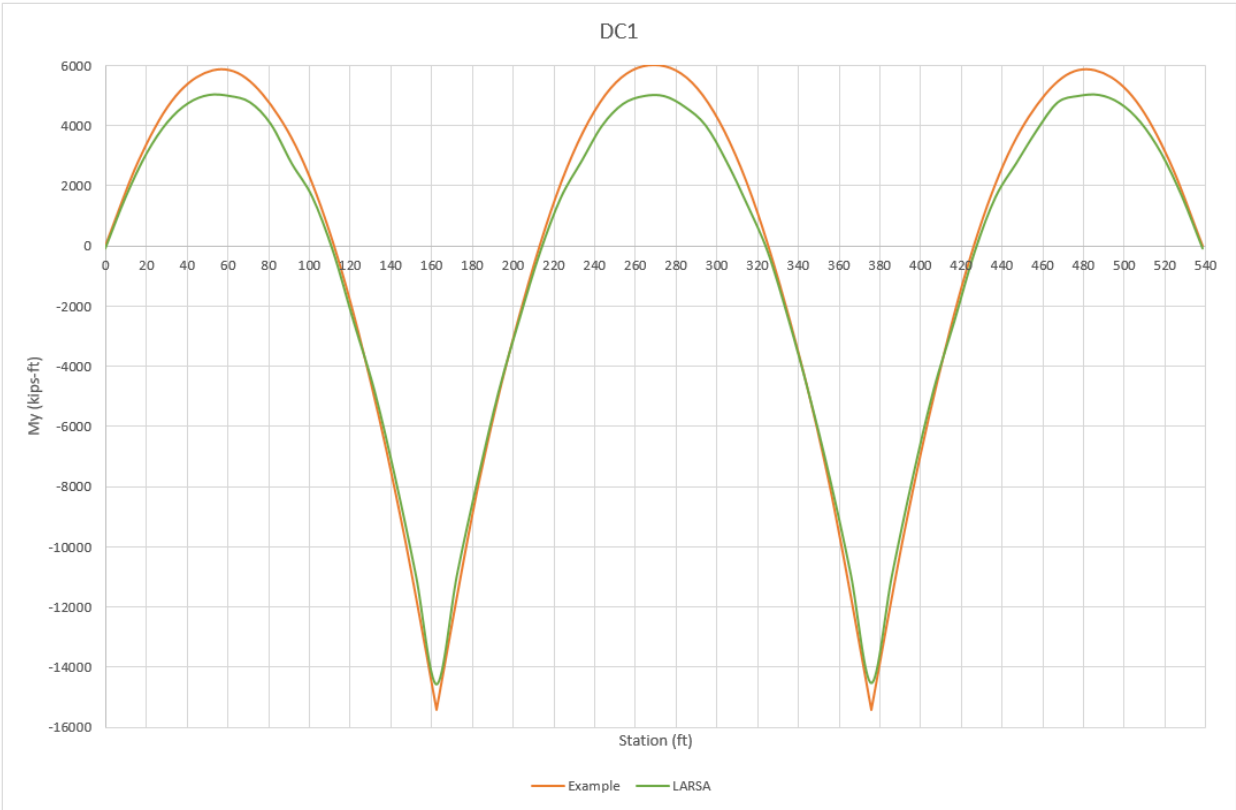


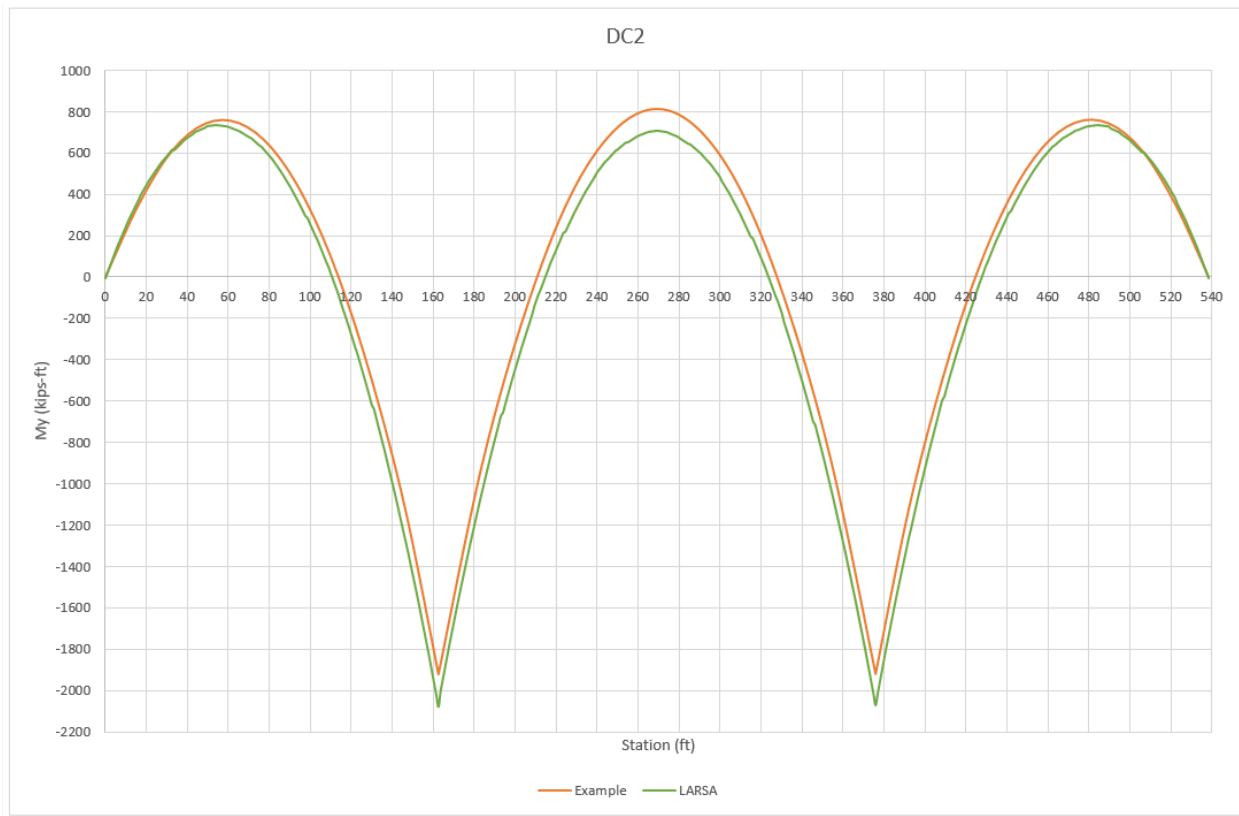
Figure 28: Girder G2 Unfactored Shears

- Unfactored major-axis bending moments for girder G1 is tabulated as “Table 4 Girder G2 Unfactored Major-Axis Bending Moments” in the reference example. Unfactored bending moments, throughout the bridge, are taken from LARSA 4D by “Compound Element Forces” after the staged construction analysis.

Graphical comparison of the results:



LARSA 4D Sample and Verification Problems



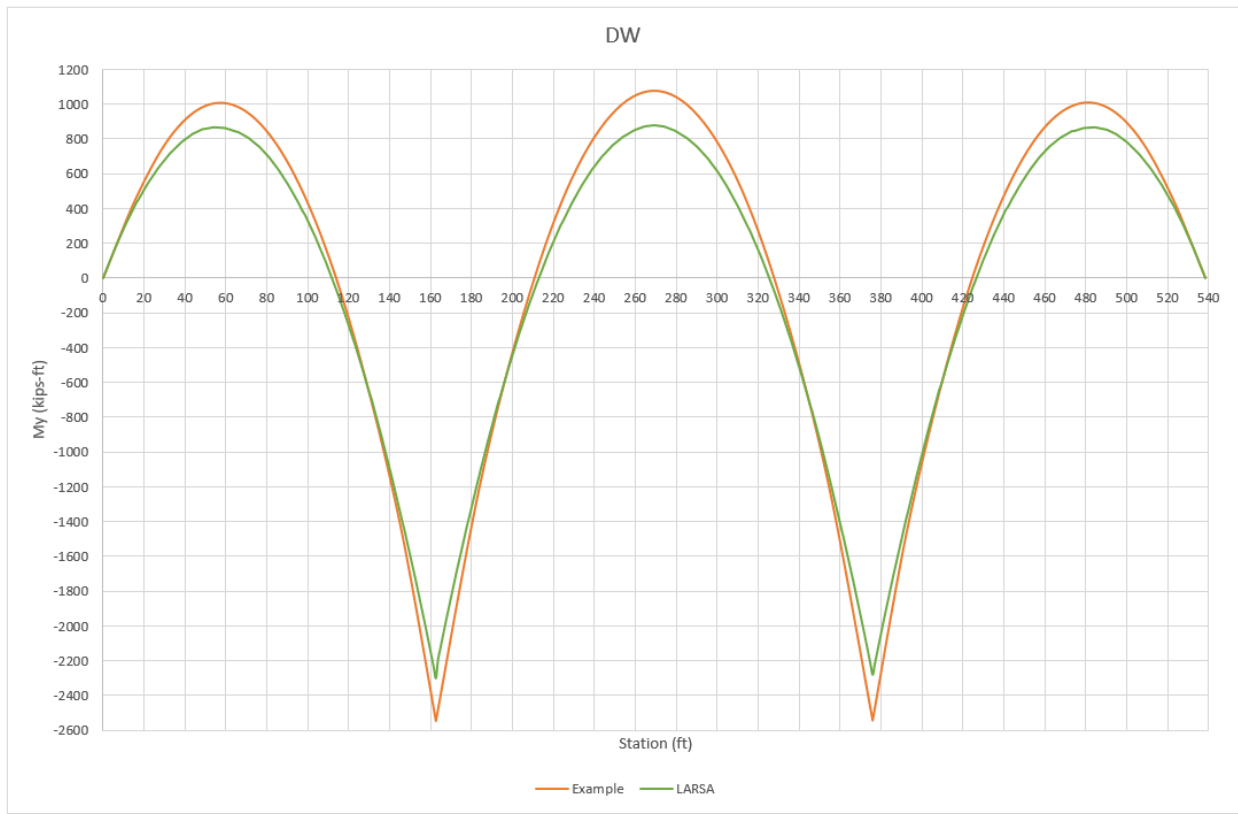


Figure 29: Girder G2 Unfactored Major-Axis Bending Moments

In the design example, bearings are modeled with “foundation elements” in 3D Finite Element Analysis Program. These elements have six different stiffnesses as explained in the example document, however there is no information regarding the stiffness values. Due to lack of information, bearings are modeled as supports with restraint conditions in LARSA 4D.

The differences between analysis results of the design example and LARSA 4D are most probably due to modeling of support conditions. It is observed that, modeling supports as springs with some arbitrary stiffness values has a significant effect on the results.

Step C – Code check per AASHTO LRFD

In this chapter, Steel Bridge Module code check inputs are illustrated for two stations which are used as positive and negative moment design sections in the reference document.

Positive moment section, G2-1 is at 57ft in the Bridge Path Coordinate System.

Negative moment section, G2-2 is at 160ft in the Bridge Path Coordinate System.

Code check is performed in LARSA 4D Steel Bridge Module per AASHTO LRFD Bridge Design Specifications.

Detailed **Verbose Report** is viewed for the positive moment code check location.

Enter →

Locations		Deck Reinforcing	Transverse Stiffeners	Longitudinal Stiffeners	Tub Data	Fatigue	Deflection Check	Girder Size Override						
	Girder Number	Station (ft)	Design Moment	Radius of Curvature (ft)	Span Length (ft)	X-Frame Spacing (Lb) (ft)	Moment Gradient Modifier (Cb)	An/Ag (Web)	An/Ag (Top Flange)	An/Ag (Bottom Flange)	Eff. Slab Width Reduction Ratio	Haunch Thickness (in)	Composite State	Override rt (6.10.8.2.3)
1	2	57.0000	Auto	700.0000	160.0000	16.0000	1.0000	1.0000	1.0000	1.0000	1.0000	Auto	Auto	-1.0000
2	2	160.0000	Auto	700.0000	160.0000	16.0000	1.0000	1.0000	1.0000	1.0000	1.0000	Auto	Auto	-1.0000

Figure 30: Locations

A_n : net cross-section area of the members

A_g : gross cross-section area of the member

r_t : effective radius of gyration

Deck Reinforcing

Top layer: #6 bars at 6 inches

Bottom layer: #4 bars at 6inches

C_{rb} and C_{rt} are not given in the example and they are not used, cover thickness from top and bottom are taken as 1 in here for 9.5in deck.

In the example, deck reinforcement is neglected in the calculation of Plastic Moment Neutral Axis for positive moment section.

Locations		Deck Reinforcing	Transverse Stiffeners	Longitudinal Stiffeners	Tub Data	Fatigue	Deflection Check	Girder Size Ove	
	Girder Number	Station (ft)	Yield Strength (kips/in ²)	Art (in ²)/(ft)	Crt (in)	Arb (in ²)/(ft)	Crb (in)	fr Factor (6.10.1.7)	
1	2	57.0000	60.0000	0.8800	1.0000	0.4000	8.5000	0.2400	
2	2	160.0000	60.0000	0.8800	1.0000	0.4000	8.5000	0.2400	

Figure 31: Deck Reinforcing

A_{rb} : area of the bottom layer of longitudinal reinforcement within the effective concrete deck width

A_{rt} : area of the top layer of longitudinal reinforcement within the effective concrete deck width

C_{rb} : distance from the top of the concrete deck to the centerline of the bottom layer of longitudinal concrete deck reinforcement

C_{rt} : distance from the top of the concrete deck to the centerline of the top layer of longitudinal concrete deck reinforcement

f_r factor : modulus of rupture factor

Transverse Stiffeners

At section G2-2, interior panel is without longitudinal stiffener and with a transverse stiffener.

Transverse stiffener: 0.5in x 5.5in

Spacing(d_o) = 62in

	Girder Number	Station (ft)	Type	Yield Strength (kips/in ²)	Spacing (in)	Width (in)	Thickness (in)	Panel
1	2	57.0000	None	50.0000	0.0000	0.0000	0.0000	Interior
2	2	160.0000	Single	50.0000	62.0000	5.5000	0.5000	Interior

Figure 32: Transverse stiffeners

☛ Longitudinal Stiffeners

T-stiffener data is to be entered under Tub Data

☛ Tub Data

T-stiffener is WT8x28.5

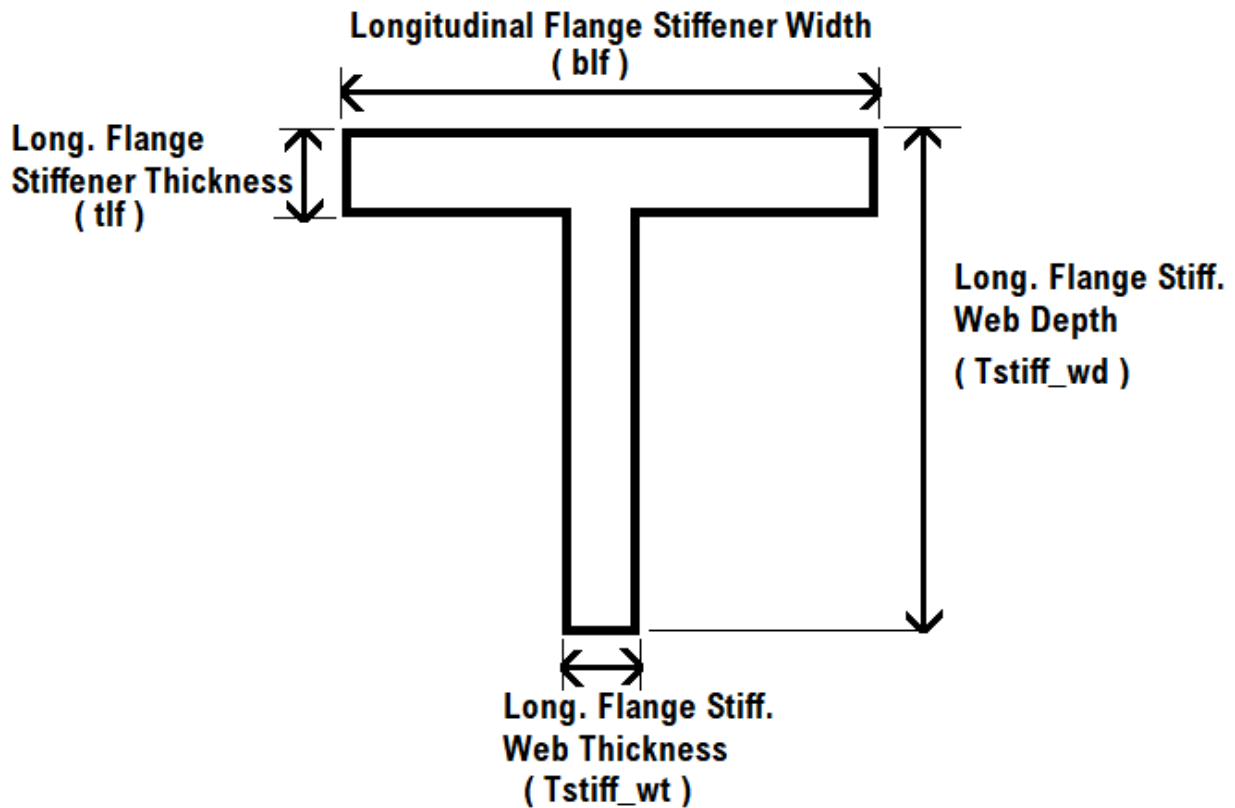


Figure 33: Bottom Flange Stiffener Definition in LARSA4D

	Girder Number	Station (ft)	theta (deg)	Transverse stiffeners within D/2 B6.5.1-1	Distance between Transverse Flange Stiffeners	# of Longitudinal Flange Stiffeners C6.11.11.2-2	Longitudinal Flange Stiffener Width (blf) (in)	Longitudinal Flange Stiffener Thickness (lf) (in)	w (6.11.8.2.3-1) (in)	Long. Flange Stiff. Web Depth (Tstiff_wd) (in)	Long. Flange Stiff. Web Thickness (Tstiff_wt) (in)
1	2	57.0000	auto	No	0.0000	0.0000	0.0000	0.0000	0.0000	8.2150	0.0000
2	2	160.0000	auto	Yes	0.0000	1.0000	7.1200	0.7150	40.5000	8.2150	0.4300

Figure 34: T-Stiffener

D : the depth of web plate measured along the slope (for inclined webs)

w : larger of the width of a box flange between longitudinal flange stiffeners or the distance from a web to the nearest longitudinal flange stiffener

☛☛ Fatigue

Fatigue I load combination is used in combination with design checks for infinite fatigue life.

Locations	Deck Reinforcing	Transverse Stiffeners	Longitudinal Stiffeners	Tub Data	Fatigue	Deflection Check	Girder Size Ove	
	Girder Number	Station (ft)	Distance from Top Flange	Distance from Bottom Flange	Detail Category	ADTTsl (3.6.1.4)	Stress Range Cycles / Passage (n)	Design Life (years)
1	2	57.0000	0.0000	0.0000	C'	infinite	0.0000	75.0000
2	2	160.0000	0.0000	0.0000	C'	infinite	0.0000	75.0000

Figure 35: Fatigue

☛☛ Result cases are assigned to load classes and load factors are modified to have Strength-I, Service-II and 1.25*(dead load) +1.5*(construction load) for constructability.

☛☛ Construction Girder Details

The top flange is continuously braced by the concrete deck for strength limit state.

The top flange is discretely braced for constructability (deck is not hardened).

Even if you leave these inputs as default, we are setting them according to your model when performing the code check.

☛☛ Click **Next** and perform the code check.

Code Check Summary

- Girder Properties

Girder Properties

Location		Girder Properties									Deck Properties				fc=	4	fy=	60	.
Girder	x	Web			Top Flange			Bottom Flange			Slab				Haunch	Reinforcing			
		D	t _w	F _{yw}	b _t	t _t	F _{yf}	b _f	t _f	F _{yf}	t _s	width L	width R	cb		th	A _{rt}	d _{rt}	A _{rb}
	(ft)	(in)	(in)	(ksi)	(in)	(in)	(ksi)	(in)	(in)	(ksi)	(in)	(ft)	(ft)	(in)	(in ²)	(in)	(in ²)	(in)	
2	57	78	0.563	50	16	1	50	83	0.625	50	9.5	10	10	1	4.	17.893	1	8.133	8.5
2	160	78	0.563	50	18	3	50	83.	1.5	50	9.5	10	10	1	4.	17.893	1	8.133	8.5

Figure 36: Summary Report Girder Properties

- Section Properties

Section Properties 1													
Location		Non-Composite						Composite w/Reinforcing					
Girder	x	A	cg _{top}	cg _{bot}	I	S _{top}	S _{bot}	A	cg _{top}	cg _{bot}	I	S _{top}	S _{bot}
	(ft)	(in ²)	(in)	(in)	(in ⁴)	(in ³)	(in ³)	(in ²)	(in)	(in)	(in ⁴)	(in ³)	(in ³)
2	57	174.35	44.469	35.156	172592.362	3881.213	4909.282	200.377	37.503	42.122	0	0	0
2	160	332.057	44.635	37.865	427385.637	9575.137	11287.07	358.084	40.871	41.629	0	0	0

Section Properties 2													
Location		Composite 3n						Composite n					
Girder	x	A	cg _{top}	cg _{bot}	I	S _{top}	S _{bot}	A	cg _{top}	cg _{bot}	I	S _{top}	S _{bot}
	(ft)	(in ²)	(in)	(in)	(in ⁴)	(in ³)	(in ³)	(in ²)	(in)	(in)	(in ⁴)	(in ³)	(in ³)
2	57	276.502	25.177	54.448	349000.03	13861.954	6409.766	480.806	11.186	68.439	477917.607	42726.222	6983.075
2	160	434.209	32.471	50.029	637004.896	19617.852	12732.63	638.513	19.819	62.681	855766.401	43179.781	13652.655

Figure 37: Summary Report Section Properties

Comparison with the design example for Section G2-2

Noncomposite Example	LARSA 4D	Composite, 3n Example	LARSA 4D	Composite, n Example	LARSA 4D
A	338.27	332.057	A	440.07	434.21
I	439269	427386	I	631237	637005
cg _{top}	43.68	44.64	cg _{top}	32.25	32.47
cg _{bot}	38.82	37.87	cg _{bot}	50.25	50.03
S _{top}	10056	9575	S _{top}	19575	19618
S _{bot}	11316	11287	S _{bot}	12561	12733

In design example, bottom flange stiffener and the longitudinal component of top flange lateral bracing area is included in section property calculations.

In LARSA 4D Code Check, section properties are calculated including the bottom flange stiffener if present. The top flange lateral bracing is not included and the reason for the difference between design example and the LARSA 4D is that.

- Force Summary

Girder Longitudinal Bending Moment Force Summary

Location		Permanent Loads			Transient Loads								Construction Loads					
Girder	x	Structure & Attach.		WS/Util	HL-93		Str II Special Vehicle		Fatigue Vehicle		Wind		Thermal		DLc ₁	DLc ₂	LLc	DLcW
		DC ₁	DC ₂	DW	LL _{max}	LL _{min}	LL _{max}	LL _{min}	LL _{max}	LL _{min}	WS _{max}	WS _{min}	TU _{max}	TU _{min}				
	(ft)	(k-ft)	(k-ft)	(k-ft)	(k-ft)	(k-ft)	(k-ft)	(k-ft)	(k-ft)	(k-ft)	(k-ft)	(k-ft)	(k-ft)	(k-ft)	(k-ft)	(k-ft)	(k-ft)	(k-ft)
2	57	5035.839	728.024	862.724	5510.913	1617.273	0	0	1336.42	-305.169	0	0	0	0	5035.839	0	0	0
2	160	14382.017	2047.597	2264.638	1304.507	8273.089	0	0	203.272	1535.775	0	0	0	0	14382.017	0	0	0

Girder Vertical Shear Force Summary

Location		Permanent Loads			Transient Loads								Construction Loads					
Girder	x	Structure & Attach.		WS/Util	HL-93		Str II Special Vehicle		Fatigue Vehicle		Wind		Thermal		DLc ₁	DLc ₂	LLc	DLcW
		DC ₁	DC ₂	DW	LL _{max}	LL _{min}	LL _{max}	LL _{min}	LL _{max}	LL _{min}	WS _{max}	WS _{min}	TU _{max}	TU _{min}				
	(ft)	(k)	(k)	(k)	(k)	(k)	(k)	(k)	(k)	(k)	(k)	(k)	(k)	(k)	(k)	(k)	(k)	(k)
2	57	-10.312	-1.44	-1.33	84.639	-83.152	0	0	26.989	-24.242	0	0	0	0	-10.312	0	0	0
2	160	-370.061	-52.23	-59.01	16.081	-260.799	0	0	5.655	-74.178	0	0	0	0	-370.061	0	0	0

Figure 38: Summary Report Force Summary

- Stress Summary

Girder Longitudinal Stress Summary (Top Flange)

Location		Permanent Loads			Transient Loads								Construction Loads			
Girder	x	Structure & Attach.		WS/Util	HL-93		Str II Special Vehicle		Wind		Thermal		DLc ₁	DLc ₂	LLc	DLcW
		DC ₁	DC ₂	DW	LL _{max}	LL _{min}	LL _{max}	LL _{min}	WS _{max}	WS _{min}	TU _{max}	TU _{min}				
	(ft)	(ksi)	(ksi)	(ksi)	(ksi)	(ksi)	(ksi)	(ksi)	(ksi)	(ksi)	(ksi)	(ksi)	(ksi)	(ksi)	(ksi)	(ksi)
2	57	-15.57	-0.63	-0.747	-1.548	0.454	0	0	0	0	0	0	-3.916	0	0	0
2	160	18.024	1.252	1.385	-0.363	2.299	0	0	0	0	0	0	8.003	0	0	0

Girder Longitudinal Stress Summary (Bottom Flange)

Location		Permanent Loads			Transient Loads								Construction Loads			
Girder	x	Structure & Attach.		WS/Util	HL-93		Str II Special Vehicle		Wind		Thermal		DLc ₁	DLc ₂	LLc	DLcW
		DC ₁	DC ₂	DW	LL _{max}	LL _{min}	LL _{max}	LL _{min}	WS _{max}	WS _{min}	TU _{max}	TU _{min}				
	(ft)	(ksi)	(ksi)	(ksi)	(ksi)	(ksi)	(ksi)	(ksi)	(ksi)	(ksi)	(ksi)	(ksi)	(ksi)	(ksi)	(ksi)	(ksi)
2	57	-12.309	-1.363	-1.615	-9.47	2.779	0	0	0	0	0	0	-12.309	0	0	0
2	160	15.29	1.93	2.134	-1.147	7.272	0	0	0	0	0	0	15.29	0	0	0

Figure 39: Summary Report Longitudinal Stress Summary

Top Flange Lateral Stress

Location		Lateral Flange Bending Moment - Analysis					Lateral Flange Bending Moment - Approximate					Lateral Flange Stress						
Girder	x	Service				Strength I	Vert. Bending			M _{approx} = Mu*L _b 2/(10*R*D)		Lateral Flange Stress						
		DC ₁	DC ₂	DW	LL	M _{analysis}	Mu(max)			D	L _b	Radius	M _{approx}	M _{lat}	b _f	t _f	S	f _{lat}
	(ft)	(k-ft)	(k-ft)	(k-ft)	(k-ft)	(k-ft)	(k-ft)			(in)	(ft)	(ft)			(in)	(in)	(in ³)	(ksi)
2	57	13.071	-0.777	-0.052	1.676	0	6294.798			78	16	700	0	173.049	16	1	42.667	4.056
2	160	12.784	11.13	-0.686	-15.817	0	-17977.521			78	16	700	0	31.998	18	3	162	0.198

Bottom Flange Lateral Stress

Location		Lateral Flange Bending Moment - Analysis					Lateral Flange Bending Moment - Approximate					Lateral Flange Stress						
Girder	x	Service				Strength I	Vert. Bending			M _{approx} = Mu*L _b 2/(10*R*D)		Lateral Flange Stress						
		DC ₁	DC ₂	DW	LL	M _{analysis}	Mu(max)			D	L _b	Radius	M _{approx}	M _{lat}	b _f	t _f	S	f _{lat}
	(ft)	(k-ft)	(k-ft)	(k-ft)	(k-ft)	(k-ft)	(k-ft)			(in)	(ft)	(ft)			(in)	(in)	(in ³)	(ksi)
2	57	21.921	-7.402	-0.044	-54.028	-55.761	0.083			78	16	8400	0	669.131	83	0.625	717.604	0.932
2	160	-160.639	129.213	-33.31	-215.842	-345.33	0.083			78	16	8400	0	4143.966	83	1.5	1722.25	2.406

Figure 40: Summary Report Lateral Stress Summary

- Flexural Resistance

Flexural Resistance - Composite Sections in Positive (6.10.7) or Negative Flexure (6.10.8)

Location		Girder Parameters											Flange Red. Parameters - 6.10.1.10		Local Flange Buckling - 6.10.8.2.1			Lateral Torsional Buckling - 6.10.8.2.2			Flexural Resistance					
Girder	x	Web		Top Flange			Bottom Flange			Composite Properties			R _h	R _b	λ _{fl}	λ _{pf}	λ _{ff}	F _{nc}	L _b	L _p	L _r	F _{nc}	F _{nc}	F _{nt}		
		D	t _w	F _{yw}	b _f	t _f	F _{yf}	b _f	t _f	F _{yf}	F _{yr}	D _c													r _t	C _b
	(ft)	(in)	(in)	(ksi)	(in)	(in)	(ksi)	(in)	(in)	(ksi)	(ksi)	(in)	(in)													
2	57	78	0.563	50	16	1	50	83	0.625	50	35	32.366	3.964	1	1	1	8	9.152	16.12	0	16	7.956	29.946	0	50	50
2	160	78	0.563	50	18	3	50	83	1.5	50	34.999	39.301	23.642	1	1	0.999	27	9.152	16.12	0	16	47.447	178.151	0	47.275	50

Figure 41: Summary Report Flexural Resistance

- Performance ratios as a result of the code check

Section Proportioning Performance Ratios

Location		Web Proportions 6.10.2.1.1-1 or 6.10.2.1.2-1				Flange Proportions																		
Girder	x	D	C	D/C	6.10.2.1.2-1				6.10.2.2-2				6.10.2.2-3				6.10.2.2-4							
					(Compression)		(Tension)		(Compression)		(Tension)		(Compression)		(Tension)									
	(ft)	D/t _w	limit	Ratio	b _{fc} / (2 * t _{fc})	12 Ratio	b _{ft} / (2 * t _{ft})	12 Ratio	D/6	b _{fc} Ratio	D/6	b _{ft} Ratio	1.1 * t _w	t _{fc} Ratio	1.1 * t _w	t _{ft} Ratio	l _{yt}	l _{yc}	l _{yt} /l _{yc}	>0.1	<10			
2	57	138.667	150	0.924	8	12	0.667	66.4	12	5.533	13	16	0.813	13	83	0.157	0.619	1	0.619	0.619	0.625	0.99	0	0
2	160	138.667	150	0.924	27.667	12	2.306	3	12	0.25	13	83	0.157	13	18	0.722	0.619	1.5	0.413	0.619	3	0.206	0	0

Strength Performance Ratios

Location		Shear			Flexural Resistance Compact Sections			Flexural Resistance Non-compact Sections			Flexural Resistance Non-compact Sections			Lateral Bending Stress		
Girder	x	D	C	D/C	D	C	D/C	D	C	D/C	D	C	D/C	D	C	D/C
		Vu	Vn	Ratio	Mu + 1/3 * fl _{tens} * Sx _{tens}	φ * Mn	Ratio	fbu	Fnc	Ratio	fbu + 1/3 * fl	φ _f * Fnt	Ratio	fl	0.6 * Fyt	Ratio
	(ft)	(kip)	(kip)		(kip-ft)	(kip-ft)		(ksi)	(ksi)		(ksi)	(ksi)		(ksi)	(ksi)	
2	57	-125.013	292.515	0.427	18317.384	0		-24.079	50	0.482	36.512	49.915	0.731	1.279	30	0.043
2	160	-579.617	1146.508	0.506	38435.217	0		-39.843	47.275	0.843	42.911	50	0.858	0.088	30	0.003

Figure 42: Performance Ratios

The Summary and the Verbose Reports

In this chapter, rather than the numerical comparisons, the code check procedures of the Steel Bridge Module will be reviewed which are verified by the design procedures of the example problem.

If you click on the station that you performed the code check from the menu, you will see pass and fail results in the **Summary Report**:

(You have an option at that page to see the verbose report)

<ul style="list-style-type: none"> Input Summary Performance Ratios Camber Deflection G:2 S:160 <li style="background-color: #e0e0e0;">G:2 S:57 	BOX GIRDER STRENGTH														
	<table border="1" style="width: 100%; border-collapse: collapse;"> <tr> <td style="width: 60%;">Shear Resistance 6.10.9.1-1</td> <td>$V_{ui} \leq \phi_{i_v} \cdot V_n$? PASSED ;</td> </tr> <tr> <td>Noncompact Sections - General Requirements 6.11.7.2.1-1</td> <td>$Abs(fbu_comp) \leq \phi_{i_f} \cdot F_{nc}$? PASSED ;</td> </tr> <tr> <td>Noncompact Sections - General Requirements 6.11.7.2.1-2</td> <td>$Abs(fbu_tens) \leq \phi_{i_f} \cdot F_{nt}$? PASSED ;</td> </tr> <tr> <td>Flexural Resistance - Composite Sections in Positive Flexure - Ductility Requirement 6.10.7.3-1</td> <td>$D_p \leq 0.42 \cdot D_t$? PASSED ;</td> </tr> <tr> <td colspan="2" style="background-color: #d3d3d3;">SECTION PROPORTIONING</td> </tr> <tr> <td>Optional Criteria for Span-To_Depth Ratio 2.5.2.6.3</td> <td>$\frac{L_{eff}}{d_a} \leq 25$? PASSED ;</td> </tr> <tr> <td>Cross Section Proportion Limits - Web Proportions 6.10.2.1.2-1</td> <td>$\frac{d_a}{t_w} < limit$? PASSED :</td> </tr> </table>	Shear Resistance 6.10.9.1-1	$V_{ui} \leq \phi_{i_v} \cdot V_n$? PASSED ;	Noncompact Sections - General Requirements 6.11.7.2.1-1	$Abs(fbu_comp) \leq \phi_{i_f} \cdot F_{nc}$? PASSED ;	Noncompact Sections - General Requirements 6.11.7.2.1-2	$Abs(fbu_tens) \leq \phi_{i_f} \cdot F_{nt}$? PASSED ;	Flexural Resistance - Composite Sections in Positive Flexure - Ductility Requirement 6.10.7.3-1	$D_p \leq 0.42 \cdot D_t$? PASSED ;	SECTION PROPORTIONING		Optional Criteria for Span-To_Depth Ratio 2.5.2.6.3	$\frac{L_{eff}}{d_a} \leq 25$? PASSED ;	Cross Section Proportion Limits - Web Proportions 6.10.2.1.2-1	$\frac{d_a}{t_w} < limit$? PASSED :
Shear Resistance 6.10.9.1-1	$V_{ui} \leq \phi_{i_v} \cdot V_n$? PASSED ;														
Noncompact Sections - General Requirements 6.11.7.2.1-1	$Abs(fbu_comp) \leq \phi_{i_f} \cdot F_{nc}$? PASSED ;														
Noncompact Sections - General Requirements 6.11.7.2.1-2	$Abs(fbu_tens) \leq \phi_{i_f} \cdot F_{nt}$? PASSED ;														
Flexural Resistance - Composite Sections in Positive Flexure - Ductility Requirement 6.10.7.3-1	$D_p \leq 0.42 \cdot D_t$? PASSED ;														
SECTION PROPORTIONING															
Optional Criteria for Span-To_Depth Ratio 2.5.2.6.3	$\frac{L_{eff}}{d_a} \leq 25$? PASSED ;														
Cross Section Proportion Limits - Web Proportions 6.10.2.1.2-1	$\frac{d_a}{t_w} < limit$? PASSED :														

[Click here to see the verbose report.](#)

Figure 43: Summary Report

The Code Check Procedures in the Verbose Report

Reference Document: AASHTO LRFD (7th Edition, 2014)

- Section Proportioning

SECTION PROPORTIONING					
Condition A [2.5.2.6.3]		<table border="1" style="width: 100%; border-collapse: collapse;"> <tr> <td>$min = MinimumValue(F_{yc}, F_{yt}, F_{yw}) = 50$</td> </tr> <tr> <td>$min \leq 50$? Yes</td> </tr> <tr> <td>Condition.4 satisfied ? Yes</td> </tr> </table>	$min = MinimumValue(F_{yc}, F_{yt}, F_{yw}) = 50$	$min \leq 50$? Yes	Condition.4 satisfied ? Yes
$min = MinimumValue(F_{yc}, F_{yt}, F_{yw}) = 50$					
$min \leq 50$? Yes					
Condition.4 satisfied ? Yes					
Optional Criteria for Span-To_Depth Ratio 2.5.2.6.3	$\frac{L_{eff}}{d_a} \leq 25$? PASSED ; where $L_{eff}= 128.0ft$, $d_a= 80.34in$	1			
The limiting ratio for section proportion checks. limit = 300 if Longitudinally Stiffened, 150 otherwise	limit = 150 = 150				
Cross Section Proportion Limits - Web Proportions 6.10.2.1.2-1	$\frac{d_a}{t_w} \leq limit$? PASSED ; where $d_a= 80.34in$, $t_w= 0.563in$, limit= 150.0	2			
Box Girder Section Proportioning					
		$isFullBox ? No$; where $isFullBox= 0.000$			
Flange Proportions 6.11.2.2-1	$\frac{bf_top}{2 \cdot tf_top} \leq 12$? PASSED ; where $bf_top= 16.00in$, $tf_top= 1.000in$				
Flange Proportions 6.11.2.2-2	$bf_top \geq \frac{d_a}{6}$? PASSED ; where $bf_top= 16.00in$, $d_a= 80.34in$	3			
Flange Proportions 6.11.2.2-3	$tf_top \geq 1.1 \cdot t_w$? PASSED ; where $tf_top= 1.000in$, $t_w= 0.563in$				
	$bf_bot > \frac{1}{5} \cdot L_{eff}$? No ; where $bf_bot= 83.00in$, $L_{eff}= 128.0ft$	4			
Web Inclination 6.11.2.1.1	$\tan(\theta) < 0.250000001$? PASSED ; where $\theta= 0.242rad$	5			

Figure 44: Section Proportioning

1) AASHTO Article 2.5.2.6.3 Optional Criteria for Span-to-Depth Ratios

“For curved girder systems, the span-to-depth ratio, L/D, of each steel girder should not exceed 25 when the specified minimum yield strength of the girder in regions of positive flexure is 50ksi or less.”

2) AASHTO Article 6.11.2.1 Web Proportions

For the case of inclined webs, the distance along the web shall be used for checking all design requirements

$$D/t_w \leq 150 \text{ (webs with longitudinal stiffener)[6.11.2.1.2-1]}$$

$$D/t_w \leq 300 \text{ (webs without longitudinal stiffener)[6.11.2.1.2-2]}$$

da: the depth of web plate measured along the slope (report)

3) AASHTO Article 6.11.2.2 Flange Proportions

$$b_f/2t_f \leq 12 \text{ [6.11.2.2.2-1]}$$

$$b_f \geq D/6 \text{ [6.11.2.2.2-2]}$$

$$b_f/2t_f \geq 1.4t_w \text{ [6.11.2.2.2-3]}$$

4) AASHTO Article 6.11.1.1 Stress Determinations

If the flange width exceeds one-fifth of the effective span, only a width equal to one-fifth of the effective span shall be considered effective in resisting flexure.

In this example, the flange width does not exceed one-fifth of the effective span where the effective length of span is 128ft, so, $b_{f_bot} = 83\text{in}$ is used for stress calculations.

5) AASHTO Article 6.11.2.1.1 General

The inclination of the web plates to a plane normal to the bottom flange should not exceed 1 to 4

- Strength Limit State - Flexural Resistance (Positive Moment Region)

6	$M_u \geq 0$? Yes ; where $M_u = 1.81e4\text{kips-ft}$
	$IsCurved$? Yes ; where $IsCurved = -1.000$
Section 6.11.7.2: Flexural Resistance of Noncompact Sections in Positive Flexure	$isFullBox$? No ; where $isFullBox = 0.000$
	The nominal flexural resistance of the compression flange 6.11.7.2.2-1 $F_{nc} = R_b \cdot R_h \cdot F_{yc} = 50$; where $R_b = 1.000$, $R_h = 1.000$, $F_{yc} = 50.00\text{kips/in}^2$
	Noncompact Sections - General Requirements 6.11.7.2.1-1 $Abs(f_{bu_comp}) \leq \phi_i \cdot F_{nc}$? PASSED ; where $f_{bu_comp} = -24.08\text{kips/in}^2$, $\phi_i = 1.000$, $F_{nc} = 50.00$
Continuation	The nominal flexural resistance of the compression flange determined as specified in Article 6.10.7.2.2 6.11.7.2.2-5 $F_{nt} = R_h \cdot F_{yt} \cdot \delta_{tens} = 49.9155$; where $R_h = 1.000$, $F_{yt} = 50.00\text{kips/in}^2$, $\delta_{tens} = 0.998$
	Noncompact Sections - General Requirements 6.11.7.2.1-2 $Abs(f_{bu_tens}) \leq \phi_i \cdot F_{nt}$? PASSED ; where $f_{bu_tens} = 36.09\text{kips/in}^2$, $\phi_i = 1.000$, $F_{nt} = 49.92$
	Flexural Resistance - Composite Sections in Positive Flexure - Ductility Requirement 6.10.7.3-1 $D_p \leq 0.42 \cdot D_t$? PASSED ; where $D_p = 8.620\text{in}$, $D_t = 92.13\text{in}$
8	

Figure 45: Flexural Resistance

6) AASHTO Article 6.11.6.2.2 Sections in Positive Flexure

Sections in horizontally curved steel girder bridges shall be considered as noncompact sections and shall satisfy the requirements of Article 6.11.7.2

Compact and noncompact sections shall satisfy the ductility requirement specified in Article 6.10.7.3

7) AASHTO Article 6.11.7.2 Noncompact Sections

Compression flanges shall satisfy: $f_{bu} \leq \phi_f F_{nc}$ [6.11.7.2.1-1]

Tension flanges shall satisfy: $f_{bu} \leq \phi_f F_{nt}$ [6.11.7.2.1-2]

$F_{nc} = R_b R_h F_{yc}$ (Tub Sections) [6.11.7.2.2-1]

$F_{nc} = R_b R_h F_{yc} \Delta$ (Closed-box Sections) [6.11.7.2.2-2]

$F_{nt} = R_h F_{yt} \Delta$ (Tub Sections and Closed-box Sections) [6.11.7.2.2-5]

8) AASHTO Article 6.10.7.3 Ductility Requirement

$D_p \leq 0.42 D_t$ [6.10.7.3-1]

- Strength Limit State - Shear Resistance(Positive Moment Region)

Vn Calculation	Shear buckling coefficient NOTE: The Girder is NOT considered stiffened since it is NOT transversely stiffened.	$k_{shear} = 5 = 5$	9
	$\frac{d_a}{t_w} > 1.4 \left(e \cdot \frac{k_{shear}}{F_{yw}} \right)^{0.5}$? Yes ; where $d_a = 80.34in$, $t_w = 0.563in$, $e = 2.90e4kips/in^2$, $k_{shear} = 5.000$, $F_{yw} = 50.00kips/in^2$		
	The ratio of the shear-buckling resistance to the shear specified minimum yield strength 6.10.9.3.2-6	$c = \left(\frac{1.57}{\left(\frac{d_a}{t_w} \right)^2} \right) \cdot \left(e \cdot \frac{k_{shear}}{F_{yw}} \right) = .2232$; where $d_a = 80.34in$, $t_w = 0.563in$, $e = 2.90e4kips/in^2$, $k_{shear} = 5.000$, $F_{yw} = 50.00kips/in^2$	
	the plastic shear force 6.10.9.3.2-3	$V_p = 0.58 \cdot f_{yw} \cdot d_a \cdot t_w = 1310.4944$ kips; where $f_{yw} = 50.00kips/in^2$, $d_a = 80.34in$, $t_w = 0.563in$	
nominal shear resistance determined as specified in Articles 6.10.9.2 and 6.10.9.3, for unstiffened and stiffened webs, respectively	$V_n = c \cdot V_p = 292.5153$ kips; where $c = 0.223$, $V_p = 1,310$ kips		
The shear projected onto the axis of the box girder web 6.11.9.1	$V_{ui} = \frac{V_u}{\cos(\theta)} = 128.7581$ kips; where $V_u = 125.0kips$, $\theta = 0.242rad$		11
for non-composite case	$a_o_{noncomp} = \frac{b_{f_{bot}} + b_{fd} - t_w}{2} \cdot (d + 0.5 \cdot t_{f_{top}} + 0.5 \cdot t_{f_{bot}}) = 8015.8352$ in ² ; where $b_{f_{bot}} = 83.00in$, $b_{fd} = 121.0in$, $t_w = 0.563in$, $d = 78.00in$, $t_{f_{top}} = 1.000in$, $t_{f_{bot}} = 0.625in$		12
for composite case	$a_o_{comp} = a_o_{noncomp} + (b_{fd} - (h_t + 0.5 \cdot t_s + 0.5 \cdot t_{f_{top}})) = 9013.9023$ in ² ; where $a_o_{noncomp} = 8,016$ in ² , $b_{fd} = 121.0in$, $h_t = 3.000in$, $t_s = 9.500in$, $t_{f_{top}} = 1.000in$		
St. Venant torsional shear 6.11.9.1	$V_{ut} = \frac{A_{bf}(M_{ux}) \cdot d_a}{2 \cdot a_o_{comp}} = 84.0457$ kips; where $M_{ux} = -1,572$ kips-ft, $d_a = 80.34in$, $a_o_{comp} = 9,014$ in ²		
Shear Resistance 6.10.9.1-1	$V_{ui} + V_{ut} \leq \phi_{t_v} \cdot V_n$? PASSED; where $V_{ui} = 128.8kips$, $V_{ut} = 84.05kips$, $\phi_{t_v} = 1.000$, $V_n = 292.5kips$		13

Figure 46: Shear Resistance

9) AASHTO Article 6.10.9.2 Nominal Resistance of Unstiffened Webs

$V_n = V_{cr} = C V_p$ [6.10.9.2-1]

V_{cr} : shear buckling resistance

$V_n = 0.58 F_{yw} D t_w$ [6.10.9.2-2]

C is the ratio of shear-buckling resistance to shear yield strength and determined according to Article 6.10.9.3.2

k taken equal to 5

10) AASHTO Article 6.10.9.3.2 Interior Panels

If $D/t_w \leq 1.12 (\sqrt{E k/F_{yw}}) \rightarrow C = 1.0$ [6.10.9.3.2-4]

If $1.12 (\sqrt{E k/F_{yw}}) < D/t_w \leq 1.4 (\sqrt{E k/F_{yw}}) \rightarrow C = (1.12/(D/t_w)) ((\sqrt{E k/F_{yw}}))$ [6.10.9.3.2-5]

If $D/t_w > 1.4 (\sqrt{E k/F_{yw}}) \rightarrow C = (1.57/(D/t_w)^2) ((\sqrt{E k/F_{yw}}))$ [6.10.9.3.2-6]

11) AASHTO Article 6.11.9 Shear Resistance

Article 6.10.9 shall apply for determining the factored shear resistance of a single web.

For the case of inclined webs, D in Article 6.10.9 shall be taken as the depth of the web plate measured along the slope ($D=da$ in the verbose report)

For the case of inclined webs, each web shall be designed for a shear, V_{ui}

$$V_{ui} = V_u / \cos\theta \text{ [6.11.9-1]}$$

For all single box sections, horizontally curved sections, and multiple box sections in bridges not satisfying the requirements of Article 6.11.2.3, or with box flanges that are not fully effective according to the provisions of Article 6.11.1.1, V_u shall be taken as the sum of the flexural and St.Venant torsional shears.

12) AASHTO Article C6.11.1.1 Stress Determinations

A_o = enclosed area within the box section

For torques applied to the noncomposite section, A_o is to be computed for the noncomposite box section. As specified in Article 6.7.5.3, if top lateral bracing in a tub section is attached to the webs, A_o is to be reduced to reflect the actual location of the bracing. Because shear connectors are required along the entire length of box sections according to these provisions, the concrete deck can be considered effective in resisting torsion at any point along the span. Therefore, for torques applied to the composite section in regions of positive or negative flexure, A_o is to be computed for the composite section using the depth from the bottom flange to the midthickness of the concrete deck. The depth may be computed using a lower bound estimate of the actual thickness of the concrete haunch, or may be determined conservatively by neglecting the thickness of the haunch.

13) AASHTO Article 6.10.9.1 General

$$V_u \leq \phi_v V_n \text{ [6.10.9.1-1]}$$

- Constructability Limit State - Flexure

A separate model with deck pouring sequence is used for constructability limit state checks

	isFullBox ? No ; where isFullBox= 0.000		
	Mu ≥ 0 ? Yes ; where Mu= 8,431.kips-ft		
15	IsDiscretelyBracedCompConstruct ? Yes ; where IsDiscretelyBracedCompConstruct=-1.000		
Fnc Calculation 16	Lb ≥ Lp & Lb ≤ Lr ? Yes ; where Lb= 16.26ft, Lp= 7.573ft, Lr= 29.84ft		
	ConstructabilityStage ? Yes		
	6.10.8.2.3-2	fnc_ltb = cb · (1 - (1 - (Fyr / Rh · Fyc) · (Lb - Lp / Lr - Lp))) · Rb · Rh · Fyc = 44.149 ; where cb= 1.000, Fyr= 35.00kips/in², Rh= 1.000, Fyc= 50.00kips/in², Lb= 16.26ft, Lp= 7.573ft, Lr= 29.84ft, Rb= 1.000	
		fnc_ltb > Rb · Rh · Fyc ? No ; where fnc_ltb= 44.15, Rb= 1.000, Rh= 1.000, Fyc= 50.00kips/in²	
		lf < lpf ? Yes	
		lf < lpf ? Yes ; where lf= 8.000, lpf= 9.152	
6.10.8.2.2-1	fnc_flb = Rb · Rh · Fyc = 50 ; where Rb= 1.000, Rh= 1.000, Fyc= 50.00kips/in²		
	The nominal flexural resistance of the compression flange	Fnc = min(fnc_ltb, fnc_flb) = 44.149 ; where fnc_ltb= 44.15, fnc_flb= 50.00	
Flexure - Discretely Braced Flanges in Compression 6.10.3.2.1-1	Abs(fbu_top) + Abs(fl_top) ≤ phi_f · Rh · Fyc ? PASSED ; where fbu_top=-26.07kips/in², fl_top= 7.138kips/in², phi_f= 1.000, Rh= 1.000, Fyc= 50.00kips/in²		
Flexure - Discretely Braced Flanges in Compression 6.10.3.2.1-2	Abs(fbu_top) + 1/3 · Abs(fl_top) ≤ phi_f · Fnc ? PASSED ; where fbu_top=-26.07kips/in², fl_top= 7.138kips/in², phi_f= 1.000, Fnc= 44.15	15	
6.10.3.2.1-3	2 · (Dc / tw) ≤ 5.7 · ((e / Fyc) ^ 0.5) ? No ; where Dc= 44.77in, tw= 0.563in, e= 2.90e4kips/in², Fyc= 50.00kips/in²		
Flexure - Discretely Braced Flanges in Compression 6.10.3.2.1-3	Abs(fbu_top) ≤ phi_f · Fcrw ? PASSED ; where fbu_top=-26.07kips/in², phi_f= 1.000, Fcrw= 37.08kips/in²		
Flange Stress And Member Bending Moments 6.10.1.6-1	Abs(fl_top) ≤ 0.6 · Fyc ? PASSED ; where fl_top= 7.138kips/in², Fyc= 50.00kips/in²	17	
Full Box Constructability 14	Constructability - Flexure 6.11.3.2-3	Abs(fbu_tens) ≤ phi_f · Rh · Fyt · delta_tens ? PASSED ; where fbu_tens= 20.61kips/in², phi_f= 1.000, Rh= 1.000, Fyt= 50.00kips/in², delta_tens= 1.000	
	Constructability - Flexure 6.11.3.2	Delta ≤ 1 / (360 · transSpan) ? PASSED ; where Delta= 0.000in, transSpan= 12115	
	Constructability - Flexure 6.11.3.2	Abs(fc) ≤ 20AndAbs(ft) ≤ 20 ? FAILED ; where fc=-26.07kips/in², ft= 20.61kips/in²	

Figure 47: Constructability - Flexure

AASHTO Article 6.11.3.1 General: The provisions of Article 6.10.3 shall apply.

14) AASHTO Article 6.11.3.2 Flexure

For critical stages of construction, the provisions of 6.10.3.2.1 through 6.10.3.2.3 shall be applied only to the top flanges of tub sections.

Continuously braced box flanges in tension or compression shall satisfy :

$$f_{bu} \leq \phi_f R_h f_{yf} \Delta \quad [6.11.3.2-3]$$

For loads applied to a composite box flange before the concrete has hardened or is made composite, the flange shall be designed as a noncomposite box flange. The maximum vertical deflection of the noncomposite box flange due to the unfactored permanent loads, including the self-weight of the flange plus the unfactored construction loads, shall not exceed 1/360 times the transverse span between webs. (Not checked in the design example)

The through-thickness bending stress in the noncomposite box flange due to the factored permanent loads and factored construction loads shall not exceed 20.0 ksi.

15) AASHTO Article 6.10.3.2.1 Discretely Braced Flanges in Compression

$$f_{bu} + f_l \leq \phi_f R_h F_{yc} \quad [6.10.3.2.1-1]$$

$$f_{bu} + 1/3 f_l \leq \phi_f F_{nc} \quad [6.10.3.2.1-2]$$

$$f_{bu} \leq \phi_f F_{crw} \quad [6.10.3.2.1-3]$$

F_{nc} shall be determined as specified in Article 6.10.8.2

In computing F_{nc} for constructability, the web load-shedding factor, R_b , shall be taken as 1.0

16) AASHTO 6.10.8.2.1 General

F_{nc} , shall be taken as the smaller of the local buckling resistance (fnc_flb in the verbose report) determined as specified in Article 6.10.8.2.2, and the lateral torsional buckling resistance (fnc_ltb in the verbose report) determined as specified in Article 6.10.8.2.3.

17) AASHTO Article 6.10.1.6 Flange Stresses and Member Bending Moments

All discretely braced flanges shall satisfy :

$$f_i \leq 0.6 F_{yf} \text{ [6.10.1.6-1]}$$

- Constructability Limit State - Shear

Similar to strength limit state except that St. Venant torsional shear is not considered.

Vn Calculation	Shear buckling coefficient NOTE: The Girder is NOT considered stiffened since it is NOT transversely stiffened.	$k_{shear} = 5 = 5$
		$\frac{d_a}{t_w} > 1.4 \cdot \left(e \cdot \frac{k_{shear}}{F_{yw}} \right)^{0.5}$? Yes ; where $d_a = 80.34in$, $t_w = 0.563in$, $e = 2.90e4kips/in^2$, $k_{shear} = 5.000$, $F_{yw} = 50.00kips/in^2$
	The ratio of the shear-buckling resistance to the shear specified minimum yield strength 6.10.9.3.2-6	$c = \left(\frac{1.57}{\left(\frac{d_a}{t_w} \right)^2} \right) \cdot \left(e \cdot \frac{k_{shear}}{F_{yw}} \right) = .2232$; where $d_a = 80.34in$, $t_w = 0.563in$, $e = 2.90e4kips/in^2$, $k_{shear} = 5.000$, $F_{yw} = 50.00kips/in^2$
	the plastic shear force 6.10.9.3.2-3	$V_p = 0.58 \cdot f_{yw} \cdot d_a \cdot t_w = 1310.4944 \text{ kips}$; where $f_{yw} = 50.00kips/in^2$, $d_a = 80.34in$, $t_w = 0.563in$
	nominal shear resistance determined as specified in Articles 6.10.9.2 and 6.10.9.3, for unstiffened and stiffened webs, respectively	$V_n = c \cdot V_p = 292.5153 \text{ kips}$; where $c = 0.223$, $V_p = 1,310.kips$
Shear buckling resistance	$V_{cr} = V_n = 292.5153 \text{ kips}$; where $V_n = 292.5kips$	
The shear projected onto the axis of the box girder web 6.11.9-1	$V_{ui} = A_b \cdot \frac{V_u}{\cos(\theta)} = 27.8584 \text{ kips}$; where $V_u = 27.05kips$, $\theta = 0.242rad$	
Shear Resistance 6.10.3.3-1	$V_{ui} \leq \phi_{i_v} \cdot V_{cr}$? PASSED ; where $V_{ui} = 27.86kips$, $\phi_{i_v} = 1.000$, $V_{cr} = 292.5kips$	

Figure 48: Constructability - Shear

AASHTO Article 6.11.3.3 Shear: the provisions of Article 6.10.3.3 and 6.11.9 apply

AASHTO Article 6.10.3.3 Shear: $V_u \leq \phi_v V_{cr}$ [6.10.3.3-1] where V_{cr} is the shear buckling resistance determined from Eq. 6.10.9.3.3-1

AASHTO 6.10.9.3.3 End Panels: $V_n = V_{cr} = C V_p$ [6.10.9.3.3-1] in which $V_p = 0.58 F_{yw} D t_w$ [6.10.9.3.3-2]

- Service Limit State

FLANGE STRESSES FOR SERVICEABILITY	
The total stress in top flange without considering flange lateral bending D6.3.1 Using the factors from Service II.	$f_{bu_top} = \frac{1 - 1 \cdot DC1_Mz - (dd - sec)}{I} - \frac{1 - 1 \cdot DC2_Mz - c3nt}{I3n} - \frac{1 - 1 \cdot DW_Mz - c3nt}{I3n} - \frac{1 - 1.3 \cdot LL_Mz - cnt}{Iln} = -18.9591 \text{ kips/in}^2$
The total stress in bottom flange without considering flange lateral bending D6.3.1 Using the factors from Service II.	$f_{bu_bot} = \frac{1 - 1 \cdot DC1_Mz - sec}{I} + \frac{1 - 1 \cdot DC2_Mz - c3nb}{I3n} + \frac{1 - 1 \cdot DW_Mz - c3nb}{I3n} + \frac{1 - 1.3 \cdot LL_Mz - cnb}{Iln} = 27.5987 \text{ kips/in}^2$
SERVICEABILITY	
The nominal flexural resistance of the compression flange determined as specified in Article 6.10.7.2.2	$F_{nt} = R_h \cdot F_{yt} = 50$; where $R_h = 1.000$, $F_{yt} = 50.00kips/in^2$
Permanent Deformations - flexure 6.10.4.2.2-1	$Abs(f_{bu_top}) \leq 0.95 \cdot R_h \cdot F_{ytop}$? PASSED ; where $f_{bu_top} = -18.96kips/in^2$, $R_h = 1.000$, $F_{ytop} = 50.00kips/in^2$
Permanent Deformations - flexure 6.10.4.2.2-2	$Abs(f_{bu_bot}) \leq 0.95 \cdot R_h \cdot F_{yBot}$? PASSED ; where $f_{bu_bot} = 27.60kips/in^2$, $R_h = 1.000$, $F_{yBot} = 50.00kips/in^2$

Figure 49: Serviceability

AASHTO Article 6.11.4 Service Limit State: The f_t term in Eq. 6.10.4.2.2-2 shall be taken equal to zero. Eq. 6.10.4.2.2-3 shall not apply. Except for sections in positive flexure in which the web satisfies the requirement of Article 6.11.2.1.2, all sections shall satisfy Eq. 6.10.4.2.2-4

18) AASHTO Article 6.10.4.2.2 Flexure

For the top steel flange of composite sections :

$$f_f \leq 0.95 R_h F_{yf} \text{ [6.10.4.2.2-1]}$$

For the bottom steel flange of composite sections:

$$f_f + f_t/2 \leq 0.95 R_h F_{yf} \text{ [6.10.4.2.2-2]}$$

- Fatigue Limit State

Fatigue Resistance (Infinite Life) (6.6.1.2.5)	19	constant-amplitude fatigue threshold taken from Table 3 (ksi) Table 6.6.1.2.5-3	$F_{\Delta} = 12 = 12$
		fatigue Resistance 6.6.1.2.5-1	$F_{\Delta} = F_{\Delta} = 12 \text{ kips/in}^2$; where $F_{\Delta} = 12.00$
Fatigue Design Criteria (6.6.1.2.2)	20	stress range at bottom flange location	$FSR_{Bot} = abs(F_{BotMax} - F_{BotMin}) = 2.821 \text{ kips/in}^2$; where $F_{BotMax} = 2.297 \text{ kips/in}^2$, $F_{BotMin} = -0.524 \text{ kips/in}^2$
		Fatigue Design Criteria @ Bottom 6.6.1.2.2	$F_{\Delta} \cdot FSR_{Bot} \leq F_{\Delta} \cdot PASSED$; where $F_{\Delta} = 1.500$, $FSR_{Bot} = 2.821 \text{ kips/in}^2$, $F_{\Delta} = 12.00 \text{ kips/in}^2$

Figure 50: Fatigue Limit State

AASHTO Article 6.11.5 Fatigue and Fracture Limit State: The provisions of Article 6.10.5 apply.

AASHTO Article 6.10.5.1 Fatigue: Details shall be investigated for fatigue as specified in Article 6.6.1. The applicable Fatigue load combination specified in Table 3.4.1-1 and fatigue live load specified in Article 3.6.1.4 shall apply. For horizontally curved I-girder bridges, the fatigue stress range due to major-axis bending plus lateral bending shall be investigated.

19) AASHTO Article 6.6.1.2.5 Fatigue Resistance

The nominal fatigue resistance for Fatigue I load combination and infinite life :

$$(\Delta F)_n = (\Delta F)_{TH} \text{ [6.6.1.2.5-1]}$$

Constant amplitude fatigue threshold for Detail Category C':

$$(\Delta F)_{TH} = 12 \text{ [Table 6.6.1.2.5-3]}$$

20) AASHTO Article 6.6.1.2.2 Design Criteria

For load-induced fatigue considerations, each detail shall satisfy :

$$\gamma (\Delta f) \leq (\Delta F)_n \text{ [6.6.1.2.2-1]}$$

γ : load factor specified in Table 3.4.1-1 for the fatigue load combination (Fgamma in the verbose report)

(Δf) : force effect, live load stress range due to the passage of the fatigue load as specified in Article 3.6.1.4 (FSRBot in the verbose report)

- Strength Limit State - Flexural Resistance (Negative Moment Region)

$\mu \geq 0$? No; where $\mu = -3.91e4$ kips-ft		
The plate buckling coefficient for shear stress	$k_s = 5.34 = 5.34$	
The compression-flange stress at the onset of nominal yielding within the cross-section, including residual stress effects, but not including compression-flange lateral bending 6.11.8.2.2-13	$F_{yr} = \min((\Delta_{comp} - 0.3) \cdot F_{yc}, F_{yw}) = 34.9744 \text{ kips/in}^2$; where $\Delta_{comp} = 0.999$, $F_{yc} = 50.00 \text{ kips/in}^2$, $F_{yw} = 50.00 \text{ kips/in}^2$	
	IsConstruct? No; where IsConstruct= 0.000	21
	IsCompFlangeLongStiffened? Yes; where IsCompFlangeLongStiffened=-1.000	
width of the compression flange. If stiffened, this will be substituted with w.	$b_{fc_local} = w = 40.5$; where $w = 40.50 \text{ in}$	
	$n = 1$? Yes; where $n = 1.000$	
The plate buckling coefficient for uniform normal stress 6.11.8.2.3-1	$k_{plate} = \left(\frac{8 \cdot I_{boxflange}}{w \cdot t_{fc}^3} \right)^{\frac{1}{3}} = 2.8013$; where $I_{boxflange} = 375.6 \text{ in}^4$, $w = 40.50 \text{ in}$, $t_{fc} = 1.500 \text{ in}$	
	$n > 2$? No; where $n = 1.000$	
The plate buckling coefficient for shear stress 6.11.8.2.3-3	$k_s = \frac{5.34 + 2.84 \cdot \left(\frac{I_{boxflange}}{w \cdot t_{fc}^3} \right)^{\frac{1}{3}}}{(n+1)^2} = 2.3295$; where $I_{boxflange} = 375.6 \text{ in}^4$, $w = 40.50 \text{ in}$, $t_{fc} = 1.500 \text{ in}$, $n = 1.000$	
	$k_s > 5.34$? No; where $k_s = 2.329$	
The slenderness ratio for the compression flange	$l_f = \frac{b_{fc_local}}{t_{fc}} = 27$; where $b_{fc_local} = 40.50$, $t_{fc} = 1.500 \text{ in}$	22
First limiting slenderness ratio per 6.11.8.2.2-9 for box flanges 6.11.8.2.2-9	$\lambda_{p} = 0.57 \cdot \left(k_{plate} \cdot \frac{e}{F_{yc} \cdot \Delta_{comp}} \right)^{0.5} = 22.9817$; where $k_{plate} = 2.801$, $e = 2.90e4 \text{ kips/in}^2$, $F_{yc} = 50.00 \text{ kips/in}^2$, $\Delta_{comp} = 0.999$	
Second limiting slenderness ratio per 6.11.8.2.2-10 for box flanges 6.11.8.2.2-10	$\lambda_{r} = 0.95 \cdot \left(e \cdot \frac{k_{plate}}{F_{yr}} \right)^{0.5} = 45.7856$; where $e = 2.90e4 \text{ kips/in}^2$, $k_{plate} = 2.801$, $F_{yr} = 34.97 \text{ kips/in}^2$	
	$l_f \leq \lambda_{p}$? No; where $l_f = 27.00$, $\lambda_{p} = 22.98$	
6.11.8.2.2-3	$F_{cb} = R_b \cdot R_h \cdot F_{yc} \cdot \left(\Delta_{comp} - \frac{\Delta_{comp} - 0.3}{R_h} \right) \cdot \left(\frac{l_f - \lambda_{p}}{\lambda_{r} - \lambda_{p}} \right) = 47.2942$; where $R_b = 0.999$, $R_h = 1.000$, $F_{yc} = 50.00 \text{ kips/in}^2$, $\Delta_{comp} = 0.999$, $l_f = 27.00$, $\lambda_{p} = 22.98$, $\lambda_{r} = 45.79$	
	$l_f < 1.12 \cdot \left(e \cdot \frac{k_s}{F_{yc}} \right)^{0.5}$? Yes; where $l_f = 27.00$, $e = 2.90e4 \text{ kips/in}^2$, $k_s = 2.329$, $F_{yc} = 50.00 \text{ kips/in}^2$	
6.11.8.2.2-5	$F_{cv} = 0.58 \cdot F_{yc} = 29$; where $F_{yc} = 50.00 \text{ kips/in}^2$	
The nominal flexural resistance of the compression flange 6.11.8.2.2-1	$F_{nc} = F_{cb} \cdot \left(1 - \left(\frac{f_{v_comp}}{\phi_v \cdot F_{cv}} \right)^2 \right)^{0.5} = 47.2703$; where $F_{cb} = 47.29$, $f_{v_comp} = 0.923 \text{ kips/in}^2$, $\phi_v = 1.000$, $F_{cv} = 29.00$	
Flexural Resistance - Sections In Negative Flexure - Box Flanges in Compression 6.11.8.1.1-1	$Abs(f_{bu_comp}) \leq \phi_f \cdot F_{nc}$? PASSED; where $f_{bu_comp} = -40.44 \text{ kips/in}^2$, $\phi_f = 1.000$, $F_{nc} = 47.27$	23
	IsFullBox? No; where IsFullBox= 0.000	
The nominal flexural resistance of the compression flange determined as specified in Article 6.10.7.2.2 6.11.8.3-1	$F_{nt} = R_h \cdot F_{yt} = 50$; where $R_h = 1.000$, $F_{yt} = 50.00 \text{ kips/in}^2$	24
Flexural Resistance Sections In Negative Flexure - Box Flanges in Compression 6.11.8.1.1-1	$Abs(f_{bu_tens}) \leq \phi_f \cdot F_{nt}$? PASSED; where $f_{bu_tens} = -43.45 \text{ kips/in}^2$, $\phi_f = 1.000$, $F_{nt} = 50.00$	25

Figure 51: Flexural Resistance

AASHTO Article 6.11.6.2.3 Sections in Negative Flexure: The provisions of Article 6.11.8 shall apply.

AASHTO Article 6.11.8.2.1 General: The nominal flexural resistance of box flanges in compression without flange longitudinal stiffeners shall be determined as specified in Article 6.11.8.2.2. The nominal flexural resistance of box flanges in compression with flange longitudinal stiffeners shall be determined as specified in Article 6.11.8.2.3.

21) AASHTO Article 6.11.8.2.3 Longitudinally Stiffened Flanges: The nominal flexural resistance of the compression flange shall be taken as equal to the nominal flexural resistance for the compression flange without longitudinal stiffeners, determined as specified in Article 6.11.8.2.2, with the following substitutions

$$b_{fc} = w$$

$$k = (8 I_s / w t_{fc}^3)^{1/3} \text{ for } n = 1 \text{ [6.11.8.2.3-1]}$$

$$k = (0.894 I_s / w t_{fc}^3)^{1/3} \text{ for } n = 2 \text{ [6.11.8.2.3-2]}$$

$$1.0 \leq k \leq 4.0$$

The plate buckling coefficient for shear stress k_s shall be taken as:

$$k_s = (5.34 + 2.84 (I_s / w t_{fc}^3)^{1/3}) / (n + 1)^2 \leq 5.34 \text{ [6.11.8.2.3-3]}$$

22) AASHTO Article 6.11.8.2.2 Unstiffened Flanges

The nominal flexural resistance of the compression flange, F_{nc} shall be taken as:

$$F_{nc} = F_{cb} \sqrt{1 - (f_v / \phi_v F_{cv})^2} \text{ [6.11.8.2.2-1]}$$

$$\text{If } \lambda_f \leq \lambda_p, F_{cb} = R_b R_h F_{yc} \Delta \text{ [6.11.8.2.2-2]}$$

$$\text{If } \lambda_p < \lambda_f \leq \lambda_r, F_{cb} = R_b R_h F_{yc} (\Delta - (\Delta - (\Delta - 0.3)/R_h) ((\lambda_f - \lambda_p)/(\lambda_r - \lambda_p))) \text{ [6.11.8.2.2-3]}$$

$$\text{If } \lambda_f > \lambda_r, F_{cb} = 0.9 E R_b k / \lambda_f^2 \text{ [6.11.8.2.2-4]}$$

$$\text{If } \lambda_f \leq 1.12 (\sqrt{E k_s / F_{yc}}), F_{cv} = 0.58 F_{yc} \text{ [6.11.8.2.2-5]}$$

$$\text{If } 1.12 (\sqrt{E k_s / F_{yc}}) < \lambda_f \leq 1.4 (\sqrt{E k_s / F_{yc}}), F_{cv} = (0.65 \sqrt{F_{yc} E k_s}) / \lambda_f \text{ [6.11.8.2.2-6]}$$

$$\text{If } \lambda_f > 1.4 (\sqrt{E k_s / F_{yc}}), F_{cv} = 0.9 E k_s / \lambda_f^2 \text{ [6.11.8.2.2-7]}$$

$$\lambda_f = b_{fc} / t_{fc} \text{ [6.11.8.2.2-8]}$$

$$\lambda_p = 0.57 \sqrt{E k / F_{yc} \Delta} \text{ [6.11.8.2.2-9]}$$

$$\lambda_r = 0.95 \sqrt{E k / F_{yr}} \text{ [6.11.8.2.2-10]}$$

23) AASHTO Article 6.11.8.1.1 Box Flanges in Compression

$$f_{bu} \leq \phi_f F_{nc} \text{ [6.11.8.1.1-1]}$$

24) AASHTO Article 6.11.8.3 Tension-Flange Flexural Resistance

The nominal flexural resistance of the tension flanges of tub sections shall be taken as:

$$F_{nt} = R_h F_{yt} \text{ [6.11.8.3-1]}$$

25) AASHTO Article 6.11.8.1.2 Continuously Braced Flanges in Tension

$$f_{bu} \leq \phi_f F_{nt} \text{ [6.11.8.1.2-1]}$$

- Strength Limit State - Shear Resistance (Negative Moment Region)

Vn Calculation	Is girder considered stiffened as defined by AASHTO? [Only Transversely Stiffened]	IsStiffened = (dos ≤ 3 · da)? Yes; where dos= 62.00, da= 80.34in	27
	Shear buckling coefficient NOTE: The Girder is considered stiffened as a result to the criteria above. [6.10.9.3.2-7]	kshear = $5 + \frac{5}{\left(\frac{dos}{da}\right)^2} = 13.3949$; where dos= 62.00, da= 80.34in	
		$\frac{da}{tw} > 1.4 \cdot \left(\epsilon \cdot \frac{kshear}{F_{yw}} \right)^{0.5}$? Yes; where da= 80.34in, tw= 0.563in, e= 2.90e4kips/in ² , kshear= 13.39, Fyw= 50.00kips/in ²	
	The ratio of the shear-buckling resistance to the shear specified minimum yield strength 6.10.9.3.2-6	$c = \frac{1.57}{\left(\frac{da}{tw}\right)^2} \left(\epsilon \cdot \frac{kshear}{F_{yw}} \right) = .598$; where da= 80.34in, tw= 0.563in, e= 2.90e4kips/in ² , kshear= 13.39, Fyw= 50.00kips/in ²	28
	the plastic shear force 6.10.9.3.2-3	Vp = 0.58 · fyw · da · tw = 1310.4944 kips; where fyw= 50.00kips/in ² , da= 80.34in, tw= 0.563in	
		IsEndPanel? No; where IsEndPanel= 0.000	
	The compression flange width 6.11.9	bfc = min $\left\{ \frac{bfc}{2}, 18 \cdot tfc \right\} = 27$ in; where tfc= 1.500in	27
6.10.9.3.2-1	$\frac{2 \cdot da \cdot tw}{bfc \cdot tfc + bfc \cdot rft} \leq 2.5$? Yes; where da= 80.34in, tw= 0.563in, bfc= 27.00in, tfc= 1.500in, bft= 18.00in, rft= 3.000in	28	
nominal shear resistance determined as specified in Articles 6.10.9.2 and 6.10.9.3, for unstiffened and stiffened webs, respectively 6.10.9.3.2-2	Vn = Vp · $c + \frac{0.87 \cdot (1 - c)}{\left(1 + \left(\frac{dos}{da}\right)^2\right)^{0.5}}$ = 1146.5084 kips; where Vp= 1,310 kips, c= 0.598, dos= 62.00, da= 80.34in		
The shear projected onto the axis of the box girder web 6.11.9-1	Vui = $\frac{Vu}{\cos(\thetaeta)} = 596.9818$ kips; where Vu=579.6kips, theta= 0.242rad	26	
for non-composite case	ao_noncomp = $\frac{bfc_{bot} + bfc_{top} - tw}{2} \cdot (d + 0.5 \cdot tf_{top} + 0.5 \cdot tf_{bot}) = 8122.4592$ in ² ; where bfc_bot= 83.00in, bfc_top= 120.0in, tw= 0.563in, d= 78.00in, tf_top= 3.000in, tf_bot= 1.500in		
for composite case	ao_comp = ao_noncomp + (bfd · (ht + 0.5 · ts + 0.5 · tf_top)) = 8992.3968 in ² ; where ao_noncomp= 8,122 in ² , bfd= 120.0in, ht= 1.000in, ts= 9.500in, tf_top= 3.000in		
St. Venant torsional shear 6.11.9-1	Vut = $\frac{Abs(M_{ux}) \cdot da}{2 \cdot ao_{comp}} = 108.8291$ kips; where Mux=-2,030 kips-ft, da= 80.34in, ao_comp= 8,992 in ²		
Shear Resistance 6.10.9.1-1	Vui + Vut ≤ phi_v · Vn? PASSED; where Vui= 597.0kips, Vut= 108.8kips, phi_v= 1.000, Vn= 1,147 kips	27	

Figure 52: Shear Resistance

26) AASHTO Article 6.11.9 Shear Resistance

Article 6.10.9 shall apply for determining the factored shear resistance of a single web.

For the case of inclined webs, D in Article 6.10.9 shall be taken as the depth of the web plate measured along the slope (D=da in the verbose report)

For the case of inclined webs, each web shall be designed for a shear, V_{ui}

$$V_{ui} = V_u / \cos\theta \text{ [6.11.9-1]}$$

For all single box sections, horizontally curved sections, and multiple box sections in bridges not satisfying the requirements of Article 6.11.2.3, or with box flanges that are not fully effective according to the provisions of Article 6.11.1.1, V_u shall be taken as the sum of the flexural and St.Venant torsional shears.

27) AASHTO Article 6.10.9.1 General

At the strength limit state, straight and curved web panels shall satisfy:

$$V_u \leq \phi_v V_n \text{ [6.10.9.1-1]}$$

Transverse intermediate stiffeners shall be designed as specified in Article 6.10.11.1.

Interior web panels of nonhybrid and hybrid I-shaped members:

-without a longitudinal stiffener and with a transverse stiffener spacing not exceeding 3D

-with one or more longitudinal stiffeners and with a transverse stiffener spacing not exceeding 1.5D

shall be considered stiffened, and the provisions of Article 6.10.9.3 shall apply.

For box flanges, b_{fc} or b_{ft} , as applicable, shall be taken as one-half of the effective flange width between webs in checking Eq. 6.10.9.3.2-1, where the effective flange width shall be taken as specified in Article 6.11.1.1, but not to exceed $18t_f$ where t_f is the thickness of the box flange.

28) AASHTO Article 6.10.9.3.2 Interior Panels

The nominal shear resistance of an interior web panel complying with the provisions of Article 6.10.9.1, and with the section along the entire panel proportioned such that:

$$2 D t_w / (b_{fc} t_{fc} + b_{ft} t_{ft}) \leq 2.5 \text{ [6.10.9.3.2-1]}$$

shall be taken as:

$$V_n = V_p (C + 0.87(1 - C) / (\sqrt{1 + (d_o / D)^2})) \text{ [6.10.9.3.2-2]}$$

$$V_p = 0.58 F_{yw} D t_w \text{ [6.10.9.3.2-3]}$$

$$\text{If } D/t_w \leq 1.12 (\sqrt{E k/F_{yw}}) \rightarrow C = 1.0 \text{ [6.10.9.3.2-4]}$$

$$\text{If } 1.12 (\sqrt{E k/F_{yw}}) < D/t_w \leq 1.4 (\sqrt{E k/F_{yw}}) \rightarrow C = (1.12/(D/t_w)) ((\sqrt{E k/F_{yw}}) \text{ [6.10.9.3.2-5]}$$

$$\text{If } D/t_w > 1.4 (\sqrt{E k/F_{yw}}) \rightarrow C = (1.57/(D/t_w)^2) ((\sqrt{E k/F_{yw}}) \text{ [6.10.9.3.2-6]}$$

$$k = 5 + 5 / (d_o / D)^2 \text{ [6.10.9.3.2-7]}$$

- Constructability Limit State - Flexure (Negative Moment Region)

	isFullBox? No ; where isFullBox= 0.000	
	Mu ≥ 0? No ; where Mu=-1.87e4kips-ft	
	IsDiscretelyBracedTensConstruct? Yes ; where IsDiscretelyBracedTensConstruct=-1.000	
Discretely Braced Flanges In Tension 6.10.3.2.2-1	Abs(fbu_tens) + Abs(fl_tens) ≤ phi_f · Rh · Fyt? PASSED ; where fbu_tens= 23.42kips/in², fl_tens= 1.163kips/in², phi_f= 1.000, Rh= 1.000, Fyt= 50.00kips/in²	29
The plate buckling coefficient for shear stress	ks = 5.34 = 5.34	
The compression-flange stress at the onset of nominal yielding within the cross-section, including residual stress effects, but not including compression-flange lateral bending 6.11.8.2.2-13	Fyw = min((delta_comp - 0.3) · Fyc, Fyw) = 34.9997 kips/in² ; where delta_comp= 1.000, Fyc= 50.00kips/in², Fyw= 50.00kips/in²	
	IsConstruct? Yes ; where IsConstruct=-1.000	
The web load-shedding factor determined as specified in Article 6.10.1.10.2	Rb = 1 = 1	
	IsCompFlangeLongStiffened? Yes ; where IsCompFlangeLongStiffened=-1.000	
width of the compression flange. If stiffened, this will be substituted with w.	bfc_local = w = 40.5 ; where w= 40.50in	
	n = 1? Yes ; where n= 1.000	
The plate buckling coefficient for uniform normal stress 6.11.8.2.3-1	kplate = $\left(\frac{8 \cdot I_{boxflange}}{w \cdot t_{fc}^3}\right)^{\frac{1}{3}} = 2.8013$; where I_boxflange= 375.6in⁴, w= 40.50in, t_fc= 1.500in	
	n > 2? No ; where n= 1.000	
The plate buckling coefficient for shear stress 6.11.8.2.3-3	ks = $\frac{5.34 + 2.84 \cdot \left(\frac{I_{boxflange}}{w \cdot t_{fc}^3}\right)^{\frac{1}{3}}}{(n + 1)^2} = 2.3295$; where I_boxflange= 375.6in⁴, w= 40.50in, t_fc= 1.500in, n= 1.000	
	ks > 5.34? No ; where ks= 2.329	
The slenderness ratio for the compression flange	lf = $\frac{bfc_local}{t_{fc}} = 27$; where bfc_local= 40.50, t_fc= 1.500in	
First limiting slenderness ratio per 6.11.8.2.2-9 for box flanges 6.11.8.2.2-9	lambda_p = $0.57 \cdot \left(kplate \cdot \frac{e}{Fyc \cdot \delta_comp}\right)^{0.5} = 22.9759$; where kplate= 2.801, e= 2.90e4kips/in², Fyc= 50.00kips/in², delta_comp= 1.000	
Second limiting slenderness ratio per 6.11.8.2.2-10 for box flanges 6.11.8.2.2-10	lambda_r = $0.95 \cdot \left(e \cdot \frac{kplate}{Fyt}\right)^{0.5} = 45.7691$; where e= 2.90e4kips/in², kplate= 2.801, Fyt= 35.00kips/in²	
	lf ≤ lambda_p? No ; where lf= 27.00, lambda_p= 22.98	
6.11.8.2.2-3	Fcb = Rb · Rh · Fyc · $\left(\delta_comp - \left(\delta_comp - \frac{\delta_comp - 0.3}{Rh}\right) \cdot \frac{lf - \lambda_p}{\lambda_r - \lambda_p}\right) = 47.3514$; where Rb= 1.000, Rh= 1.000, Fyc= 50.00kips/in², delta_comp= 1.000, lf= 27.00, lambda_p= 22.98, lambda_r= 45.77	
	lf < 1.12 · $\left(e \cdot \frac{ks}{Fyc}\right)^{0.5}$? Yes ; where lf= 27.00, e= 2.90e4kips/in², ks= 2.329, Fyc= 50.00kips/in²	
6.11.8.2.2-5	Fcv = 0.58 · Fyc = 29 ; where Fyc= 50.00kips/in²	
The nominal flexural resistance of the compression flange 6.11.8.2.2-1	Fnc = Fcb · $\left(1 - \left(\frac{fv_comp}{\phi_{fv} \cdot Fcv}\right)^2\right)^{0.5} = 47.3511$; where Fcb= 47.35, fv_comp= 0.105kips/in², phi_v= 1.000, Fcv= 29.00	
Constructability - Flexure 6.11.3.2-1	Abs(fbu_comp) ≤ phi_f · Fnc? PASSED ; where fbu_comp=-19.87kips/in², phi_f= 1.000, Fnc= 47.35	
6.10.1.10.2-4	2 · $\frac{Dc}{tw} < 5.7 \cdot \left(\frac{e}{Fyc}\right)^{0.5}$? Yes ; where Dc= 37.45in, tw= 0.563in, e= 2.90e4kips/in², Fyc= 50.00kips/in²	30

Figure 53: Constructability-Flexure

29) AASHTO Article 6.10.3.2.2 Discretely Braced Flanges in Tension

$$f_{bu} + f_l \leq \phi_f R_h F_{yt} \quad [6.10.3.2.2-1]$$

30) AASHTO Article 6.11.3.2 Discretely Braced Flanges in Tension

$$f_{bu} \leq \phi_f F_{nc} \quad [6.11.3.2-1]$$

$$f_{bu} \leq \phi_f F_{crw} \quad [6.11.3.2-2]$$

For sections with compact or noncompact webs, Eq. 6.11.3.2-2 shall not be checked.

- Constructability Limit State - Shear (Negative Moment Region)

Similar to strength limit state except that St. Venant torsional shear is not considered.

Vn Calculation	Is girder considered stiffened as defined by AASHTO? [Only Transversely Stiffened]	IsStiffened = (dos ≤ 3 · da) ? Yes ; where dos= 62.00, da= 80.34in
	Shear buckling coefficient NOTE: The Girder is considered stiffened as a result to the criteria above. [6.10.9.3.2-7]	kshear = $5 + \frac{5}{\left(\frac{dos}{da}\right)^2} = 13.3949$; where dos= 62.00, da= 80.34in
		$\frac{da}{tw} > 1.4 \cdot \left(e \cdot \frac{kshear}{Fyw} \right)^{0.5}$? Yes ; where da= 80.34in, tw= 0.563in, e= 2.90e4kips/in ² , kshear= 13.39, Fyw= 50.00kips/in ²
	The ratio of the shear-buckling resistance to the shear specified minimum yield strength 6.10.9.3.2-6	$c = \left(\frac{1.57}{\left(\frac{dos}{da}\right)^2} \right) \cdot \left(e \cdot \frac{kshear}{Fyw} \right) = .598$; where da= 80.34in, tw= 0.563in, e= 2.90e4kips/in ² , kshear= 13.39, Fyw= 50.00kips/in ²
	the plastic shear force 6.10.9.3.2-3	Vp = 0.58 · fyw · da · tw = 1310.4944 kips ; where fyw= 50.00kips/in ² , da= 80.34in, tw= 0.563in
		IsEndPanel ? No ; where IsEndPanel= 0.000
	The compression flange width 6.11.9	bfc = $\min\left(\frac{bfc}{2}, 18 \cdot tfc\right) = 27$ in ; where tfc= 1.500in
6.10.9.3.2-1	$\frac{2 \cdot da \cdot tw}{bfc \cdot tfc + bft \cdot tft} \leq 2.5$? Yes ; where da= 80.34in, tw= 0.563in, bfc= 27.00in, tfc= 1.500in, bft= 18.00in, tft= 3.000in	
nominal shear resistance determined as specified in Articles 6.10.9.2 and 6.10.9.3, for unstiffened and stiffened webs, respectively 6.10.9.3.2-2	$Vn = Vp \cdot \left[c + \frac{0.87 \cdot (1 - c)}{1 + \left(\frac{dos}{da}\right)^2} \right] = 1146.5084$ kips ; where Vp= 1,310.kips, c= 0.598, dos= 62.00, da= 80.34in	
Shear buckling resistance	Vcr = Vn = 1146.5084 kips ; where Vn= 1,147.kips	
The shear projected onto the axis of the box girder web 6.11.9-1	Vui = $\text{Abs}\left(\frac{Vu}{\text{Cos}}(\text{theta})\right) = 240.4142$ kips ; where Vu=-233.4kips, theta= 0.242rad	
Shear Resistance 6.10.3.3-1	Vui ≤ phi_v · Vcr ? PASSED ; where Vui= 240.4kips, phi_v= 1.000, Vcr= 1,147.kips	

Figure 54: Constructability-Shear

Note: According to AASHTO Article 6.11.7.2.1 the maximum longitudinal compressive stress in the concrete deck at the strength limit state is limited. This check is to be added inside the Steel Bridge Module Code Check Procedures in the next release.

References

- U.S. Department of Transportation Federal Highway Administration. (2015, December). *Steel Bridge Design Handbook Design Example 5*. Retrieved from www.fhwa.dot.gov: <https://www.fhwa.dot.gov/bridge/steel/pubs/hif16002/designexample06.pdf>
- AASHTO LRFD Bridge Design Specifications (7th Edition, 2014)

Samples for Composite Construction

These samples provide an overview of the composite section construction.

C01: Single Span with Roller under Vertical Load	501
Cross-Section Definition	501
Model	503
Cross-Sectional Properties	504
Self-Weight Loading	505
C02: Staged Construction Analysis	509
Composite Sequence States	509
Self-Weight Loading	510
Standard Staged Construction Analysis	511
C03: Time-Dependent Material Properties	517
Cross-Section Definition	517
Model	517
Cross-Sectional Properties	518
Self-Weight Loading	519
Time Effect on Elastic Modulus	520
Shrinkage	522
Creep	525
References	525
C04: Thermal Loads	527
Cross-Section Definition	527
Model	529
Analysis of Thermal Loads	529
Uniform Thermal Load	530
Linear Gradient Thermal Load	531
Nonlinear Gradient Thermal Load	533

C01: Single Span with Roller under Vertical Load

A simply supported beam is used to verify several aspects of the analysis of composite sections in a static analysis. The length of the span is 300 ft, and it has a composite cross-section comprised of a steel I-shape girder and a concrete rectangular-shape deck. Section properties of the composite cross-section and behavior of the beam (displacement, member force, and member stress) under self-weight loading is verified.

Example Project: The example described here can be found in the Composite Construction folder of your LARSA 4D Samples directory (generally My Documents\LARSA Projects\Samples) in the file C01.

Cross-Section Definition

The cross-section used in this problem is composed of a steel I-shape and a concrete slab on top. The dimensions are:

- **I-Shape:** 5 ft deep; 2 ft wide; 0.2 ft flange and web thickness
- **Rectangle Shape:** 0.8 ft deep; 4 ft wide

This is created in **LARSA Section Composer**. Stress Recovery Points must be set on the section at this point to determine where LARSA 4D will report stresses later. This example includes six Stress Recovery Points: 1-4 clockwise around the I-shape, and 5 and 6 at the upper-right and upper-left of the concrete slab, respectively.

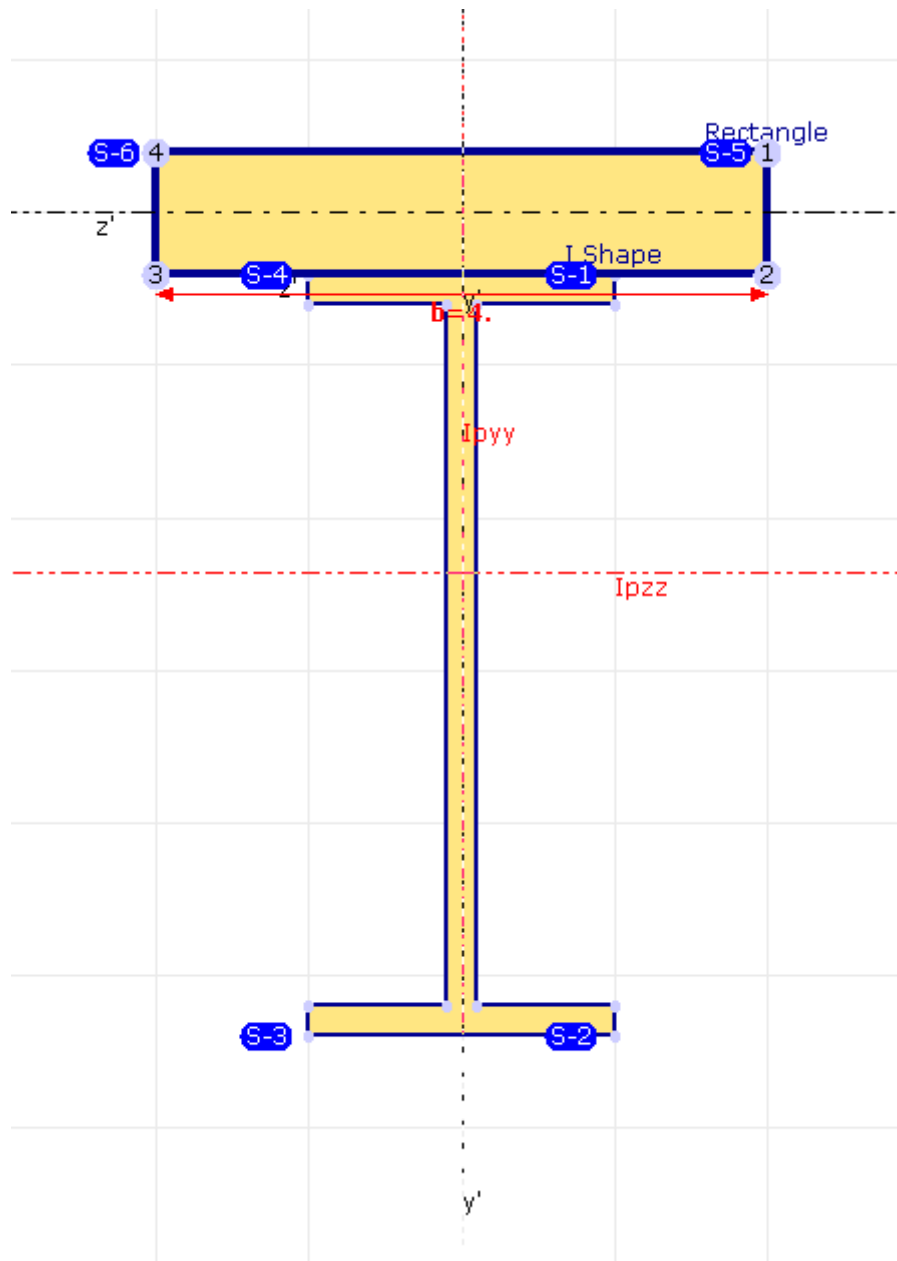


Figure 1: Cross-Section

Note that the shapes are placed such that the reference axes (the joint-to-joint line) are at the centroid of the deck slab.

Two additional steps are taken for composite sections.

The material of each shape is set in LARSA Section Composer. For a composite section with multiple materials, it is not possible to set the member's materials in LARSA 4D. The materials of all shapes must be set in Section Composer. The materials **A36** (for the I-Shape) and **Fc_4** (for the Rectangle Shape) are set in **Section** → **Composite Materials**. A Base Material can be chosen at this point which is used in the display of the cross-section properties (here and in LARSA 4D) but ultimately does not affect the analysis.

Model

The girder and deck system is modeled as a single composite beam as defined in the previous section. The beam is supported by a pin on one end and a roller at the other, with the supports level with the centroid of the deck. The length of the span is 300 ft. The span is divided into 10 segments. This is a 2D problem: TY, RX, and RZ are fixed as universal restraints.

The composite model is not assigned a material in LARSA 4D as the materials of the shapes have been set in LARSA Section Composer. Although the model has no member end offsets, because the reference axes of the cross-section are positioned in Section Composer to align with the centroid of the deck shape, the I girder shape is located below the joints, i.e., shifted down, automatically. The girder is along the x-axis with the z-axis parallel to the web. The members have an orientation angle of 90 degrees.

A verification of the results of a composite section model is made by comparing the results to hand calculations and to roughly equivalent reference models using non-composite elements.

Non-composite reference models A and B are each made using a line of member elements for the concrete part and a separate line of member elements for the steel part. The two lines are divided into ten segments and are rigidly connected at the eleven points along those lines. Two options for rigid connections exist in LARSA 4D. **Reference model A** uses member elements with high stiffness between pairs of joints to connect the two lines of members at the 11 intermediate joints. There are 22 joints in this model and 30 member elements. The joints are positioned at the centroids of the members.

Reference model B uses member end offsets to connect the two lines of members to the same joints while still positioning the members at their appropriate locations. The deck elements go from joint 1 to joint 2, from joint 2 to joint 3, and so on. The girder elements have identical connectivity (joint 1 to joint 2, joint 2 to joint 3, etc.), except member end offsets are used to shift the I-shaped elements down by 2.9 ft, the distance from the centroid of the slab to the centroid of the girder. (In other words, the I-Offset Z and the J-Offset Z are set to -2.9 for the girder elements.) There are 11 joints and 20 member elements in this model.

Reference model C is made entirely using shell elements, one for the web, two for the flanges (one top, one bottom), and one for the slab. Shell end offsets are used so that the shell connective in each cross-section is to the same joint. This is highly unusual but appropriate for a comparison with the composite model. In other words, the connectivity of the first shell for the slab is joint 1-joint 1-joint 2-joint 2. Shell end offsets set the Y offset of the shell to -2 ft, 2 ft, 2 ft, -2 ft. In other words, the I-coordinate of the shell is joint 1 minus 2 ft in the y direction. The J-coordinate is joint 1 plus 2 ft in the y direction. And so on. This will mimic the behavior of member element cross sections in which plane sections remain plane. The Thick (PQ2) with Drilling shell formulation is used.

The C01 project file includes the composite model and the reference models together. The composite model is on the left, followed by the reference models A, B, and C from left to right.

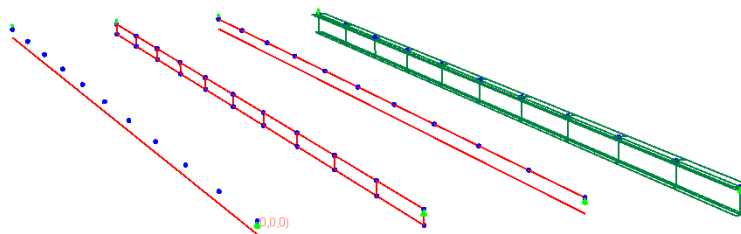


Figure 3: Models

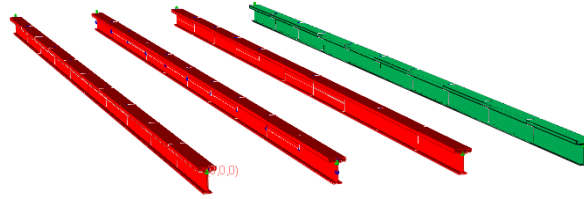


Figure 4: Models with Rendering

Cross-Sectional Properties

Cross-sectional properties of the composite section are computed for the section as a whole as well as for each construction sequence state.

The centroid of the cross-section is computed by Section Composer as 2.356 ft below the reference axes (at the centroid of the concrete part). This is readily verified by hand as the sum of the centroid locations of the shapes (relative to the reference axes) times their modulus of elasticity and area divided by the total $E \times A$.

Section Centroid Computation and Basic Shape Properties

	Centroid Location (c) (ft)	E (kip/ft²)	A (ft²)	c×E×A (kip-ft)	c×E×A/ΣEA (ft)
Concrete	0	519,120	3.20	0	0
Steel	-2.9	4,176,000	1.72	-20,829,888	-2.355
Total E×A:		8,843,904			

The properties for the section as a whole as given by Section Composer, with concrete as the reference material, are given in the table below. Units are feet. Hand calculations verify A , I_{yy} , and I_{zz} easily. The total cross-sectional area is the sum of the factored properties of the two shapes. Each shape's properties are factored by the ratio of its modulus of elasticity to that of the reference material. The moment of inertia in y is computed in this same way. In z , the moment of inertia is additionally transformed by adding the shape's area times the square of the distance from the shape's centroid to the section centroid, and is then factored.

Section Properties Computation

	Concrete Part		Steel Part		Factored	Composite
	Base	Transformed	Base	Transformed		
A (ft ²)	3.20	---	1.72	---	13.8	17.0
I_{yy} (ft ⁴)	4.27	---	0.270	---	2.17	6.44
I_{zz} (ft ⁴)	0.171	17.9	6.23	6.74	54.2	72.2

	Concrete Part		Steel Part		Composite	
J (ft ⁴)	0.588	---	0.0229	---	---	1.49

LARSA 4D's computations match the hand calculation to within rounding error. There is no hand verification for the torsion constant J at this time. The value for J computed by the Section Composer is listed above for reference.

Self-Weight Loading

The results of the test model and the reference models in LARSA 4D are compared to hand calculations.

The total magnitude of self-weight on the structure is the sum of the self-weight for each piece.

Hand Calculation of Total Self-Weight Load

	Area (ft ²)	Length (ft)	Density (kip/ft ³)	Total Weight (kip)
Steel	1.72	300	0.49	253
Concrete	3.20	300	0.15	144
				397

We can compare this with the sum of the z-reactions reported in the three reference models and the composite test model. The reactions sum to the correct total within three significant digits.

The next verification is for displacements. The maximum deflection at mid-span is given by

$$\delta = 5/384 \times (W \times L^3) / (E \times I)$$

W = 397 kip, as given in the previous table. L = 300 ft. E is the modulus of elasticity of the reference material (given above). I is the moment of inertia about Z for the composite section (based on the choice of reference material). A similar hand calculation is given for deflection at 20% of the length of the span.

Deflections

	@ 20% of Span		@ Mid-Span (ft)	
	Deflection (ft)	Error (%)	Deflection (ft)	Error (%)
Hand Calc.	2.21		3.72	
Composite	2.21	<1%	3.73	<1%
Reference A	2.23	1%	3.75	1%
Reference B	2.23	1%	3.75	1%
Reference C	2.06	-6%	3.47	-8%

The axial force acting on each of the two shapes is computed. Because of the end restraints, there is no pure axial force at the centroid of the composite beam. However, bending of the beam causes strain at other locations, and consequently the

two shapes that make up the composite beam are carrying axial force, with the I-Shape in tension and the rectangular-shape in compression. The strain distribution on the shapes is computed by

$$\epsilon = cM/EI_{zz}$$

where M is the moment acting at the centroid of the beam, c is the distance between the centroid and a particular fiber, and EI_{zz} is the property of the composite section. Then, multiplying the strain with the elastic modulus of the corresponding shape provides the stress at the chosen fiber. Integrating the stress distribution over the area of each shape gives the total axial force acting on that shape due to bending.

The non-composite and composite models differ significantly in the reported axial force in the members. The reference models show step-wise variation. The force within each member element is constant, and there are large breaks at the discrete points of rigid connections. On the other hand, the composite model shows a smooth axial force curve across the entire length of the model. The force at the end of each element is equal to the force at the start of the next.

However, we can see that the computations agree at a larger scale. The average of the start and end force of each member in the composite model is close to the corresponding force in either of the two member reference models. But because the axial force curve in the composite model is parabolic and not linear, the correct comparison is not the average of the end forces but the average value of the parabolic force curve (i.e., the area under the curve divided by the member length), F' . The start and end forces, the F' force, and the axial forces in the two member-based reference models, are shown below at two locations on the models. For Reference Model C, Compound Element Forces are used to obtain the forces at the composite element centroid of the shell elements that make up the I-Section shape.

Axial Force in Steel I-Shape. Units are kip

Location	Member 1			Member 5		
	Start	End	F'	Start	End	F'
Hand Calc.	0	560	290	1,492	1,554	1,533
Composite	0	560		1,492	1,554	
Reference A	290	290		1,533	1,533	
Reference B	290	290		1,533	1,533	
Reference C	280	280		1,497	1,497	

The next comparison is **member stresses**. Care must be taken to compare stresses at equivalent stress recovery points, as they may not be numbered in the same manner between the three member-based models.

Stresses at the start of the model and at mid-span are given below. Note that Stress Recovery Points 1-4 are in the steel I-shape while points 5-6 are in the concrete slab. Stresses in the deck (point 5) in Reference Model C are reported from the Shell Stresses at Joints, maximum Principal Stress.

There is no strain at the compound centroid in a model with loading such as this. Stresses are due entirely to the bending stress. Further, at the pin supports there is no bending stress.

The stress at mid-span can be computed by first computing the rotational strain, the slope of the strain curve along the member's y-axis. The rotational strain of the compound section is assumed to be the same as the rotational strain of each shape in a composite section in order to enforce the requirement of plane sections remaining plane (assuming the shapes were constructed at the same time). The rotational strain is given by

$$M/EI_{zz} = 3.97e-4$$

where

$$M = WL/8 = 14,888 \text{ kip-ft}$$

and E and I_{zz} are the composite section properties as given in the table above. This can be converted into a stress for each shape by multiplying it by the modulus of elasticity of the shape and the distance from the stress recovery point to the section centroid (point 3: 3.044 ft; point 5: 2.756 ft).

Stresses. Units are kip/ft²

Stress Point	@ Start		@ Mid-Span	
	3	5	3	5
Hand Calc.	0	0	5,050	568
Composite	0	0	5,050	568
Reference A	152	185	5,077	479
Reference B	152	185	5,077	479
Reference C	939	97	1,497	1,497

The differences between the non-composite models on the one hand and the hand calc and composite model on the other are significant here. The stresses follow a similar pattern as the shape axial forces: the reference models exhibit step-wise changes at the joints, while the composite model has a smooth stress curve over the length of the span.

C02: Staged Construction Analysis

A beam with fully fixed supports on both ends is used to verify several aspects of the analysis of composite sections in static and standard Staged Construction Analysis. The length of the span is 300 ft, and it has a composite cross-section comprised of a steel I-shape girder and a concrete rectangular-shape deck.

Example Project: The example described here can be found in the Composite Construction folder of your LARSA 4D Samples directory (generally My Documents\LARSA Projects\Samples) in the file C02.

The model in this verification sample is identical to that in problem C01: Single Span with Roller under Vertical Load (page 501) except that the span is fully supported on both ends and composite sequence states are added to the cross-section definition in LARSA Section Composer.

Composite Sequence States

The shapes of the cross-section will be added at different times during construction in the Staged Construction Analysis verification. Construction Sequence States must be defined. A Construction Sequence State is a configuration of the cross-section that will be needed later. In each configuration, each shape is either:

- **Active**
- **Active with Stiffness Only (self-weight is deferred)**
- **Weight Only (no stiffness)**
- **Inactive**

No Construction Sequence State is needed specifically for the case when all shapes are active. In this example, where the girder is erected first, a Construction Sequence State is needed that includes the I girder as active and the slab as inactive. Since the deck pour is modeled in a weight-only then stiffness manner, two Construction Sequence States are needed:

State A

- I Girder: Active
- Slab: Inactive

State B

- I Girder: Active
- Slab: Weight Only

State C

- I Girder: Active
- Slab: Active

The state with both shapes Active is implicitly defined. Consequently, it is not necessary to define State C explicitly.

Construction Sequence States can be defined in any order (i.e. what is State A versus what is State B doesn't matter).

To define a Construction Sequence State, change to the **Const. Seq.** tab of the Shapes Explorer:

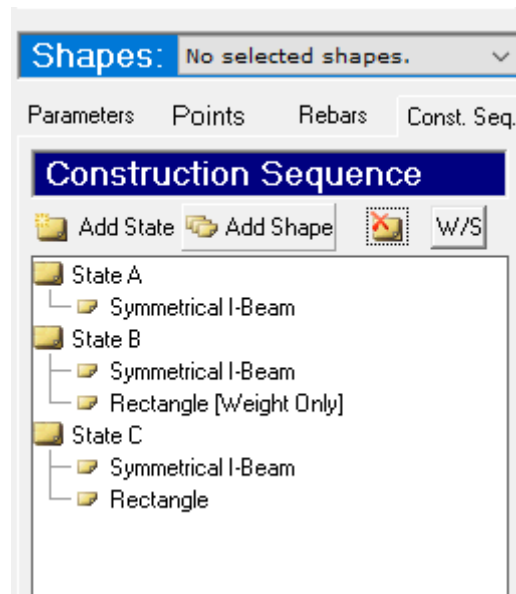


Figure2: Construction Sequence

To add a state, click on **Add State**. Then for each shape active in the state, select the shape in the drawing canvas, and then click **Add Shape** in the construction sequence panel.

To toggle a shape through the different shape modes like weight-only, click the name of the shape in the list and then click the **WS** button at the top of the list.

In the two Construction Sequence States, the concrete slab is omitted from the cross-section analysis. As a result, the total properties of the cross-section are the same as that of the steel I-shape alone. The centroid of the cross section in these states is located at the centroid of the I-shape (2.9 ft below the reference axis).

Self-Weight Loading

The first verification is for **displacements**. The maximum deflection at mid-span is given by

$$\delta = 1/384 \times (W \times L^3) / (E \times I)$$

where W = 397 kips, L = 300 ft., E is the modulus of elasticity of the reference material, and I is the moment of inertia about Z for the composite section (based on the choice of reference material), all as in C01 (page 501).

The results of the test model and the reference models in LARSA 4D are compared to hand calculations.

Deflections

	@ Mid-Span (ft)	
	Deflection (ft)	Error (%)
Hand Calc.	0.745	
Composite	0.749	1%
Reference A	0.767	3%

	@ Mid-Span (ft)	
Reference B	0.767	3%
Reference C	0.682	-8%

The next comparison is **member stresses**. Stresses at the start of the model and at mid-span are given below. Note that Stress Recovery Points 1-4 are in the steel I-shape while points 5-6 are in the concrete slab. Stresses in the deck (point 5) in Reference Model B are reported from the Shell Stresses at Joints, **Principal Stress**.

There is no strain at the compound centroid in a model such as this. Stresses are due entirely to the bending stress. The stress at mid-span can be computed by first computing the bending strain. The bending strain of the compound section is assumed to be the same as the bending strain of each shape in a composite section (assuming the shapes were constructed at the same time). The bending strain is given by

$$\epsilon = cM/EI_{zz}$$

where at the start

$$M = WL/12 = 9,925 \text{ kip-ft}$$

yielding a bending strain of $2.65e-4$, and at mid span

$$M = WL/24 = 4,963 \text{ kip-ft}$$

giving a bending strain of $1.32e-4$. E and I_{zz} are the composite section properties as given in the table at the start of C01 (page 501). This can be converted into a stress for each shape by multiplying it by the modulus of elasticity of the shape and the offset of the stress recovery point from the section centroid (point 3: 3.044 ft; point 5: 2.756 ft).

Stresses. Units are kip/ft²

Stress Point	@ Start		@ Mid-Span	
	3	5	3	5
Hand Calc.	3,370	379	1,680	189
Composite	3,367	379	1,683.4	189
Reference A	3,520	383	1,710	100.3
Reference B	3,519.7	382.9	1,709.8	100.3
Reference C	2,483.2	251	1,649	178.2

Standard Staged Construction Analysis

The model can be run in a standard Staged Construction Analysis. The span is divided into three segments comprising 4, 2, and 4 members each, and each segment is assembled in separate stages. The three I-girder segments are constructed first starting with the segments at the supports, and then the three deck segments are constructed.

This verification illustrates two aspects of composite section construction. First, member cross-sectional properties will change over time as shapes are added. Second, stress computation will recognize that the shapes have different strain values because they were added at different times.

The construction sequence is as follows:

Stage 1: Girders

- Step A: The leftmost I-girder segment is constructed.
- The first three I-girder member/shell elements are constructed.
- In the composite model, a Composite State Activity is used to set the section to “State A”, in which only the I-shape is active.
- Step B: The rightmost I-girder segment is constructed.
- Step C: The center I-girder segment is constructed.
- The Hinged Assembly option is used to initialize the joint coordinates.
- Step D: Dead load of 0.5 kip/ft is applied along the entire girder.

Stage 2: Deck Weight

- Step A: The leftmost deck segment is casted.
- Weight of last three I-girder member/shell elements are added.
- In the composite model, a Composite State Activity is used to set the section to “State B” in order to add the weight of the rectangular shape.
- Step B: Weight of the rightmost deck segment is added.
- Step C: Weight of the center deck segment is added.
- The Hinged Assembly option is used to initialize the joint coordinates.

Stage 3: Deck Assembly (Weight + Stiffness)

- Step A: The leftmost deck segment is assembled.
- The last three I-girder member/shell elements are assembled.
- In the composite model, a Composite State Activity is used to set the section to “Whole Section” in order to add the rectangular shape.
- Step B: The rightmost deck segment is assembled.
- Step C: The center deck segment is assembled.
- Step D: Dead load of 0.5 kip/ft is applied along the entire girder (again).

Self-weight is included in each step in which an element is casted or constructed.

Comparison of Results:

Incremental Deflection at Mid Span at Each Stage. Units are ft.

	1-C	1-D	2-A	2-B	2-C	3-A,B,C	3-D
Composite	-0.265	-0.407	-0.120	-0.120	-0.151	0.0	-0.283
Reference A	-0.266	-0.409	-0.122	-0.122	-0.149	0.0	-0.290
Reference B	-0.266	-0.409	-0.122	-0.122	-0.149	0.0	-0.290

	1-C	1-D	2-A	2-B	2-C	3-A,B,C	3-D
Reference C	-0.236	-0.366	-0.109	-0.109	-0.133	0.0	-0.258

Incremental Stresses at Stress Point 3 at Station 0 at Each Stage. Units are kips/ft².

	1-A	1-B	1-C	1-D	2-A	2-B	2-C	3-A,B,C	3-D
Composite	-2,434	0.0	-750	-1,504	-758	-259	-427	0.0	-1,273
Reference A	-2,434	0.0	-750	-1,504	-741	-264	-424	0.0	-1,336
Reference B	-2,434	0.0	-750	-1,504	-741	-264	-425	0.0	-1,336
Reference C	-1,931	0.0	-609	-1,108	-497	-221	-0.345	0.0	-939

Incremental Stresses at Stress Point 5 at Station 0 at Each Stage. Units are kips/ft².

	3-A,B,C	3-D
Composite	0.0	143
Reference A	0.0	113
Reference B	0.0	113
Reference C	0.0	103

Verification of Step D dead load results

The purpose of Step D in Stages 1 and 3, which have the same uniform load distribution over the span, is to compare the incremental deflections before and after the deck is included, to show the effect of changing cross-sectional properties. An approximate hand-calculation is made by assuming the girder is a continuous beam (because it is assembled in stages, this assumption is not true) and in Stage 1 assuming the support is level with the centroid of the I-shape. The approximate deflection at mid-span is given by

$$\delta = 1/384 \times (w \times L^4) / (EI)$$

where $w = 0.5$ kip/ft. In Stage 1, E and I are the properties of the I-shape alone, whereas in Stage 3 the properties are that of the composite section.

Incremental Deflection in Step D

	Stage 1	Stage 3
Approx. Hand Calc.	0.405	0.281
Composite	0.407	0.283

	Stage 1	Stage 3
Reference A	0.409	0.290
Reference B	0.409	0.290
Reference C	0.366	0.258

The computation of member stresses will show that although the composite section is treated as a single line element at the core of the finite element analysis, strain is recorded independently for each shape. In this model, the girder is elongated in three stages, while the deck experiences only elongation during Stage 3. Strain values are accumulated from one stage into the next.

There is no strain at the compound centroid in a model such as this with only dead load. Stresses are due entirely to the bending stress. To compute a stress by hand calculation, the same procedure is used as in the last section. The incremental rotational strain, labeled as $\Delta\epsilon_y$ below, is computed first, again as M/EI , where $M=wL^2/12$ at the start and $wL^2/24$ at mid-span. In Stage 1, only the I-shape is included, so E is that of steel and I is the base I_{zz} of the I-shape. In Stage 3, E and I are the composite section reference material and properties as given in the table at the start of C01 (page 501). This is computed for each stage separately in the following table:

		@ Start	@ Mid-Span
Stage 1	M (kip-ft)	-3,750	1,875
	EI	steel E, I	
	$\Delta\epsilon_y$	1.44e-4	7.21e-5
Stage 3	M (kip-ft)	-3,750	1,875
	EI	composite section	
	$\Delta\epsilon_y$	1.00e-4	5.00e-5

The rotational strain in each stage can be converted into an incremental stress for each shape by multiplying it by the modulus of elasticity of the shape and the offset of the stress recovery point from the section centroid. In Stage 1, the Stress Recovery Point offsets are the distance from the I-shape centroid to the point, 2.5 ft for point 3. Point 5 is in the concrete shape so its stress is not applicable at this point.

Incremental Stresses, Stage 1 Step D. Units are kips/ft².

	@ Start		@ Mid-Span	
Stress Point	3	5	3	5
Hand Calc.	1,505	n/a	752	n/a
Composite	1,504	n/a	752	n/a
Reference A	1,504	n/a	752	n/a
Reference B	1,504	n/a	752	n/a

	@ Start		@ Mid-Span	
Reference C	1,108	n/a	736	n/a

In Stage 3, the Stress Recovery Point offsets are again what they have been in previous examples (point 3: 3.044 ft; point 5: 2.756 ft).

Incremental Stresses, Stage 3 Step D. Units are kips/ft².

	@ Start		@ Mid-Span	
Stress Point	3	5	3	5
Hand Calc.	-1,273	143	636	-71.5
Composite	-1,273	143	636	-71.5
Reference A	-1,336	113	641	-69.8
Reference B	-1,336	113	641	-69.8
Reference C	-939	103	623	-67.3

C03: Time-Dependent Material Properties

This verification problem tests composite sections in a cantilever and guided design and in a Time-Dependent Staged Construction Analysis. The cross-section in this model is a box girder modeled as a composite of two concrete shapes: a tub and a rectangle.

Example Project: The example described here can be found in the Composite Construction folder of your LARSA 4D Samples directory (generally My Documents\LARSA Projects\Samples) in the file C03.

Cross-Section Definition

The box girder has total width 14 ft, total depth 9 ft, and 1 ft thickness of the webs, base, and deck. The top flanges are 2 ft wide. The base is 6 ft wide. The width at the top of the tub is 12 ft from the outer edges of the flanges.

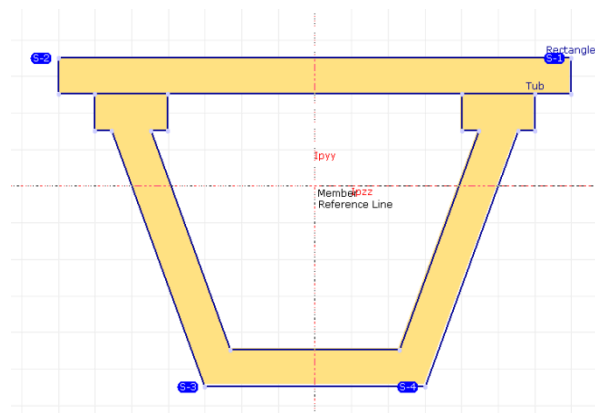


Figure1: Cross-Section

This example includes four stress recovery points, as indicated in the figure, counter-clockwise around the exterior-most points starting at the top right.

The shapes are placed such that the reference axes are at the centroid of the composite section.

The shear area is set to zero in this section so that results can be compared to simple hand calculations.

Model

This model is a cantilever beam which is 60 ft long. One end of the beam is fully fixed and the other one is free. (This is a 2D problem: TY, RX, and RZ are fixed as universal restraints.)

Besides the composite model, two reference models are used for comparison. **Reference Model A** is the same as the composite model but the cross-section is modeled as a single concrete shape, rather than two shapes. **Reference Model B** is made up of two lines of member elements connected at 6 ft intervals, one line of members tub-shape elements and one rectangle-shape elements. The members are connected to the same 11 joints. The centroids of the two shapes

are offset from the joints by offsetting the shapes from the reference axis in Section Composer. This is shown for the tub section in the figure below:

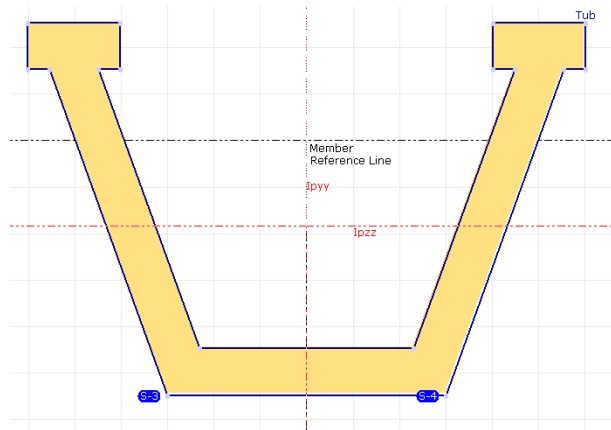


Figure2: Cross-Section of tub

The members all have an orientation angle of 90 degrees.

To activate time-dependent material effects, a **Material Time Effect** record is added to the project in the **Properties** spreadsheets. It does not need to be configured for CEB-FIP90, which we will use. This record is then assigned to the **FC_4** material record in the **More Properties** section of the **Materials** spreadsheet. Additionally, ensure that **FC_4** is marked as “**Normal**” under **Concrete Cement Hardening Type**. Its **Fc_28** is 4 kip/in². The default relative humidity is left at 80% in the **Construction Stages**. In **Analysis** → **Time Dependent Analysis Options**, set the code to CEB-FIP 90 and turn on Time Effect on **Elastic Modulus**, **Creep**, and **Shrinkage** and turn off all other time-dependent material effects.

The construction sequence consists of four steps:

Stage1: Day5 - Cast the concrete of the tub.

Stage2: Day10 - Cast the concrete of the deck.

Stage3: Day15 - a) Assemble the tub. b) Tub self-weight is applied.

Stage4: Day25 - a) Assemble the deck. b) Deck self-weight is applied.

Besides these steps, additional construction stages are placed on days **50**, **100**, **400**, and **1000**. These stages have no activities but are used to compute the long-term effects of creep.

Cross-Sectional Properties

A summary of the computation of cross-sectional properties is given below. Since the cross-section has a single material, the modulus of elasticity of concrete is not relevant. In the tables below, y_c is the distance from a shape centroid to the composite centroid.

Computation of the composite cross-section centroid

	yc (ft)	A (ft ²)
Tub	-1.83	23.1
Deck	3.02	14.0

Computation of compound properties

	Tub		Deck		Composite
	Base	Transformed	Base	Transformed	
A (ft ²)	23.1	---	14.0	---	37.1
I _{zz} (ft ⁴)	163	240	1.17	129	369
J (ft ⁴)	7.84	---	4.44	---	580

LARSA 4D's computations match the hand calculation to within rounding error. There is no hand verification for the torsion constant J at this time.

Self-Weight Loading

The results of a static self-weight load case are reported below, as well as a hand calculation using

$$\delta = WL^4/8EI$$

The unit weight of concrete is taken as 0.15 kip/ft³.

Deflection at free end

	Deflection (ft)
Hand Calc.	0.047
Composite	0.047
Reference A	0.047
Reference B	0.047

The same method will be used to verify stresses as in C01: Single Span with Roller under Vertical Load (page 501). The stress at the left end of the cantilever is

$$\sigma = \gamma WL^2/2I$$

where γ is the fiber location relative to the centroid. Stress point 1 is at the top of the deck and stress point 3 is at the bottom of the tub.

Stresses

	Stress Point 1	Error (%)	Stress Point 3	Error (%)
y (ft)	3.52		-5.48	
Hand Calc. (kip/ft ²)	95.6		-149	
Composite (kip/ft ²)	95.6	<1%	-149	<1%
Reference A (kip/ft ²)	95.6	<1%	-149	<1%
Reference B (kip/ft ²)	92.0	-4%	-156	4%

Time Effect on Elastic Modulus

In this part, results of Stage 4 with the time effect on elastic modulus included will be verified. A **Time-Dependent Staged Construction Analysis** is run.

At this point, the tub is 20 days old and the deck is 15 days old. First, the cross-sectional properties will be computed based on the revised elastic modulus for each shape. (The revised cross-sectional properties are not reported by LARSA 4D.) The effect of time is modeled by multiplying E by

$$f = \sqrt{\text{age}/(4.0+0.857 \times \text{age})}$$

where "age" is in days and is no greater than 28. Because the original E is constant throughout the cross-section and cancels out in all computations, it can be replaced below by just the time factor, f.

Computation of the new cross-section centroid location relative to the previous location

	Area (ft ²)	Age (day)	f	Centroid Location (distance to original composite centroid)
Tub	23.1	20	0.973	-1.83
Deck	14.0	15	0.943	3.02
New Composite				-0.0347

The **Transformed** column reflects the moment of inertia transformed to the composite centroid (i.e. $I_{zz} + A \times y_c^2$). For the new section properties we will use the original modulus of elasticity as the base material, which is reflected in the **Factored** columns below which is the product of the transformed properties multiplied by f.

The new composite properties about the new centroid

	Tub		Deck		Composite	Original Value		
	Base	Transformed	Factored	Base	Transformed	Factored		
A (ft ²)	23.1	--	22.5	14.0	--	13.2	35.7	37.1

	Tub			Deck			Composite	Original Value
I_{zz} (ft ⁴)	163	237	231	1.17	132	124	356	369

In Step 4 the deck is constructed and its self weight is applied. The incremental displacements at the far end of the cantilever are given in the table below, along with a hand calculation ($\delta = WL^4/8EI$, $W=2.1$ kip/ft) and, for comparison, a hand calculation for a similar model with the original day-28 properties.

Reference Model A is not applicable in this comparison because it could only be assembled in one step, as it is made of a single shape, and therefore could not have self-weight applied for just one shape in this step.

Deflection at free end (**Incremental**)

	Deflection (ft)	Error (%)
Hand Calc.	0.0184	
Composite	0.0184	<1%
Reference B	0.0185	<1%
Day 28 Hand Calc.	0.0178	

Similar method will be used to verify stresses as in previous sections. Now that the two shapes have different material properties, the member-end moment

$$M = WL^2/2$$

must be converted to a curvature first

$$\kappa = WL^2/2EI$$

using the composite I_{zz} and the corresponding original (28-day) E . The curvature is multiplied by the fiber location y and the 15- or 20-day modulus of elasticity at the fiber to find the stress. The fiber locations of the stress points are changed here to reflect the new centroid location. Hand calculations assuming all 28-day concrete is also provided for comparison. Stress point 1 is at the top of the deck and stress point 3 is at the bottom of the tub.

Stresses (**Incremental**)

	Stress Point 1	Stress Point 3
y (ft)	3.55	-5.44
Hand Calc. (kip/ft ²)	35.5	-56.2
$(yfWL^2/2I)$		
Composite (kip/ft ²)	35.7	-56.3
Reference B (kip/ft ²)	36.0	-58.8
Day 28 Hand Calc. (kip/ft ²)	36.1	-56.0

Shrinkage

To verify shrinkage, total effect on stress of shrinkage though day 400 will be checked. Shrinkage, ϵ_s as given below according to CEB-FIP90, is an additional strain added into the cross-section accumulated from time t_0 to time t_1 . **In this part, the time effect on elastic modulus is not included.**

$$\epsilon_s = \epsilon_{cs0}[\beta_s(t_1) - \beta_s(t_0)]$$

$$\epsilon_{cs0} = (160 + 10 \times \beta_{sc} \times (9 - F_{c28}/10)) / 1e6 \times (-1.55 \times (1.0 - (RH/100)^3))$$

$$\beta_s(t) = \text{sqrt}((t - TS) / (350 \times ((H/100)^2) + (t - TS)))$$

where $TS = 3$, $\beta_{sc} = 5$, $H = 2 \times \text{Area/Perimeter}$ converted to millimeters, RH is the relative humidity (80%), and t_0 , t_1 are the ages of the section in days. $F_{c28} = 27.6 \text{ MPa}$ (576 kip/ft^2).

The shrinkage must be computed in two parts. From days 15 to 25, the tub alone is constructed. The shrinkage results in deformation due to pure strain but neither bending nor stress. From days 25 to 400, the tub and the deck are subject to different amounts of shrinkage. Because the shapes are connected, this creates bending strain and eigenstresses. Additionally, strain compatibility must be considered. Because of “plane sections remain plane,” shrinkage must be considered as the sum of two virtual strain components.

The first component called the “**external**” component, with magnitude ϵ_s , and is responsible for causing deformation. In Ghali, Favre, and Elbadry (2002) example 5.2, this corresponds to the forces and moments that undo the artificial restraint on shrinkage. The second or “**internal**” component has magnitude $-\epsilon_s$ but does not cause deformation. (It corresponds to Ghali, Favre, and Elbadry’s strain in the section when shrinkage is restrained.) Initially, the external and internal virtual strains cancel out.

Next replace the external strain with an equivalent force and moment at the beam end. The external stresses are integrated across the cross-section to determine an equivalent force

$$F = \epsilon_s \times E \times A$$

and moment

$$M = F \times y_c$$

imposed at the beam end, which in turn determines the actual deformation of the beam as the combination of pure

$$\epsilon_p = F / EA$$

and rotational

$$\epsilon_r = M / EI$$

strains (E , A , and I are properties of the entire cross-section, with E unmodified for time). In this way, the original external strains which have sharp changes at the boundaries of shapes are turned into a linear strain profile across the entire cross-section, which satisfies strain compatibility (i.e. plane sections remain plane).

The table below shows the relevant computations for the external virtual strain. The perimeters used in the hand calculation include the interior perimeter of the tub and the unexposed perimeters at the interface of the two shapes in order to match the computations in LARSA 4D.

Because the original external strains are constant throughout each individual shape, a lumped force at each shape’s centroid,

$$F = \epsilon_s EA$$

is given in the table below in order to compute the moment about the cross-section centroid.

Computation of External Strain, Day 400

	Tub	Deck
Area (ft ²)	23.1	14.0
Perimeter (ft)	48.1	30
Age on Day 15 (day)	10	n/a (no stiffness)
Age on Day 25 (day)	20	15
Shrinkage (ϵ_{s1}), days 15-25	-9.57e-6	n/a
Age on Day 400 (day)	395	390
Shrinkage (ϵ_{s2}), days 25-400	-9.46e-5	-1.01e-4
Equivalent Force $F = \epsilon_{s2}EA$ (kip)	-1,134	-734
cy (ft)	-1.83	3.02
Equivalent Moment $M = Fcy$ (kip-ft)	2076	-2217
Total Pure Strain ($\epsilon_p = F/EA + \epsilon_{s1}$)	-1.07e-4	-1.07e-4
Total Rotational Strain ($\epsilon_r = M/EI$) (per ft)	-7.4e-7	-7.4e-7

The deformation of the centroid of the span is circular with a radius of curvature r equal to the reciprocal of the total rotational strain. At the same time, the arc-length of the span, s , is reduced according to the pure strain, therefore

$$s = 60 \times (1 + \epsilon_p)$$

A hand computation for displacement (Δx , Δy) is explained in the diagram below.

$$\theta = s/r$$

$$x1 = r \times \cos(\pi/2 - \theta)$$

$$y1 = r \times \sin(\pi/2 - \theta)$$

$$\Delta x = x1 - 60$$

$$\Delta y = r - y1$$

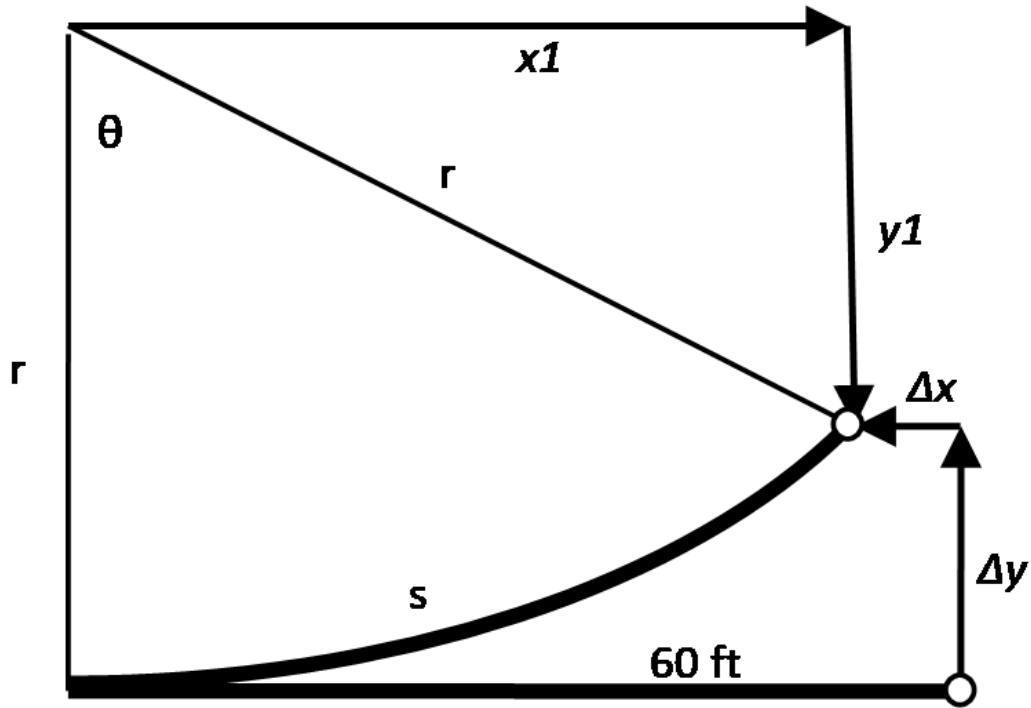


Figure3: Deformed Shape due to Shrinkage

The displacement at the free end of the cantilever is given in the table below, from hand calculations and as reported by LARSA 4D in the composite model and the two reference models. In LARSA 4D, `Extract Shrinkage` is used to report the cumulative effects of shrinkage alone.

Displacement

	Δx (ft)	Δy (ft)
Hand Calc.	-6.38e-3	1.26e-3
Composite	-6.38e-3	1.25e-3
Reference A	-5.74e-3	0.00
Reference B	-6.38e-3	1.25e-3

The stress in any fiber is then given essentially by

$$\sigma = E \times ((\epsilon_p - \epsilon_{s1}) + \gamma \times \epsilon_r - \epsilon_{s2})$$

the sum of the external and internal components of stress at each fiber. For stresses we subtract ϵ_{s1} from ϵ_p in the external component of stress because when the tub alone is constructed shrinkage does not create stress. Similarly, it is not included in the internal component of stress. Stresses at the free end of the cantilever are given below.

Stresses

	Stress Point 1	Stress Point 3
y (ft)	3.52	-5.47
Hand Calc. (kip/ft ²)	0.688	0.791
Composite (kip/ft ²)	0.691	0.790
Reference A (kip/ft ²)	0.00	0.00
Reference B (kip/ft ²)	0.691	0.79

Creep

The computation of creep is significantly more complex than that of shrinkage, and creep involves an integration of stresses over time. Rather than presenting a hand calculation, simply compare the results of the composite model to the two reference models.

Recall that Reference A is a single-member representation of the composite model in which the whole section is cast on day 5. This differs from the composite model and Reference B in which the two shapes are cast at different times.

The cumulative effect of creep alone on day 1000 (i.e. “**extract creep**”) is reported in the table below. Joint displacements in vertical direction at the far end of the cantilever and stresses at the fixed end are reported. As in previous models, we expect joint displacements in the composite model and Reference B to match exactly but we expect non-composite models to report different stresses due to the distribution of forces in the rigid connections not present in the composite model.

Stresses

	Displacement (ft)	Stress Point 1 (kip/ft ²)	Stress Point 3 (kip/ft ²)
Composite	-0.097	63.6	55.2
Reference A	-0.094	0.00	0.00
Reference B	-0.097	55.6	49.0

References

Ghali, A., Favre, R., and Elbadry, M. Concrete Structures: Stresses and Deformations: Analysis and Design for Serviceability (2002).

C04: Thermal Loads

This verification problem tests composite sections for uniform, linear, and nonlinear thermal gradients in a linear static analysis.

Example Project: The example described here can be found in the Composite Construction folder of your LARSA 4D Samples directory (generally My Documents\LARSA Projects\Samples) in the file C04.

Cross-Section Definition

The cross-section definition is the same in problems C01: Single Span with Roller under Vertical Load (page 501) and C02: Staged Construction Analysis (page 509). The cross-section used in this problem is composed of a steel I-shape and a concrete slab on top. The dimensions are:

- **I-Shape:** 5 ft deep; 2 ft wide; 0.2 ft flange and web thickness
- **Rectangle Shape:** 0.8 ft deep; 4 ft wide

This example includes six Stress Recovery Points: 1-4 clockwise around the I-shape, and 5-6 at the upper-right and upper-left of the concrete slab, respectively.

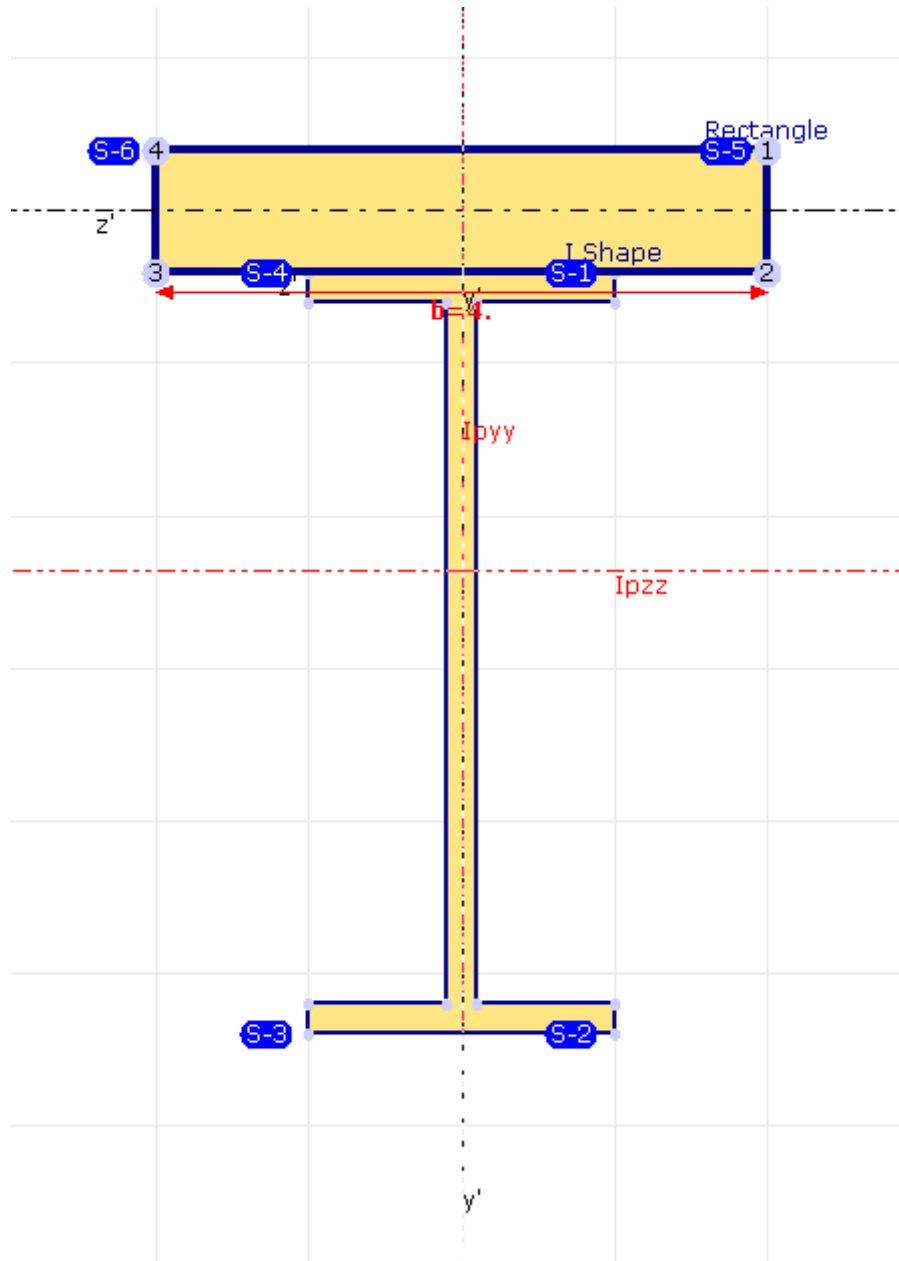


Figure1: Cross-Section

The shapes are placed such that the reference axes are at the centroid of the deck slab.

The properties for the section as a whole, with concrete as the reference material, are given in the table below.

Section Properties

A (ft ²)	17.0
I_{yy} (ft ⁴)	6.44

I_{zz} (ft ⁴)	72.2
J (ft ⁴)	1.49

Model

The model is the same as in problem C01 (page 501). The girder and deck system is supported by a pin on one end and a roller at the other (the supports are level with the centroid of the deck). The length of the span is 300 ft.

A verification of the results of a composite section model is made by comparing the results to hand calculations and to roughly equivalent reference models using non-composite beam elements connected rigidly at intervals using rigid members (**A**), non-composite beam elements connected at intervals using member end offsets (**B**), and shell elements connected at intervals using shell end offsets (**C**) (left to right, below).

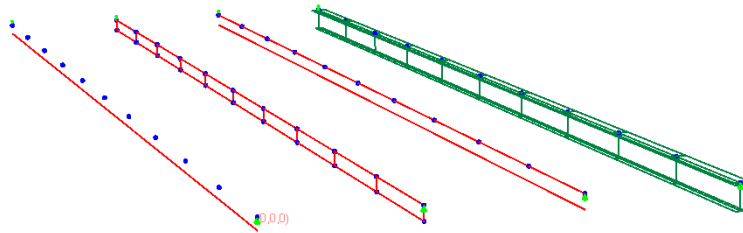


Figure2: Models

Analysis of Thermal Loads

The analysis of thermal loads is performed similarly to that of shrinkage (see C03: Time-Dependent Material Properties (page 517)). At each fiber we split the thermal load into an “**external**” component of stress and an equal and opposite “**internal**” component, each with magnitude $E\alpha t$. The external component is responsible for the deformation of the beam, and so the external components are integrated over the cross-section area to determine the resultant force and moment at the whole-member cross-section centroid, and from there the total pure

$$\epsilon_p = F/EA$$

and rotational

$$\epsilon_r = M/EI$$

strains (where E , A , and I are properties of the entire cross-section).

The total stress in any fiber is the sum of “external” component of stress

$$E^*(\epsilon_p + y^*\epsilon_r)$$

and the “internal” component of stress

$$-E\alpha t$$

Uniform Thermal Load

This section verifies the uniform thermal load. A uniform +20 °F thermal change is applied to the entire cross-section. Steel has a larger coefficient of thermal expansion. Thus we expect the steel I shape, which is below the composite centroid, to cause the entire model to have an upward curvature. Because of the vertical supports at the ends, there will be negative vertical displacements along the model.

Vertical Displacements. Units are ft

	@ 20%	@ Mid-Span
Composite	-0.0150	-0.0235
Reference A	-0.0150	-0.0235
Reference B	-0.0150	-0.0235
Reference C	-0.0456	-0.0292

Since plane sections remain plane, the deformation of the two shapes that make up the composite section must be related. The steel part is restrained from expanding as much as it would unrestrained, so we should expect a compressive stress at the centroid of the steel shape. Similarly, we expect a tensile stress at the centroid of the concrete shape.

The integration of the “**external**” component of stress is given in the following table. The moment and rotational strain are at the compound centroid.

	Steel I	Concrete Slab
E (kip/ft ²)	4,176,000	519,120
A (ft ²)	1.72	3.2
α (1/°F)	6.5e-6	5.5e-6
Force (αTEA) (kip)	933.8	182.7
Centroid Location (ft)	-0.544	2.356
Moment (kip-ft)	-508.0	-430.5
Total Pure Strain (ϵ_p)	-1.262e-4	-1.262e-4
Total Rotational Strain (ϵ_r) (per ft)	-2.069e-6	-2.069e-6

The total stress in each shape is computed in the following table by summing the internal and external components of stress. Note that stress recovery point 3 is in the steel shape and stress recovery point 5 is in the concrete shape and so each stress recovery point uses a different E value.

	I Shape Centroid	Slab Centroid	Stress Point 3	Stress Point 5
y (ft)	-0.544	2.356	-3.044	2.756
$E*(\epsilon_p + y*\epsilon_r)$ (kip/ft ²)	532	63.0	553.3	62.54

	I Shape Centroid	Slab Centroid	Stress Point 3	Stress Point 5
$-\alpha TE$ (kip/ft ²)	-543	-57.1	-543	-57.1
Total Stress (kips/ft ²)	-11.2	5.88	10.4	5.44

Stresses. Units are kip/ft².

	Stress Point 3	Error (%)	Stress Point 5	Error (%)
Composite	10.9	5%	5.44	0%
Reference A	10.9	5%	5.44	0%
Reference B	10.9	5%	5.44	0%
Reference C	23.5	-	13.12	-

Linear Gradient Thermal Load

This section verifies the linear gradient thermal load. A thermal change is applied to the entire cross-section with a $T_0 = +20$ °F change at the cross-section centroid and a $T_{\text{slope}} = 5$ °F/ft slope in the vertical axis. (That results in a temperature change of +4.8 °F at the bottom of the steel I shape, 29.8 °F at the meeting of the two shapes, and 33.8 °F at the top of the concrete slab.) A linear thermal gradient cannot be applied in the shell-based reference model because a thermal load cannot be entered to vary along the shell's surface.

In the non-composite reference models, the linear thermal load is broken down into a part for the I shape member and a part for the slab member.

Displacements

	@ 20%	@ Mid-Span
Composite (ft)	0.210	0.328
Reference A (ft)	0.210	0.328
Reference B (ft)	0.210	0.328

To compute the “external” component of stress at the composite cross-section centroid, the stress at each fiber $E\alpha t$ is integrated over the area of the section, i.e.

$$F = \int E_a \alpha_a (20 + 5y) da$$

and

$$M = \int E_a \alpha_a y (20 + 5y) da$$

where E_a and α_a are the elastic modulus and coefficient of thermal expansion of fiber a , and y is the location of the fiber relative to the centroid of the composite section. This can be computed by breaking the cross-section down into its rectangular pieces which have constant E , α , and y for each horizontal strip with width w , so that

$$F = \sum_{\text{rect}} w E \alpha \int (20 + 5y) dy$$

$$M = \sum_{\text{rect}} wE\alpha \int y(20+5y)dy$$

Computation of “External” Force and Moment

Rectangular Part	y ₀ (ft)	y ₁ (ft)	width (w) (ft)	E (kip/ft ²)	α (1/°F)	F (kip)	M (kip-ft)
Bottom Flange	0.0	0.2	2.0	4,176,000	6.5e-6	57.6	-169
Web	0.2	4.8	0.2	4,176,000	6.5e-6	432	-14.8
Top Flange	4.8	5.0	2.0	4,176,000	6.5e-6	318	590
Slab	5.0	5.8	4.0	519,120	5.5e-6	290	686

The sum of the forces and moments at the section centroid and the corresponding total pure strain

$$\epsilon_p = F/EA$$

and rotational strain

$$\epsilon_r = M/EI$$

(with E and I here the properties of the cross-section) are given below.

Computation of “External” Force and Moment

F (kip)	1098
M (kip-ft)	1093
ε _p	1.24e-4
ε _r	2.92e-5

The total stress in each shape is computed in the following table by adding the “external” stress as given by the total strains above and the “internal” stress based on the value of the linear curve at the fiber. Note that stress recovery point 3 is in the steel shape and stress recovery point 5 is in the concrete shape and have **E** and **α** set accordingly. The **y** values are relative to the cross-section centroid.

Hand Calculation of Stress

	Stress Point 3	Stress Point 5
y (ft)	-3.044	2.756
E*(ε _p +y*ε _r) (kip/ft ²)	147	106
-αE(T ₀ +y*T _{slope}) (kip/ft ²)	-130	-96.5
Total Stress (kips/ft ²)	16.2	9.63

Stresses. Units are kip/ft²

	Stress Point 3	Error (%)	Stress Point 5	Error (%)
Composite	17.4	-7%	9.68	-1%
Reference A	17.4	-7%	9.68	-1%
Reference B	17.4	-7%	9.68	-1%

The same results are reported by LARSA 4D when the linear variation is entered as a nonlinear thermal curve with two points.

Nonlinear Gradient Thermal Load

This section verifies the nonlinear gradient thermal load. A thermal change is applied to the entire cross-section with formula

$$T = y^2$$

where y is the distance measured from the lower extreme fiber of the section in feet (0-5.8 ft) and T is in °F. The temperature change at the top is 33.64 °F; the temperature change at the intersection of the two shapes is 25 °F. For the purposes of entering the temperature curve into LARSA 4D, it has been discretized into 30 points equally spaced on the section y -axis.

In the reference models, the thermal load is broken down into a part for the I shape member and a part for the slab member. The shell-based reference model is not used.

Displacements

	@ 20%	@ Mid-Span
Composite (ft)	0.236	0.369
Reference A (ft)	0.236	0.369
Reference B (ft)	0.236	0.369

To compute the “external” component of stress at the composite cross-section centroid, the stress at each fiber $E\alpha t$ is integrated over the area of the section, i.e.

$$F = \int E\alpha y^2 da$$

$$M = \int E\alpha y^2(y-3.044)da$$

where E and α are the elastic modulus and coefficient of thermal expansion (which are functions of the fiber), y is the location of the fiber relative to the lowest fiber of the section, and 3.044 ft is the distance from the lowest fiber to the centroid of the composite section. This can be computed by breaking the cross-section down into its rectangular pieces which have constant E , α , and y for each horizontal strip with width w , so that

$$F = \sum_{\text{rect}} wE\alpha \int y^2 dy$$

$$M = \sum_{\text{rect}} wE\alpha \int y^2(y-3.044)dy$$

Computation of “External” Force and Moment

Rectangular Part	y_0 (ft)	y_1 (ft)	width (w) (ft)	E (kip/ft ²)	α (1/°F)	F (kip)	M (kip-ft)
Bottom Flange	0.0	0.2	2.0	4,176,000	6.5e-6	0.145	-0.419
Web	0.2	4.8	0.2	4,176,000	6.5e-6	200	111
Top Flange	4.8	5.0	2.0	4,176,000	6.5e-6	261	484
Slab	5.0	5.8	4.0	519,120	5.5e-6	267	634

The sum of the forces and moments and the total pure strain

$$\epsilon_p = F/EA$$

and rotational strain

$$\epsilon_r = M/EI$$

(with E and I here the properties of the cross-section) are given below.

Computation of Nonlinear Gradient Effect

F (kip)	728
M (kip-ft)	1229
ϵ_p	8.23e-5
ϵ_r	3.28e-5

The total stress in each shape is computed in the following table by adding the “external” stress as given by the total strains above and the “internal” stress based on the value of the nonlinear curve at the fiber. Note that stress recovery point 3 is in the steel shape and stress recovery point 5 is in the concrete shape and have E set accordingly.

Hand Calculation of Stress

	Stress Point 3	Stress Point 5
y (ft)	-3.044	2.756
$E*(\epsilon_p+y*\epsilon_r)$ (kip/ft ²)	-73.4	89.6
$-\alpha E(y-3.044)^2$ (kip/ft ²)	0	-96.0
Total Stress (kips/ft ²)	-73.4	-6.39

Stresses. Units are kip/ft²

	Stress Point 3	Error (%)	Stress Point 5	Error (%)
Composite	-72.8	<1%	-6.49	3%

	Stress Point 3	Error (%)	Stress Point 5	Error (%)
Reference A	-73.1	1%	-6.39	1%
Reference B	-73.1	1%	-6.39	1%

Samples for Buckling Analysis

These samples provide an overview of linear and nonlinear buckling analysis.

For More Information, please refer to the following documentation.

- For help on nonlinear buckling analysis, see Nonlinear Buckling Analysis in *LARSA 4D Reference Manual*.

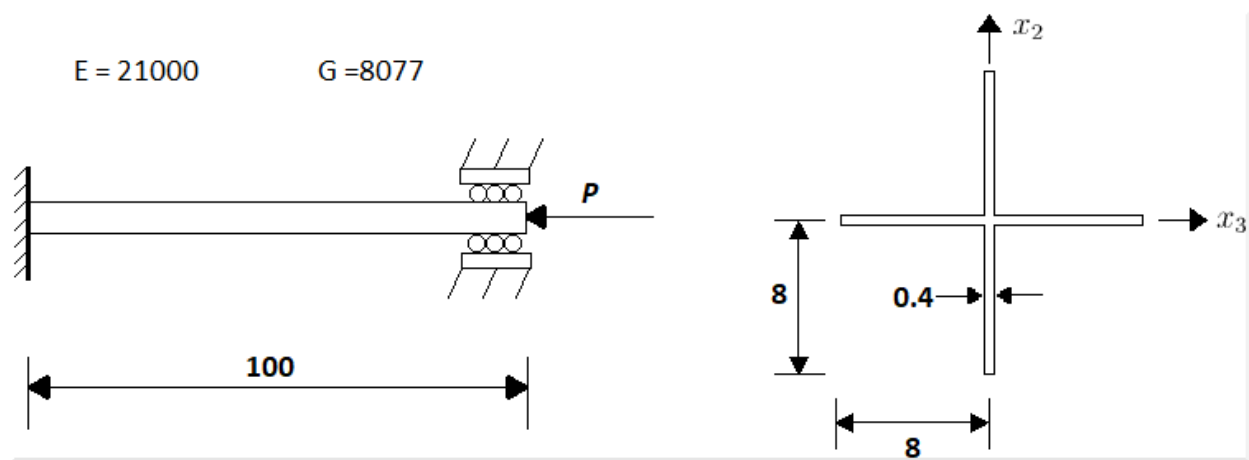
B01: Torsional Buckling of Crucifix Section with Shell Elements	539
Problem Description	539
Solution Comparison	540
References	540
B02: Lateral Buckling of I Section with Shell Elements	541
Problem Description	541
Solution Comparison	542
References	542
B03: Lateral Torsional Buckling of C Section with Shell Elements	543
Problem Description	543
Solution Comparison	544
References	544

B01: Torsional Buckling of Crucifix Section with Shell Elements

A fixed-fixed girder with a crucifix cross-section is modeled with nonlinear shell elements. The girder is subjected to an incrementally increasing axial load. Determine the torsional buckling load by analyzing the model with Nonlinear Buckling Analysis.

Example Project: The example described here can be found in the Buckling folder of your LARSA 4D Samples directory (generally My Documents\LARSA Projects\Samples) in the file B01.

Problem Description



Fixed-Fixed girder and its cross-section

The girder consists of 160 nonlinear shell elements. Each blade of the section is 40 shells. All the translational and rotational degrees of freedom are restrained for the joints at the left end of the section. For the right end of the section, only axial translation is free to see the behavior of the section under axial loading.

The blades of the cross-section have 0.4 in. thickness and 8 in. width. The total length of the girder is 100 inches.

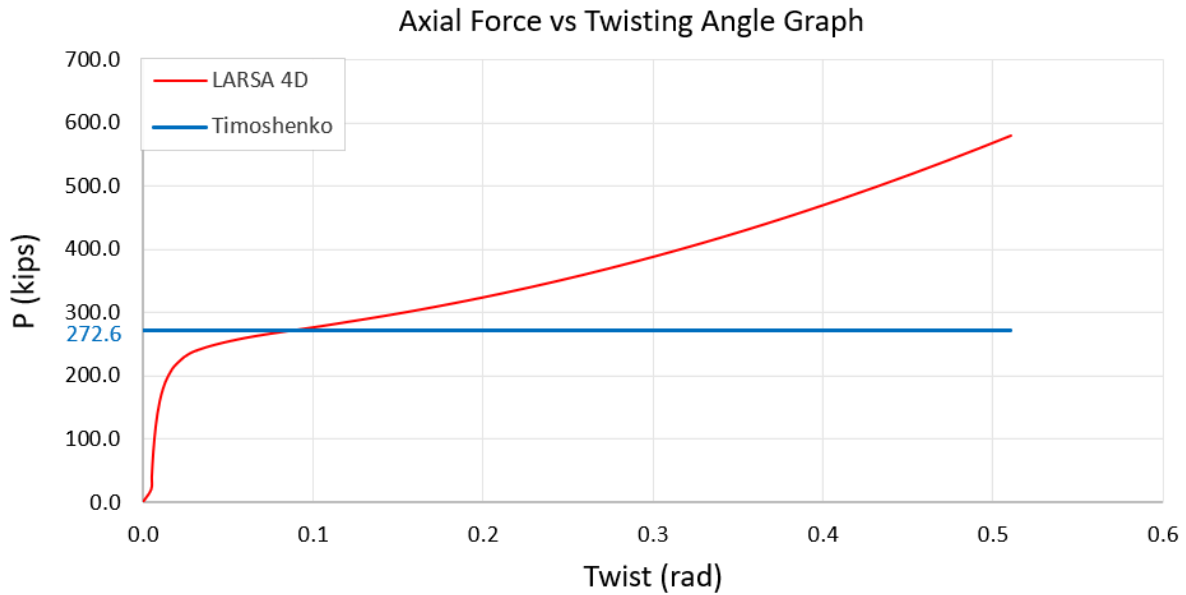
The material has 21,000 kips/in² elastic modulus with 0.3 Poisson's ratio.

In order to achieve nonlinear behavior, the MITC4 element formulation is used.

A small 1 kip-in perturbation is applied at the middle of the cross-section as a small torsional load to initiate the twisting. Loading is applied axially by gradually increasing it until it reaches 580 kips. At every step, the load is increased by 20 kips. It is modeled as a 1 kip load divided equally across the 5 nodes at the tip of each blade and the node at the intersection of the blades at the free end of the member. Perturbation and loading are defined in separate load cases. Each step is created as a load combination. Perturbation is only applied in first load combination. The axial load is applied in each step by increasing its magnitude 20 times. The model is analyzed using Nonlinear Buckling Analysis.

Solution Comparison

The results are obtained from the axial loading versus twisting angle (R_x of joint 26) curve of the model. The load where the rate of the curve changes remarkably may be counted as buckling load. In order to compare the results, the independent solution which is given by Timoshenko and Gere based on Bernoulli beam theory with Vlasov warping is shown in the graph.



Load deflection curve

References

- S.P. Timoshenko, J.M. Gere, Theory of Elastic Stability, second ed., McGraw-Hill, Tokyo, 1961

For More Information, please refer to the following documentation.

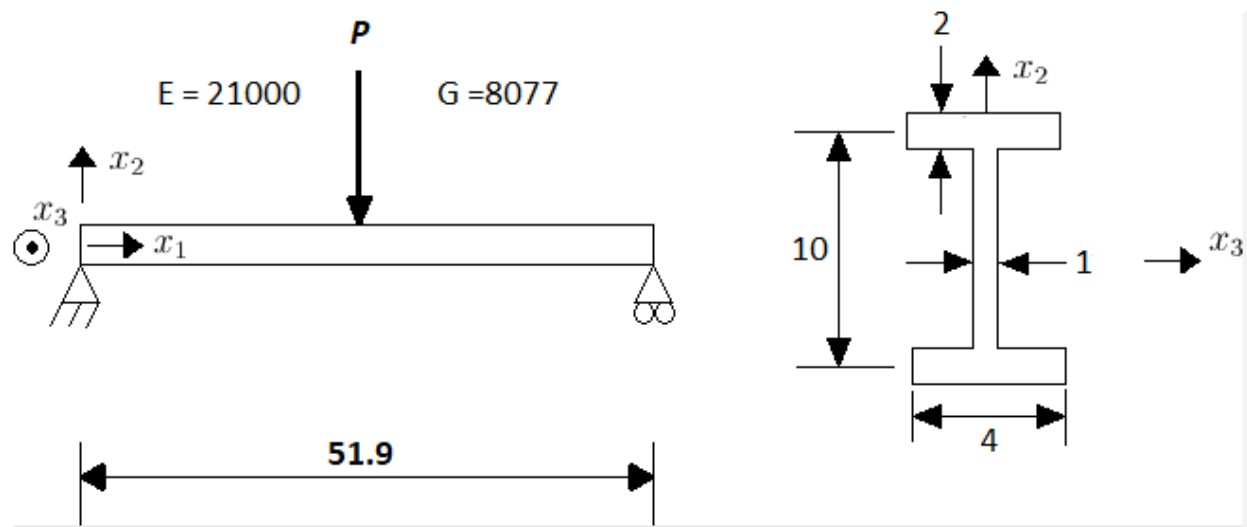
- For help on nonlinear buckling analysis, see Nonlinear Buckling Analysis in *LARSA 4D Reference Manual*.
- For help on nonlinear plate elements, see Shells in *LARSA 4D Reference Manual*.

B02: Lateral Buckling of I Section with Shell Elements

A simply supported girder with an I-shaped cross-section is modeled with nonlinear shell elements. The girder is subjected to an incrementally increasing vertical point load. Determine the lateral buckling load by analyzing the model with Nonlinear Buckling Analysis.

Example Project: The example described here can be found in the Buckling folder of your LARSA 4D Samples directory (generally My Documents\LARSA Projects\Samples) in the file B02.

Problem Description



Simple supported girder and its cross-section

The girder consists of a total of 960 nonlinear shell elements. Each flange has 320 shells. The web of the section has 320 shell elements. In order to obtain the simply supported behavior, the middle of the web at the left end of the section (67th joint) is restrained for translation in x and z directions and the middle of the web at the right end of the section (77th joint) is restrained for translation in the z direction. Also, to stabilize the model, corners of the web element (1st, 4th, 61st and 64th joints) are restrained in translation in the y direction.

The flanges have 4 in. width and 2 in. thickness. The web has 8 in. depth and 1 in. thickness. The total length of the girder is 51.9 inches.

The material has 21,000 kips/in² elastic modulus with 0.3 Poisson's ratio.

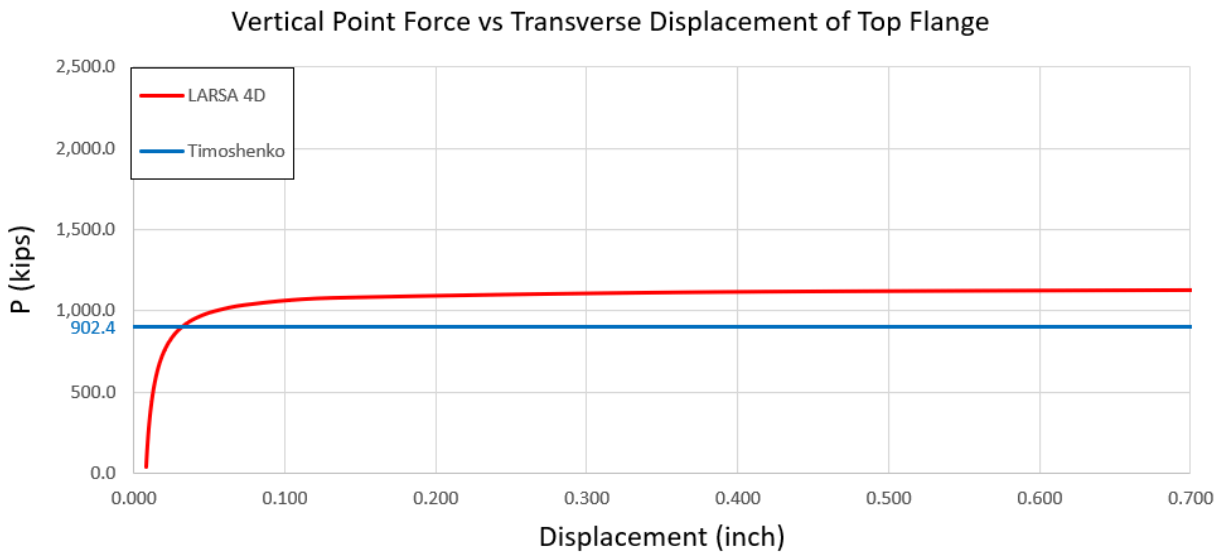
In order to achieve nonlinear behavior, the MITC4 element formulation is used.

A small 1 kip perturbation is applied at middle of the top flange as small lateral point load to initiate the lateral movement. Loading is applied at the center of the top surface of the top flange by gradually increasing it by 40 kips in each step. A one kip load is divided on three nodes equally: the left, right, and middle of the cross-section of top flange

at the middle end of the member. Perturbation and loading are defined in separate load cases. Each step is created as a load combination. Perturbation is only applied in first load combination. The vertical point load is applied in each step by increasing its magnitude 40 times. The model is analyzed using Nonlinear Buckling Analysis.

Solution Comparison

The results are obtained from axial loading versus lateral displacement of top flange(U_y of joint 31) curve of the model. The load where the rate of the curve changes remarkably may be counted as buckling load. In order to compare the results, the independent solution which is given by Timoshenko and Gere is shown in the graph.



Load deflection curve

References

- S.P. Timoshenko, J.M. Gere, Theory of Elastic Stability, second ed., McGraw-Hill, Tokyo, 1961

For More Information, please refer to the following documentation.

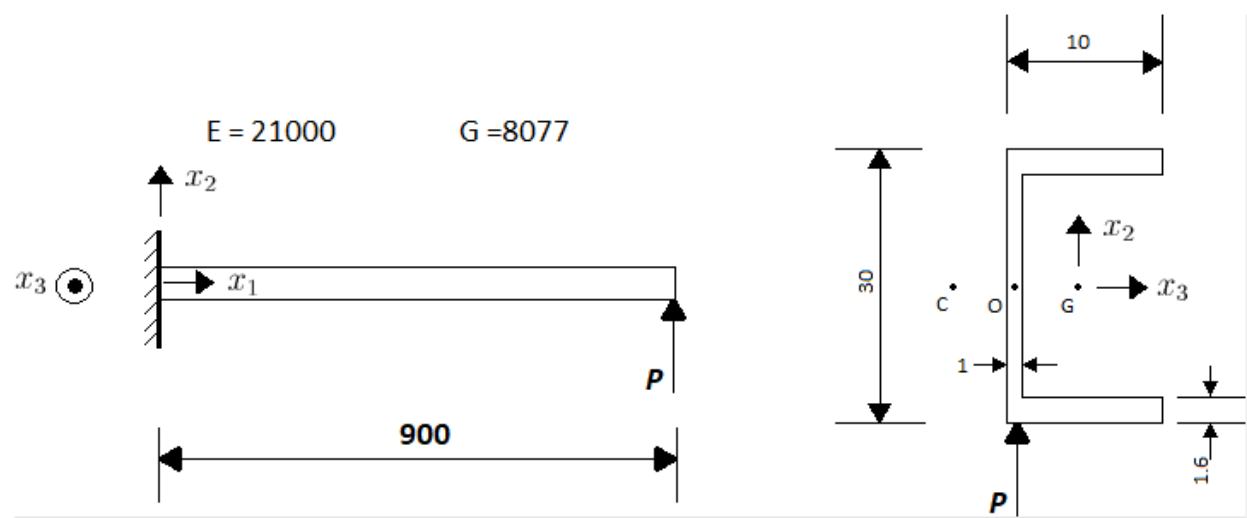
- For help on nonlinear buckling analysis, see Nonlinear Buckling Analysis in *LARSA 4D Reference Manual*.
- For help on nonlinear plate elements, see Shells in *LARSA 4D Reference Manual*.

B03: Lateral Torsional Buckling of C Section with Shell Elements

A cantilever girder with a C-shaped cross-section is modeled with nonlinear shell elements. The girder is subjected to an incrementally increasing vertical tip load. Determine the lateral-torsional buckling load by analyzing the model with Nonlinear Buckling Analysis.

Example Project: The example described here can be found in the Buckling folder of your LARSA 4D Samples directory (generally My Documents\LARSA Projects\Samples) in the file B03.

Problem Description



Cantilever girder and its cross-section

The girder consists of a total of 640 nonlinear shell elements. Each flange has 160 shells. The web of the section has 320 shell elements. In order to obtain the cantilever behavior, the corners of the top and bottom flanges at the left end of the girder (1st, 2nd, 3rd and 4th joints) are fixed in both translation and rotation. Joints at the right end of the girder are free to rotate and translate.

Flanges have 10 in. width and 1.6 in. thickness. The web has 26.8 in. depth and 1 in. thickness. The total length of the girder is 900 inches.

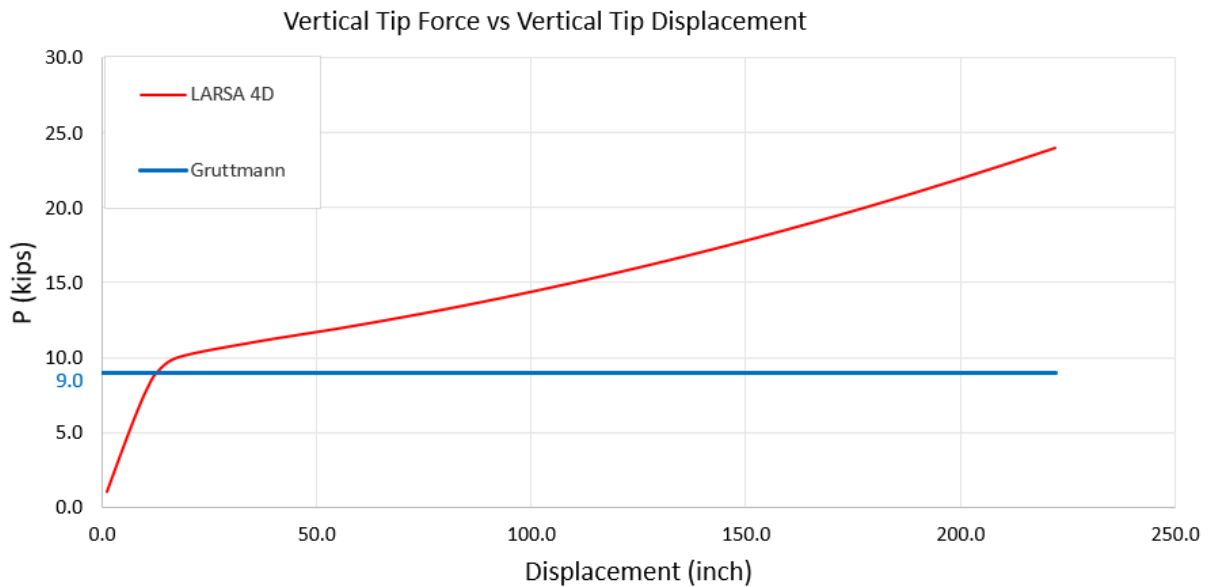
The material has 21,000 kips/in² elastic modulus with 0.3 Poisson's ratio.

In order to achieve nonlinear behavior, the MITC4 element formulation is used.

Loading is applied where the web element and the bottom flange coincides at the free end of the girder vertically by gradually increasing until it reaches 24 kips. Each step is created as a load combination. Vertical load is applied in each step. The model is analyzed by using Nonlinear Buckling Analysis.

Solution Comparison

The results are obtained from axial loading versus vertical displacement of free end (U_z of joint 287) curve of the model. The load where the rate of the curve changes remarkably may be counted as buckling load. In order to compare the results, the independent solution which is given by Gruttmann is shown in the graph.



Load deflection curve

References

- R. Gruttmann, R. Sauer, W. Wagner, Theory and numerics of three-dimensional beams with elastoplastic behaviour, *Int. J. Numer. Methods Engrg.* 48 (2000) 1675–1702.

For More Information, please refer to the following documentation.

- For help on nonlinear buckling analysis, see Nonlinear Buckling Analysis in *LARSA 4D Reference Manual*.
- For help on nonlinear plate elements, see Shells in *LARSA 4D Reference Manual*.

Index

- arch, 171
- barrel vault, 47
- beams, 201
- bridge path, 377
- buckling, 537
- cable roof, 165
- cables, 159
- cantilever
 - E01: Triangular Cantilever Plate Eigenvalues, 193
 - E02: Square Cantilever Plate Eigenvalues, 197
- circular arch, 171
- circular plate, 41
- composite construction
 - C01: Single Span with Roller under Vertical Load, 501
 - C02: Staged Construction Analysis, 509
 - C03: Time-Dependent Material Properties, 517
 - C04: Thermal Loads, 527
 - Samples for Composite Construction, 499
- compression-only foundation springs, 161
- concentrated mass, 239
- cylindrical roof, 47
- diamond shaped frame, 167
- dynamic loads, 239
- eigenvalue analysis, 191
- elastic foundation
 - L03: Beam on Elastic Foundation, 21
 - N03: Beam on an Elastic Soil Foundation, 161
- element space truss, 27
- geometric nonlinearity
 - N06: Diamond Shaped Frame - Geometric Nonlinear, 167
 - N08: A High Arch Structure - Geometric Nonlinear, 171
- geometric stiffening
 - L10: Tie Beam without Geometric Stiffening, 39
 - N01: Tie Beam with Geometric Stiffening, 157
- hemispherical shell, 43
- holes, 41
- influence lines and surfaces, 369
- linear elastic static, 13
- linear gradient thermal load, 527
- linear time history analysis, 235
- live load analysis, 369
- lumped masses, 209
- mass elements, 209
- nonlinear elastic static, 155
- nonlinear gradient thermal load, 527
- nonlinear thermal load, 53
- nonlinear time history analysis, 235
- pin connection
 - L02: Beam with Elastic Supports, 19
 - L06: Static Analysis of a Space Frame, 31
- plate
 - B01: Torsional Buckling of Crucifix Section with Shell Elements, 539

- B02: Lateral Buckling of I Section with Shell Elements, 541
- B03: Lateral Torsional Buckling of C Section with Shell Elements, 543
- N13: Straight Cantilever Girder with Nonlinear Shell Elements in Membrane Action, 175
- N14: Straight Cantilever Girder with Nonlinear Shell Elements in Plate Action, 179
- N15: Slit Annular Plate with Vertical Load, 183
- plate thermal loads, 35
- plates
 - E01: Triangular Cantilever Plate Eigenvalues, 193
 - E02: Square Cantilever Plate Eigenvalues, 197
 - L07: Plate Thermal Analysis, 35
 - L08: Shell-Bending of a Tapered Cantilever, 37
 - L11: Circular Plate with a Hole Static Analysis, 41
- point loads
 - L02: Beam with Elastic Supports, 19
 - L06: Static Analysis of a Space Frame, 31
- reactions, 159
- reinforced concrete, 47
- response spectra analysis, 225
- settlement, 51
- simply supported beam, 21
- space truss, 27
- span break markers, 377
- spring mass system, 237
- springs, 209
- staged construction analysis
 - C02: Staged Construction Analysis, 509
 - Samples for Staged Construction Analysis, 293
- steel bridge, 387
- stressed eigenvalue analysis, 221
- tapered cantilever, 37
- temperature loads
 - L14: 2D Truss - Thermal Loads and Settlement, 51
 - L16: Nonlinear Thermal Load, 53
- tensile force, 157
- tension, 159
- thermal loads
 - C04: Thermal Loads, 527
 - L05: 2D Truss with Thermal Load, 29
 - L14: 2D Truss - Thermal Loads and Settlement, 51
 - L16: Nonlinear Thermal Load, 53
- tie beam
 - L10: Tie Beam without Geometric Stiffening, 39
 - N01: Tie Beam with Geometric Stiffening, 157
- time history analysis, 235
- time-dependent material properties, 517
- time-dependent staged-construction analysis, 517
- torsional system, 219
- truss
 - L01: 2D Truss with Static Loads, 17
 - L05: 2D Truss with Thermal Load, 29
 - L14: 2D Truss - Thermal Loads and Settlement, 51
- uniform lateral load
 - L10: Tie Beam without Geometric Stiffening, 39
 - N01: Tie Beam with Geometric Stiffening, 157
- uniform load, 21
- uniform loads, 47
- uniform thermal load, 527
- yielding elastic supports

LARSA 4D Sample and Verification Problems

L02: Beam with Elastic Supports, 19

L06: Static Analysis of a Space Frame, 31